

Bone Densitometry for Technologists

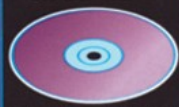
Sydney Lou Bonnicks, MD, FACP

Lori Ann Lewis, MRT, CDT

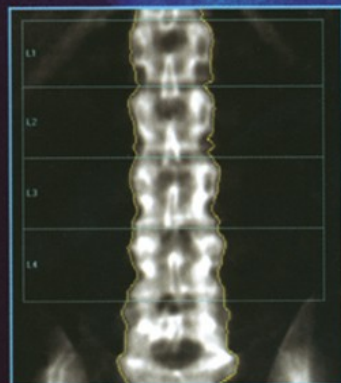
SECOND EDITION



*Includes CE Test
on CD-ROM*



15 Hrs Category A ASRT Credit



 HUMANA PRESS

BONE DENSITOMETRY FOR TECHNOLOGISTS

BONE DENSITOMETRY FOR TECHNOLOGISTS

Second Edition

SYDNEY LOU BONNICK, MD, FACP
LORI ANN LEWIS, MRT, CDT

*Clinical Research Center of North Texas
Denton, TX*



HUMANA PRESS
TOTOWA, NEW JERSEY

© 2006 Humana Press Inc.
999 Riverview Drive, Suite 208
Totowa, New Jersey 07512
www.humanapress.com

For additional copies, pricing for bulk purchases, and/or information about other Humana titles, contact Humana at the above address or at any of the following numbers: Tel.: 973-256-1699; Fax: 973-256-8341, E-mail: orders@humanapr.com; or visit our Website: www.humanapress.com

All rights reserved. No part of this book may be reproduced, stored in a retrieval system, or transmitted in any form or by any means, electronic, mechanical, photocopying, microfilming, recording, or otherwise without written permission from the Publisher.

All articles, comments, opinions, conclusions, or recommendations are those of the author(s), and do not necessarily reflect the views of the publisher.

Due diligence has been taken by the publishers, editors, and authors of this book to assure the accuracy of the information published and to describe generally accepted practices. The contributors herein have carefully checked to ensure that the drug selections and dosages set forth in this text are accurate and in accord with the standards accepted at the time of publication. Notwithstanding, as new research, changes in government regulations, and knowledge from clinical experience relating to drug therapy and drug reactions constantly occurs, the reader is advised to check the product information provided by the manufacturer of each drug for any change in dosages or for additional warnings and contraindications. This is of utmost importance when the recommended drug herein is a new or infrequently used drug. It is the responsibility of the treating physician to determine dosages and treatment strategies for individual patients. Further it is the responsibility of the health care provider to ascertain the Food and Drug Administration status of each drug or device used in their clinical practice. The publisher, editors, and authors are not responsible for errors or omissions or for any consequences from the application of the information presented in this book and make no warranty, express or implied, with respect to the contents in this publication.

Production Editor: Tracy Catanese
Cover design by Patricia F. Cleary

Cover Illustration: Top left: a vertebral fracture assessment image, acquired on the Hologic Delphi, showing vertebral deformities in the lower thoracic spine as well as spurring of the lower lumbar vertebra and aortic calcification to the lumbar spine. Top right: total body bone density image, acquired on the Hologic Discovery. Both images courtesy of Hologic, Inc., Bedford, MA. Bottom: posterior-anterior spine image acquired on the GE Lunar Prodigy. Image courtesy of the author.

This publication is printed on acid-free paper. 
ANSI Z39.48-1984 (American National Standards Institute) Permanence of Paper for Printed Library Materials.

Photocopy Authorization Policy:

Authorization to photocopy items for internal or personal use, or the internal or personal use of specific clients, is granted by Humana Press Inc., provided that the base fee of US \$30.00 per copy is paid directly to the Copyright Clearance Center at 222 Rosewood Drive, Danvers, MA 01923. For those organizations that have been granted a photocopy license from the CCC, a separate system of payment has been arranged and is acceptable to Humana Press Inc. The fee code for users of the Transactional Reporting Service is: [1-58829-670-9/06 \$30.00].

Printed in the United States of America. 10 9 8 7 6 5 4 3 2 1

e-ISBN: 1-59259-992-3

Library of Congress Cataloging-in-Publication Data

Bonnick, Sydney Lou.

Bone densitometry for technologists / Sydney Lou Bonnick, Lori Ann Lewis.-- 2nd ed.
p. cm.

Includes bibliographical references and index.

ISBN 1-58829-670-9 (alk. paper)

1. Bone densitometry. I. Lewis, Lori Ann. II. Title.

RC930.5.B678 2006

616.7'10754--dc22

2005007778

DEDICATION

*For Momma, Daddy and Sissy and Bo and his family
L.A.L.*

*For Mom and Dad, Tooney and Charles
S.L.B.*

PREFACE

Bone densitometry is an extraordinary clinical and research tool. Most of us think of densitometry as a relatively recent technological development, but in fact, its history began more than 100 years ago. In the field of dentistry, crude devices by today's standards were developed in the late 19th century to evaluate the density of the bone in the mandible. The advances in technology continued, albeit slowly, for the first half of the 20th century, gaining some speed in the 1960s and 1970s. The introduction of dual-energy X-ray absorptiometry in the late 1980s truly opened the door to clinicians' offices for bone densitometry. In the last 10 years, the advances in technology and the introduction of new machines of various types has occurred with almost blinding speed compared with the pace of development during most of the 20th century.

As densitometry has matured as a field, the number of disease states in which bone density is known to be affected has increased. With this knowledge, physicians in many different fields of medicine now recognize the need to measure bone density as part of the management of their patients. More studies are being requested now than ever before. This demand for densitometry has also led to an increased need for qualified technologists to operate the machines.

Densitometry is a quantitative technique, as are measurements of blood pressure and cholesterol. That is, the technology is used to measure a quantity. But of all the quantitative techniques in use in clinical medicine today, there is none that has the potential to be more accurate or precise than bone densitometry. The technology is highly sophisticated. All of the devices in use today employ computer technology. In spite of this mechanical sophistication, however, the technology will only be as good as the technologist.

The densitometry technologist must have knowledge of skeletal anatomy, densitometry techniques, radiation safety, basic statistics, quality control procedures, and the processes of various diseases such as osteoporosis. The technologist must often make decisions about the conduct of testing without immediate input from the physician. The circumstances in which densitometry is usually performed create the opportunity for extended technologist-patient interaction and discussion. For technologists accustomed to performing radiologic procedures, this degree of interaction is unprecedented. Today's densitometry technologist must be prepared for these encounters.

There is no substitute for the thoughtful training provided by the manufacturers of the various types of densitometry equipment when the devices are installed. There is also no substitute for careful study of the operator's manuals that are supplied with these machines. The exact operation of each machine is different. To be proficient on any densitometry device, the technologist must be trained on that specific device. There is a broad knowledge base, however, that all technologists

should possess. *Bone Densitometry for Technologists, Second Edition* is intended to help provide that base.

It is always difficult to know where to begin. Like so many other fields of medicine, densitometry has its own language and conventions that must be explained so that in-depth discussions can be understood. Chapter 1 is an introduction to the terminology and conventions used in bone densitometry. In Chapter 2, a review of the various techniques and technologies used in quantifying bone mass is presented. This review provides some of the historical development of the field as well as discussing the attributes of the various technologies and the differences between them. In Chapter 4, descriptions provided by the manufacturers of all the devices that were approved by the Food and Drug Administration at the time this book went to press can be found, along with photographs of the devices. New models that have become available since the first edition of this book was published in 2002 have been added. This summary description should be useful in determining what skeletal regions can be studied with any particular device, the nature of the technology employed in the device, the patient radiation exposure during a study, as well as other machine specifics. Chapter 5 covers computer basics. Although technologists and physicians are becoming more comfortable using computers and some of us consider ourselves quite “computer-literate,” many of us are not. All of our machines are computer-driven. A basic knowledge of computers is almost mandatory for a densitometry technologist. This chapter cannot substitute for learning the nuances of the specific software that operates any given device, but it should help those who consider themselves beginners or even intermediate computer users. Since the first edition of *Bone Densitometry for Technologists*, processing speeds have become faster, hard drives larger, and new types of removable storage media have become available. This chapter has been updated to reflect these developments.

In Chapter 3, the skeletal anatomy of commonly measured densitometry sites is discussed, with an emphasis on those attributes of anatomy that are either unique to densitometry or would have an effect on the measurement of bone density at that site.* This knowledge is indispensable for the densitometry technologist. It is equally important that the technologist understand the concept of precision and how to measure it. This is presented in Chapter 6.† Without the technologist’s careful attention to precision, those factors that affect it, and knowledge of how to calculate it, the physician to whom the results are given will not be able to interpret followup bone density studies to determine if the bone density has changed.

All densitometers, as sophisticated as they are, are mechanical devices. Things can and do go wrong. It is imperative that machine malfunctions be recognized as

* Portions of this chapter were adapted from Bonnick SL. Skeletal anatomy in densitometry. In: Bonnick SL, *Bone Densitometry in Clinical Practice*, 2nd ed. Totowa, NJ: Humana Press, 2004:31–64. With permission of the publisher.

† Adapted from Bonnick, S.L., Johnston, C.C., Kleerekoper, M., et al. The importance of precision in bone density measurements. *J Clin Densitom* 2001;4:105–110. With permission of the publisher.

soon as possible. Otherwise, the data from the machine that is provided by the technologist to the physician will be flawed. This means that a good quality control program must be in place. It is normally the responsibility of the technologist to not only to create this program but also to monitor it. Quality control procedures are discussed in Chapter 8. Almost all quality control procedures involve scanning a phantom. A discussion of the various types of phantoms has been added to *Bone Densitometry for Technologists, Second Edition*.

Most, but not all, densitometers are also X-ray devices. Radiation safety then must be a concern. Fortunately, both patient and technologist exposures from X-ray densitometry are incredibly small. Nevertheless, the concept of *ALARA* (as low as reasonably achievable) demands that the patient, the public, and the technologist be protected from unnecessary exposure to ionizing radiation. In Chapter 7, radiation safety concepts are discussed, with recommendations made for radiation safety procedures at densitometry facilities.

Two of the chapters may seem unusual in a book for technologists. Chapter 9 is a review of the disease for which densitometry is most commonly used, osteoporosis. Chapter 10 is a review of how the data that come from these machines are actually interpreted to diagnose osteoporosis and predict fracture risk. These chapters might at first seem more appropriate in a book written for physicians. However, the densitometry technologist normally spends a significant amount of time with the patient. There is ample opportunity for the patient to ask questions of the technologist about osteoporosis and about the test that he or she is about to undergo. The knowledgeable technologist can be a vital link in the education of the patient. He or she can allay unnecessary fears and encourage appropriate medical followup. The technologist is not usurping the role of the physician by doing so if the technologist understands the issues involved. Indeed, the complete medical care of the patient must involve a partnership between the technologist and the physician. The final diagnosis and treatment recommendations for any patient must be left to the physician, but within those bounds there is much that the technologist can do that will actually strengthen the patient's trust in the quality of their care and improve compliance with the medical recommendations. The technologist who understands as much as possible about what the physician will consider as he or she looks at the densitometry report will only be better able to aid that physician in the performance of their profession. Since the publication of the first edition of *Bone Densitometry for Technologists*, new drugs have been approved for the prevention and/or treatment of osteoporosis and new guidelines have been issued for bone density testing and pharmacologic intervention based on that testing. This information has been added to Chapter 9 in this edition.

In the last few years, densitometry has been applied increasingly in pediatrics. The technical considerations for pediatric densitometry are different from those of adult densitometry and the interpretation of data even more complex. This is an area that is expected to grow, however, and so many of the confounding issues in pediatric densitometry are addressed in Chapter 11 for the first time in this second edition.

Finally, in Chapter 12, there is a review of skeletal morphometry performed with dual-energy X-ray absorptiometry as well as body composition analysis.

These two applications of dual-energy X-ray absorptiometry take the technology beyond the measurement of bone density. Skeletal morphometry, particularly vertebral fracture assessment, is expected to become an integral part of the fracture risk assessment of the postmenopausal woman. Body composition analysis with DXA is an application that is only beginning to achieve some prominence in clinical practice, but its advantages become obvious when compared with other body composition methods. This chapter, like Chapter 11, is completely new in *Bone Densitometry for Technologists, Second Edition*.

The 12 appendices have been updated wherever necessary to reflect the most current information available. Contact information for densitometry equipment manufacturers and organizations of interest can be found in Appendix I. Every attempt was made to verify the accuracy of this information at the time this book went to press. Guidelines for bone density testing and CPT codes have been updated in Appendices III and V, respectively. New conversion equations have been added to Appendix VII and new terms have been added to Appendix XI. Finally, in Appendix XII, the contents of the new CD-ROM are reviewed. On this CD, you will find the Precision Calculator Companion that was first included with *Bone Densitometry in Clinical Practice, Second Edition*, and with which you will be able to calculate the short-term precision and least significant change values for your facility as well as the statistical confidence level for any measured change in BMD. These concepts are discussed thoroughly in Chapter 6. There is also a patient questionnaire that may be customized for your facility. A continuing education review is also found on the CD, which, if successfully completed, may result in the awarding of 15 hours of Category A credit acceptable to the American Society of Radiologic Technologists.

As a technology, bone densitometry is really quite extraordinary. The ability to quantify the density of the bones at a variety of skeletal sites has truly revolutionized the approach to a number of diseases, the most important of which is osteoporosis. Using the information from the machines, physicians can recommend and prescribe interventions that will stop bone loss and prevent disabling fractures. The remarkable advances in skeletal imaging with densitometry devices have made possible quantitative and diagnostic assessments of skeletal structure. But it is in fact the skill and concern of the technologist that enables all of this to happen. It is our hope that *Bone Densitometry for Technologists, Second Edition* assists you in your pursuit of excellence in your profession.

Sydney Lou Bonnick, MD, FACP
Lori Ann Lewis, MRT, CDT

ACKNOWLEDGMENTS

Our gratitude is extended to the following individuals for their assistance and support in the production of this work: Joyce Paucek, Mary Ann Barrick, John Jenkins of Hologic, Inc.; Thomas Hessel of Osteometer Meditech; Louai Al-Dayeh of Compumed, Inc.; Diane King and Jeff Prellwitz of Alara, Inc.; Ken Faulkner and Linda Weynand of GE Healthcare; Daniel Michaeli of Schick Technologies, Inc.; Jody Spear of Quidel Corp.; Tom Sanchez of CooperSurgical Norland; Roger Schulte of Image Analysis, Inc., Colin Miller of Bio-Imaging Technologies, Inc.; Anders Rosholm of Sectra Pronosco; Varda Green of Sunlight Medical, Ltd., and Harry Genant of the University of California San Francisco. And a very special thanks to Cathy Heist, RT of the American Society for Radiologic Technologists for her assistance in the preparation of the continuing educational material for technologists.

We would also like to thank those authors and publishers who allowed us to reproduce their work in the interest of continuing education.

CONTENTS

Dedication	v
Preface	vii
Acknowledgments	xi
Continuing Education	xxi
Chapter 1: An Introduction to Conventions in Densitometry	1
Densitometry as a Quantitative Measurement Technique	2
Accuracy and Precision	2
The Skeleton in Densitometry	4
Weight Bearing or Non-Weight Bearing	4
Axial or Apppendicular	4
Central or Peripheral	6
Cortical or Trabecular	6
What Do the Machines Actually Measure?	8
The Effect of Bone Size on Areal Densities	9
Bone Mineral Apparent Density	10
Calculating “Average” Spine Bone Densities	11
Ultrasound Parameters	11
The Densitometry Printout	12
The Percentage Comparisons	13
The Standard Score Comparisons	15
The Age-Regression Graph	19
The Standardized BMD	20
The Utility of the sBMD	22
The National Health and Nutrition Examination Survey (NHANES) III Database for the Proximal Femur	23
Nomenclature Guidelines From the International Society for Clinical Densitometry	25
References	26
Chapter 2: Densitometry Techniques	29
Plain Radiography in the Assessment of Bone Density	30
Qualitative Morphometry	30
Qualitative Spinal Morphometry	30
The Singh Index	31
Quantitative Morphometric Techniques	32
Calcar Femorale Thickness	32
Radiogrammetry	33
The Radiologic Osteoporosis Score	35

Radiographic Photodensitometry	35
Radiographic Absorptiometry	37
Photon Absorptiometry Techniques	39
Single-Photon Absorptiometry	40
Dual-Photon Absorptiometry	42
Dual-Energy X-Ray Absorptiometry	45
Peripheral DXA	51
Single-Energy X-Ray Absorptiometry	52
Quantitative Computed Tomography	53
Peripheral QCT	58
Quantitative Ultrasound Bone Densitometry	58
References	61
Chapter 3: Skeletal Anatomy in Densitometry	67
The Spine in Densitometry	67
Vertebral Anatomy	68
Artifacts in PA or AP Spine Densitometry	73
Vertebral Fractures	73
Effect of Osteophytes on BMD	76
Effect of Aortic Calcification on BMD	77
Effect of Facet Sclerosis on BMD	80
Effect of Vertebral Rotation on PA Lumbar Spine Bone Density	81
Other Causes of Artifacts in PA and AP Lumbar Spine Studies	84
The Spine in the Lateral Projection	84
The Proximal Femur in Densitometry	88
Proximal Femur Anatomy	88
Effect of Rotation on BMD in the Proximal Femur	89
Effect of Leg Dominance on BMD in the Proximal Femur	93
Effect of Scoliosis, Osteoarthritis, Osteophytes, Surgery, and Fracture on BMD in the Proximal Femur	93
The Forearm in Densitometry	94
Nomenclature	94
Effect of Arm Dominance on Forearm BMD	97
Effect of Artifacts on BMD in the Forearm	98
The Metacarpals, Phalanges, and Calcaneus	100
References	102
Chapter 4: FDA-Approved Densitometry Devices	105
Computer-Enhanced Radiogrammetry	105
Computer-Enhanced Radiographic Absorptiometry	107
Central X-Ray Densitometers	109
Peripheral X-Ray Densitometers	138
Ultrasound Bone Densitometers	148

Chapter 5: Computer Basics	163
Types of Computers	164
Desktops, Towers, Minitowers, and Laptops	164
PCs and MACs	165
Major Components of a Computer System	166
Important Components Inside the Computer Housing	167
Motherboard, Random Access Memory, and Slots	167
Central Processing Units	167
Hard Drives	168
Internal Disk Drives	169
Input Devices	170
The Keyboard	170
The Mouse	172
The Trackball	172
Output Devices	173
Monitors	173
Printers	174
Computer Ports	175
Keyboard and Mouse Ports	175
Parallel Ports	175
Serial Ports	176
Universal Serial Bus Ports	177
Power, Monitor, Modem, and Network Ports	177
Types of Storage Media	179
Magnetic Media	180
Optical Storage Media	182
Flash Memory	183
Protecting the Data	184
Computer Maintenance	186
Chapter 6: The Importance of Precision	189
The Concept of Precision	189
Performing a Precision Study	190
Short-Term Precision Studies	192
Mathematical Procedures Used to Calculate Precision	195
Long-Term Precision Studies	197
Applying the Precision Value to Serial Measurements	197
Determination of Least Significant Change	197
Using the Least Significant Change to Determine the Timing of Repeat Measurements	200
A Case in Point	201
More Sophisticated Issues of Statistical Confidence	203
for the Measured Change	203
Determining the Level of Confidence for Any Change and Precision	203

The Confidence Interval for the Change in BMD Between Two Measurements	204
The Importance of Precision	206
Which Skeletal Sites Should Be Used for Monitoring	207
How Frequently Should Measurements Be Repeated?	210
A Final Consideration	211
References	212
Chapter 7: Radiation Safety in X-Ray Densitometry	213
Radiation Basics	213
Radiation Quantities	214
The Curie	214
The Roentgen	214
The Rad	215
The Rem	215
The Effective Dose Equivalent	216
Harmful Effects of Ionizing Radiation	217
Acute Lethal Radiation Syndromes	217
Local Tissue Damage From Radiation	218
Skin	218
Ovaries and Testes	218
Bone Marrow and Blood	219
Late Effects of Ionizing Radiation	219
Radiation Doses in Densitometry	220
Radiation Protection Programs	222
Protection of the Public	223
Protection of the Patient	224
Protection of the Technologist	227
Time, Distance, and Shielding	227
Personnel Monitoring Devices	228
The Pregnant Technologist	229
References	229
Chapter 8: Quality Control	231
Phantoms	232
European Spine Phantom	233
Bona Fide Spine Phantom	234
Hologic Spine and Hip Phantoms	235
Lunar Spine Phantom	235
Using the Phantom to Create Control Tables and Charts	237
Shewhart Rules and CUSUM Charts	241
Shewhart Rules	242
CUSUM Charts	245
Automated Quality Control Procedures	249
Replacing a Densitometer	254
References	255

Chapter 9: An Overview of Osteoporosis	257
The Definition of Osteoporosis	258
The 1991 and 1993 Consensus Development Conferences	258
The 1994 World Health Organization Criteria for Diagnosis of Osteoporosis	259
The 2000 National Institutes of Health Consensus Conference Definition of Osteoporosis	261
Prevalence of Osteoporosis	262
Consequences of Osteoporosis	263
Risk Factors for Osteoporosis	264
Attainment of Peak Bone Density	264
Maintenance of Bone Density	265
Guidelines for Bone Mass Measurements	266
The National Osteoporosis Foundation Guidelines for Bone Mass Measurements	266
Guidelines From Specialty Societies	267
The 1997 Bone Mass Measurement Act	268
Treatment Guidelines for Postmenopausal Osteoporosis	271
NOF Guidelines	271
Treatment Guidelines From AACE and NAMS	271
Interventions in Osteoporosis	272
Nonprescription Interventions	272
Lifestyle Modifications	272
Calcium, Vitamin D, and Exercise	273
Prescription Interventions	276
Estrogen Replacement	276
The Selective Estrogen Receptor Modulator Raloxifene	277
Synthetic Salmon Calcitonin	278
Bisphosphonates	278
Alendronate	279
Risedronate	280
Ibandronate	281
Dosing, Contraindications, and Safety	282
Teriparatide	283
Patient Education Materials	284
References	285
Chapter 10: Interpretation of Bone Densitometry Data	289
The Results	290
The Skeletal Image	290
Measured and Calculated Bone Density Parameters	292
Comparisons to the Reference Database	296
Standardized BMD	300
Age-Regression Graph	300

Assignment of Diagnostic Category Based on WHO Criteria	303
Conflicting Diagnoses From the Measurement of Multiple Sites	305
Report Review	308
References	312
Chapter 11: Considerations in Pediatric Densitometry	313
Scan Acquisition and Analysis Considerations	314
Bone Age	315
Sexual Maturation Stage	317
Considerations of Bone Size and Shape	317
Skeletal Development and the Use of Standard Scores in Pediatric Densitometry	319
Skeletal Development	320
Use of Standard Scores in Pediatric Densitometry	322
Pediatric Reference Databases	324
International Society for Clinical Densitometry Guidelines for Children	325
The Specialty of Pediatric Densitometry	325
References	326
Chapter 12: Moving Beyond Bone Density With Bone Densitometers: Skeletal Morphometry and Body Composition Assessments	329
Skeletal Morphometry for Structural Diagnoses and Prediction of Fracture Risk	329
Vertebral Morphometry and Fractures	330
Relationship Between Prevalent Spine Fractures and Future Fracture Risk	330
Diagnosing Vertebral Fractures	330
Vertebral Fracture Assessment With Genant's Semiquantitative Technique	332
Vertebral Fracture Assessment With Quantitative Techniques	332
Performance Comparisons of Semiquantitative and Quantitative Techniques	334
Fan-Array Spine Imaging With DXA	335
Proximal Femur Morphometry	339
Hip Axis Length	339
The Femoral Neck-Shaft Angle	342
Femoral Neck Width	342
The Upper Femoral Neck	342
Hip Strength Analysis	344
Body Composition Analysis	345
The Body Mass Index	346
Body Composition Methods	347

Two-Compartment Body Composition Measurement Techniques	349
Underwater Weighing	349
Skinfold Measurements	350
Bioelectrical Impedance Analysis	351
Air Displacement Plethysmography	352
Three-Compartment Body Composition Measurement Techniques	352
Near Infrared Interactance	352
Dual Energy X-Ray Absorptiometry	353
References	361
<i>Appendix I: Contacts for Bone Densitometry Manufacturers and Organizations of Interest</i>	<i>367</i>
<i>Appendix II: World Health Organization Criteria for the Diagnosis of Osteoporosis Based on the Measurement of Bone Density</i>	<i>373</i>
<i>Appendix III: Guidelines for Bone Density Testing</i>	<i>375</i>
<i>Appendix IV: Bone Mass Measurement Act of 1997</i>	<i>379</i>
<i>Appendix V: CPT Codes for Bone Densitometry</i>	<i>381</i>
<i>Appendix VI: Dual-Energy X-Ray Absorptiometry Posteroanterior Lumbar Spine Labeling Guidelines</i>	<i>383</i>
<i>Appendix VII: Conversion Formulas</i>	<i>385</i>
<i>Appendix VIII: Recommended Procedures for Short-Term Precision Studies</i>	<i>389</i>
<i>Appendix IX: Least Significant Change</i>	<i>393</i>
<i>Appendix X: Quality Control Shewhart Rules</i>	<i>395</i>
<i>Appendix XI: Glossary of Computer Terms</i>	<i>397</i>
<i>Appendix XII: The CD-ROM Companion</i>	<i>407</i>
Index	409
About the Authors	417

CONTINUING EDUCATION

The Companion CD for this book contains a continuing education test good for 15 hours of Category A credit from the The American Society of Radiologic Technologists (ASRT). Instructions for the test are contained within the program. The Program also includes links to a Patient Questionnaire in Word format and a Precision Calculator for Bone Densitometry Technologists in Excel format.

The CD-ROM program requires one of the following:

- A PC running windows 98 or higher
- Mac OSX 10.2 or later
- Mac OS 9.2

Additional software is required for use with the linked Word and Excel documents. A printer is required to print the results of the test.

1

An Introduction to Conventions in Densitometry

CONTENTS

DENSITOMETRY AS A QUANTITATIVE MEASUREMENT TECHNIQUE
ACCURACY AND PRECISION
THE SKELETON IN DENSITOMETRY
WEIGHT BEARING OR NON-WEIGHT BEARING
AXIAL OR APPENDICULAR
CENTRAL OR PERIPHERAL
CORTICAL OR TRABECULAR
WHAT DO THE MACHINES ACTUALLY MEASURE?
THE EFFECT OF BONE SIZE ON AREAL DENSITIES
BONE MINERAL APPARENT DENSITY
CALCULATING “AVERAGE” SPINE BONE DENSITIES
ULTRASOUND PARAMETERS
THE DENSITOMETRY PRINTOUT
THE PERCENTAGE COMPARISONS
THE STANDARD SCORE COMPARISONS
THE AGE-REGRESSION GRAPH
THE STANDARDIZED BMD
THE NATIONAL HEALTH AND NUTRITION EXAMINATION SURVEY (NHANES) III DATABASE FOR THE PROXIMAL FEMUR
NOMENCLATURE GUIDELINES FROM THE INTERNATIONAL SOCIETY FOR CLINICAL DENSITOMETRY
REFERENCES

In any discussion of bone densitometry, many terms and conventions are used that are unique to this field. In the chapters that follow, these terms and conventions will be used repeatedly. In an effort to facilitate the

reading and comprehension of those chapters, a preliminary review of some of these unique aspects of bone densitometry is offered here.

DENSITOMETRY AS A QUANTITATIVE MEASUREMENT TECHNIQUE

Bone densitometry is primarily a quantitative measurement technique. That is, the technology is used to measure a quantity, in this case, the bone mass or density. Other quantitative measurement techniques used in clinical medicine are sphygmomanometry; spirometry; and the measurement of hemoglobin, cholesterol, glucose, and other substances found in the blood. Some of today's highly sophisticated densitometers are capable of producing extraordinary skeletal images that may be used for structural diagnoses. Nevertheless, densitometry primarily remains a quantitative measurement technique, rather than an imaging technique such as plain radiography. As such, quality control measures in densitometry are not only concerned with the mechanical operation of the devices, but also with attributes of quantitative measurements such as precision and accuracy.

Accuracy and Precision

Accuracy and precision are easily understood using a target analogy shown in Fig. 1-1. To hit the bull's-eye of the target is the goal of any archer. In a sense, the bull's-eye is the "gold standard" for accuracy. In Fig. 1-1 on target A, one of the archer's arrows has, in fact, hit the bull's-eye. Three of the other four arrows are close to the bull's-eye as well, although none has actually hit it. One arrow is above and to the right of the bull's-eye in the second ring. A second arrow is to the right and below the bull's-eye in the second ring, and a third arrow is below and to the left of the bull's-eye straddling rings 1 and 2. The last arrow is straddling rings 2 and 3, above and to the left of the bull's-eye. This archer can be said to be reasonably accurate but he has been unable to reproduce his shot. Target A illustrates accuracy and lack of precision. In target B, another archer has attempted to hit the bull's-eye. Unfortunately, he has not come close. He has, however, been extremely consistent in the placement of his five arrows. All five are tightly grouped together in the upper right quadrant of the target. In other words, although not accurate, this archer's shots were extremely reproducible, or precise. Target B illustrates precision and lack of accuracy. Ideally, an archer would be both accurate and precise, as shown in target C in Fig. 1-1. Here, all five arrows

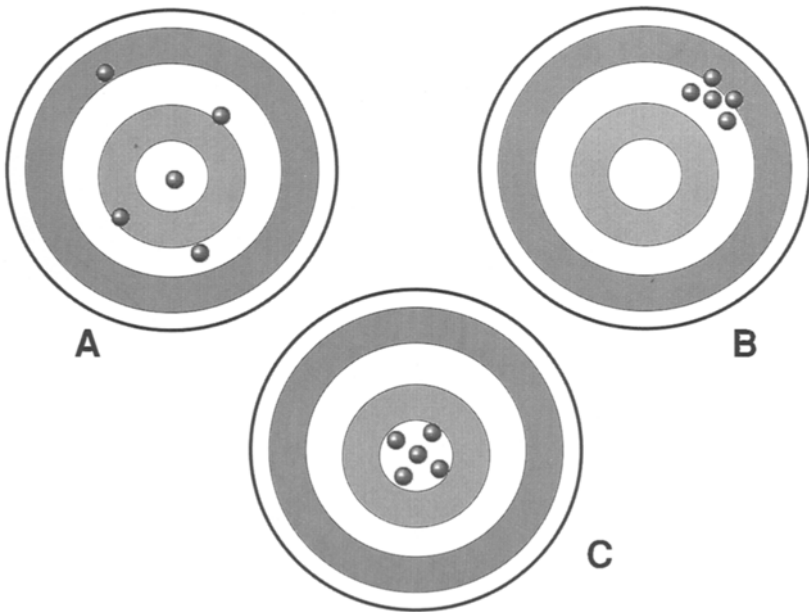


Fig. 1-1. Accuracy and precision. Target A illustrates accuracy without precision, target B illustrates precision without accuracy, and target C illustrates a high degree of both accuracy and precision.

are grouped together within the bull's-eye, indicating a high degree of both accuracy and precision.

When bone densitometry is used to quantify the bone density for the purpose of diagnosing osteoporosis or predicting fracture risk, it is imperative that the measurement be accurate. On the other hand, when bone densitometry is used to follow changes in bone density over time, precision becomes paramount. Strictly speaking, the initial accuracy of the measurement is no longer of major concern. It is only necessary that the measurement be reproducible or precise because it is the change between measurements that is of interest. Bone densitometry has the potential to be the most precise quantitative measurement technique in clinical medicine. The precision that is actually obtained, however, is highly dependent upon the skills of the technologist. Precision itself can be quantified in a precision study, as discussed in Chapter 6. The performance of a precision study is imperative in order to provide the physician with the necessary information to interpret serial changes in bone density. Precision values are usually provided by the manufacturers of the various types of densitometry equipment. Most manufacturers express precision as a percent coefficient of variation

(%CV). The %CV expresses the variability in the measurement as a percentage of the average value for a series of replicate measurements. These values are the values that the manufacturers have obtained in their own precision studies. This is not necessarily the precision that will be obtained at a clinical densitometry facility. That value must be established by the facility itself. As will be discussed in Chapter 6, it is preferable to use the root-mean-square standard deviation (RMS-SD) or root-mean-square coefficient of variation (RMS-CV) to express precision rather than the arithmetic mean or average standard deviation (SD) or coefficient of variation (CV). It is not always clear whether the manufacturer's precision value is being expressed as the RMS or arithmetic average. In general, the arithmetic mean SD or CV will be better than the RMS-SD or RMS-CV. Manufacturers also do not usually state the average bone density of the population in the precision study or the exact number of people and number of scans per person, making the comparison of such values with values obtained at clinical facilities difficult.

THE SKELETON IN DENSITOMETRY

Virtually every part of the skeleton can be studied with the variety of densitometers now in clinical use. The bones of the skeleton can be characterized in four different ways, one of which is unique to densitometry. The characterizations are important, as this often determines which site is the most desirable to measure in a given clinical situation. A skeletal site may be characterized as weight bearing or non-weight bearing, axial or appendicular, central or peripheral, and predominantly cortical or trabecular.

Weight Bearing or Non-Weight Bearing

The distinction between weight bearing and non-weight bearing is reasonably intuitive. The lower extremities are weight bearing as is the cervical, thoracic, and lumbar spine. Often forgotten, although it is the most sensitive weight bearing bone, is the calcaneus or os calcis. Portions of the pelvis are considered weight bearing as well. The remainder of the skeleton is considered non-weight bearing.

Axial or Appendicular

The axial skeleton includes the skull, ribs, sternum, and spine, as shown in Fig. 1-2 (1). In densitometry, the phrase *axial skeleton* or *axial bone density study* has been used to refer to the lumbar spine and

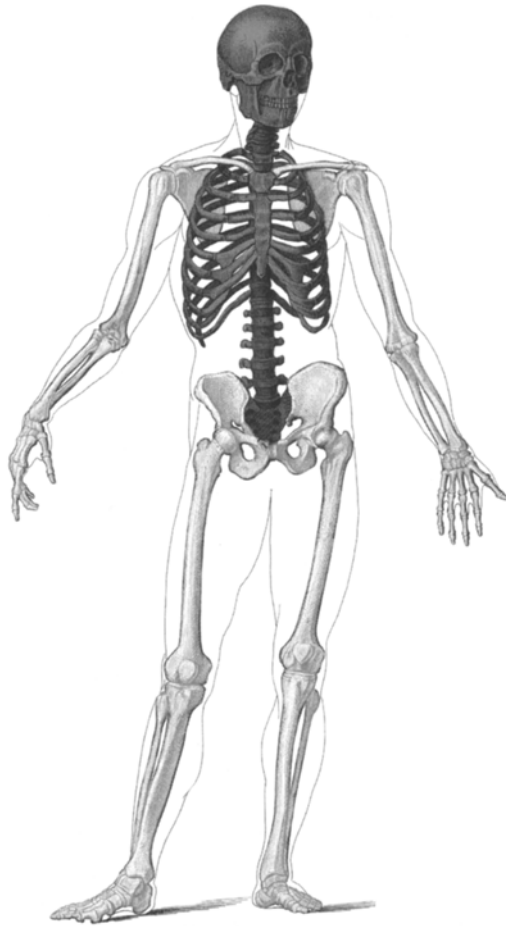


Fig. 1-2. The axial and appendicular skeleton. The darker shaded bones comprise the axial skeleton. The lighter shaded bones comprise the appendicular skeleton. Image adapted from EclectiCollections™.

posteroanterior (PA) lumbar spine bone density studies. This limited use is no longer appropriate since the lumbar spine can also be studied in the lateral projection and the thoracic spine can be measured as well. The skull and the ribs are quantified only as part of a total body bone density study and as a consequence, the phrase *axial bone density study* has never implied a study of those regions. The appendicular skeleton includes the extremities and the limb girdles, as shown in Fig. 1-2. The scapulae and the pelvis are therefore part of the appendicular skeleton. The proximal femur is also obviously part of the appendicular skeleton, although it is often

mistakenly included in the axial skeleton. Contributing to this confusion is the current practice of including dual-energy X-ray bone density studies of the proximal femur under the CPT code 76075 used for dual-energy X-ray absorptiometry (DXA) spine bone density studies (see Appendix V).

Central or Peripheral

The characterization of skeletal sites as either central or peripheral is unique to densitometry. Central sites are the thoracic and lumbar spine in either the PA or lateral projection and the proximal femur. By extension, those densitometers that have the capability of measuring the spine and proximal femur are called central densitometers. As a matter of convention, this designation is generally not applied to quantitative computed tomography (QCT), even though spine bone density measurements are made with QCT. Peripheral sites are the commonly measured distal appendicular sites such as the calcaneus, tibia, metacarpals, phalanges, and forearm. Again, by extension, densitometers that measure only these sites are called peripheral densitometers. Some central devices also have the capability of measuring peripheral sites. Nevertheless, they retain their designation as central bone densitometers. The central and peripheral skeleton is illustrated in Fig. 1-3.

Cortical or Trabecular

The characterization of a site as predominantly cortical or trabecular bone is important in densitometry. Some disease states show a predilection for one type of bone over the other, making this an important consideration in the selection of the site to measure when a particular disease is present or suspected. Similarly, the response to certain therapies is greater at sites that are predominantly trabecular because of the greater metabolic rate of trabecular bone. There are also circumstances in which a physician desires to assess the bone density at both a predominantly cortical and predominantly trabecular site in order to have a more complete evaluation of a patient's bone mineral status.

It is relatively easy to characterize the commonly measured sites as either predominantly cortical or predominantly trabecular, as shown in Table 1-1. It is more difficult to define exact percentages of cortical and trabecular bone at each site. The values given in Tables 1-2 and 1-3 should be considered clinically useful approximations of these percentages. Slightly different values may appear in other texts depending upon the references used, but the differences tend to be so small that they are not clinically important.

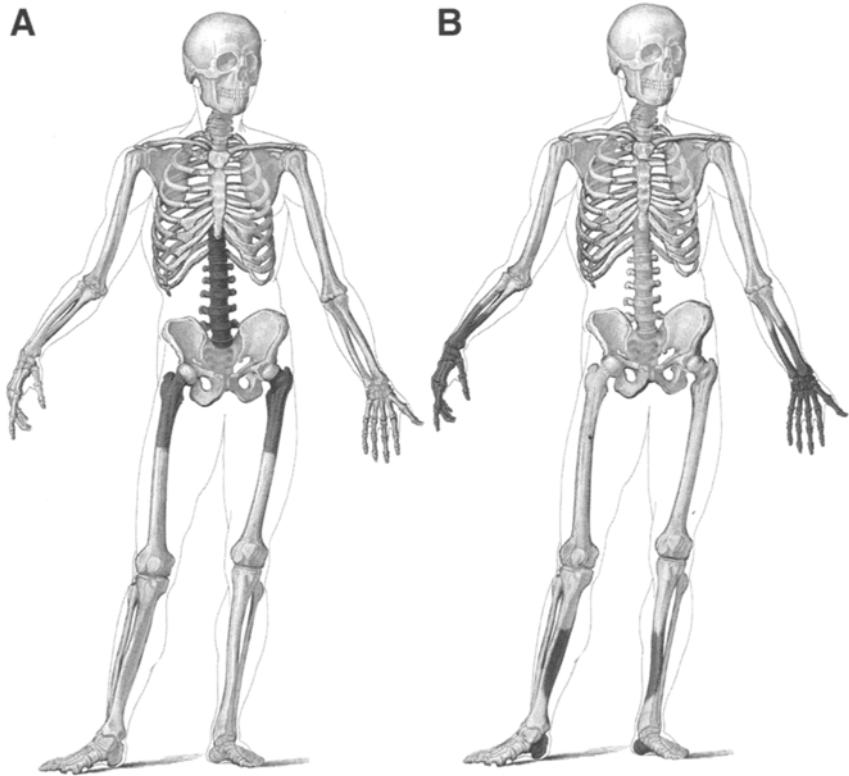


Fig. 1-3. The central and peripheral skeleton. (A) The darker shaded bones comprise the central skeleton. (B) The darker shaded bones comprise the peripheral skeleton. Images adapted from EclectiCollections.

Table 1-1
Predominantly Trabecular or Cortical Skeletal Sites

<i>Trabecular</i>	<i>Cortical</i>
Posteroanterior spine	Total body
Lateral spine	Femoral neck
Ward's	33% Forearm ^a
4–5% Forearm ^a	10% Forearm ^a
Calcaneus	5- and 8-mm Forearm ^b
	Phalanges

^aindicates the location of the region of interest on either the radius, ulna, or both combined as a percentage of the length of the ulna, measured from the ulnar styloid. See Chapter 3 for a discussion of naming conventions for forearm sites.

^bDistance in millimeters indicates the separation distance between the radius and ulna at the site in question.

Table 1-2
Percentage of Trabecular Bone at Central Sites as Measured
by Dual-Energy X-Ray Absorptiometry (DXA)

PA spine ^a	66%
Lateral spine ^b	?
Femoral neck	25%
Trochanter	50%
Ward's ^b	?
Total body	20%

^aThese percentages are for DXA posteroanterior (PA) spine studies only. A volumetric measurement of 100% trabecular bone could be obtained with quantitative computed tomography.

^bThese sites are considered to be highly trabecular but the exact percentage of trabecular bone is not known.

Table 1-3
Percentage of Trabecular Bone at Peripheral Sites as Measured
by Single- or Dual-Energy X-Ray Absorptiometry

Calcaneus	95%
33% Radius or ulna ^{a,b}	1%
10% Radius or ulna ^{a,c}	20%
8-mm Radius or ulna ^{a,c}	25%
5-mm Radius or ulna ^{a,c}	40%
4-5% Radius or ulna ^{a,d}	66%
Phalanges	40%

^aSee Chapter 3 for naming convention for forearm bone density sites.

^bThis site is often called the *proximal* site.

^cThis site is often called the *distal* site.

^dThis site is often called the *ultradistal* site, but may be called simply *distal* as well.

Any given skeletal site can thus be characterized in four different ways. For example, the calcaneus is a weight bearing, appendicular, peripheral, predominantly trabecular site. The femoral neck is a weight bearing, appendicular, central, predominantly cortical site. The lumbar spine, in either the PA or lateral projection, is a weight bearing, axial, central, predominantly trabecular site.

WHAT DO THE MACHINES ACTUALLY MEASURE?

Although all of today's X-ray densitometers ultimately report bone mineral density (BMD), none actually measure BMD. Instead, the quantities that are actually measured are the bone mineral content (BMC) and

the length or area of bone. BMC is usually expressed in grams (g) although it is measured in milligrams (mg) when quantified by QCT or peripheral quantitative computed tomography (pQCT). Length is generally measured in centimeters (cm) and area in square centimeters (cm²). In the case of QCT and pQCT, volume, not area, is measured and reported in cubic centimeters (cm³). The BMD is calculated from the measurement of BMC and area or BMC and volume as shown in eqs. 1 and 2:

$$\text{BMC(g)/Area(cm}^2\text{)} = \text{BMD(g/cm}^2\text{)} \quad (1)$$

$$\text{BMC(mg)/Volume(cm}^3\text{)} = \text{BMD(mg/cm}^3\text{)} \quad (2)$$

The Effect of Bone Size on Areal Densities

It should be clear then that BMD measurements with DXA are two-dimensional or areal measurements, whereas BMD measurements with QCT are three-dimensional, or volumetric. Because DXA measurements are areal, bone size can affect the apparent BMD. In other words, it is possible for two vertebrae with identical volumetric densities to have different areal densities because of a difference in size. This is illustrated in Fig. 1-4. In Fig. 1-4A, each of the eight components of the cube is identical with a mineral weight of 2 g and dimensions of 1 × 1 × 1 cm. Therefore, the face of the cube has a width of 2 cm and a height of 2 cm for a projected area* of 4 cm². The cube also has a depth of 2 cm. Its volume† then, is 8 cm³. Because there are eight components of the cube, each weighing 2 g, the entire mineral weight of the cube is 16 g. Using eq. 1, the areal density of this cube, such as might be seen with a DXA measurement, would be calculated as shown in eq. 3:

$$16 \text{ g}/4 \text{ cm}^2 = 4.0 \text{ g/cm}^2 \quad (3)$$

The volumetric density of this cube, however, would be calculated using eq. 2. This calculation is shown in eq. 4:

$$16 \text{ g}/8 \text{ cm}^3 = 2 \text{ g/cm}^3 \quad (4)$$

This eight-component cube has an areal density of 4 g/cm² and a volumetric density of 2 g/cm³. The cube in Fig. 1-4B has identical individual components as the cube in Fig. 1-4A, but the entire cube is larger. Instead of eight components, the cube in Fig. 1-4B has twenty-seven. Each of the components, however, is identical in size and mineral weight to the components that make up the cube in Fig. 1-4A. The areal density and volumetric density of the cube in Fig. 1-4B are calculated in eqs. 5 and 6:

*Area is calculated by multiplying the height × width

†Volume is calculated by multiplying the height × width × depth.

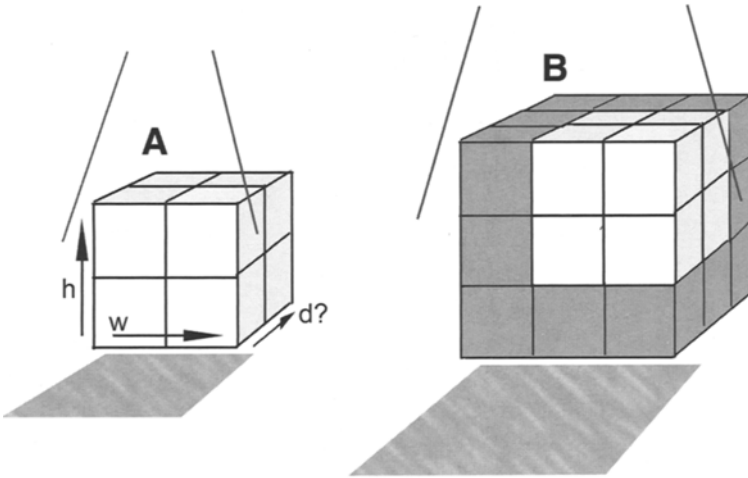


Fig. 1-4. The effect of bone size on areal bone mineral density. (A) The individual components of cube A are identical in size and volumetric density to the components of the larger cube (B). Note that cube A will fit within cube B. The volumetric densities of cubes A and B are identical but a dual-energy X-ray absorptiometry areal density for cube A will be less than for cube B because of its greater depth. The depth of both cubes is unknown. Formulas in the text used to calculate the bone mineral apparent density are based on assumptions about the relationship between the depth and height of the vertebrae. h, height; w, width; d, depth.

$$54 \text{ g}/9 \text{ cm}^2 = 6 \text{ g}/\text{cm}^2 \quad (5)$$

$$54 \text{ g}/27 \text{ cm}^3 = 2 \text{ g}/\text{cm}^3 \quad (6)$$

In this case, then, the volumetric densities of the two cubes are identical, but the larger cube has the greater areal density. This reflects the effect of bone size on the two-dimensional areal measurement.

Bone Mineral Apparent Density

This issue has been recognized for some time, although no consensus has been reached on how to best correct for the effects of bone size on areal measurements. Different approaches have been proposed to calculate a volumetric bone density from the DXA areal measurement, which is then called the bone mineral apparent density (BMAD) (2,3). An approach suggested by Carter et al. (2) is shown in eq. 7 and by Jergas et al. (3) in eq. 8.

$$\text{BMAD} = \text{BMC}/pA^{1.5} \text{ in which } pA = h \times w \quad (7)$$

$$\text{BMAD} = \text{BMC}/pA \times w \text{ in which } w = pA/h \quad (8)$$

The dimensions used in these equations are illustrated in Fig. 1-4A. The effect of bone size on areal density is particularly important in pediatric densitometry, both in interpreting the results of single measurements and in following changes in bone density in growing children. It is also relevant in looking at the differences in bone density between men and women. At its most basic, smaller bones may have a lower areal bone density because of the effect of bone size. In addition, a change in bone size may cause a change in areal bone density, even though the volumetric bone density has not changed.

Calculating “Average” Spine Bone Densities

When bone density measurements are made in the lumbar spine in the PA projection by DXA, the BMD for three or four contiguous vertebrae is generally reported rather than the BMD for any single vertebra. In other words, the L1–L4 or L2–L4 BMD is reported for the lumbar spine rather than only using L1, L2, L3 or L4. The accuracy and precision for L1–L4 or L2–L4 are superior to the accuracy and precision for a single vertebrae. But how is the L1–L4 or L2–L4 BMD derived? The BMD is calculated by the densitometry software for each individual vertebra and these values are provided on the bone density report as shown in Figs. 1-5 and 1-6. It is tempting to assume that the individual BMDs for each of the vertebrae included in the three or four vertebrae value are simply added and then the total divided by the number of vertebrae to find the “average” BMD. This is not correct, however. Remember that BMD is not measured directly; it is calculated from the measurement of BMC and area. The correct approach is to add the BMC values for each of the vertebrae included in the three or four vertebrae value and divide this total by the sum of the individual areas of each of the included vertebrae. This is illustrated in eq. 9 for the L1–L4 BMD.

$$\text{BMD}_{L1-L4} = \frac{(\text{BMC}_{L1} + \text{BMC}_{L2} + \text{BMC}_{L3} + \text{BMC}_{L4})}{(\text{Area}_{L1} + \text{Area}_{L2} + \text{Area}_{L3} + \text{Area}_{L4})} \quad (9)$$

It is an accepted convention in densitometry to call the L1–L4 BMD and the L2–L4 BMD “average” BMD values, even though they do not truly represent the average of the BMD at each vertebral level.

Ultrasound Parameters

Quantitative ultrasound (QUS) measurements of bone density do not measure BMC or area. Instead two parameters of the passage of sound through bone are measured: speed of sound (SOS) and broadband ultrasound

TEXAS WOMAN'S UNIVERSITY
Denton, Texas

AP SPINE BONE DENSITY

Facility: TWU	Acquired: 09/15/2000 (4.7a)
47 years	Analyzed: 09/15/2000 (4.7a)
64 in 125 lbs White Female	Printed: 09/15/2000 (4.7a)
Physician: Bonnick	

Region	BMD g/cm ²	Young %	Adult T	Age %	Matched Z
L1	1.039	92	-0.8	94	-0.6
L2	1.081	90	-1.0	92	-0.8
L3	1.080	90	-1.0	92	-0.8
L4	1.048	87	-1.3	89	-1.1
L1-L2	1.062	92	-0.7	94	-0.5
L1-L3	1.069	91	-0.8	93	-0.7
L1-L4	1.063	90	-1.0	92	-0.8
L2-L3	1.080	90	-1.0	92	-0.8
L2-L4	1.069	89	-1.1	91	-0.9
L3-L4	1.063	89	-1.1	90	-1.0

Fig. 1-5. A dual-energy X-ray absorptiometry posteroanterior spine bone density report showing the calculated bone mineral density values for each lumbar vertebra and every combination of contiguous vertebrae. Percentage comparisons and standard scores are also shown. This is the detailed data for the summary report in Fig. 1-6.

attenuation (BUA). The SOS is derived by determining the speed with which the sound wave passes through the bone. This requires a measurement of time and distance from which the SOS is then calculated and usually expressed in meters/second (m/sec). BUA refers to the amount of energy lost from the sound wave as it passes through bone. It is expressed in decibels/megahertz (db/Mhz). An ultrasound bone density report is shown in Fig. 1-7. Some manufacturers will mathematically combine the SOS and BUA into a proprietary index such as the Stiffness Index, also shown in Fig. 1-7.

THE DENSITOMETRY PRINTOUT

A complete printout for a PA lumbar spine study is shown in Figs. 1-5 and 1-6. In addition to reporting the measured and calculated parameters, comparisons are made by the densitometry software, using the databases contained within the computer. The purpose of these comparisons is to place the measured and calculated values into some context. Are these values good or bad? Do they indicate the presence of disease or not? Two

TEXAS WOMAN'S UNIVERSITY
Denton, Texas

AP SPINE BONE DENSITY

Facility: TWU
47 years
64 in 125 lbs White Female
Physician: Bonnick

Acquired: 09/15/2000 (4.7a)
Analyzed: 09/15/2000 (4.7a)
Printed: 09/15/2000 (4.7a)

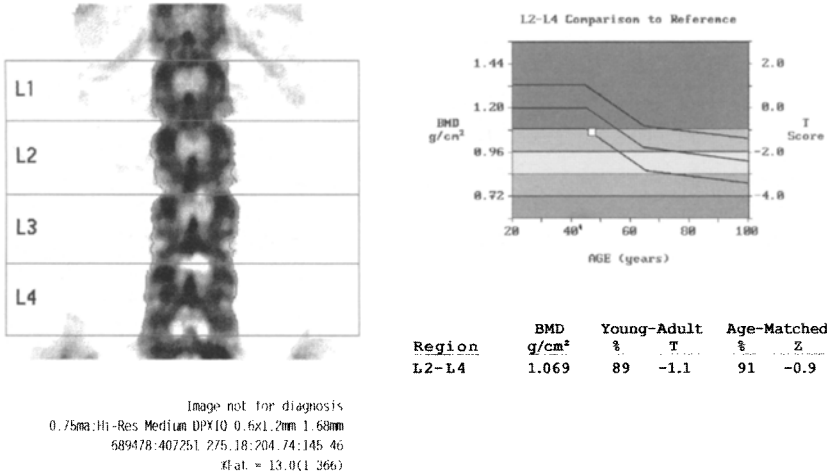


Fig. 1-6. A summary dual-energy X-ray absorptiometry posteroanterior spine bone density report showing the skeletal image, age-regression graph, and data for the selected region of interest, L2–L4. Detailed data is shown for this study in Fig. 1-5.

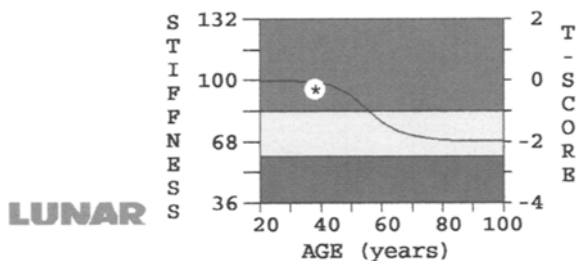
types of comparisons are made. The first is in the form of a percentage of the average peak value for a young adult and the average value for an individual the same age as the patient. The second comparison again compares the value to the expected peak value for a young adult and the expected average value for an individual the same age, but the comparisons are in the form of standard scores called T-scores and z-scores.

The Percentage Comparisons

The expression of the patient’s value as a percentage of the average peak value for a young adult of the same sex is called the “% Young Adult” or the “% Young Reference” comparison. This percentage may also be found in parentheses next to the T-score. The age or age range at which peak bone density is assumed to have occurred is sometimes not clear. The age used by the manufacturers may vary for any given skeletal site and certainly varies between different skeletal sites. The age or age range for peak bone

Clinical Research Center of North Texas
Denton, Texas

PATIENT ID: 0000	SCAN: 3.02	03/09/2003
NAME: LAS	ANALYSIS: 3.02	03/09/2003



Stiffness Index	95 ± 2
% Young Adult	95 ± 2
% Age Matched	96 ± 2

LEFT HEEL

Age (Years).....38	Weight (kg).....90	Ethnic.....W
Sex.....F	Height (cm).....165	System.....20255
STIFFNESS INDEX.....95	SOS (m/s).....1599	BUA (dB/MHz).....102

Stiffness Index

Young Adult	95 %	-0.29	T-score
Age Matched	96 %	-0.23	Z-score

Fig. 1-7. An ultrasound bone density report. The values for speed of sound (SOS) and broadband ultrasound attenuation (BUA) can be seen in the middle section of the report. SOS and BUA have been mathematically combined to produce a proprietary index by this manufacturer called the Stiffness Index. The value for this index is plotted on the age-regression graph. The background of the age-regression graph is divided into green, yellow, and red areas. The dividing lines for these areas correspond to the World Health Organization diagnostic categories based on the T-score. This can be helpful but should be interpreted cautiously in younger individuals.

density used for the % Young Adult comparison can be determined by reviewing information on the database that has been provided by the manufacturer or by studying the age-regression graph.

If the % Young Adult value for an L2–L4 PA spine BMD is 89%, as shown in Fig. 1-6, the patient's BMD is 89% of the average peak bone density for a young adult of the same sex. The BMD is 11% below the average peak bone density. This % Young Adult value should not be interpreted as meaning that the patient has lost 11% of her bone density. After all, the patient's actual peak bone density as a young adult is not known. The patient's peak bone density could have been higher or lower than the average peak bone density. How much the patient's bone density has actually changed, if at all, cannot be determined from a single bone density study. One can only conclude that her bone density is 11% lower than the average peak.

The second comparison made in the form of a percentage is to compare the patient's value to the average value for an individual of the same age and sex. This is usually called the "% Age-Matched" comparison or it may be listed in parentheses next to the z -score. This percentage indicates how the patient compares to other people of the same age. Unfortunately, this value can be misinterpreted resulting in a false sense of security. Individuals tend to lose bone density with age. While this is an expected phenomenon, it is not a desirable one. To have a bone density that compares favorably to other individuals of the same age who may have also lost bone density, is not necessarily good. Ideally, an individual's bone density will be better than expected for their age. If the % Age-Matched comparison is quite poor, it raises the specter of some underlying cause of bone loss other than age or, for women, estrogen deficiency. The effects of both age and estrogen deficiency are already reflected in the values that are established as expected in the database. When the % Age-Matched comparison is poor, something other than age or estrogen deficiency should be suspected. Nothing may necessarily be found, but other causes of bone loss should certainly be considered. It is difficult to say exactly what constitutes a "poor" comparison but certainly anything less than 80% should raise a red flag and prompt a very thorough evaluation for other causes of bone loss.

The Standard Score Comparisons

Standard scores are not unique to densitometry but they are not used routinely in any other field of clinical medicine. As a consequence, densitometry is usually a technologist's and physician's first exposure to standard scores. Standard scores take their name from their dependence upon the "standard" deviation, a statistical measure of variability about an average value. The calculation of the standard deviation and its utility in expressing the variability of measurements about an average value is discussed more thoroughly in Chapter 6 in the context of precision.

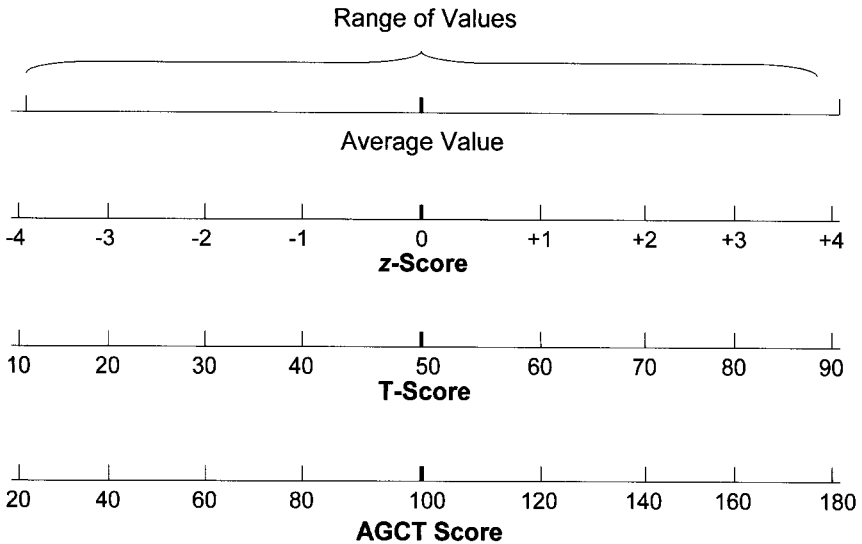


Fig. 1-8. Standard score scales. These scales are based on the standard deviation.

Standard scores indicate how many standard deviations above or below the average value the value in question actually lies. Several different standard score scales have been created, as illustrated in Fig. 1-8 (4). At the center of each scale is the average (also called mean) value for whatever set of values is being considered. Remember that standard scores and scales are not unique to densitometry. These scales can be applied to any kind of numerical values.

In the z -score scale, the z -score value increases by 1 for each standard deviation increase or decrease from the average value. The average value is arbitrarily assigned a z -score value of 0. A plus (+) sign or minus (-) sign is placed in front of the z -score value to indicate whether the value lies above or below the average value. If the actual value were 2 standard deviations above the average, the z -score would be +2. If the value were 1.5 standard deviations below the average, the z -score would be -1.5.

In the T-score scale, as it was originally designed, the average value was arbitrarily assigned a T-score value of 50. For each standard deviation change in the actual value from the average, the T-score would increase or decrease by 10. If the actual value was 1 standard deviation above the average, the T-score would be 60. If it was 2 standard deviations below the average, the T-score would be 30. Another type of standard score scale is the Army General Classification Test (AGCT) scale in which the average value is assigned an AGCT score of 100 and each

standard deviation increase or decrease from the average changes the AGCT score by 20.

Both the original T-score and AGCT scales utilize whole numbers and neither requires the use of a plus or minus sign. The z -score scale, on the other hand, does require the use of small numbers, decimal points, and either a plus or minus sign. It is perhaps unfortunate, but at present the z -score scale is the basis for the standard score comparisons used in densitometry.

In densitometry, if a patient's z -score is -2 , the implication is that the patient's value is 2 standard deviations below the average value. But to what average value is the comparison being made? There is nothing in the definition of the z -score that specifies the average to which the comparison is being made. Is it the average peak value of the young adult or the average value that is expected for the patient's age? In years past, this dilemma was addressed by labeling the comparisons "Young-Adult Z" and "Age-Matched Z" in order to make clear what comparison was being made. This is no longer done today. By convention in densitometry, it is understood that the z -score comparison is the comparison to the average value expected for the patient's age. The z -score scale is still used for comparisons of the patient's value to the average peak value for a young adult, but this comparison, by convention, is now called the T-score. This is clearly a misuse of the term T-score because it is the z -score scale that is being used, but it has served to shorten the terminology required to distinguish between the two comparisons without using a different standard score scale. In the bone density report shown in Fig. 1-9, the patient's L1-L4 T-score is -1.3 and her z -score, -0.5 . Her L1-L4 BMD, then, is 1.3 standard deviations below the peak value for a young adult and 0.5 standard deviations below the value predicted for her age.

Like the % Young Adult comparison, the T-score should not be used to suggest a certain magnitude of bone loss. It is the T-score, however, on which current diagnostic criteria are based. Like the % Age-Matched comparison, the z -score only indicates how the patient compares to their age-matched peers. A poor z -score should prompt a thorough evaluation for causes of bone loss other than age and estrogen deficiency. Statistically, a poor z -score is anything below -2 , but certainly such an evaluation should be pursued at any time the physician deems necessary.

Because both peak bone density and the expected bone density for any age can be affected by the race and weight of an individual, the % comparisons and standard scores can be adjusted to take these factors into

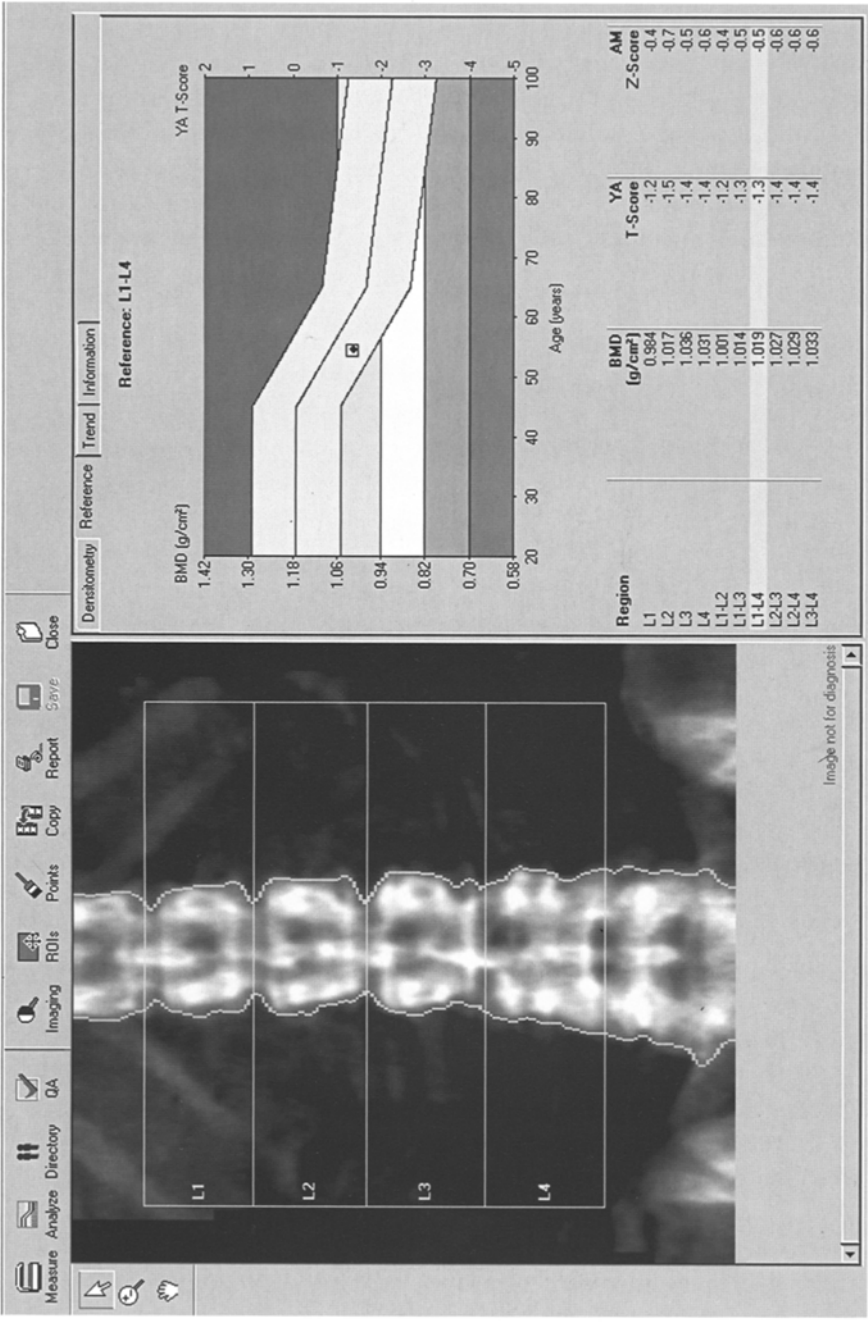


Fig. 1-9. A DXA PA lumbar spine study acquired on the GE Lunar Prodigy. The L1-L4 T-score is -1.3 and the z-score is -0.5 . The upper and lower limits for the age-regression represent a 1 SD change from the BMD predicted for any given age.

account. The various manufacturers approach this issue differently, however. In some cases, the % Young Adult and T-score comparisons can be adjusted for race, whereas in other cases it is the % Age-Matched and z-score that are adjusted. The weight adjustment may be made similarly in either set of comparisons. A careful reading of the device manufacturer's description of the comparisons is the only way to know with certainty where these adjustments are being made.

The Age-Regression Graph

The age-regression graph on densitometry reports, although usually quite colorful, is only a graphic representation of the selected calculated parameter and the standard score comparisons for a particular region of interest. Consequently, it actually provides little to no additional information beyond the printed numbers. On these graphs, the patient's BMD (or ultrasound value) will be plotted above their age. This is superimposed on a line graph of the expected change in BMD with advancing age, called the *age-regression line*. The highest point on this graph will represent the peak BMD (or ultrasound parameter) for the young adult. On both sides and paralleling the age-regression line is an outer limiting line that denotes a 1 or 2 SD change in BMD from the predicted value for any age. Some manufacturers have used a 1 SD limit for this line whereas others have used a 2 SD limit. The limits shown on the age-regression graphs in Figs. 1-6 and 1-9 represent a 1 SD change. These limits allow a visual estimation of the z-score. In the background of the graph, many manufacturers are now utilizing a red, yellow, and green color scheme. If the BMD or other chosen parameter lies in the red area, the World Health Organization (WHO) criteria for a diagnosis of osteoporosis have been met. If the plotted value is in the yellow area, the diagnosis is osteopenia, and if in the green area, the diagnosis is normal. Red, yellow, and green are also used to denote high, medium, and low risk of fracture, respectively. This is the scheme used in Fig. 1-7, although the image is in black and white here. This is also illustrated in Fig. 10-6. The WHO criteria for the diagnosis of osteoporosis are discussed more thoroughly in Chapter 9 and are listed again in Appendix II for easy reference. Although the red, yellow, and green color schemes can be useful, these colored areas extend across the entire age range represented on the graph. The WHO criteria were intended to be applied to postmenopausal women only. In addition, fracture risk at younger ages is clearly not the same as fracture risk at older ages even at the same BMD. As a consequence, this aspect of the graph must be interpreted with caution.

The Standardized BMD

The bone density values at any one skeletal site when obtained on devices from different manufacturers will not be the same. This is not because one device is more accurate than another; all the various devices are highly accurate as long as good quality control is maintained. The differences occur because the devices are calibrated to slightly different standards and because of slight differences in how the edges of the bones are detected. It has been shown repeatedly that the results for a skeletal site on one manufacturer's device are highly correlated with the results for that site from another manufacturer's device. In other words, the devices are indeed measuring the same thing. Although the absolute values reported are different, they are predictably different. A useful analogy would be a certain amount of money expressed as either US dollars, Canadian dollars, or British pounds. The numbers will be different even though the actual amount of money is the same.

Because the values are different, however, there has been a great deal of interest in developing a standardized BMD (sBMD) to which all DXA values could be converted regardless of which manufacturer's machine was used. In November 1990, the major manufacturers of DXA equipment agreed to work together in the area of standards as part of an international committee, known as the International Committee for Standards in Bone Measurement. Under the auspices of this committee a study of 100 healthy women was performed in which each of the women underwent PA spine and proximal femur studies on the Hologic QDR-2000, the Norland XR-26 Mark II, and the Lunar DPX-L (5). The women ranged in age from 20 to 80, with an average age of 52.6 years. The difference in BMD in the spine was greatest between the Norland XR-26 and the Lunar DPX-L, averaging 0.118 g/cm^2 , or 12.2%, with Lunar values being higher than Norland values. The difference between the Lunar DPX-L and the Hologic QDR-2000 averaged 0.113 g/cm^2 , or 11.7%, with Lunar values again being higher. Between the Norland XR-26 and the Hologic QDR-2000, the average difference in BMD in the lumbar spine was only 0.012 g/cm^2 , or 1.3%.

Based on this data, equations were derived for the conversion of PA lumbar spine BMD obtained on one manufacturer's machine to the BMD that would be expected on each of the other two. These equations for each of the three pairs of scanners are shown in Table 1-4 and again in Appendix VII for easy reference.

In order to convert each manufacturer's absolute BMD to a sBMD, a specially designed phantom called the European Spine Phantom (ESP)

Table 1-4

Conversion Formulas for Bone Mineral Densities (BMDs) of the Posteroanterior Spine Between Dual-Energy X-Ray Absorptiometry Devices

Hologic QDR-2000 Spine _{BMD}	$= (0.906 \times \text{Lunar DPX-L Spine}_{\text{BMD}}) - 0.025$
Hologic QDR-2000 Spine _{BMD}	$= (0.912 \times \text{Norland XR 26 Spine}_{\text{BMD}}) + 0.088$
Lunar DPX-L Spine _{BMD}	$= (1.074 \times \text{Hologic QDR 2000 Spine}_{\text{BMD}}) + 0.054$
Lunar DPX-L Spine _{BMD}	$= (0.995 \times \text{Norland XR 26 Spine}_{\text{BMD}}) + 0.135$
Norland XR-26 Spine _{BMD}	$= (0.983 \times \text{Lunar DPX-L Spine}_{\text{BMD}}) - 0.112$
Norland XR-26 Spine _{BMD}	$= (1.068 \times \text{Hologic QDR 2000 Spine}_{\text{BMD}}) - 0.070$

Adapted from the *Journal of Bone and Mineral Research* 1994;9:1503–1514 with permission from the American Society for Bone and Mineral Research.

Table 1-5

Formulas for the Conversion of Manufacturer-Specific AP Spine Bone Mineral Densities (BMDs) to the Standardized BMD (sBMD)

sBMD _{SPINE}	$= 1000(1.076 \times \text{Norland XR-26 BMD}_{\text{SPINE}})$
sBMD _{SPINE}	$= 1000(0.9522 \times \text{Lunar DPX-L BMD}_{\text{SPINE}})$
sBMD _{SPINE}	$= 1000(1.0755 \times \text{Hologic QDR-2000 BMD}_{\text{SPINE}})$

Adapted from the *Journal of Bone and Mineral Research* 1994;9:1503–1514 with permission from the American Society for Bone and Mineral Research.

was scanned on each of the three devices.[‡] Based on those results, formulas for converting each manufacturer's absolute BMD in the spine to a standardized spine BMD were derived, as shown in Table 1-5.

The value for the standardized BMD or sBMD is multiplied by 1000 to convert it to mg/cm² rather than reporting it in g/cm² to distinguish the sBMD from the nonstandardized value. For example, if the L2–L4 BMD obtained in the PA spine on a Lunar DXA device is 1.069 g/cm², as shown in Fig. 1-6, this value becomes 1018 mg/cm² when reported as the sBMD (1.069 × 0.9522 = 1.0179 g/cm² × 1000 = 1018 mg/cm²). When these formulas were used to convert the average PA lumbar spine BMD for the 100 women in the study population to the sBMD, the differences in BMD among the three machines were greatly reduced. Instead of an average difference of 12.2% between the Norland and Lunar values, the difference using the sBMD was only 2.8%. The difference between Hologic and Lunar was reduced to 2.2%, and the difference between Hologic and Norland was 2.7%.

[‡]See Chapter 8 for a discussion of the European Spine Phantom.

Table 1-6
Conversion Formulas for Bone Mineral Densities (BMDs) in the Proximal Femur Between Dual-Energy X-Ray Absorptiometry Devices

Hologic QDR-2000 Neck _{BMD}	= (0.836 × Lunar DPX-L Neck _{BMD}) – 0.008
Hologic QDR-2000 Neck _{BMD}	= (0.836 × Norland XR 26 Neck _{BMD}) + 0.051
Lunar DPX-L Neck _{BMD}	= (1.013 × Hologic QDR 2000 Neck _{BMD}) + 0.142
Lunar DPX-L Neck _{BMD}	= (0.945 × Norland XR 26 Neck _{BMD}) + 0.115
Norland XR-26 Neck _{BMD}	= (0.961 × Lunar DPX-L Neck _{BMD}) – 0.037
Norland XR-26 Neck _{BMD}	= (1.030 × Hologic QDR 2000 Neck _{BMD}) + 0.058

Adapted from the *Journal of Bone and Mineral Research* 1994;9:1503–1514 with permission from the American Society for Bone and Mineral Research.

Conversion formulas were also developed for the femoral neck for each pair of scanners, as shown in Table 1-6.

In December 1996, the International Committee for Standards in Bone Measurement approved the sBMD for the total femur region of interest(6). The total femur region of interest includes the femoral neck, Ward's area, the trochanter, and the shaft of the proximal femur. This region appears to have equal diagnostic utility but better precision than the femoral neck. The formulas for the sBMD for the total femur, shown in Table 1-7, were based on the work by Genant et al. from which the formulas for sBMD of the spine were also derived (5). The sBMD from any one of the three central DXA devices should fall within 3–6% of the sBMD on any of the other two. The sBMD calculation is generally provided as an option in most densitometry software that can be turned on and off by the technologist.

Other formulas have been developed to calculate a sBMD for the various subregions of the proximal femur (7). In addition, formulas exist for calculating the sBMD for various regions in the forearm (8). These formulas are also shown in Appendix VII. These additional formulas are not in widespread use.

THE UTILITY OF THE sBMD

The sBMD is attractive as a means of comparing a BMD value obtained on one manufacturer's device with a BMD value obtained on another. This is useful in large population studies and clinical trials in which devices from several manufacturers must be used. The root-mean-square error in the calculation of the sBMD is estimated to be 4% for the PA spine and total femur and even larger for the proximal femur subregions (7). This error is simply too large to base important clinical decisions on the comparison of sBMD values obtained on different devices for an individual.

Table 1-7
Formulas for the Conversion of Manufacturer-Specific Total Femur Bone
Mineral Density (BMD) to the Standardized BMD (sBMD)

$$\text{sBMD}_{\text{TOTAL FEMUR}} = 1000[(1.008 \times \text{Hologic BMD}_{\text{TOTAL FEMUR}}) + 0.006]$$

$$\text{sBMD}_{\text{TOTAL FEMUR}} = 1000[(0.979 \times \text{Lunar BMD}_{\text{TOTAL FEMUR}}) - 0.031]$$

$$\text{sBMD}_{\text{TOTAL FEMUR}} = 1000[(1.012 \times \text{Norland BMD}_{\text{TOTAL FEMUR}}) + 0.026]$$

Adapted from the *Journal of Bone and Mineral Research* 1997;12:1316-1317 with permission from the American Society for Bone and Mineral Research.

But, if nothing else, these formulas illustrate that the measured BMD at a given site cannot be directly compared to the measured BMD at that same site from another manufacturer's device.

THE NATIONAL HEALTH AND NUTRITION EXAMINATION SURVEY (NHANES) III DATABASE FOR THE PROXIMAL FEMUR

Although the development of the sBMD reduced the apparent discrepancies between the reported values for BMD at the PA spine and total femur between the three major DXA device manufacturers, discrepancies still remained between the % comparisons and standard scores. These discrepancies were seen at both the lumbar spine and the proximal femur, but the problem was clearly greatest at the proximal femur.

In 1992 it was noted by Pocock et al. that the % comparisons for the spine were similar in 46 women studied on the Hologic QDR-1000 and the Lunar DPX (9). At the femoral neck, however, the % Young Adult comparisons were 6.2% lower on the QDR-1000 compared to the Lunar DPX. The % Age-Matched comparisons were 3.3% lower on the QDR-1000 than on the Lunar DPX.

Other authors confirmed these observations. Laskey et al. evaluated 53 subjects undergoing spine and proximal femur bone density measurements on the same day on the Lunar DPX and Hologic QDR-1000 (10). Like Pocock, Laskey found that the young-adult and age-matched comparisons to the reference database at the spine were similar. At the proximal femur, however, the differences were substantial. The magnitude of the differences approximated 1 standard deviation. This was a sufficient difference to potentially have profound clinical ramifications. Depending on which manufacturer's machine was used for the measurement, a patient could potentially be given a different diagnosis. Faulkner et al. compared the young adult standard scores at the spine in 83 women and at the proximal

femur for 120 women who underwent bone density studies on a Lunar DPX and Hologic QDR-1000/W (11). The difference between the young adult standard scores on the QDR-1000/W and the Lunar DPX at the spine was not statistically or clinically significant. At the femoral neck, however, there was a systematic difference of almost 1 standard deviation.

Faulkner et al. observed that these differences in % comparisons and standard scores could be due to a combination of factors: different inclusion criteria for the two databases, relatively small numbers of individuals used to calculate the average and standard deviation young-adult values, and different statistical methods employed in the calculation of the reference curves. Faulkner suggested correcting the proximal femur data from both manufacturers by replacing the manufacturer's data with proximal femur bone density data that were obtained during the NHANES III study of the United States population.[§] This was data that was collected between 1988 and 1991 using the Hologic QDR-1000 (12). As originally reported, there were 194 non-Hispanic white women aged 20–29 whose BMD values were used to calculate the young-adult average BMD value and standard deviation in the five regions in the proximal femur. The average BMD in the femoral neck for these young adults from NHANES III was reported as 0.849 g/cm² with a standard deviation of 0.11 g/cm². Faulkner substituted these values for the average and standard deviation values used in the QDR-1000 reference database of 0.895 g/cm² and 0.10 gm/cm², respectively. The equivalent Lunar DPX BMD young-adult BMD was then calculated using the cross-calibration equation from Genant et al (5). This resulted in a Lunar value of 1.000 g/cm² for the average young-adult BMD in the femoral neck compared to the value of 0.980 g/cm² used in the Lunar-supplied database prior to October 1997. The standard deviation for the young adult of 0.11 g/cm² from NHANES III was substituted for the Lunar reported standard deviation of 0.12 g/cm². When the young-adult standard scores were recalculated for each machine using the new values

[§]NHANES III was conducted by the National Center for Health Statistics, Centers for Disease Control and Prevention. During the study, proximal femur bone density data was collected on 7116 men and women aged 20 and older (12). There were a total of 3217 non-Hispanic whites, 1831 non-Hispanic blacks, and 1840 Mexican-Americans in this study population. There were no specific inclusion or exclusion criteria used to select individuals for bone density measurements in this study other than the presence of prior hip fracture or pregnancy, which were grounds for exclusion. The individuals who received bone density measurements were otherwise part of a random sample of the population.

based on the NHANES III data, the differences between the two manufacturer's databases largely disappeared.

With the development of the crosscalibration equations between manufacturers and the sBMD for the total femur, it became possible for the proximal femur data from NHANES III to be adopted as a common femur database by the different manufacturers even though the original data was obtained solely on Hologic DXA devices. Based on the equations for sBMD, the average total femur sBMD for US non-Hispanic white women aged 20–29 is 955 mg/cm² with a standard deviation of 123 mg/cm² (6,13). Standardized NHANES III proximal femur data were offered as part of the reference databases by DXA manufacturers, either in conjunction with the manufacturer-derived databases or as a replacement for the manufacturer-derived proximal femur data after September 1997.

NOMENCLATURE GUIDELINES FROM THE INTERNATIONAL SOCIETY FOR CLINICAL DENSITOMETRY

In 2004, the International Society for Clinical Densitometry (ISCD) issued guidelines for densitometry nomenclature as it applied to studies performed specifically with dual-energy X-ray absorptiometry (14). ISCD addressed three issues: the use of the acronym DEXA or DXA, the appropriate form of the notation used to refer to standard scores in densitometry, and the number of decimal places used in expressing the quantitative data from densitometry studies.

ISCD recommended that the acronym DXA be used instead of DEXA. This has increasingly been the convention for many years among medical journals and equipment manufacturers, however, some authorities have continued to use DEXA. The preferred use of the acronym DXA over DEXA has little importance in the application of densitometry in clinical practice, but it is relevant when performing searches of the medical literature in which one must enter one or the other of the two terms.

ISCD also recommended that the standard scores used in densitometry be written using the format T-score and Z-score, although they noted that this was largely a matter of esthetics. This is the format commonly used on DXA printouts from the various manufacturers. This book, however, utilizes the format commonly found in texts on statistics in which the Z-score is denoted as the *z*-score. The meaning is the same and certainly an understanding of the meaning is the more important issue. As noted

Table 1-8
Dual-Energy X-Ray Absorptiometry Quantitative Reporting Conventions
Recommended by the International Society for Clinical Densitometry

<i>Quantity</i>	<i>Number of decimal places</i>	<i>Example</i>
BMD	3	1.045 g/cm ²
T-score	1	-2.5
z-score	1	-1.4
BMC	2	25.33 g
Area	2	15.67 cm ²
% Reference database	0	94%

BMD, bone mineral density; BMC, bone mineral content.

previously in this chapter, the way in which we use the term T-score in densitometry is not actually correct and more a matter of convenience. The format used to denote the T-score in this book, however, is the format now recommended by ISCD.

The number of places to the right of the decimal point associated with the reporting of quantities measured with densitometry that are recommended by ISCD are shown in Table 1-8. These recommendations are based both on convention and mathematical guidelines for reporting only the number of places to the right of the decimal point for a quantity that are justified by the nature of the measurement.

REFERENCES

1. Recker, R. R. (1992) Embryology, anatomy, and microstructure of bone, in Disorders of Bone and Mineral Metabolism (Coe, F. L. and Favus, M. J., eds.), Raven, New York, pp. 219–240.
2. Carter, D. R., Bouxsein, M. L., Marcus, R. (1992) New approaches for interpreting projected bone densitometry data. *J. Bone Miner. Res.* **7**, 137–146.
3. Jergas, M., Breitenseher, M., Gluer, C. C., Yu, W., Genant, H. K. (1995) Estimates of volumetric bone density from projectional measurements improve the discriminatory capability of dual X-ray absorptiometry. *J. Bone Miner. Res.* **10**, 1101–1110.
4. Phillips, J. L. (1982) Interpreting individual measures, in Statistical Thinking, WH Freeman, New York. 62–78.
5. Genant, H. K., Grampp, S., Gluer, C. C., et al. (1994) Universal standardization for dual X-ray absorptiometry: patient and phantom cross-calibration results. *J. Bone Miner. Res.* **9**, 1503–1514.
6. Hanson, J. (1997) Standardization of femur BMD. *J. Bone Miner. Res.* **12**, 1316–1317.
7. Lu, Y., Fuerst, T., Hui, S., Genant, H. K. (2001) Standardization of bone mineral density at femoral neck, trochanter and Ward's triangle. *Osteoporos Int.* **12**, 438–444.

8. Shepherd, J. A., Cheng, X. G., Lu Y., et al. (2002) Universal standardization of forearm bone densitometry. *J. Bone Miner. Res.* **17**, 734–745.
9. Pocock, N. A., Sambrook, P. N., Nguyen, T., Kelly, P., Freund, J., Eisman, J. A. (1992) Assessment of spinal and femoral bone density by dual X-ray absorptiometry: comparison of Lunar and Hologic instruments. *J. Bone Miner. Res.* **7**, 1081–1084.
10. Laskey, M. A., Crisp, A. J., Cole, T. J., Compston, J. E. (1992) Comparison of the effect of different reference data on Lunar DPX and Hologic QDR-1000 dual-energy X-ray absorptiometers. *Br. J. Radiol.* **65**, 1124–1129.
11. Faulkner, K. G., Roberts, L. A., McClung, M. R. (1996) Discrepancies in normative data between Lunar and Hologic DXA systems. *Osteoporos Int.* **6**, 432–436.
12. Looker, A. C., Wahner, H. W., Dunn, W. L., et al. (1995) Proximal femur bone mineral levels of US adults. *Osteoporos Int.* **5**, 389–409.
13. Looker, A. C., Wahner, H. W., Dunn, W. L., et al. (1998) Updated data on proximal femur bone mineral levels of US adults. *Osteoporos Int.* **8**, 468–489.
14. The Writing Group for the ISCD Position Development Conference. (2004) *J. Clin. Densitom.* **7**, 45–49.

2

Densitometry Techniques

CONTENTS

- PLAIN RADIOGRAPHY IN THE ASSESSMENT OF BONE DENSITY
- QUALITATIVE MORPHOMETRY
 - QUALITATIVE SPINAL MORPHOMETRY
 - THE SINGH INDEX
- QUANTITATIVE MORPHOMETRIC TECHNIQUES
 - CALCAR FEMORALE THICKNESS
 - RADIOGRAMMETRY
 - THE RADIOLOGIC OSTEOPOROSIS SCORE
- RADIOGRAPHIC PHOTODENSITOMETRY
- RADIOGRAPHIC ABSORPTIOMETRY
- PHOTON ABSORPTIOMETRY TECHNIQUES
 - SINGLE-PHOTON ABSORPTIOMETRY
 - DUAL-PHOTON ABSORPTIOMETRY
 - DUAL-ENERGY X-RAY ABSORPTIOMETRY
 - PERIPHERAL DXA
 - SINGLE-ENERGY X-RAY ABSORPTIOMETRY
 - QUANTITATIVE COMPUTED TOMOGRAPHY
 - PERIPHERAL QCT
- QUANTITATIVE ULTRASOUND BONE DENSITOMETRY
- REFERENCES

Clinical densitometry is relatively new, but densitometry itself is actually quite old. It was first described over 100 years ago in the field of dental radiology as dentists attempted to quantify the bone density in the mandible (1,2). With today's techniques, bone density can be quantified in almost every region of the skeleton. The extraordinary technical advances in recent years have expanded the realm of densitometry from that of a quantitative technique to that of an imaging technique as well. But even the oldest techniques remain both viable and valuable with computer

modernization. Densitometry technologies have evolved as our understanding of relevant disease processes has increased. In a complementary fashion, our understanding of the disease processes has increased as the technologies have evolved.

PLAIN RADIOGRAPHY IN THE ASSESSMENT OF BONE DENSITY

The earliest attempts to quantify bone density utilized plain skeletal radiography. When viewed by the unaided eye, plain skeletal radiographs can only be used in an extremely limited fashion to quantify bone density. Demineralization becomes visually apparent only after 40% or more of the bone density has been lost (3). If demineralization is suspected from a plain film, a great deal of demineralization is presumed to have occurred. A more precise statement cannot be made. Plain radiographs have been used for qualitative and quantitative skeletal morphometry. Plain radiographs were also used to assess bone density based on the optical densities of the skeleton when compared with simultaneously X-rayed standards of known density made from ivory or aluminum. With the advent of the photon absorptiometric techniques, most of these early methods as originally performed have fallen into disuse. Nevertheless, a brief review of these techniques should enhance the appreciation of the capabilities of modern testing and provide a background for understanding modern technologies.

QUALITATIVE MORPHOMETRY

Qualitative Spinal Morphometry

Qualitative morphometric techniques for the assessment of bone density have been in limited use for over 50 years. Grading systems for the spine relied on the appearance of the trabecular patterns within the vertebral body and the appearance and thickness of the cortical shell (4). Vertebrae were graded from IV down to I as the vertical trabecular pattern became more pronounced with the loss of the horizontal trabeculae and the cortical shell became progressively thinned. The spine shown in Fig. 2-1 demonstrates a pronounced vertical trabecular pattern. The cortical shell appears as though it was outlined in white around the more radiotranslucent vertebral body. These vertebrae would be classified as Grade II.



Fig. 2-1. Qualitative spine morphometry. The vertebrae on this lateral lumbar spine X-ray demonstrate marked accentuation of the vertical trabecular pattern and thinning of the cortical shell. This is a Grade II spine.

The Singh Index

The Singh Index is a qualitative morphometric technique that was similarly based on trabecular patterns, but based on those seen in the proximal femur (5). Singh and others noted that there was a predictable order in the disappearance of the five groups of trabeculae from the proximal femur in osteoporosis. Based on the order of disappearance, radiographs of the proximal femur could be graded 1 through 6 with lower values indicating a greater loss of the trabecular patterns normally seen in the proximal femur. Studies evaluating prevalent fractures demonstrated an association between Singh Index values of 3 or less and the presence of fractures of the hip, spine, or wrist. Figure 2-2 shows a proximal femur with a Singh Index of 2. Only the trabecular pattern known as the principle compressive group, which extends from the medial cortex of the shaft to the upper portion of the head of the femur, remains. This patient was



Fig. 2-2. The Singh Index and calcar femorale thickness. A Grade 2 Singh index would be assessed based on having only remnants of the principle compressive and principle tensile trabecular groups visible. This is indicative of osteoporosis. The arrow points to the calcar femorale, which was 4 mm thick. Values <5 mm are associated with hip fracture. This patient had experienced a contralateral hip fracture.

known to have osteoporotic spine fractures as well as a contralateral proximal femur fracture. Later attempts to demonstrate an association between Singh Index values and proximal femur bone density measured by dual-photon absorptiometry were not successful (6).

Both of these qualitative morphometric techniques are highly subjective. In general, the best approach to their use required the creation of a set of reference radiographs of the various grades of vertebrae for spinal morphometry or proximal femurs for the Singh Index to which all other radiographs could be compared.

QUANTITATIVE MORPHOMETRIC TECHNIQUES

Calcar Femorale Thickness

A little known quantitative morphometric technique involves the measurement of the thickness of the calcar femorale. The calcar femorale is the band of cortical bone immediately above the lesser trochanter in the proximal

femur. In normal subjects, this thickness is greater than 5 mm. In femoral fracture cases, it is generally less than 5 mm in thickness (7). The arrow in Fig. 2-2 is pointing to the calcar femorale. This patient had previously suffered a femoral neck fracture. The thickness of the calcar femorale measured 4 mm.

Radiogrammetry

Radiogrammetry is the measurement of the dimensions of the bones using skeletal radiographs. Metacarpal radiogrammetry has been in use for almost 50 years. As originally practiced, the dimensions of the metacarpals were measured using a plain radiograph of the hand and fine calipers or a transparent ruler. The total width and medullary width of the metacarpals of the index, long, and ring fingers were measured at the midpoint of the metacarpal. The cortical width was calculated by subtracting the medullary width from the total width. Alternatively, the cortical width could be measured directly. A variety of different calculations were then made such as the metacarpal index (MI) and the hand score (HS). The MI is the cortical width divided by the total width. The HS, also known as the percent cortical thickness, is the metacarpal index expressed as a percentage. Measurements of the middle three metacarpals of both hands were also made and used to calculate the six metacarpal hand score (6HS). Other quantities derived from these measurements included the percent cortical area (%CA), the cortical area (CA) and the cortical area to surface area ratio (CA:SA). The main limitation in all of these measurements is that they were based on the false assumption that the point at which these measurements were made on the metacarpal was a perfect hollow cylinder. Nevertheless, using these measurements and knowledge of the gravimetric density of bone, the bone density could be calculated. The correlation* between such measurements and the weight of ashed bone was good, ranging from 0.79 to 0.85 (8,9). The precision of metacarpal radiogrammetry was quite variable depending upon the measurement used†. The measurement of total width is very reproducible.

*Correlation indicates the strength of the association between two values or variables. The correlation value is denoted with the letter r . A perfect correlation would be indicated by an r value of +1.00 or -1.00.

†Techniques are compared on the basis of accuracy and precision, which can be described using the percent coefficient of variation (%CV). The %CV is the standard deviation divided by the average of replicate measurements expressed as a percentage. The lower the %CV, the better the accuracy or precision.

The measurement of medullary width or the direct measurement of cortical width is less reproducible because the delineation between the cortical bone and medullary canal is not as distinct as the delineation between the cortical bone and soft tissue. Precision was variously reported as excellent to poor, but in expert hands it was possible to achieve a precision of 1.9% (10).

Although metacarpal radiogrammetry is an old technique and somewhat tedious to perform, it remains a viable means of assessing bone density in the metacarpals. Metacarpal radiogrammetry demonstrates a reasonably good correlation to bone density at other skeletal sites measured with photon absorptiometric techniques (11). The technique is very safe as the biologically significant radiation dose from a hand X-ray is extremely low at only 1 mrem.

Radiogrammetry can also be performed at other sites such as the phalanx, distal radius, and femur (12-14). Combined measurements of the cortical widths of the distal radius and the second metacarpal are highly correlated with bone density in the spine as measured by dual-photon absorptiometry (12).

Today, plain films of the hand and forearm can be digitized using flatbed optical scanners and radiogrammetry performed with computerized analysis of the digitized images. Using such a digital radiogrammetry (DXR) system, Bouxsein et al. (15) evaluated the utility of metacarpal radiogrammetry in predicting fracture risk and the correlation between metacarpal DXR-bone mineral density (BMD) and BMD measured by other techniques at other sites. The authors used a case-cohort approach to identify three groups of 200 women based on their having experienced a hip fracture, wrist fracture or spine fracture during the first five years of the Study of Osteoporotic Fractures (16). DXR-BMD of the metacarpals was strongly correlated with distal and proximal radial BMD measured by single-photon absorptiometry* ($r = 0.68$ and 0.75 , respectively). The correlation with femoral neck and lumbar spine BMD measured by dual-energy X-ray absorptiometry* was more modest ($r = 0.50$ and 0.44 , respectively). Metacarpal DXR-BMD predicted spine and wrist fracture risk as well as single-photon absorptiometry BMD measurements of the distal or proximal radius or heel or dual-energy X-ray absorptiometry measurements of the posteroanterior (PA) lumbar spine or femoral neck. The increase in risk for wrist fracture was 1.6 for each standard deviation decline in DXR-BMD and 1.9 for spine fracture. Although femoral neck BMD was the

*This technique is discussed later in this chapter.

strongest predictor of hip fracture risk, metacarpal DXR-BMD predicted hip fracture risk as well as the other BMD measurements with an increase in risk of 1.8 for each standard deviation decline in BMD. This type of DXR system is available commercially from Sectra Pronosco in Denmark as part of a Picture Archiving and Communications system.

The Radiologic Osteoporosis Score

The radiologic osteoporosis score combined aspects of both quantitative and qualitative morphometry (14). Developed by Barnett and Nordin, this scoring system utilized radiogrammetry of the femoral shaft and metacarpal as well as an index of biconcavity of the lumbar vertebrae. In calculating what Barnett and Nordin called a peripheral score, the cortical thickness of the femoral shaft divided by the diameter of the shaft and expressed as a percentage, was added to a similar measurement of the metacarpal. A score of 88 or less was considered to indicate peripheral osteoporosis. The biconcavity index was calculated by dividing the middle height of the third lumbar vertebra by its anterior height and expressing this value as a percentage. A biconcavity index of 80 or less indicated spinal osteoporosis. Combining both the peripheral score and biconcavity index resulted in the total radiologic osteoporosis score, which indicated osteoporosis if the value was 168 or less.

RADIOGRAPHIC PHOTODENSITOMETRY

Much of the development of the modern techniques of single- and dual-photon absorptiometry and dual-energy X-ray absorptiometry actually came from early work on the X-ray-based method of photodensitometry (17). In photodensitometry, broad-beam X-ray exposures of radiographs were obtained and the density of the skeletal image was quantified using a scanning photodensitometer. One such early device at Texas Woman's University is shown in Fig. 2-3. The effects of variations in technique such as exposure settings, beam energy, and film development were partially compensated by the simultaneous exposure of a step wedge of known densities on the film. An aluminum wedge was most often used, but other materials such as ivory were also employed (13). This technique could only be applied to areas of the skeleton in which the soft tissue coverage was less than 5 cm, such as the hand, forearm, and heel. This restriction was necessary because of technical limitations from scattered radiation in thicker parts of the body and "beam hardening" or the preferential

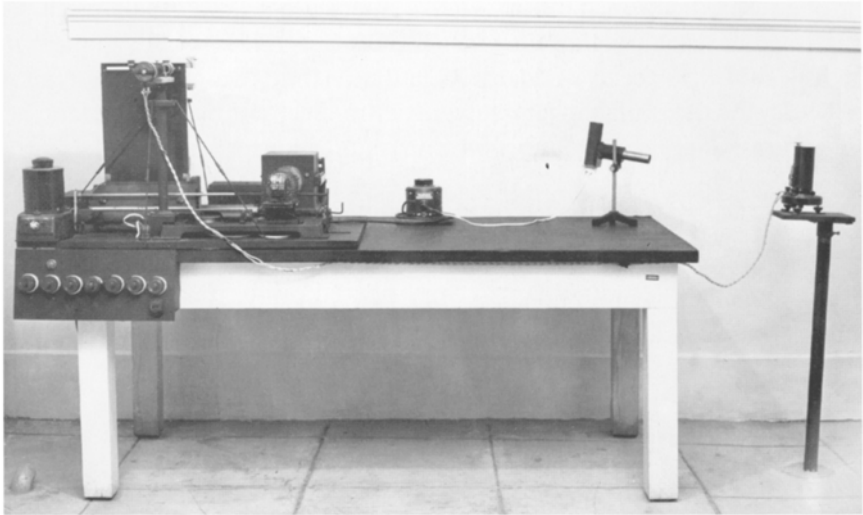


Fig. 2-3. Radiographic photodensitometer at Texas Woman's University from the early 1950s.

attenuation of the softer energies of the polychromatic X-ray beam as it passed through the body. Photodensitometry was also used in cadaver studies of the proximal femur (18). Such studies noted the predictive power for hip fracture of the density of the region in the proximal femur known as Ward's triangle* 30 years before studies using the modern technique of dual-energy X-ray absorptiometry in 1993 (19). The accuracy of such measurements was fairly good with a %CV of 5%. The correlation between metacarpal photodensitometry and ashed bone was also high at 0.88 (8). This was a slightly better correlation than seen with metacarpal radiogrammetry. The precision of photodensitometry was not as good, however, ranging from 5 to 15% (20). In this regard, the six metacarpal radiogrammetry hand score was superior (4). Radiation dose to the hand was the same for metacarpal radiogrammetry and radiographic photodensitometry. In both cases, the biologically significant radiation dose was negligible.

Radiographic photodensitometry was developed and used extensively by researchers Pauline Beery Mack and George Vose (21). Many of the

*Ward's triangle was first described by F.O. Ward in *Outlines of Human Osteology*, Henry Renshaw, London, 1838. It is a triangular region created by the intersection of three groups of trabeculae in the femoral neck. See Fig. 3-22.

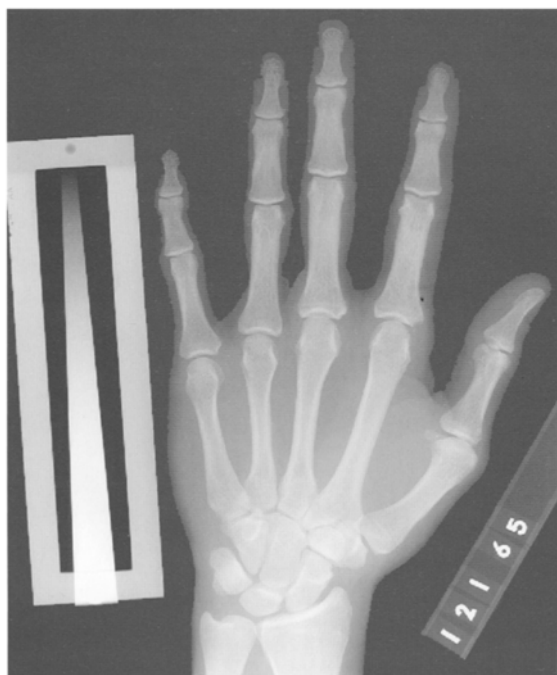


Fig. 2-4. Radiographic photodensitometry hand film taken in 1965 of one of the *Gemini* astronauts. The Texas Woman's University aluminum wedge is seen next to the little finger.

original studies of the effects of weightlessness on the skeleton in the *Gemini* and *Apollo* astronauts were performed by Pauline Beery Mack and colleagues at Texas Woman's University (22). The photodensitometry hand film of one of the *Gemini* astronauts is shown in Fig. 2-4.

RADIOGRAPHIC ABSORPTIOMETRY

Radiographic absorptiometry (RA) is the modern-day descendent of radiographic photodensitometry (23,24). The ability to digitize high resolution radiographic images and to perform computerized analysis of such images largely eliminated the errors introduced by differences in radiographic exposure techniques and overlying soft tissue thickness. In an early version of RA, two X-rays of the left hand using nonscreened film were taken at slightly different exposures. Standard X-ray equipment was used to perform the hand films. The initial recommended settings were 50 kVp at 300 mA for 1 second and 60 kVp at 300 mA for 1 second. The



Fig. 2-5. Radiographic absorptiometry hand film. The small aluminum wedge, originally known as the Fel's wedge, is seen next to the index finger.

exact settings varied slightly with the equipment used and were adjusted so that the background optical density of each of the two hand films matched a quality control film. An aluminum alloy reference wedge was placed on the film prior to exposure, parallel to the middle phalanx of the index finger. After development, the films were sent to a central laboratory where they were digitized and analyzed by computer. The average bone mineral density in arbitrary RA units of the middle phalanges of the index, long, and ring fingers was reported. Figure 2-5 illustrates the X-ray appearance of the hand and aluminum alloy reference wedge.

In cadaveric studies, the accuracy of RA for the assessment of bone mineral content of the middle phalanges was good at 4.8% (25). The authors of this study noted that the very thick soft tissue that might be seen in very obese subjects could potentially result in an underestimation of RA values. The correlation between the RA values and the ashed weight in the phalanges was excellent with $r = 0.983$. The short-term reproducibility of these measurements was also excellent at 0.6%.

The ability to predict bone density at other skeletal sites from hand radiographic absorptiometry is as good as that seen with other techniques such as single-photon absorptiometry, dual-photon absorptiometry, dual-energy X-ray absorptiometry or quantitative computed tomography of the spine (23,26). This does not mean that RA hand values can be used to accurately predict bone density at other skeletal sites. Although the correlations between the different sites as measured by the various techniques are correctly said to be statistically significant, the correlations are too weak to allow clinically useful predictions of bone mass or density at one site from measurement at another.

The utility of modern-day radiographic absorptiometry in predicting hip fracture risk was suggested by an analysis of data acquired during the first National Health and Nutrition Examination Survey (NHANES I, 1971–1975). During this survey, 1559 hand radiographs of Caucasian women were obtained with the older technique of photodensitometry using the Texas Woman's University wedge (27). During a median follow-up of 14 years that extended through 1987, 51 hip fractures occurred. Based on radiographic photodensitometry of the second phalanx of the small finger of the left hand, the risk for hip fracture per standard deviation decline in bone density increased 1.66-fold. These films were then reanalyzed using radiographic absorptiometry with some compensation for the differences in technique. This reanalysis yielded an increase in the risk for hip fracture per standard deviation decline in RA bone density of 1.81-fold. Huang and colleagues (28) evaluated the utility of RA in the prediction of vertebral fractures. They followed 560 postmenopausal women, average age 73.7 years, for an average of 2.7 years in the Hawaii Osteoporosis Study. The risk for vertebral fracture in this study using RA was 3.41-fold for each standard deviation decline in bone density.

RA systems are commercially available. The automated Osteogram[®] system from Compumed, Inc. consists of the computer hardware, software, and film cassette with hand template and reference wedge needed to perform radiographic absorptiometry of the phalanges. A filmless, self-contained system is also in development. The Metriscan[™] from Alara, Inc. is a self-contained device that utilizes storage phosphor technology in place of X-ray film to perform RA of the phalanges. Both systems are discussed in Chapter 4.

PHOTON ABSORPTIOMETRY TECHNIQUES

In radiology, attenuation refers to a reduction in the number and energy of photons in an X-ray beam. Attenuation, then, is a reduction in an X-ray

beam's intensity. To a large extent, the attenuation of X-rays is determined by tissue density. The difference in tissue densities is responsible for creating the images seen on an X-ray. The more dense the tissue, the more electrons it contains. The number of electrons in the tissue determines the ability of the tissue to either attenuate or transmit the photons in the X-ray beam. The differences in the pattern of transmitted or attenuated photons creates the contrast necessary to discern images on the X-ray. If all the photons were attenuated (or none were transmitted), no image would be seen because the film would be totally white. If all of the photons were transmitted (or none were attenuated), no image would be seen because the film would be totally black. The difference in the attenuation of the X-ray photon energy by different tissues is responsible for the contrast on an X-ray, which enables the images to be seen. If the degree of attenuation could be quantified, it would be possible to quantitatively assess the tissue density as well. This is the premise behind the measurement of bone density with photon absorptiometric techniques. The earliest photon absorptiometric techniques employed radionuclides to generate photon energy. These radionuclide-based techniques have given way to X-ray based techniques. The basic principles on which they operate, however, remain the same.

Single-Photon Absorptiometry

Writing in the journal *Science* in 1963, Cameron and Sorenson (29) described a new method for determining bone density in vivo by passing a monochromatic or single-energy photon beam through bone and soft tissue. The amount of mineral encountered by the beam could be quantified by subtracting the beam intensity after passage through the region of interest from the initial beam intensity. In these earliest single-photon absorptiometry (SPA) units, the results of multiple scan passes at a single location, usually the midradius, were averaged (30). In later units, scan passes at equally spaced intervals along the bone were utilized such that the mass of mineral per unit of bone length could be calculated. A scintillation detector was used to quantify the photon energy after attenuation by the bone and soft tissue in the scan path. After the photon attenuation was quantified, a comparison to the photon attenuation seen with a calibration standard derived from dried defatted human ashed bone of known weight was made in order to determine the amount of bone mineral.

The photon beam and the detector were highly "collimated" or restricted in size and shape. The beam source and detector moved in tandem across the region of interest on the bone, coupled by a mechanical drive system.

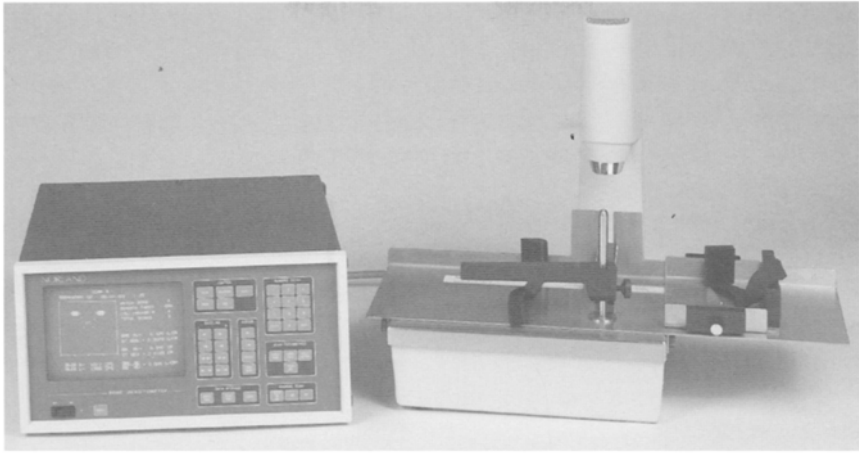


Fig. 2-6. Early Norland model 2780 single photon absorptiometer. This device utilized ^{125}I to generate photon energy. (Photo courtesy of CooperSurgical Norland, Trumbull, CT.)

Iodine-125 at 27.3 keV or americium-241 at 59.6 keV were originally used to generate the single-energy photon beam although most SPA units subsequently developed in the United States employed only ^{125}I .

The physical calculations for SPA determinations of bone mineral were valid only when there was uniform thickness of the bone and soft tissue in the scan path. In order to artificially create this kind of uniform thickness, the limb to be studied had to be submerged in a water bath or surrounded by a tissue-equivalent material. As a practical matter, this limited SPA to measurements of the distal appendicular skeleton such as the radius and later, the calcaneus. Figure 2-6 is a photograph of an old SPA device, the Norland 2780, that was in use in the 1980s.

Single-photon absorptiometry was both accurate and precise, although the parameters varied slightly with the site studied. For SPA measurements of the midradius accuracy ranged from 3 to 5%, and precision from 1 to 2% (29,31–33). Early measurements of the distal and ultradistal radius with SPA did not demonstrate the same high degree of precision primarily because of the marked changes in the composition of the bone with very small changes in location within the distal and ultradistal radius.* With later instruments that employed computer enhanced localization routines and rectilinear scanning, SPA measurements of the distal

*See Chapter 1 for a discussion of the composition of the radius and ulna.

and ultradistal radius approached a precision of 1% (34). Accuracy and precision of measurements at the calcaneus with SPA were reported to be less than 3% (32). The skin radiation dose for both the radius and calcaneus was 5 to 10 mrem (32,33). The biologically important radiation dose, the effective dose, was negligible. Results were reported as either bone mineral content (BMC) in g or as BMC per unit length (BMC/l) in g/cm. The time required to perform such studies was approximately 10 minutes (35).

SPA is rarely performed today, having been supplanted first by single-energy X-ray absorptiometry (SXA) and now dual-energy X-ray absorptiometry (DXA). The demise of SPA was due to improvements in ease of use and precision seen with SXA and DXA. SPA was an accurate technology that could be used to predict fracture risk. The ability to predict the risk of appendicular fractures with SPA measurements of the radius was convincingly established (36–38). SPA measurements of the radius were also good predictors of spine fracture risk and global* fracture risk (36,39,40). Indeed, the longest fracture trials published to date demonstrating the ability of a single bone mass measurement to predict fracture were performed using SPA measurements of the radius.

Dual-Photon Absorptiometry

The basic principle involved in dual-photon absorptiometry (DPA) for the measurement of bone density was the same as for SPA quantifying the degree of attenuation of a photon energy beam after passage through bone and soft tissue. In dual-photon systems, however, an isotope that emitted photon energy at two distinct photoelectric peaks or two isotopes, each emitting photon energy at separate and distinct photoelectric peaks, were used. When the beam was passed through a region of the body containing both bone and soft tissue, attenuation of the photon beam occurred at both energy peaks. If one energy peak was preferentially attenuated by bone, however, the contributions of soft tissue to beam attenuation could be mathematically subtracted (41). As in SPA, the remaining contributions of beam attenuation from bone were quantified and then compared to standards created from ashed bone. The ability to separate bone from soft tissue in this manner finally allowed quantification of the bone density in

*Global fracture risk refers to the risk of having any and all types of fractures combined. This is in contrast to a site-specific fracture risk prediction in which the risk for a fracture at a specific skeletal site is given, such as spine fracture risk or hip fracture risk.

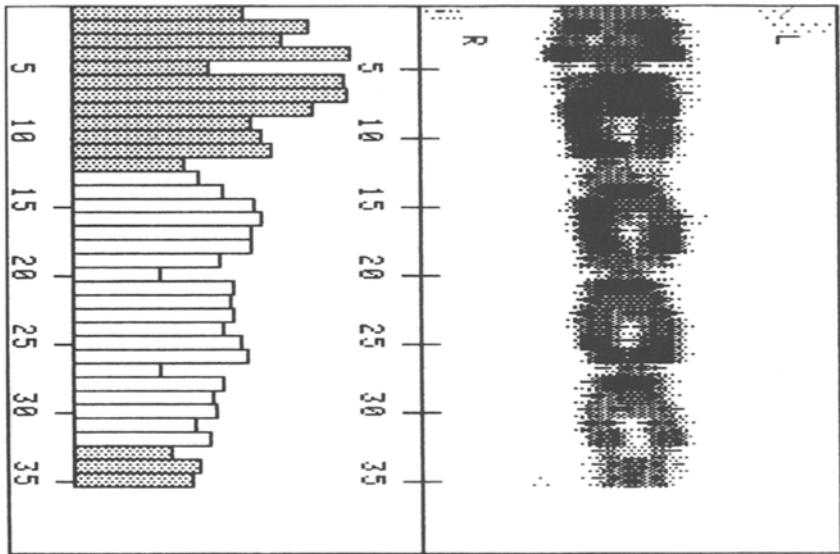


Fig. 2-7. Dual-photon absorptiometry posteroanterior spine study obtained on a device as shown in Fig. 2-8. The spine image is upside down. The histogram on the left was used to place the intervertebral disc space markers. The shortest bar in the vicinity of the disc space was identified and the marker was placed there.

those areas of the skeleton that were surrounded by large or irregular soft tissue masses, notably the spine and proximal femur. DPA was also used to determine total body bone density. The development of DPA and its application to the spine, proximal femur, and total body is attributed to a number of investigators: B. O. Roos, G. W. Reed, R. B. Mazess, C. R. Wilson, M. Madsen, W. Peppler, B. L. Riggs, W. L. Dunn, and H. W. Wahner (42–47).

The isotope most commonly employed in the United States was gadolinium-153, which naturally emitted photon energy at two photoelectric peaks, 44 keV and 100 keV. At the photoelectric peak of 44 keV bone preferentially attenuated the photon energy. The attenuated photon beams were detected by a NaI scintillation detector and quantified after passage through pulse-height analyzers set at 44 and 100 keV. The shielded holder for the ^{153}Gd source, which was collimated and equipped with a shutter that was operated by a computer, moved in tandem with the NaI detector in a rectilinear scan path over the region of interest. A point-by-point calculation of bone density in the scan path was made. Figure 2-7 is an intensity-modulated image of the spine created with an early DPA device.

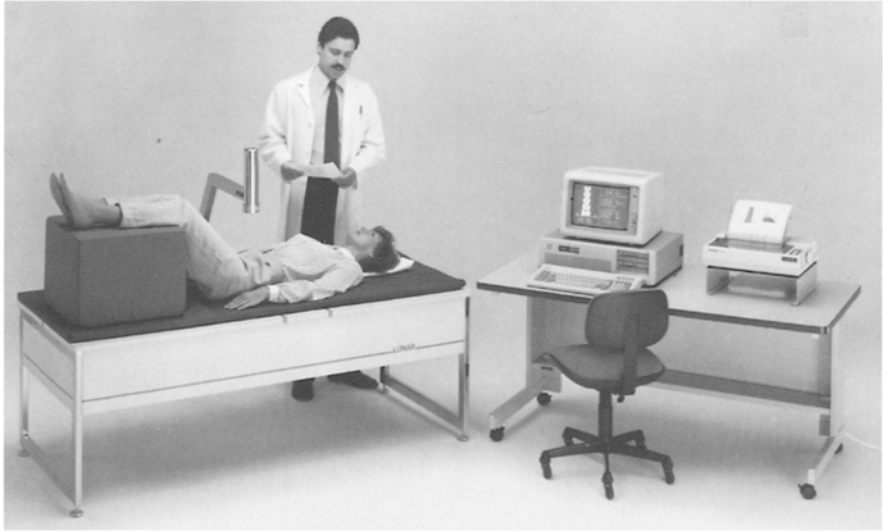


Fig. 2-8. Early GE Lunar DP3 dual photon absorptiometer. This device utilized ^{153}Gd to generate photon energy. (Photo courtesy of GE Healthcare, Madison, WI.)

DPA bone density studies of the lumbar spine were performed with the photon energy beam passing in a posterior to anterior direction. Because of the direction of the beam, the vertebral body and the posterior elements were included in the scan path. The transverse processes were eliminated. This resulted in a combined measurement of cortical and trabecular bone, or an integral measurement, that included the more trabecular vertebral body surrounded by its cortical shell and the highly cortical posterior elements. The results were reported as an areal density in g/cm^2 . The bone mineral density of the proximal femur was also an areal density that was acquired with the beam passing in a posterior to anterior direction. Figure 2-8 shows an early dual-photon absorptiometer with the patient positioned for a study of the lumbar spine.

DPA studies of the spine required approximately 30 minutes to complete. Studies of the proximal femur took 30–45 minutes to perform. Total body bone density studies with DPA required 1 hour. Skin radiation dose was low during spine or proximal femur studies at 15 mrem. Accuracy of DPA measurements of the spine ranged from 3 to 6% and for the proximal femur, 3 to 4% (48). Precision for measurements of spine bone density was 2–4% and around 4% for the femoral neck.

Dual-photon absorptiometry was considered a major advance from single-photon absorptiometry because it allowed the quantification of

bone density in the spine and proximal femur. DPA did have several limitations, however. Machine maintenance was expensive. The ^{153}Gd source had to be replaced yearly at a cost of \$5000 or more. It had also been noted that as the radioactive source decayed, values obtained with DPA increased by as much as 0.6% per month (49). With replacement of the source, values could fall by as much as 6.2%. Although mathematical formulas were developed to compensate for the effect of source decay, it remained a cause for concern, potentially affecting both accuracy and precision. The precision of 2–4% for DPA measurements of the spine and proximal femur limited its application in detecting changes in bone density. With a precision of 2%, a change of at least 5.5% from the baseline value had to be seen before one could be certain at the 95% confidence level that any change had occurred at all (50). With a precision of 4%, this figure increased to 11.1%. At a lower 80% confidence level, the required change for precision values of 2% and 4% were 3.6% and 7.2%, respectively. As a practical matter, this meant that DPA bone density studies would not show significant changes for up to 5 years. This was too long a period to wait to be clinically useful.

In DPA spine bone density studies in which the photon beam passed in a PA direction the highly trabecular vertebral body could not be separated from its more cortical posterior elements. In addition, the cortical shell of the vertebral body could not be separated from its trabecular interior. Calcifications in the overlying soft tissue or abdominal aorta will attenuate such a beam, falsely elevating the bone density values. Arthritic changes in the posterior elements of the spine also affect the measurement (51). These effects are discussed in greater detail in Chapter 3. PA DXA studies of the spine are not immune to these effects either but lateral DXA spine studies can be performed to overcome these limitations. Studies of the spine in the lateral projection were never available with DPA.

The ability to make site-specific predictions of fracture risk of the spine and proximal femur or global fracture risk predictions with dual photon absorptiometry was established in prospective trials (19,39). Like SPA, DPA is rarely performed in the United States now because of the availability of DXA with its technological improvements.

Dual-Energy X-Ray Absorptiometry

The underlying principles DXA are the same as those of dual-photon absorptiometry. With DXA, however, the radioactive isotope source of photon energy has been replaced by an X-ray tube. There are several advantages of X-ray sources over radioactive isotopes. There is no source

decay that would otherwise require costly replacement of the radioactive source. Similarly, there is no concern of a drift in patient values resulting from source decay. The greater source intensity or “photon flux” produced by the X-ray tube and the smaller focal spot allows for better beam collimation resulting in less dose overlap between scan lines and greater image resolution. Scan times are faster and precision is improved.

Because X-ray tubes produce a beam that spans a wide range of photon energies, the beam must be narrowed in some fashion in order to produce the two distinct photoelectric peaks necessary to separate bone from soft tissue. The major manufacturers of central dual-energy X-ray absorptiometers in the United States have chosen to do this in one of two ways. GE Healthcare (Madison, WI) and CooperSurgical Norland (Trumbull, CT) use rare earth K-edge filters to produce two distinct photoelectric peaks. Hologic, Inc. (Bedford, MA) uses a pulsed power source to the X-ray tube to create the same effect.

K-edge filters produce an X-ray beam with a high number of photons in a specific range. The energy range that is desired is the energy range that is just above the K-absorption edge of the tissue in question. The K-edge is the binding energy of the K-shell electron. This energy level varies from tissue to tissue. The importance of the K-edge is that at photon energies just above this level the transmission of photons through the tissue in question drops dramatically. That is, the photons are maximally attenuated at this energy level (52). Therefore, to separate bone from soft tissue in a quantifiable fashion, the energy of the photon beam should be just above the K-edge of bone or soft tissue for maximum attenuation. GE Healthcare uses a cerium filter in its central* devices that has a K-shell absorption edge at 40 keV. A cerium-filtered X-ray spectrum at 80 kV will contain two photoelectric peaks at about 40 and 70 keV. The samarium K-edge filter employed by Norland in its central devices has a K-shell absorption edge of 46.8 keV. The samarium-filtered X-ray beam at 100 kV produces a low-energy peak at 46.8 keV. In the Norland system, the high-energy peak is variable because the system employs selectable levels of filtration but the photons are limited to less than 100 keV by the 100 kV employed. The K-edge of both cerium and samarium results in a low-energy peak that approximates the 44 keV low-energy peak of gadolinium-153 used in old dual-photon systems.

*A central device is a bone densitometer that can be used to quantify bone density in the spine and proximal femur. The distinction between central and peripheral devices is discussed in Chapter 1.

Hologic central DXA devices utilize a different system to produce the two photoelectric peaks necessary to separate bone from soft tissue. Instead of employing K-edge filtering of the X-ray beam, Hologic employs alternating pulses to the X-ray source at 70 kV and 140 kV.

Most regions of the skeleton are accessible with dual-energy X-ray absorptiometry. Studies can be made of the spine in both an anterior-posterior (AP)* and lateral projection. Lumbar spine studies acquired in the lateral projection are not affected by the confounding effects of dystrophic calcification on densities measured in the PA direction (53). Lateral scans also eliminate the highly cortical posterior elements, which contribute as much as 47% of the mineral content measured in the PA direction (54). The utility of lateral DXA lumbar spine studies can be limited by rib overlap of L1 and L2 and pelvic overlap of L4, more so when performed in the left lateral decubitus position than the supine position (53,55). Bone density in the proximal femur, forearm, calcaneus and total body can also be measured with DXA.

Scan times are dramatically shorter with DXA compared with DPA. Early DXA units required approximately 4 minutes for studies of the PA lumbar spine or proximal femur. Total body studies required 20 minutes in the medium scan mode and only 10 minutes in the fast scan mode. Newer DXA units scan even faster, with studies of the PA spine or proximal femur requiring less than a minute to perform.

The values obtained with dual-energy X-ray studies of the skeleton are highly correlated with values from earlier studies performed with dual-photon absorptiometry. Consequently, the accuracy of DXA is considered comparable with that of DPA (56–59). DXA spine values and Hologic and Norland DXA proximal femur values are consistently lower than values obtained previously with DPA. There are also differences in the values obtained with DXA equipment from the three major manufacturers as noted in Chapter 1. Values obtained with either a Hologic or Norland DXA unit are consistently lower than those obtained with a Lunar DXA unit, although all are highly correlated with each other (60–62). Comparison studies using all three manufacturers' central DXA devices have resulted in the development of formulas that make it possible to convert values for

*Although spine bone density studies with dual-energy X-ray absorptiometry are often referred to as AP spine studies, the beam actually passes in a posterior to anterior direction. Such studies are correctly characterized as PA spine studies, but it has become an accepted convention to refer to them as AP spine bone density studies. The GE Lunar Expert, a fan-array DXA scanner, does acquire spine bone density studies in the AP projection.

the lumbar spine and femoral neck obtained on one manufacturer's device to the expected value on another manufacturer's device (see Appendix VII) (63). The margin of error in such conversions is still too great to use such values in following a patient over time, however. Such values should only be viewed as "ball park" figures. Another set of formulas makes the conversion of any manufacturer's BMD value at the lumbar spine or total hip to a second value called the "standardized bone mineral density" (sBMD) (see Appendix VII) (63,64). As noted in Chapter 1, the sBMD is always reported in mg/cm^2 to distinguish it from the manufacturer's BMD, which is reported in g/cm^2 .

Perhaps the most significant advance seen with DXA compared with DPA is the marked improvement in precision. Expressed as a coefficient of variation, short-term precision in normal subjects has been reported as low as 0.9% for the PA lumbar spine and 1.4% for the femoral neck (56). Precision studies over the course of 1 year have reported values of 1% for the PA lumbar spine and 1.7–2.3% for the femoral neck (59).

Radiation exposure is extremely low for all types of DXA scans. Expressed as skin dose, radiation exposure during a PA lumbar spine or proximal femur study is only 2–5 mrem.* The biologically important effective dose or whole-body equivalent dose is only 0.1 mrem (65).

Dual-energy X-ray absorptiometry has been used in prospective studies to predict fracture risk. In one of the largest studies of its kind, DXA studies of the proximal femur were demonstrated to have the greatest short-term predictive ability for hip fracture compared to measurements at other sites with SPA or DPA (19).

DXA central devices are called pencil-beam or fan-array scanners. Examples of pencil-beam scanners are the GE Lunar DPX® Plus, DPX®-L, DPX-IQ™, DPX®-SF, DPX®-A, DPX-MD™, DPX-MD+™, and DPX-NT™; the Hologic QDR® 1000 and QDR® 2000; and the Norland XR-36™, XR-46™, Excell™, and Excell™plus.† Examples of fan-array DXA scanners are the GE Lunar Expert® and Prodigy™; DPX Bravo™ and DPX Duo™; and the Hologic QDR® 4500 A, QDR® 4500 C, QDR® 4500 W, and QDR® 4500 SL; and the Delphi™, Explorer™, and Discovery™. The difference between the pencil-beam and fan-array scanners is illustrated in Figs. 2-9 and 2-10. Pencil-beam scanners employ a collimated or narrowed X-ray beam (narrow like a pencil) that moves in tandem in a rectilinear pattern with the detector(s). Fan-array scanners utilize a much broader or fan-shaped beam and an array of detectors, so that

*See Chapter 4 for a listing of radiation dose according to device and scan type.

†Specific descriptions and photographs of these scanners can be found in Chapter 4.

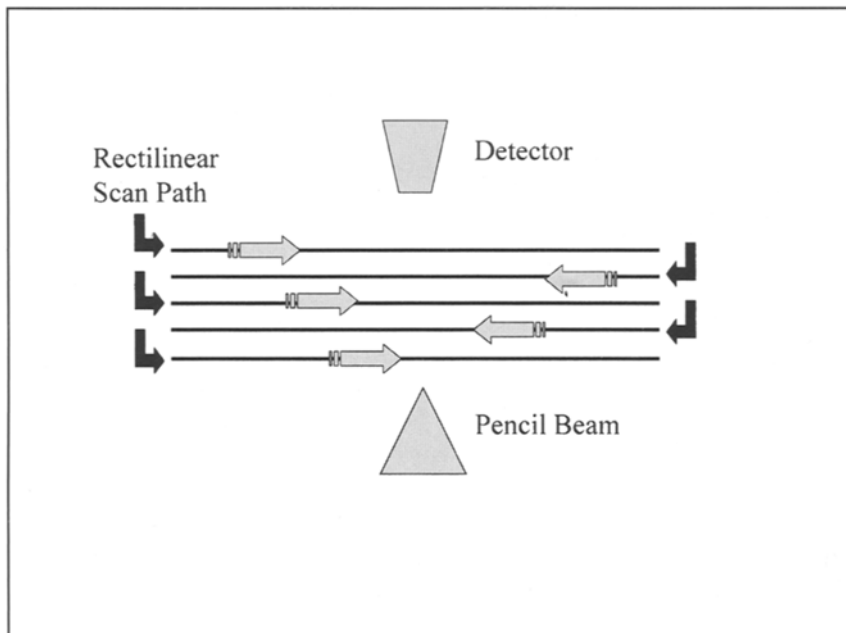


Fig. 2-9. Pencil-beam dual-energy X-ray absorptiometry densitometers. The single detector or sequential detectors move in tandem with the narrowed X-ray beam in a rectilinear scan path.

an entire scan line can be instantly quantified. Scan times are reduced to as little as 30 seconds for a PA study of the lumbar spine. Image resolution is also enhanced with the fan-array scanners, as evinced by the extraordinary images in Fig. 2-11. This has created a new application for bone densitometry scanning called morphometric X-ray absorptiometry (MXA), which is discussed more fully in Chapter 12. With MXA, images of the spine obtained in the lateral projection can be used for computer analysis of the vertebral dimensions and diagnosis of vertebral fracture. Fan-array scanners have also been developed to image the lateral spine in its entirety to allow a visual assessment of vertebral size and shape. Examples of scanners with this capability are the Hologic Delphi, Discovery, and the GE Lunar Prodigy. Figures 2-12 and 2-13 are lateral spine images from the Lunar Prodigy. In the Dual-energy Vertebral Assessment (DVA™) image in Fig. 2-12 a fracture is suggested at T12. In Fig. 2-13, the dimensions of the suspect vertebra are measured with morphometry software. Figure 2-14 and 2-15 are Instant Vertebral Assessment (IVA™) images from the Hologic Delphi. No fractures are apparent in Fig. 2-14. Note the multiple thoracic deformities in Fig. 2-15.

DXA has effectively replaced DPA in both research and clinical practice. The shortened scan times, improved image resolution, lower radiation

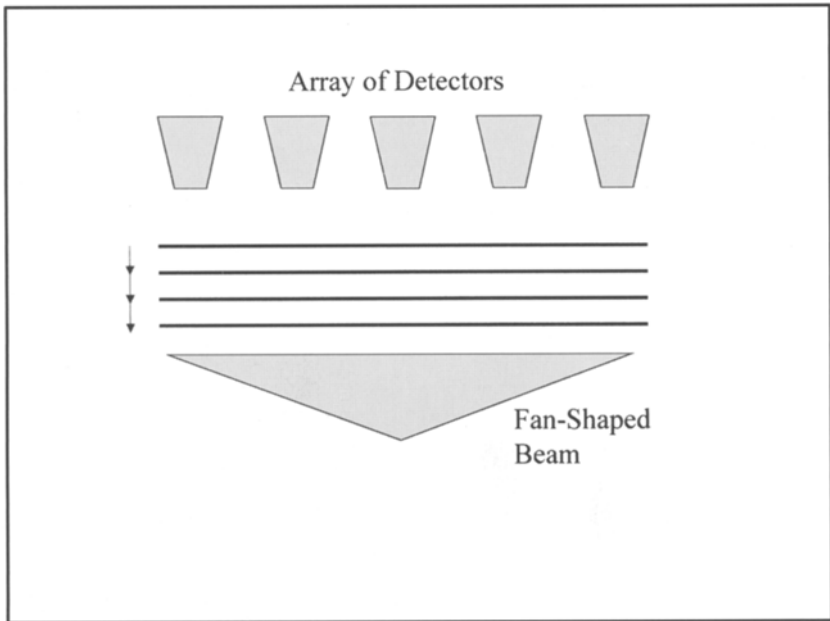


Fig. 2-10. Fan-array dual-energy X-ray absorptiometry densitometers. An array of detectors and fan-shaped beam make possible the simultaneous acquisition of data across an entire scan line.

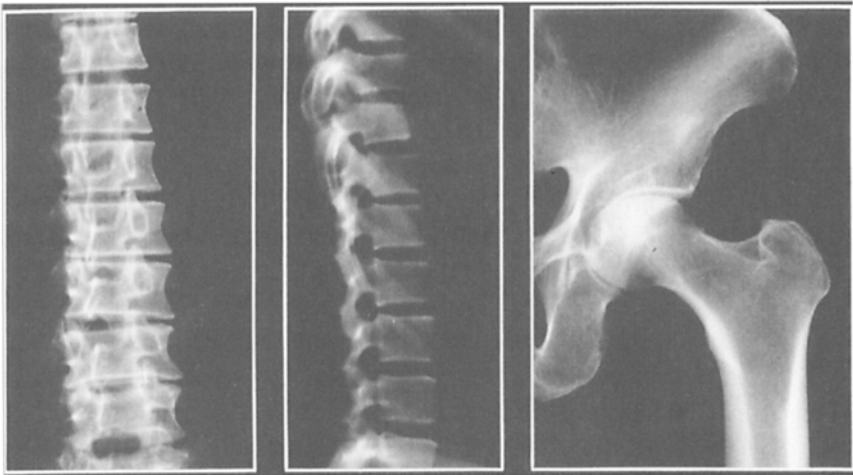


Fig. 2-11. Images from the fan-array imaging densitometer, the GE Lunar EXPERT-XL. (Images courtesy of GE Healthcare, Madison, WI.)

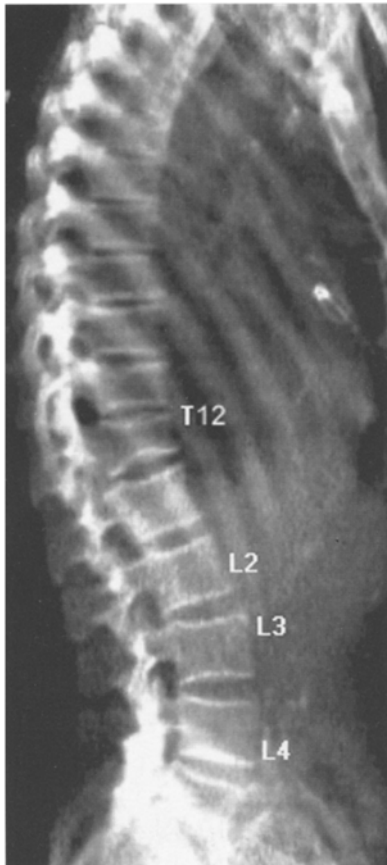


Fig. 2-12. LVA™ image acquired on the GE Lunar Prodigy™ A fracture is apparent at T12. These images are now called DVA™ images. (Case courtesy of GE Healthcare, Madison, WI.)

dose, improved precision, application to more skeletal sites, and lower cost of operation with DXA have relegated DPA to an honored place in densitometry history.

Peripheral DXA

Dual-energy X-ray technology is also employed in portable devices dedicated to the measurement of one or two appendicular sites. As such, these devices are characterized as “peripheral” devices or pDXA devices. Because these devices employ dual-energy X-ray, they do not require a water bath or tissue-equivalent gel surrounding the region of the skeleton



Fig. 2-13. LVA™ image acquired on the GE Lunar Prodigy™. Morphometric software allows the user to define the vertebral edges and measure the vertebral heights to quantitatively diagnose fracture. These images are now called DVA™ images. (Case courtesy of GE Healthcare, Madison, WI.)

being studied. As a consequence, they are somewhat easier to maintain and use than SXA devices. Examples of pDXA units are the Lunar PIXI®; the Norland pDEXA® and the Norland Apollo™; and the Schick accuDEXA™ and the Osteometer DEXACare® DTX-200 and G4. These devices are discussed in detail in Chapter 4.

Single-Energy X-Ray Absorptiometry

SXA is the X-ray-based counterpart of single-photon absorptiometry, much as dual-energy X-ray absorptiometry is the X-ray-based counterpart of dual-photon absorptiometry. SXA units were used to measure bone density in the distal radius, ulna, and calcaneus. Like their DXA counterparts, SXA units did not utilize radioactive isotopes but did require a water bath or tissue-equivalent gel surrounding the region of the skeleton being measured. The accuracy and precision of SXA were comparable with SPA (66). With the development of portable DXA devices for the measurement of forearm and heel bone density that do not require a water bath or tissue-equivalent gel, SXA is largely obsolete, as is its predecessor SPA.

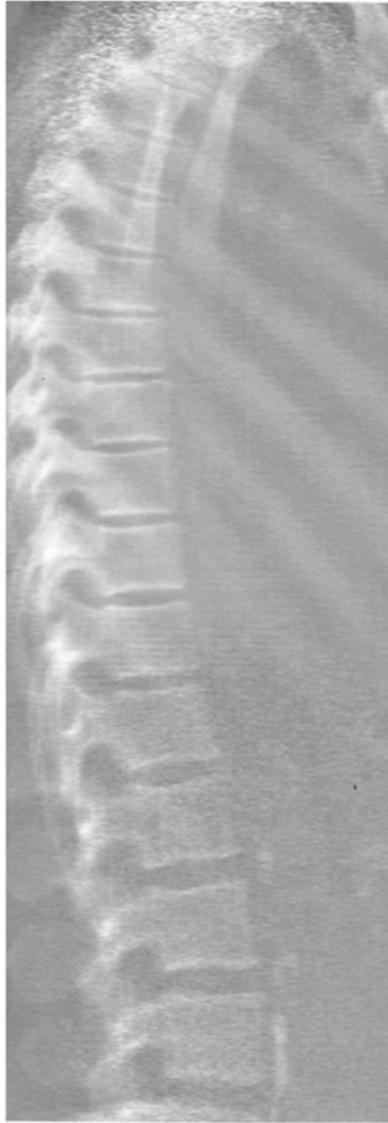


Fig. 2-14. IVA™ image acquired on the Hologic Delphi™. No fractures are apparent in the thoracic and lumbar spine although aortic calcification is seen anterior to the lumbar spine. (Case courtesy of Hologic, Inc., Bedford, MA.)

Quantitative Computed Tomography

Although quantitative computed tomography (QCT) is a photon absorptiometric technique like SPA, SXA, DPA, and DXA, it is unique in that it provides a three-dimensional or volumetric measurement of bone

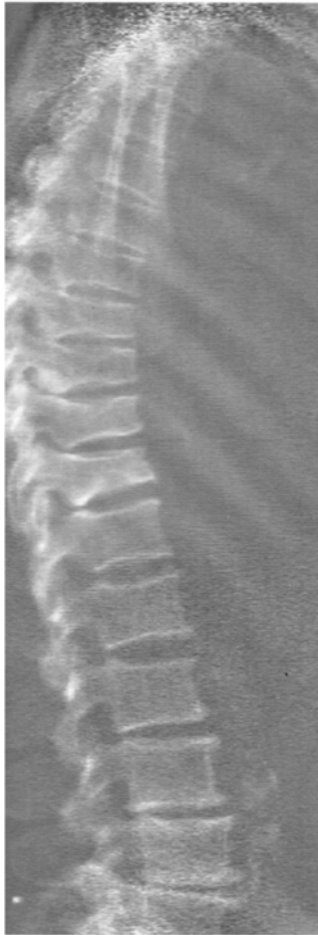


Fig. 2-15. IVA™ image acquired on the Hologic Delphi™. There are multiple deformities in the thoracic spine as well as osteophytes in the lower lumbar spine. Aortic calcification is also seen anterior to the lumbar spine. (Case courtesy of Hologic, Inc., Bedford, MA.)

density and a spatial separation of trabecular from cortical bone. In 1976, Ruegsegger et al. (67) developed a dedicated peripheral quantitative CT scanner using ^{125}I for measurements of the radius. Cann and Genant (68,69) are credited with adapting commercially available CT scanners for the quantitative assessment of spinal bone density. It is this approach that has received the most widespread use in the United States, although dedicated CT units for the measurement of the peripheral skeleton, or peripheral QCT (pQCT) units, are in use in clinical centers. QCT studies

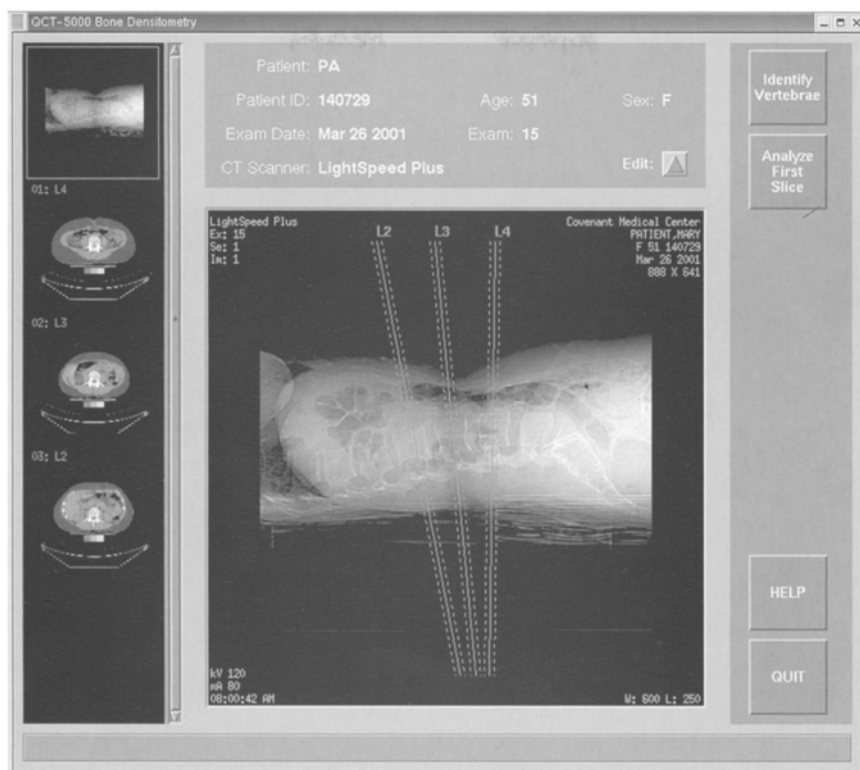


Fig. 2-16. QCT-5000™ scout image. (Reproduced courtesy of Image Analysis, Inc., Columbia, KY.)

of the spine utilize a reference standard or phantom that is scanned simultaneously with the patient. The phantom contains varying concentrations of K_2HPO_4 and is placed underneath the patient during the study. A scout view, shown in Fig. 2-16, is required for localization and then an 8- to 10-mm-thick slice is measured through the center of two or more vertebral bodies that are generally selected from T12 to L3 (70). A region of interest within the anterior portion of the vertebral body is analyzed for bone density and is reported as mg/cm^3 K_2HPO_4 equivalents, as shown in Fig. 2-17. This region of interest is carefully placed to avoid the cortical shell of the vertebral body. The result is a three-dimensional trabecular density unlike the two-dimensional areal mixed cortical and trabecular densities reported with PA studies of the spine utilizing DPA or DXA.

A study of the spine with QCT requires about 10 minutes (35). The skin radiation dose is generally 100–300 mrem. This overestimates the biolog-



Fig. 2-17. QCT-5000™ axial spine image. This is a three-dimensional volumetric measurement, reported in mg/cm^3 or mg/cc . The L2 bone mineral density shown here is 120.2 mg/cc . This measurement is 100% trabecular. (Reproduced courtesy of Image Analysis, Inc., Columbia, KY.)

ically important effective dose because only a small portion of marrow is irradiated during a QCT study of the spine (65). The effective dose or whole-body equivalent dose is generally in the range of only 3 mrem (30 μSv). The localizer scan that precedes the actual QCT study will add an additional 3 mrem to the effective dose. These values are quite acceptable in the context of natural background radiation of approximately 20 mrem per month. Older CT units, that by their design are unable to utilize low kVp settings for QCT studies, may deliver doses 3–10 times higher.

The accuracy of QCT for measurements of spine bone mineral density can be affected by the presence of marrow fat (70–72). Marrow fat increases with age resulting in an increasingly large error in the accuracy of spine QCT measurements in older patients. The accuracy of QCT is

reported to range from 5% to 15%, depending upon the age of the patient and percentage of marrow fat. The presence of marrow fat results in an underestimation of bone density in the young of about 20 mg/cm³ and as much as 30 mg/cm³ in the elderly (70). The error introduced by marrow fat can be partially corrected by applying data on vertebral marrow fat with aging originally developed by Dunnill et al. (73). In an attempt to eliminate the error introduced by marrow fat, dual-energy QCT (DEQCT) was developed by Genant and Boyd (74). This method clearly reduced the error introduced by the presence of marrow fat to as low as 1.4% in cadaveric studies (71,72). In vivo, the accuracy with DEQCT is 3–6% (35,70). Radiation dose with DEQCT is increased approximately 10-fold compared to regular or single-energy QCT (SEQCT), but precision is not as good. The precision of SEQCT for vertebral measurements in expert hands is 1–3%, and for DEQCT, 3–5% (70,75).

The measurement of bone density in the proximal femur with QCT is not readily available. Using both dedicated QCT and standard CT units, investigators have attempted to utilize QCT for measurements of the proximal femur but this capability remains restricted to a few research centers (76,77).

QCT of the spine has been used in studies of prevalent osteoporotic fractures and it is clear that such measurements can distinguish osteoporotic individuals from normal individuals as well or even better than DPA (78–81). Fractures are rare with values above 110 mg/cc and extremely common below 60 mg/cm³ (82). Because QCT can isolate and measure trabecular bone, which is more metabolically active than cortical bone, rates of change in disease states observed with QCT spine measurements tend to be greater than those observed with PA spine studies performed with DPA or DXA (68,83). This greater magnitude of change partially offsets the effects of the poorer precision seen with QCT compared to DXA.* The correlations between spine bone density measurements with QCT and skeletal sites measured with other techniques are statistically significant but too weak to allow accurate prediction of bone density at another site from measurement of the spine with QCT (26,80,81). This is no different, however, from attempting to use BMD at the spine obtained with DXA to predict BMD at other skeletal sites.

*See Chapter 6 for a detailed discussion on the interaction between precision and rate of change in determining the time interval required between measurements to demonstrate significant change.

Peripheral QCT

pQCT is becoming more widely available. pQCT devices are utilized primarily for the measurement of bone density in the forearm. Like QCT scans of the spine, pQCT makes possible true 3D or volumetric measurements of bone density in the forearm, which may be particularly useful when the size of the bone is changing, as in pediatric populations. Information on a commercially available pQCT device, the Stratec XCT 2000™, can be found in Chapter 4.

QUANTITATIVE ULTRASOUND BONE DENSITOMETRY

Research in quantitative ultrasound (QUS) bone densitometry has been ongoing for over 40 years. Only in the last few years, however, has QUS begun to play a role in the clinical evaluation of the patient. Ultrasound technologies in clinical medicine have traditionally been imaging technologies used, for example, to image the gall bladder or the ovaries. Like photon absorptiometric technologies, however, the application of ultrasound in bone densitometry is not primarily directed at producing an image of the bone. Instead, a quantitative assessment of bone density is desired with the image being secondary in importance.

In theory, the speed with which sound passes through bone is related not only to the density of the bone, but to the quality of the bone as well. Both bone density and bone quality determine a bone's resistance to fracture. Therefore, the speed of sound through bone can be related to the risk of fracture. These relationships can be illustrated mathematically. For example, the bone's ability to resist fracture (R) can be described as the amount the bone deforms when it is subjected to a force (F) that is moderated by the bone's ability to resist that force, the elastic modulus (E) as shown in eq. 1.

$$R = \frac{F}{E} \quad (1)$$

Studies have shown that the E is determined by both bone density and bone quality. Mathematically, this is represented in eq. 2, where K is a constant representing bone quality and ρ represents bone density.

$$E = K\rho^2 \quad (2)$$

From such an equation, it becomes clear that the bone's ability to resist a force and not fracture is determined by changes in bone density and

bone quality. When ultrasound passes through a material, the velocity of the sound wave is also related to the elastic modulus (84,85) and density of the material as shown in eq. 3.

$$V = \sqrt{\frac{E}{\rho}} \quad (3)$$

When eqs. 2 and 3 are combined, it becomes clear that the velocity of ultrasound through bone is directly related to the square root of the product of bone density and bone quality.

$$V = \sqrt{\frac{K\rho^2}{\rho}} \quad (4)$$

$$V = \sqrt{K\rho} \quad (5)$$

The velocity with which ultrasound passes through normal bone is quite fast and varies depending on whether the bone is cortical or trabecular. Speeds of 3000–3600 m/sec are typical in cortical bone with speeds of 1650–2300 m/sec typical of trabecular bone.

In order to calculate velocity, ultrasound densitometers must measure the distance between two points and the time required for the sound wave to travel between these two points. The velocity is reported as the speed of sound (SOS). Higher values of SOS indicate greater values of bone density.

A second ultrasound parameter is broadband ultrasound attenuation (BUA). This parameter is reported in decibels per megahertz (dB/MHz). BUA is perhaps best understood using the analogy of a child's slinky toy. When the toy is stretched out and then suddenly released, the energy imparted to the rings by stretching them causes the rings to oscillate for a period of time, with the oscillations becoming progressively less and finally stopping as the energy is lost. The same thing happens to the sound wave as it passes through bone. Some of the energy is lost from the sound wave and the oscillations of the sound wave are diminished. How much energy is lost is again related to the density of the bone and to architectural qualities such as porosity and trabecular connectivity (84,85). Like SOS, higher BUA values indicate greater bone density.

Most devices report both SOS and BUA. However, one manufacturer has mathematically combined SOS and BUA into a proprietary index

called the Stiffness Index. Another manufacturer reports a proprietary index called the Quantitative Ultrasound Index (QUI) and an estimated BMD that is derived from the measurements of SOS and BUA. QUS devices are considered peripheral devices and are generally quite portable. They employ no ionizing radiation, unlike their SXA or DXA peripheral counterparts. The calcaneus is the most common skeletal site assessed with QUS, but devices exist that can be applied to the radius, finger, and tibia. In heel QUS measurements, heel width apparently has little, if any, effect on BUA but may have a slight effect on SOS (86). Most ultrasound devices require some type of coupling medium between the transducers and the bone. This is often accomplished with water when the heel is placed directly into a water bath. Ultrasound gel may be used in place of direct contact with water for heel measurements and measurements at other skeletal sites. Systems that utilize water baths into which the foot is placed are called “wet” systems. Systems that do not require water submersion but utilize gel instead, are called “dry” systems. There is one system for the heel in which neither water submersion nor gel are required, making it truly “dry.” The GE Lunar Achilles+™, the Lunar Achilles Express™, the Lunar Insight™, the Sunlight Omnisense™ 7000S, the Quidel QUS-2™, the McCue C.U.B.A. Clinical™, the Hologic Sahara™ Clinical Bone Sonometer, and the Osteometer DTU-one Ultrasure® are all examples of QUS densitometers currently available for clinical use. These devices are discussed in more detail in Chapter 4.

The technical differences between QUS devices from various manufacturers are even greater than those seen with DXA devices. Different frequency ranges and transducer sizes may be employed from device to device. Within the same skeletal site, slightly different regions of interest may be measured. As a consequence, values obtained on one QUS device are not necessarily comparable to values obtained on another QUS device.

The physics of ultrasound suggest that it should provide information about the bone that goes beyond a simple measurement of mass or density. Clinical research has tended to confirm this assumption, although perhaps not to the extent that was originally hoped. In a very large study of 5662 older women, both SOS and BUA predicted the risk of hip fracture as well or better than did measurements of BMD at the femoral neck using DXA (87). Similar findings were reported in the Study of Osteoporotic Fractures by Bauer et al. (88).

The precision of QUS measurements is generally excellent. In addition, because of the speed with which measurements can be made and the lack of any ionizing radiation, measurements can be made in duplicate or

triplicate at any one examination. The average value of such replicate studies can be used, which dramatically improves precision. In a study from Njeh et al. (89). in which the precision of six different calcaneal QUS devices was determined, the short-term precision for SOS, expressed as the root-mean-square percent coefficient of variation (RMS-%CV) ranged from 0.11 to 0.42. For BUA, the RMS-%CV ranged from 1.39 to 6.30. Typically, better precision values are seen for SOS than for BUA.

REFERENCES

1. Dennis, J. (1897) A new system of measurement in X-ray work. *Dental Cosmos* **39**, 445–454.
2. Price, W. A. (1901) The science of dental radiology. *Dental Cosmos* **43**, 483–503.
3. Johnston, C. C. and Epstein, S. (1981) Clinical, biochemical, radiographic, epidemiologic, and economic features of osteoporosis. *Orthop. Clin. North Am.* **12**, 559–569.
4. Aitken, M. (1984) Measurement of bone mass and turnover, in Osteoporosis in Clinical Practice. John Wright & Sons Ltd, Bristol, pp. 19,20.
5. Singh, J., Nagrath, A. R., Maini, P. S. (1970) Changes in trabecular pattern of the upper end of the femur as an index of osteoporosis. *J. Bone Joint Surg. Am.* **52-A**, 457–467.
6. Bohr, H. and Schadt, O. (1983) Bone mineral content of femoral bone and lumbar spine measured in women with fracture of the femoral neck by dual photon absorptiometry. *Clin. Ortho.* **179**, 240–245.
7. Nordin, B. E. C. Osteoporosis with particular reference to the menopause, in The Osteoporotic Syndrome (Avioli, L. V. ed.), Grune & Stratton, New York, pp. 13–44.
8. Shimmins, J., Anderson, J. B., Smith, D. A., et al. (1972) The accuracy and reproducibility of bone mineral measurements “in vivo.” (a) The measurement of metacarpal mineralisation using an X-ray generator. *Clin. Radiol.* **23**, 42–46.
9. Exton-Smith, A. N., Millard, P. H., Payne, P. R., Wheeler, E. F. (1969) Method for measuring quantity of bone. *Lancet* **2**, 1153–1154.
10. Dequeker, J. (1982) Precision of the radiogrammetric evaluation of bone mass at the metacarpal bones, in Non-invasive Bone Measurements: Methodological Problems (Dequeker, J., Johnston, C. C., eds.), IRL Press, Oxford, pp. 27–32.
11. Aitken, J. M., Smith, C. B., Horton, P. W., et al. (1974) The interrelationships between bone mineral at different skeletal sites in male and female cadavera. *J. Bone Joint Surg. Br.* **56B**, 370–375.
12. Meema, H. E. and Meindok, H. (1992) Advantages of peripheral radiogrammetry over dual-photon absorptiometry of the spine in the assessment of prevalence of osteoporotic vertebral fractures in women. *J. Bone. Miner. Res.* **7**, 897–903.
13. Bywaters, E. G. L. (1948) The measurement of bone opacity. *Clin. Sci.* **6**, 281–287.
14. Barnett, E. and Nordin, B. E. C. (1961) Radiologic assessment of bone density. 1.-The clinical and radiological problem of thin bones. *Br. J. Radiol.* **34**, 683–692.
15. Bouxsein, M. L., Palermo, L., Yeung, C., Black, D. M. (2002) Digital X-ray radiogrammetry predicts hip, wrist, and vertebral fracture risk in elderly women: a prospective analysis from the Study of Osteoporotic Fractures. *Osteoporos. Int.* **12**, 358–365.

16. Cummings, S., Black, D., Nevitt, M., et al. (1990) Appendicular bone density and age predict hip fractures in women. *JAMA* **263**, 665–668.
17. Mack, P. B., Brown, W. N., Trapp, H. D. (1949) The quantitative evaluation of bone density. *Am. J. Roentgenol Rad. Ther.* **61**, 808–825.
18. Vose, G. P. and Mack, P. B. (1963) Roentgenologic assessment of femoral neck density as related to fracturing. *Am. J. Roentgenol Rad. Ther. Nucl. Med.* **89**, 1296–1301.
19. Cummings, S. R., Black, D. M., Nevitt, M. C., et al. (1993) Bone density at various sites for prediction of hip fractures. *Lancet* **341**, 72–75.
20. Mazess, R. B. (1983) Noninvasive methods for quantitating trabecular bone, in *The Osteoporotic Syndrome* (Avioli L. V. ed.), Grune & Stratton, New York, pp. 85–114.
21. Mack, P. B., O'Brien, A. T., Smith, J. M., Bauman, A. W. (1939) A method for estimating degree of mineralization of bones from tracings of roentgenograms. *Science* **89**, 467.
22. Mack, P. B. and Vogt, F. B. (1971) Roentgenographic bone density changes in astronauts during representative Apollo space flight. *Am. J. Roentgenol Rad. Ther. Nucl. Med.* **113**, 621–633.
23. Cosman, F., Herrington, B., Himmelstein, S., Lindsay, R. (1991) Radiographic absorptiometry: a simple method for determination of bone mass. *Osteoporos Int.* **2**, 34–38.
24. Yates, A. J., Ross, P. D., Lydick, E., Epstein, R. S. (1995) Radiographic absorptiometry in the diagnosis of osteoporosis. *Am. J. Med.* **98**, 41S–47S.
25. Yang, S., Hagiwara, S., Engelke, K., et al. (1994) Radiographic absorptiometry for bone mineral measurement of the phalanges: precision and accuracy study. *Radiology* **192**, 857–859.
26. Kleerekoper, M., Nelson, D. A., Flynn, M. J., Pawluszka, A. S., Jacobsen, G., Peterson E. L. (1994) Comparison of radiographic absorptiometry with dual-energy X-ray absorptiometry and quantitative computed tomography in normal older white and black women. *J. Bone Miner. Res.* **9**, 1745–1749.
27. Mussolino, M. E., Looker, A. C., Madans, J. H., et al. (1997) Phalangeal bone density and hip fracture risk. *Arch. Intern. Med.* **157**, 433–438.
28. Huang, C., Ross, P. D., Yates, A. J., et al. (1998) Prediction of fracture risk by radiographic absorptiometry and quantitative ultrasound: a prospective study. *Calcif. Tissue Int.* **6**, 380–384.
29. Cameron, J. R. and Sorenson, G. (1963) Measurements of bone mineral in vivo: an improved method. *Science* **142**, 230–232.
30. Vogel, J. M. (1987) Application principles and technical considerations in SPA, in *Osteoporosis Update 1987* (Genant, H. K., ed.), University of California Printing Services, San Francisco, pp. 219–231.
31. Johnston, C. C. (1983) Noninvasive methods for quantitating appendicular bone mass, in *The Osteoporotic Syndrome* (Avioli, L., ed.), Grune & Stratton, New York, pp. 73–84.
32. Barden, H. S. and Mazess, R. B. (1989) Bone densitometry of the appendicular and axial skeleton. *Top Geriatric Rehabil.* **4**, 1–12.
33. Kimmel, P. L. (1984) Radiologic methods to evaluate bone mineral content. *Ann. Intern. Med.* **100**, 908–911.
34. Steiger, P. and Genant, H. K. (1987) The current implementation of single-photon absorptiometry in commercially available instruments, in *Osteoporosis Update 1987* (Genant, H. K., ed.), University of California Printing Services, San Francisco, pp. 233–240.

35. Chesnut, C. H. (1993) Noninvasive methods for bone mass measurement, in *The Osteoporotic Syndrome*, 3rd ed. (Avioli, L., ed.), Wiley-Liss, New York, pp. 77–87.
36. Gardsell, P., Johnell, O., Nilsson, B. E. (1991) The predictive value of bone loss for fragility fractures in women: a longitudinal study over 15 years. *Calcif. Tissue Int.* **49**, 90–94.
37. Hui, S. L., Slemenda, C. W., Johnston, C. C. (1989) Baseline measurement of bone mass predicts fracture in white women. *Ann. Intern. Med.* **111**, 355–361.
38. Ross, P. D., Davis, J. W., Vogel, J. M., Wasnich, R. D. (1990) A critical review of bone mass and the risk of fractures in osteoporosis. *Calcif. Tissue Int.* **46**, 149–161.
39. Melton, L. J., Atkinson, E. J., O’Fallon, W. M., Wahner, H. W., Riggs, B. L. (1993) Long-term fracture prediction by bone mineral assessed at different skeletal sites. *J. Bone Miner. Res.* **8**, 1227–1233.
40. Black, D. M., Cummings, S. R., Genant, H. K., Nevitt, M. C., Palermo, L., Browner, W. (1992) Axial and appendicular bone density predict fracture in older women. *J. Bone Miner. Res.* **7**, 633–638.
41. Nord, R. H. Technical considerations in DPA, in *Osteoporosis Update 1987* (Genant, H. K., ed.), University of California Printing Services, San Francisco, pp. 203–212.
42. Dunn, W. L., Wahner, H. W., Riggs, B. L. (1980) Measurement of bone mineral content in human vertebrae hip by dual photon absorptiometry. *Radiology* **136**, 485–487.
43. Reed, G. W. (1966) The assessment of bone mineralization from the relative transmission of ^{241}Am and ^{137}Cs radiations. *Phys. Med. Biol.* **11**, 174.
44. Roos, B. and Skoldborn, H. (1974) Dual photon absorptiometry in lumbar vertebrae. I. Theory and method. *Acta. Radiol. Ther. Phys. Biol.* **13**, 266–290.
45. Mazess, R. B., Ort, M., Judy, P. (1970) Absorptiometric bone mineral determination using ^{153}Gd , in *Proceedings of Bone Measurements Conference* (Cameron, J. R., ed.), U.S. Atomic Energy Commission, pp. 308–312.
46. Wilson, C. R. and Madsen, M. (1977) Dichromatic absorptiometry of vertebral bone mineral content. *Invest. Radiol.* **12**, 180–184.
47. Madsen, M., Peppler, W., Mazess, R. B. (1976) Vertebral and total body bone mineral content by dual photon absorptiometry. *Calcif. Tissue Res.* **2**, 361–364.
48. Wahner, W. H., Dunn, W. L., Mazess, R. B., et al. (1985) Dual-photon Gd-153 absorptiometry of bone. *Radiology* **156**, 203–206.
49. Lindsay, R., Fey, C., Haboubi, A. (1987) Dual photon absorptiometric measurements of bone mineral density increase with source life. *Calcif. Tissue Int.* **41**, 293–294.
50. Cummings, S. R. and Black, D. B. (1986) Should perimenopausal women be screened for osteoporosis? *Ann. Intern. Med.* **104**, 817–823.
51. Drinka, P. J., DeSmet, A. A., Bauwens, S. F., Rogot, A. (1992) The effect of overlying calcification on lumbar bone densitometry. *Calcif. Tissue Int.* **50**, 507–510.
52. Curry, T. S., Dowdey, J. E., Murry, R. C. (1990) *Christensen’s Physics of Diagnostic Radiology*. Lea & Febiger, Philadelphia.
53. Rupich, R. C., Griffin, M. G., Pacifici, R., Avioli, L. V., Susman, N. (1992) Lateral dual-energy radiography: artifact error from rib and pelvic bone. *J. Bone Miner. Res.* **7**, 97–101.
54. Louis, O., Van Den Winkel, P., Covens, P., Schoutens, A., Osteaux, M. (1992) Dual-energy X-ray absorptiometry of lumbar vertebrae: relative contribution of body and posterior elements and accuracy in relation with neutron activation analysis. *Bone* **13**, 317–320.

55. Peel, N. F. A., Johnson, A., Barrington, N. A., Smith, T. W. D., Eastell, R. (1993) Impact of anomalous vertebral segmentation of measurements of bone mineral density. *J. Bone Miner. Res.* **8**, 719–723.
56. Lees, B. and Stevenson, J. C. (1992) An evaluation of dual-energy X-ray absorptiometry and comparison with dual-photon absorptiometry. *Osteoporos Int.* **2**, 146–152.
57. Kelly, T. L., Slovik, D. M., Schoenfeld, D. A., Neer, R. M. (1988) Quantitative digital radiography versus dual photon absorptiometry of the lumbar spine. *J. Clin. Endocrinol. Metab.* **76**, 839–844.
58. Holbrook, T. L., Barrett-Connor, E., Klauber, M., Sartoris, D. (1991) A population-based comparison of quantitative dual-energy X-ray absorptiometry with dual-photon absorptiometry of the spine and hip. *Calcif. Tissue Int.* **49**, 305–307.
59. Pouilles, J. M., Tremollieres, F., Todorovsky, N., Ribot, C. (1991) Precision and sensitivity of dual-energy X-ray absorptiometry in spinal osteoporosis. *J. Bone Miner. Res.* **6**, 997–1002.
60. Laskey, M. A., Cirsp, A. J., Cole, T. J., Compston, J. E. (1992) Comparison of the effect of different reference data on Lunar DPX and Hologic QDR-1000 dual-energy X-ray absorptiometers. *Br. J. Radiol.* **65**, 1124–1129.
61. Pocock, N. A., Sambrook, P. N., Nguyen, T., Kelly, P., Freund, J., Eisman, J. (1992) Assessment of spinal and femoral bone density by dual X-ray absorptiometry: comparison of Lunar and Hologic instruments. *J. Bone Miner Res.* **7**, 1081–1084.
62. Lai, K. C., Goodsitt, M. M., Murano, R., Chesnut, C. C. (1992) A comparison of two dual-energy X-ray absorptiometry systems for spinal bone mineral measurement. *Calcif. Tissue Int.* **50**, 203–208.
63. Genant, H. K., Grampp, S., Gluer, C. C., et al. (1994) Universal standardization for dual X-ray absorptiometry: patient and phantom cross-calibration results. *J. Bone Miner. Res.* **9**, 1503–1514.
64. Hanson, J. (1997) Standardization of femur BMD. *J. Bone Miner. Res.* **12**, 1316–1317.
65. Kalender, W. A. (1992) Effective dose values in bone mineral measurements by photon-absorptiometry and computed tomography. *Osteoporos. Int.* **2**, 82–87.
66. Kelly, T. L., Crane, G., Baran, D. T. (1994) Single X-ray absorptiometry of the forearm: precision, correlation, and reference data. *Calcif. Tissue Int.* **54**, 212–218.
67. Ruegsegger, P., Elsasser, U., Anliker, M., Gnehn, H., Kind, H., Prader, A. (1976) Quantification of bone mineralisation using computed tomography. *Radiology* **121**, 93–97.
68. Genant, H. K., Cann, C. E., Ettinger, B., Gorday, G. S. (1982) Quantitative computed tomography of vertebral spongiosa: a sensitive method for detecting early bone loss after oophorectomy. *Ann. Intern. Med.* **97**, 699–705.
69. Cann, C. E. and Genant, H. K. (1980) Precise measurement of vertebral mineral content using computed tomography. *J. Comput. Assist. Tomogr.* **4**, 493–500.
70. Genant, H. K., Block, J. E., Steiger, P., Gluer, C. (1987) Quantitative computed tomography in the assessment of osteoporosis, in *Osteoporosis Update 1987* (Genant, H. K., ed.), University of California Printing Services, San Francisco. pp. 49–72.
71. Laval-Jeantet, A. M., Roger, B., Bouysse, S., Bergot, C., Mazess, R. B. (1986) Influence of vertebral fat content on quantitative CT density. *Radiology* **159**, 463–466.
72. Reinbold, W., Adler, C. P., Kalender, W. A., Lente, R. (1991) Accuracy of vertebral mineral determination by dual-energy quantitative computed tomography. *Skeletal Radiol.* **20**, 25–29.

73. Dunnill, M. S., Anderson, J. A., Whitehead, R. (1967) Quantitative histological studies on age changes in bone. *J. Pathol. Bacteriol.* **94**, 274–291.
74. Genant, H. K. and Boyd, D. (1977) Quantitative bone mineral analysis using dual energy computed tomography. *Invest. Radiol.* **12**, 545–551.
75. Cann, C. E. (1987) Quantitative computed tomography for bone mineral analysis: technical considerations, in *Osteoporosis Update 1987* (Genant, H. K., ed.), University of California Printing Services, San Francisco, pp. 131–144.
76. Sartoris, D. J., Andre, M., Resnick, C., Resnick, D. (1986) Trabecular bone density in the proximal femur: quantitative CT assessment. *Radiology* **160**, 707–712.
77. Reiser, U. J. and Genant, H. K. (1984) Determination of bone mineral content in the femoral neck by quantitative computed tomography. 70th Scientific Assembly and Annual Meeting of the Radiological Society of North America, Washington, DC.
78. Gallagher, C., Golgar, D., Mahoney, P., McGill, J. (1985) Measurement of spine density in normal and osteoporotic subjects using computed tomography: relationship of spine density to fracture threshold and fracture index. *J. Comput. Assist. Tomogr.* **9**, 634–635.
79. Raymaker, J. A., Hoekstra, O., Van Putten, J., Kerkhoff, H., Duursma, S. A. (1986) Osteoporosis fracture prevalence and bone mineral mass measured with CT and DPA. *Skeletal Radiol.* **15**, 191–197.
80. Reinbold, W. D., Reiser, U. J., Harris, S. T., Ettinger, B., Genant, H. K. (1986) Measurement of bone mineral content in early postmenopausal and postmenopausal osteoporotic women. A comparison of methods. *Radiology* **160**, 469–478.
81. Sambrook, P. N., Bartlett, C., Evans, R., Hesp, R., Katz, D., Reeve, J. (1985) Measurement of lumbar spine bone mineral: a comparison of dual photon absorptiometry and computed tomography. *Br. J. Radiol.* **58**, 621–624.
82. Genant, H. K., Ettinger, B., Harris, S. T., Block, J. E., Steiger, P. (1988) Quantitative computed tomography in assessment of osteoporosis, in *Osteoporosis: Etiology, Diagnosis and Management*, (Riggs, B. L., Melton, L. J., eds.), Raven Press, New York, pp. 221–249.
83. Richardson, M. L., Genant, H. K., Cann, C. E., et al. (1985) Assessment of metabolic bone disease by quantitative computed tomography. *Clin. Orth. Rel. Res.* **195**, 224–238.
84. Gluer, C., Wu, C., Jergas, M., Goldstein, S., Genant, H. (1994) Three quantitative ultrasound parameters reflect bone structure. *Calcif. Tissue Int.* **55**, 46–52.
85. Nicholson, P., Haddaway, M., Davie, M. (1994) The dependence of ultrasonic properties on orientation in human vertebral bone. *Phys. Med. Biol.* **39**, 1013–1024.
86. Njeh, C. F., Boivin, C. M., Langton, C. M. (1997) The role of ultrasound in the assessment of osteoporosis: a review. *Osteoporos. Int.* **7**, 7–22.
87. Hans, D., Dargent-Molina, P., Schott, A. M., et al. (1996) Ultrasonographic heel measurements to predict hip fracture in elderly women: the EPIDOS prospective study. *Lancet* **348**, 511–514.
88. Bauer, D. C., Gluer, C. C., Cauley, J. A., et al. (1997) Bone ultrasound predicts fractures strongly and independently of densitometry in older women: a prospective study. *Arch. Intern. Med.* **157**, 629–634.
89. Njeh, C. F., Hans, D., Li, J., et al. (2000) Comparison of six calcaneal quantitative ultrasound devices: precision and hip fracture discrimination. *Osteoporos. Int.* **11**, 1051–1062.

3

Skeletal Anatomy in Densitometry

CONTENTS

THE SPINE IN DENSITOMETRY
VERTEBRAL ANATOMY
ARTIFACTS IN PA OR AP SPINE DENSITOMETRY
THE SPINE IN THE LATERAL PROJECTION
THE PROXIMAL FEMUR IN DENSITOMETRY
PROXIMAL FEMUR ANATOMY
EFFECT OF ROTATION ON BMD IN THE PROXIMAL FEMUR
EFFECT OF LEG DOMINANCE ON BMD IN THE PROXIMAL FEMUR
EFFECT OF SCOLIOSIS, OSTEOARTHRITIS, OSTEOPHYTES, SURGERY, AND FRACTURE ON BMD IN THE PROXIMAL FEMUR
THE FOREARM IN DENSITOMETRY
NOMENCLATURE
EFFECT OF ARM DOMINANCE ON FOREARM BMD
EFFECT OF ARTIFACTS ON BMD IN THE FOREARM
THE METACARPALS, PHALANGES, AND CALCANEUS
REFERENCES

THE SPINE IN DENSITOMETRY

Studies of the lumbar spine performed with dual-photon absorptiometry (DPA) or dual-energy X-ray absorptiometry (DXA) are generally acquired by the passage of photon energy from the posterior to anterior direction. They are properly characterized as posteroanterior (PA) spine studies. Nevertheless, these studies are often called anterior-posterior (AP) spine studies, probably because plain films of the lumbar spine are acquired in the AP projection. The GE Lunar Expert[®], a fan-array scanner, actually does acquire lumbar spine bone density images in the AP direction. Compared to

plain radiography, however, the beam direction in a DXA study of the spine has less influence on the appearance of the image and little, if any, influence on the measured bone mineral content (BMC) or bone mineral density (BMD). Studies of the lumbar spine may also be acquired in the lateral projection using DXA. Such studies may be performed with the patient in the supine or left lateral decubitus position, depending on the type of DXA unit employed.

Vertebral Anatomy

The whole vertebra can be divided into two major components: the body and the posterior elements. The posterior elements consist of the pedicles, the lamina, the spinous process, the transverse processes, and the inferior and superior articulating surfaces. The appearance of the image of the spine on an AP or PA spine study is predominantly determined by the relative density of the various elements that make up the entire vertebra. Figure 3-1A is a photograph of a posterior view of the lumbar spine with the intervertebral discs removed. Figure 3-1B and 3-1C demonstrate the appearance of the spine as first the transverse processes and then the vertebral bodies are removed from the photograph. What remains in Figure 3-1C is characteristic of the appearance of the lumbar spine on a PA DXA lumbar spine study and consists largely of the posterior elements. The posterior elements form the basis of the DXA lumbar spine image seen in Fig. 3-2. The transverse processes are eliminated from the scan field and the vertebral bodies are not well seen because they are both behind and equally or less dense than the posterior elements. In a study of 34 lumbar vertebrae taken from 10 individuals aged 61–88, the average mineral content of the posterior elements was 47% of the mineral content of the entire vertebra (1).

The unique shapes of the posterior elements of the various lumbar vertebrae can be used as an aid in identifying the lumbar vertebrae. The posterior elements of L1, L2, and L3 have a U- or Y-shaped appearance. L4 can be described as looking like a block H or X. L5 has the appearance of a block I on its side. Figure 3-3 is a graphic illustration of these shapes. Compare these shapes to the actual posterior elements seen in Fig. 3-1C and the DXA lumbar spine study shown in Fig. 3-2. Although the transverse processes are generally not seen on a spine bone density study, the processes at L3 will sometimes be partially visible, because this vertebra tends to have the largest transverse processes. This fact can also be helpful in lumbar vertebral identification. Figure 3-4 is the spine image only

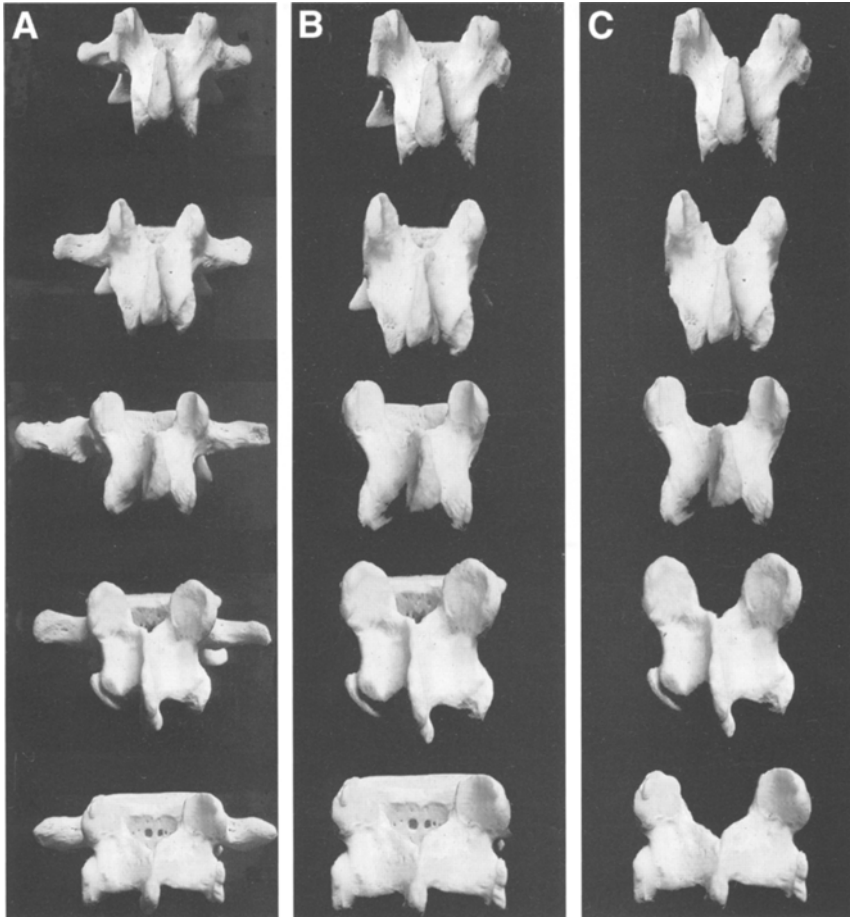


Fig. 3-1. Lumbar spine in the posterior view. (A) Intact vertebrae; (B) the transverse processes have been removed; (C) The vertebral bodies have been removed, leaving only the posterior elements. (Adapted with permission from *Colour Atlas of Human Anatomy*, [1993] 3rd edition, p. 83.)

from the study shown in Fig. 3-2. In Fig. 3-4B, the shapes of the posterior elements have been outlined for emphasis.

On PA or AP DXA lumbar spine studies, L1 through L4 are quantified. Although L5 can be seen, it is not usually quantified because of potential interference from the pelvis. In fact, even if labeled on the scan, some software programs will not analyze L5 unless it is deliberately mislabeled L4. L1 frequently has the lowest BMC and BMD of the first four lumbar vertebrae. In a study of 148 normal women aged 50–60, Peel et al. (2) found

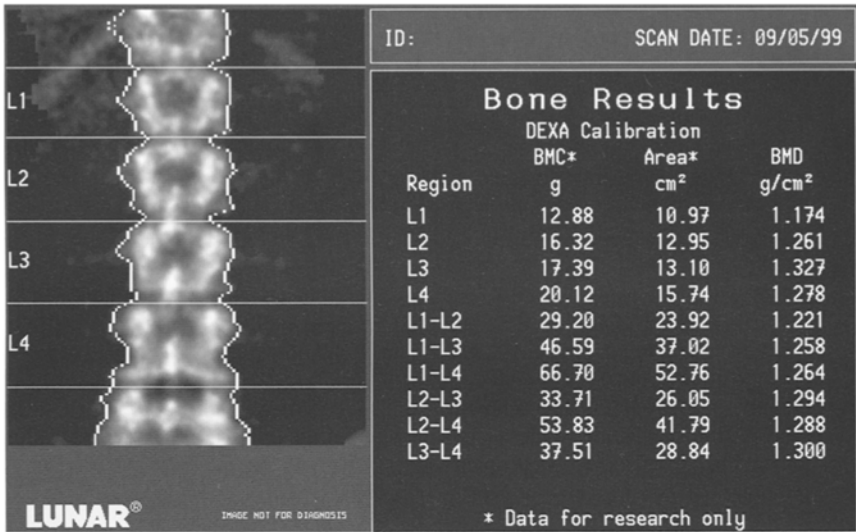


Fig. 3-2. DXA PA spine study acquired on the GE Lunar DPX. The shapes of the vertebrae in this image are primarily created by the posterior elements. The shapes in this study are classic. The expected increase in bone mineral content and area is also seen from L1 to L4. The increase in bone mineral density from L1 to L3, with a decline from L3 to L4, is also typical.

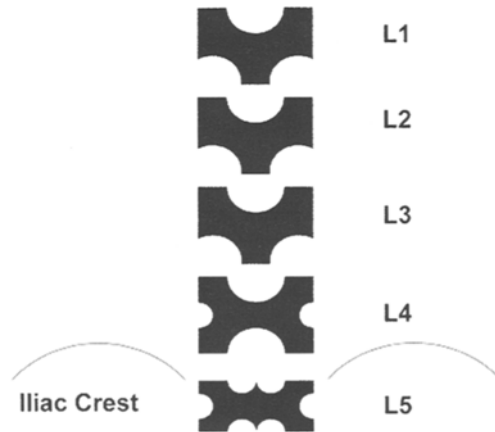


Fig. 3-3. Graphic illustration of the characteristic shapes of the lumbar vertebrae as seen on a dual-energy X-ray absorptiometry posteroanterior spine study.

that the BMC increased between L1-L2, L2-L3 and L3-L4, although the increase between L3-L4 was roughly half that seen at the other levels, as shown in Table 3-1. BMD increased between L1-L2 and L2-L3 but

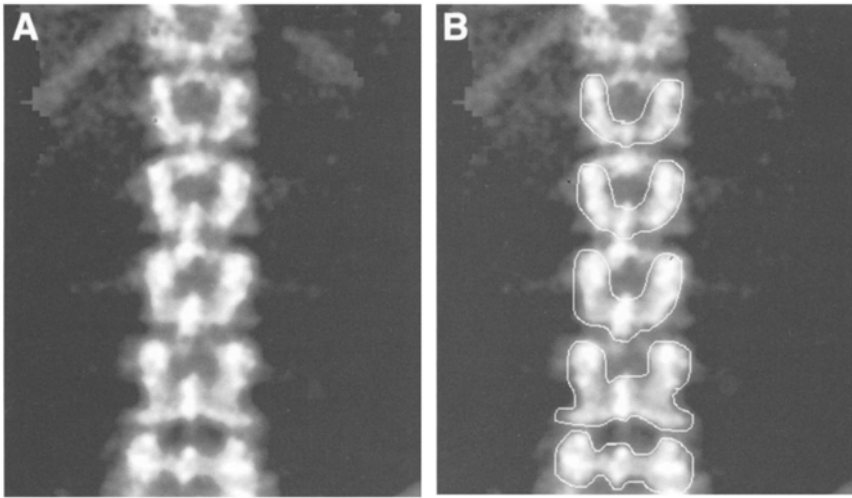


Fig. 3-4. (A) Dual-energy X-ray absorptiometry posteroanterior spine image acquired on the GE Lunar DPX. This is the spine image from the study shown in Fig. 3-2, with the intervertebral disk markers and bone-edge markers removed for clarity. (B) The shapes have been outlined for emphasis.

showed no significant change between L3–L4. The average change between L3–L4 was actually a decline of 0.004 g/cm^2 . The largest increase in BMD occurred between L1–L2. The apparent discrepancies in the magnitude of the change in BMC and BMD between the vertebrae are the result of the progressive increase in area of the vertebrae from L1 to L4. The DXA PA lumbar spine study shown in Fig. 3-2 illustrates the progressive increase in BMC and area from L1 to L4 and the expected pattern of change in BMD between the vertebral levels.

Studies from both Peel et al. (2) and Bornstein and Peterson (3) suggest that the majority of individuals have five lumbar vertebrae with the lowest set of ribs on T12. Bornstein and Peterson (3) found that only 17% of 1239 skeletons demonstrated a pattern of vertebral segmentation and rib placement other than five lumbar vertebrae with the lowest ribs on T12. Similarly, Peel et al. (2) found something other than the expected pattern of five lumbar vertebrae with the lowest ribs on T12 in only 16.5% of 375 women. An additional 7.2% had five lumbar vertebrae but had the lowest level of ribs on T11. Therefore, 90.7% of the women in this study had five lumbar vertebrae. Only 1.9% (or 7) women had six lumbar vertebrae. In three of these women ribs were seen on L1. This was the only circumstance in which ribs were seen on L1. Of the entire group, 7.5% had only

Table 3-1
Incremental Change in Bone Mineral Content (BMC) and Bone Mineral Density (BMD) Between Adjacent Vertebrae in 148 Normal Women Ages 50–60 as Measured by Dual X-Ray Absorptiometry

<i>Vertebrae</i>	<i>Increase in BMC (g)</i>	<i>Increase in BMC (%)</i>	<i>Increase in BMD (g/cm²)</i>	<i>Increase in BMD (%)</i>
L1–L2	2.07	13.7	0.090	7.9
L2–L3	2.43	14.8	0.050	4.3
L3–L4	1.13	5.0	–0.004 ^a	–0.8 ^a

^aNot statistically significant.

Reprinted with permission from the *J. Bone Miner. Res.* 1993;8:719–723.

Table 3-2
Percentage of Women With Various Combinations of Numbers of Lumbar Vertebrae and Position of Lowest Ribs

<i>No. of lumbar vertebrae</i>	<i>Position of lowest ribs</i>	<i>Women (%)</i>
5	T12	83.5
5	T11	7.2
4	T12	2.1
4	T11	5.3
6	T12	1.1
6	L1	0.8

Reprinted with permission from the *J. Bone Miner. Res.* 1993;8:719–723.

four lumbar vertebrae. In the majority of cases here, the lowest ribs were seen on T11. Table 3-2 summarizes these findings.

Knowledge of the frequency of anomalous vertebral segmentation, the characteristic shapes created by the posterior lumbar elements on a PA lumbar spine study, and the expected incremental change in BMC and BMD can be used to label the vertebrae correctly. If the vertebrae are mislabeled, comparisons to the normative databases will be misleading. The expected effect of mislabeling T12 as L1 is a lowering of the BMC or BMD at L1, which would then compare less favorably to the reference values for L1. The BMC and BMD averages for L1–L4 or L2–L4 would also be lowered. The degree to which BMC is lowered by mislabeling is substantially greater than BMD as shown in Table 3-3 (2). The assumption that the lowest set of ribs is found at level T12 is often used as the basis for label-

Table 3-3
Effect of Mislabeling T12 as L1 on Bone Mineral Content
and Bone Mineral Density in AP DXA Spine Measurements

<i>Measurement</i>	<i>Difference</i>	<i>Mean %</i>
BMC		
L1	1.61 g	11.5%
L2-L4	3.47 g	8.4%
L1-L4	4.8 g	8.4%
BMD		
L2-L4	0.035 g/cm ²	3.6%
L1-L4	0.039 g/cm ²	3.5%

Reprinted with permission from the *J. Bone Miner. Res.* 1993;8:719-723.

ing the lumbar vertebrae. As can be seen from Table 3-2, this assumption would result in the vertebrae being labeled incorrectly in 13.3% of the population. As a consequence, all of the criteria noted above should be employed in determining the correct labeling of the lumbar vertebrae. This should obviate the need for plain films for the sole purpose of labeling the vertebrae in the vast majority of instances. Figure 3-5 is a PA spine study in which the labeling of the lumbar vertebra was not straightforward. The characteristic shapes of the vertebrae are easily seen, but no ribs appear to be projecting from what should be T12. Note the block H shape of the vertebra labeled L4 and the visible transverse processes on the vertebra labeled L3. Statistically, it is likely that there are five lumbar vertebrae here with the lowest set of ribs on T11. The appearance of L3 and L4 would also support this labeling. Plain films, acquired for the purpose of diagnosing spine fracture, confirmed that the labeling shown in Fig. 3-5 is correct.

Artifacts in PA or AP Spine Densitometry

The PA lumbar spine has been, and continues to be, used extensively in densitometry for diagnosis, fracture prediction and monitoring. Unfortunately, it is also the skeletal site most often affected by structural changes and artifacts that may limit its utility.

VERTEBRAL FRACTURES

The BMD of a fractured vertebra will be increased because of the fracture itself. This increase in density could erroneously lead the physician

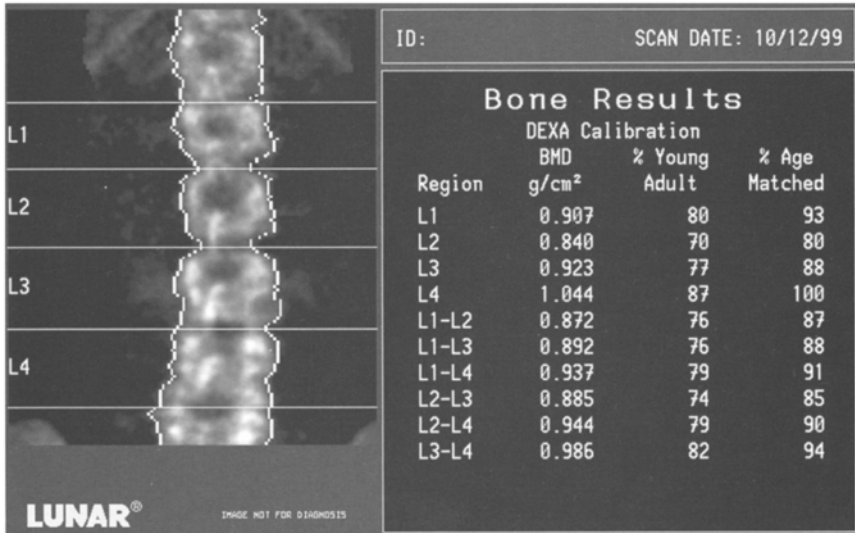


Fig. 3-5. Dual-energy X-ray absorptiometry posteroanterior spine study acquired on the GE Lunar DPX. The vertebra labeled L4 has a classic block H or X shape. However, no ribs are seen protruding from the vertebra that should be T12. It is far more likely that this represents five lumbar vertebrae with the lowest ribs on T11 than six lumbar vertebrae with the lowest ribs on T12. Also note that the BMD at L1 is higher than at L2, which is unusual. A lateral lumbar spine X-ray of this patient, shown in Fig. 3-7, confirmed a fracture at L1.

to conclude that the bone strength is better and that risk for fracture is lower than is the case. Vertebral fractures in osteoporosis frequently occur in the T7–T9 region and in the T12–L2 region (4,5). Because DXA measurements of the lumbar spine are often employed in patients with osteoporosis, osteoporotic fractures in the lumbar spine, particularly at L1 and L2, are a common problem, rendering the measurement of BMD inaccurate if the fractured vertebrae are included. An increased precision error would also be expected if the fractured vertebrae were included in BMD measurements performed as part of a serial evaluation of BMD. Although a fractured lumbar vertebra can be excluded from consideration in the analysis of the data, this reduces the maximum number of contiguous vertebrae in the lumbar spine available for analysis. For reasons of statistical accuracy and precision, the BMD for three or four contiguous vertebrae is preferred over two-vertebrae averages or the BMD of a single vertebra. Figure 3-6 illustrates a PA lumbar spine study in which a fracture was apparent at L3. Although the BMD at L3

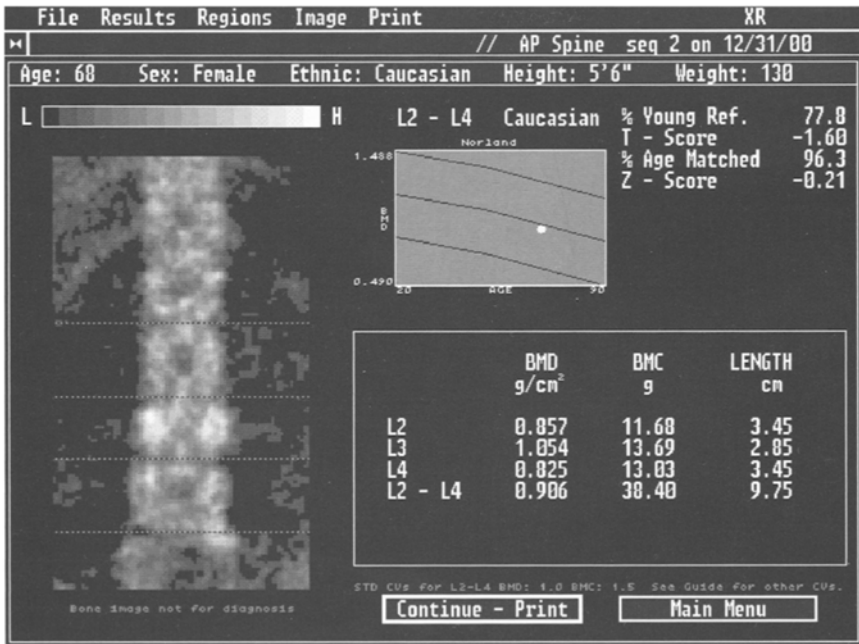


Fig. 3-6. Dual-energy X-ray absorptiometry posteroanterior spine study acquired on the Norland XR-36. The image suggests a loss of vertebral height and increased sclerosis at L3. Although the BMD at L3 is expected to be higher than at L2, the BMD at L3 here is markedly higher. These findings suggest a fracture at this level but this must be confirmed. In any case, the L2–L4 BMD will be increased by this structural change. (Case courtesy of CooperSurgical Norland, Trumbull, CT.)

is expected to be higher than either L2 or L4, it is disproportionately higher. The L2–L4 BMD will be increased because of the effect of the fracture on the BMD at L3. In the DXA PA lumbar spine study shown in Fig. 3-5, the image does not readily suggest a fracture. The BMD at L1, however, is higher than the BMD at L2, which is unusual. A plain lateral film of the lumbar spine of this patient, shown in Fig. 3-7, confirmed a fracture at L1.

Other structural changes within the spine can affect BMD measurements. Osteophytes and facet sclerosis can increase the BMD when measured in the AP or PA projection. Aortic calcification will also potentially affect the BMD when measured in the AP or PA spine because the X-ray beam will detect the calcium in the aorta as it passes through the body on an anterior to posterior or posterior to anterior path. It is therefore useful to note how often these types of changes are expected in the general population and the

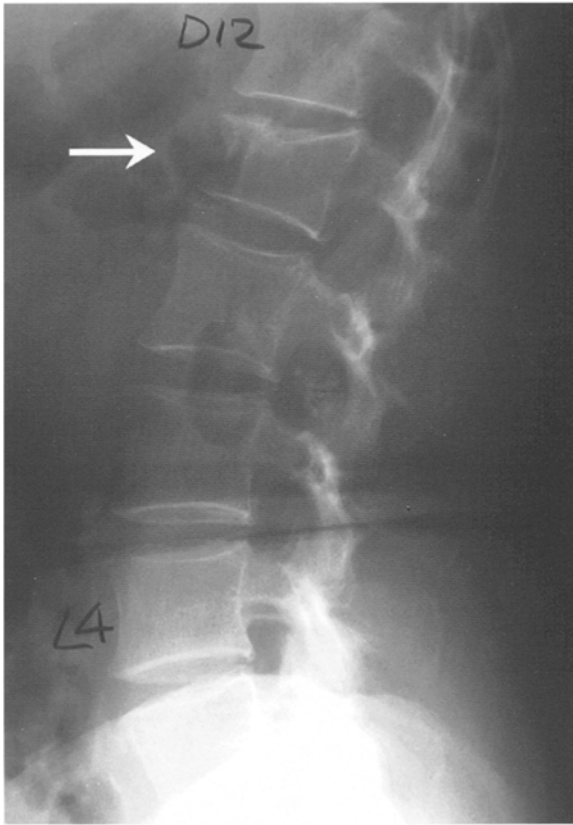


Fig. 3-7. Lateral lumbar spine X-ray of the patient whose dual-energy X-ray absorptiometry study is shown in Fig. 3-5. A fracture at L1 is indicated by the arrow.

potential magnitude of the effect these changes may have on the measured BMD in the lumbar spine.

EFFECT OF OSTEOPHYTES ON BMD

In 1982, Krolner et al. (6) observed that osteophytes caused a statistically significant increase in the BMD in the AP spine when compared to controls without osteophytes. More recently, Rand et al. (7) evaluated a population of 144 postmenopausal women aged 40–84 years, with an average age of 63.3 years, for the presence of osteophytes, scoliosis, and aortic calcification. These were generally healthy women referred for evaluation of BMD because of suspected postmenopausal osteoporosis. Table 3-4 lists the percentages of these women found to have these types of degenerative changes. Based on these findings, Rand et al. estimated

Table 3-4
Frequency of Specific Types of Degenerative Changes in the
Spines of 144 Women Aged 40–84

<i>Type of degenerative change</i>	<i>% with change (n)</i>
Osteophytes	45.8 (66)
Osteochondrosis	21.5 (31)
Vascular calcification	24.3 (35)
Scoliosis	22.2 (32)
Any type	59.0 (72)

Adapted with permission from *Calcif. Tissue Int.* 1997;60:430–433.

the likelihood of degenerative changes in the spine as being less than 10% in women under the age of 50. In 55-year-old women, however, the likelihood jumped to 40%, and in 70-year-old women, to 85%. Of these types of degenerative changes, however, only the presence of osteophytes significantly increased the BMD. The magnitude of the increase caused by the osteophytes ranged from 9.5% at L4 to 13.9% at L1. Cann et al. (8) also estimated the increase in BMD from osteophytes in the spine at 11%. In 1997, Liu et al. (9) studied 120 men and 314 women, aged 60–99 years. Lumbar spine osteophytes were found in 75% of the men and 61.1% of the women. The effect of osteophytes on the BMD was sufficiently great to cause 50% of the men and 25% of the women with osteopenia to be misdiagnosed. About 20% of the men and 10% of the women with osteoporosis were misdiagnosed because of the effect of osteophytes on the BMD. In Fig. 3-8 osteophytes are clearly visible at L2 on the lateral lumbar radiograph. The appearance of this region on the DXA PA lumbar spine study in Fig. 3-9 suggests a sclerotic process at this level. Osteophytes and end-plate sclerosis are also seen on the plain film in Fig. 3-10. The effect on the DXA image of the lumbar spine, shown in Fig. 3-11 is dramatic. There is also a disproportionate increase in the BMD at L2 and L3 compared to L1 and L4.

EFFECT OF AORTIC CALCIFICATION ON BMD

Although it did not significantly increase BMD, vascular calcification was seen in 24.3% of the 144 postmenopausal women studied by Rand et al. (7). In a study of aortic calcification in 200 women aged 50 or older by Frye et al. (10), the percentage of women with aortic calcification and the effect on BMD measured in the PA lumbar spine was noted. A grading system for both linear calcifications and calcified plaques was applied to lateral

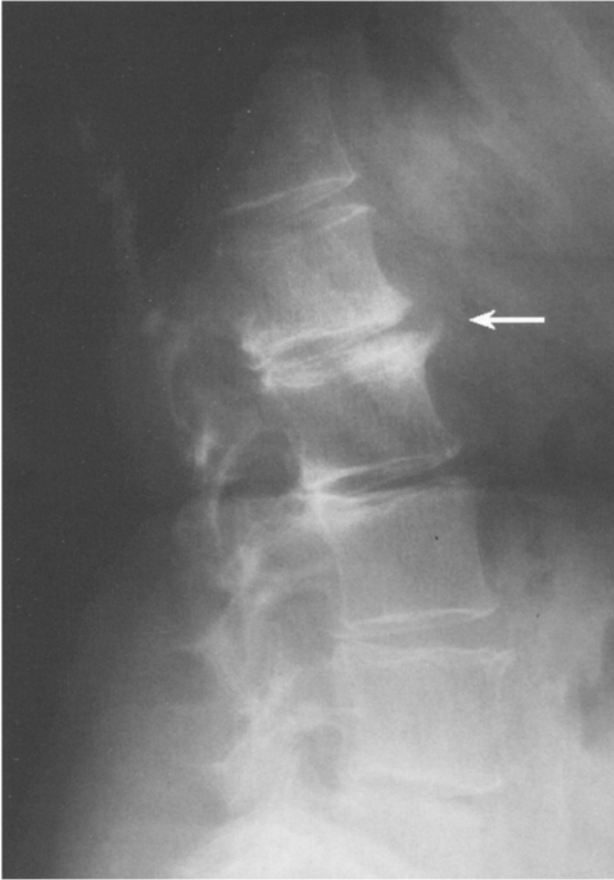


Fig. 3-8. Lateral lumbar spine X-ray of the patient whose dual-energy X-ray absorptiometry study is shown in Fig. 3-9. The arrow indicates a region of endplate sclerosis and osteophyte formation.

spine films with a grade of 0 indicating neither type of calcification and a grade of 2 indicating the most severe degree. The percentage of women with any degree of aortic calcification and severe calcification is shown in Fig. 3-12. The percentage with any degree of aortic calcification was extremely low under age 60 but increased dramatically in women aged 60 and older. The percentage of women with severe aortic calcification, however, remained low throughout the 50s, 60s, and 70s. Even in women aged 80 and older, the percentage did not exceed 30%. Table 3-5 summarizes the effect of any degree of aortic calcification and severe aortic calcification on BMD in women. Neither effect was statistically significant.

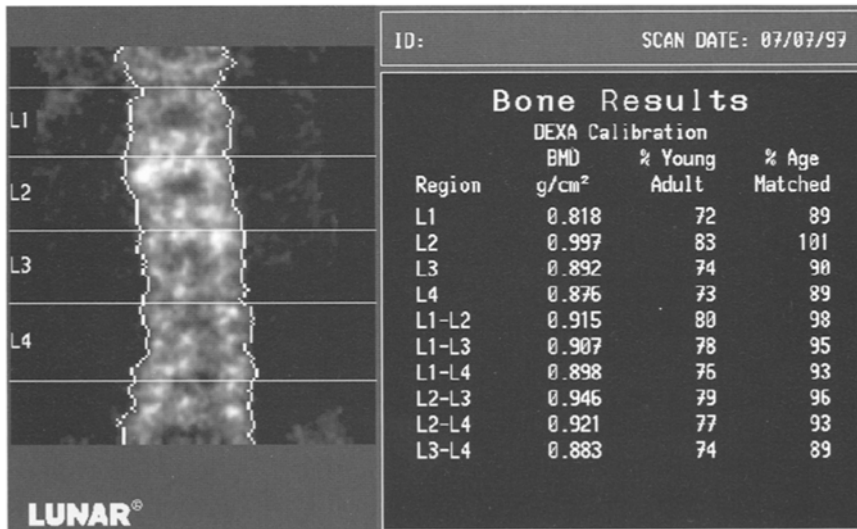


Fig. 3-9. DXA PA spine study acquired on the GE Lunar DPX. A sclerotic process is suggested at L2 by the image. The bone mineral density is also increased more than expected in comparison to L1 and is higher than L3, which is unusual. These findings are compatible with the endplate sclerosis and osteophytes seen in Fig. 3-8.

These findings are similar to those of Frohn et al. (11), Orwoll et al. (12), Reid et al. (13), Banks et al. (14), and Drinka et al. (15), in which no significant effect of aortic calcification was seen on the BMD measured in the PA spine. The studies from Orwoll et al. (12) and Drinka et al. (15) were performed in men. A recent ex vivo study from Cherney et al. (16) quantified the effect of removal of the aorta on PA lumbar spine bone density. After choosing eight cadavers at random, PA lumbar spine DXA bone density studies were performed before and after the removal of the aorta. The age at death ranged from 67 to 87 years, with an average age of 79 years. Removal of the aorta resulted in an average decrease in PA lumbar spine BMD of 4.64%. The authors do not describe the severity of any observed aortic calcification. Nevertheless, their results are in keeping with those from Frye et al. (10), in which a small effect on lumbar spine bone density was observed with severe aortic calcification.

Aortic calcification is not easily seen on most DXA PA lumbar spine studies. In Fig. 3-13A, however, the faint outline of the calcified aorta is visible. The aorta is easily seen on the lateral DXA image in Fig. 3-13B. Figure 3-14 shows both studies. In this case, the effects of the calcified aorta on the BMD measurement can be eliminated on the DXA lateral spine study.



Fig. 3-10. Lateral lumbar spine X-ray of the patient whose dual-energy X-ray absorptiometry study is shown in Fig. 3-11. The arrow indicates a region of marked endplate sclerosis.

EFFECT OF FACET SCLEROSIS ON BMD

Unlike aortic calcification, facet sclerosis can have a profound effect on the measured BMD in the AP or PA projection. In the study by Drinka et al. (15) noted earlier, 113 elderly men were evaluated with standard AP and lateral lumbar spine films and DPA of the lumbar spine. A grading system for facet sclerosis was developed with a grade of 0 indicating no sclerosis and a grade of 3 indicating marked sclerosis. As shown in Table 3-6, grade 1 sclerosis had no significant effect on the BMD. Grades 2 and 3, however, markedly increased the BMD at the vertebral levels at which the facet sclerosis was found. Figure 3-15 is a PA spine BMD study in which facet sclerosis is suggested at L3 by the appearance of the image. The BMD values at L3 and L4 are also markedly higher than expected based on the values at L1 and L2. The plain film of this patient shown in Fig. 3-16 confirms facet sclerosis at the lower lumbar levels.

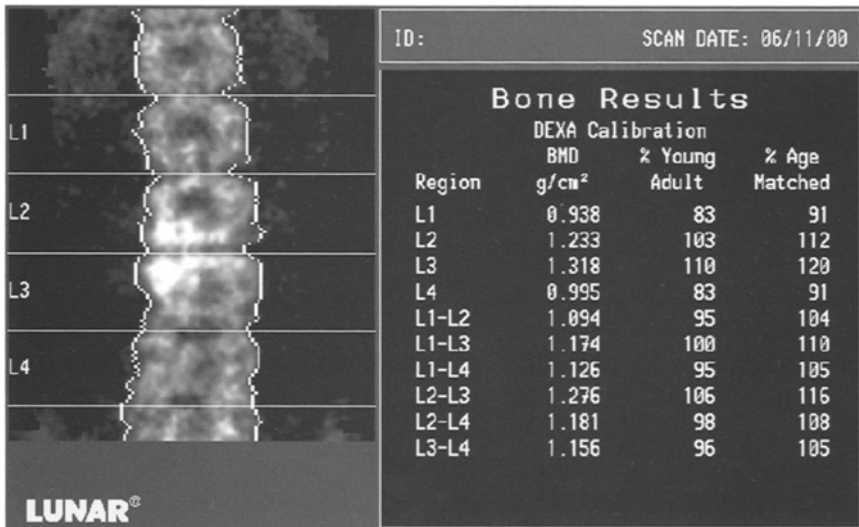


Fig. 3-11. Dual-energy X-ray absorptiometry spine study acquired on the GE Lunar DPX. The image dramatically suggests the sclerotic process seen on the X-ray in Fig. 3-10. There is a marked increase in the bone mineral density at L2 and L3 compared to L1 and L4.

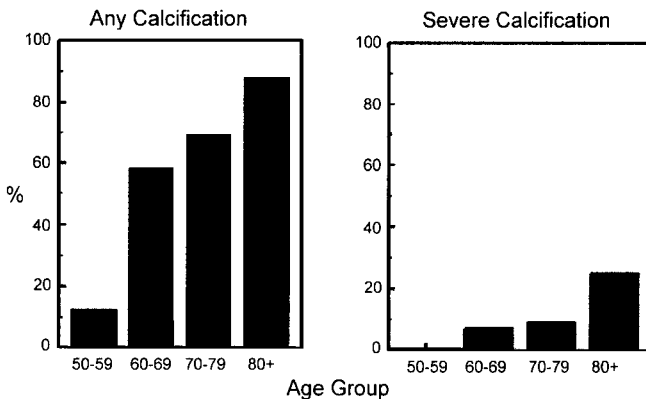


Fig. 3-12. The prevalence of aortic calcification in women aged 50 and over. (Reprinted with permission from *Bone Miner.* 19;185-194.

EFFECT OF VERTEBRAL ROTATION ON PA LUMBAR SPINE BONE DENSITY

Rotation of the vertebral bodies is often a component of idiopathic scoliosis, although it is not frequently seen in adult-onset degenerative scoliosis. To study the effect of vertebral body rotation on bone density measured in the lumbar spine with DXA, Girardi and colleagues (17)

Table 3-5
Effect of Aortic Calcification on Bone Mineral Density in Spine

Site	BMD			
	Observed	Expected	Difference	Expected (%)
BMD spine				
Any Grade 1 or 2	0.93	0.92	0.01	101.4
Any Grade 2	0.94	0.89	0.05	106.7

Adapted with permission from *Bone Min.* 1992;19:185-194.

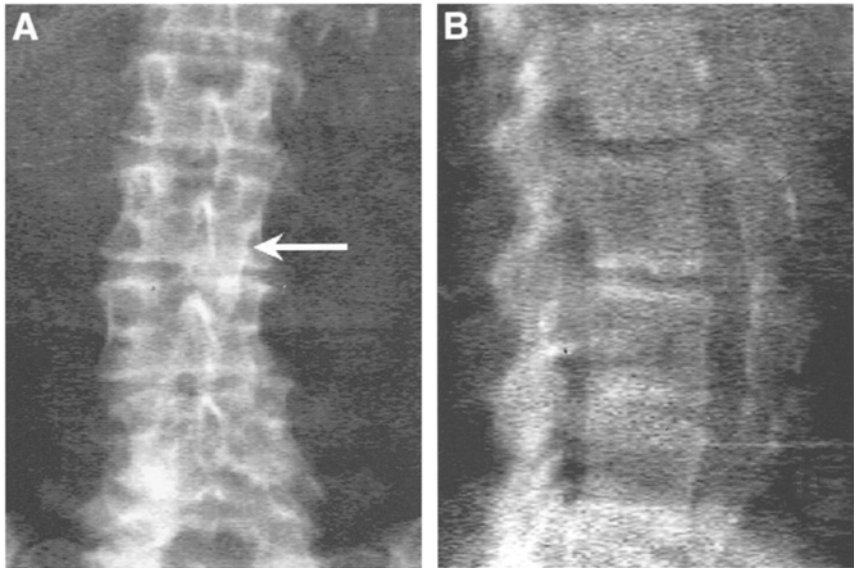


Fig. 3-13. Posteroanterior and lateral dual-energy X-ray absorptiometry lumbar spine images acquired on the Hologic QDR-4500. The arrow seen in (A) indicates the faint outline of the calcified aorta that is easily seen on the lateral study in (B). (Case courtesy of Hologic, Inc., Bedford, MA.)

used a cadaveric spine with intact soft tissue. The spine, which spanned the ninth thoracic vertebra to the sacrum, was mounted at both ends in the neutral midline position. Calibration markings on the mounts allowed for the spine to be rotated in 10° increments to a maximum of 60° in either direction. The bone density of L1 through L4 was measured with DXA in duplicate in the neutral position and at each 10° increment in both directions.

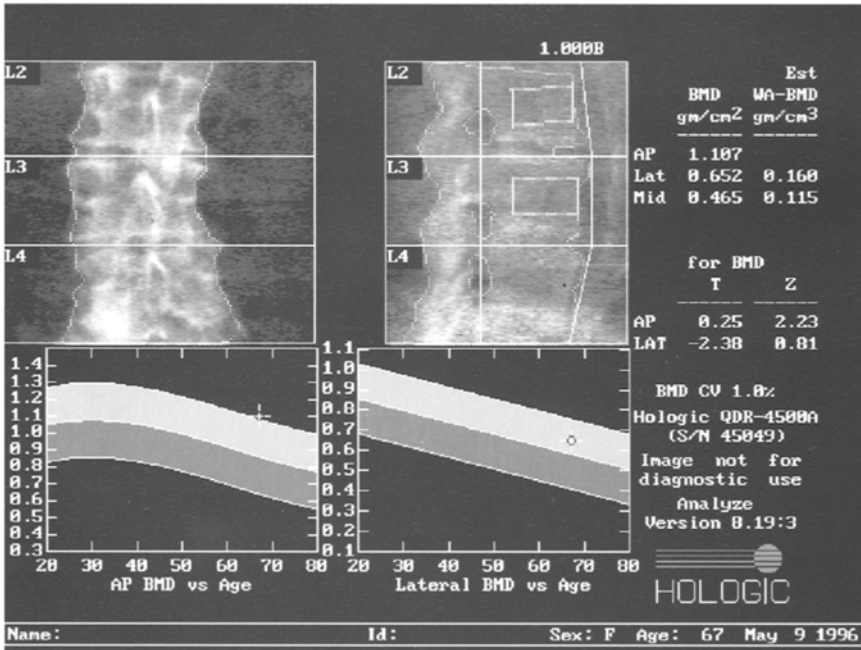


Fig. 3-14. Dual-energy X-ray absorptiometry posteroanterior and lateral lumbar spine study acquired on the Hologic QDR-4500. These are the analyzed studies for the images shown in Fig. 3-13. (Case courtesy of Hologic, Inc., Bedford, MA.)

Table 3-6
 Increase in Bone Mineral Density From Facet Sclerosis

	Grade 2	Grade 3
L1	0.275	0.465
L2	0.312	0.472
L3	0.184	0.343
L4	0.034	0.247
Average	0.201	0.382

Values are in gm/cm².

Adapted with permission from *Calcif. Tissue Int.* 1992;50:507-510.

The vertebral segment area increased with increasing rotation up to 50° in either direction from midline and then decreased between 50° and 60°. The BMC remained relatively constant throughout rotation except at the extreme of 60° on either side of the midline at which point it decreased.

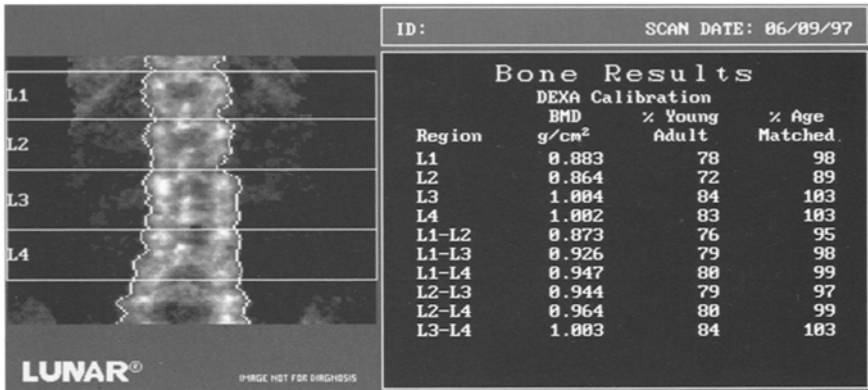


Fig. 3-15. Dual-energy X-ray absorptiometry posteroanterior lumbar spine study acquired on the GE Lunar DPX. There is a marked increase in the bone mineral density between L2 and L3, which is maintained at L4. The image faintly suggests sclerosis in the region of the facet joints at L3 and L4. This is more dramatically seen in the plain film of this patient shown in Fig. 3-16.

Because BMD is determined by dividing the BMC by the area, the increasing area with rotation resulted in BMD decreasing with rotation to either side of the midline. From neutral to 60°, the decrease in BMD was almost 20%. In clinical practice then, rotation of the spine for any reason, should be expected to cause an apparent decrease in bone density when measured with DXA.

OTHER CAUSES OF ARTIFACTS IN PA AND AP LUMBAR SPINE STUDIES

Potential causes of apparent increases in the BMD in the AP or PA lumbar spine have been identified by Stutzman et al. (18). These include pancreatic calcifications, renal stones, gall stones, contrast agents, and ingested calcium tablets in addition to osteophytes, aortic calcification, and fractures. Figures 3-17 to 3-19 illustrate other structural changes in the spine that will affect the BMD measured in the PA projection.

The Spine in the Lateral Projection

The effect on BMD measured in the AP or PA projection from aortic calcification, facet sclerosis, osteophytes and other degenerative changes in the spine can be nullified by quantifying the bone density of the spine in the lateral projection, as shown in Fig. 3-13B. In addition, the highly

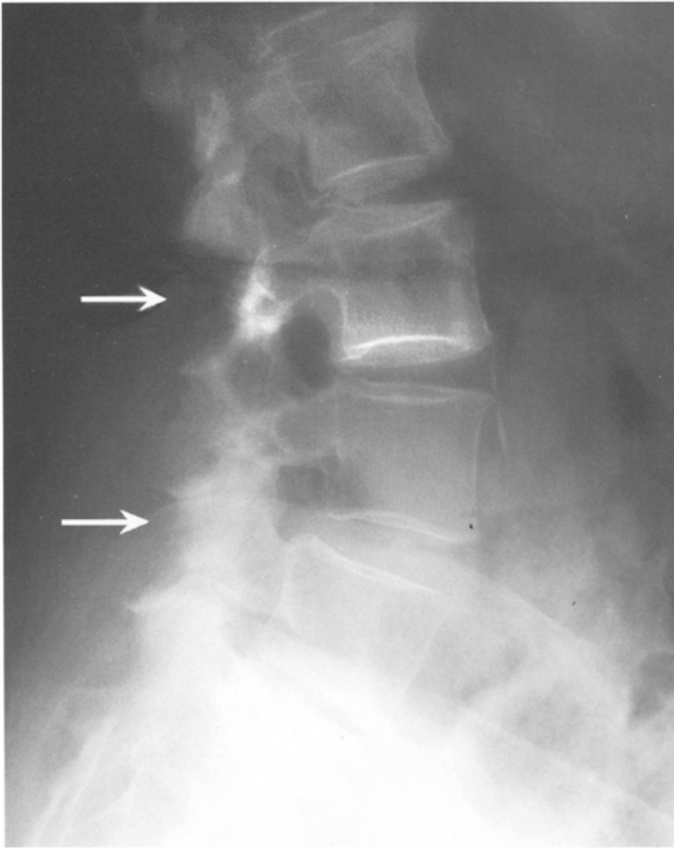


Fig. 3-16. Lateral lumbar spine X-ray of the patient whose bone density study is shown in Fig. 3-15. The arrows indicate sclerotic regions in the posterior elements.

cortical posterior elements and a portion of the cortical shell of the vertebral body can be eliminated from the measurement, resulting in a more trabecular measure of bone density in the spine. The measurement is not a 100% trabecular measure, because portions of the cortical vertebral body shell will still be included in the measurement. In addition to the elimination of artifact or confounding degenerative changes, the lateral spine BMD measurement is desirable in those circumstances in which a trabecular measure of bone density is indicated, and particularly in circumstances in which changes in trabecular bone are being followed over time. The higher metabolic rate of trabecular bone compared to cortical bone should result in a much larger magnitude of change in this more trabecular

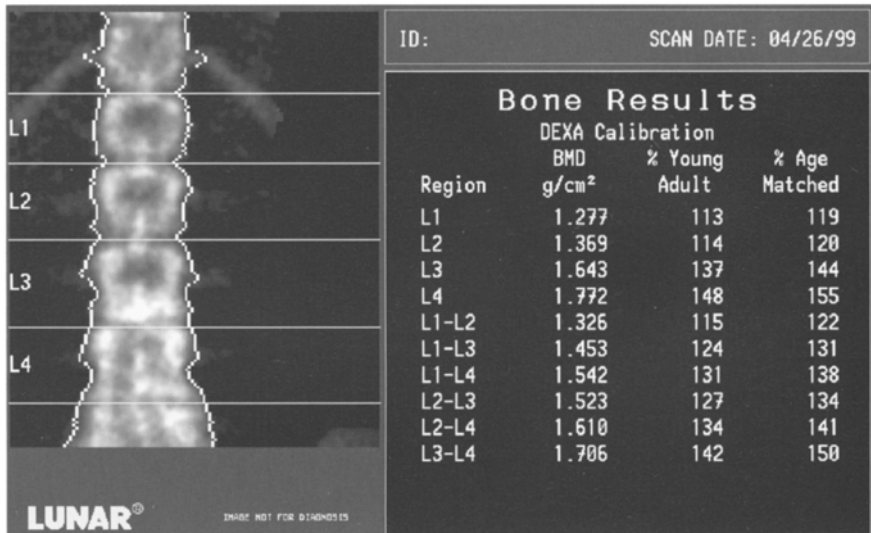


Fig. 3-17. Dual-energy X-ray absorptiometry posteroanterior lumbar spine study acquired on the GE Lunar DPX. The image suggests increased density at L3 and L4, but there is also a linear vertical lucency over L4. The bone mineral density (BMD) values are markedly increased at L3 and L4. This patient had previously undergone an L3–L4, L4–L5 interbody fusion and laminectomy at L4. Although the laminectomy alone would decrease the BMD at L4, the fusion mass has increased the BMD at L3 and L4 dramatically.

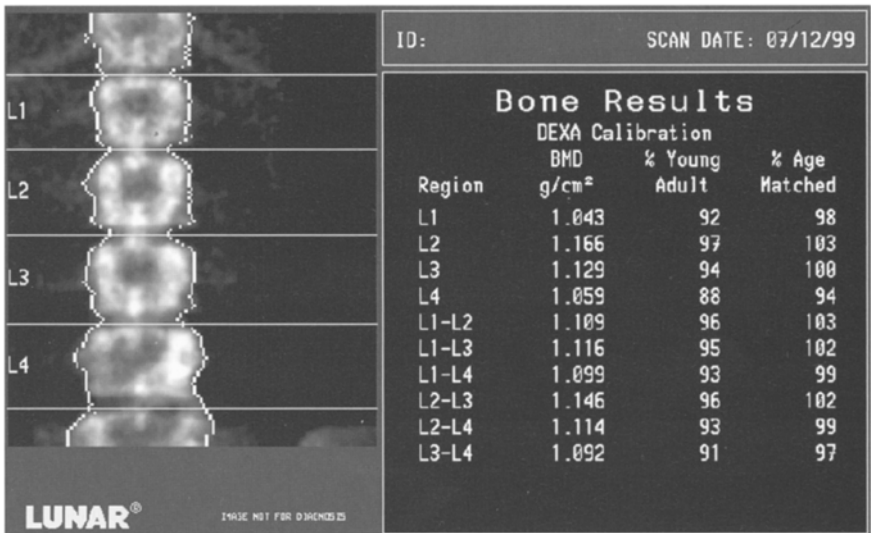


Fig. 3-18. Dual-energy X-ray absorptiometry posteroanterior spine study acquired on the GE Lunar DPX. The image is unusual at L4, with what appears to be an absence of part of the posterior elements. This was confirmed with plain films. This should decrease the bone mineral density at L4.

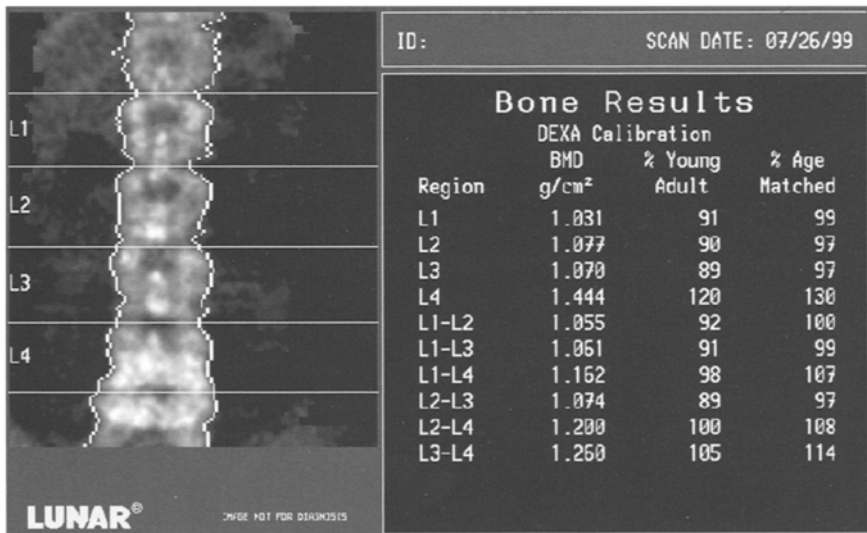


Fig. 3-19. Dual-energy X-ray absorptiometry posteroanterior spine study acquired on the GE Lunar DPX. The image suggests a marked sclerotic reaction at L4 and L5. There is also a marked increase in the bone mineral density at L4, compared to L3. This sclerotic process was thought to be the result of an episode of childhood discitis. The patient was asymptomatic.

measure of bone density compared to the mixed cortical-trabecular measure of bone density in the PA spine.

Vertebral identification in the lateral projection can be difficult. The lumbar vertebrae are generally identified by the relative position of the overlapping pelvis and the position of the lowest set of ribs. The position of the pelvis tends to differ, however, when the study is performed in the left lateral decubitus position compared to the supine position. Rupich et al. (19) found that the pelvis overlapped L4 in only 15% of individuals when studied in the supine position. Jergas et al. (20) reported a figure of 19.7% for L4 overlap for individuals studied in the supine position. In DXA studies performed in the left lateral decubitus position, pelvic overlap of L4 occurred in 88% of individuals in the study by Peel et al. (2). In the other 12%, the pelvis overlapped L5 in 5%, and the L3-L4 disc space, or L3 itself, in 7%. Consequently, although the position of the pelvis tends to identify L4 in most individuals scanned in the left lateral decubitus position, it also eliminates the ability to accurately measure the BMD at L4 in those individuals. The ribs are less useful than the pelvis in identifying the lumbar vertebrae. Rib overlap of L1 can be expected in the majority of individuals, whether they are studied in the supine or left

lateral decubitus position (2). This may not be seen, however, in the 12.5% of individuals whose lowest set of ribs in on T11.

Although the location of the pelvis and the presence of rib overlap aid in identification of the vertebrae, they also limit the available vertebrae for analysis. When a lateral spine DXA study is performed in the left lateral decubitus position, L4 cannot be analyzed in the majority of individuals because of pelvic overlap. L1 is generally not analyzed because of rib overlap, regardless of whether the study is performed supine or in left lateral decubitus position. Rupich et al. (19) also found that rib overlay L2 in 90% of individuals studied in the supine position. It was estimated that rib BMC added 10.4% to the L2 BMC. Thus, when lateral DXA studies are performed in the left lateral decubitus position, L3 may be the only vertebra that is not affected by either pelvic or rib overlap. In the supine position, L3 and L4 are generally unaffected. This means that depending on the positioning required by the technique, the value from a single vertebra or from only a two-vertebrae average may have to be used. This is undesirable, although sometimes unavoidable, from the standpoint of statistical accuracy and precision.

If the vertebrae are misidentified in the lateral projection, the effect on BMD can be significant. In the study by Peel et al. (2), misidentification of the vertebral levels would have occurred in 12% of individuals in which the pelvis did not overlap L4 in the left lateral decubitus position. If L2 was misidentified as L3, the BMD of L3 was underestimated by an average of 5.7%. When L4 was misidentified as L3, the BMD at L3 was overestimated by an average of 3.1%. Although spine X-rays are rarely justified for the sole purpose of vertebral identification on a DXA study performed in the PA or AP projection, this may occasionally be required for DXA lumbar spine studies performed in the lateral projection. Analysis may be restricted to only one or two vertebrae because of rib and pelvic overlap. This reduces the statistical accuracy and precision of the measurement. Because of this reduction in accuracy, consideration should be given to combining lateral DXA spine studies with bone density assessments of other sites for diagnostic purposes.

THE PROXIMAL FEMUR IN DENSITOMETRY

Proximal Femur Anatomy

The gross anatomy of the proximal femur is shown in Fig. 3-20. In densitometry, the proximal femur has been divided into specific regions

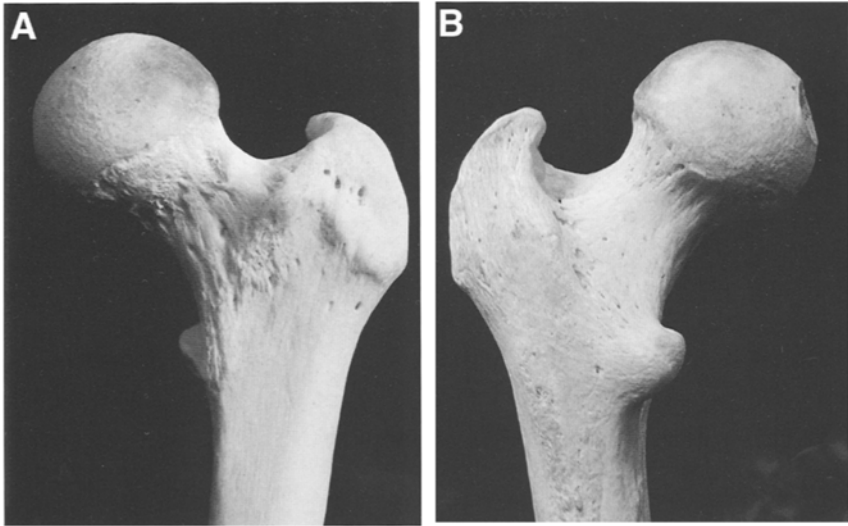


Fig. 3-20. (A) Proximal femur as viewed from the front. The lesser trochanter is behind the shaft of the femur. (B) Proximal femur as viewed from behind. The lesser trochanter is clearly seen to be a posterior structure. (Adapted with permission from *Colour Atlas of Human Anatomy*, [1993] 3rd edition, pp. 267–268.)

of interest (ROIs). The proximal femur studies shown in Fig. 3-21 illustrate these regions, which are based on the anatomy shown in Fig. 3-20. Ward's area is a region with which most physicians and technologists are not familiar. Ward's triangle, as it was originally called, is an anatomic region in the neck of the femur that is formed by the intersection of three trabecular bundles as shown in Fig. 3-22. In densitometry, Ward's triangle is a calculated region of low density in the femoral neck rather than a specific anatomic region. Because the region in densitometry is identified as a square, the region is generally now called Ward's area, instead of Ward's triangle. The total femur ROI encompasses all of the individual regions: the femoral neck, Ward's area, the trochanteric region, and the shaft. Each of these regions within this one bone contains a different percentage of trabecular and cortical bone as noted in Table 1-2 in chapter 1.

Effect of Rotation on BMD in the Proximal Femur

The lesser trochanter is an important anatomic structure from the perspective of recognizing the degree to which the femur has been rotated during positioning for a proximal femoral bone density study. Precision in

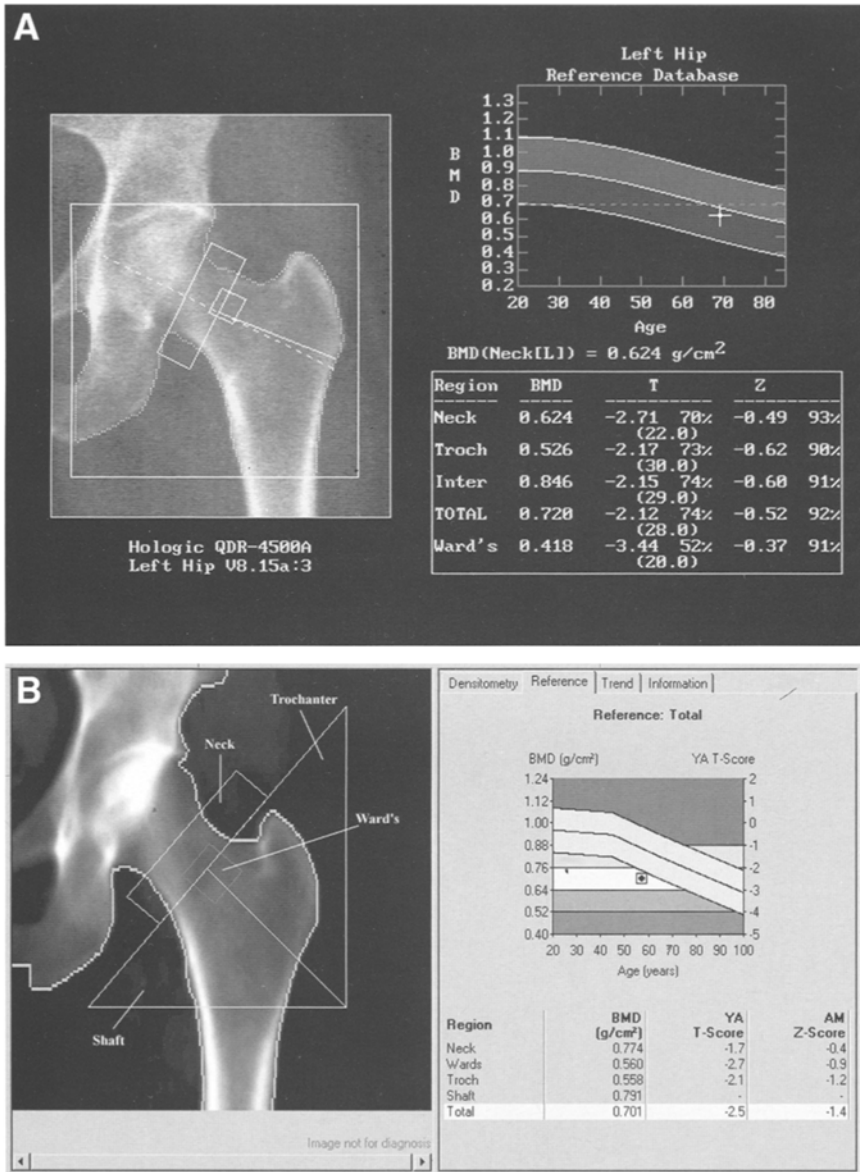


Fig. 3-21. Dual-energy X-ray absorptiometry proximal femur studies. Five regions of interest (ROIs) are defined. **(A)** Hologic QDR 4500 DXA study. (Case courtesy of Hologic, Inc., Bedford, MA.) **(B)** Lunar Prodigy. Four ROIs are labeled for emphasis on this study. The total ROI, which is not outlined, includes the neck, trochanter, and shaft.



Fig. 3-22. Ward's triangle, indicated by the letter *W*, is formed by the intersection of bundles of trabeculae in the femoral neck. (Adapted with permission from *Colour Atlas of Human Anatomy*, [1993] 3rd edition, p. 271.)

proximal femur bone density testing is highly dependent on reproduction of the degree of rotation of the proximal femur from study to study. In positioning the patient for a proximal femur study, internally rotating the femur 15–20° will bring the femoral neck parallel to the plane of the scan table. This rotation is accomplished with the aid of positioning devices provided by the manufacturers. In this position, BMD values in the femoral neck are the lowest. If the femoral neck rotation is increased or decreased from this position, the femoral neck BMD value will increase. This is because the apparent length of the neck of the femur will decrease as rotation is increased or decreased from the basic position. When the neck of the femur is parallel to the plane of the scan table, the X-ray beam passes through the neck at a 90° angle to the neck. With changes in rotation, the neck is no longer parallel to the scan table and the beam enters the neck at an angle that is greater or lesser than 90°. The result is an apparent shortening of the length of the neck and an increase in the mineral content in the path of the beam. The combination results in an apparent increase in BMD. Table 3-7 illustrates the magnitude of the increase in BMD in a

Table 3-7
Effect of Increasing Internal or External Rotation From the Neutral Position on the Femoral Neck Bone Mineral Density (g/cm^2) of Cadaveric Femurs

Cadaver no.	Neutral	External rotation from neutral of			Internal rotation from neutral of		
	0°	15°	30°	45°	15°	30°	45°
1	0.490	0.524	0.549	0.628	0.510	0.714	0.845
2	0.574	0.567	0.632	0.711	0.581	0.619	0.753
3	0.835	0.872	0.902	1.071	0.874	1.037	1.222
4	0.946	0.977	1.005	1.036	1.102	1.283	1.492

Reproduced with permission from *Calcif. Tissue Int.* 1995;57:340–343.

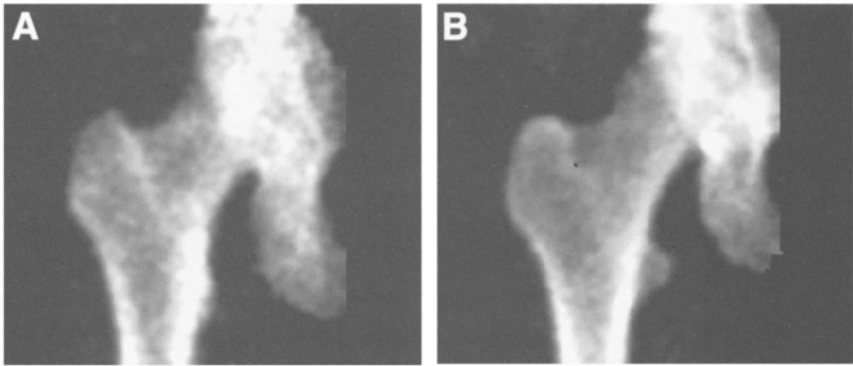


Fig. 3-23. Images of the proximal femur acquired during dual-energy X-ray absorptiometry studies on the Lunar DPX. (A) The lesser trochanter is clearly seen but is small and rounded, indicating proper internal rotation of the proximal femur during positioning. Compare this lesser trochanter to the lesser trochanter seen in (B). This is the same patient seen in (A) but here the proximal femur was not rotated internally sufficiently causing the lesser trochanter to appear large and pointed.

cadaver study from Goh et al. (21) The only visual clue to consistent rotation is the reproduction of the size and shape of the lesser trochanter.

Because the trochanter is a posterior structure, leg positioning in which the femur has not been rotated sufficiently internally tends to produce a very large and pointed lesser trochanter. Excessive internal rotation of the proximal femur will result in a total disappearance of the lesser trochanter. The size of the lesser trochanter in the DXA proximal femur image in Fig. 3-23A indicates correct internal rotation. This can be compared to the size of the lesser trochanter seen in the DXA proximal femur study in Fig. 3-23B. The

lesser trochanter is very large and pointed, indicating insufficient internal rotation. Although this would be undesirable in a baseline study of the proximal femur, follow-up studies using the proximal femur in this patient should be done with this same degree of rotation. Any change in rotation from the baseline study would be expected to affect the magnitude of change in the BMD, decreasing the precision of the study.

Effect of Leg Dominance on BMD in the Proximal Femur

In general, there does not seem to be a significant difference in the BMD in the regions of the proximal femur between the right and left legs of normal individuals (22–25). Leg dominance, unlike arm dominance, does not appear to exert a significant effect on the bone densities in the proximal femur and is not used to determine which femur should be studied. When proximal femur bone density studies first became available, the default or automatic positioning mode for the proximal femur was the right side. This was subsequently changed to the left side. The reason for the change, however, only reflected the orientation of the machine and the technologist's ease of access to the left leg.

Effect of Scoliosis, Osteoarthritis, Osteophytes, Surgery, and Fracture on BMD in the Proximal Femur

Structural changes and artifacts that interfere with DXA proximal femoral BMD measurements occur less often than at the spine. Osteoarthritic change in the hip joint may cause thickening of the medial cortex and hypertrophy of the trabeculae in the femoral neck, which may increase the BMD in the femoral neck and Ward's area (26). The trochanteric region apparently is not affected by such change and has been recommended as the preferred site to evaluate in patients with osteoarthritis of the hip (27). Osteophytes in the proximal femur are apparently much less common than osteophytes in the lumbar spine (9). They also appear to have little effect on the bone densities measured in the proximal femur. In patients with scoliosis, however, lower bone densities have been reported on the side of the convexity (28). If a worst-case measurement is desired, the bone density in the proximal femur should be measured in the femur on the side of the convexity. Proximal femur fracture and surgically implanted prostheses will render measurements of bone density in the proximal femur inaccurate.

If osteoarthritis or some other process restricts the ability of the patient to rotate the femur properly, the study should not be done. An attempt

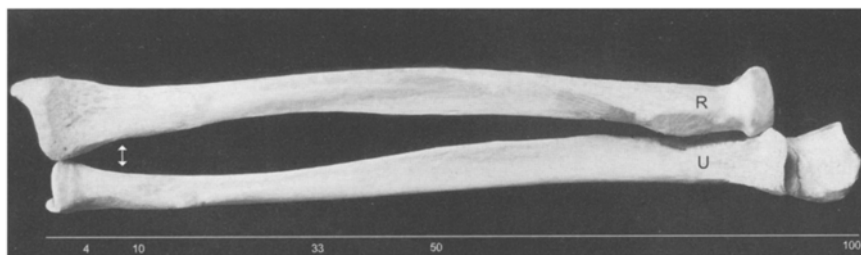


Fig. 3-24. Forearm. The scale at the bottom of the figure indicates ulnar length. The numbers reflect the percentage of ulnar length at which commonly measured sites are centered on either bone. The arrow between the two bones indicates the 8-mm separation point. R, radius; U, ulna. (Adapted with permission from *Colour Atlas of Human Anatomy*, [1993] 3rd edition, p. 110.)

should be made to scan the opposite proximal femur if possible. Similarly, if pain restricts the patient's range of motion such that the femur cannot be properly positioned, the study should not be done because the results will be not be valid.

THE FOREARM IN DENSITOMETRY

Nomenclature

The nomenclature used to describe the various sites in the forearm that are assessed with densitometry is confusing. Commonly measured sites are the 33% or 1/3 site,* the 50% and 10% sites, the 5-mm and 8-mm sites, and the ultradistal site. The sites designated by a percentage are named based on the location of the site in relationship to the overall length of the ulna. This is true for the site regardless of whether the site is on the ulna or the radius. In other words, the 50% site on the radius is located at a site on the radius which is directly across from the site on the ulna that marks 50% of the overall ulnar length, not 50% of the overall radial length. The 5-mm and 8-mm sites, are located on either bone at the point where the

*Although a mathematical conversion of 1/3 to a percentage would result in a value of 33.3%, the site when named as a percentage is called the 33% site and is located on the radius or forearm at a location that represents 33%, not 33.3%, of the length of the ulna.

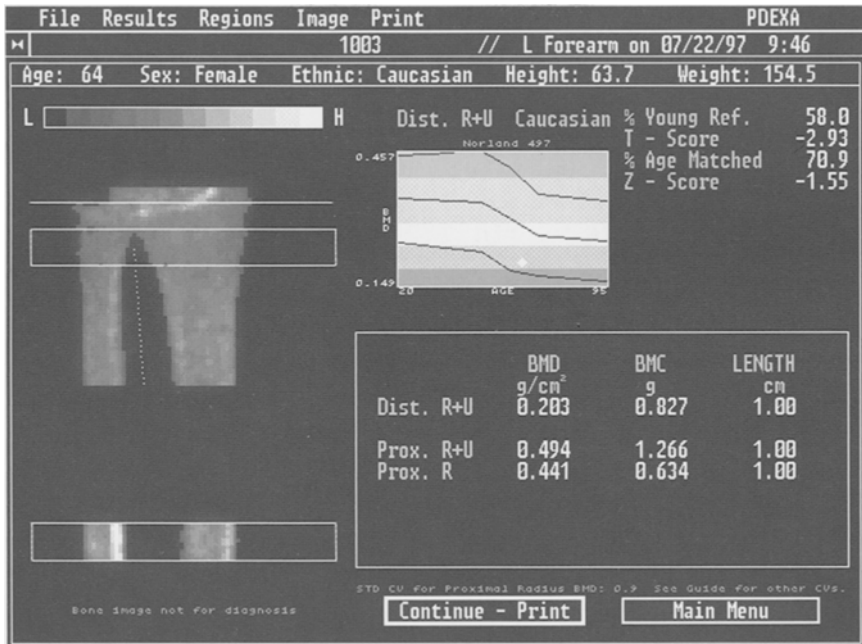


Fig. 3-25. Dual-energy X-ray absorptiometry study of the forearm acquired on the Norland pDEXA. Note the location of the regions of interest (ROIs) called the distal (dist.) and proximal (prox.). BMD values are given for the radius and ulna combined at both regions and for the radius alone at the proximal ROI.

separation distance between the radius and ulna is 5- or 8-mm, respectively. In Fig. 3-24 the approximate location of these sites is indicated. The 33% and 50% sites are both characterized as midradial sites, whereas the 10% site is considered a distal site. The ultradistal site is variously centered at a distance of either 4 or 5% of the ulnar length. There is nothing inherent in the definition of distal, ultradistal, and proximal, however, that specifies the exact location of sites bearing these names. In Figs. 3-25 to 3-28, the location of variously named ROIs from several different DXA forearm devices can be compared.

The clinically important difference between these sites is the relative percentages of cortical and trabecular bone found at the site. Table 1-3 in chapter 1 summarizes the percentages of trabecular bone at the various sites on the radius. These values are transferable to sites at the same location on the ulna as indicated in the table.

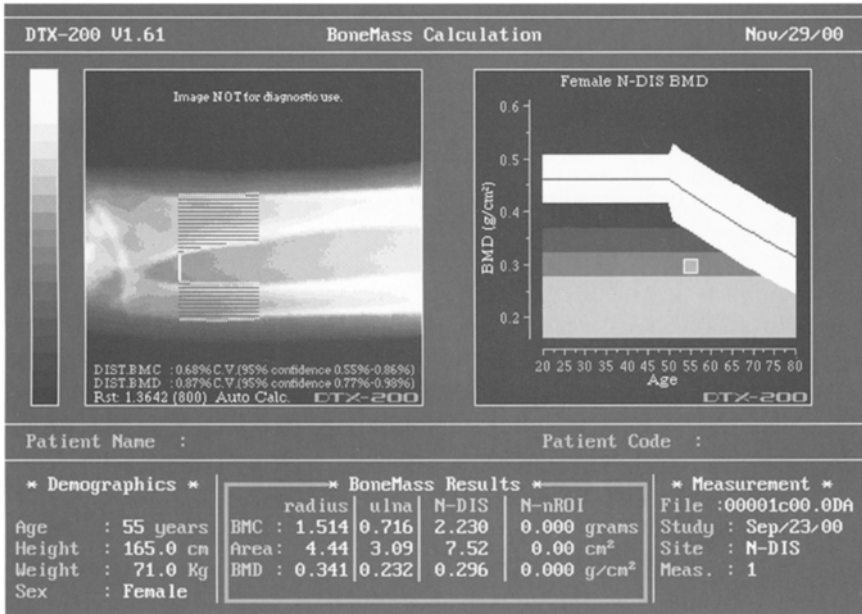


Fig. 3-26. Dual-energy X-ray absorptiometry study of the forearm acquired on the Osteometer DTX-200 DEXA Care[®]. The ROI is called the distal (DIS) region and begins at the 8-mm separation point. Values are given for each bone and for both bones combined. This distal region of interest (ROI) is not the same as the distal ROI shown in Fig. 3-25.

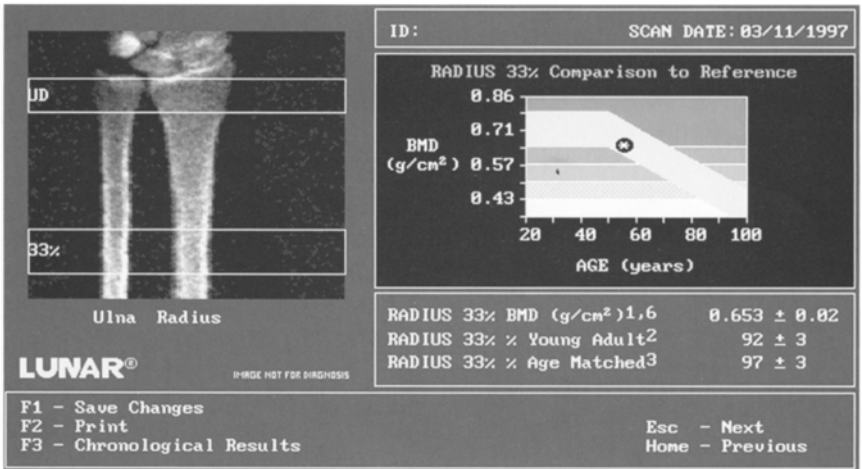


Fig. 3-27. Dual-energy X-ray absorptiometry study of the forearm acquired on the GE Lunar DPX. The two primary regions of interest are the ultradistal (UD) and 33% regions. These are similar but not identical in location to the distal and proximal regions seen in the study in Fig. 3-25.

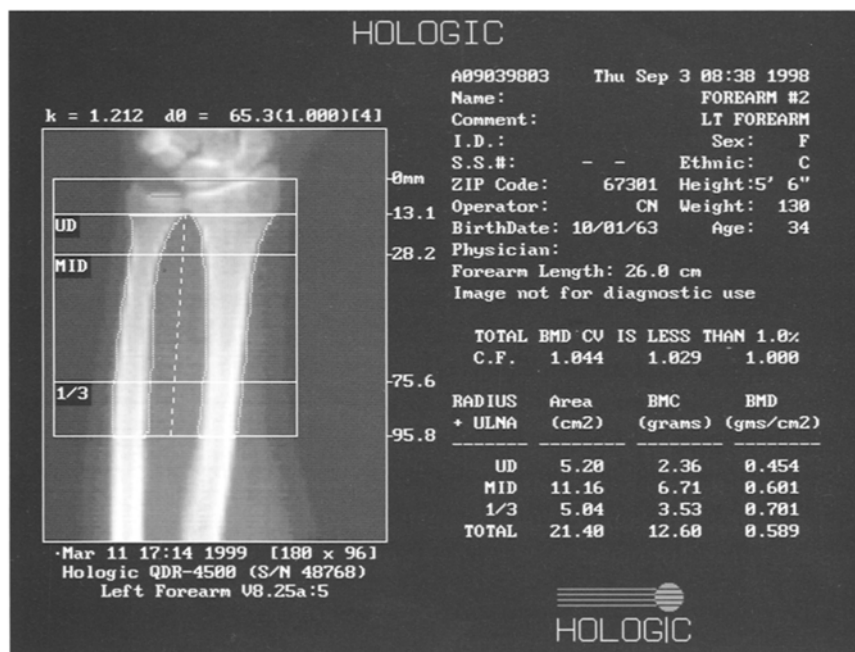


Fig. 3-28. Dual-energy X-ray absorptiometry study of the forearm acquired on the Hologic QDR-4500. Three ROIs are shown here. An ultradistal (UD), mid- and 1/3 ROI are indicated. The 1/3 region of interest is located similarly to the 33% ROI shown in Fig. 3-27. Note that the midregion here is clearly not located at a point that would correspond to 50% of ulnar length. It is between the ultradistal and 1/3 sites.

Effect of Arm Dominance on Forearm BMD

Unlike the proximal femur, arm dominance has a pronounced effect on bone density in the forearm. In healthy individuals, the BMC at the 33% radial site differs by 6–9% between the dominant and nondominant arms (29). A difference of 3% has been reported at the 8-mm site (30). If the individual is involved in any type of repetitive unilateral arm activity, the difference between the dominant and nondominant arm densities will be magnified to an even greater extent. Two studies of tennis players, an activity in which the dominant arm is subjected to repeated loading and impact, illustrated the effect of unilateral activity. In a study by Huddleston et al. (31), the BMC in the dominant forearm at the 50% radial site measured by SPA was 13% greater than in the nondominant arm. In a more recent study from Kannus et al. (32) using DXA, the side-to-side difference in BMD in tennis players averaged 10.8% at the

distal radius and 9.9% at the midradius. The corresponding values in the nontennis-playing controls were only 3.4% and 2.5%, respectively. Because of these recognized differences, the nondominant arm has traditionally been studied when the bone content or density is quantified for the purposes of diagnosis or assessment of fracture risk. Most reference databases for the machines in current use have been created using the nondominant arm. Comparisons of the dominant arm to these reference databases would not be valid. Some manufacturers supply databases for the dominant arm that can be used for comparisons if the dominant arm is to be studied. The operator's manual for the densitometry device should be consulted to determine which arm was used to create the database(s) provided by the manufacturer.

Effect of Artifacts on BMD in the Forearm

The forearm sites are relatively free from the confounding effects of most of the types of artifacts that are often seen in the lumbar spine. The presence of a prior fracture in the forearm will affect the BMC or BMD measurements in the forearm close to the prior fracture site. A study from Akesson et al. (33), suggested that in women with a prior fracture of the distal radius, the BMC was increased by 20% at the distal radius of the fractured arm in comparison to the nonfractured arm, irrespective of arm dominance. It is obviously important for the technologist to ask if the patient has experienced a prior wrist or forearm fracture. Unfortunately, this same study from Akesson et al. (33) noted that in a group of older women who were known to have had a distal radial fracture previously, many of the women did not recall the fracture or incorrectly recalled which arm was fractured. It was noted, however, that the forearm most often fractured was the dominant forearm.

The effect of movement during a forearm scan was quantified by Berntsen et al. (34), using single-energy X-ray absorptiometry forearm studies performed as part of the Tromsø Study.[†] Over 7900 forearm studies were evaluated for the presence of movement artifacts, which were graded I to III depending on the severity. Movement artifacts were found in 14.2% of the studies. Berntsen et al. (34) found that movement was more likely in older individuals with the prevalence of movement artifact increasing to 20% of

[†]The Tromsø Study is a population-based study conducted in Tromsø Norway, that focuses on lifestyle-related diseases such as osteoporosis.



Fig. 3-29. Dorsal surface of the hand. The numbering on the index finger would apply to the long, ring, and small fingers as well. 1, 2, and 3: distal, mid-, and proximal phalanges, respectively; 4: metacarpal; R, radius; U, ulna. (Adapted with permission from *Colour Atlas of Human Anatomy*, [1993] 3rd edition, p. 112.)

the scans in the oldest age group. Movement artifact appeared to slightly decrease the measured BMD. The effect on precision was studied in a subset of 111 patients. The authors found a doubling of precision[§] when movement was present, which was independent of the severity of the movement artifact. Although this study was performed utilizing only one type of forearm densitometer, the authors noted that these results should be applicable to any forearm scan for which data acquisition requires 3–5 minutes.

[§]See chapter 6 for a discussion of precision. Because precision is a measure of variability, an increase in precision is undesirable.

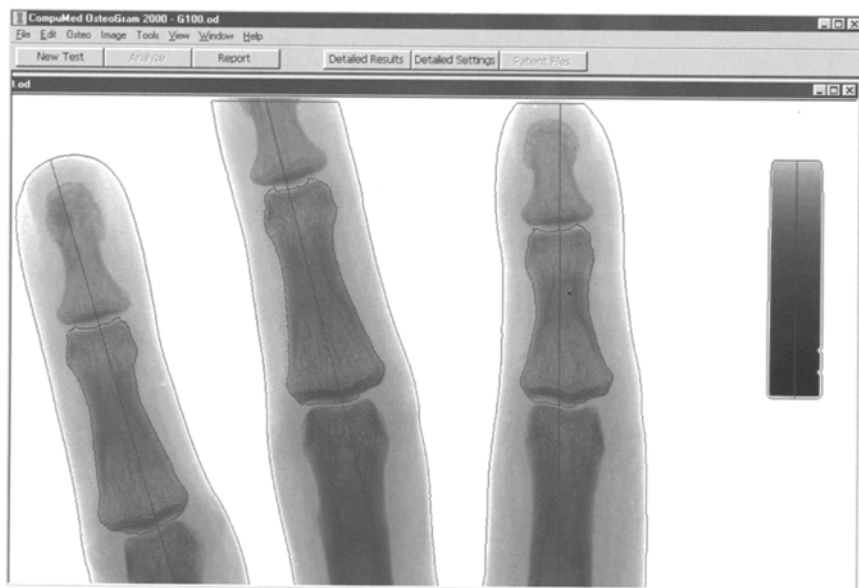


Fig. 3-30. A radiographic absorptiometry analysis of the midphalanges of the index, long, and ring fingers. (Case provided courtesy of CompuMed, Inc., Los Angeles, CA.)

THE METACARPALS, PHALANGES, AND CALCANEUS

Other skeletal sites can be studied using the techniques available today. The metacarpals, phalanges, and calcaneus were among the very first sites studied with the older techniques of radiographic photodensitometry and radiogrammetry. These sites are increasingly used today with the advent of computerized radiographic absorptiometry, computerized radiogrammetry, and peripheral DXA and ultrasound units. Figure 3-29 illustrates the anatomy of the hand and the location of the metacarpals and phalanges. The middle phalanges of the index, long, and ring fingers are the phalangeal regions most often quantified. Figure 3-30 illustrates the appearance of the phalanges on a computerized radiographic absorptiometry study, whereas, Fig. 3-31 illustrates the appearance of the metacarpals on a computer-assisted radiogrammetry study. The anatomy of the calcaneus[¶] is illustrated in Fig. 3-32. The calcaneus contains an extremely high percentage of trabecular bone and is exquisitely sensitive to weightbearing activities. Both the phalanges and the calcaneus have been shown to be useful sites for the prediction of hip fracture risk (35–37). The percentage of trabecular bone found in the phalanges and calcaneus is listed in Table 1-3 in chapter 1.

[¶]The calcaneus is also known as the os calcis or heel.



Fig. 3-31. X-ray image from computer-assisted radiogrammetry of the metacarpals of the index, long, and ring finger. (Case provided courtesy of Sectra Pronosco, Denmark.)

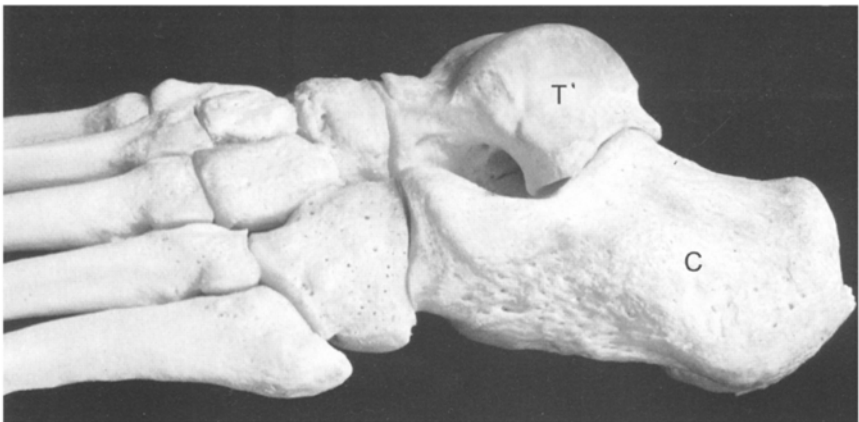


Fig. 3-32. Lateral view of the bones of the left foot. T, talus; C, calcaneus. (Adapted with permission from *Colour Atlas of Human Anatomy*, [1993] 3rd edition, p. 284.)

REFERENCES

1. Louis, O., Van Den Winkel, P., Covens, P., Schoutens, A., Osteaux, M. (1992) Dual-energy X-ray absorptiometry of lumbar vertebrae: relative contribution of body and posterior elements and accuracy in relation with neutron activation analysis. *Bone* **13**, 317–320.
2. Peel, N. F. A., Johnson, A., Barrington, N. A., Smith, T. W. D., Eastell, R. (1993) Impact of anomalous vertebral segmentation of measurements of bone mineral density. *J. Bone Miner. Res.* **8**, 719–723.
3. Bornstein, P. E. and Peterson, R. R. (1996) Numerical variation of the presacral vertebral column in three population groups in North America. *Am. J. Phys. Anthropol.* **25**, 139–146.
4. Davis, J. W., Grove, J. S., Wasnich, R. D., Ross, P. D. (1999) Spatial relationships between prevalent and incident fractures. *Bone* **24**, 261–264.
5. Nevitt, M. C., Ross, P. D., Palermo, L., Musliner, T., Genant, H. K., Thompson, D. E. (1999) Association of prevalent vertebral fractures, bone density, and alendronate treatment with incident vertebral fractures: effect of number and spinal location of fractures. *Bone* **25**, 613–619.
6. Krolner, B., Berthelsen, B., Nielsen, S. P. (1982) Assessment of vertebral osteopenia—comparison of spinal radiography and dual-photon absorptiometry. *Acta Radiol. Diagn.* **23**, 517–521.
7. Rand, T., Seidl, G., Kainberger, F., et al. (1997) Impact of spinal degenerative changes on the evaluation of bone mineral density with dual energy X-ray absorptiometry (DXA). *Calcif. Tissue Int.* **60**, 430–433.
8. Cann, C. E., Rutt, B. K., Genant, H. K. (1983) Effect of extrasosseous calcification on vertebral mineral measurement. *Calcif. Tissue Int.* **35**, 667.
9. Liu, G., Peacock, M., Eilam, O., Dorulla, G., Braunstein, E., Johnston, C. C. (1997) Effect of osteoarthritis in the lumbar spine and hip on bone mineral density and diagnosis of osteoporosis in elderly men and women. *Osteoporos. Int.* **7**, 564–569.
10. Frye, M. A., Melton, L. J., Bryant, S. C. et al. (1992) Osteoporosis and calcification of the aorta. *Bone Miner.* **19**, 185–194.
11. Frohn, J., Wilken, T., Falk, S., Stutte, H. J., Kollath, J., Hor, G. (1990) Effect of aortic sclerosis on bone mineral measurements by dual-photon absorptiometry. *J. Nucl. Med.* **32**, 259–262.
12. Orwoll, E. S., Oviatt, S. K., Mann, T. (1990) The impact of osteophytic and vascular calcifications on vertebral mineral density measurements in men. *J. Clin. Endocrinol. Metab.* **70**, 1202–1207.
13. Reid, I. R., Evans, M. C., Ames, R., Wattie, D. J. (1991) The influence of osteophytes and aortic calcification on spinal mineral density in post-menopausal women. *J. Clin. Endocrinol. Metab.* **72**, 1372–1374.
14. Banks, L. M., Lees, B., MacSweeney, J. E., Stevenson, J. C. (1991) Do degenerative changes and aortic calcification influence long-term bone density measurements? Abstract. 8th International Workshop on Bone Densitometry, Bad Reichenhall, Germany.
15. Drinka, P. J., DeSmet, A. A., Bauwens, S. F., Rogot, A. (1992) The effect of overlying calcification on lumbar bone densitometry. *Calcif. Tissue Int.* **50**, 507–510.
16. Cherney, D. D., Laymon, M. S., McNitt, A., Yuly, S. (2002) A study on the influence of calcified intervertebral disk and aorta in determining bone mineral density. *J. Clin. Densitom.* **5**, 193–198.

17. Girardi, F. P., Parvataneni, H. K., Sandhu, H. S., et al. (2001) Correlation between vertebral body rotation and two-dimensional vertebral bone density measurement. *Osteoporos. Int.* **12**, 738–740.
18. Stutzman, M. E., Yester, M. V., Dubovsky, E. V. (1997) Technical aspects of dual-photon absorptiometry of the spine. *Technique* **15**, 177–181.
19. Rupich, R. C., Griffin, M. G., Pacifici, R., Avioli, L. V., Susman, N. (1992) Lateral dual-energy radiography: artifact error from rib and pelvic bone. *J. Bone Miner. Res.* **7**, 97–101.
20. Jergas, M., Breitenseher, M., Gluer, C. C., et al. (1995) Which vertebrae should be assessed using lateral dual-energy X-ray absorptiometry of the lumbar spine? *Osteoporos. Int.* **5**, 196–204.
21. Goh, J. C. H., Low, S. L., Bose, K. (1995) Effect of femoral rotation on bone mineral density measurements with dual energy X-ray absorptiometry. *Calcif. Tissue Int.* **57**, 340–343.
22. Bonnick, S. L., Nichols, D. L., Sanborn, C. F., Payne, S. G., Moen, S. M., Heiss, C. J. (1996) Right and left proximal femur analyses: is there a need to do both? *Calcif. Tissue Int.* **58**, 307–310.
23. Faulkner, K. G., Genant, H. K., McClung, M. (1995) Bilateral comparison of femoral bone density and hip axis length from single and fan beam DXA scans. *Calcif. Tissue Int.* **56**, 26–31.
24. Rao, A. K., Reddy, S., Rao, D. S. (2000) Is there a difference between right and left femoral bone density? *J. Clin. Densitom.* **3**, 57–61.
25. Petley, G. W., Taylor, P. A., Murrills, A. J., Dennison, E., Pearson, G., Cooper, C. (2000) An investigation of the diagnostic value of bilateral femoral neck bone mineral density measurements. *Osteoporos. Int.* **11**, 675–679.
26. Nevitt, M. C., Lane, N. E., Scott, J. C., et al. (1995) Radiographic osteoarthritis of the hip and bone mineral density. *Arth. Rheum.* **38**, 907–916.
27. Preidler, K. W., White, L. S., Tashkin, J., et al. (1997) Dual-energy X-ray absorptiometric densitometry in osteoarthritis of the hip. Influence of secondary bone remodeling of the femoral neck. *Acta Radiol.* **38**, 539–542.
28. Hans, D., Biot, B., Schott, A. M., Meunier, P. J. (1996) No diffuse osteoporosis in lumbar scoliosis but lower femoral bone density on the convexity. *Bone* **18**, 15–17.
29. Karjalainen, P. and Alhava, E. M. (1976) Bone mineral content of the forearm in a healthy population. *Acta Radiol. Oncol. Radiat. Phys. Biol.* **16**, 199–208.
30. Borg, J., Mollgaard, A., Riis, B. J. (1995) Single X-ray absorptiometry: performance characteristics and comparison with single photon absorptiometry. *Osteoporos. Int.* **5**, 377–381.
31. Huddleston, A. L., Rockwell, D., Kulund, D. N., Harrison, B. (1980) Bone mass in lifetime tennis athletes. *JAMA* **244**, 1107–1109.
32. Kannus, P., Haapasalo, H., Sievanen, H., Oja, P., Vuori, I. (1994) The site-specific effects of long-term unilateral activity on bone mineral density and content. *Bone* **15**, 279–284.
33. Akesson, K., Gardsell, P., Sernbo, I., Johnell, O., Obrant, K. J. (1992) Earlier wrist fracture: a confounding factor in distal forearm bone screening. *Osteoporos. Int.* **2**, 201–204.
34. Berntsen, G. K. R., Tollan, A., Magnus, J. H., Sjøgaard, A. J., Ringberg, T., Fønnebo, V. (1999) The Tromsø study: artifacts in forearm densitometry—prevalence and effects. *Osteoporos. Int.* **10**, 425–432.
35. Mussolino, M. E., Looker, A. C., Madans, J. H., et al. (1997) Phalangeal bone density and hip fracture risk. *Arch. Intern. Med.* **157**, 433–438.

36. Huang, C., Ross, P. D., Yates, A. J., et al. (1998) Prediction of fracture risk by radiographic absorptiometry and quantitative ultrasound: a prospective study. *Calcif. Tissue Int.* **6**, 380–384.
37. Cummings, S. R., Black, D. M., Nevitt, M. C. (1993) Bone density at various sites for prediction of hip fractures. *Lancet* **341**, 72–75.

4

FDA-Approved Densitometry Devices

CONTENTS

COMPUTER-ENHANCED RADIOGRAMMETRY
COMPUTER-ENHANCED RADIOGRAPHIC ABSORPTIOMETRY
CENTRAL X-RAY DENSITOMETERS
PERIPHERAL X-RAY DENSITOMETERS
ULTRASOUND BONE DENSITOMETERS

The devices discussed in this chapter are available in the United States for clinical use. The specifications were provided by the manufacturers and are subject to change without notice because devices are continually upgraded to reflect advances in the technology. The categories of information provided by each manufacturer may vary slightly. All categories are not relevant to every device. This listing of devices is not intended to reflect all devices in use in the United States. This listing may also reflect devices in use in clinical and research settings, but not necessarily still sold by manufacturers. Every attempt was made to ensure the accuracy of the information. The manufacturer should be contacted for the latest specifications. The devices are grouped by type and listed alphabetically by model name.

COMPUTER-ENHANCED RADIOGRAMMETRY

Sectra Osteoporosis Package™ IDS5™ Workstation Clinical Application (Fig. 4-1)

- Manufacturer: Sectra Pronosco, Herlev, Denmark.
- Technique: Computerized radiogrammetry utilizing a standard digitized X-ray image of the hand as part of an integrated Picture Archiving and Communication System (PACS) workstation.
- Skeletal application(s): Metacarpals of the index, long, and ring fingers.



Fig. 4-1. Sectra Osteoporosis Package™ IDS5™ Workstation Clinical Application. The analysis is performed as part of an integrated Picture Archiving and Communication System workstation. (Photograph courtesy of Sectra Pronosco, Denmark.)

- Results
 - Bone mineral density (BMD) estimate (g/cm^2).
 - Metacarpal Index.
 - T-score and z-score.
 - Graphical representation of the T- and z-score.
 - Graphical representation of the Metacarpal Index.
- Patient scan time: Not applicable.
- Analysis time: 5 seconds.
- Precision: 0.35%.
- Radiation exposure: 1 μSv limited to the hand during plain film acquisition.
- Operation: Data from a hand image is analyzed and stored in a PACS system. The hand image data file is opened for viewing on the IDS5 workstation. The radiogrammetry analysis is begun with a mouse click and complete in approximately 5 seconds. The report can then be printed. The system is equipped with an Internet update feature for reference databases and DICOM modality on-line support.



Fig. 4-2. CompuMed Automated OsteoGram® Analysis System. The system consists of the computer, monitor, mouse, flatbed scanner, and analysis software to perform computer-assisted radiographic absorptiometry of the phalanges. (Photograph courtesy of CompuMed Inc., Los Angeles, CA.)

COMPUTER-ENHANCED RADIOGRAPHIC ABSORPTIOMETRY

Automated OsteoGram® (Fig. 4-2)

- Manufacturer: CompuMed Inc., Los Angeles, CA.
- Technique: Radiographic absorptiometry (RA) utilizing plain films of the hand with a computerized analysis. The system consists of a desktop computer with OsteoGram software installed, 15-in. flat panel display monitor, AGFA DuoScan T1200 scanner, keyboard, and mouse. A DICOM version is also available.
- Skeletal application(s): Middle phalanges of the index, long, and middle fingers.
- Results
 - BMD in arbitrary RA units.
 - T-score and z-score.
 - Diagnostic classification based on World Health Organization (WHO) criteria.

- Patient scan time: Not applicable.
- Analysis time: Approximately 1 minute, excluding film digitization time.
- Precision: <1%.
- Quality control: Automated system checks to ensure quality and accuracy of image digitalization.
- Operation: Two hand films are taken. Data is entered into the computer program with the computer keyboard. The plain film is scanned into the computer. Scanning is not necessary when using the DICOM system. The data are analyzed by proprietary software installed on the computer. The results are then printed.
- Accessories provided with the standalone system.
 - SCSI interface connector.
 - CMI/AGFA Ortho 400 Green Cassette with the OsteoGram film. Template mounted with the reference wedge.
 - Mouse pad.
 - Clinical Overview CD.
 - Procedure video.
 - Instruction manual.

MetriScan™ (Fig. 4-3)

- Manufacturer: Alara, Inc., Hayward, CA.
- Technique: Radiographic absorptiometry with storage phosphor technology.
- Skeletal application(s): Middle phalanges of the index, long, and ring fingers.
- Scan time: 1 second.
- Results
 - Estimated phalangeal BMD in arbitrary RA units.
 - % Young Adult and % Age-Matched comparisons.
 - T-score and z-score.
 - Diagnostic classification based on WHO criteria.
- Precision: 1.1%.
- Radiation exposure: 0.0001 mrem/scan (0.001 μ Sv/scan).
- Dimensions: 16 × 16 × 16 in. (40.6 × 40.6 × 40.6 cm).
- Weight: 41.5 lb (18.8 kg).
- Environmental operating temperature: 64°F to 95°F (18° to 35°C).
- Environmental operating humidity: 5 to 80%, noncondensing.
- Scatter radiation: 0.0001 mrem/scan (0.001 μ Sv/scan) at 1 m.
- Quality control: Automated.

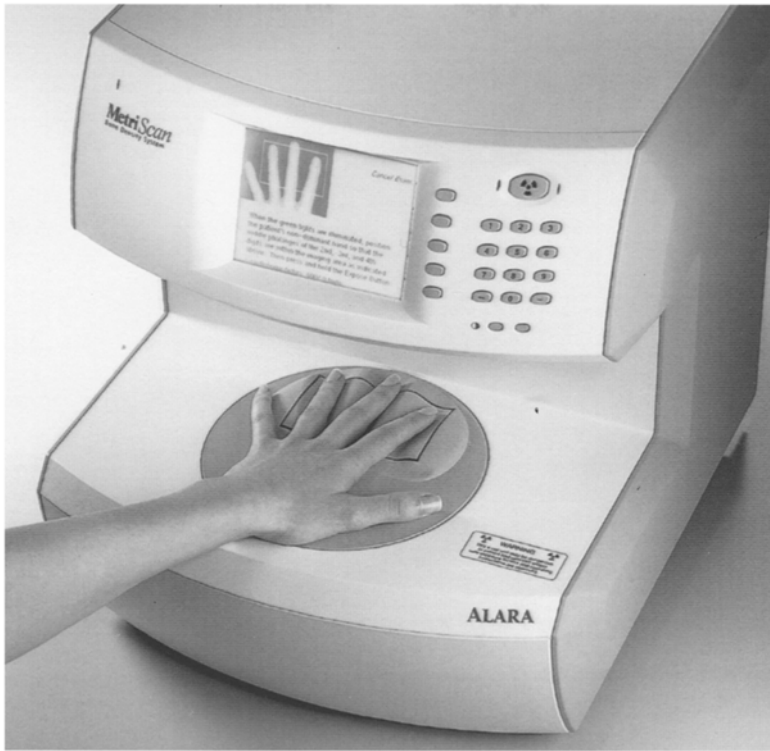


Fig. 4-3. Alara MetriScan™. This is a self-contained X-ray unit used to perform radiographic absorptiometry of the phalanges. (Photograph courtesy of Alara, Inc., Hayward, CA.)

- **Operation:** The unit is self-contained and does not require a standard hand film. Data input from keypad on unit. Separate HP DeskJet® 697C or 710C printer or printer as specified by Alara, Inc. is needed for results output.

CENTRAL X-RAY DENSITOMETERS

Delphi™ (Fig. 4-4)

- **Manufacturer:** Hologic, Inc., Bedford, MA.
- **Technology:** Dual-energy X-ray absorptiometry.
- **Skeletal regions studied**
 - Posteroanterior (PA) lumbar spine.
 - Proximal femur.

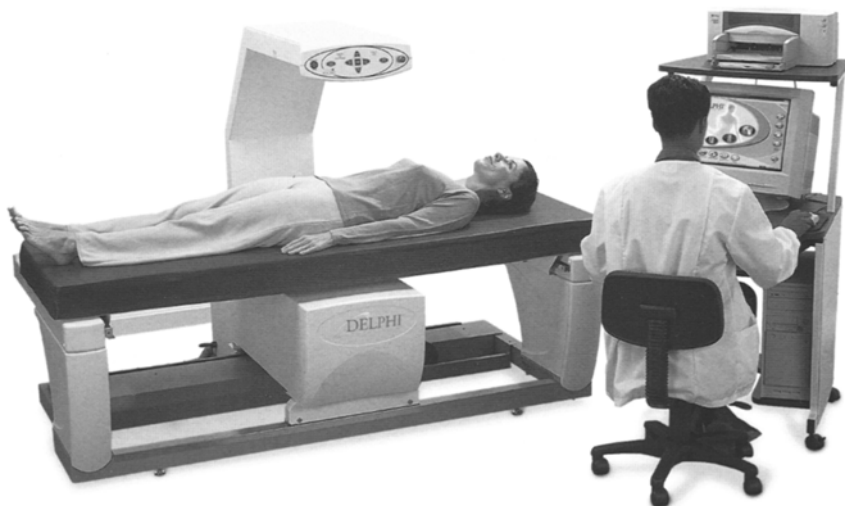


Fig. 4-4. Hologic Delphi™. A central fan-array dual-energy X-ray absorptiometer. (Photograph courtesy of Hologic, Inc., Bedford, MA.)

- Forearm.
- IVA™ lateral spine imaging (T4–L4).
- Dual Hip™.
- Whole body (on Delphi with Whole Body).
- Scan time (in the 60-Hz scan mode)
 - PA lumbar spine and proximal femur: 15 seconds.
 - Forearm: 30 seconds.
 - Whole body: 6.8 minutes.
 - Single energy IVA™: 10 seconds (for 15-in. scan length).
- Results
 - BMD (g/cm^2).
 - Bone mineral content (BMC) (g).
 - Area (cm^2).
 - T-score and z-score.
 - Standardized BMD (sBMD) (mg/cm^2).
 - National Health and Nutrition Examination Survey (NHANES) III reference data for hip.
 - Trend reports for serial monitoring.
- Precision: <1.0%.
- Radiation dose (in the 60-Hz scan mode)
 - PA lumbar spine and proximal femur: 5 mR.
 - Forearm: 10 mR.

- Whole body: 1.5 mR.
- IVA: 7 mR (15-in. scan length).
- Dimensions
 - Delphi: 76 × 49.5 × 28 in. (193 × 126 × 71 cm).
 - Delphi with Whole Body: 79.5 × 48 × 28 in. (202 × 122 × 71 cm), 119 × 59 × 28 in. (302 × 150 × 71 cm) table extended.
- Weight
 - Delphi: 650 lb (296 kg).
 - Delphi with whole body: 680 lb (310 kg).
- Recommended dedicated floor space: 8 × 8 ft (2.4 × 2.4 m).
- Scatter radiation: <1.0 mR/hr (0.01 mSv/hr) measured at 6.6 ft (2.0 m) from the examination table for most scan modes.
- Operating environmental temperature: 60° to 90°F (15° to 32°C).
- Operating environmental relative humidity: 20 to 80%, noncondensing.
- X-ray source: Switched pulse at 140 kVp and 100 kVp for dual energy, 140 kVp for single energy IVA.
- X-ray beam geometry: Fan.
- Detectors: Multielement detector array.
- Scan path: Linear.
- Quality control: Self-calibrating with Hologic Automatic Internal Reference system and automated quality control program.
- Operation: IBM-compatible Pentium™ computer, Windows 98®-based operating system, HP DeskJet printer, 17-in. monitor.
- Accessories provided
 - Anthropomorphic spine phantom.
 - Medical imaging printer.
- Options: Magneto optical disk storage; HP LaserJet® black-and-white printer; flat panel monitor; whole body, body composition analysis, and quantitative morphometry software; modem or network options.

Discovery™ (Fig. 4-5)

- Manufacturer: Hologic, Inc., Bedford, MA.
- Technology: Dual-energy X-ray absorptiometry.
- Models: *Ci*, *Wi*, *C*, *W*, *SL*, and *A*.
- Skeletal regions studied
 - PA lumbar spine, all models.
 - Proximal femur, all models.
 - Forearm, all models.
 - Dual Hip™, all models.

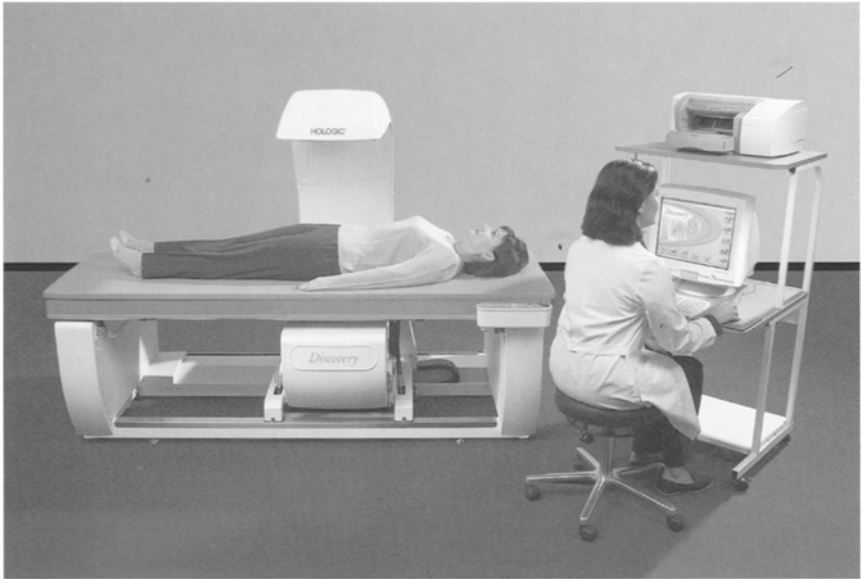


Fig. 4-5. The Hologic Discovery™. A central fan-array dual-energy X-ray absorptiometry scanner. (Photograph courtesy of Hologic, Inc., Bedford, MA.)

- IVA™, on models C, W, SL, and A.
- CADfx, on models C, W, SL, and A.
- Whole body, on models Wi, W, and A.
- Scan time on models Ci and Wi (in the 60 Hz scan mode)
 - PA lumbar spine and proximal femur: 30 seconds.
 - Forearm: 30 seconds.
 - Whole body: 6.8 minutes.
- Scan time on models C, W, SL, and A (in the 60-Hz scan mode)
 - PA lumbar spine and proximal femur: 10 seconds.
 - Forearm: 30 seconds.
 - Single-energy IVA™: 30 seconds.
 - Whole Body: 6.8 minutes (model W); 180 seconds (model A).
- Results
 - BMD (g/cm²).
 - BMC (g).
 - Area (cm²).
 - T-score and z-score.
 - NHANES III reference data for hip.
 - Diagnosis using WHO criteria.

- Fracture risk assessment.
- Vertebral fracture assessment (with IVA™).
- Trend reports for serial monitoring.
- Precision: <1.0%.
- Radiation dose (in the 60-Hz scan mode)
 - Models *Ci* and *Wi* PA lumbar spine and proximal femur: 0.10 mGy.
 - Models C, W, SL, and A: PA lumbar spine, 0.007 mGy.
 - Models C, W, SL, and A: Proximal femur, 0.07 mGy.
 - Models *Ci* and *Wi*: Forearm, 0.010 mGy.
 - Models C, W, SL, and A: Forearm, 0.005 mGy.
 - Models *Wi*, W, and A: Whole body, 0.015 mGy.
 - Models C, W, SL, and A: IVA™, 0.07 mGy.
- Dimensions
 - Models *Ci* and C: 76 × 41 in. (1.93 × 1.05 m).
 - Models *Wi*, W, SL, and A: 79.5 × 41 in. (2.02 × 1.05 m).
 - Models *Wi* and W, table extended: 119 × 59 in. (3.02 × 1.50 m).
 - Model SL, table extended and C-arm rotated: 79.5 × 59 in. (2.02 × 1.50 m).
 - Model A, table extended and C-arm rotated: 119 × 59 in. (3.02 × 1.50 m).
- Weight
 - Control console, all models: 150 lb (68 kg).
 - Models *Ci* and C: 650 lb (296 kg).
 - Models *Wi* and W: 680 lb (310 kg).
 - Models SL and A: 800 lb (365 kg).
- Recommended dedicated floor space: 8 × 8 ft (2.4 × 2.4 m) to 8 × 10 ft (2.4 × 3.1 m), depending on model.
- Scatter radiation: <1.0 mR/hr (0.01 mSv/hr) measured at 6.6 ft (2.0 m) from the examination table for most scan modes.
- Operating environmental temperature: 60° to 90°F (15° to 32°C).
- Operating environmental relative humidity: 20 to 80%, noncondensing.
- X-ray source: Switched pulse with 140 kVp peak.
- X-ray beam geometry: Fan.
- Detectors: Multielement detector array.
- Quality control: Self-calibrating with Hologic Automatic Internal Reference system and automated quality control program.
- Operation: IBM-compatible Pentium computer, QDR for Windows XP® operating system, HP DeskJet printer, 17-in. monitor, mouse, 56K modem, and CD-RW drive.



Fig. 4-6. GE Lunar DPX Bravo[®]. A central fan-array dual-energy X-ray absorptiometer. (Photograph courtesy of GE Healthcare, Madison, WI.)

- Options: Magneto optical disk storage; HP LaserJet[®] black-and-white printer; 15-in. flat panel monitor; modem or network options; IRIS package (includes DICOM, and Physician's Report Writer); prosthetic hip software; and, depending on model, decubitus lateral BMD, body composition and subregion analysis software and small animal capability.

DPX Bravo[®] (Fig. 4-6)

- Manufacturer: GE Medical Systems, Madison, WI.
- Technology: Dual-energy X-ray absorptiometry.
- Skeletal application(s)
 - PA spine.
 - Proximal femur.
- Scan time
 - PA spine: 90 seconds.
 - Proximal femur: 90 seconds.
- Results
 - BMD (g/cm^2).
 - BMC (g).

- Area (cm^2).
- % Young Adult and % Age-Matched comparisons.
- T-score and z-score.
- NHANES III total hip comparisons.
- Precision
 - PA spine: <1%.
 - Hip: <1%.
- Radiation dose: PA spine or proximal femur: 3 mR.
- Dimensions: 73.2 × 33.9 × 51.2 in. (186 × 86 × 130 cm).
- Power: 100–240 VAC +/- 10%, THD <5%, 600 VA.
- X-ray filtration: constant potential, cerium K-edge filter.
- X-ray beam geometry: SmartBeam™.
- Quality control: Block phantom and aluminum spine phantom supplied by manufacturer. Automated quality assurance (QA) program with daily precision monitoring.
- Software platform: Windows XP.
- Accessories provided
 - PA spine-positioning block.
 - Foot positioner for proximal femur studies.
 - Block phantom.
 - Aluminum spine phantom.
 - Washable table pad.
- Options: DualFemur™, Forearm, OneVision, CAD, OneScan, Physician's Composer, TeleDensitometry, DEXTER PDA.

DPX Duo® (Fig. 4-7)

- Manufacturer: GE Medical Systems, Madison, WI.
- Technology: Dual-energy X-ray absorptiometry/gynecology exam table.
- Skeletal application(s)
 - PA spine.
 - Proximal femur.
- Scan time
 - PA spine: 90 seconds.
 - Proximal femur: 90 seconds.
- Results
 - BMD (g/cm^2).
 - BMC (g).
 - Area (cm^2).
 - % Young Adult and % Age-Matched comparisons.



Fig. 4-7. GE Lunar DPX Duo[®]. A central fan-array dual-energy X-ray absorptiometer. This is a combination DXA scanner and examination table. (Photograph courtesy of GE Healthcare, Madison, WI.)

- T-score and z -score.
- NHANES III total hip comparisons.
- Precision
 - PA spine: <1%.
 - Hip: <1%.
- Radiation dose: PA spine or proximal femur: 3 mR.
- Dimensions: 73.2 × 33.9 × 57.9 in. (186 × 86 × 147 cm).
- Power: 100–240 VAC +/- 10%, THD <5%, 600 VA.
- X-ray beam geometry: SmartBeam[™].
- Quality control: Block phantom and aluminum spine phantom supplied by manufacturer. Automated QA program with daily precision monitoring.

- Software platform: Windows XP.
- Accessories provided
 - PA spine-positioning block.
 - Foot positioner for proximal femur studies.
 - Block phantom.
 - Aluminum spine phantom.
- Exam table features
 - Two storage drawers.
 - Paper roll disperser.
 - Washable table pad.
 - Extendable leg rests.
 - Treatment pan.
- Options: DualFemur™, Forearm, OneVision, CAD, OneScan, Physician's Composer, TeleDensitometry, DEXTER PDA.

DPX-IQ™ (Fig. 4-8)

- Manufacturer: GE Medical Systems, Madison, WI.
- Technology: Dual-energy X-ray absorptiometry.
- Skeletal application(s)
 - PA spine.
 - Proximal femur.
 - Total body with soft tissue quantification (with full size table only).
- Scan time
 - PA spine: 2 minutes.
 - Proximal femur: 2 minutes.
 - Total body: 11 minutes.
- Results
 - BMD (g/cm^2).
 - BMC (g).
 - Area (cm^2).
 - % Young Adult and % Age-Matched comparisons.
 - T-score and z-score.
 - sBMD (mg/cm^2) for L2–L4 and total hip.
 - NHANES III total hip comparisons.
- Precision
 - PA spine: 0.5%.
 - Hip: 1%.
 - Total body: 0.5%.
- Radiation dose
 - PA spine or proximal femur: <3 mRem.
 - Total body: 0.02 mRem.

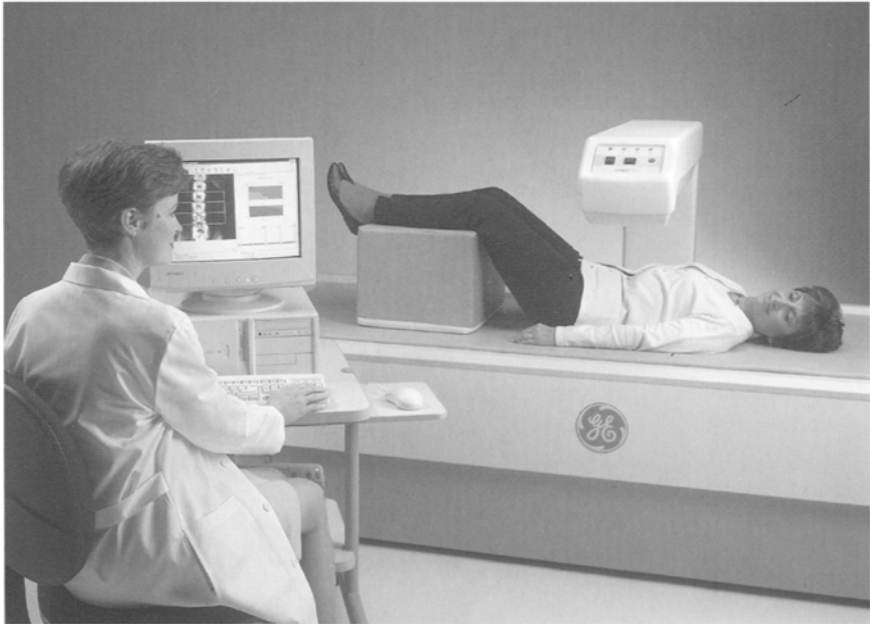


Fig. 4-8. GE Lunar DPX Pro™. A central pencil-beam dual-energy X-ray absorptiometer. This device is available in both a full-size and compact model. (Photograph courtesy of GE Healthcare, Madison, WI.)

- Dimensions
 - Full-size table: 95 × 42 × 52 in. (242 × 107 × 133 cm).
 - Compact table: 71 × 40 × 52 in. (181 × 100 × 133 cm).
- Weight
 - Full-size table: 598 lbs (272 kg).
 - Compact table: 550 lbs (250 kg).
- Recommended dedicated floor space
 - Full-size table: 9 × 7 ft (2.7 × 2.1 m).
 - Compact table: 7 × 7 ft (2.1 × 2.1 m).
- Operating environmental temperature: 65° to 80°F (18° to 27°C).
- Operating environmental relative humidity: 30 to 75%, noncondensing.
- X-ray source: 134 KVp; 3.0 mA for PA spine and proximal femur studies (mA varies by skeletal site and scan mode).
- X-ray filtration: constant potential, cerium K-edge filter.
- X-ray beam geometry: Pencil-beam.
- Detectors: NaI.
- Scan path: Rectilinear.

- Quality control: Block phantom and aluminum spine phantom supplied by manufacturer.
- Operation: IBM compatible desktop Pentium computer, SVGA monitor, printer.
- Accessories provided
 - PA spine-positioning block.
 - Foot positioner for proximal femur studies.
 - Block phantom.
 - Aluminum spine phantom.
- Options: Forearm, hand, lateral spine, and orthopedics software; forearm positioner; lateral spine positioner; encapsulated spine phantom.

DPX MD™

- Manufacturer: GE Medical Systems, Madison, WI.
- Technology: Dual-energy X-ray absorptiometry.
- Skeletal application(s)
 - PA spine.
 - Proximal femur.
 - DualFemur™ (not available on compact model).
 - Total body (not available on compact model).
- Scan time
 - PA spine and proximal femur: 2 minutes.
 - DualFemur™: 4 minutes.
 - Total body: 8 minutes.
- Results
 - BMD (g/cm^2).
 - BMC (g).
 - % Young Adult and % Age-Matched comparisons.
 - T-score and z-score.
 - sBMD (mg/cm^2).
 - NHANES III reference data.
 - WHO diagnostic classification.
- Precision
 - PA spine and total femur: 1.0%.
 - DualFemur™: 0.7%.
 - Total body: 0.5%.
- Radiation dose
 - PA spine: 1 mrem.
 - Femur: 1 mrem.
 - Total body: 0.02 mrem.

- Dimensions
 - Full size table: 95 × 42 × 52 in. (242 × 107 × 133 cm).
 - Compact table: 71 × 40 × 52 in. (181 × 100 × 133 cm).
- Weight
 - Full-size table: 598 lbs (272 kg).
 - Compact table: 550 lbs (250 kg).
- Recommended dedicated floor space
 - Full size table: 9 × 7 ft (2.7 × 2.1 m).
 - Compact table: 7 × 7 ft (2.1 × 2.1 m).
- Operating environmental temperature: 65° to 80°F (18° to 27°C).
- Operating environmental relative humidity: 30 to 75%, noncondensing.
- X-ray source: 134 kV; 0.75 mA for PA spine, proximal femur, and DualFemur™ (mA varies by skeletal site and scan mode).
- X-ray filtration: Constant potential, cerium K-edge filter.
- X-ray beam geometry: Pencil beam.
- Detectors: NaI.
- Scan path: Rectilinear.
- Quality control: Automatic test program.
- Operation: IBM-compatible computer and printer.
- Accessories provided
 - PA spine positioner.
 - Proximal femur positioner.
 - DualFemur™ positioner.
 - Aluminum spine phantom.
- Options: Lateral spine, forearm/hand, pediatrics, orthopedics and small animal software; and encapsulated phantom.

DPX MD+™

- Manufacturer: GE Medical Systems, Madison, WI.
- Technology: Dual-energy X-ray absorptiometry.
- Skeletal application(s)
 - PA spine.
 - Proximal femur.
- Results
 - BMD (g/cm²).
 - BMC (g).
 - % Young Adult and % Age-Matched comparisons.
 - T-score and z-score.
 - sBMD (mg/cm²).

- NHANES III reference data.
- WHO diagnostic classification.
- Precision
 - PA spine, proximal femur, and total body: 1.0%.
 - DualFemur™: <1.0%.
- Radiation dose
 - PA spine and proximal femur: 3.0 mrem.
 - Total body: 0.02 mrem.
- Dimensions
 - Full-size table: 95 × 42 × 52 in. (242 × 107 × 133 cm).
 - Compact table: 71 × 40 × 52 in. (181 × 100 × 133 cm).
- Weight
 - Full-size table: 598 lbs (272 kg).
 - Compact table: 550 lbs (250 kg).
- Recommended dedicated floor space
 - Full-size table: 9 × 7 ft (2.7 × 2.1 m).
 - Compact table: 7 × 7 ft (2.1 × 2.1 m).
- Operating environmental temperature: 65° to 80°F (18° to 27°C).
- Operating environmental relative humidity: 30 to 75%, non-condensing.
- X-ray source: 134 kV; 0.75 mA for PA spine, proximal femur, and DualFemur™.
- X-ray filtration: Constant potential, cerium K-edge filter.
- X-ray beam geometry: Pencil beam.
- Detectors: NaI.
- Scan path: Rectilinear.
- Quality control: Automatic test program.
- Operation: IBM-compatible computer and printer.
- Accessories provided
 - PA spine positioner.
 - Proximal femur positioner.
 - Aluminum spine phantom.
- Options: DualFemur™ with positioner (not available on compact model), total body with body composition (not available on compact model), encapsulated phantom.

DPX-NT™

- Manufacturer: GE Medical Systems, Madison, WI.
- Technology: Dual-energy X-ray absorptiometry.

- Skeletal application(s)
 - PA spine.
 - Proximal femur.
 - DualFemur™.
 - Total body with body composition.
- Scan time
 - PA spine: 1 minute.
 - Proximal femur: 2 minutes.
 - DualFemur™: 4 minutes.
 - Total body: 8 minutes.
- Results
 - BMD (g/cm^2).
 - sBMD (mg/cm^2).
 - T-score and z-score.
 - NHANES III reference data.
 - WHO diagnostic classification.
- Precision
 - PA spine: 1.0%.
 - Proximal femur: 1.0%.
 - Total body: 1.0%.
 - DualFemur™: <1.0%.
- Radiation dose
 - PA spine: 3.0 mrem.
 - Proximal femur: 3.0 mrem.
 - Total body: 0.02 mrem.
- Dimensions: 95 × 42 × 52 in. (242 × 107 × 133 cm).
- Weight: 598 lbs (272 kg).
- Recommended dedicated floor space: 9 × 7 ft (2.7 × 2.1 m).
- Operating environmental temperature: 65° to 80°F (18° to 27°C).
- Operating environmental relative humidity: 30 to 75%, noncondensing.
- X-ray source: 134 kV; 1.5 mA for PA spine, proximal femur, and DualFemur™ (mA varies by skeletal site and scan mode).
- X-ray filtration: Constant potential, cerium cerium K-edge filter.
- X-ray beam geometry: Pencil beam.
- Detectors: NaI.
- Scan path: Rectilinear.
- Quality control: Automated QA program.
- Operation: IBM-compatible computer running Windows NT.
- Accessories provided
 - PA spine positioner.
 - Proximal femur positioner.

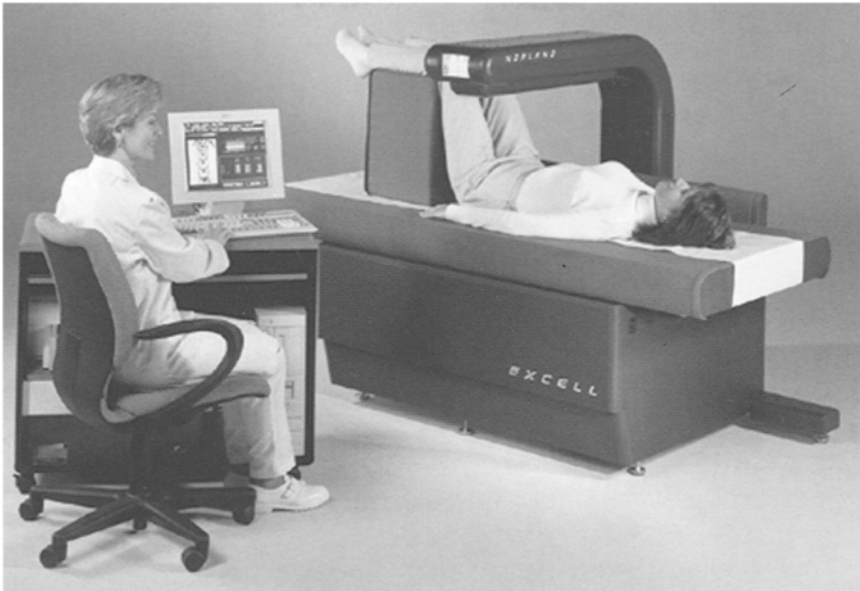


Fig. 4-9. Norland Excell™. A central pencil-beam dual-energy X-ray absorptiometer. (Photograph courtesy of CooperSurgical Norland, Trumbull, CT.)

- DualFemur positioner.
- Aluminum spine phantom.
- Options: Encapsulated phantom.

Excell™ (Fig. 4-9)

- Manufacturer: CooperSurgical Norland, Trumbull, CT.
- Technology: Dual-energy X-ray absorptiometry.
- Standard application(s)
 - PA spine.
 - Proximal femur.
- Scan time
 - PA spine: <1.5 minutes.
 - Proximal femur: <2 minutes.
- Results
 - BMD (g/cm^2).
 - BMC (g).
 - Length (cm).
 - % Young Reference and % Age-Matched comparisons.
 - T-score and z-score.
 - sBMD (mg/cm^2) for L2–L4 and total hip.

- NHANES III total hip comparisons.
- Fracture risk based on WHO diagnostic classification.
- Precision
 - PA spine: 1.0%.
 - Hip: 1.2%.
- Radiation dose: <1.0 mRem in high-speed scan mode.
- Dimensions: 72 × 48 × 49 in. (182.8 × 122.0 × 124.5 cm).
- Weight: 400 lbs (181 kg).
- Recommended dedicated floor space: 7 × 7 ft (2.1 × 2.1 m).
- Operating environmental temperature: 60° to 104°F (15° to 40°C).
- Operating environmental relative humidity: up to 80%, noncondensing.
- X-ray source: 100 kV, 1.3 mA.
- X-ray filtration: Samarium.
- X-ray beam geometry: Pencil-beam.
- Detectors: Two NaI scintillation detectors.
- Scan path: Rectilinear.
- Quality control: Automated with 77-step calibration standard and quality control phantom.
- Operation: IBM-compatible PC computer and HP DeskJet printer.
- Accessories provided
 - PA spine-positioning block.
 - Hip sling with foot separator.
 - 77-step calibration standard.
 - Quality control phantom.
- Options: Laptop computer.

Excell™plus

- Manufacturer: CooperSurgical Norland, Trumbull, CT.
- Technology: Dual-energy X-ray absorptiometry.
- Skeletal application(s)
 - PA spine.
 - Proximal femur.
 - Forearm.
 - Lateral spine.
- Scan time
 - PA spine: <1.5 minutes.
 - Proximal femur: <2 minutes.
 - Forearm: <3 minutes.
 - Lateral spine: <4 minutes.

- Results
 - BMD (g/cm^2).
 - BMC (g).
 - Length (cm).
 - % Young Reference and % Age-Matched comparisons.
 - T-score and z-score.
 - sBMD (mg/cm^2) for L2–L4 and total hip.
 - NHANES III total hip comparisons.
- Precision
 - PA spine: 1.0%.
 - Hip: 1.2%.
 - Forearm: 0.8%.
 - Lateral spine: 2.4%.
- Radiation dose
 - PA spine, proximal femur, and forearm: <1.0 mrem.
 - Lateral spine: <2 mrem.
- Dimensions: 72 × 48 × 49 in. (182.8 × 122.0 × 124.5 cm).
- Weight: 400 lbs (181 kg).
- Recommended dedicated floor space: 7 × 7 ft (2.1 × 2.1 m).
- Operating environmental temperature: 60° to 104°F (15° to 40°C).
- Operating environmental relative humidity: up to 80%, non-condensing.
- X-ray source: 100 kV, 1.3 mA.
- X-ray filtration: Samarium.
- X-ray beam geometry: Pencil-beam.
- Detectors: Two NaI scintillation detectors.
- Scan path: Rectilinear.
- Quality control: Automated with 77-step calibration standard and quality control phantom.
- Operation: IBM-compatible computer with Windows operating system, DeskJet printer, 15-in. SVGA monitor.
- Accessories provided
 - PA spine-positioning block.
 - Hip sling with foot separator for use in proximal femur studies.
 - Lateral and forearm positioning aids.
 - 77-step calibration standard.
 - Quality control phantom.
- Options: Software for research, small subject or body composition, laptop computer, flat screen monitor, 17-in. SVGA monitor.

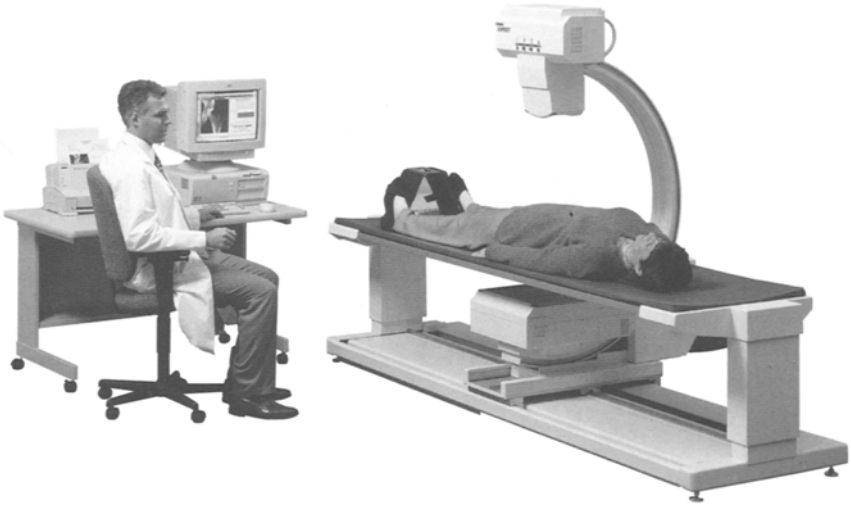


Fig. 4-10. GE Lunar Expert[®]-XL. A central fan-array dual-energy X-ray absorptiometer. (Photograph courtesy of GE Healthcare, Madison, WI.)

EXPERT[®]-XL (Fig. 4-10)

- Manufacturer: GE Medical Systems, Madison, WI.
- Technology: Dual-energy X-ray absorptiometry.
- Skeletal regions studied
 - PA spine.
 - Lateral lumbar spine.
 - Proximal femur.
 - Forearm and hand.
 - Total body.
 - Orthopedic hip.
 - Vertebral morphometry.
- Scan time
 - PA spine and proximal femur: 6 seconds.
 - Forearm/hand: 10 seconds.
 - Lateral spine: 24 seconds.
 - Total body: 160 seconds.
 - Vertebral morphometry: 38 seconds.
- Results
 - BMD (g/cm^2).
 - BMC (g).

- Area (cm²).
- % Young adult and % Age-Matched comparisons.
- T-score and z-score.
- Vertebral heights (mm) and vertebral height ratios.
- Precision: 1.0%.
- Radiation dose
 - PA spine and proximal femur: 27 mrem.
 - Forearm/hand: 12 mrem.
 - Lateral spine: 190 mrem.
 - Total body: 5 mrem.
 - Morphometry: 120 mrem.
- Dimensions: 108 × 71 in. (2.7 × 1.8 m). Motorized C-arm 140° rotation with 78 in. (198 cm) longitudinal travel and 14 in. (36 cm) transverse travel.
- Weight: 750 lb (340.2 kg).
- Recommended dedicated floor space: 12 × 10 ft (3.7 × 3.1 m).
- Operating environmental temperature: 65° to 80°F (18° to 27°C).
- Operating environmental relative humidity: 30 to 75%, noncondensing.
- X-ray source: 134 kV, 5 mA for PA spine, proximal femur, lateral spine, and morphometry.
- X-ray beam geometry: Fan-beam.
- Detectors: Dual-energy solid state.
- Scan path: Linear.
- Image resolution: 0.5 mm.
- Quality control: Internal hydroxyapatite and automated quality assurance program with spine phantom.
- Operation: IBM-compatible, Pentium-based computer; Windows operating system; SVGA monitor; black-and-white laser printer; handheld motor controller for C-arm rotation and table elevation.
- Accessories provided: Spine phantom.
- Options: Color printer and DICOM utilities.

Explorer™ (Fig. 4-11)

- Manufacturer: Hologic, Inc., Bedford, MA.
- Technology: Dual-energy X-ray absorptiometry.
- Skeletal regions studied
 - PA lumbar spine.
 - Proximal femur.
 - Dual Hip™.
 - Forearm.

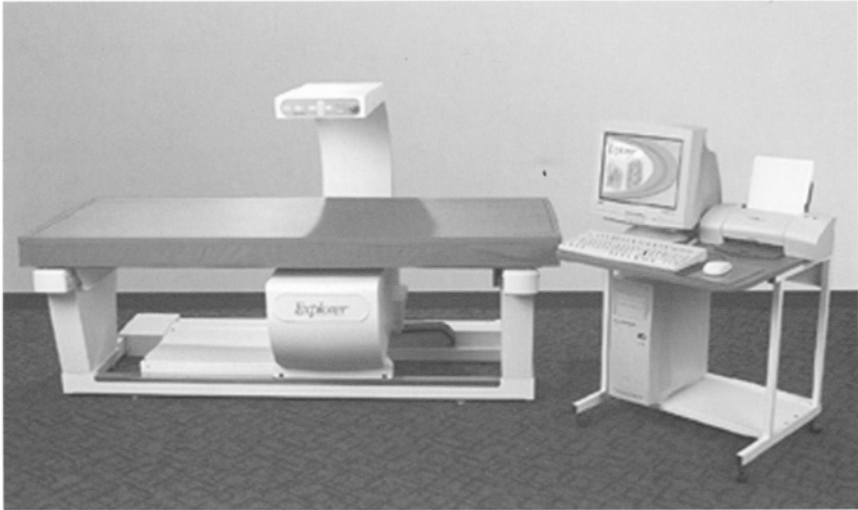


Fig. 4-11. Hologic Explorer™. A central fan-array dual-energy X-ray absorptiometer. (Photograph courtesy of Hologic, Inc., Bedford, MA.)

- Decubitus lateral spine.
- Whole body.
- Scan time
 - PA lumbar spine: 122–163 seconds.
 - Proximal femur: 92–123 seconds.
 - Forearm: 62 seconds.
 - Whole body: 6.7 minutes.
 - Decubitus lateral spine: 163 seconds.
- Results
 - BMD (g/cm^2).
 - BMC (g).
 - Area (cm^2).
 - T-score and z-score.
 - NHANES III reference data for hip.
- Precision: <1.0% for PA spine and proximal femur.
- Radiation dose (typical skin entrance dose)
 - PA spine: 0.07–0.25 mGy.
 - Proximal femur: 0.07–0.094 mGy.
 - Forearm: 0.05 mGy.
 - Whole body: 0.012 mGy.
 - Decubitus lateral spine: 0.25 mGy.
- Scan region dimensions at pad surface: 77.5 × 25.6 in. (1.97 × 0.65 m).

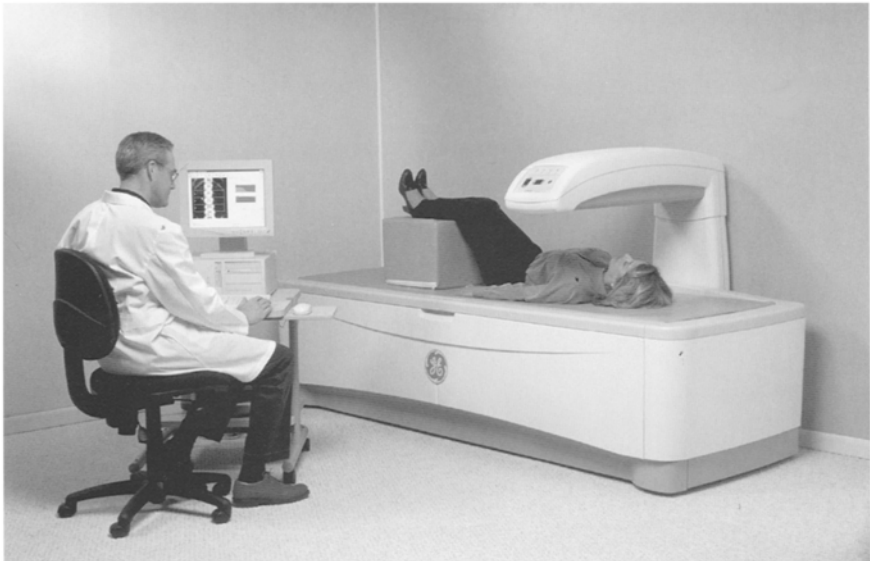


Fig. 4-12. GE Lunar Prodigy™. A central fan-array dual-energy X-ray absorptiometer. (Photograph courtesy of GE Healthcare, Madison, WI.)

- Weight
 - System: 720 lb (327 kg).
 - Console (Computer, Printer, and Monitor): 75 lb (34.1 kg).
- Scatter radiation: Nominal 10 mGy/hr at 3.3 ft (1.0 m) from the examination table.
- Operating environmental temperature: 59° to 90°F (15° to 32°C).
- Operating environmental relative humidity: 20 to 80%, noncondensing.
- Operating footprint: 119 × 59 × 56 in. (3.02 × 1.50 × 1.42 m).
- X-ray source: Switched pulse at 100 and 140kVp.
- X-ray beam geometry: Fan beam.
- Detectors: Multidetector array.
- Quality control: Self-calibrating with Hologic Automatic Internal Reference system and automated quality control program.
- Operation: IBM-compatible Pentium computer.
- Options: Multiple reporting options. Forearm, prosthetic hip, decubitus lateral spine, body composition, and subregion analysis, pediatric software.

Prodigy™ (Fig. 4-12)

- Manufacturer: GE Healthcare, Madison, WI.
- Technology: Dual-energy X-ray absorptiometry.

- Skeletal application(s)
 - PA spine.
 - Proximal femur.
 - DualFemur™.
 - Customized regions of interest with metal removal.
 - Total body and body composition.
- Scan time
 - PA spine and proximal femur: 30 seconds.
 - DualFemur™: 1 minute.
 - Total body: 5 minutes.
- Results
 - BMD (g/cm^2).
 - sBMD (mg/cm^2).
 - T-score and z-score.
 - Fracture risk assessment based on WHO diagnostic classification.
 - LUNAR® and NHANES III databases.
- Precision
 - PA spine and proximal femur: 1.0%.
 - DualFemur™: <1.0%.
 - Total body: <1.0%.
- Radiation dose
 - PA spine and proximal femur: 3.7 mrem.
 - Total body: 0.037 mrem.
- Dimensions: 103.5 × 43.5 × 50 in. (263 × 111 × 127 cm).
- Weight: 600 lbs (272 kg).
- Recommended dedicated floor space: 9 × 7.5 ft (2.8 × 2.3 m).
- Scatter radiation: <0.3mR/hr (3 $\mu\text{Sv}/\text{hr}$) at 39 in. (1 m).
- Operating environmental temperature: 65° to 80°F (18° to 27°C).
- Operating environmental relative humidity: 20 to 80%, non-condensing.
- X-ray source: 134 kV; 3.0 mA for PA spine, proximal femur, and Lateral Vertebral Assessment (mA varies by skeletal site and scan mode).
- X-ray filtration: Constant potential cerium K-edge filter.
- X-ray beam geometry: Narrow-angle fan-beam.
- Detectors: Cadmium-zinc-telluride (CZT).
- Scan path: Rectilinear.
- Quality control: Automatic test program with QA trending.
- Operation: Windows operating system on IBM-compatible Pentium computer, and printer.



Fig. 4-13. Hologic QDR® 4500 A. A central fan-array dual-energy X-ray absorptiometer. (Photograph courtesy of Hologic, Inc., Bedford, MA.)

- Accessories provided
 - PA spine positioner.
 - DualFemur™ positioner.
 - Aluminum spine phantom.
- Options: Pediatric, forearm, lateral spine, and LateralView™ software; encapsulated phantom.

QDR® 4500 A (Figs. 4-13 and 4-14)

- Manufacturer: Hologic, Inc., Bedford, MA.
- Technology: Dual-energy X-ray absorptiometry.
- Skeletal regions studied
 - PA spine.
 - Proximal femur.
 - Forearm.
 - Whole body.
 - Supine lateral lumbar spine.
- Scan time (in the 60-Hz scan mode)
 - PA lumbar spine and proximal femur: 10 seconds.
 - Lateral spine: 120 seconds.
 - Forearm: 30 seconds.
 - Whole body: 3 minutes.
 - Lateral imaging with morphometric X-ray absorptiometry (MXA): 7.5 seconds.

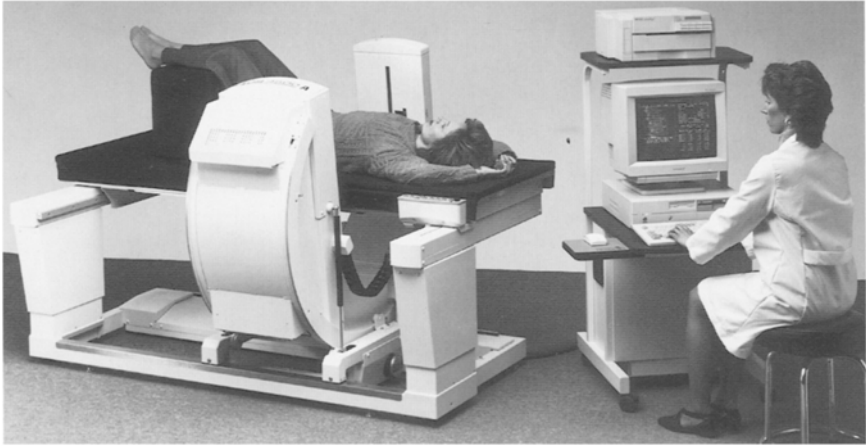


Fig. 4-14. Hologic QDR® 4500 A. The gantry is rotated to perform supine lateral lumbar spine studies. (Photograph courtesy of Hologic, Inc., Bedford, MA.)

- Results
 - BMD (g/cm^2).
 - BMC (g).
 - Area (cm^2).
 - % Young Adult and % Age-Matched comparisons.
 - T-score and z-score.
 - sBMD (mg/cm^2) for L2–L4 and total hip.
 - NHANES III total hip comparisons.
- Precision: <1%.
- Radiation dose (in the 60-Hz scan mode)
 - PA lumbar: 7 mR.
 - Proximal femur: 7 mR.
 - Lateral spine: 35 mR.
 - Forearm: 5 mR.
 - Whole body: 1 mR.
 - Lateral imaging with MXA: 7 mR.
- Dimensions: 79.5 × 41 × 28 in. (202 × 104 × 71 cm), 118.9 × 57 in. (302 × 145 cm) with C-arm rotated and table extended.
- Weight: 800 lb (364 kg).
- Recommended dedicated floor space: 8 × 10 ft (2.4 × 3.1 m).
- Scatter radiation: <1.0 mR/hr (0.01 mSv/hr) measured at 6.6 ft (2.0 m) from the examination table for most scan modes.
- Operating environmental temperature: 60° to 90°F (15° to 32°C).

- Operating environmental relative humidity: 20 to 80%.
- X-ray source: Switched pulse, dual energy.
- X-ray beam geometry: Fan-beam.
- Detectors: Multielement detector array.
- Scan path: Linear.
- Quality control: Self-calibrating with patented Hologic Automatic Internal Reference System and automated quality control program.
- Operation: IBM-compatible Pentium computer with Windows operating system, 17-in. monitor, HP LaserJet® black-and-white printer.
- Accessories provided: Anthropomorphic spine phantom.
- Options: Magneto optical disk storage, network configurations, body composition analysis software, MXA software, small animal software.

QDR® 4500 C

- Manufacturer: Hologic, Inc., Bedford, MA.
- Technology: Dual-energy X-ray absorptiometry.
- Skeletal application(s)
 - PA spine.
 - Proximal femur.
 - Forearm.
- Scan time (in the 60-Hz scan mode)
 - PA lumbar spine and proximal femur: 15 seconds.
 - Forearm: 30 seconds.
- Results
 - BMD (g/cm^2).
 - BMC (g).
 - Area (cm^2).
 - % Young Adult and % Age-Matched comparisons.
 - T-score and z-score.
 - sBMD (mg/cm^2) for L2–L4 and total hip.
 - NHANES III total hip comparisons.
 - Fracture risk and diagnostic classification based on WHO criteria.
- Precision: <1%.
- Radiation dose (in the 60-Hz scan mode)
 - PA lumbar spine: 5 mR.
 - Proximal femur: 5 mR.
 - Forearm: 10 mR.
- Dimensions: 79.5 × 41 × 28 in. (202 × 104 × 71 cm).
- Weight: 650 lb (296 kg).
- Recommended dedicated floor space: 8 × 8 ft (2.4 × 2.4 m).

- Scatter radiation: <1.0 mR/hr (0.01 mSv/hr) measured at 6.6 ft (2.0 m) from the examination table for most scan modes.
- Operating environmental temperature: 60° to 90°F (15° to 32°C).
- Operating environmental relative humidity: 20 to 80%, noncondensing.
- X-ray source: Switched pulse, dual energy, 140 V peak.
- X-ray beam geometry: Fan-beam.
- Detectors: Multielement detector array.
- Scan path: Linear.
- Quality control: Self-calibrating with patented Hologic Automatic Internal Reference System and automated quality control program.
- Operation: IBM-compatible Pentium computer with Windows operating system, 17-in. monitor, HP DeskJet® printer.
- Accessories provided: Anthropomorphic spine phantom.
- Options: Magneto optical disk storage, network configuration, HP LaserJet® black-and-white printer.

QDR® 4500 SL

- Manufacturer: Hologic, Inc., Bedford, MA.
- Technology: Dual-energy X-ray absorptiometry.
- Skeletal application(s)
 - PA spine.
 - Proximal femur.
 - Forearm.
 - Supine lateral lumbar spine.
- Scan time (in the 60-Hz scan mode)
 - PA lumbar spine and proximal femur: 10 seconds.
 - Lateral spine: 120 seconds.
 - Forearm: 30 seconds.
 - Lateral imaging with MXA: 7.5 seconds.
- Results
 - BMD (g/cm^2).
 - BMC (g).
 - Area (cm^2).
 - % Young Adult and % Age-Matched comparisons.
 - T-score and z-score.
 - sBMD (mg/cm^2) for L2–L4 and total hip.
 - NHANES III total hip comparisons.
- Precision: <1%.
- Radiation dose (in the 60-Hz scan mode)
 - PA lumbar spine: 7 mR.

- Proximal femur: 7 mR.
- Lateral spine: 35 mR.
- Forearm: 5 mR.
- Lateral imaging with MXA: 7 mR.
- Dimensions: 79.5 × 41 × 28 in. (202 × 104 × 71 cm), 79.5 × 57 in. (202 × 145 cm) with C-arm rotated and table extended.
- Weight: 800 lb (364 kg).
- Recommended dedicated floor space: 8 × 8 ft (2.4 × 2.4 m).
- Scatter radiation: <1.0 mR/hr (0.01 mSv/hr) measured at 6.6 ft (2.0 m) from the examination table for most scan modes.
- Operating environmental temperature: 60° to 90°F (15° to 32°C).
- Operating environmental relative humidity: 20 to 80%.
- X-ray source: Switched pulse, dual energy.
- X-ray beam geometry: Fan-beam.
- Detectors: Multielement detector array.
- Scan path: Linear.
- Quality control: Self-calibrating with patented Hologic Automatic Internal Reference System and automated quality control program.
- Operation: IBM-compatible Pentium computer with Windows operating system, 17-in. monitor, HP DeskJet® printer.
- Accessories provided: Anthropomorphic spine phantom.
- Options: Magneto optical disk storage, network configurations, HP LaserJet® black-and-white printer, MXA software.

QDR® 4500 W

- Manufacturer: Hologic, Inc., Bedford, MA.
- Technology: Dual-energy X-ray absorptiometry.
- Skeletal regions studied
 - PA spine.
 - Proximal femur.
 - Forearm.
 - Whole body.
- Scan time (in the 60-Hz scan mode)
 - PA lumbar spine and proximal femur: 15 seconds.
 - Forearm: 30 seconds.
 - Whole body: 6.8 minutes.
- Results:
 - BMD (g/cm²).
 - BMC (g).
 - Area (cm²).

- % Young Adult and % Age-Matched comparisons.
- T-score and z-score.
- sBMD (mg/cm^2) for L2–L4 and total hip.
- NHANES III total hip comparisons.
- Precision: <1%.
- Radiation dose (in the 60-Hz scan mode)
 - PA lumbar spine: 5 mR.
 - Proximal femur: 5 mR.
 - Forearm: 10 mR.
 - Whole body: 1.5 mR.
- Dimensions: $79.5 \times 48 \times 28$ ($202 \times 122 \times 71$ cm), $118.9 \times 59 \times 28$ in. ($302 \times 150 \times 71$ cm) with table extended.
- Weight: 680 lb (310 kg).
- Recommended dedicated floor space: 8×10 ft (2.4×3.1 m).
- Scatter radiation: <1.0 mR/hr (0.01 mSv/hr) measured at 6.6 ft (2.0 m) from the examination table for most scan modes.
- Operating environmental temperature: 60° to 90°F (15° to 32°C).
- Operating environmental relative humidity: 20 to 80%.
- X-ray source: Switched pulse, dual energy.
- X-ray beam geometry: Fan-beam.
- Detectors: Multi-element detector array.
- Scan path: Linear.
- Quality control: Self-calibrating with patented Hologic Automatic Internal Reference System and automated quality control program.
- Operation: IBM-compatible Pentium computer with Windows operating system, 17-in. monitor, HP DeskJet™ printer.
- Accessories provided: Anthropomorphic spine phantom.
- Options: Magneto optical disk storage, network configurations, HP LaserJet™ black-and-white printer, body composition analysis software.

XR-46™ (Fig. 4-15)

- Manufacturer: CooperSurgical Norland, Trumbull, CT.
- Technology: Dual-energy X-ray absorptiometry.
- Skeletal regions studied
 - PA spine.
 - Lateral spine.
 - Proximal Femur.
 - Forearm.
 - Whole body with soft tissue composition.



Fig. 4-15. Norland XR-46™. A central pencil-beam dual-energy X-ray absorptiometer. (Photograph courtesy of CooperSurgical Norland, Trumbull, CT.)

- Scan time
 - PA spine: <1.5 minutes.
 - Hip: <2 minutes.
 - Forearm: <3 minutes.
 - Lateral spine: <4 minutes.
 - Whole body: 5 minutes.
- Results
 - BMD (g/cm^2).
 - BMC (g).
 - % Young Reference and % Age-Matched comparisons.
 - T-score and z-score.
 - sBMD (mg/cm^2) for L2–L4 and total hip based on NHANES III reference data.
- Precision
 - PA spine: 1.0%.
 - Hip: 1.2%.
 - Forearm: 0.8%.
 - Lateral spine: 2.4%.
 - Whole-body BMD: 1%.
- Radiation dose
 - PA spine, hip, and forearm: <1.0 mrem.
 - Lateral spine: <5 mrem.
 - Whole body: <0.1 mrem.

- Dimensions: 103 × 48 × 51 in. (261.6 × 122.0 × 129.5 cm).
- Weight: 556.5 lbs (252.4 kg).
- Recommended dedicated floor space: 10 × 7 ft (3.1 × 2.1 m).
- Operating environmental temperatures: 60° to 90°F (15° to 32°C).
- Operating environmental relative humidity: Up to 80%, noncondensing.
- X-ray source: 100 kV, 1.3 mA.
- X-ray filtration: Eight-level automated samarium.
- X-ray beam geometry: Pencil-beam.
- Detectors: Two NaI detectors.
- Scan path: Rectilinear.
- Quality control: Automatic with supplied calibration standard and quality control phantom.
- Operation: IBM-compatible computer with HP color DeskJet® printer. DOS program with Microsoft® Windows resident.
- Accessories provided
 - 77-Step calibration standard.
 - Quality control phantom.
 - PA spine positioning block.
 - Hip sling with foot separator.
 - Lateral spine positioner.
 - Forearm positioner.
- Options: Flat panel display, 17 in. SVGA monitor, laptop configuration, research and small subject software.

PERIPHERAL X-RAY DENSITOMETERS

accuDEXA™ (Fig. 4-16)

- Manufacturer: Schick Technologies, Inc., Long Island City, NY.
- Technology: Dual-energy X-ray absorptiometry.
- Skeletal application(s): Middle phalanx of the long finger.
- Scan time: <1 minute.
- Results
 - BMD (g/cm^2).
 - % Young Adult and % Age-Matched comparisons.
 - T-score and z-score.
 - Diagnostic classification based on WHO criteria.
- Precision: <1%.
- Radiation dose: 0.0003 μSv .
- Dimensions: 14 × 15 × 14 in. (35.56 × 38.1 × 35.56 cm).

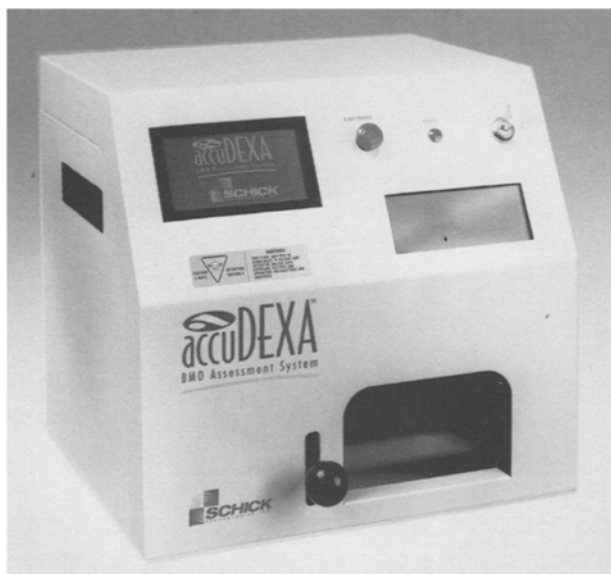


Fig. 4-16. Schick accuDEXA™. A peripheral dual-energy X-ray absorptiometer used to measure bone density in the phalanges. (Photograph courtesy of Schick Technologies, Inc., Long Island City, NY.)

- Weight: 66 lbs (29.7 kg).
- Environmental Operating Temperature: 70° to 85°F (21° to 29°C).
- Environmental Operating Relative Humidity: 20 to 80%.
- X-ray source
 - Low energy: 50 kVp, 0.5 mA.
 - High energy 70 kVp, 0.9 mA.
- X-ray filtration (high energy only): Zinc.
- Scatter radiation: 6.1 mR/hr at 1 m.
- Quality control: Automatic, no user intervention required.
- Operation: Data input with touch pad on the device, data output with printer supplied by user (list of compatible printers available from manufacturer).

Apollo™ (Fig. 4-17)

- Manufacturer: CooperSurgical Norland, Trumbull, CT.
- Technology: Dual-energy X-ray absorptiometry.
- Skeletal application(s): Calcaneus.
- Scan time: 15 seconds.



Fig. 4-17. Norland Apollo™. A peripheral dual-energy X-ray absorptiometer used to measure bone density in the calcaneus. (Photograph courtesy of CooperSurgical Norland, Trumbull, CT.)

- Results
 - BMD (g/cm^2).
 - BMC (g).
 - Area (cm^2).
 - % Young Reference and % Age-Matched comparisons.
 - T-score and z-score.
 - Fracture risk based on WHO diagnostic classification.
- Precision: 1.8%.
- Radiation dose: <0.2 mrem.
- Dimensions: $22.5 \times 17.5 \times 14$ in ($57.2 \times 44.5 \times 35.6$ cm).
- Weight: 64 lbs (29 kg).
- Operating environmental temperature: 50° to 90°F (10° to 32°C).
- Operating environmental relative humidity: 20 to 95%, noncondensing.
- X-ray source: 60kV, <0.3 mA.
- X-ray filtration: Tin.
- Detectors: Two solid state.

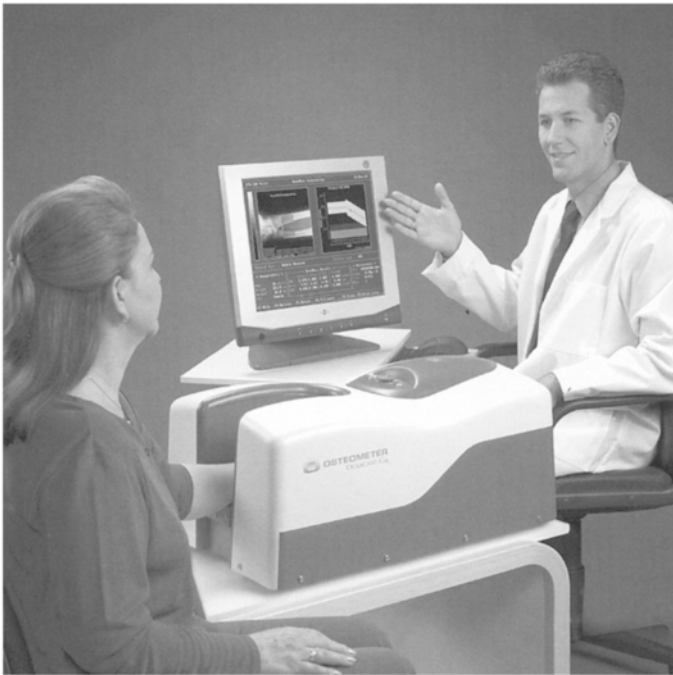


Fig. 4-18. Osteometer DEXaCare® G4. A peripheral dual-energy X-ray absorptiometer used to measure bone density in the forearm. (Photograph courtesy of Osteometer MediTech, Hawthorne, CA.)

- Quality control: Automatic with internal phantoms requiring <5 minutes.
- Operation: Handheld console with fluorescent display, unit on wheels with retractable handle, built-in floppy disk drive for data transfer, built-in parallel printer port for Canon BJC color printer or equivalent.
- Options: Laptop configuration.

DEXaCare® G4 (Figs. 4-18 and 4-19)

- Manufacturer: Osteometer MediTech, Inc., Hawthorne, CA.
- Technology: Dual-energy X-ray absorptiometry.
- Skeletal application(s): Forearm.
- Scan time: 2 minutes, distal forearm.
- Results
 - BMD (g/cm^2).
 - BMC (g), area (cm^2).



Fig. 4-19. Osteometer DEXACARE® G4. A peripheral dual-energy X-ray absorptiometer used to measure bone density in the forearm. The forearm is placed into the well on the top of the machine. (Photograph courtesy of Osteometer MediTech, Hawthorne, CA.)

- % Young adult and % Age-Matched comparisons.
- T-score and z-score.
- Precision: <1%.
- Radiation dose: 0.1 μSv per scan.
- Dimensions: 12.5 \times 26 \times 15.5 in. (32 \times 66 \times 40 cm).
- Weight: 49 lbs (22 kg).
- Environmental operating temperature: 58° to 86°F (15° to 30°C).
- X-ray source: 55 kV, 300 μA .
- X-ray filtration: K-edge filtration.
- Detectors: Solid state.
- Imaging resolution: 0.4 \times 0.4 mm.
- Scatter radiation: <0.25 $\mu\text{Sv/hr}$ at 1 m.
- Calibration system: Line-by-line internal reference calibration.
- Operation: IBM-compatible computer, HP DeskJet™ 600C or equivalent printer, VGA display.

DTX-200 DEXACARE® (Figs. 4-20 and 4-21)

- Manufacturer: Osteometer MediTech, Inc., Hawthorne, CA.
- Technology: Dual-energy X-ray absorptiometry.



Fig. 4-20. Osteometer DTX-200 DexaCare®. A peripheral dual-energy X-ray absorptiometer used to measure bone density in the forearm. (Photograph courtesy of Osteometer MediTech, Hawthorne, CA.)

- Skeletal application(s): Forearm.
- Scan time: 4.5 minutes.
- Results
 - BMD (g/cm^2).
 - BMC (g), area (cm^2).
 - % Young Adult and % Age-Matched comparisons.
 - T-score and z-score.
- Precision: <1%.
- Radiation dose: $0.1 \mu\text{Sv}$ per scan.
- Dimensions: $32 \times 24 \times 12$ in. ($80 \times 62 \times 30$ cm).
- Weight: 114 lbs (52 kg).
- Environmental operating temperature: 58° to 86°F (15° to 30°C).
- X-ray source: 55 kV, $300 \mu\text{A}$.
- X-ray filtration: Tin, K-edge filtration.
- Detectors: Solid state.



Fig. 4-21. Osteometer DTX-200 DexaCare®. The forearm is placed into the well in the top of the machine. (Photograph courtesy of Osteometer MediTech, Hawthorne, CA.)

- Imaging resolution: 0.4×0.4 mm.
- Scatter radiation: $<0.25 \mu\text{Sv/hr}$ at 1 m.
- Quality control: Automated with forearm phantom supplied by manufacturer.
- Operation: IBM-compatible computer, HP DeskJet™ 600C or equivalent printer, VGA monitor, unit on wheels for easy mobility.

pDEXA® (Fig. 4-22)

- Manufacturer: CooperSurgical Norland, Trumbull, CT.
- Technology: Dual-energy X-ray absorptiometry.
- Skeletal application(s): Forearm.
- Scan time: <5 minutes.
- Results
 - BMD (g/cm^2).
 - BMC (g).
 - Area (cm^2).
 - % Young Reference and % Age-Matched comparisons.
 - T-score and z-score.
- Precision: $<2.0\%$.
- Radiation dose: <1.5 mrem at high speed.
- Dimensions: $20.5 \times 17 \times 16.7$ in. ($52 \times 43 \times 42.5$ cm).
- Weight: 59.4 lbs (27 kg).

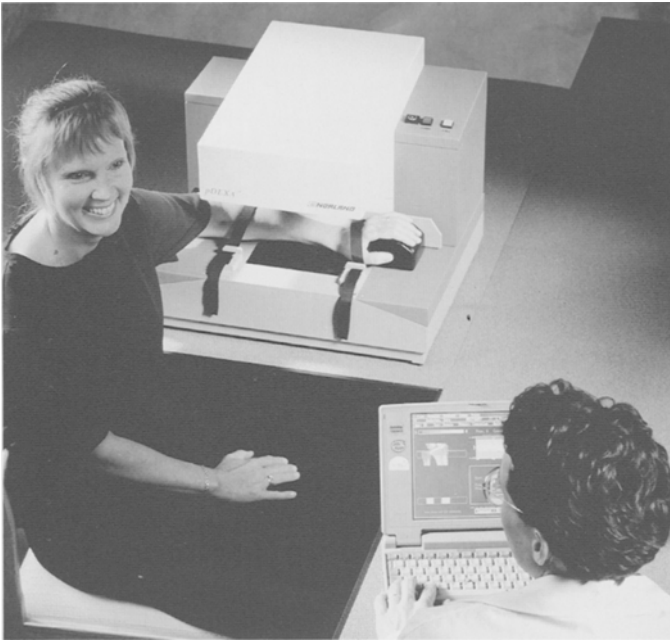


Fig. 4-22. Norland pDEXA[®]. A peripheral dual-energy X-ray absorptiometer used to measure bone density in the forearm. (Photograph courtesy of CooperSurgical Norland, Trumbull, CT.)

- Environmental operating temperature: 60° to 82°F (15° to 28°C).
- Environmental operating relative humidity: up to 80%, noncondensing.
- X-ray source: 60 kV, <0.3 mA.
- X-ray filtration: Tin.
- Detectors: Two solid state.
- Quality control: Automatic with manufacturer-supplied calibration standard and quality control phantom.
- Operation: IBM-compatible laptop computer with Windows operating system, HP DeskJet™ printer and mouse.
- Options: IBM-compatible desktop computer with Windows operating system, 15-in. SVGA monitor, 15-in. flat panel display, 17-in. SVGA monitor, HP DeskJet™ printer.

PIXI[®] (Peripheral Instantaneous X-ray Imager) (Fig. 4-23)

- Manufacturer: GE Medical Systems, Madison, WI.
- Technology: Dual-energy X-ray absorptiometry.
- Skeletal application(s): Calcaneus, forearm.



Fig. 4-23. GE Lunar PIXI®. A peripheral dual-energy X-ray absorptiometer shown here in the configuration used to measure bone density in the calcaneus. The device can be reconfigured and used to measure bone density in the forearm. (Photograph courtesy of GE Healthcare, Madison, WI.)

- Scan time: 5 seconds.
- Results
 - BMD (g/cm^2).
 - % Young Adult and % Age-Matched comparisons.
 - T-score and z-score.
- Precision: $<1.5\%$.
- Radiation dose: $0.032 \mu\text{Sv}$.
- Dimensions: $12 \times 25 \times 13$ in. ($30 \times 63 \times 33$ cm).



Fig. 4-24. Stratec XCT 2000™. A peripheral quantitative computed tomography device used to measure bone density in the forearm. (Photograph courtesy of CooperSurgical Norland, Trumbull, CT.)

- Weight: 66 lb (<30 kg).
- Environmental operating temperature: 64° to 81°F (18° to 27°C).
- X-ray source: Cone-beam geometry, 250 μ A current.
- Image resolution: 0.2 \times 0.2 mm.
- Quality control: Aluminum os calcis and forearm phantoms supplied by the manufacturer.
- Operation: Laptop computer, printer.
- Options: Portable color printer, reusable hard shipping case, soft-sided portability case and cart.

XCT 2000™ (Fig. 4-24)

- Manufacturer: Stratec Medizintechnik, Pforzheim, Germany.
- Distributor: Orthometrix, Inc., White Plains, NY.
- Technology: Computerized tomography.
- Skeletal application(s): Forearm.
- Scan time: 80 seconds.

- Results: BMD (mg/cm^3) for total bone and trabecular and cortical compartments.
- Precision: $\pm 3 \text{ mg}/\text{cm}^3$ for trabecular bone; $\pm 9 \text{ mg}/\text{cm}^3$ for cortical bone.
- Radiation dose: 0.03 mSv per scan.
- Dimensions: $21.7 \times 36.6 \times 24.4 \text{ in.}$ ($55 \times 93 \times 62 \text{ cm}$).
- Weight: $<100 \text{ lbs}$ ($<45 \text{ kg}$).
- X-ray source: 55 to 60 kV, $<0.3 \text{ mA}$.
- Detectors: 12 semiconductor detectors with amplifiers.
- Operation: Pentium computer, monitor, and color printer.
- Options: Magneto opticals for data backup.

ULTRASOUND BONE DENSITOMETERS

Achilles+™ (Figs. 4-25 and 4-26)

- Manufacturer: GE Medical Systems, Madison, WI.
- Technology
 - Ultrasound.
 - Transmitted through bone.
 - Wet.
- Skeletal application(s): Calcaneus.
- Scan time: 1 minute.
- Results
 - Speed of Sound (SOS) (m/sec).
 - Broadband ultrasound attenuation (BUA) (db/MHz).
 - Stiffness Index.
 - % Young-Adult and % Age-Matched comparisons.
 - T-score and z-score.
- Precision: 2.0% for Stiffness Index.
- Dimensions: $20 \times 13 \times 24 \text{ in.}$ ($51 \times 33 \times 61 \text{ cm}$).
- Weight: 44 lbs (20 kg).
- Operating environmental temperature: 59° to 95°F (15° to 35°C).
- Operating environmental relative humidity: 20 to 80%.
- Operation: Self-contained LCD touch screen, thermal printer, 50-measurement memory, built-in carrying handle.
- Accessories provided
 - Water-soluble ultrasonic gel.
 - Premeasured surfactant.
- Options: Laptop computer, external printer.



Fig. 4-25. GE Lunar Achilles+™. A peripheral quantitative ultrasound device used to measure the calcaneus, shown here in the closed position. (Photograph courtesy of GE Healthcare, Madison, WI.)

Achilles Express™ (Fig. 4-27)

- Manufacturer: GE Medical Systems, Madison, WI.
- Technology
 - Ultrasound.
 - Transmitted through bone.
 - Dry.
- Skeletal application(s): Calcaneus.
- Scan time: 1 minute.
- Results
 - Stiffness Index.
 - % Young Adult and % Age-Matched comparisons.
 - T-score and z-score.
- Precision: 2.0%.
- Dimensions: 10 × 12 × 24 in. (25 × 31 × 61 cm).
- Weight: 22 lbs (10 kg).
- Operating environmental temperature: 59° to 95°F (15° to 35°C).
- Operating environmental relative humidity: 20 to 80%.
- Operation: Self-contained LCD swiveling touch screen, thermal printer, 100-measurement memory; built-in carrying handle.
- Accessories: Water-soluble ultrasonic gel.

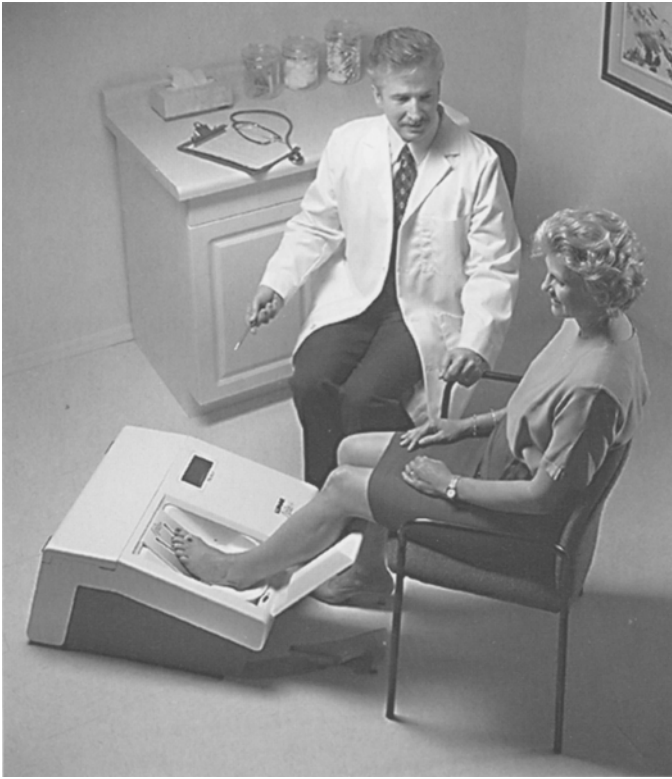


Fig. 4-26. GE Lunar Achilles+™. A peripheral quantitative ultrasound device used to measure the calcaneus, shown here in use. (Photograph courtesy of GE Healthcare, Madison, WI.)

Achilles InSight™ (Fig. 4-28)

- Manufacturer: GE Medical Systems, Madison, WI.
- Technology
 - Ultrasound.
 - Transmitted through bone.
 - Dry.
- Skeletal application(s): Calcaneus.
- Scan time: 15 seconds.
- Results
 - Stiffness Index.
 - % Young Adult and % Age-Matched comparisons.
 - T-score and z-score.
 - WHO classification.



Fig. 4-27. GE Lunar Achilles Express™. A peripheral quantitative ultrasound device used to measure the calcaneus. (Photograph courtesy of GE Healthcare, Madison, WI.)



Fig. 4-28. GE Lunar Achilles InSight™. A peripheral quantitative ultrasound device used to measure the calcaneus. (Photograph courtesy of GE Healthcare, Madison, WI.)



Fig. 4-29. GE Lunar InSight™. A peripheral quantitative ultrasound device used to measure the calcaneus, shown in use. (Photograph courtesy of GE Healthcare, Madison, WI.)

- Heel image.
- Reference graph.
- Precision: <2.0% coefficient of variation (CV).
- Dimensions: 10 × 12 × 24 in. (25 × 31 × 61 cm).
- Weight: 22 lbs (10 kg).
- Operating environmental temperature: 59° to 95°F (15° to 35°C).
- Operation: Self-contained LCD swiveling touch screen, thermal printer, 100-measurement memory; built-in carrying handle. No gel required.
- Options: External computer, external color printer, Windows XP user interface, PC software.

DTU-one UltraSure® (Figs. 4-30 and 4-31)

- Osteometer MediTech, Inc., Hawthorne, CA.
- Technology
 - Imaging ultrasound.
 - Transmitted through bone.
 - Wet.



Fig. 4-30. Osteometer DTU-one UltraSure®. A peripheral quantitative ultrasound device used to measure the calcaneus. (Photograph courtesy of Osteometer MediTech, Hawthorne, CA.)

- Skeletal application(s): Calcaneus.
- Scan time: 3 minutes.
- Results
 - SOS (m/sec).
 - BUA (dB/MHz).
 - % Young Adult and % Age-Matched comparisons.
 - T-score and z-score.
- Precision
 - SOS: 0.2%.
 - BUA: 1.6%.
- Dimensions: 21 × 11 × 17 in. (53 × 28 × 44 cm).
- Weight: 64 lbs (29 kg).
- Environmental operating temperature: 59° to 86°F (15° to 30°C).
- Image resolution: 0.6 mm.
- Quality control: Automated with supplied phantom.

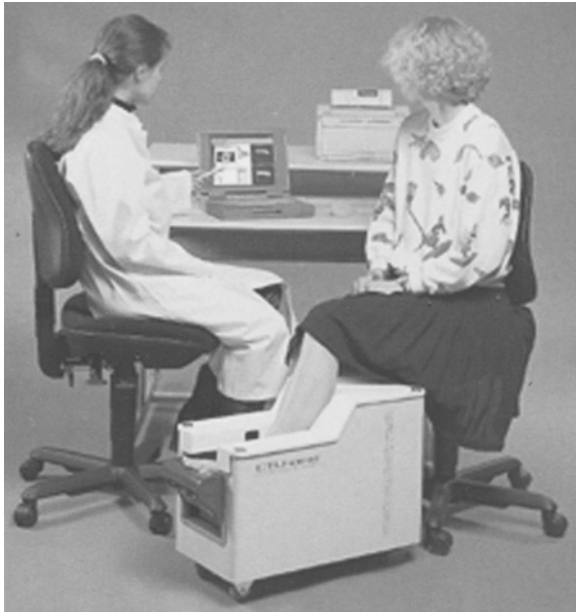


Fig. 4-31. Osteometer DTU-one UltraSure®. A peripheral quantitative ultrasound device used to measure the calcaneus, shown here in use. (Photograph courtesy of Osteometer MediTech, Hawthorne, CA.)

- Operation: IBM-compatible Pentium computer with Windows operating system, SVGA 15-in. monitor, printer.
- Accessories provided: Phantom.

McCue C.U.B.A. Clinical™ (Contact Ultrasound Bone Analyzer)
(Fig. 4-32)

- Distributor: CooperSurgical Norland, Trumbull, CT.
- Technology
 - Ultrasound.
 - Transmitted through bone.
 - Dry.
- Skeletal application(s): Calcaneus.
- Scan time: 1 minute.
- Results
 - BUA in db/MHz.
 - % Young Reference and % Age-Matched comparisons.
 - T-score and z-score.



Fig. 4-32. McCue C.U.B.A. Clinical™. A peripheral quantitative ultrasound device used to measure the calcaneus. (Photograph courtesy of CooperSurgical Norland, Trumbull, CT.)

- Precision: 1.3% for BUA.
- Dimensions: 17.8 × 13.9 × 10.2 in. (45.2 × 35.3 × 25.9 cm).
- Weight: 22 lb (10 kg).
- Environmental storage temperature: 23° to 122°F (−5° to 50°C).
- Environmental storage humidity: 10 to 95%.
- Quality control: Internal phantom and external QA phantom.
- Operation: IBM-compatible computer with a minimum of 10 MB free hard drive space, 486DX2 microprocessor at 66 MHz, 1.44 MB floppy disk drive, serial port, Windows 3.1 or higher (Windows NT not supported) and Microsoft® Windows supported printer (all computer equipment supplied by end user).
- Accessories provided
 - Padded carrying bag for C.U.B.A.
 - Padded carrying bag for QA phantom, QA phantom.
 - Bottle of ultrasound gel.
 - Two anatomical foot inserts.

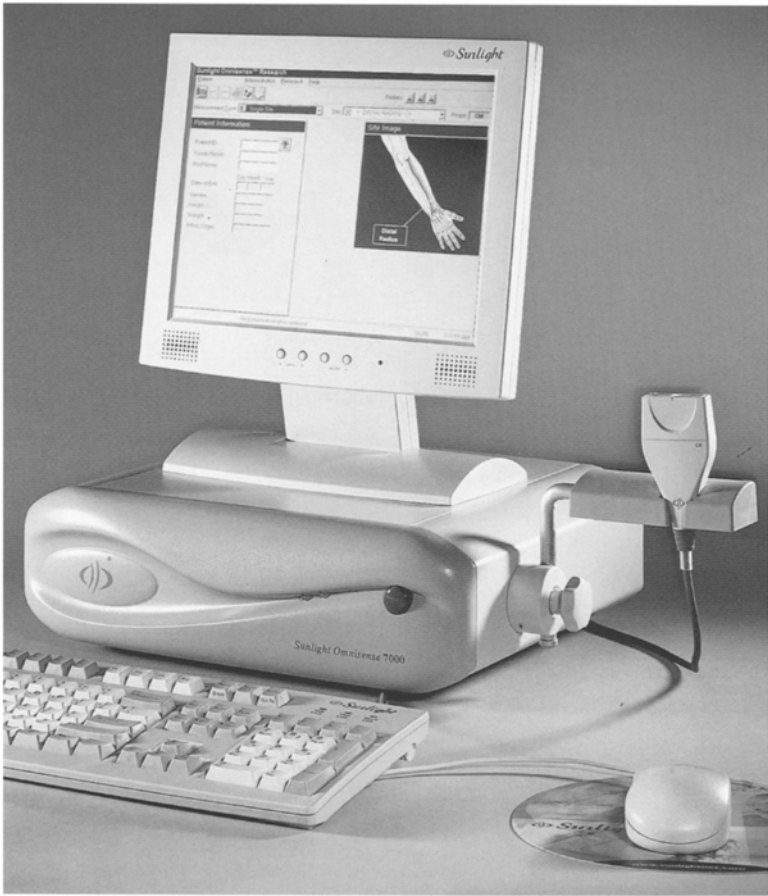


Fig. 4-33. Sunlight Omnisense™ 7000S. A peripheral quantitative ultrasound device used to measure the radius. (Photograph courtesy of Sunlight Medical Ltd., Rehovot, Israel.)

- C.U.B.A. plus+ software.
- Serial cable.
- Power cable.
- User's manual.

Omnisense™ 7000S Ultrasound Bone Sonometer (Figs. 4-33 and 4-34)

- Manufacturer: Sunlight Medical, Israel.
- Technology
 - Ultrasound.
 - Axially transmitted along bone.
 - Dry.



Fig. 4-34. Sunlight Omnisense™ 7000S. A peripheral quantitative ultrasound device used to measure the radius, shown here in use. (Photograph courtesy of Sunlight Medical Ltd., Rehovot, Israel.)

- Skeletal application(s): Distal radius, proximal phalanx (third finger), metatarsal.
- Scan time: Approximately 1 minute.
- Results
 - SOS (m/sec).
 - T-score and z-score.
- Precision: 0.4 to 0.8% as the root-mean-square %CV, depending on the site.
- Main unit dimensions: 15.4 × 5.1 × 13 in. (39 × 13 × 33 cm).
- Main unit weight: 15 lbs (7 kg).
- Operating environmental temperature: 50° to 95°F (10° to 35°C).
- Operating environmental relative humidity: 30 to 75%, noncondensing.



Fig. 4-35. Quidel QUS-2[®]. A peripheral quantitative ultrasound device used to measure the calcaneus. (Photograph courtesy of Quidel Corporation, Mountain View, CA.)

- Quality control: Calibration free. Daily system verification with phantom required.
- Operation: PC with Windows XP interface, 15 in. flat color display monitor, mouse or trackball, printer.
- Accessories provided
 - System quality verification phantom.
 - Aquasonic[®] Clear[®] Ultrasound Gel.
 - Hand rest.
 - Skin marker.
- Options: Mobile version also available.

QUS-2[®] Calcaneal Ultrasonometer (Fig. 4-35)

- Manufacturer: Quidel Corp., San Diego, CA.
- Technology
 - Ultrasound.
 - Transmitted through bone.
 - Dry.
- Skeletal application(s): Calcaneus.

- Scan time: Approximately 1 minute.
- Results
 - BUA (dB/MHz).
 - T-score.
- Precision: 2.6%.
- Dimensions: 7.5 × 16.0 × 9.0 in. (19.1 × 40.6 × 22.9 cm).
- Weight: 7 lbs (3.2 kg).
- Environmental operating temperature: 59° to 95°F (15° to 35°C).
- Environmental operating relative humidity: 30 to 75%, noncondensing.
- Quality control: Automated with supplied test object.
- Operation: Self-contained unit with messages displayed on LCD screen. Keyboard on unit allows data entry. Results printed by on-board printer. Foot size accommodated ranges from women's shoe size 5 to men's shoe size 12. Onboard storage capacity of approximately 8000 scan summary files. RS232 interface for download of scan data to a computer.
- Accessories provided
 - QUS-2 power supply.
 - Rechargeable battery.
 - AC cable.
 - Operator's manual.
 - Printer paper.
 - Aqueous gel.
 - Alcohol prep pads.
 - Test object.
- Options: Carrying case.

Sahara Clinical Bone Sonometer® (Figs. 4-36 and 4-37)

- Manufacturer: Hologic, Inc., Bedford, MA.
- Technology
 - Ultrasound.
 - Transmitted through bone.
 - Dry.
- Skeletal application(s): Calcaneus.
- Scan time: <10 seconds.
- Results
 - Estimated BMD (g/cm²).
 - Quantitative Ultrasound Index (QUI) obtained from BUA and SOS.
 - T-score and z-score.



Fig. 4-36. Hologic Sahara Clinical Bone Sonometer®. A peripheral quantitative ultrasound device used to measure the calcaneus. (Photograph courtesy of Hologic, Inc., Bedford, MA.)

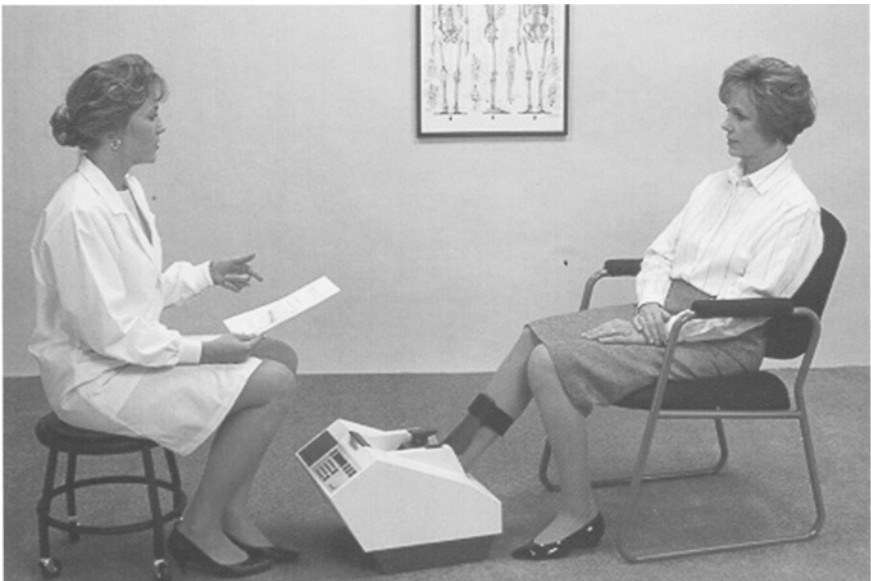


Fig. 4-37. Hologic Sahara Clinical Bone Sonometer®. A peripheral quantitative ultrasound device used to measure the calcaneus, shown here in use. (Photograph courtesy of Hologic, Inc., Bedford, MA.)

- Precision
 - BMD 3% or 0.014 g/cm².
 - QUI 2.6% or 2.2.
- Dimensions: 17 × 14 × 12 in. (43 × 36 × 30 cm).
- Weight: 22 lbs (10 kg).
- Environmental operating temperature: 60° to 100°F (15° to 37.7°C).
- Environmental operating relative humidity: 20 to 80%, noncondensing.
- Quality control: Daily, with supplied quality control phantom.
- Operation: Embedded microprocessor. Data and command input from touch pad on unit. Built-in strip printer.
- Accessories provided
 - Quality control phantom.
 - Sahara coupling gel.
 - Alcohol wipes.
 - Patient report forms.
 - Operator training video.
- Options
 - Carrying case.
 - AC power cable.
 - Spare battery.

5

Computer Basics

CONTENTS

- TYPES OF COMPUTERS
 - DESKTOPS, TOWERS, MINITOWERS, AND LAPTOPS
 - PCS AND MACS
- MAJOR COMPONENTS OF A COMPUTER SYSTEM
 - IMPORTANT COMPONENTS INSIDE THE COMPUTER
 - HOUSING
 - INPUT DEVICES
 - OUTPUT DEVICES
- COMPUTER PORTS
 - KEYBOARD AND MOUSE PORTS
 - PARALLEL PORTS
 - SERIAL PORTS
 - UNIVERSAL SERIAL BUS PORTS
 - POWER, MONITOR, MODEM, AND NETWORK PORTS
- TYPES OF STORAGE MEDIA
 - MAGNETIC MEDIA
 - OPTICAL STORAGE MEDIA
 - FLASH MEMORY
- PROTECTING THE DATA
- COMPUTER MAINTENANCE

A basic knowledge of computer components, terminology, and functions is not only desirable for a technologist but absolutely necessary in the practice of densitometry today. Appendix XI is a glossary of computer terms that should be part of the vocabulary of the densitometry technologist. In the 21st century, dual X-ray absorptiometry (DXA), single X-ray absorptiometry (SXA), and ultrasound devices are computer-driven. Even techniques such as some forms of radiographic absorptiometry and radiogrammetry that require plain skeletal radiographs utilize computer systems with special software to analyze the films. Some peripheral X-ray and ultrasound devices are self-contained; that is, the computer and bone

densitometer are blended into one machine. Many of these devices can be configured to operate with a separate computer if the technologist so desires. The use of a separate computer may be desirable when there is a need to store data on a large number of patients for an indefinite period of time. The computers that control the operation of X-ray densitometers are considered by the Food and Drug Administration (FDA) to be the X-ray controllers. Consequently, the computer systems that are used to operate X-ray bone densitometers are sold as part of a package with the densitometer itself. In fact, using a nondensitometry manufacturer-supplied computer to operate an X-ray densitometry system is a violation of FDA regulations. With that said, there is generally nothing special about the computers used to operate densitometers that distinguishes them from a computer that might be found in someone's home.

TYPES OF COMPUTERS

Desktops, Towers, Minitowers, and Laptops

Personal computers are often called desktops or towers, depending on the size and shape of the computer housing. A desktop computer, as the term implies, is a computer that can comfortably be placed on top of a desk. The term also implies, however, that the computer housing is deeper and wider than it is tall. A tower is a computer that is much taller than it is wide, as shown in Fig. 5-1. A minitower is not quite as tall, but it will still be more tall than wide. Towers and minitowers are usually placed on the floor, although some minitowers are placed on top of a desk. One style of computer housing is not necessarily better than the other. A laptop computer is a portable computer that opens like a notebook to reveal the monitor screen and keyboard. Most laptops will weigh 7 lbs or less. As laptop technology has improved, the monitor screens on laptops have approached the size of the small screens on monitors used with desktop and tower personal computers. The keyboard on a laptop is necessarily smaller than the full size keyboards that accompany desktop or tower computers. For the data entry required in performing densitometry, this smaller keyboard generally presents no problems. When typing large amounts of text, however, the full size keyboard is unquestionably easier to use. Many peripheral densitometers can be purchased with either desktop or tower computers or laptops. If portability in the peripheral densitometer is important, a laptop computer instead of a desktop or tower is preferable.

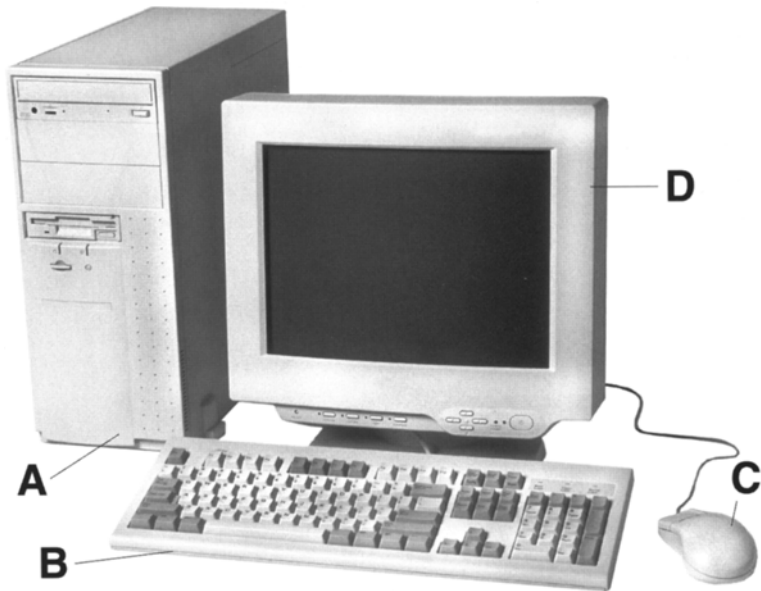


Fig. 5-1. Basic computer system. This is a tower computer (A) with a flat panel display monitor (D), keyboard (B), and mouse (C). (Photograph[®] Hemera Technologies, Inc.)

PCs and Macs

In addition to being characterized based on the size and shape of the computer housing, personal computers are also characterized by their operating system. In today's personal computer world, the computers are generally either PCs or Macs. Although *PC* is actually the abbreviation for personal computer, it has become synonymous with an IBM-compatible computer in which the operating system of the computer was either the character-based PC-DOS or MS-DOS. Mac is short for the Macintosh operating system found in computers manufactured by Apple. The Macintosh operating system employs a graphical user interface (GUI) that distinguishes it from the character-based PC-DOS or MS-DOS. Although most PCs now employ the graphical user interface known as Windows, distinct differences exist between the Macintosh and Windows operating systems. Peripheral devices, software utilities, and applications may run on a computer utilizing one type of operating system but not the other. Diskettes must be formatted for one type of system or the other. The computers utilized in densitometry are generally IBM-compatible computers or PCs that utilize DOS or Windows.

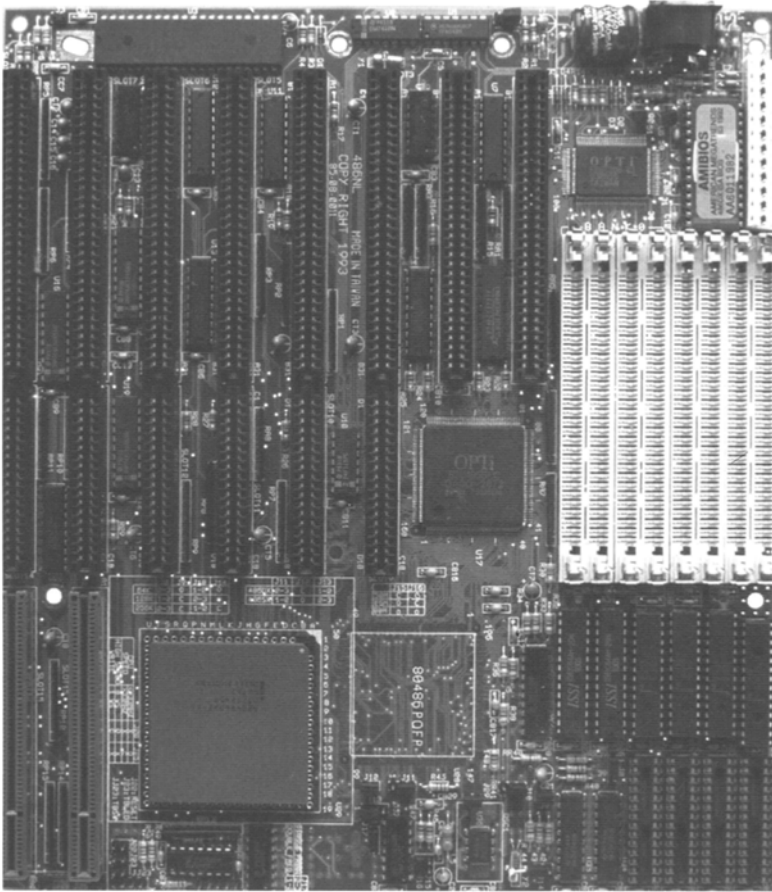


Fig. 5-2. Computer motherboard. (Photograph[®] 2000 IMS Communications Ltd: www.picture-gallery.com.)

MAJOR COMPONENTS OF A COMPUTER SYSTEM

A basic computer system is shown in Fig. 5-1. It is customary to refer to all the various devices as a whole as the computer, but the term *computer* really refers only to device A in Fig. 5-1. The keyboard is device B and the mouse is device C. The keyboard and mouse are both *input* devices because they are used to “input” information into the computer. Device D is the monitor. The monitor, keyboard, and mouse are called *peripherals*. Any device that is attached to the computer by a cable or communicates with a computer using radio waves or infrared waves can

legitimately be called a peripheral device, including a bone densitometer. All of the physical components of a computer system are collectively called *hardware*. This is in contrast to *software*, which refers to the computer programs such as operating systems, utilities, and applications.

Important Components Inside the Computer Housing

MOTHERBOARD, RANDOM ACCESS MEMORY, AND SLOTS

The motherboard found inside the computer housing is illustrated in Fig. 5-2. The motherboard is the main circuit board in the computer. On the motherboard is the microprocessor or central processing unit (CPU) and all the microcircuitry that carries information from the microprocessor to the other components. The hard drive and internal disk drives will also be found here. The random access memory (RAM) is located on the motherboard as well. Depending on the particular type of computer, the RAM will be comprised of small boards called SIMMS, DIMMS, or SDRAM. There may be more than one of these, grouped together, depending on the amount of memory found in the computer. There are also slots, called ISA or PCI slots as shown in Fig. 5-2. Cards can be inserted into these slots to attach different types of peripheral devices to the computer. An ISA card is shown in Fig. 5-3. An internal modem card may be found inserted in a slot. Audio cards and video cards may also be present in various slots. A number of cables will be found on the motherboard, through which the various drives communicate with the CPU.

CENTRAL PROCESSING UNITS

The CPU, as previously noted, is found on the motherboard inside the computer housing. It is the brain of the computer. In one analogy, the CPU is like the conductor of a symphony orchestra. The conductor directs the interpretation of the music (the software programs) by the members of the orchestra (all the other components and attached peripheral devices). Without the conductor, there would be chaos in the orchestra. Without the CPU, the computer can do nothing. CPUs are also often called chips. Major manufacturers include Intel, AMD, and Cyrix. Each manufacturer has different kinds of chips with their own trade names such as Intel's well-known Celeron and Pentium IV chips and AMD's Athlon 64. CPUs are also characterized by their clock speed, generally measured in MHz or GHz. The clock speed reflects the electrical cycles per second sent to the CPU, which essentially controls the rate at which the CPU processes

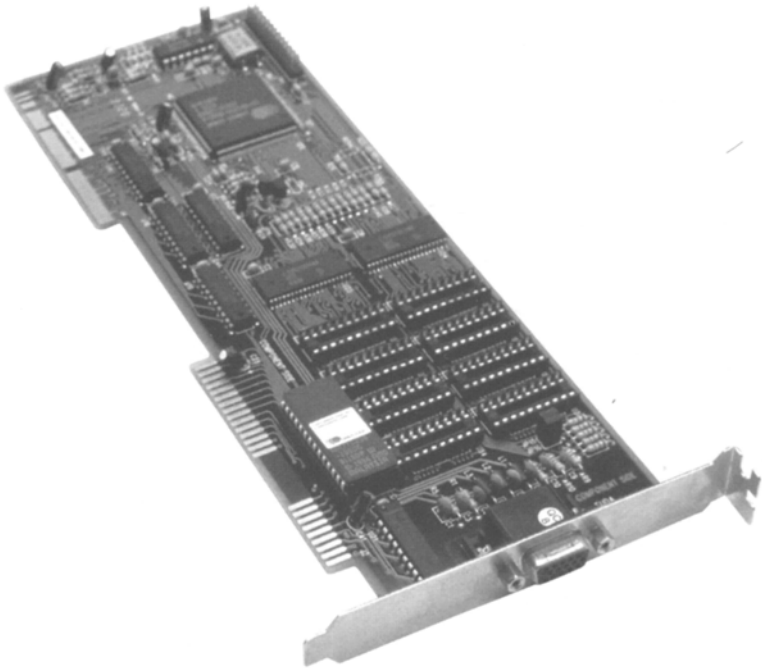


Fig. 5-3. ISA card. (Photograph[©] 2000 IMS Communications Ltd: www.picture-gallery.com.)

instructions. CPUs found in personal computers today commonly have speeds of 2 GHz or higher.

HARD DRIVES

The hard drive is the primary data storage medium inside the computer. Because it is inside the computer, it is considered a *fixed* or *internal* storage medium. Today's hard drives can hold an incredible amount of information. Some of the very first personal computers and laptops had hard drives of 20 to 40 MB. Fifteen years ago, this size hard drive was considered large. A small hard drive today is a 3-GB drive, which can hold 75 times more data than a 40-MB drive. Personal computers commonly have hard drives of 70 GB or more.

Unlike other disk drives and the magnetic or optical storage media they use, the term *hard drive* refers to both the drive that reads and writes the data as well as to the magnetic media to which the data is written. The hard drive itself is remarkably similar to an old record player. Inside the hard drive is a round, polished platter that has a magnetic coating. Much like an old 45 or 78 rpm record, the platter has concentric circles on it

called tracks that cover the entire surface. The platter is also divided into sectors, which are analogous to slices of pie. When the computer is powered up or *booted*, the platter begins to spin at extremely high speeds. Hanging over the platter is the drive actuator arm, which functions like the needle arm of an old record player. At the end of the drive actuator arm is a device called the read-write head. The head is normally separated from the platter by no more than 2 millionths of an inch and is never supposed to touch the platter. To put this in perspective, a human hair is about 10 millionths of an inch thick. Data is written to the hard drive by an electric current that comes through the write head on the actuator arm and is transmitted to the magnetic coating on the platter. The hard drive is usually assigned the capital letter *C* in computer terminology.

INTERNAL DISK DRIVES

The internal disk drives are drives that are contained within the computer housing, but that will open externally to allow the user to insert a diskette or other type of removable storage media into the drive. In this case, the term *disk drive* refers only to the drive and not to the storage media that is used by the drive. Before the advent of zip disks and compact disks (CDs), internal disk drives accommodated diskettes that were either 3½-in. or 5¼-in. square. Whichever disk drive was uppermost in the computer housing was assigned the lowercase letter *a* and the other drive was assigned the lowercase letter *b*. The 5¼-in. diskettes are no longer used. Consequently, the 5¼-in. disk drive has largely disappeared from today's computers. The disk drive for 3½-in. diskettes is still traditionally assigned the letter *a*, however, even if it is not the uppermost drive in the computer housing.

There are internal drives for other types of magnetic storage media as well. Zip drives read and write data on zip disks, tape drives read and write data on magnetic tape, and super floppy drives read and write data on super floppies as well as standard floppies. Optical drives employ a laser to read indentations or pits on a compact disk. The pits reflect varying degrees of light, which are translated into information that the computer can understand. A CD-ROM drive that will read data or play audio from a CD-ROM is a type of optical drive. Some of the newest internal optical drives are CD-R and CD-RW drives, which will not only read data and play audio from CD-ROM disks but also read and write data and audio on a new type of CD, called either a CD-R or CD-RW. In a CD-R or CD-RW drive, the laser actually heats a dye on the CD, causing less light to be reflected at that location. The effect is the same as the pit created on a



Fig. 5-4. External zip drive and zip disk. (Photograph[®] Hemera Technologies, Inc.)

CD-ROM. The differences in light reflectivity are translated into digital information when the disk is read.

These magnetic and optical drives are assigned letters of their own, which can be any letter other than *C* or *a*. If these drives are not present inside the computer housing, but instead are attached to the computer by a cable, they are called external disk drives. An external zip drive is shown in Fig. 5-4.

Input Devices

THE KEYBOARD

The basic layout of the alphabetical and numeric keys on the computer keyboard shown in Fig. 5-5 is the same as found on old QWERTY typewriters. The keys of the QWERTY typewriter account for only 54 of the 104 keys found on standard computer keyboards. The keys on the top row of the keyboard are called *function keys*. They are numbered F1 through F12. These keys have different actions depending on the software program being run. Other special keys found on the bottom row include the control key, abbreviated *Ctrl*, and the alternate key, abbreviated *Alt*. On laptop computer keyboards a Function key, abbreviated *Fn*, is also found. These



Fig. 5-5. Computer keyboard. (Photograph©Hemera Technologies, Inc.)

keys are depressed in combination with other keys in order to initiate a particular action. Another special key is the Escape key, abbreviated *Esc*, found on the top row on the far left. This key, when depressed, will generally stop an action or return the user to the previous viewing screen. In one densitometry manufacturer's software program, however, the *Esc* key is used to advance the user to the next screen in the program. There are three other groups of keys, which are normally set apart from the alphabetical and numeric keys on a full size keyboard. On laptop keyboards, these separate groups may be absent, but their functions are replicated by depressing certain alphabetical keys in combination with the *Fn* key. The first group is simply a separate set of numeric keys and functions as found on a calculator. The second group are keys labeled *Page Up*, *Page Down*, *Insert*, *Delete*, *Home*, and *End*. These keys, again, will have different functions depending on the software program being run. Finally, there is a group of keys called *arrow keys*. This is a set of four keys with arrows pointing up, down, right, and left. These keys can be used in a variety of ways, depending on the software program being run, but generally will initiate some type of directional action. There are three special keys found on the bottom row of keyboards for computer systems using the Windows operating system. Two of these keys have the Windows logo on them and the third key has a document logo on it. Once again, these keys will have slightly different actions depending on the particular software being run. There are two other keys that are worth noting, only because they are so commonly confused. The backslash key, or “\” key, and the forward slash key, or “/” key, are often used in computer commands and web addresses. They mean very different things to a computer and must not be interchanged. In recent years, even more keys have been added to full-size computer keyboards. These keys usually have specific functions to facilitate use of the Internet.

THE MOUSE

In early computers all computer commands were character-based; that is, the commands were entered by typing characters found on the keyboard. The development of GUIs made it possible for a whole series of commands to be initiated by simply activating a single graphic symbol. This was simpler and faster than typing in a series of characters from the keyboard and also eliminated the need to be familiar with the location of the various keys. One simply needed a device that could be used to point to the graphic symbol on the screen and then activate it. This is exactly what is done with the mouse, labeled C in Fig. 5-1. It is used to point at the graphic symbol and then, by depressing a button on the mouse either once or twice in succession, the series of commands represented by the symbol will be initiated.

A mouse generally has two buttons, designated left and right. The left mouse button is the button most often used to initiate programs as well as other actions. The left mouse button will rest under the index finger of a right-handed person, making it easier to use. The right mouse button tends to be reserved for specialized actions that will differ depending on the program being run. It is usually possible to change which button is used for most functions if the user is left-handed and wishes to do so. Newer mice also have a wheel, which can be used in word processor and spreadsheet programs to move or scroll through documents quickly. This type of mouse is often called a *wheel mouse*.

THE TRACKBALL

Trackballs perform exactly the same function as mice. The arrow on the screen is moved by rolling the trackball within its holder rather than by moving a mouse across a surface. The advantage of a trackball is that the holder remains stationary no matter how much the trackball is moved, so the space required for a trackball is less than the space required for a mouse, which must be rolled around on a desktop surface. If desktop space is limited, a trackball may be preferable to a mouse. There are buttons on the trackball holder that mimic the left and right buttons on a mouse, and some new trackballs also have a wheel.

The keyboard and mouse or trackball are the main input devices for every computer. They will generally attach to the computer by a cable, each having a specialized connection or port on the back of the computer. There are keyboards and mice, however, that can use either radio waves or infrared waves to communicate with the computer, eliminating the need for a cable connection.

Output Devices

MONITORS

Monitors are peripheral output devices. Although much more emphasis is generally placed on the internal components of the computer system than the monitor, it is the monitor on which the work is displayed. A poor quality monitor can make working on an otherwise superb computer quite frustrating. Monitor sizes are described like televisions. The dimension that is given is the diagonal dimension in inches of the viewing area. Some manufacturers of monitors provide two measurements: the diagonal dimension of the screen and the diagonal dimension of the casing surrounding the screen. For example, a monitor may be described as a 19-in. monitor with a 17-in. viewable image size. This means that the diagonal dimension of the casing that surrounds the screen is 19-in. whereas the actual viewing screen has a diagonal dimension of 17-in. Equally important is the resolution of the display, which is usually described as the number of dots per square inch (dpi). A monitor with a resolution of 1024×768 is a monitor with a horizontal dpi of 1024 and a vertical dpi of 768. With higher resolutions, more information can be seen on any one screen. Dot pitch and vertical scan refresh rate are two other important characteristics of a monitor. The dot pitch in millimeters is the distance between two pixels of the same color on the monitor screen. The smaller the distance, the sharper the image. An example of a dot pitch measurement is 0.25 mm. The vertical scan refresh rate is the number of times per second that the entire screen is refreshed or renewed. This is measured in hertz (Hz). A higher refresh rate results in less screen dimming and flickering. An example of a vertical scan refresh rate is a measurement such as 48 to 120 Hz.

Conventional monitors employ cathode ray tube (CRT) technology in which magnetic fields control the patterns created by electrons on the viewing screen. New monitors employ liquid crystal display (LCD) technology. LCD technology was employed in the screens in laptops long before it was incorporated into full size monitors for personal computers. With LCD technology, the screen can be flat rather than curved, giving rise to the term *flat panel display* monitor. LCD screens employ active- or passive-matrix technology. Active-matrix technology is also called *thin film transistor* (TFT) technology. In TFT, transistors control each pixel on the screen making these screens much brighter and more colorful than passive-matrix technology. Flat-panel LCD monitors are smaller in overall size compared to CRT monitors with the same size screen. They weigh much less and require less space on the desktop. Prices have fallen

dramatically in the last several years for flat-panel monitors, making them attractive options to their larger CRT counterparts.

Monitors should be turned off when not in use, even if the computer is left on for some reason. In the past, it was imperative that the monitor be turned off to avoid an image being burned into the screen. This is no longer the case, but there is no justification for wasting the electricity. The screens should be kept clean but should only be cleaned with soft, lint-free, antistatic cloths. Depending on the location of the monitor and the lighting in the room, a glare screen may be helpful in improving viewing.

PRINTERS

Printers are peripheral output devices that usually communicate with the computer through the parallel port. Some of the earliest printers were dot-matrix and daisy-wheel printers, neither commonly used today. Dot-matrix printers printed characters as a series of dots. Daisy wheel printers used a wheel that rotated to print characters. Most printers in use today are inkjet or laser printers. Inkjet printers actually embed ink into the paper. These printers will use ink cartridges of various colors that must be replaced as the ink is consumed. Print and graphics quality with inkjet printers is excellent, although the use of poor quality paper can result in the ink bleeding into the paper, reducing the clarity of the text or image. Laser printers tend to be more expensive than inkjet printers. Laser printers use a laser beam to generate an image which is then transferred to paper by using an electrostatic charge to put toner or ink on the paper.

Several factors should be considered in purchasing a printer. Overall cost is always a consideration, but beyond that the resolution and speed of the printer should be considered as well. Printer resolution is given in dpi. This refers to how many dots can be placed in one square inch. For text, a resolution of 600 dpi is desirable. For graphics, a higher minimum resolution of 1200×600 dpi is preferred. Color pages take longer to print than black-and-white pages. Graphics generally take longer to print than text. With those basic tenets in mind, print speeds can vary by model, so the primary use of the printer should be considered before purchasing a printer. Most densitometry reports contain both text and graphics and some color as well as black text.

The system requirements, which will be found on the box containing the printer, should always be checked prior to the purchase. It is imperative that the printer be compatible with the operating system of the computer. Not all new printers today will work with all types of operating systems. This can be particularly problematic if the operating system is

Windows NT®, Windows 95® or even Windows 98®. The port required by the printer must also be available on the computer. Although the parallel port has traditionally been reserved for the printer connection, many new printers utilize a universal serial bus (USB) port. In the past, the cable that attached the printer to the computer was sold with the printer. This is no longer the case, so printer cables must be purchased separately. The printer specifications should be checked to determine what type of cable is recommended by the printer manufacturer. Depending on the system specifications, this may be a parallel cable or a USB cable. If the printer is purchased as part of the densitometry system, the printer cable should be supplied as part of the purchase.

COMPUTER PORTS

The various ports to which the cables from peripheral devices and the computer power cable attach are found on the back of the computer housing. Each type of port has a reasonably consistent appearance from computer to computer. Different devices will utilize the same type of port from computer to computer as well. Ports and the cable plugs that attach to them are typically described as being male or female, depending on whether they have pins or pin receptacles. Care must always be taken when attaching cable plugs to ports to ensure that the pins are correctly oriented to the pin receptacles to avoid bending the pins and permanently damaging either the port or cable plug.

Keyboard and Mouse Ports

As noted earlier, there are usually specific, dedicated ports for the keyboard and mouse cable. These ports are very similar in appearance and often next to each other. Care must be taken to ensure that the correct cable is plugged into the correct port. A typical keyboard or mouse port is shown in Fig. 5-6. This is a female port. The mouse port is often called a PS/2 port. This style port was originally introduced by IBM in its PS/2 line of computers and came to be known as a PS/2 port. This port has since become the standard style mouse port on all manufacturers' computers.

Parallel Ports

The parallel port, as illustrated in Fig. 5-7, is also a female port. It is called a parallel port because it is used by cables having parallel wires.

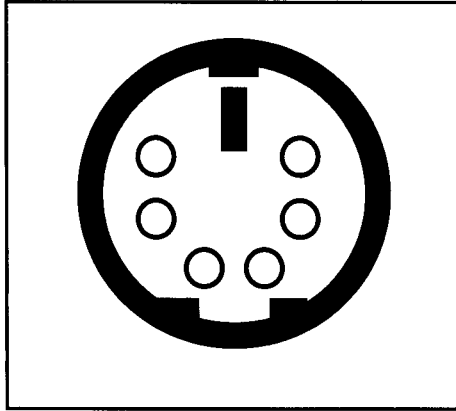


Fig. 5-6. Keyboard or mouse port. This is the standard PS/2 port. The keyboard and mouse each have its own port. Although identical in appearance, they are not interchangeable.

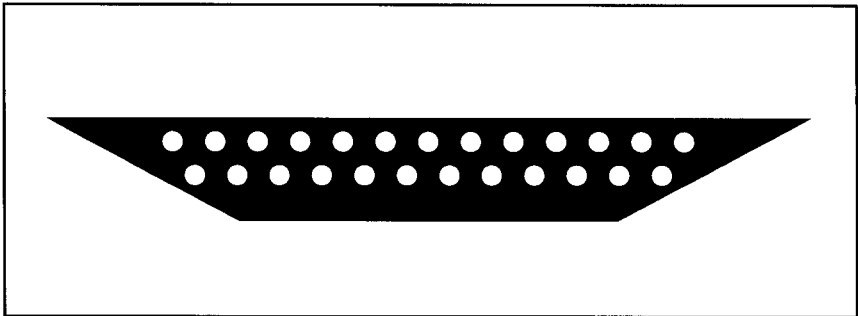


Fig. 5-7. Parallel port. Often used to connect printers to the computer, this is a 25-pin receptacle, female port.

Parallel ports generally have two rows of pin receptacles for a total of 25 receptacles. Parallel ports are commonly used to connect printers to the computer. Computers may have more than one parallel port, in which case the ports are designated as LPT1, LPT2, and so on.

Serial Ports

Serial ports are male ports, with two rows of pins totaling either 9 or 25, as shown in Fig. 5-8. Computers typically have more than one serial port, which are designated as COM1, COM2, and so on, as necessary. A variety of different devices may utilize a serial port. Bone densitometers generally communicate with the computer through a serial port. If a computer has a 9-pin serial port and a device requires a 25-pin serial port, an

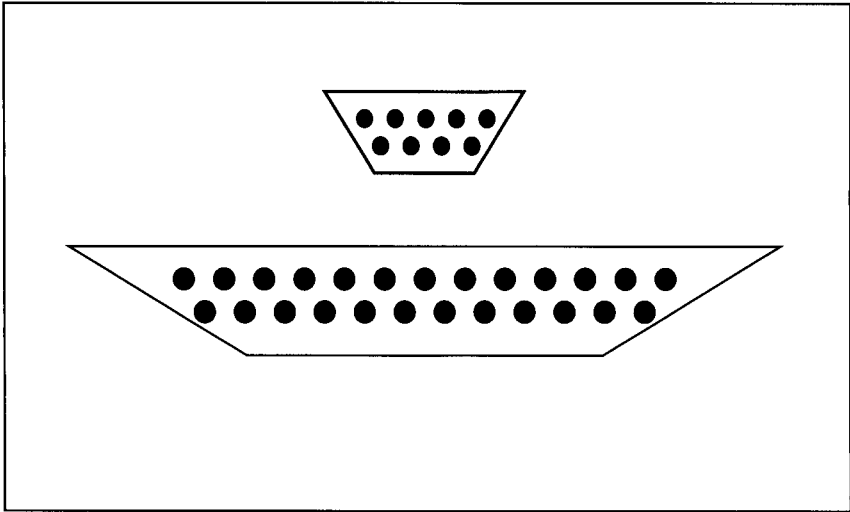


Fig. 5-8. 9-pin and 25-pin serial port. Densitometers often communicate with the computer through the serial port. Adapters can be purchased to change the 9-pin port to a 25-pin port or the 25-pin port to a 9-pin port.

adapter can be purchased that will convert the 9-pin port to a 25-pin port. The reverse is also true if a computer has a 25-pin port and a 9-pin port is required.

Universal Serial Bus Ports

The appearance of a USB port is quite different from parallel and serial ports as shown in Fig. 5-9. USB ports are designed to enable the computer to communicate with devices using USB architecture. USB is a different type of communication language that was intended to simplify the installation of various devices. It was thought that USB would replace the other bus architectures or languages used by peripheral devices that required special cards to be inserted into slots in the computer before the device could be attached to the computer. This has certainly not happened yet. USB ports are, however, increasingly being used to connect the printer to the computer, instead of the more traditional parallel port. This usually results in much faster transfer of data between the computer and printer.

Power, Monitor, Modem, and Network Ports

Other, perhaps more recognizable ports, are shown in Figs. 5-10 and 5-11. The power cord outlet port looks very much like a wall socket for any

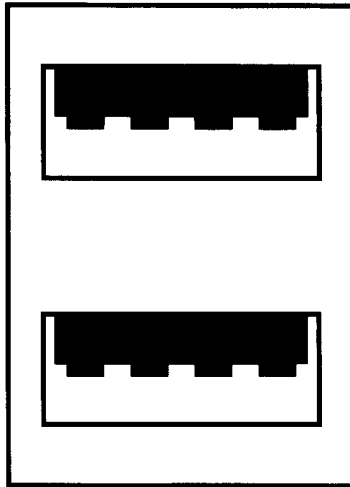


Fig. 5-9. Universal serial bus (USB) port. Many new peripheral devices utilize the USB port.

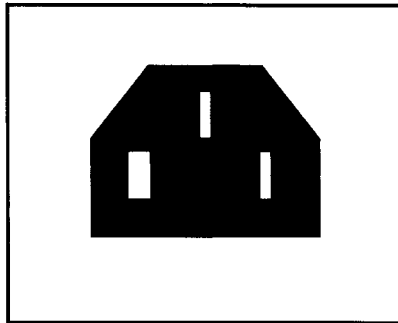


Fig. 5-10. Computer power cord port.

electrical cord. The modem port looks like the typical wall telephone jack. One end of the telephone cable is inserted into this port and the other end into the wall jack. The network interface port is very similar in appearance to the modem port but there are twice as many pin receptacles than found in the modem port. The network interface port is used to connect the computer to a network, rather than a telephone line. Care must be taken not to confuse the two communication ports as damage could result to both the port and telephone line. The monitor will also have its own port, shown in Fig. 5-12.

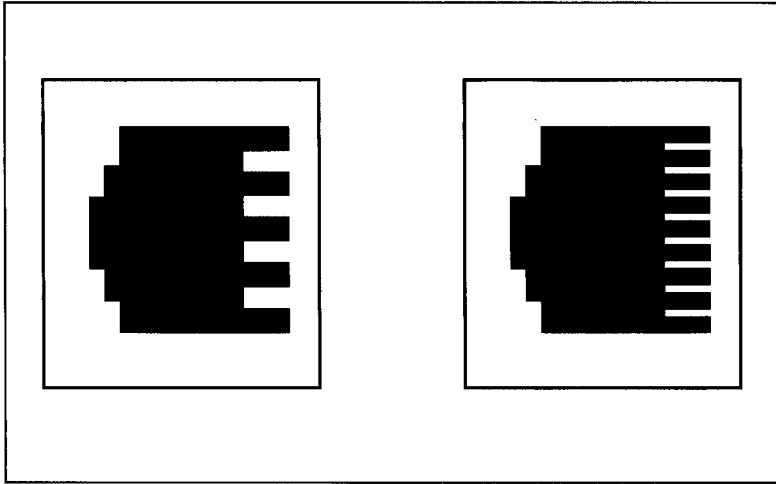


Fig. 5-11. Modem and network communication ports. These two ports are similar in appearance but the network port has twice as many pin receptacles as the modem port. Care must be taken not to confuse the two ports.

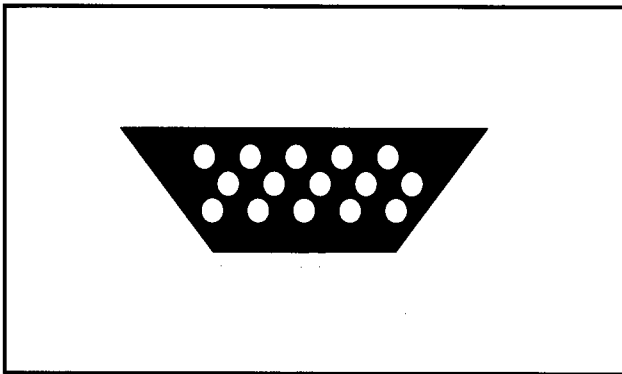


Fig. 5-12. VGA port. The monitor cable attaches here. This is a female port with three rows of pin receptacles.

TYPES OF STORAGE MEDIA

Storage media is the media onto which data is written. There are four basic types: magnetic, optical, tape, and flash. Some storage media is fixed and some is removable. Optical storage media is increasingly replacing magnetic media as removable storage media, but magnetic storage media



Fig. 5-13. Standard 1.44 MB, 3½-in. floppy disks. The designation HD can be seen in the upper right-hand corner. The read-write protect tab is seen on the lower left and is accessible from the back of the disk. (Photograph[®] Hemera Technologies, Inc.)

is still the mainstay for fixed data storage. Flash memory devices are rapidly increasing in popularity as removal storage media for laptop computers as well as desktop computers.

Magnetic Media

The hard drive is a type of magnetic storage media. The most common magnetic media is the floppy diskette, often simply called a floppy, shown in Fig. 5-13. In spite of the name, a standard floppy diskette is actually quite hard. It measures about $3\frac{1}{2} \times 3\frac{11}{16} \times \frac{1}{8}$ in. This size diskette is known as a 3½-in. floppy. The average 3½-in. floppy will hold 1.44 MB of data, but is called a 1-MB floppy in the vernacular. In the past, a similar physical size floppy diskette was available that would only hold 750 KB of data. These were called double-sided, double-density diskettes (DS, DD). The 1-MB diskettes were called double-sided, high-density diskettes (DS, HD), in order to distinguish them from the otherwise outwardly identical DS, DD disks. Today, most 3½-in. floppies that are sold are the 1-MB disks, but the HD designation on the diskette remains as shown in Fig. 5-13. Floppy diskettes come in all colors, besides basic

black. They also are generally preformatted for either IBM-compatible or Macintosh computers. In the past, diskettes were sold that were not formatted, requiring the user to do so before data could be written to the diskette. When formatted diskettes became available, they were slightly more expensive than nonformatted diskettes. Today, almost all 3½-in. diskettes that are sold are already formatted for either IBM-compatible or Macintosh computers. The type of computer for which they have been formatted will be noted on the box. Because most densitometer computers utilize IBM-compatible computers or PCs, they will also utilize IBM-formatted diskettes.

On the floppy diskette there are two physical items to inspect. There is metal door on each floppy that slides back to give the disk drive access to the magnetic media inside the diskette. This door should slide easily. If the door is bent or does not slide easily, it should not be used because it may damage the disk drive. The small tab on the back of the diskette at the bottom, called the *write-protect tab*, should be checked to ensure that it is in the proper position. In the up or write position, data can be written to the diskette. In the down or protect position, data cannot be written or erased from the diskette.

There is also a diskette called a *super floppy*. These are diskettes that are roughly the same size as the 3½-in. standard floppy, but hold 120 MB or more of data. To use super floppies, the computer must have a disk drive that is specifically designed for that type of super floppy. Such drives are also generally able to read standard 3½-in. 1-MB floppy disks. Super floppies are a type of magnetic storage media, although optical technology is used to read and write data to the diskette.

Floppy disks are commonly used in all computer applications. But because of the increasing demand for larger file storage capability, they are struggling to maintain their viability against the optical data storage devices discussed below. In fact, some computer manufacturers are no longer including floppy disk drives as part of the basic computer package. They can be added, but at an additional cost.

A zip disk is another type of diskette with a far greater storage capacity than a standard floppy, measuring roughly 3 7/8 in. square × 1/4 in. thick. A zip disk is shown in Fig. 5-4. Zip disks cannot be used in floppy disk drives. A specific zip drive must be available, either installed as an internal drive in the computer or attached to the computer as a peripheral device. Zip disks come in either 100-MB or 250-MB sizes. This means that one zip disk can hold an amount of data equivalent to 100 or 250 1-MB standard floppy diskettes. If the 250-MB zip disks are used, the

zip drive must be a 250-MB zip disk drive. This drive also reads the 100-MB zip disks. The 100 MB zip disk drive only reads 100-MB zip disks. Zip disk drives cannot read standard or super floppy disks. Like floppy diskettes, zip disks are preformatted for either IBM-compatible computers or Macs.

Super floppies and zip disks enable the storage of a much greater amount of data on one diskette when compared to a standard 1-MB floppy. They are more expensive than the standard 3½-in. floppy diskette, but the increase in price is generally proportional to the number of standard floppies that they replace. The upside is that they allow the user to store a great deal of information in one place. The downside is that they cost more per diskette, require specific disk drives, and, if damaged, result in the loss of a lot of information rather than a little. They are particularly useful for storing graphics files, which are often very large files, easily exceeding the 1-MB storage capacity of the standard floppy. Diskettes of any kind should never be stored near magnets or stereo speakers. They should be protected from extreme heat and never packed tightly together once used. They should not be left in disk drives when not in use. Although this is not necessarily bad for the diskette, it causes the drive door to remain open, unnecessarily exposing the drive to dust and other debris.

Magnetic tape is primarily used for backing up data, rather than routine data storage. Tape cartridges, somewhat larger than the standard audiocassette, come in a variety of storage sizes, ranging from several hundred MB to several GB. The tape drive can be either internal or external. Utilizing the tape drive and tape cartridge requires software designed to be used with the specific tape drive, unlike other magnetic storage media drives.

Optical Storage Media

CD-ROMs are compact disks from which data can only be read. Although a CD-ROM can hold an enormous amount of data, the user cannot write data to the CD. CD-Rs and CD-RWs are types of CDs to which the user can write data. The computer must have a CD-R or CD-RW drive to use this type of media. An enormous amount of data can be stored on a single disk, as much as 650 MB. The CD-writable or CD-R disk allows data to be written to it only once. The CD-rewritable or CD-RW disk can be erased and rewritten thousands of times. CD-R and CD-RW disks can be read by a regular CD-ROM drive. Similarly, a CD-R drive or a CD-RW drive can read CD-ROMs as well as CD-Rs and CD-RWs. The outward appearance of CD-Rs and CD-RWs is almost indistinguishable from that



Fig. 5-14. CD-ROM. The appearance of CD-R and CD-RW disks is basically identical. (Photograph© 2000 IMS Communications Ltd: www.picture-gallery.com.)

of the CD-ROM, shown in Fig. 5-14. The back of the CD-R or CD-RW disk, where the data is written, will reflect the color of the dye used on the disk.

CDs in general are very durable but they should always be handled by the edges to avoid damaging the read/write surface. Special cloths are available to clean dusty CDs to avoid scratching them. They should be stored in plastic cases when not in use. With proper care, the expected life span of a CD-RW disk is 30 years. For a CD-R, the expected life span is 100 years. Either way, the data on them should be preserved for a very long time.

Flash Memory

Flash memory devices are solid state electronic devices with no moving parts. Although some flash memory devices can be found inside the computer, flash memory devices that are removal memory storage devices have increased in popularity and utility in recent years. One of the most common types of flash memory is the Compact Flash card. This is a small card measuring approximately 43 mm wide × 36 mm long. A type I card is 3.3 mm thick and a type II card is 5.5 mm thick. This type of flash memory card can hold as much as 6 GB of data in spite of its very small size. Another type of flash memory card is a Smart Media card. This card is

also called a solid state floppy disk card. The Smart Media card resembles a miniature floppy disk. It measures approximately 45 mm long \times 37 mm wide, but it is less than 1 mm thick. This type of flash memory card holds less data than the compact flash card but considering its size, this may still be up to an impressive 128 MB.

Flash memory devices usually conform to standards set by the Personal Computer Memory Card International Association (PCMCIA). There are also cards that are simply called PCMCIA cards, either type I or type II. These cards may be inserted into special slots on laptop computers. Flash memory devices, because of their large data storage capacity and small size, are often used as removable and portable hard drives. Solid state technology is quiet and generally allows for faster data access. Compact flash and smart media cards require a special flash memory card reader, which is analogous to a disk drive for a specific type of disk. Although card readers in the past were specific for one type of card, some readers can be purchased today that read many different types of cards. Flash memory card readers may be built-in in some of the newer computers. Flash memory devices that simply plug into an existing USB port are also available.

PROTECTING THE DATA

The hard drive inside the computer is the primary location for data storage, but it should never be the only location for data storage. It is absolutely imperative that the technologist both back up and archive data from the hard drive. Copies should be made of the backup and archive media. The original and copied backup and archive media should be stored in two different locations. Remember: back up, archive, copy, and separate. Why?

The data should be backed up and copied to protect the data from being lost should some disaster befall the hard drive. The backup and archive media should be copied because they too can eventually be damaged, resulting in an irretrievable loss of data. The copies should be stored in separate locations so that if a physical disaster occurs, such as a fire or flood, the chances of one set surviving are improved.

Hard drives are built to take a lot of wear and tear. The term *crash* is often used to describe any and every problem that might occur with the hard drive or computer, in general. Originally, however, the term referred to the circumstance in which the read/write head made contact with the hard drive platter where data was stored. This is similar to dropping the

needle arm of the record player onto the record itself. The track on the record where the needle hit would be damaged and the record would skip when it was played. A similar loss of the data will occur where the hard drive is touched by the head. Hard drive crashes are fortunately rare in today's computers. Hard drives are sealed to keep out dust, hair, smoke, and other unwanted particles. The platters are coated with a much firmer material than they used to be, making them more resistant to gouging by the heads. It is still possible to jar the hard drive enough to cause the head to damage the platter, but it takes some effort. Nevertheless, it should go without saying that dropping the computer is a very bad idea. Hard drives can eventually fail, however. Failure to back up and copy the data is to court disaster.

Temperature extremes and high humidity are detrimental to hard drives as well as densitometers. The ambient temperature and humidity in the room in which the computer and bone densitometer are housed need to be kept within the ranges specified by the manufacturer. A combination thermometer-hygrometer can generally be purchased at hardware stores for less than \$20. Because densitometers also have specific temperature and humidity operating ranges*, such a device is a wise investment to ensure that the computer and densitometer are protected.

Hard drives can also be irreparably damaged by power surges and static discharges. The shut down sequence required by the operating system should always be followed whenever possible. To this end, surge protectors and uninterruptible power supply (UPS) units are absolute necessities. Surge protectors will protect the devices plugged into it from electrical spikes or power surges. A surge protector is plugged into a wall outlet and then the computer and its peripheral devices are plugged into the surge protector. The amount of protection offered by a surge protector will vary depending on the model. UPS units are a form of backup power for the computer that, in case of a power outage, will continue to provide power to the computer to allow the user to properly shut the computer down and avoid the loss of any data. A UPS unit will provide 10–30 minutes of power, depending on the particular model. Some UPS units also provide surge protection for the computer, monitor, and modem or network connections. Remember to keep all forms of magnets away from the computer and magnetic storage media.

*See Chapter 4, FDA-approved devices for the environmental operating temperature and humidity ranges for bone densitometers.

COMPUTER MAINTENANCE

Some general computer system maintenance is advisable. The computer and its peripherals should be turned off when not in use. Some years ago it was thought that booting up the computer caused wear and tear on the hard drive, so users would leave the computer on for days at a time, rather than shut down and boot up on a daily basis. This is unnecessary and simply wastes electricity. Scandisk programs (programs that check for errors on the hard drive) should be run often, although how often depends on how much the computer is used. Similarly, disk defragmenter programs should also be run periodically. The hard drive becomes fragmented over time because the computer will store bits and pieces of files where it finds room to do so. The so-called clusters of data, however, are not necessarily next to each other but may instead be scattered over the hard drive. This ultimately slows down the performance of the computer because it takes the computer longer to locate all these file fragments when needed. Defragmentor programs attempt to bring all these clusters of data together to improve machine performance. There is a defragmentor program included with the Windows operating system. If the computer is used daily with frequent installation and uninstallation of programs and downloading of files from the Internet, scandisk and defragmenter programs should be run once a week and at least twice a year, respectively. If this type of activity is infrequent, once a month will suffice for a scandisk program and perhaps once a year for a defragmenter program. Make sure that the computer and every peripheral device has surge protection at all times. If the computer has a modem, utilize a surge protector that also offers protection for telephone lines, because these lines can carry an electrical surge as well as the power cable itself. Surge protectors and UPS units must generally be purchased separately from the computer system but are wise safeguards against equipment damage and data loss, particularly in areas of the country that experience frequent thunderstorms.

There are very few if any user-serviceable components inside the computer housing. Although opening the housing is quite safe when done properly, there is little that the average user can accomplish in the way of repairs when something goes wrong. Some general preventive maintenance that requires opening the computer housing should be done once or twice a year. Dust and debris can accumulate inside the housing and are detrimental to the computer components. Cans of compressed air or ozone-safe compounds like tetrafluoroethane can be purchased and used to blow out the dust and debris safely. It is imperative that the user is

grounded when the computer housing is opened before touching any part of the interior of the housing. This can be accomplished by touching some nonpainted metal surface. Many computers that accompany bone densitometers have dire warnings attached that the warranty will be voided if the computer housing is opened. If this warning is present, call the densitometry manufacturer technical support division and ask permission to open the housing without voiding the warranty.

Make sure that the openings on the back of the computer housing that allow air in are not blocked. Today's microprocessors generate heat that must be dissipated or the computer will crash. This is accomplished by cooling fans that draw cool air in through the vents and send hot air out. If the vents are blocked, either by dust and debris or by the computer being placed too close to a wall, this necessary cooling will not occur. In the absence of proper cooling either because of blocked vents or fan failure, the computer itself will crash in only 15 or 20 minutes. The gentle humming or whirring noise that is usually heard when the computer is in operation is the sound of the cooling fan. Learn this sound. If this sound is not normal, it is cause for immediate concern as it may indicate the failure of the fan and imminent disaster for the computer. In this case, back up the data and obtain professional assistance immediately. An additional safeguard is a heat sensor with a front-panel read-out. This type of sensor is physically connected to the CPU and can warn you of increases in temperature. Installation of such a sensor is not difficult but does require some familiarity with the internal components of the computer. The cost is generally under \$50.

6

The Importance of Precision

CONTENTS

THE CONCEPT OF PRECISION
PERFORMING A PRECISION STUDY
SHORT-TERM PRECISION STUDIES
MATHEMATICAL PROCEDURES USED TO CALCULATE PRECISION
LONG-TERM PRECISION STUDIES
APPLYING THE PRECISION VALUE TO SERIAL MEASUREMENTS
DETERMINATION OF LEAST SIGNIFICANT CHANGE
USING THE LEAST SIGNIFICANT CHANGE TO DETERMINE THE TIMING OF REPEAT MEASUREMENTS
A CASE IN POINT
MORE SOPHISTICATED ISSUES OF STATISTICAL CONFIDENCE FOR THE MEASURED CHANGE
DETERMINING THE LEVEL OF CONFIDENCE FOR ANY CHANGE AND PRECISION
THE CONFIDENCE INTERVAL FOR THE CHANGE IN BMD BETWEEN TWO MEASUREMENTS
THE IMPORTANCE OF PRECISION
WHICH SKELETAL SITES SHOULD BE USED FOR MONITORING?
HOW FREQUENTLY SHOULD MEASUREMENTS BE REPEATED?
A FINAL CONSIDERATION
REFERENCES

THE CONCEPT OF PRECISION

Precision is the attribute of a quantitative measurement technique such as bone densitometry that refers to the ability to reproduce the same

numerical result in the setting of no real biologic change when the test is repeatedly performed in an identical fashion. Like all quantitative tests in clinical medicine, no bone densitometry technique is perfectly reproducible. This is true even when the bone density test is performed in exact accordance with the manufacturer's recommendations every time. If the test is not consistently performed in accordance with the manufacturer's recommendations, the technique becomes less reproducible.

The precision of bone density testing assumes great importance when the technique is used to follow changes in bone density over time. Because densitometry is not perfectly reproducible, the results on any given patient are not expected to be identical, even if the bone density in the patient has not actually changed. The only way that a physician can know that a real biologic change has occurred is to know if the precision error of the technique has been exceeded. This means that the precision must be quantified by performing a precision study. The precision, expressed as the root-mean-square standard deviation (RMS-SD) with the same units as the measurement or the root-mean-square percent coefficient of variation (RMS-%CV), is then used to determine the minimum change in bone density that constitutes a real biologic change. This is called the least significant change (LSC). The LSC can then be used to determine the minimum interval between follow-up measurements.

PERFORMING A PRECISION STUDY

The results of three PA lumbar spine DXA bone density measurements are shown in Table 6-1. These measurements on Mrs. B were all performed within a few minutes of each other, with only enough time between studies to allow Mrs. B to get off the scan table and be repositioned by the technologist. The same technologist positioned Mrs. B perfectly for all three studies and also analyzed all three studies according to the manufacturer's recommendations. The mean or average value for these three studies was 1.021 g/cm^2 .

Note that the numerical results of the three studies are not identical, even though each study was performed perfectly and no biologic change could have occurred in Mrs. B in the brief period that elapsed between tests. This reflects the imperfect precision of bone densitometry. In looking at Mrs. B's measurements in Table 6-1 it is reasonable to ask, By how much do each of the three measurements vary from the mean value? This can be found by subtracting each of the three measurements from the mean value, as shown in Eqs. 1-3.

Table 6-1
Results From a Series of Three PA Lumbar Spine Dual-Energy
X-Ray Absorptiometry Studies on Patient Mrs. B

<i>PA spine DXA study</i>	<i>Value</i>
Study no.1	1.011 g/cm ²
Study no.2	1.030 g/cm ²
Study no.3	1.022 g/cm ²
Mean	1.021 g/cm ²
SD	0.010 g/cm ²
CV	0.010
%CV	1.0

$$\text{Scan no. 1: } 1.011 \text{ g/cm}^2 - 1.021 \text{ g/cm}^2 = -0.010 \text{ g/cm}^2 \quad (1)$$

$$\text{Scan no. 2: } 1.030 \text{ g/cm}^2 - 1.021 \text{ g/cm}^2 = 0.009 \text{ g/cm}^2 \quad (2)$$

$$\text{Scan no. 3: } 1.022 \text{ g/cm}^2 - 1.021 \text{ g/cm}^2 = 0.001 \text{ g/cm}^2 \quad (3)$$

The question then becomes, what is the representative variation from the mean for each of these measurements? An intuitive approach would be to find the average difference by adding the three differences found in Eqs. 1–3 and dividing the sum by 3. This is neither mathematically correct nor possible, because the sum of the differences is 0, which cannot be divided. Instead, the formula in eq. 4 is used. The three differences are squared, to remove the minus signs. After squaring, they are added and the resulting total is divided by the number of measurements minus 1 (or in this case, 2). Then the square root is taken. The resulting value is the SD for the set of three measurements on Mrs. B. The SD has the units of the measurement, g/cm², and is the appropriate expression of the representative variability about the mean for the three measurements on Mrs. B. The SD is also the appropriate expression of the precision of the three measurements.

$$SD_B = \sqrt{\frac{\sum_{i=1}^{n_B} (X_{iB} - \bar{X}_B)^2}{n_B - 1}} \quad (4)$$

In eq. 4, n_B is the number of measurements on Mrs. B, X_{iB} is the actual value of the i th measurement, and \bar{X}_B (pronounced “ex bar”) is the mean bone mineral density (BMD) value for Mrs. B. The sum of the squared differences is divided by $n - 1$ rather than n because, in this case, only two

of the three measurements actually contribute independently to the calculation of the mean. In other words, if the average value and two of the three measured values that were used to calculate the average were known, the third measured value could always be determined mathematically. The third value is thus not independent. In the example presented, the SD for the set of three measurements on Mrs. B is 0.010 g/cm^2 , as shown in Table 6-1.

Now that the SD and mean value for the three measurements on Mrs. B are known to be 0.010 g/cm^2 and 1.021 g/cm^2 respectively, it can be asked, What proportion or percentage of the mean does the SD represent? This is found by dividing the SD by the mean as shown in eq. 5. This quantity is the coefficient of variation (CV). When multiplied by 100 and expressed as a percentage, it is called the %CV, as shown in eq. 6. The CV and %CV are alternative expressions of the precision of the measurement. For Mrs. B, the CV was 0.010 (after rounding) and the %CV, 1.0%.

$$CV = SD/\bar{X} \quad (5)$$

$$\%CV = (SD/\bar{X}) \times 100 \quad (6)$$

Although the SD, CV, or %CV for Mrs. B could be used in determining significant changes in PA lumbar spine bone density over time for Mrs. B, calculating individual precision values for every patient in a clinical practice that might be followed with bone densitometry is not practical. It is necessary to establish representative precision values for each skeletal site used for monitoring at a bone densitometry facility. This is done by performing a short-term precision study.

Short-Term Precision Studies

A separate precision study must be done for each skeletal site that might be used in following a patient. The precision for multiple regions within a skeletal site, such as the five regions of interest within the proximal femur, can be determined from a single proximal femur precision study.

The number of individuals and number of scans per individual needed for a precision study is determined by the degrees of freedom necessary to achieve the narrowest confidence limits for the precision estimate that are practical. Remember that one of the measurements on an individual will not contribute independently to the calculation of the mean for that individual. The number of measurements that independently contribute are called the degrees of freedom (d.f.) for the study. For statistical validity,

Table 6-2
 Combination of Number of Patients and Scans/Patient for 30
 Degrees of Freedom in a Precision Study

<i>No. of Patients</i>	<i>No. of scans/patient</i>
1	31
5	7
10	4
15	3
30	2

it is recommended that a short-term precision study have 30 d.f. (1). Thirty d.f. are chosen to ensure that the upper limit for the 95% confidence interval of the precision value is no more than 34% greater than the calculated precision value. If only one person is studied, 31 tests must be performed to obtain 30 d.f. because one test will not contribute independently to the calculation of the mean. If 15 patients are studied, three tests per patient must be done because again, only two of the three tests per patient will be independent ($15 \times 2 = 30$). The specific combinations of the number of patients and number of scans per patient that are recommended for a short-term precision study are shown in Table 6-2. A short-term precision study should be completed in 2 weeks to 1 month. All the scans on any one patient can be completed on the same day if desired.

The following is the method for determining short-term precision as recommended by Gluer et al. (2). Using the combination of 15 patients and three scans each for the sake of example, the average value, SD, and CV should be found for each of the 15 sets of three measurements, just as was done for the set of three measurements on Mrs. B. Rather than reporting the arithmetic mean of the 15 SDs or 15 CVs (adding the 15 values and dividing by 15) as the precision value, the RMS-SD or the RMS-CV is calculated as shown in Eqs. 7 and 8. The RMS-SD and RMS-CV are preferred to the arithmetic mean, SD, and CV because the latter quantities tend to underestimate the Gaussian error.*

*The Gaussian distribution is the symmetrical bell-shaped curve that is obtained from a plot of values of a variable in which the variation in the value is caused by several independent factors. It was named after Gauss, the individual who originally described it. If the variation in the value of a variable is primarily from only one factor, the distribution will not be a symmetrical bell-shaped curve. Instead, it may be skewed in one direction or the other.

Table 6-3
Measured and Mean Posteroanterior Lumbar Spine Values for 15 Patients
in a Short-Term Precision Study

<i>Patient</i>	<i>Scan no.1</i>	<i>Scan no.2</i>	<i>Scan no.3</i>	<i>Mean</i>
1	1.011	1.030	1.022	1.021
2	0.925	0.940	0.918	0.928
3	1.164	1.160	1.170	1.165
4	0.999	1.010	1.008	1.006
5	0.900	0.920	0.905	0.908
6	0.955	0.960	0.960	0.958
7	1.000	1.010	1.150	1.053
8	0.875	0.849	0.869	0.864
9	0.898	0.920	0.901	0.906
10	1.111	1.009	1.100	1.073
11	0.964	0.949	0.960	0.958
12	1.000	0.985	0.992	0.992
13	1.200	1.185	1.205	1.197
14	1.165	1.170	1.180	1.172
15	0.909	0.915	0.904	0.909

All values are in g/cm²

$$SD_{RMS} = \sqrt{\frac{\sum_{i=1}^m (SD^2)}{m}} \quad (7)$$

$$CV_{RMS} = \sqrt{\frac{\sum_{i=1}^m (CV^2)}{m}} \quad (8)$$

In Eqs. 7 and 8, m is the number of patients. Using these equations, the 15 SDs or 15 CVs would be squared, summed, and then divided by the number of patients, 15. Then the square root is taken resulting in the RMS-SD or RMS-CV for the group of 15 patients. The RMS-CV can be expressed as a percentage, the RMS-%CV, by multiplying by 100.

In the following example, the short-term precision for the PA lumbar spine was calculated after three PA lumbar spine studies were performed on each of 15 patients within 4 weeks. The same technologist scanned all of the patients. Between each scan, the patient was repositioned. The individual values and the average value for each of the 15 patients are listed in Table 6-3. In all, 45 PA spine studies were performed (15 patients \times 3 scans/patient = 45 scans).

Table 6-4
Mean, Standard Deviation (SD), Coefficient of Variation (CV), and Percent
Coefficient of Variation (%CV) for Each of 15 Patients
in a Short-Term Precision Study

<i>Patient</i>	<i>Mean (g/cm²)</i>	<i>SD (g/cm²)</i>	<i>CV</i>	<i>%CV</i>
1	1.021	0.010	0.010	1.0
2	0.928	0.011	0.012	1.2
3	1.165	0.005	0.004	0.4
4	1.006	0.006	0.006	0.6
5	0.908	0.010	0.011	1.2
6	0.958	0.003	0.003	0.3
7	1.053	0.084	0.080	8.0
8	0.864	0.014	0.016	1.6
9	0.906	0.012	0.013	1.3
10	1.073	0.056	0.052	5.2
11	0.958	0.008	0.008	0.8
12	0.992	0.008	0.008	0.8
13	1.197	0.010	0.009	0.9
14	1.172	0.008	0.007	0.7
15	0.909	0.006	0.006	0.6

Mathematical Procedures Used to Calculate Precision

Step 1. The mean or average BMD, SD, CV, and %CV for the set of three scans for each of the 15 patients must be calculated. These results are shown in Table 6-4. Note that patient no.1 in Tables 6-3 and 6-4 is Mrs. B, for whom this calculation was made earlier.

Step 2. Although the precision for each of the 15 patients is now known, the precision for the group as a whole must now be calculated. This is done by finding the RMS-SD or RMS-CV for the group of 15 patients, using Eqs. 7 and 8, noted above.

Using Eq. 7, each of the 15 SDs are squared. The 15 squared SDs are summed beginning with Mrs. B, who is patient no. 1, and continuing through the total number of patients, m , which in this case is 15. The sum is divided by m , the number of patients, or 15. Finally, the square root is taken. This is the RMS-SD in g/cm^2 and is the precision for the entire group. For the short-term precision study illustrated in Tables 6-3 and 6-4, the RMS-SD is 0.027 g/cm^2 .

Because the precision may also be expressed as the CV, the RMS-CV for the entire group of 15 patients is determined using Eq. 8. The steps are analogous to those described above for Eq. 7 and the calculation of the RMS-SD, except that the CV for each set of scans is used instead of the SD.

Using Eq. 8, each of the 15 CVs previously calculated are squared and then added. This sum is divided by the number of patients, m , and then the square root is taken. This is the RMS-CV for the entire group. To convert this value to the RMS-%CV, the RMS-CV is multiplied by 100. The RMS-%CV for the group of 15 patients is 2.61%.

The average BMD for the entire group used to determine the precision should be stated in addition to the RMS-SD, RMS-CV, or RMS-%CV. The average BMD for the group of 15 patients is found simply by adding all 45 values and dividing by 45. This value is 1.007 g/cm^2 . The average BMD for the group should be stated because the precision may not be as good in osteopenic or osteoporotic populations as it is in normal populations. When the precision is expressed as a CV or %CV, part of the poorer precision in groups with a lower average BMD is a function of the smaller denominator in the calculation of the CV for each patient. For example, in the group of 15 patients with an average BMD of 1.007 g/cm^2 shown in Tables 6-3 and 6-4, the precision was found to be 0.027 g/cm^2 when the RMS-SD was used and 2.61% when the RMS-%CV was used. If a precision study was done in a different group of 15 individuals and the RMS-SD for this group was also 0.027 g/cm^2 , it would be correct to conclude that the precision was equal in the two groups. However, if the average BMD in the second group was lower, the RMS-%CV would appear to be poorer.

Part of the poorer precision may be real, however. As the bones become progressively demineralized and the BMD falls, the precision may not be as good as the precision in individuals with higher levels of BMD. In ideal circumstances, a precision study would be performed on different groups of individuals in which the average BMDs of the various groups spanned normal to osteoporotic values. The appropriate precision value could then be applied in clinical circumstances based on the BMD of the patient in question. Another approach is to perform a precision study in each individual patient that will be followed. Neither are clinically practical suggestions. It is therefore important to remember that the precision value obtained in a short-term study of young, normal individuals represents the best possible precision. Nevertheless, this is an excellent population to test the basic skills of the technologist in positioning and analysis. If a young, healthy population is not representative of the patient population in whom the precision values would be used, a second precision study should be performed using individuals who more closely resemble the patient population in age and BMD.

Most authorities agree that precision should be expressed as the RMS-SD in the units of the measurement. Nevertheless, use of the arithmetic mean SD as well as the arithmetic mean %CV remains common in the

literature. The arithmetic mean SD, CV, and %CV will appear better than their RMS counterparts.

Long-Term Precision Studies

A long-term precision study in which patients are followed over the course of at least a year would be preferable to a short-term precision study, but is logistically much more difficult to do. The calculation of the precision value is also different, requiring the use of a statistical technique called linear regression because biological changes would be expected to occur during the longer time frame. Instead of the SD, a different quantity called the standard error of the estimate is calculated and used to express precision (3). Because of the longer time involved, the possibility of other errors in the test increases, such as errors from machine drift and differences in operator techniques. Consequently, long-term precision estimates tend to be poorer than short-term precision estimates. Although a long-term precision study is a more appropriate reflection of the relevant circumstances in clinical practice, the logistical difficulties of performing such a study make it impractical to do.

APPLYING THE PRECISION VALUE TO SERIAL MEASUREMENTS

Assume that a postmenopausal woman, Mrs. C, underwent a PA lumbar spine bone density study and her physician elected to begin a bone active therapy for the treatment of osteoporosis. Her baseline study revealed a BMD of 0.734 g/cm^2 . When should the PA spine bone density study be repeated in the hope of seeing a significant change in BMD? When the repeat bone density study was performed, the PA spine bone density was 0.760 g/cm^2 . This represented an absolute increase of 0.026 g/cm^2 or 3.54% from baseline. Was this a statistically significant increase given that the technology cannot perfectly reproduce the results of any bone density test even when there has been no real change in the BMD? Answering these questions begins with establishing the precision value for PA lumbar spine bone density testing and then using this value to determine the least significant change.

Determination of Least Significant Change

Once the precision of the measurement at any given skeletal site is known, the magnitude of the change in bone density at that site that

Table 6-5
Z' Values for Various Levels of Statistical Confidence

<i>Statistical confidence level</i>	<i>Z' value</i>
99	2.58
95	1.96
90	1.65
85	1.44
80	1.28

indicates real biologic change can be determined. This is called the LSC. To determine the LSC, a decision must be made as to what level of statistical confidence is needed and how many measurements will be done at baseline and follow-up. Ideally, 95% statistical confidence is chosen, but 80% statistical confidence is generally more than adequate for clinical decisions. The formula for determining the LSC is as follows:

$$\text{LSC} = Z'(Pr) \sqrt{\frac{1}{n_1} + \frac{1}{n_2}} \quad (9)$$

where Z' (pronounced "Z prime") is the value chosen based on the desired level of statistical confidence, Pr is the precision value as either the RMS-SD or the RMS-CV, n_1 is the number of baseline measurements, and n_2 is the number of follow-up measurements. Z' values are chosen from tables of such values usually found in statistical or mathematical texts. Z' values for various levels of confidence are shown in Table 6-5.

For any precision value and any number of baseline and follow-up measurements, the magnitude of the change needed for statistical significance, the LSC, will be less at lower levels of statistical confidence. The magnitude of the LSC can also be reduced for any level of statistical confidence by increasing the number of measurements performed at baseline and follow-up. In clinical practice, one measurement is commonly done at baseline and again at follow-up. When 1 is substituted for both n_1 and n_2 in Eq. 9, the sum under the square root sign becomes 2 as shown in Eq. 10.

$$\text{LSC} = Z'(Pr) \sqrt{\frac{1}{1} + \frac{1}{1}} = Z'(Pr) \sqrt{2} \quad (10)$$

The situation then, of one measurement at baseline and one measurement at follow-up effectively changes Eq. 10 to Eq. 11, used for the calculation of the 1×1 LSC:

$${}_{1 \times 1} \text{LSC} = Z'(Pr)1.414 \quad (11)$$

If two measurements are done at baseline and again at follow-up, the sum under the square root sign in Eq. 9 becomes 1 as shown in Eq. 12 for the calculation of the ${}_{2 \times 2}$ LSC.

$${}_{2 \times 2} \text{LSC} = Z'(Pr)\sqrt{\frac{1}{2} + \frac{1}{2}} = Z'(Pr)\sqrt{1} \quad (12)$$

This effectively changes the equation for the calculation of the ${}_{2 \times 2}$ LSC to:

$${}_{2 \times 2} \text{LSC} = Z'(Pr)1 = Z'(Pr)1 = Z'(Pr) \quad (13)$$

Thus, for any level of statistical confidence, the magnitude of the LSC is reduced by performing duplicate measurements at baseline and follow-up rather than single measurements because the product of the Z' and precision values is being multiplied by only 1 instead of 1.414. The LSC is effectively reduced by approximately 30%.

If the Z' values shown in Table 6-5 for 95% and 80% are substituted in the formulas for the ${}_{1 \times 1}$ LSC and the ${}_{2 \times 2}$ LSC the formulas become:

$${}_{1 \times 1} \text{LSC}^{95} = 1.96 (Pr)1.414 = 2.77 (Pr) \quad (14)$$

$${}_{1 \times 1} \text{LSC}^{80} = 1.28 (Pr)1.414 = 1.81 (Pr) \quad (15)$$

$${}_{2 \times 2} \text{LSC}^{95} = 1.96 (Pr)1 = 1.96 (Pr) \quad (16)$$

$${}_{2 \times 2} \text{LSC}^{80} = 1.28 (Pr)1 = 1.28 (Pr) \quad (17)$$

For example, if the RMS-SD precision of PA lumbar spine DXA studies at a facility was determined to be 0.015 g/cm², this value would be substituted in Eq. 14 if 95% confidence was desired and one measurement was performed both at baseline and follow-up. In that case, the changes in Eq. 14 are reflected in Eqs. 18 and 19.

$${}_{1 \times 1} \text{LSC}^{95} = 2.77 (Pr) = 2.77 (0.015 \text{ g/cm}^2) \quad (18)$$

$${}_{1 \times 1} \text{LSC}^{80} = 0.042 \text{ g/cm}^2 \quad (19)$$

For 80% confidence, the precision value of 0.015 g/cm² is substituted in Eq. 15, resulting in an LSC of 0.027 g/cm². The RMS-%CV can be substituted in a similar fashion for the precision value in Eqs. 14 through 17

to give the LSC as a percent change from baseline for the various levels of confidence and numbers of measurements.

Using the Least Significant Change to Determine the Timing of Repeat Measurements

The timing of the repeat measurement is a direct consequence of the LSC. The follow-up measurement(s) should be done when enough time has passed for the LSC to be achieved. Therefore, once the magnitude of the LSC has been determined, the time required between measurements is:

$$\text{Time Interval} = \text{LSC} \sqrt{\text{Expected rate of change per year}} \quad (20)$$

The expected rate of change per year for the various therapeutic agents or disease states is determined from the available literature. For example, if the average increase in bone density after 1 year of therapy with some agent is 0.03 g/cm^2 and the LSC of 0.042 g/cm^2 is used in Eq. 19, the time interval required is:

$$\text{Time Interval} = \frac{0.042 \text{ g/cm}^2}{0.03 \text{ g/cm}^2/\text{yr}} = 1.4 \text{ years} \quad (21)$$

The follow-up measurement should not be made for 1.4 years because it will take at least that long before the LSC can be expected to be reached. The LSC and expected rate of change can also be given as percentages. To calculate the LSC as a percentage change from baseline, the RMS-%CV value must be used as the precision value rather than the RMS-SD.

It is clear then, that the time interval required to see a significant change is not only dependent on the precision at a site, but also on the expected rate of change at that site as well. Therefore, if the precision at a particular site is excellent but the anticipated rate of change is very slow, the required time interval may be far too long to be acceptable for clinical purposes. Table 6-6 illustrates the interaction between precision and rate of change and the time interval to the LSC at the 95% confidence level for one measurement at both baseline and follow-up. Precision tends to be the best, and therefore the precision values the lowest at the PA lumbar spine, total hip, proximal radius, and heel. Rates of changes at these sites may be quite different, however. The preferred skeletal site for monitoring any particular therapy or disease state will be the site that provides the combination of superior precision and greatest rate of change.

Table 6-6
Interval Between Bone Mineral Density Measurements Required to Obtain
the $1_{\times 1}$ LSC⁹⁵ for Various Levels of Precision and Expected Rates of Change

Precision (%CV)	Change per year (%)	Interval between BMD measurements	
		Months	Years
0.5	1	16.7	1.39
	3	5.60	0.46
	5	3.30	0.28
1.0	1	33.2	2.77
	3	11.0	0.92
	5	6.70	0.55
1.5	1	50.0	4.16
	3	16.6	1.39
	5	10.0	0.83
2.0	1	66.5	5.54
	3	22.2	1.85
	5	13.3	1.11
2.5	1	83.2	6.93
	3	27.7	2.31
	5	16.6	1.39

A Case in Point

This case study illustrates the application of the precision and LSC values in clinical practice in order to answer the questions posed earlier in this chapter about Mrs. C, the postmenopausal woman who has begun therapy for the treatment of osteoporosis. Assume that the precision for PA lumbar spine studies at a bone densitometry facility was previously determined to be 1.5%. This is the RMS-%CV that was calculated from a study of 15 people, each of whom underwent three studies of the PA lumbar spine.[†] Such a precision study provides 30 d.f. This means that the calculated precision of 1.5%, at a statistical confidence level of 95%, is at worst actually 34% higher than that, or 2.01% ($[1.5\% \times 34\%] + 1.5\%$). At

[†]Although the RMS-SD is preferred to the RMS-5CV, the change in bone density from baseline seen with various therapeutic agents is generally given as a percentage in the medical literature, necessitating the use of the RMS-%CV for the calculation of the time to the LSC.

this same facility, the precision for femoral neck bone density studies was established as 2.4%. At 95% confidence, the worst this precision figure might actually be is 3.2%.

Mrs. C, who has a recent diagnosis of osteoporosis, has just received a prescription for a potent antiresorptive agent as treatment for her osteoporosis. Her physician has requested that she have repeat bone density studies to assess the effectiveness of the therapy. When should Mrs. C's bone density studies be repeated? The follow-up measurements to assess therapeutic efficacy should not be made until sufficient time has passed to allow the LSC to be reached.

There are several factors to be considered in answering what would seem to be a straightforward question. First, what magnitude of change in bone density at the PA lumbar spine and femoral neck is expected over the course of a year with the particular agent that has been prescribed for Mrs. C? How many measurements will be done at both baseline and follow-up? And finally, what level of statistical confidence is required for the clinical decision-making process. Ninety-five percent confidence is the most stringent criterion, but 80% confidence is often more than sufficient.

For this example, assume that the therapeutic agent in question has been shown to produce an average increase of 5% from baseline in PA lumbar spine bone density and 2% in femoral neck bone density during the first year of treatment. One measurement of the PA lumbar spine and femoral neck has already been made and no additional baseline measurements are planned. Only one measurement of either the PA lumbar spine or femoral neck or both is planned at the time of follow-up. The time to the $_{1 \times 1}$ LSC for both 95% and 80% confidence can be calculated.

The first step is to find the $_{1 \times 1}$ LSC for 80% confidence and the $_{1 \times 1}$ LSC for 95% confidence for each of the skeletal sites using the precision values that have been previously established. Equations 14 and 15 can be used to find these values by substituting the RMS-%CV precision values of 1.5% for the PA lumbar spine and 2.4% for the femoral neck into each of the equations. For the lumbar spine, the $_{1 \times 1}$ LSC⁹⁵ is 4.16% and the $_{1 \times 1}$ LSC⁸⁰ is 2.72%. At the femoral neck, the $_{1 \times 1}$ LSC⁹⁵ is 6.65% and the $_{1 \times 1}$ LSC⁸⁰ is 4.34%. Given the anticipated rate of change from the chosen therapeutic agent, the length of time it will take to equal or exceed any of these values is the earliest time that the follow-up study at either site should be performed.

If the average increase in PA lumbar spine bone density with this agent is 5% in the first year, then the $_{1 \times 1}$ LSC⁹⁵ of 4.16% should be exceeded within one year. Using Eq. 20, the exact time can be determined to be 0.8 years. The $_{1 \times 1}$ LSC⁸⁰ at the lumbar spine can be reached even more quickly, by 0.54 years. At the femoral neck, however, given that the average increase in bone

density is only 2% in the first year and the precision is slightly poorer than at the PA lumbar spine, the 1×1 LSC⁹⁵ of 6.65% would not be reached for 3.33 years. Even the 1×1 LSC⁸⁰ of 4.34% will not be reached for 2.17 years. It would be reasonable then to advise repeating only the PA lumbar spine bone density study in one year in anticipation of seeing a change in bone density sufficiently great to conclude that a significant change has occurred with 95% statistical confidence. Repeating the proximal femur bone density study in one year would not be reasonable since a significant change in bone density would probably not be detected then, given the precision of testing at the femoral neck and the relatively small anticipated change at that site.

One year later, Mrs. C returns for her repeat PA spine bone density study. At the time of her original study, her L1–L4 PA lumbar spine bone density was 0.734 g/cm². On her repeat study, the L1–L4 BMD was 0.760 g/cm². Is this a significant change? For the change to be significant, the LSC must be equaled or exceeded. In this example, the LSC has been given as a percentage, so the percent increase from baseline for Mrs. C must be calculated. In order to do this, the baseline BMD value is subtracted from the follow-up value. This difference is divided by the baseline value and multiplied by 100 to express it as a percentage. The formula and the practical application are shown in Eqs. 22 through 24.

$$\% \text{ Change from baseline} = [(\text{Follow-up BMD} - \text{Baseline BMD}) / \text{Baseline BMD}] \times 100 \quad (22)$$

$$\% \text{ Change from baseline} = [(0.760 \text{ g/cm}^2 - 0.734 \text{ g/cm}^2) / 0.734 \text{ g/cm}^2] \times 100 \quad (23)$$

$$\% \text{ Change from Baseline} = 3.54\% \quad (24)$$

The % change from baseline of 3.54% does not equal or exceed the 1×1 LSC⁹⁵ of 4.16% so the change cannot be said to be significant at the 95% confidence level. It does exceed the 1×1 LSC⁸⁰ of 2.72%, however, so the change can be said to be significant at the 80% confidence level.

MORE SOPHISTICATED ISSUES OF STATISTICAL CONFIDENCE FOR THE MEASURED CHANGE

Determining the Level of Confidence for Any Change and Precision

In its 2002 position statement, the International Society for Clinical Densitometry (ISCD) recommended that the LSC be calculated for 95%

confidence and that changes in bone density be considered significant only if they equal or exceed this value. This is a stringent requirement. It is imperative to know how confident one can be that a real change has occurred, but the level of statistical confidence necessary to influence clinical decisions is generally not required to be 95%. For example, 80% is often more than adequate. If the change in BMD has not equaled or exceeded the LSC for 95% or even 80% confidence, the question then becomes how confident can you be that there has been a real change in the BMD? It is possible to calculate the level of confidence for any given precision value and change in BMD. This is essentially done by using Eq. 9. The measured change, no matter what it is, is considered the LSC. Because the precision of the measurement and the number of measurements made at baseline and follow-up are also known, the equation can be solved for Z' . Once that is done, the confidence level can be determined. That is what has been done in the Statistical Confidence Calculator spreadsheet on the CD that accompanies this book. Table 6-7, from Dr. Ken Faulkner, is this type of calculation in tabular form for specific combinations of precision and change in BMD. For example, if the RMS-SD precision is 0.010 g/cm^2 and the measured change in BMD is 0.015 g/cm^2 , the physician may be 71% confident that a real change in BMD has occurred. Whether the confidence is sufficient to warrant clinical consideration is a matter of judgment on the part of the physician.

The Confidence Interval for the Change in BMD Between Two Measurements

Once it has been determined that a measured change in BMD is significant at some level of statistical confidence, the question remains as to what the actual change in BMD really is. As noted in the example above, with a precision of 0.010 g/cm^2 and a measured change of 0.015 g/cm^2 , a physician may be 71% confident that a real change has occurred. The physician cannot be 71% confident that a change of exactly 0.015 g/cm^2 has actually occurred. Because there is some statistical uncertainty in both the baseline and follow-up measurements, there is also uncertainty in the magnitude of the measured change. So how can the range of values in which the true change may lie be calculated? Table 6-8 illustrates the range of values for 99%, 95%, 90%, 85%, and 80% confidence intervals for a change in BMD between two measurements at various levels of precision. The values shown in the table for the various levels of precision and confidence are added and subtracted from the actual measured

Table 6-7
Levels of Statistical Confidence for Various Combinations of Precision
and Change in Bone Mineral Density

Change in BMD (g/cm ²)	Precision (g/cm ²)									
	0.005	0.010	0.015	0.020	0.025	0.030	0.035	0.040	0.045	0.050
0.005	52%	28%	19%	14%	11%	9%	8%	7%	6%	6%
0.010	84%	52%	36%	28%	22%	19%	16%	14%	12%	11%
0.015	97%	71%	52%	40%	33%	28%	24%	21%	19%	17%
0.020	100%	84%	65%	52%	43%	36%	31%	28%	25%	22%
0.025	100%	92%	76%	62%	52%	44%	39%	34%	31%	28%
0.030	100%	97%	84%	71%	60%	52%	46%	40%	36%	33%
0.035	100%	99%	90%	78%	68%	59%	52%	46%	42%	38%
0.040	100%	100%	94%	84%	74%	65%	58%	52%	47%	43%
0.045	100%	100%	97%	89%	80%	71%	64%	57%	52%	48%
0.050	100%	100%	98%	92%	84%	76%	69%	62%	57%	52%
0.055	100%	100%	99%	95%	88%	81%	73%	67%	61%	56%
0.060	100%	100%	100%	97%	91%	84%	77%	71%	65%	60%
0.065	100%	100%	100%	98%	93%	87%	81%	75%	69%	64%
0.070	100%	100%	100%	99%	95%	90%	84%	78%	73%	68%
0.075	100%	100%	100%	99%	97%	92%	87%	82%	76%	71%
0.080	100%	100%	100%	100%	98%	94%	89%	84%	79%	74%
0.085	100%	100%	100%	100%	98%	95%	91%	87%	82%	77%
0.090	100%	100%	100%	100%	99%	97%	93%	89%	84%	80%
0.095	100%	100%	100%	100%	99%	97%	95%	91%	86%	82%
0.100	100%	100%	100%	100%	100%	98%	96%	92%	88%	84%

Table created by and reproduced courtesy of Ken Faulkner, PhD

change. For example, if the precision of testing is 1.5% and the measured change is 3%, the actual range of change for the 95% confidence interval is $3\% \pm 4.16$, or -1.16 to $+7.16$. Because the range of possible values contains 0, the measured change of 3% with a precision of 1.5% is not statistically significant at the 95% confidence level. On the other hand, if the precision is 1.25% and the change between two measurements is 4%, the 95% confidence interval for the change is $4\% \pm 3.46$, or 0.54 to 7.46%. This range of values does not contain 0 and therefore the change of 4% is significant at the 95% confidence level. Obviously this is a very wide confidence interval. It is perhaps disconcerting to note that, although the measured change is statistically significant, the actual change may range

Table 6-8
Confidence Intervals for Measured Change in Bone Mineral Density
for Different Values of Precision

<i>Confidence interval%</i>	<i>Precision (%CV)</i>				
	<i>1</i>	<i>1.25</i>	<i>1.5</i>	<i>1.75</i>	<i>2.0</i>
99	±3.65	±4.56	±5.48	±6.39	±7.30
95	±2.77	±3.46	±4.16	±4.85	±5.54
90	±2.33	±2.91	±3.50	±4.08	±4.66
85	±2.04	±2.55	±3.06	±3.57	±4.08
80	±1.81	±2.26	±2.72	±3.17	±3.62

from as little as 0.54% to as much as 7.46%. The 85% confidence interval is narrower. In this case, the range of values is $4\% \pm 2.76$, or 1.24 to 6.76%. Defining these ranges is certainly less important than recognizing whether the measured change is statistically significant.

THE IMPORTANCE OF PRECISION

When properly performed, bone density measurements are the most precise quantitative measurements in use in clinical medicine today. But it should be clear that until precision studies are performed at a facility, the LSC cannot be determined for any level of statistical confidence, making the interpretation of serial studies impossible. The calculations necessary to determine precision are somewhat tedious but not complex. Such calculations are simple with a relatively inexpensive statistical calculator. On the CD-ROM that accompanies this book, a precision calculator program is included that utilizes Microsoft® Excel. A similar program is available from the ISCD.[§] Some densitometry manufacturers have incorporated the calculation of the LSC based on a facility's precision into their software so significant changes in BMD may be flagged in trend results.

[§]An Excel spreadsheet is available for download at no cost that allows the physician to enter the bone density values obtained during a precision study at: www.iscd.org. The precision is calculated automatically by formulas imbedded in the spreadsheet. The spreadsheet can only be used with Microsoft® Excel.

Precision studies do not need to be done on a regular basis, but they should be done at least once. They should be repeated if a new technologist begins scanning or if there is a major equipment change. The patients who participate in precision studies to derive the values that will be used clinically should be representative of the patient population that will be subsequently monitored with the technique. If a densitometry facility employs two or more technologists who are equally likely to perform a patient's bone density study on any given day, then the precision study should be performed by all of the technologists because this will be more representative of what is likely to occur in actual practice. It should be anticipated that the precision will not be quite as good as when only one technologist performs all the studies. It is not uncommon for precision studies to be performed with healthy young adults of normal body size and normal bone density. This type of precision study should be done to allow the technologist to test his or her skills in positioning and analysis. The precision value that results from such a study should not be used as the representative precision value for the facility, unless that is the type of patient the facility sees.

Which Skeletal Sites Should Be Used for Monitoring?

There are four basic rules that govern the choice of skeletal site for the purposes of monitoring the effects of disease or drugs on the skeleton.

1. Measure the skeletal site or type of bone (trabecular or cortical) that is expected to be affected by the disease process or therapy.
2. Of the sites potentially affected, measure the site at which the greatest change in BMD is expected.
3. Of the sites potentially affected, use the site at which the BMD can be measured with the best precision.
4. Peripheral sites are not used for monitoring by any technique.

Rule 1 is simply common sense. If a disease, drug, or procedure is not known to affect bone density in a particular region of the skeleton, it makes no sense to monitor that region. Rule 1 requires the ordering physician to know what the anticipated effect of a disease, drug, or procedure on the skeleton may be. Knowing the skeletal site at which the greatest effect is likely to be seen, as required by rule 2, is necessary to pick the skeletal site at which a change in BMD is most likely to be detected. This is because a certain magnitude of change is necessary to

equal or exceed the LSC, as discussed earlier. In addition, the greater the magnitude of the change, the sooner the change can be detected, making monitoring a more efficient process. Better precision, as required by rule 3, also increases the likelihood of detecting a significant change and detecting it more quickly. Table 6-6, seen earlier in this chapter, illustrates the relationship between rate of change, precision, and the time to the LSC. Ideally, the site that is chosen for monitoring is the site with the greatest anticipated rate of change and the best precision. Peripheral sites are not used for monitoring, regardless of the technique by which they are measured. Precision is generally excellent at peripheral sites but the anticipated rates of change are too slow to make monitoring clinically useful. Guidelines[¶] for monitoring changes in bone density from the ISCD in both 2002 and 2004, from the American Association of Clinical Endocrinologists (AACE) in 2001 and 2003, and from the North American Menopause Society (NAMS) in 2002 all recommend that peripheral sites not be used for this purpose (4–7). As a practical matter then, rule 4 means that the skeletal sites used for monitoring are the spine and proximal femur.

As noted in Chapter 1, the spine and proximal femur are both weight bearing, central sites. The spine is part of the axial skeleton and the proximal femur is part of the appendicular skeleton. In considering the requirements of rules 1 and 2, however, the percentages of cortical and trabecular bone within the spine and various regions in the proximal femur are most pertinent. The area or size of the various regions of interest is relevant to rule 3. The PA spine is generally considered to be 66% trabecular bone. In the proximal femur, the regions of interest with the greatest percentage of trabecular bone are Ward's area and the trochanteric region. The exact percentage of trabecular bone in Ward's area is not defined, but it is considered highly trabecular. The percentage of trabecular bone in the trochanteric region is approximately 50%. The greatest rates of change are usually seen in skeletal regions that contain higher percentages of trabecular bone. This is because trabecular bone has a much higher metabolic rate than cortical bone. Precision, however, is often a function of the size of the area being measured. The larger the size, the better the precision tends to be. The greatest area is found in the PA spine by considering three or four of the lumbar vertebrae as one

[¶]See Table 9–3 for a comparison of these guidelines.

block. In the proximal femur, the greatest area is in the total femur region, followed by the trochanteric region.

In a position statement from the ISCD published in 2002 (4) and again in 2004 (5), the PA lumbar spine was described as the preferred site for monitoring. The total femur region of interest was an alternate choice when the PA spine could not be measured for any reason. In recommending the PA lumbar spine as the preferred choice in 2002, the ISCD panel members noted that the PA lumbar spine provided the best combination of magnitude of change and precision. In the original publication there was no recommendation to use L1–L4 in preference to L2–L4. The precision of L1–L4 has rarely been compared to the precision of L2–L4. The area of L1–L4 will clearly be greater than that for L2–L4, and in general, the greater the area, the greater the precision will be. There is a point, however, past which further increases in area will not have a significant effect on improving precision. In a precision study in which the precision at L1–L4 was compared to that of L2–L4 on the Lunar Prodigy, Bonnicksen and Lewis (8) found excellent precision at for both L1–L4 and L2–L4. In women aged 50–70, the RMS-SD and RMS-%CV values were 0.012 g/cm² and 1.1% for both combinations of vertebrae. In a younger group of women aged 20–49 years, the RMS-SD and RMS-%CV values were 0.009 g/cm² and 0.7% for L1–L4 and 0.011 g/cm² and 0.9% for L2–L4. Although these differences are statistically significant, their clinical significance is doubtful. It would seem then, that either L1–L4 or L2–L4 is appropriate for monitoring purposes in the PA lumbar spine.

The total femur was recommended by ISCD because of its greater area in the proximal femur. This does indeed result in excellent precision at the total femur. In the precision study from Bonnicksen and Lewis (8) noted above, the precision of the total femur on the Lunar Prodigy was 0.007 g/cm² and 0.7% in younger women (RMS-SD and RMS-%CV, respectively). In the group of older women the precision was 0.006 g/cm² and 0.7%. Rates of change at the total femur tend to be slow. They are often less than those seen in the femoral neck, a region with a much smaller area and certainly less than those seen in the trochanteric region. This slower rate of change is, in part, offset by the excellent precision, enabling the physician to detect a significant change in bone density within a reasonable period of time. The trochanteric region of interest, however, potentially offers a reasonable alternative to the PA lumbar spine for monitoring. Rates of change in the trochanteric region of interest are often similar to those seen in the

PA lumbar spine, because of its similar trabecular composition. The area of the trochanteric region is greater than that of the femoral neck although not as great as that of the total femur. With the advent of fan-array DXA scanning, the precision of trochanteric measurements has been dramatically improved. The precision of the trochanteric region of interest on the Lunar Prodigy was 0.008 g/cm^2 and 0.9% (RMS-SD and RMS%CV, respectively) in younger women and 0.009 g/cm^2 and 1.3% in the older women (8). Note that these RMS-SD values are even smaller than those seen at the PA lumbar spine and comparable to those seen at the total femur. The combination of rate of change and precision at the trochanter make it a suitable site for monitoring in the proximal femur and a reasonable choice if the PA lumbar spine cannot be monitored.

How Frequently Should Measurements Be Repeated?

The frequency with which measurements should be made is determined by the time to the LSC, as discussed earlier. The time to the LSC is determined by the anticipated rate of change and the precision at the skeletal site being measured as well as the number of measurements made at baseline and at follow-up and the desired level of statistical confidence for the measured change. In the 2002 ISCD position statement on serial bone density measurements, it was noted that an interval of less than 1 year was rarely indicated when measurements were made at the PA lumbar spine. It was also noted that an interval of 2 years at the total femur might not be sufficient to demonstrate a statistically significant change. Both of these statements are correct. The precision of PA lumbar spine bone density measurements is sufficiently good when combined with the rates of change generally seen at the PA lumbar spine to justify repeat measurements at the end of 1 year in anticipation of seeing a significant change in most circumstances, even at the 95% confidence level. In spite of superb precision at the total femur, the slower rates of change generally seen at this site may preclude seeing a significant change even after 2 years. The same statement would be true regarding the femoral neck region of interest. The potentially superb precision of the trochanteric region of interest with the newer DXA devices combined with rates of change comparable to those seen in the PA lumbar spine suggest that monitoring of the trochanteric region could be done in many cases at an interval of 1 year.

Once it has been determined that the bone density is stable or has significantly changed, the frequency with which testing should be repeated is

unclear. In the context of assessing therapeutic efficacy of bone active agents, there is no evidence to date that suggests that therapeutic efficacy, once established, may subsequently be lost. As a consequence, the frequency of monitoring in this circumstance must be left to the discretion of the physician.

A FINAL CONSIDERATION

All of these careful considerations may be rendered moot, however, if the follow-up study is performed on a different manufacturer's bone densitometer. Even a different device from the same manufacturer is less desirable than using the exact same densitometer for the follow-up study as was used for the baseline study. Under ideal circumstances, the same technologist would perform both the baseline and follow-up study. Although sometimes difficult, the best medical practice demands that the follow-up study is performed under the exact conditions of the baseline study. Serial measurements made on devices from different manufacturers cannot be interpreted with any degree of clinical accuracy. The conversion equations described in Chapter 1 cannot be used for this purpose, as there is still too great a margin for error. The use of a different device for the follow-up study even though it is from the same manufacturer of the device used for the baseline study has the potential to increase the precision error and therefore, increase the LSC. The magnitude of any increase is difficult to quantify in clinical practice. As a consequence, it is desirable to avoid this situation if at all possible.

The 2004 ISCD guidelines for precision assessment (5) also recommended that each DXA center perform its own precision study and calculate the LSC for every relevant skeletal site. The ISCD recommended that precision be expressed as the RMS-SD and that this value be used to calculate the LSC at 95% confidence. Finally, they also recommended that, in the case of multiple technologists performing densitometry studies, the values for the precision studies from individual technologists be averaged to determine the precision for the facility. Whether this approach is used or whether multiple technologists participate in a single precision study to calculate the LSC for a facility as suggested earlier in this chapter, it must be recognized that the resulting precision, both in the study and in practice, will not be as good as that from a single, skilled technologist.

REFERENCES

1. (1999) Assessment of instrument performance: precision, installation of new equipment and radiation dose, in *The Evaluation of Osteoporosis* (Blake, G. M., Wahner, H. W., Fogelman, I., eds.), Martin Dunitz Ltd., London; pp. 47–172.
2. Glüer, C. C., Blake, G., Lu, Y., Blunt, B. A., Jergas, M., Genant, H. K. (1995) Accurate assessment of precision errors: how to measure the reproducibility of bone densitometry techniques. *Osteoporos. Int.* **5**, 262–270.
3. Verheij, L. F., Blokland, J. A. K., Papapoulos, S. E., Zwinderman, A. H., Pauwels, E. K. J. (1992) Optimization of follow-up measurements of bone mass. *J. Nucl. Med.* **33**, 1406–1410.
4. Lenchik, L., Kiebzak, G. M., Blunt B. A. (2002) What is the role of serial bone mineral density measurements in patient management? *J. Clin. Densitom.* **5**, S29–S38.
5. The Writing Group for the ISCD Position Development Conference. (2004) Technical standardization for dual-energy X-ray absorptiometry. *J. Clin. Densitom.* **7**, 27–36.
6. AACE. (2003) American Association of Clinical Endocrinologists medical guidelines for clinical practice for the prevention and treatment of postmenopausal osteoporosis: 2001 edition, with selected updates for 2003. *Endocr. Pract.* **9**, 545–564.
7. (2002) Management of postmenopausal osteoporosis: position statement of The North American Menopause Society. *Menopause* **9**, 84–101.
8. Bonnicks, S. L. and Lewis, L. A. (2002) The precision of PA spine, dual femur and single femur bone density studies on the GE Lunar Prodigy, a DXA fan-array device. Abstract. *J. Clin. Densitom.* **5**, S48.

7

Radiation Safety in X-Ray Densitometry

CONTENTS

- RADIATION BASICS
 - RADIATION QUANTITIES
- HARMFUL EFFECTS OF IONIZING RADIATION
 - ACUTE LETHAL RADIATION SYNDROMES
 - LOCAL TISSUE DAMAGE FROM RADIATION
 - LATE EFFECTS OF IONIZING RADIATION
- RADIATION DOSES IN DENSITOMETRY
- RADIATION PROTECTION PROGRAMS
 - PROTECTION OF THE PUBLIC
 - PROTECTION OF THE PATIENT
 - PROTECTION OF THE TECHNOLOGIST
- REFERENCES

X-ray densitometers expose patients to extremely small amounts of radiation in comparison to plain X-ray techniques. These amounts are often so small that they are biologically insignificant. Similarly, the technologist operating an X-ray densitometer on a regular basis is extremely unlikely to be exposed to a significant amount of radiation. Nevertheless, no amount of radiation should be considered inconsequential. The principle of “as low as reasonably achievable” (ALARA) should always be given the highest priority in the operation of these devices.

RADIATION BASICS

X-rays are a form of electromagnetic energy. Other forms of electromagnetic energy are radio and television waves; microwaves; radar; infrared; visible and ultraviolet light; and gamma (γ) radiation. These types

of energies form the electromagnetic spectrum of energy. When energy is released and then transmitted through a substance it is called *radiation*. The substance through which the radiation has passed is said to have been “irradiated” or “exposed” to radiation. Ionizing radiation is radiation that causes the release of an electron from its orbit around an atom when the radiation passes through the substance containing that atom (1). X-rays and γ -rays are also forms of ionizing radiation.

Radiation Quantities

In X-ray densitometry the technologist must be concerned with the amount of ionizing radiation to which both the patient and technologist are exposed. A review of the terminology describing these quantities is necessary before discussing the potential effects of ionizing radiation on living tissue and the exposure levels produced during various densitometry exams.

THE CURIE

The most basic unit of radiation is the Curie (Ci). This is used to quantify the amount of a radioactive material, not the radiation emitted by the material. The SI* unit equivalent to the Ci is the Becquerel (Bq). The formula for converting Ci to Bq is shown in Eq. 1:

$$\text{Ci } (3.7 \times 10^{10}) = \text{Bq} \quad (1)$$

To use this equation, multiply the number of Ci by 3.7×10^{10} to determine the number of Bq. Amounts of radioactive material are often described as being a certain number of milliCuries (mCi) or even microCuries (μCi).

THE ROENTGEN

The Roentgen (R), named for Wilhelm Roentgen who discovered X-rays, is used to describe a quantity of radiation exposure, but it is only used to describe the interaction of X-rays and γ -rays with air. The Roentgen is based on the electrical charge created by the liberation of electrons that occurs during ionization. In densitometry, the Roentgen is rarely used except to describe measured amounts of scatter radiation in the air when the devices are in use. This quantity is quite low and generally expressed in milliRoentgens (mR). The Roentgen also has an SI counterpart, called the

*The system of units known as Le Systeme International d’Unites, or SI, is considered the preferred method of expressing scientific quantities.

coulomb per kilogram (C/kg). The mathematical conversion of Roentgens to coulombs per kilogram is shown in Eq. 2:

$$R (2.58 \times 10^{-4}) = C/kg \quad (2)$$

THE RAD

Rad is both an abbreviation and acronym for radiation absorbed dose. It is used in conjunction with any kind of ionizing radiation and any type of substance that has been exposed to ionizing radiation. The rad is commonly used to express the quantity of radiation received by a patient. The biologic effects of radiation are often associated with various quantities of radiation given as rads. The SI rad equivalent is the Gray[†] (Gy). The mathematical relationship between the rad and Gy is simple: 100 rads equal 1 Gy. This is expressed in Eq. 3:

$$\text{rad} (0.01) = \text{Gy} \quad (3)$$

For medical X-rays, 1 R is considered to be approximately equal to 1 rad because the radiation exposure to human tissue from 1R is only about 5% more than 1 rad.

THE REM

Rem is also both an abbreviation and acronym for rad equivalent man. The rem expresses the quantity of radiation received by a patient but unlike the rad, the quantity has been adjusted to reflect the type or quality of radiation involved (2). This recognizes that different types of ionizing radiation have different potentials to do harm. The conversion of rads to rems is expressed in Eq. 4:

$$\text{Rem} = \text{rad} \times \text{quality factor} \quad (4)$$

Medical X-rays are assigned a quality factor of 1. As a consequence, multiplying the number of rads by a medical X-ray quality factor of 1 does not change the value. For medical X-rays, then, in the context of whole body exposure, a rad is equal to a rem. By extension, for medical X-rays, 1 R is also approximately equal to 1 rem. This is not true for all types of ionizing radiation, however. For example, alpha particle radiation as seen with radon exposure, has a quality factor of 20. Because radon is a gas, this exposure reflects the dose to the lungs. The exposure from medical X-rays in rads or rems is often called the skin dose.

[†]The Gray is named for Louis Gray (1905–1965), one of the creators of the Bragg-Gray Theory used in radiation therapy.

The SI equivalent of the rem is the Sievert[§] (Sv). The mathematical relationship between the rem and Sievert is the same as between the rad and the Gray: 100 rems are equal to 1 Sv. This is expressed in Eq. 5:

$$\text{rem (0.01)} = \text{Sv} \quad (5)$$

THE EFFECTIVE DOSE EQUIVALENT

The effective dose equivalent (H_E) is a concept, rather than a particular unit of measure. The concept was introduced in 1987 in an attempt to relate the magnitude of an exposure in rems or Sv to the *risk created by that exposure* (3). As noted in the discussion of the rem, the dose in rads must be multiplied by a quality factor for the type of ionizing radiation, recognizing that different types of radiation have different potentials to do harm. Similarly, different tissues or organs within the human body have different sensitivities to radiation. Some tissues are more sensitive than others. It matters, then, what tissues are being irradiated in determining what the risk of that irradiation truly is. This is the concept behind the effective dose equivalent. Tissue weighting factors are assigned to the various tissues in the body. The H_E is determined by multiplying the value in rems or Sv by the tissue sensitivity weighting factor. Because the tissue weighting factor has no units of its own, the H_E is still expressed in rems or Sv.

The body as a whole is assigned a tissue weighting factor of 1. Individual tissues or organs have sensitivity weighting factors <1 and vary widely. The ovaries and testes are assigned one of the highest values at 0.25 (4). The thyroid's sensitivity is relatively low at 0.03. The red bone marrow is assigned a sensitivity weighting factor of 0.12. The H_E that is calculated for the exposure of any given area of the body is an expression of the risk that would result if the *entire body* were exposed to the same amount of radiation. For example, the H_E for a radiographic absorptiometry study of the phalanges on the MetriscanTM is stated as being <0.0001 mrem or 0.012 μSv (5). This means that the risk of the radiation exposure from such a densitometry study of the phalanges is the same as if the entire body was exposed to <0.0001 mrem. This is not a measure of the amount of radiation exposure to the phalanges. The effective dose equivalent is an expression of the biologically important risk associated with any given amount of radiation exposure.

[§]The Sievert is named for a Swedish scientist who was a member of the International Committee on Radiation Protection.

HARMFUL EFFECTS OF IONIZING RADIATION

Ionizing radiation has the potential to harm living tissue. In addition to medical X-rays, there are other sources of ionizing radiation. One important source found naturally in the environment is radon. Radon is a gas formed by the decay of uranium, which is normally found in small amounts in the earth. Materials that are derived from the earth, like concrete and brick, will therefore contain small amounts of radon to which everyone is exposed. The largest source of man-made ionizing radiation is medical X-rays. Other man-made sources include nuclear power generators, consumer products such as smoke detectors and televisions, and industrial sources. In comparison to natural environmental radiation, man-made sources of ionizing radiation contribute very little to the total annual radiation exposure of an individual. Nevertheless, ionizing radiation does have the potential to do harm. The decision to expose a patient to ionizing radiation, no matter how small in amount, should not be made lightly.

Although ionizing radiation can cause an increase in the expected number of mutations, the mutations that result are not unique. In spite of the frightening and bizarre images seen in movies of giant crickets devouring Chicago after being exposed to ionizing radiation, the types of mutations that are actually seen are those that occur in nature. They simply will occur more frequently. Similarly, cancers that can result from high doses of ionizing radiation are not unique. The incidence of almost all types of cancer is increased after exposure to high doses of ionizing radiation, but these are the same cancers seen in individuals who have not been exposed.

Acute Lethal Radiation Syndromes

Acute lethal radiation syndromes are mentioned here only for the sake of completeness. They cannot occur with the devices used in densitometry, because the radiation doses required to produce them are thousands of times greater than those used in densitometry. Dual-energy X-ray absorptiometry (DXA) and single-energy X-ray absorptiometry (SXA) X-ray tubes are incapable of producing the high doses of radiation necessary to cause these syndromes because of their relatively low applied voltage and current. The peak kilovoltage (kVp) of the tube determines the amount of radiation that can be delivered by the tube. The X-ray tube current (mA) determines the number of X-rays that are produced, which also affects the amount of radiation produced. In densitometry X-ray tubes, the kVp and mA are far too low to cause any of these syndromes. Nevertheless, the

technologist should be aware of them, if only to reassure the anxious patient that they *cannot occur* with X-ray densitometry.

There are three different acute syndromes that ultimately result in death. The syndromes are called hematologic death, gastrointestinal (GI) death, and central nervous system (CNS) death. Doses of 200 to 1000 rads can cause nausea, vomiting and diarrhea, hemorrhage, and a decrease in the white blood cell count leading to infection and fever. Hematologic death occurs within 10 to 60 days. Higher doses of 1000 to 5000 rads result in GI death in 4 to 10 days preceded by lethargy and shock as well as all the signs and symptoms seen with the hematologic death syndrome. Doses of >5000 rads results in CNS death within 3 days of exposure. Loss of coordination, meningitis, and the signs and symptoms seen in the GI and hematologic syndromes are also present. These types of syndromes were seen in the unfortunate victims of the Chernobyl nuclear power plant accident in 1986.

Local Tissue Damage From Radiation

Any tissue can suffer acute radiation damage if the dose is high enough. Like the acute lethal radiation syndromes, the doses employed in bone densitometry are much too low to cause immediate tissue damage but it may be necessary for the technologist to reassure the patient that such damage cannot occur.

SKIN

Reddening of the skin, or erythema, can follow a single dose of 300 to 1000 rads. Persons who have undergone radiation therapy for cancer may have experienced erythema in the course of their therapy. The erythema may be followed by a sloughing of the skin called desquamation. The dose that has been determined to cause erythema in about 50% of the persons exposed is 600 rads (6 Gy) (6). This is again a dose that is thousands of times higher than the doses given with bone densitometry and as a consequence, erythema of the skin after a bone density study simply cannot occur.

OVARIES AND TESTES

The sensitivity of the ovaries to radiation changes with age. The ovaries are very sensitive in childhood and again after the age of 30 up until menopause. A radiation dose of 10 rads in a mature woman can cause a delay in menstruation (6). A higher dose of 200 rads can cause temporary sterility and a dose of 500 rads can cause permanent sterility. It is also possible that doses of 25 to 50 rads can produce genetic mutations in the

oocytes without killing the oocytes such that birth defects could result if fertilization of one of these damaged oocytes was to occur. For this reason, some authorities have recommended delaying attempts at pregnancy for several months after receiving such a radiation dose.

The testes are also sensitive to radiation. Doses of 10 rads have been reported to cause a decrease in the number of sperm. A dose of 200 rads can produce temporary sterility and 500 rads can cause permanent sterility. Like the oocytes in the ovary, genetic mutations in surviving sperm are reason to advise men receiving such radiation doses to avoid attempts at inducing pregnancy for several months.

BONE MARROW AND BLOOD

Irradiation of the bone marrow can cause a drop in the number of red cells, white cells, and platelets. The most sensitive cell appears to be the white blood cell, known as the lymphocyte. Another type of white blood cell, the granulocyte, is less sensitive. The platelets, the small cells responsible for clot initiation are less sensitive than white blood cells, and the red blood cells are the least sensitive of all. Radiation doses generally in excess of 25 rads are required to see a demonstrable effect on the most sensitive lymphocytes. The effect on the lymphocytes is rapid and recovery is slow. The drop in the number of the other cell types is less rapid and recovery is quicker.

Late Effects of Ionizing Radiation

As a practical matter, the late effects of ionizing radiation are more of a concern to those who work with radiation rather than to patients who undergo an occasional X-ray. Although late effects can follow a single high dose of radiation, there is greater concern that they will follow low doses received over a prolonged period of time such as might be seen in a radiologic technologist or physician working with an X-ray device. A technologist who works solely with X-ray densitometry, again because of the very low doses employed, will not accumulate sufficient radiation exposure to be at increased risk for these late effects.

The late effect of most concern is cancer. As noted earlier, radiation has been implicated as a cause of almost every type of cancer. Leukemia, thyroid cancer, skin cancer, bone cancer, lung cancer, and liver cancer have been strongly associated with certain types of ionizing radiation. It is difficult to state with certainty the exact amount of radiation that one must receive to be at increased risk for cancer. What does seem clear is that this amount is hundreds or even thousands of times higher than the amount to

which a DXA or SXA technologist would be exposed. Even the most basic radiation safety program will reduce the risk further still.

RADIATION DOSES IN DENSITOMETRY

The X-ray tubes used in densitometry devices have kVp and mA characteristics that prohibit the generation of high doses of radiation. The kVp and mA specifications for various devices are listed in the descriptions of the devices in Chapter 4. The technologist should be familiar with the patient doses for the various types of X-ray densitometry studies and how these doses compare to other types of radiation exposure. The point here is not to minimize the importance of any radiation exposure but to put the amount of exposure in perspective to allay inappropriate fears about the exposure.

A certain amount of radiation exposure occurs as a result of sources in the environment. The effective dose from natural background sources is estimated to be 0.6 to 0.7 mrem/day (6 to 7 μ Sv/day) or about 240 mrem/year (2400 μ Sv/year) (4). Living at higher altitudes such as a mile above sea level increases this environmental radiation by about 5 mrem/mos (50 μ Sv/mos). A PA spine DXA pencil-beam study generally results in an effective dose of only 0.1 mrem (1 μ Sv). Quantitative computed tomography (QCT) bone density studies do result in slightly higher effective doses than pencil-beam DXA PA spine studies. A QCT spine study may have an effective dose of about 3 mrem (30 μ Sv). By comparison, the effective dose for an AP chest X-ray is about 5 mrem (50 μ Sv) and for a plain lateral lumbar spine film, about 70 mrem (700 μ Sv). The radiation doses for various types of densitometry studies, as provided by the manufacturers, are listed in Chapter 4. In some cases these are the skin doses and in others, the effective dose equivalents.

The kVp and mA of an X-ray tube was noted earlier as determining the amount of radiation produced by the tube. The skin and effective doses seen in bone densitometry studies will vary depending on the scan speed and scan length (7). The dose will increase as the scan speed decreases and the scan length increases. On many devices, the technologist can select the mA as well as the scan speed and scan length. Although decreasing the mA and increasing the scan speed decreases the skin and effective radiation doses, it also tends to reduce the precision of the measurement.[¶]

[¶]See Chapter 6 for a discussion of precision in bone densitometry.

The effect of increasing scan length on increasing dose, however, makes it even more important that the technologist both perform and recognize a technically good study to avoid repeat starts and excessive scanning.

Multiple bone density studies will also result in greater effective dose equivalents. For example, it is not uncommon for a woman to undergo both a PA spine and proximal femur bone density study on the same day. The total effective dose for that patient is the sum of the effective doses for the individual studies. It also makes a difference whether the woman is pre- or postmenopausal. The effective dose during a DXA proximal femur study will be greater for a premenopausal woman because the effect on the ovaries must be considered. For a postmenopausal woman, the effect on the ovaries need not be considered. Skin doses may be higher in some projections because of higher mA values used in that scan mode, but if the scan length is shorter and important tissues are no longer in the beam path, the effective dose can still be comparable to other projections using lower mA values with resulting lower skin doses.

Fan-array DXA scanners tend to have higher effective doses per scan than pencil-beam scanners.** This is because of higher X-ray tube voltages and currents that are employed in these scanners. For example, the effective dose for a PA lumbar spine study of L1–L4 on a Hologic QDR-1000, a pencil-beam DXA device, is estimated to be 0.05 mrem (0.5 μ Sv) (8). On a QDR-4500, a fan-array DXA device, this dose may increase to 0.67 mrem (6.7 μ Sv) (9). Although the effective dose on the fan-array scanner is more than 10 times higher than the pencil-beam scanner, it is still no more than the effective dose from natural background radiation for 1 day.

The effective dose during a QCT spine bone density, like that of its DXA counterpart, will depend on the kVp and mA. It will also depend on the number of slices made during the study and the thickness of those slices. Usually three slices are made that are 8- to 10-mm thick. Consequently, the area that is irradiated is quite small and the effective dose is much lower than might otherwise be anticipated. If a scout scan precedes the actual QCT examination for localization purposes, the effective dose is the sum of the effective doses of the scout scan and the actual QCT study. This total effective dose has been estimated at 6 mrem (60 μ Sv), but this may be an underestimation (4,7).

Plain lumbar spine films are occasionally obtained either prior to or after DXA spine studies to aid in vertebral identification or the assessment of

**See Chapter 2 for a discussion of pencil-beam vs fan-array DXA scanners.

vertebral deformities. This adds significantly to the effective radiation dose received by the patient. The effective dose from a lateral lumbar spine film alone may be 60 to 70 mrem (600 to 700 μ Sv). If a lateral thoracic film is obtained as well, the effective dose will be even higher. It is imperative, then, that the technologist learn to identify the vertebrae based on their appearance on the densitometry image, their spatial relationships to other skeletal structures, and the various probabilities of types of segmentation to avoid needing plain spine film solely for the purpose of vertebral labeling.^{††} Morphometry and vertebral imaging without morphometry as performed on some of the newest DXA devices may also reduce the need for plain films in the assessment of vertebral deformities. These types of DXA scans can be performed rapidly with much lower effective doses than plain films of the thoracic or lumbar spine. In addition to the added clinical value of assessing vertebral deformities at the time of the bone density study, the lower effective dose makes these new DXA applications a safer alternative to plain films. The effective dose for vertebral morphometry on a Hologic QDR 4500 has been estimated as 4.1 mrem (41 μ Sv) in one of the slower scan modes. On the Lunar Expert-XL, the effective dose for vertebral morphometry has been estimated at 3.8 mrem (38 μ Sv). Both of these doses are considerably lower than the 60 to 70 mrem (600 to 700 μ Sv) for lateral thoracic and lumbar spine films. Spine imaging performed with newer modalities such as Hologic's Radiographic Vertebral Assessment™ and GE Lunar's Dual-energy Vertebral Assessment™ can be performed at a fraction of the effective dose for plain lateral spine films.

RADIATION PROTECTION PROGRAMS

Radiation protection programs, even in bone densitometry facilities, are based on the premise that any unnecessary radiation exposure is unacceptable, no matter how small. The guiding principle of all such programs is ALARA. There are three aspects to any radiation protection program. One aspect is the protection of the public. Another is the protection of the patient. The final aspect is the protection of the technologists and physicians involved in the operation of radiologic devices. Limits for radiation exposure have been set for members of the public and for radiation workers such as technologists and physicians. *Members of the public* refers to

^{††}See Chapter 3 for a discussion of skeletal anatomy and identification of the vertebrae.

individuals not undergoing radiologic procedures and who do not work with radiation producing devices or substances. These limits have changed over the years to reflect increasing knowledge about the effects of ionizing radiation. A member of the public may receive a dose of 0.1 rem (1 mSv) per year, whereas a radiation worker may receive a dose of 5 rem (50 mSv) per year and still be considered to have exposures within permissible limits (10). The lifetime effective dose limit in rems for a radiation worker should not exceed his or her age in years. Although it is extremely unlikely that a member of the public who is consistently in the vicinity of a DXA device or a radiation worker dealing solely with DXA devices would ever exceed those limits, radiation protection programs can be designed to ensure this.

The exact requirements for any radiation protection program may vary from state to state. It is imperative, therefore, that the state regulations be reviewed to ensure compliance. In facilities in which the only radiologic device is a DXA densitometer, the regulations pertaining to radiation safety are generally minimal. But even in the absence of any regulations there are some simple but appropriate measures that should be considered.

Protection of the Public

The first measure is to “post” the room in which the densitometer is kept. *Posting* means placing radiation warning signs on the entrances to the room and restricting access. This is generally a requirement when radiation levels are 5 mrem/hour or more in the area housing the X-ray device. With most densitometers, radiation levels won’t approach this threshold. Nevertheless, it seems reasonable to place warning signs on the entrances to the room and restrict access. This is simply a matter of fully informing the public and protecting expensive medical devices. The traditional X-ray warning sign is shown in Fig. 7-1. The fan blades of the sign are normally magenta on a yellow background. Professionally produced signs are inexpensive and available from a variety of X-ray supply companies.

Consideration should also be given to a radiation survey. A radiation physicist can document readings with a counter in and around the densitometer when the densitometer is in operation. Such readings should be taken at specific distances from the X-ray tube within the room and outside of the room as well. If there are offices or hallways that the public has occasion to frequent that are next to the densitometry room, readings should be taken there as well. This would include offices on floors both above and below the densitometry room. The readings at each location

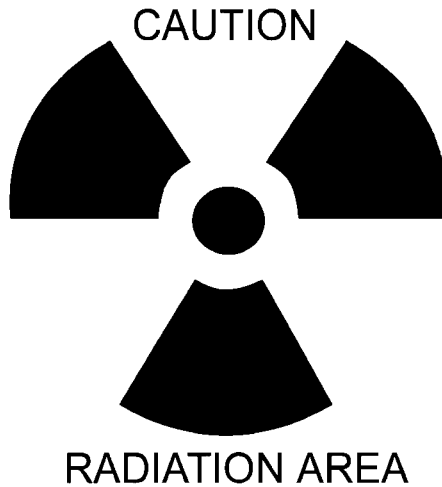


Fig. 7-1. Radiation warning sign. The fan blades are traditionally magenta on a yellow background.

should be documented in some way and signed and dated by the individual making the readings. It is quite likely that there will be no detectable counts on the counter when this is done. Nevertheless, this documentation can be invaluable in allaying unjustified fears about radiation exposure among members of the public.

Individuals who are not directly involved in the performance of a bone density test should not be in the densitometry room during testing. This is again an additional safeguard against even the smallest amount of unnecessary radiation exposure. If a radiation survey has been done so that no detectable counts have been documented at a specific distance from the X-ray tube, exceptions can be made on a case-by-case basis as long as the individual stays the documented safe distance away from the tube. If a radiation survey has not been done, allowing members of the public in the room is not advisable under any circumstances.

Protection of the Patient

The patient undergoing a bone density study is not technically considered a member of the public for radiation protection purposes. The technologist must assume a major role in protecting these individuals from unnecessary radiation as well. It is not the responsibility of the technologist to order the bone density study in the first place. This is the responsibility of the physician. In a sense, the technologist cannot control the ordering of

unnecessary bone density studies. This does not mean, however, that the technologist should abandon all thoughts of what he or she knows to be appropriate once the patient has arrived for testing. The knowledgeable technologist can aid the physician, enhance the care of the patient, and protect the patient from unnecessary radiation exposure without intruding on the physician–patient relationship or undermining the patient’s confidence in his or her physician.

Patients should always be asked if they have had a previous bone density study and if so, where, when, and on what type of machine. It is not uncommon for the patient to have had a bone density study by any technique of the peripheral skeleton that suggests bone loss prompting the physician to request a study of the spine or proximal femur almost immediately. This is appropriate in many circumstances. On the other hand, if the patient is undergoing treatment for bone loss and being followed with bone density measurements, the bone density measurements should ideally be made on exactly the same machine every time. If the same machine is not used, then the next best choice is the same type of machine. If the patient’s previous bone density study was at another facility on a different type of machine, it would be in the patient’s best interests to return to that facility if possible. A test on another type of machine will not be interpretable in the context of judging a change in bone density, rendering that radiation exposure unjustified. The timing of the repeat study is also an issue. Rarely are repeat studies justified more often than once a year at the spine and more often than every 2 years at the proximal femur. The most notable exception is patients receiving corticosteroids who may indeed undergo a follow-up spine bone density study after only 6 months. The appropriate timing of the repeat bone density study is determined by the precision of the measurement at the bone density facility at the particular skeletal site in question and by the expected rate of change in the bone density at that site.^{§§} If the study appears to have been ordered too soon, such that significant change in bone density is unlikely, it is appropriate for the technologist to confirm the physician’s desire to have this test done now. Once again, a test done too soon for the purposes of following therapy is a test that exposes the patient to unnecessary radiation.

It is also incumbent on the technologist to perform every test correctly. This includes the correct choice of scan mode and speed when these

^{§§}See Chapter 6 for a discussion of issues surrounding precision and the timing of repeat measurements.

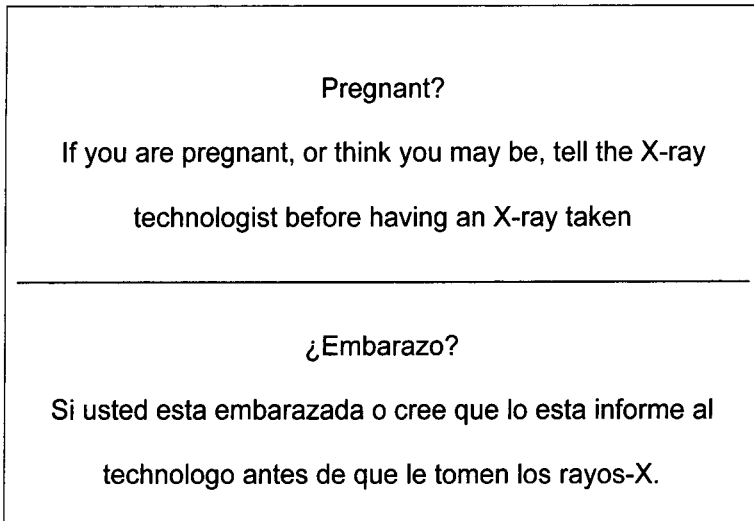


Fig. 7-2. Pregnancy warning sign in English and Spanish.

attributes are modifiable, correct patient positioning, correct data acquisition and analysis. If it is not possible to position the patient correctly because of some arthritic or disease process, then the particular study should not be done. This is not the fault of the technologist. This is the expertise of the technologist in preventing the performance of an inappropriate bone density study. The physician should simply be notified, the reasons given and a request made for suggestions as to how to proceed.

Within the area there should also be signs that prompt a woman to disclose a pregnancy or the possibility of pregnancy. The wording for such a sign is shown in Fig. 7-2 in both English and Spanish. In clinical medicine, there is very little reason if any to perform a bone density study on a woman who is pregnant or who might be pregnant. There are simply no emergency bone density studies. Although it has been suggested that the effective doses are so low to the fetus that even asking about pregnancy is not necessary, there is simply no reason to abandon this precautionary measure (11). Do not assume because the sign is posted on the wall that the patient has read it. Ask the question directly, explaining that the risk is virtually negligible but that their safety is paramount. Another approach to this issue is the "10-day rule," which states that a radiologic exam should only be performed within 10 days of a woman's last menstrual period. In any case, it is far better to err on the side of caution in deciding whether to proceed with the examination, so whenever there is any doubt about the possibility of a pregnancy, the test should be postponed.

Although not routinely used in X-ray densitometry, protective aprons, gonadal shields, and thyroid collars should be available. On occasion it becomes clear that no amount of explanation will sufficiently allay a patient's fears about radiation. In that circumstance, a protective apron or shield should be made available to the patient if it will not interfere with the test. It is a simple matter with many of the peripheral X-ray densitometers to allow the patient to wear an apron during the study. This should always be used with children. In this circumstance, an apron with a thyroid collar is desirable. Gonadal shields can generally be used for men undergoing spine and proximal femur bone density studies without compromising either study.

Protection of the Technologist

The technologist who works solely with X-ray bone densitometers is unlikely to ever receive significant exposures. The concept of ALARA applies here as well, however. Protection for a technologist involves three concepts: time, distance, and shielding. Tracking radiation exposure over time is an additional safeguard.

TIME, DISTANCE, AND SHIELDING

Longer scan times result in greater exposure, both for the patient and the technologist, for any given exposure rate. Whereas the patient is exposed directly to the X-ray beam, the technologist is only concerned with any potential radiation leakage or scatter radiation. As noted previously, the choice of the correct scan speed for a study is an integral part of radiation protection for the patient. It is also part of radiation protection for the technologist. Radiation leakage and scatter radiation are very low for X-ray densitometers, if they occur at all. The concept of ALARA demands, however, that the shortest appropriate scan speed be chosen for any particular study. This may not necessarily be the shortest scan speed of which the machine is capable. It should simply be the shortest appropriate scan speed for that particular patient undergoing that particular study.

Shielding and distance can be considered together for X-ray densitometers in the context of the protection of the technologist. Because the leakage and scatter radiation are low to nonexistent for pencil-beam DXA devices, the radiation exposure of a technologist should be well below permissible limits at distances of 3 ft (1 m) or more from the X-ray tube (12). For fan-array devices, this distance increases to about 10 ft (3 m). Ideally, then, the technologist should remain this minimum distance away

from the X-ray tube when the machine is in operation. These recommended distances are based on the assumption that the densitometer is being maximally utilized. If studies are infrequent, the potential radiation exposure of the technologist is greatly reduced. In any case, the technologist should not stand or sit within 3 ft of the X-ray tube when the machine is in operation. If this is not possible, a protective barrier should be utilized. When central DXA devices are considered, it should be recognized that the X-ray tube moves during patient scanning. The position of the tube during the entire scan must be considered in determining the necessary distance from the tube. This movement can also be used to the advantage of the technologist. For example, when the tube is homed to the head of the scan table, the technologist's workstation may be an unacceptably short distance from the tube. When the tube is moved into position for a spine or proximal femur study, however, this distance will automatically increase. Similarly, additional distance may be obtained by performing right proximal femur studies rather than left.

PERSONNEL MONITORING DEVICES

Radiation monitoring devices, often called personnel monitoring devices, are inexpensive safeguards that allow a technologist to track exposure over a lifetime. A monitoring device does not protect the technologist from exposure, but the record that it provides can be used to ensure that the maximum permissible doses are not exceeded. These devices are generally required when it is anticipated that an individual may receive more than 1/4 of the maximum permissible dose. However, they should be provided to any technologist who requests one even if such exposures are not anticipated. The most common types of devices are film badges and thermoluminescence dosimeters (TLDs).

Film badges have been in use since the mid-1940s, but they are giving way to TLDs. Special radiation dosimetry film is placed in the badge, which is then worn for no more than 1 month. Film badges are not as sensitive to small exposures as are TLDs, which makes them less useful for the densitometry technologist. The TLD contains an entirely different material, such as lithium fluoride. The TLD can generally be worn for up to 3 months at a time. Both the film badge and the TLD should be worn with their proper side to the front. Ideally they should be clipped to the collar, but a chest pocket or waist band is acceptable as long as a protective apron is not being worn.

Film badges and TLDs are obtained from certified laboratories to which they are then sent for analysis. The laboratory will provide a report

back to the facility documenting the exposure of the wearer. A control badge or control TLD is provided with each shipment of new personnel monitors. This control should be kept at a location that is distant from the radiation-producing device. The purpose of the control is to document any radiation exposure during the mailing of the personnel monitors. This purpose is defeated if the control is kept in the room with the radiation-producing device. Film badges and TLDs should not be exposed to extreme heat or high humidity, left in cars, or worn during activities not related to the performance of the technologist's professional duties.

THE PREGNANT TECHNOLOGIST

If the technologist becomes pregnant, there are specific measures that can be taken to ensure the protection of the fetus, even though the risk is extraordinarily low if bone densitometry is the only potential source of occupational exposure. First, the technologist should inform her employer in writing that she is pregnant. A protective apron can be provided that should be worn by the technologist. It is also reasonable to wear a second personnel monitoring device at waist level under the apron to monitor exposure of the fetus. The maximum permissible dose to the fetus according to the 1993 NCRP recommendations is 500 mrem (5 mSv) (10). It is extremely unlikely that a densitometry technologist would even remotely approach this level of exposure to a fetus but the concept of ALARA should always guide radiation protection efforts.

REFERENCES

1. (1993) Concepts of radiation, in *Radiologic Science for Technologists* (Bushong, S. C.), Mosby, St. Louise, pp. 3–17.
2. (1990) Protection, in *Christensen's Physics of Diagnostic Radiology* (Curry, T. S., Dowdey, J. E., Murry, R. C., eds.), Lea & Febiger, Philadelphia, pp. 372–391.
3. National Council on Radiation Protection and Measurements. (1993) Ionizing radiation exposure of the population of the United States. NCRP Report No. 93. NCRP Publications, Bethesda, MD.
4. Kalendar, W. A. (1992) Effective dose values in bone mineral measurements by photon absorptiometry and computed tomography. *Osteoporos. Int.* **2**, 82–87.
5. Information on file. Alara, Inc., 2545 Barrington Court, Hayward, CA 94545.
6. (1993) Early effects of radiation, in *Radiologic Science for Technologists* (Bushong, S. C.), Mosby, St. Louise, pp. 559–576.
7. Njeh, C. R., Fuerst, T., Hans, D., Blake, G. M., Genant, H. K. (1999) Radiation exposure in bone mineral density assessment. *Appl. Radiat. Isot.* **50**, 215–236.
8. Lewis, M. D., Blake, G. M., Fogelman, I. (1994) Patient dose in dual X-ray absorptiometry. *Osteoporos. Int.* **1**, 11–15.

9. Patel, R., Lewis, M. D., Blake, G. M., Batchelor, S., et al. (1996) New generation DXA scanners increase dose to patient and staff, in *Current Research in Osteoporosis and Bone Mineral Measurement IV*, British Institute of Radiology, London, p. 99.
10. National Council on Radiation Protection and Measurements. (1993) *Limitations of exposure to ionizing radiation*. NCRP Report No. 116. NCRP Publications, Bethesda, MD.
11. Lloyd, T., Egli, D. F., Miller, K. L., Egli, K. D., Dodson, W. C. (1998) Radiation dose from DXA scanning to reproductive tissues of females. *J. Clin. Densitom.* **1**, 379–383.
12. Patel, R., Blake, G. M., Batchelor, S., Fogelman, I. (1996) Occupational dose to the radiographer in dual X-ray absorptiometry: a comparison of pencil-beam and fan-beam systems. *Br. J. Radiol.* **69**, 539–543.

8

Quality Control

CONTENTS

- PHANTOMS
 - EUROPEAN SPINE PHANTOM
 - BONA FIDE SPINE PHANTOM
 - HOLOGIC SPINE AND HIP PHANTOMS
 - LUNAR SPINE PHANTOM
- USING THE PHANTOM TO CREATE CONTROL TABLES AND CHARTS
- SHEWHART RULES AND CUSUM CHARTS
 - SHEWHART RULES
 - CUSUM CHARTS
- AUTOMATED QUALITY CONTROL PROCEDURES
- REPLACING A DENSITOMETER
- REFERENCES

Although much has been written about quality control procedures in densitometry, many of these articles have been concerned with data collection in clinical research rather than patient data collected as part of medical care. Quality control, although absolutely necessary in clinical research, is no less necessary in clinical practice. The original indications for bone mass measurements from the National Osteoporosis Foundation published in 1989 and the guidelines for the clinical applications of bone densitometry from the International Society for Clinical Densitometry published in 1996 called for strict quality control procedures at clinical sites performing densitometry (1,2). The Canadian Panel* of the International Society for Clinical Densitometry published specific guidelines for quality control procedures in 2002 (3). Such

*The Canadian Panel of the International Society for Clinical Densitometry represents the International Society for Clinical Densitometry in Canada and oversees the Society's programs in Canada.

procedures are crucial to the generation of accurate and precise bone density data. When quality control is poor or absent, the bone density data may be incorrect. The interpretation made by the physician based on that incorrect information would be in error. The medical management of the patient may be adversely affected. The patient will also have been exposed to a small amount of radiation inappropriately and wasted time and money. In clinical trials, the results from hundreds or thousands of individuals are usually averaged and conclusions based on the average values. Small errors in machine performance are made insignificant by the averaging of so many results. In clinical practice, this luxury does not exist. Decisions are made based on one measurement from one patient, which means that strict quality control in clinical practice is even more important than in clinical trials. In spite of inherently superb accuracy and precision in today's densitometers, alterations in the functioning of the machines can and will occur. Quality control procedures to detect these alterations in machine function should be utilized by every clinical site performing densitometry regardless of the frequency with which measurements are performed.

The quality control procedures used in densitometry were derived from procedures originally developed for quality control in analytical chemistry and industry (4). The adaptation of these procedures for use in bone densitometry is generally credited to Drs. Orwoll and Oviatt (5). The most commonly used methods are control tables, visual inspection of a Shewhart chart, Shewhart rules, and the cumulative sum (CUSUM) chart. All of these methods require that a phantom be scanned to establish a baseline value and then regularly, to establish longitudinal values.

PHANTOMS

Manufacturers of X-ray-based bone densitometers routinely provide phantoms for use with their machines. Some phantoms, like the anthropomorphic Hologic spine phantom, are used with densitometers from other manufacturers. Other phantoms, such as the European Spine Phantom (ESP) or the Bona Fide phantom were developed independently of any one manufacturer and intended for use on multiple machines. The manufacturer-supplied phantom is often designed with the specific attributes of the manufacturer's machine in mind, making it the preferred phantom to use with that machine. The perfect phantom that could be used on all machines to test all things does not yet exist.

Some, but not all, manufacturers provide two phantoms to be used for different purposes. One phantom may be used for daily quality assurance functions, during which the mechanical operation and calibration of the machine are tested. The second phantom may be designed to mimic a region of the skeleton and used for quality control to detect a shift or drift in bone mineral density (BMD) values.

Phantoms that attempt to replicate a particular region of the skeleton are called *anthropomorphic phantoms*. These phantoms are made of hydroxyapatite or aluminum. Although hydroxyapatite is preferred by the Food and Drug Administration for such a phantom, aluminum is also appropriate because it behaves very much like bone when X-rayed. The phantom may be encased in an epoxy-resin or plastic block or placed within some other type of material to simulate human soft tissue. Water or uncooked rice can be used for this purpose. The perfect anthropomorphic phantom would replicate the size and shape of the bone or bones in question, have varying densities within a single bone or region, contain a range of densities likely to be encountered clinically, and be surrounded by a material that adequately mimics human soft tissue. Replicating the size and shape of the particular bone or bones and having a nonuniform density throughout the bone tests the edge-detection methodology of the particular system. In other words, it tests the machine's ability to distinguish bone from soft tissue. If the phantom bears no resemblance in size or shape to the particular bone or has very sharp, smooth edges, or if the density of the material is uniform within the bone, the edge-detection program of the machine will not be adequately tested. If the material surrounding the phantom does not adequately replicate human soft tissue, once again the ability of the machine to tell bone from soft tissue will not be not maximally tested. In order to test a system's abilities at various levels of bone density, it is desirable to have a range of densities contained within the phantom. At the same time, this range should reflect values that are likely to be encountered in clinical practice for the test to truly be useful. Most of the manufacturer-supplied phantoms in use today have some of these attributes, but not all. The attributes emphasized by a manufacturer generally depends on those attributes that the manufacturer wishes to test as a part of the routine quality control program for their machine.

European Spine Phantom

The development of the ESP was one attempt to develop a more perfect spine phantom that could be used on all central devices. It was

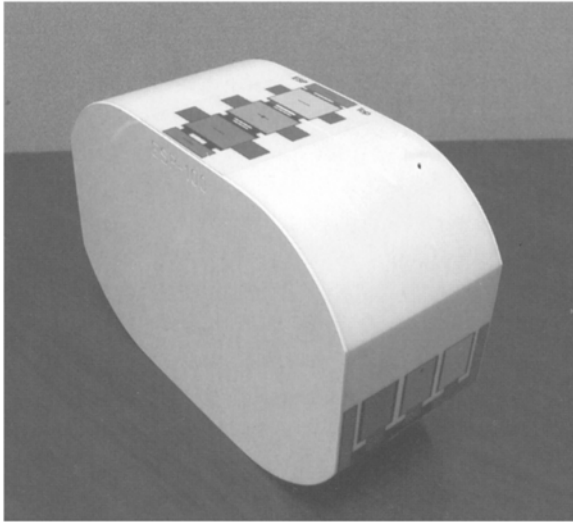


Fig. 8-1. European Spine Phantom. (Photo courtesy of Bio-Imaging Technologies Inc., Newtown, PA.)

developed independently of any manufacturer under the direction of the Committee d'Actions Concertées-Biomedical Engineering. (6). The ESP is a semianthropomorphic phantom. Its three vertebrae are made of hydroxyapatite and vary in density, with standardized BMDs of 500, 1000, and 1500 mg/cm^2 (7). The vertebrae are encased in a plastic and epoxy-resin material equivalent to about 10% fat that is molded into an oval shape with flattened sides measuring 28 \times 18 cm. The phantom is shown in Fig. 8-1. The use of the ESP has generally been restricted to clinical research trials, primarily because of its expense. It was originally hoped that the ESP could be used to standardize BMD on any central bone densitometer. Unfortunately, this has not proven to be the case. It is an excellent phantom for cross-calibration of central DXA densitometers, however.

Bona Fide Spine Phantom

The Bona Fide phantom is a calcium hydroxyapatite step wedge encased within an acrylic block. The acrylic provides a soft tissue equivalent of 26% fat, and the phantom spans a range of densities from 0.7 to 1.5 g/cm^2 (8). The block may remain in its cloth carrying case during scanning, increasing ease of use. Like the ESP phantom, the Bona Fide phantom is not manufacturer-specific and is an excellent phantom for cross-calibration of central DXA devices. This phantom is shown in Fig. 8-2.

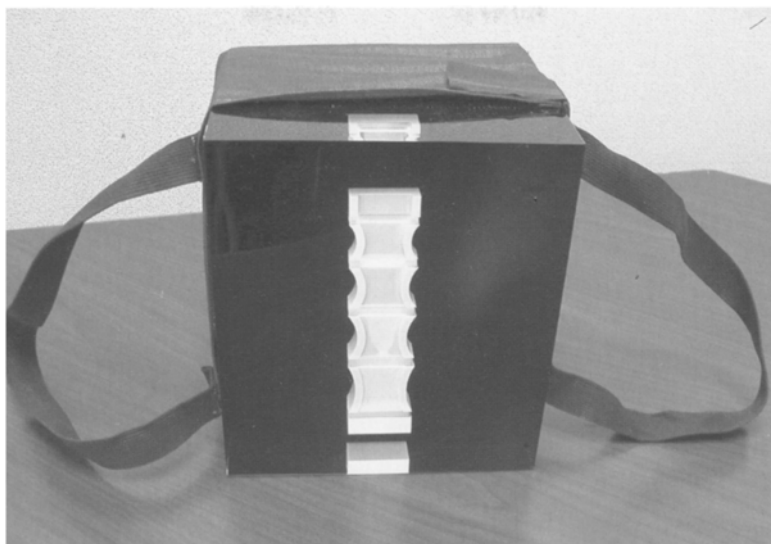


Fig. 8-2. Bona Fide Spine Phantom. (Photo courtesy of Bio-Imaging Technologies Inc., Newtown, PA.)

Hologic Spine and Hip Phantoms

The Hologic anthropomorphic spine phantom, although intended for use with Hologic DXA devices, is often used with DXA devices from other manufacturers. The phantom itself consists of four anatomically correct vertebrae made of calcium hydroxyapatite. The vertebrae are encased in an epoxy-resin to simulate soft tissue. The four vertebrae have similar densities and areas and the soft tissue simulation of the epoxy-resin approaches 60% fat. Each Hologic spine phantom will have a factory-specified L1–L4 BMD. Consistent daily calibration can be obtained with the Hologic anthropomorphic spine phantom, although the lack of a range of BMD values make it less suitable for cross-calibration of central DXA devices. The Hologic spine phantom is shown in Fig. 8-3. The Hologic anthropomorphic hip phantom has found less of a role in clinical medicine. It does not offer any quality control testing capabilities to the clinician that cannot be obtained with the anthropomorphic spine phantom other than proximal femur edge detection, which is under the control of the machine software, rather than the hardware (8).

Lunar Spine Phantom

The Lunar spine phantom, shown in Fig. 8-4, is a rectangular aluminum bar that is intended to replicate the lower half of T12, all of L1, L2, L3,

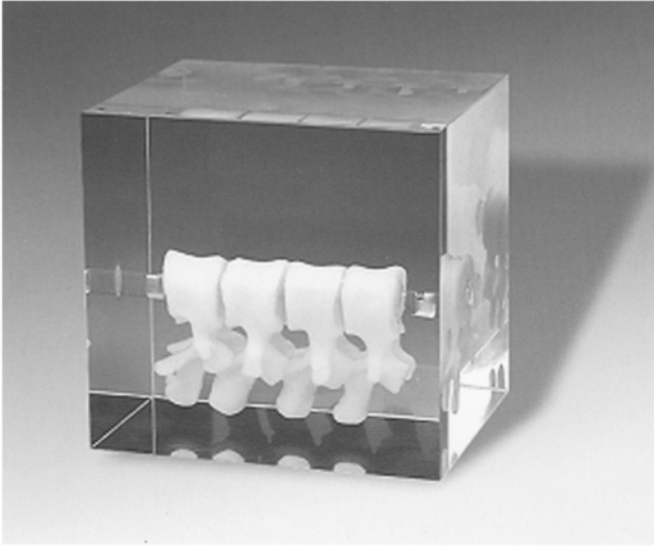


Fig. 8-3. Hologic Spine Phantom. (Photo courtesy of Hologic, Inc., Bedford, MA.)

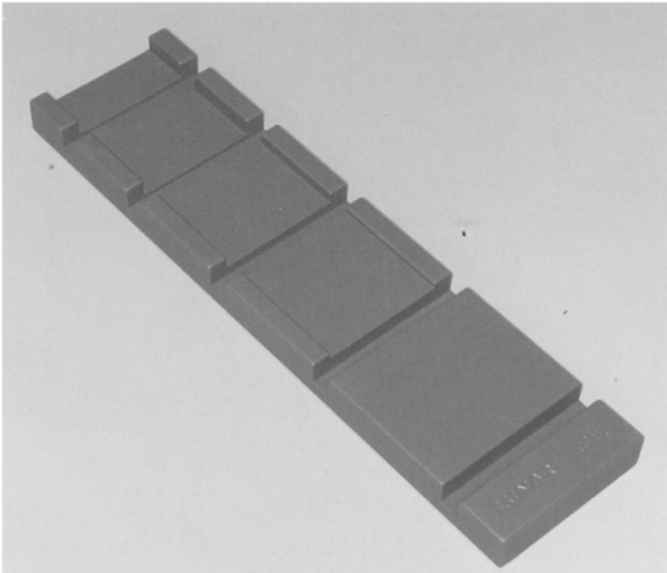


Fig. 8-4. Lunar Aluminum Spine Phantom. (Photo courtesy of Bio-Imaging Technologies Inc., Newtown, PA.)

and L4, and the upper half of L5. Each vertebra has a different density that is achieved by varying the thickness of the aluminum. The area of each vertebra is different as well. The densities of L1–L4 are 0.92, 1.076, 1.239, and 1.403 g/cm², respectively. The L2–L4 BMD is 1.256 g/cm². To simulate soft tissue, the aluminum phantom is submerged in a water bath with a depth of approximately 15 cm. The aluminum phantom is also available encased in an epoxy-resin block, avoiding the necessity of a water bath and improving ease of use.

USING THE PHANTOM TO CREATE CONTROL TABLES AND CHARTS

Most daily quality assurance procedures to detect mechanical failures on today's densitometers are automated. The program will indicate a passing or failing condition. Before outright mechanical failure occurs, however, regular scanning of the quality control phantom and the application of Shewhart charts and rules or CUSUM charts can detect drifts or shifts in machine values that require correction in order to ensure continued accuracy and precision. Abrupt shifts in values are generally easy to detect. Drifts can be more subtle and therefore, more insidious. The confirmed occurrence of either indicates that the machine is out of control (OOC).

Manufacturers generally recommend scanning the phantom 10 times on the same day without repositioning the phantom in between studies. This is also the procedure often used as part of quality control procedures in longitudinal clinical research trials. Subsequent phantom scans are then performed at least three times a week and on every day that a patient is scanned.

The average value of the 10 phantom scans should be calculated. The range that represents the average value $\pm 1.5\%$ should also be calculated. The average value $+1.5\%$ and the average value -1.5% become the upper and lower limits of BMD within which all subsequent measurements of the phantom should fall. These upper and lower limits are called *control limits*. A control table as shown in Table 8-1 can then be created. One column lists the date of the phantom scan. The second column gives the actual BMD value. In the third column, a yes or no entry indicates whether the phantom BMD value fell within the established control limits.

A control graph offers some advantages over the control table. A control graph is created using the same average value from 10 consecutive phantom scans and control limits based on $\pm 1.5\%$ of the average value. The vertical or y-axis of the graph reflects the BMD values in g/cm². The

Table 8-1
Control Table

<i>Date</i>	<i>Phantom value (g/cm²)</i>	<i>Within control limits</i>
10/09/2000	1.179	Yes
10/10/2000	1.187	Yes
10/11/2000	1.162	No
10/11/2000	1.170	Yes
10/12/2000	1.184	Yes

Control limits of $\pm 1.5\%$ or 1.164 to 1.200 g/cm² were established based on a 10-phantom average bone mineral density of 1.182 g/cm².

horizontal or *x*-axis reflects time in days. The BMD that corresponds to the 10-phantom average should be indicated by drawing a solid horizontal line across the graph. The upper and lower control limits values are similarly indicated by drawing a dashed line across the graph. Subsequent phantom values are easily tracked by plotting the results on the control graph. Such a graph is called a Shewhart chart.

The results of 10 scans of the anthropomorphic Hologic spine phantom that were performed on a Lunar DPX are shown in Table 8-2. The average value for the 10 scans was calculated as 1.182 g/cm². To find the upper and lower control limits, the average value was multiplied by 1.5%. This was determined to be 0.018 g/cm² (1.182 g/cm² \times 0.015). Therefore the range of values within which all subsequent phantom scan values should fall is 1.182 \pm 0.018 gm/cm² or from 1.164 to 1.200 g/cm². Figure 8-5 is the Shewhart chart that was created for this set of 10 phantom scans onto which subsequent phantom scan values have been plotted. The phantom BMD values obtained over time from a scanner that is operating perfectly should randomly fall on either side of the 10-phantom BMD average value but remain within the control limit boundaries of $\pm 1.5\%$. If a value falls outside the boundaries, the phantom scan should immediately be repeated. If it falls outside the boundaries again, or “fails”, the manufacturer should be contacted for additional instructions.

A visual inspection of the Shewhart chart can also provide more subtle clues to machine malfunction or a machine going OOC. The pattern of the values should be reviewed to ensure that the values appear to be randomly falling on either side of the average value in addition to being within the control limits. If this randomness appears to be lost, the machine may be

Table 8-2
Ten Hologic Spine Phantom Scans Performed on a Lunar DPX
on the Same Day to Establish a Baseline Phantom Bone Mineral Density
Value for Quality Control

<i>Phantom scan no.</i>	<i>Date</i>	<i>L1-L4 BMD (g/cm²)</i>
1	4/22/00	1.181
2	4/22/00	1.173
3	4/22/00	1.176
4	4/22/00	1.180
5	4/22/00	1.190
6	4/22/00	1.174
7	4/22/00	1.189
8	4/22/00	1.192
9	4/22/00	1.177
10	4/22/00	1.187

The average value for the 10 phantom scans is 1.182 g/cm². The standard deviation is 0.007 g/cm² and 1.5% of the average value is 0.018 g/cm².

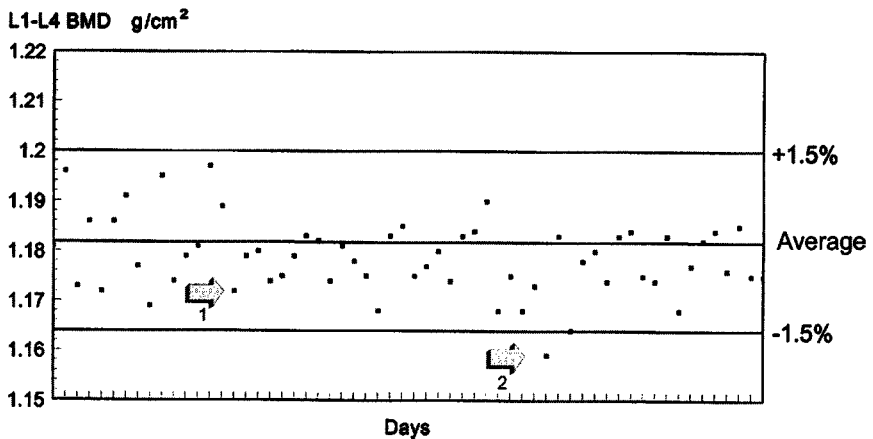


Fig. 8-5. Shewhart control chart. The average bone mineral density of the phantom was established by scanning the phantom 10 times on the same day without repositioning between scans. The control limits were established as $\pm 1.5\%$. The warning level for application of Shewhart rules was set at $\pm 1.5\%$. Arrow 1 indicates the point at which it appears that the values are beginning to drift downward rather than maintaining their random scatter on either side of the average. Arrow 2 indicates the point at which the warning rule was actually violated, triggering the application of the Shewhart rules.

drifting. If an imaginary straight line drawn through the center of the phantom values is above or below the average value, a shift may have occurred. In either of these cases, the manufacturer should again be contacted for instructions. An inspection of the Shewhart chart in Fig. 8-5 suggests a possible drift in values. Arrow 1 on the graph in Fig. 8-5 indicates a point at which it appears that the phantom values are no longer randomly scattered on either side of the average but instead are concentrated below the average. This suggests that the scan values may be starting to drift downward. These situations can and do occur even though the absolute BMD values obtained from the daily phantom scans remain within the established range and other daily quality assurance procedures continue to give "PASS" indications.

The control table described earlier is simpler to create and maintain than the Shewhart chart but the ability to visually inspect the data for drifts or shifts is lost. The creation of a Shewhart control table or chart constitutes the minimum quality control program that should be in use in every facility performing densitometry.

The creation of an average baseline phantom value by scanning the phantom 10 times on the same day without repositioning may not reflect the day to day variability in machine values and the effects of repositioning that would be expected as the phantom is scanned over time. Several groups have consequently recommended that the baseline phantom value be established by scanning the phantom once a day for 15 to 25 consecutive days and then averaging these 15 to 25 scans. It is thought that this will more accurately reflect the day-to-day variability in machine values and result in fewer "false alarm failures." For example, the average BMD of the same Hologic spine phantom when scanned on 25 consecutive days as shown in Table 8-3 was 1.177 g/cm^2 resulting in a range for the average $\pm 1.5\%$ of 1.159 g/cm^2 to 1.195 g/cm^2 . In both cases, 1.5% of the mean value was 0.018 g/cm^2 but the range of acceptable values was different from that seen when the phantom was scanned 10 times on the same day without repositioning. Figure 8-6 is the graph of subsequent scans now plotted against the baseline phantom value obtained after scanning the phantom once on each of 25 consecutive days.

Notice in Fig. 8-6, when the mean was calculated using 25 scans performed on consecutive days, the same phantom values do not give any indication of a loss of random scatter. More sophisticated evaluations of this type of data can be done to determine if, in fact, there has been a shift in values. Nevertheless, this type of chart is the foundation of a good quality control program.

Table 8-3
25 Hologic Spine Phantom Scans Performed on a Lunar DPX
on 25 Consecutive Days to Establish a Baseline Phantom Value
for Quality Control

<i>Phantom scan no.</i>	<i>Date</i>	<i>(L1-L4) BMD (g/cm²)</i>
1	4/22/00	1.181
2	4/23/00	1.172
3	4/24/00	1.176
4	4/25/00	1.172
5	4/29/00	1.180
6	4/30/00	1.185
7	5/01/00	1.179
8	5/02/00	1.176
9	5/06/00	1.177
10	5/07/00	1.169
11	5/08/00	1.180
12	5/09/00	1.167
13	5/13/00	1.179
14	5/14/00	1.189
15	5/15/00	1.174
16	5/16/00	1.186
17	5/20/00	1.181
18	5/21/00	1.170
19	5/22/00	1.179
20	5/23/00	1.178
21	5/28/00	1.180
22	5/29/00	1.181
23	5/30/00	1.168
24	6/03/00	1.182
25	6/04/00	1.172

The average value for the 25 phantom scans is 1.177 g/cm². The standard deviation (SD) is 0.006 g/cm² and 1.5% of the average value is 0.018 g/cm². Compare these average and SD values to those calculated for the 10 scans in Table 8-2.

SHEWHART RULES AND CUSUM CHARTS

The field of analytical chemistry recognized the need for strict quality control many years ago. Like bone densitometry, analytical chemistry involves the use of machines for quantitative measurements. Techniques had to be developed to determine that the machines continued to function

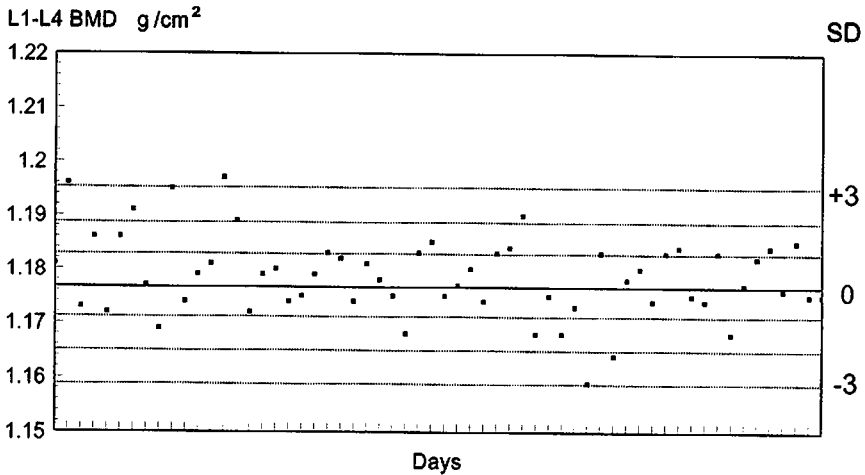


Fig. 8-6. Shewhart control chart. The average bone mineral density of the phantom was established by scanning the phantom once on 25 consecutive days. The values appear to be randomly scattered on either side of the average value. If the warning rule was set at 3 standard deviations, the application of Shewhart rules would have been triggered on two occasions, seen early in the plot. No other rules were violated, however. As a consequence, the violations were not confirmed and were considered false alarms.

properly over long periods of time in order to ensure consistency in the results (4). The methods common to analytical chemistry have been adapted for use in bone densitometry (5). These methods utilize the BMD values from the phantom scans as described earlier: the average phantom value and the values from phantom scans performed over time. The two most commonly used methods for tracking machine performance are Shewhart rules and the CUSUM chart.

Shewhart Rules

Shewhart[†] rules have been used in analytical chemistry since the 1950s. In order to utilize Shewhart rules it is necessary to establish a baseline value and control limits for the phantom measurement and create a Shewhart chart as described earlier. Establishing the baseline phantom value by scanning the phantom on each of 15 to 25 consecutive days,

[†]Dr. William Andrew Shewhart (1891–1967) as a scientist with Western Electric devised the basis for the application of statistical methods to quality control. In 1931, his book, *Economic Control of Quality of Manufactured Product*, was published in which he presented his methods for statistical sampling.

rather than multiple times on the same day is recommended. If, for some reason, this is impractical, a 10-phantom average created by scanning the phantom 10 times on the same day can certainly be used. Once the average value of the phantom scans is determined, the standard deviation (SD) for the set of scans should be calculated. A Shewhart chart can then be created onto which the BMD data from subsequent phantom measurements is plotted as was done in Fig. 8-6. The y-axis of the graph should reflect both the actual BMD values and SD units as shown in Fig. 8-6. To utilize SD units, the average BMD is assigned a value of 0 on the y-axis of the graph and the SD tics are labeled +1 or -1, +2 or -2, and so on. In other words, the y-axis reflects both the measured BMD and the z -score[§] of the daily phantom BMD measurements. The average phantom value used to construct the Shewhart chart in Fig. 8-6 was previously found to be 1.177 g/cm². The SD was also previously found to be 0.006 g/cm² for this set of measurements. It is not necessary to calculate the z -score for each of the phantom measurements. When the measured BMD is plotted on the graph, it becomes visually apparent how many SDs from the average the value actually lies because of the SD or z -score scale on the y-axis. Remember that with a perfectly functioning machine, the values plotted on the graph are expected to be randomly scattered on either side (that is, above and below) of the average BMD or z -score of 0.

As these values are being plotted, “rules” are applied to detect trends or “failures” that may indicate a change in machine performance. These are called *Shewhart rules* or *sensitizing rules* (9). Different combinations of rules have been tested in densitometry in order to minimize false alarms and increase the ability of the Shewhart rules to detect true alterations in machine performance (5,10,11).

Shewhart rules are usually “set” at a certain level. In other words, a triggering or warning level is selected. When this level is exceeded, the Shewhart rules are applied. For example, Shewhart rules may be set at a warning level of the average ± 2 SDs (4). If the phantom BMD value is more than 2 SDs above or below the average BMD, the Shewhart rules are applied to detect potential machine failures. A machine failure is then deemed to have occurred if any one or more of the following Shewhart rules have been violated:

[§]In this context, z -score has nothing to do with reference population BMD data. It is simply the number of standard deviations above or below the average value. See Chapter 1, for a discussion of the z -score scale.

1. A phantom BMD value exceeding the average ± 3 SDs.
2. Two consecutive phantom BMD values on the same side of the average exceeding the average by ± 2 SDs.
3. Two consecutive phantom BMD values differing by more than 4 SDs.
4. Four consecutive phantom BMD values on the same side of the average exceeding the average by ± 1 SD.
5. Ten consecutive phantom BMD values falling on the same side of the average regardless of their distance from the average.

Not all violations of the rules will be found to be machine failures that require correction and as such, are considered false alarms. In order to reduce the false alarms, a filter is sometimes applied to the sensitizing rules. One such filter is to calculate the average BMD for 10 consecutive phantom measurements after a violation of one of the Shewhart rules has occurred. If this 10-scan average differs by more than 1 SD from the baseline average value, the violation is confirmed. Another method is to set the triggering of the rules at a higher level, such as the 3 SD deviation level. When this approach is employed, the occurrence of a single value outside the 3 SD limit then triggers the application of the other rules.

Without such filters or triggers, Shewhart rules, although easy to use, produce a high false alarm rate. Even if a machine is in perfect working order, a violation of the Shewhart rules is expected to occur once every 39 scans (11). When the filter is added, the false alarm rate drops to once every 631 scans. Unfortunately, although the addition of the filter to Shewhart rules reduces the number of false alarms, it may also have the undesirable effect of delaying detection of true shifts in machine performance.

Shewhart rules may also be utilized by calculating the average \pm a percentage of the average as was done in the quality control chart in Fig. 8-5 (12). For most of the central DXA scanners in clinical use today, repeat phantom measurements will generally result in an SD for the baseline set of phantom measurements that is roughly 0.5% of the average value. Consequently, 1.5% of the average value for the phantom BMD will approximately equal 3 SDs. For example, when the statistics were calculated for the 10 phantom measurements performed on the same day shown in Table 8-2, the average was 1.182 g/cm², with a SD of 0.007 g/cm², and 1.5% of the average was found to be 0.018 g/cm². In this case, 1.5% of the average is equal to 2.6 SDs. In the case of the 25 phantom scans shown in Table 8-3 with a SD of 0.006, the 1.5% value of 0.018 g/cm² is equal to 3 SDs. The percentage values can be used to invoke the Shewhart rules. Using a value of 0.5% of the average as equaling 1 SD, the Shewhart rules

would be applied if a phantom value exceeded the baseline average value $\pm 1\%$ (instead of the average ± 2 SDs). A violation would be deemed to have occurred in any of the following circumstances:

1. A phantom BMD value exceeds the average by $\pm 1.5\%$.
2. Two consecutive phantom BMD values on the same side of the average exceed the average by $\pm 1\%$.
3. Two consecutive phantom BMD values differ by more than 2% .
4. Four consecutive phantom BMD values on the same side of the average exceed the average by $\pm 0.5\%$.
5. Ten consecutive phantom BMD values fall on the same side of the average regardless of their distance from the average.

The 10-scan average filter described above would confirm a failure if the 10-scan average differed from the baseline average by more than 0.5% (instead of 1 SD).

In quality control jargon, each of these rules has its own name. In the order listed above, the rules are known as:

1. 3 SD or 1.5% rule.
2. 2 SD twice or 1.0% twice rule.
3. Range of 4 SD or range of 2% rule.
4. Four ± 1 SD or four $\pm 0.5\%$ rule.
5. Mean $\times 10$ rule.

When any of the Shewhart rules are confirmed, the machine is OOC and the manufacturer should be consulted to determine the cause and corrective action. Once corrective action has been taken, a new phantom baseline BMD must be established by scanning the phantom as described earlier. A new Shewhart chart can then be constructed to monitor machine performance.

CUSUM Charts

CUSUM charts are not as easy to use as Shewhart charts and rules, but these are the types of charts employed by many professional densitometry quality control centers. This technique was originally developed for use in industry (13) and was subsequently adapted for use in bone densitometry (11,14,15). The principle underlying CUSUM charts is the expected random variation in the phantom measurement. Remember that even in a perfectly functioning machine, daily phantom BMD values are expected to randomly fall above or below the average phantom value. In other words, the daily phantom BMD value is expected to vary about the average value.

The magnitude of the variation, however, even though some measurements will be above (or greater) than the average value and some will be below (or less) than the average value, should remain relatively constant.

In order to utilize the CUSUM chart, a baseline spine phantom value must again be established by scanning the phantom 10 times consecutively or once on each of 15 to 25 consecutive days as was done previously for the application of Shewhart rules. For all subsequent scans, the difference between the average value and the subsequent value is calculated. The differences are progressively summed and plotted on the CUSUM chart. Mathematically, this is expressed in Eq. 1 as:

$$CS_n = \sum_{p=1}^n \left(BMD_p - BMD_{Mean} \right) \quad (1)$$

where CS is the cumulative sum, n is the total number of measurements, BMD_{Mean} is the average phantom value, and BMD_p is the phantom value for each of the n measurements. Each sequential value of CS is plotted on the graph. The vertical axis of the graph is marked in SD units of the average value. For a properly functioning machine, the values plotted on the CUSUM chart should be scattered in a horizontal pattern around 0 (0 is equal to the average phantom value). If the pattern is rising or falling, the machine is not functioning properly.

The construction of a CUSUM chart begins again with the data in Table 8-3. The phantom was scanned once each day for 25 consecutive days. The average value of the phantom was found to be 1.177 g/cm² and the SD was calculated to be 0.006 g/cm². Table 8-4 illustrates the calculations of the cumulative sum for the next 10 phantom measurements. Figure 8-7 illustrates the CUSUM plot for these 10 measurements and 30 additional measurements that followed. In Fig. 8-7, instead of BMD on the vertical axis, SD units or z-scores are utilized. The CUSUM plot for these 40 phantom scans clearly appears to be rising rather than being horizontal.

Although the CUSUM chart is inspected visually to determine machine malfunction indicated by the nonhorizontal plot, two methods have been developed to determine mathematically when control limits have been exceeded. One method involves the superimposition of a V-mask in which the slope of the arms on the mask is determined mathematically (14). The slope is normally some multiple of the standard error of the average phantom value. The stringency of the mask can be changed by increasing or decreasing the slope of the V-mask. The other method, called tabular CUSUM, involves the mathematical calculation of upper and lower control limits (11). In either case, when values fall outside the control limits

Table 8-4
Calculation of the Cumulative Sum (CUSUM) for Sequential Phantom Scans

Date	Phantom BMD (g/cm ²)	Difference from average phantom value (g/cm ²)	Cumulative sum of differences (g/cm ²)	Cumulative sum of differences expressed in SD units (z-score)
6/05/00	1.181	0.004	0.004	0.67 (0.004 ÷ 0.006)
6/06/00	1.196	0.019	0.023 (0.004 + 0.019)	4.33 (0.023 ÷ 0.006)
6/10/00	1.173	-0.004	0.019 (0.019 - 0.004)	3.17 (0.019 ÷ 0.006)
6/11/00	1.186	0.009	0.028 (0.019 + 0.009)	4.67 (0.028 ÷ 0.006)
6/12/00	1.172	-0.005	0.023 (0.028 - 0.005)	3.83 (0.023 ÷ 0.006)
6/13/00	1.186	0.009	0.032 (0.023 + 0.009)	5.33 (0.032 ÷ 0.006)
6/17/00	1.191	0.014	0.046 (0.032 + 0.014)	7.66 (0.046 ÷ 0.006)
6/21/00	1.169	-0.008	0.038 (0.046 - 0.008)	6.33 (0.038 ÷ 0.006)
6/24/00	1.195	0.018	0.056 (0.038 + 0.018)	9.33 (0.056 ÷ 0.006)
6/25/00	1.174	-0.003	0.053 (0.056 - 0.003)	8.83 (0.053 ÷ 0.006)

The z-score of the cumulative sum is plotted on the CUSUM chart. The average phantom value is 1.177 g/cm² and the standard deviation is 0.006 g/cm².

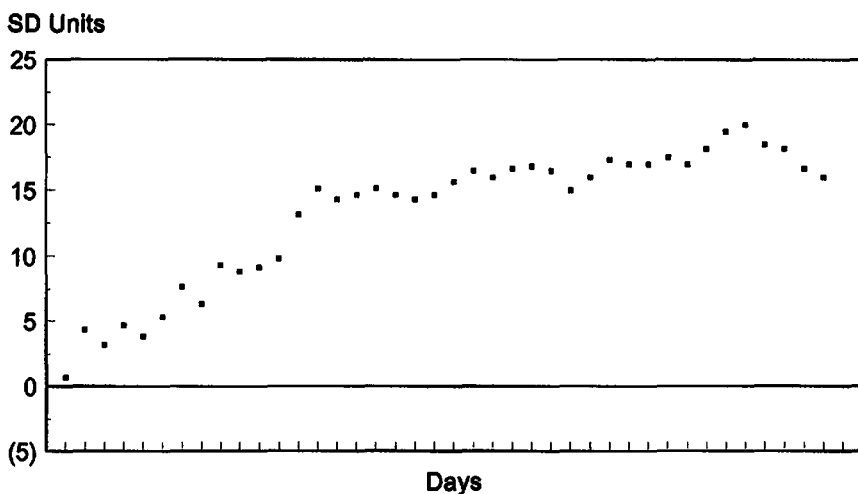


Fig. 8-7. CUSUM quality control plot. The plot clearly appears to be rising, indicating a drift in values.

or the arms of the mask, an alarm is triggered indicating that the machine is OOC and that the manufacturer should be contacted.

The calculation of the control limits for tabular CUSUM is more tedious than complex although the equations used for these calculations appear somewhat intimidating at first. The upper control limit is calculated using Eq. 2:

$$CS_{H_{max}(i)} = \frac{X_i - \mu_0}{\sigma} - k + CS_{H_{max}(i-1)} \quad (2)$$

In other words, to calculate the upper limit of the maximum cumulative sum for scan i ($CS_{H_{max}}$), subtract the average phantom value (μ_0) from the phantom value for scan i (X_i) and then divide this difference by the SD (σ) from the baseline phantom data. Now subtract the value of k , which is 0.5 (this has the effect of subtracting half a standard deviation). The resulting value is then added to the value of $CS_{H_{max}}$ that had been calculated for the previous phantom scan (scan $i - 1$). The lower limit of the maximum cumulative sum is calculated in an analogous fashion using Eq. 3:

$$CS_{L_{max}(i)} = \frac{\mu_0 - X_i}{\sigma} - k + CS_{L_{max}(i-1)} \quad (3)$$

The process is identical except that in this case, the value for phantom scan i is subtracted from the average phantom value, which is the opposite of what was done in order to calculate the upper control limit. When either

Table 8-5
Tabular (CUSUM) Limits for 10 Phantom Scans Previously Shown in Table 8-4

<i>Date</i>	<i>Phantom BMD (g/cm²)</i>	<i>CS_{Hmax}</i>	<i>CS_{Lmax}</i>
6/5/00	1.181	0.167	0
6/6/00	1.196	2.834	0
6/10/00	1.173	1.667	0.167
6/11/00	1.186	2.667	0
6/12/00	1.172	1.334	0.333
6/13/00	1.186	2.334	0
6/17/00	1.191	4.167	0
6/21/00	1.169	2.334	0.833
6/24/00	1.195	4.834	0
6/25/00	1.174	3.834	0

The CS_{Hmax} approached but did not exceed 5. The CS_{Lmax} was reset to 0 on seven occasions because the value fell below 0. The mean and standard deviation for the baseline phantom values used in these calculations are 1.177 g/cm² and 0.006 g/cm², respectively.

of the two control limits falls below 0, the CS for that limit is set back to 0, the value that is then used for subsequent calculations for that CS. When either of the CS limits exceeds a value of 5, a possible machine failure is deemed to have occurred. Table 8-5 illustrates the calculation of the upper and lower CS control limits for 10 scans that were performed after the initial establishment of the baseline phantom mean value and SD previously shown in Table 8-3.

CUSUM charts or tabular CUSUM are most easily performed with the help of sophisticated statistical software programs. There is no reason, however, that clinical densitometry centers cannot employ CUSUM methodology, even though it is certainly less intuitive to use than Shewhart charts and rules.

AUTOMATED QUALITY CONTROL PROCEDURES

In recent years, densitometry manufacturers have increasingly automated quality control procedures. Calibration standards may be contained within the devices and checked routinely at the touch of a button. Quality control graphs may be generated by the system software, on which phantom values over time are plotted. Shewhart rules may be automatically applied to the results, prompting messages of Pass, Fail, or notification of specific rule failures. Such innovations are indeed welcome, but they are

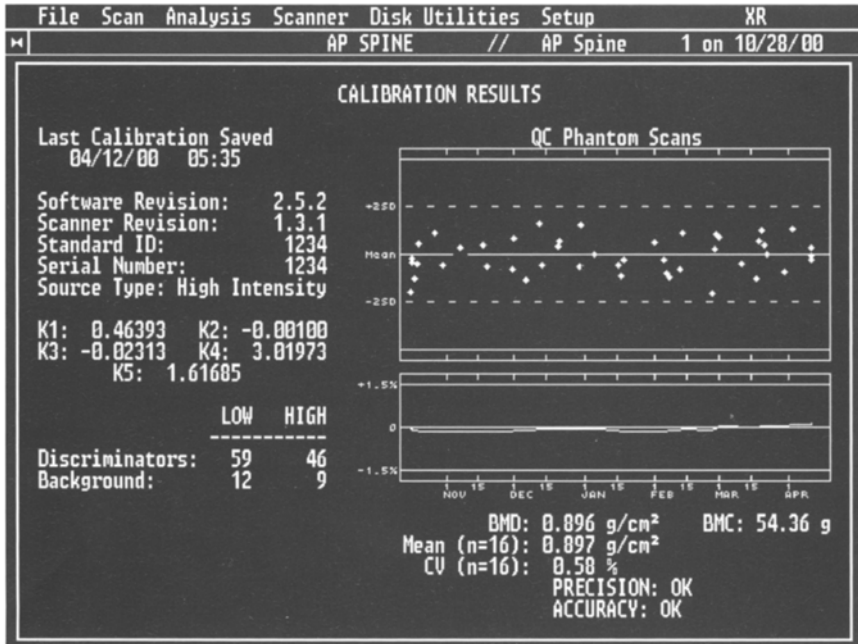


Fig. 8-8. Quality control plot from a Norland XR-series central densitometer. This is a Shewhart chart with control limits of ± 2 standard deviations (SDs) for precision on the upper graph and $\pm 1.5\%$ for accuracy on the lower graph. The software automatically calculates the average and SD of the last 16 phantom measurements and applies Shewhart rules to determine possible shifts and drifts. The indication of “OK” after accuracy and precision indicates that no rules have been violated.

useless unless these procedures are performed on a regular basis. It is also imperative that the densitometrist knows what to look for and understand the information presented.

A quality control graph from a Norland XR-Series densitometer is shown in Fig. 8-8. The upper graph reflects the precision of the system (16). In the upper graph, the solid horizontal line reflects the average value for the 16 most recent scans. The dashed horizontal lines indicate ± 2 SDs about the average. The value of the SD used to establish this range is a value for the phantom that is entered into the computer during the setup of the system. The BMD values of the individual scans are plotted on the graph. Approximately 1 out of every 20 scans is expected to fall outside the range defined by the average ± 2 SDs simply because, statistically, this range will contain only 95% of the values. The computer will also calculate the SD for each set of 16 scans. This value is not plotted, but is used

by the computer. Clearly, the average and SD will change as new phantom scans are performed and added to the set of the 16 most recent scans. This type of calculation is called a *moving average*. The results are monitored for changes in the BMD as well as increases in the SD. Shewhart rules are applied to detect unacceptable changes in the BMD. The acceptable limits for an increase in the SD are calculated mathematically. If the system passes all tests, the notation of “OK” is seen after “PRECISION” at the bottom of the graph. Other messages may be seen, however, which should prompt a call to the manufacturer. For example, an “OUT OF RANGE” notation indicates that the SD from the most recent 16 scans has increased beyond acceptable limits. A “WARNING 1” notation indicates that a single phantom BMD value is more than 3 SDs from the average. This is a violation of the Shewhart 3 SD rule. “WARNING 2” is a violation of either the Shewhart 2 SD twice or Range of 4 SD rule and “WARNING 3” is a violation of the Shewhart Four ± 1 SD rule.

The lower graph reflects the accuracy of the system (16). The solid horizontal line represents the phantom BMD value that was entered into the computer during the setup of the system. The dashed horizontal lines indicate a range of $\pm 1.5\%$ about this value. The values plotted on this graph are the average BMD values for the last 16 phantom scans. If the average value for the 16 most recent phantom scans falls within $\pm 1.5\%$ of the true phantom value, “OK” will be seen next to the word “ACCURACY” at the bottom of the graph. An “OUT OF RANGE” message will appear if the value falls outside those limits. If eight consecutive values fall on the same side of the true phantom value, a “TREND WARNING” message will appear.

The quality control graphs and calculations for the Norland pDEXA[®] are very similar to those of the XR-Series. The control limits for the accuracy of the pDEXA system are $\pm 2.5\%$ instead of 1.5% (17).

Hologic scanners also provide automated quality control graphing procedures (18). The BMD of a phantom is established during the initial calibration procedures for the scanner. The control limits of $\pm 1.5\%$ of the phantom BMD value are defined on a graph onto which subsequent spine phantom BMD data is plotted. Underneath the graph, two tables are displayed. The table titled “Reference Values” lists the average or mean value and SD for the spine phantom established during machine calibration. The table titled “Plot Statistics” lists the number of phantom scans plotted (n), the mean, SD, and percent coefficient of variation for those scans. There are no sensitizing rules built into the quality control program in the computer. With this automated plot, however, Shewhart rules are easy to apply.

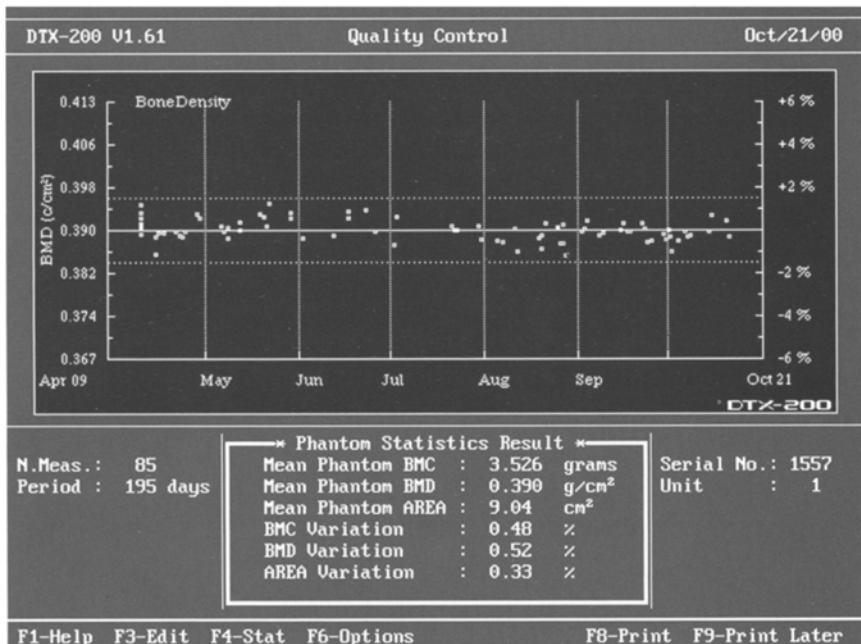


Fig. 8-9. Quality control plot from a DTX-200 DexaCare[®] peripheral densitometer. This is a Shewhart chart with control limits of $\pm 1.5\%$.

Other manufacturers have automated charting of phantom values. Figure 8-9 is such a chart from the Osteometer DTX-200 DexaCare[®], a dedicated DXA forearm scanner. The dashed horizontal lines on the graph represent control limits of $\pm 1.5\%$. None of the 85 phantom values has fallen outside the control limits and the values appear to be randomly scattered about the average value. If such charts are not available, they are easily created using the information in this chapter.

All densitometry centers should implement quality control procedures that minimally consist of control tables or charts with defined control limits of $\pm 1.5\%$ for the average of 10 phantom scans performed on 1 day or 25 scans performed on consecutive days. Shewhart rules with a filter can then be implemented, using rules defined on the basis of percentage or SD, to further strengthen the quality control program. The application of CUSUM charts and calculations as performed at professional quality control centers is more labor intensive and not necessarily of greater benefit to the clinical densitometry center. The recommendations (3) from the Canadian Panel of the International Society for Clinical Densitometry

Table 8-6
**Recommendations from the Canadian Panel of the International Society
for Clinical Densitometry for Documentation of a Quality Control Program**

1. Current operating manual from equipment manufacturer
 2. Appropriate positioning devices
 3. Appropriate calibration standard
 4. Calibration history for specific densitometer
 5. Precision data and estimates of site-specific precision errors
 6. Maintenance and upgrade records
 7. Software version/upgrade records
 8. Cross-calibration records in the event of an equipment change
 9. Data and database archiving procedures
 10. Local, provincial, and federal licensures of equipment as required
 11. Medical physicist inspection reports as required
-

Reproduced with permission from *J. Clin. Densitom.* 2002;5:247–257.

Table 8-7
**2004 International Society for Clinical Densitometry Guidelines for Quality
Control Requirements for Dual-Energy X-Ray Absorptiometry Facilities**

- Follow manufacturer's guidelines for system maintenance
 - Perform weekly phantom scans, unless required more often by the manufacturer
 - Establish a quality control chart for phantom scans showing upper and lower control limits of $\pm 1.5\%$
 - Recheck and verify the mean phantom BMD after any service performed on the densitometer has not deviated from the prior mean BMD by more than 1%
 - Establish corrective thresholds to trigger a repair request, such as two consecutive failing phantom scans
 - Maintain all service logs
 - Comply with all government inspections, surveys and requirements
-

(ISCD) for a complete quality control program include not only the creation of a control chart with limits of 1.5% but the maintenance of logs and manuals for each densitometer that include the items listed in Table 8-6. These recommendations are certainly appropriate for densitometry facilities in the United States as well as Canada. In 2004, the full ISCD (19) issued guidelines for densitometry facility quality control programs. ISCD recommended that the manufacturer's specific guidelines for system maintenance be followed. Their additional recommendations are shown in Table 8-7.

REPLACING A DENSITOMETER

Replacing a densitometer in clinical practice is not, of necessity, a frequent event. Densitometers are extremely durable and rarely subject to such widespread component failure that replacement of the equipment becomes necessary. Software updates and upgrades to a device purchased years ago can keep that device's applications as current as most new models. Periodically, however, a densitometer must be replaced or a replacement simply becomes desirable. This creates a clinical dilemma for facilities at which patients are being followed and the original bone density measurement was made with the device being replaced.

Under ideal circumstances, provisions should be made to keep the old machine in use after the installation of the new machine until all patients who are currently being followed can be recalled and measured on both devices. This completes the follow-up on the old machine and creates a baseline on the new device. Alternatively, an *in vivo* or *in vitro* cross-calibration study can be performed. For an *in vivo* cross-calibration study, between 60 and 100 patients will be needed whose bone densities span peak to osteoporotic values. Linear regression methods[¶] can be used to develop cross-calibration equations with a standard error of the estimate^{**} of around 3% (20). Once the cross-calibration equation is created, it can be used to predict the value on the old machine from the value that is obtained on the new machine. With the help of a statistician or statistical software program, the 95% confidence interval for a predicted value for an individual can be calculated.^{††} If an *in vivo* cross-calibration study is not feasible, an *in vitro* study may be done using a phantom. The phantom should be scanned on both devices, 60 to 100 times over a similar period of days. Linear regression is again used to create the predictive equation. It is important to remember that linear regression equations are useful for prediction only within the range of values that were used to

[¶]Linear regression involves the development of a mathematical model in order to predict one value from the measurement of another. Such models are useful but they are never perfect. Many statistical calculators or software programs can be used to calculate the regression equation.

^{**}The standard error of the estimate is also known as the standard deviation from the regression line. It is an estimate of the variability about the line of means predicted by the regression equation.

^{††}The 95% confidence interval describes the range of values within which we can be 95% confident that the true value actually lies.

create the equation in the first place. In vivo and in vitro cross-calibration studies and the predictive equations that come from such studies are extremely useful but not as desirable as scanning patients being followed on both devices, as difficult as that may be. In a recent study by Pearson, et al. (21), after comparing both in vivo and in vitro phantom cross-calibrations, it was concluded that applying such calibrations to individual patients being followed over time was simply not possible because the error in such calibrations was too similar to the expected annual change in BMD. These authors noted that a new baseline BMD must be obtained for each patient when a new scanner is put into use. In 2004, the International Society for Clinical Densitometry (19) also stated as an official position of the Society that a new baseline BMD must be established on the new or replacement scanner rather than relying on cross-calibration formulas to predict the new baseline value.

REFERENCES

1. Johnston, C. C., Melton, L. J., Lindsay, R., Eddy, D. M. (1989) Clinical indications for bone mass measurements: a report from the scientific advisory board of the National Osteoporosis Foundation. *J. Bone Miner. Res.* **4**, S1–S28.
2. Miller, P. D., Bonnick, S. L., Rosen, C. J. (1996) Consensus of an international panel on the clinical utility of bone mass measurements in the detection of low bone mass in the adult population. *Calcif. Tissue Int.* **58**, 207–214.
3. Khan, A. A., Brown, J., Faulkner, K., et al. (2002) Standards and guidelines for performing central dual x-ray densitometry from the Canadian Panel of International Society for Clinical Densitometry. *J. Clin. Densitom.* **5**, 247–257.
4. Westgard, J. O., Barry, P. L., Hunt, M. R., Groth, T. (1981) A multirule Shewhart Chart for quality control in clinical chemistry. *Clin. Chem.* **27**, 493–501.
5. Orwoll, E. S., Oviatt, S. K., and the Nafarelin Bone Study Group. (1991) Longitudinal precision of dual-energy X-ray absorptiometry in a multicenter trial. *J. Bone Miner. Res.* **6**, 191–197.
6. Kalender, W., Felsenberg, D., Genant, H. K., Fischer, M., Dequeker, J., Reeve, J. (1995) The European spine phantom—a tool for standardization and quality control in spine bone mineral measurements by DXA and QCT. *Eur. J. Radiol.* **20**, 83–92.
7. Pearson, J., Dequeker, J., Henley, M., et al. (1995) European semi-anthropomorphic spine phantom for the calibration of bone densitometers: assessment of precision, stability and accuracy. The European Quantitation of Osteoporosis Study group. *Osteoporos. Int.* **5**, 174–184.
8. Pearson, D. (2002) Standardization and pre-trial quality control, in *Clinical Trials in Osteoporosis*. (Pearson, D., Miller, C. G., eds.) Springer, London, England, pp. 43–65.
9. Montgomery, D.C. (1992) Introduction to statistical quality control. Wiley, New York.
10. Orwoll, E. S., Oviatt, S. K., Biddle, J. A. (1993) Precision of dual-energy X-ray absorptiometry: development of quality control rules and their application in longitudinal studies. *J. Bone Miner. Res.* **8**, 693–699.

11. Lu, Y., Mathur, A. K., Blunt, B. A., et al. (1998) Dual X-ray absorptiometry quality control: comparison of visual examination and process-control charts. *J. Bone Miner. Res.* **11**, 626–637.
12. Faulkner, K. G., Glüer, C., Estilo, M., Genant, H. K. (1993) Cross-calibration of DXA equipment: upgrading from a Hologic QDR 1000/W to a QDR 2000. *Calcif. Tissue Int.* **52**, 79–84.
13. (1980) BS5703: Guide to Data Analysis and Quality Control Using Cusum Techniques. British Standards Institution, London.
14. Pearson, D. and Cawte, S. A. (1997) Long-term quality control of DXA: a comparison of Shewhart rules and CUSUM charts. *Osteoporos. Int.* **7**, 338–343.
15. Garland, S. W., Lees, B., Stevenson, J. C. (1997) DXA longitudinal quality control: a comparison of inbuilt quality assurance, visual inspection: multi-rule Shewhart charts and Cusum analysis. *Osteoporos. Int.* **7**, 231–237.
16. (1993) XR-Series X-Ray Bone Densitometer Operator's Guide, Norland Medical Systems, Inc., Ft. Atkinson, WI.
17. (1996) Model pDEXA Forearm X-ray Bone Densitometer Operator's Guide. Norland Medical Systems, Inc., Ft. Atkinson, WI.
18. QDR 4500 X-Ray Bone Densitometer User's Guide. Hologic, Inc., Waltham, MA.
19. The Writing Group for the ISCD Position Development Conference. (2004) Technical standardization for dual-energy X-ray absorptiometry. *J. Clin. Densitom.* **7**, 27–36.
20. Pearson, D. and Lawson, N. (2002) Laboratory and instrument quality control, in *Clinical Trials in Osteoporosis*. (Pearson, D. and Miller, C. G., eds.) London, England, Springer, pp. 137–154.
21. Pearson, D., Horton, B., Green, D. J., Miller, C. G., Jackson, S. A. (2004) A strategy for DXA cross calibration during equipment upgrade. Abstract. *J. Bone Miner. Res.* **19**, S367.

9

An Overview of Osteoporosis

CONTENTS

THE DEFINITION OF OSTEOPOROSIS
THE 1991 AND 1993 CONSENSUS DEVELOPMENT CONFERENCES
THE 1994 WORLD HEALTH ORGANIZATION CRITERIA FOR DIAGNOSIS OF OSTEOPOROSIS
THE 2000 NATIONAL INSTITUTES OF HEALTH CONSENSUS CONFERENCE DEFINITION OF OSTEOPOROSIS
PREVALENCE OF OSTEOPOROSIS
CONSEQUENCES OF OSTEOPOROSIS
RISK FACTORS FOR OSTEOPOROSIS
ATTAINMENT OF PEAK BONE DENSITY
MAINTENANCE OF BONE DENSITY
GUIDELINES FOR BONE MASS MEASUREMENTS
THE NATIONAL OSTEOPOROSIS FOUNDATION GUIDELINES FOR BONE MASS MEASUREMENTS
GUIDELINES FROM SPECIALTY SOCIETIES
THE 1997 BONE MASS MEASUREMENT ACT
TREATMENT GUIDELINES FOR POSTMENOPAUSAL OSTEOPOROSIS
NOF GUIDELINES
TREATMENT GUIDELINES FROM AACE AND NAMS
INTERVENTIONS IN OSTEOPOROSIS
NONPRESCRIPTION INTERVENTIONS
PRESCRIPTION INTERVENTIONS
PATIENT EDUCATION MATERIALS
REFERENCES

Osteoporosis is not the only disease process in which bone densitometry is used in diagnosis and management. Osteoporosis is perhaps the most important disease in which this technology is used, from the standpoint of the prevalence of the disease itself and the number of individuals referred for testing in the context of osteoporosis. It is not the responsibility of the technologist to discuss disease processes with patients referred for testing. In fact, some physicians would consider this intrusive and inappropriate. Nevertheless, the setting in which densitometry is usually performed and the interaction between the technologist and patient is conducive to patients asking questions of the technologist about osteoporosis. In these circumstances, it would be inappropriate for a technologist to fail to respond within reason or appear to be uninformed. Knowledge of the disease process and the approved therapies for osteoporosis should be part of the densitometry technologist's education. In any discussion with patients, however, it should also be emphasized that the patient's physician is the final authority on the interpretation of bone density results and the need for prescription or nonprescription interventions to prevent or treat osteoporosis.

THE DEFINITION OF OSTEOPOROSIS

The 1991 and 1993 Consensus Development Conferences

The most widely accepted formal definition of osteoporosis was originally proposed in 1991 and reaffirmed in 1993 at consensus development conferences sponsored by the National Osteoporosis Foundation, European Foundation for Osteoporosis and Bone Disease, and the National Institute of Arthritis and Musculoskeletal and Skin Diseases. At those conferences osteoporosis was defined as "a systemic skeletal disease, characterized by low bone mass and microarchitectural deterioration of bone tissue with a consequent increase in bone fragility and susceptibility to fracture" (1,2). This definition of osteoporosis was a departure in many respects from previous definitions of the disease. Prior to 1991, osteoporosis was often described as an "age-related" disorder, which implied that the inevitability of advancing age alone was reason to develop the disease. This also implied an inability to prevent or even successfully treat osteoporosis. In the 1991 and 1993 consensus conference definitions, there is no longer any mention of aging as a causative factor.

Some definitions of osteoporosis also required that a fracture be present before the disease could be said to exist. The 1991 and 1993 consensus

conference definition does not require the presence of a fracture. The definition requires only that the skeleton be sufficiently fragile that an individual is at increased risk for fracture. This approach separates the undesirable outcome of a fragile skeleton—fracture—from the disease process itself. This is similar to the approaches taken with hypertension and hypercholesterolemia. For example, the disease hypertension is based on the finding of an increased blood pressure, a quantity that is measured clinically. Once the blood pressure exceeds a certain limit, hypertension is said to exist. Having hypertension places the individual at increased risk for a stroke, although hypertension is not the only cause of stroke. The undesirable outcome of hypertension, then, is a cerebrovascular accident or stroke. The presence of a stroke, however, is not required before it can be said that the disease hypertension exists. The same is true with hypercholesterolemia. This diagnosis is based on the finding of increased levels of cholesterol in the blood, a quantity that is measured clinically. The undesirable outcome of hypercholesterolemia is myocardial infarction or heart attack. It is not necessary for a heart attack to have occurred, however, before the diagnosis of hypercholesterolemia is made.

Hypertension and hypercholesterolemia are both diseases that are based on finding abnormal values of quantities that can be measured clinically, blood pressure, and cholesterol. Like these diseases, the 1991 and 1993 consensus conference definition of osteoporosis suggested that osteoporosis could, at least in part, be defined on the basis of a quantity that could be measured such as the bone mass or density. The clinical measurement of microarchitectural deterioration of bone tissue *in vivo* remains difficult even today. But the bone mass or density can be readily measured by any one of several different techniques. It only remained to define the level of bone density that resulted in an increased risk for fracture to complete a clinically useful definition of osteoporosis.

The 1994 World Health Organization Criteria for Diagnosis of Osteoporosis

The World Health Organization (WHO) criteria for the diagnosis of osteoporosis based on the measurement of bone density were published in 1994 (3). At the time the criteria were developed, the WHO was attempting to devise criteria that would allow them to estimate the prevalence or percentage of individuals in different countries who might have osteoporosis. In order to do this, some common objective definition of osteoporosis was required. The WHO was actually not attempting to specify a

level of bone density that would be used clinically in individuals to diagnose osteoporosis.

The levels of bone density that were ultimately chosen by the WHO were based on reviewing the medical literature that was available at the time. After considering several different approaches to establishing the level of bone density that would be called osteoporosis, the WHO stated that a bone mass or bone density that was 2.5 standard deviations (SDs)* or more below the average peak bone mass or density of the young adult was sufficiently low to be called osteoporosis (3). This was based on the finding that the percentage of women in the United States and Great Britain who were thought to have a bone density this low at the hip or at the hip, spine, and forearm combined was very similar to the lifetime risk of hip fracture and the lifetime global fracture risk.† The bone mass or bone density was considered normal if it was not more than 1 SD below the average peak bone density of the young adult. Bone mineral densities that were more than 1 but less than 2.5 SDs below the average young adult value were called osteopenic. A fourth category, called severe or established osteoporosis, referred to individuals who had bone densities that were 2.5 SDs or more below the average for a young adult and who also had a fracture. These criteria are summarized in Table 9-1 and again in Appendix II for easy reference. The WHO did not restrict the application of these criteria to measurements at any particular skeletal site while noting that measurements at different sites could result in different diagnoses. The original WHO criteria were given as the number of SDs below the average peak bone mass or density for each diagnostic category. These criteria can readily be converted to T-scores, as shown in Table 9-1, because the definition of the T-score in bone densitometry indicates the number of SDs above or below the average peak bone mass or density.§

The WHO criteria were based on information that was relevant only to Caucasian women. Strictly speaking, then, the WHO criteria themselves should be applied only to Caucasian women. In addition, they are relevant only to postmenopausal Caucasian women. They should not be applied to premenopausal women of any race or ethnicity. The WHO did note in 1994 that in the absence of other criteria, it might not be inappropriate to

*An SD is a measure of variability about an average value. See Chapter 6 for a discussion of the mathematical definition of an SD.

†Global fracture risk refers to the risk of developing any and all types of fractures rather than any one type of fracture.

§See Chapter 1 for a discussion of the T-score and other standard score scales.

Table 9-1
World Health Organization Criteria for the Diagnosis of Osteoporosis Based on the Measurement of Bone Density

<i>Diagnosis</i>	<i>Bone density criteria</i>	<i>T-score criteria</i>
Normal	Not more than 1 SD below the average peak young adult value	Better than or equal to -1
Osteopenia (low bone mass)	More than 1 but not yet 2.5 SDs below the average peak young adult value	Poorer than -1 but better than -2.5
Osteoporosis	2.5 SDs or more below the average peak young adult value	-2.5 or poorer
Severe (established) osteoporosis	2.5 SDs or more below the average peak young adult value + a fracture	-2.5 or poorer + a fracture

apply the WHO criteria to mature Caucasian men. It should be noted again that the WHO was not attempting to establish diagnostic criteria for the clinician to use in diagnosing individual patients. With the increasing usage of bone densitometry, however, and the consensus conference definitions of osteoporosis that included a finding of low bone mass without an objective level being specified, clinicians understandably began to apply the WHO criteria to individual patients. The restriction of the criteria to Caucasian women, however, left the clinician ill prepared to interpret bone density results in women of other races. This dilemma remains unresolved. It is not clear whether different criteria should exist for men as opposed to women and for different races. There is little disagreement that the criteria should not be applied to otherwise healthy children, adolescents, and young adults of either sex or any race.

The 2000 National Institutes of Health Consensus Conference Definition of Osteoporosis

In March 2000, a consensus development conference on osteoporosis prevention, diagnosis, and therapy was sponsored by the National Institutes of Health (NIH) (4). During this conference osteoporosis was redefined as a “skeletal disorder characterized by compromised bone strength predisposing to an increased risk of fracture.” This new definition of osteoporosis, although more succinct than its 1991 and 1993 predecessors, was actually intended to be more expansive. Bone strength was considered as being determined not only by bone density but by bone

quality as well. Although bone quality referred to bone architecture as mentioned in the 1991 and 1993 Consensus Conference definitions, it also referred to bone turnover, microfractures, and mineralization. Consistent with the 1991 and 1993 definitions, osteoporosis was not considered an age-related disorder and fracture was not a prerequisite to the diagnosis. As a practical matter, the 2000 NIH Consensus Development Panel definition of osteoporosis has not affected the clinical implementation of the WHO criteria for the diagnosis of osteoporosis based on the measurement of bone density.

PREVALENCE OF OSTEOPOROSIS

Prevalence is a statistical term that is best understood as an expression of how common a disease is in any population. Prevalence is often expressed as a percentage. This was actually the question that originally concerned the WHO. How many people, or what percentage of a population, would ultimately be said to have osteoporosis? The answer clearly depended on what level of bone density was chosen as the diagnostic threshold for osteoporosis. It could also depend on which skeletal site or combination of sites is measured.

In 1992, it was estimated that 45% of Caucasian women in the United States aged 50 and older had osteoporosis, if osteoporosis was defined as a bone density more than 2 SDs below the average peak bone density at the spine, hip, or forearm (5). If the skeletal sites were considered separately, 32% would have osteoporosis at the spine, 29% at the hip, and 26% at the forearm. After the publication of the 1994 WHO criteria, in which osteoporosis was defined as a bone density 2.5 SDs or more below the average peak bone density, these estimates were revised (6). Approximately 30% of postmenopausal Caucasian women in the United States were now estimated to have osteoporosis at the spine, hip, or forearm and 54% were estimated to have osteopenia. When the numbers of postmenopausal Caucasian women with osteopenia and osteoporosis were combined, the number of postmenopausal Caucasian women at risk for fracture was estimated to be 26 million.

In 2002, the National Osteoporosis Foundation published a revised status report, in which it was estimated that osteoporosis and osteopenia affect 44 million men and women aged 50 and older in the United States (7). These 44 million men and woman represent 55% of all the individuals aged 50 and older in the United States. Based on current trends, the number of

men and women aged 50 and older with osteopenia or osteoporosis is expected to increase to over 61 million by the year 2020.

Being at risk for fracture does not guarantee that a woman will fracture. The risks, however, are substantial. When all types of osteoporotic fractures are considered, one out of every two Caucasian women is expected to experience an osteoporotic fracture in her lifetime (8). The lifetime risk of hip fracture for a Caucasian woman age 50 is 17.5% (5). The lifetime risk for a clinical spine fracture is 15.6%. The risk for a morphometric spine fracture is almost certainly much higher but more difficult to estimate.[¶] Some estimates place this risk as high as 35% (8).

Not surprisingly, the number of osteoporotic fractures that occur each year in the United States is staggering. Over 1.5 million fractures are attributed to osteoporosis every year. Spine fractures account for more than 700,000 fractures and hip fractures account for more than 300,000 fractures (7). In 1995, the total cost of treating these fractures was estimated to be \$13.8 billion (9). In 2001 dollars, this cost is approximately \$17 billion (7). Costs associated with hip fracture account for 63.1% of the total.

CONSEQUENCES OF OSTEOPOROSIS

The consequences of osteoporosis are not restricted to the immediate pain caused by the fracture. Multiple spinal compression fractures lead to a permanent change in the curvature of the spine known as kyphosis. This spinal curvature is commonly called a widow's hump or dowager's hump. Loss of height also results from compression fractures of the spine. As more height is lost and kyphosis increases, the function of the lungs and gastrointestinal tract is compromised because the organs are being compressed. This can result in a restrictive lung defect leading to shortness of breath (10). The compression of the intestinal tract can lead to early satiety and weight loss. Patients become undernourished, frail, and depressed. The change in the curvature of the spine also results in abnormal mechanical stress being placed on the musculature of the back causing chronic back pain. Quality of life is greatly diminished.

[¶]A clinical spine fracture is a fracture of the spine that causes symptoms. A morphometric spine fracture is a fracture that is diagnosed on the basis of changes seen on X-ray without accompanying symptoms.

The consequences of hip fracture are equally if not more devastating. The treatment of hip fracture generally involves surgery with its attendant morbidity and mortality. It is estimated that 1/2 of the women who fracture their hip cannot walk independently 1 year after the fracture. As many as 60% cannot perform the activities of daily living that they could perform before the fracture (11). This leads to a loss of independence, which can result in referral to a nursing home environment. An excess mortality** of up to 20% has been associated with osteoporotic hip fractures (12).

RISK FACTORS FOR OSTEOPOROSIS

The factors that increase the risk for bone loss or osteoporotic fracture are numerous. They can be factors that either inhibit the development of a normal peak bone density as a young adult or that cause bone loss after the attainment of peak bone mass. Some factors can affect both.

Attainment of Peak Bone Density

Peak bone density^{††} refers to the maximum bone mass or density that is attained in life. It is the average peak bone density at any given skeletal site that is used as the reference for the T-score. The average age at which peak bone density is reached is the subject of some controversy. It is likely that the age differs depending on the skeletal site being considered. There is little disagreement that peak bone density is reached by the age of 35. The disagreement begins as that age is revised downward. Many authorities believe that peak bone density is reached in the spine and proximal femur by the age of 20 (13–15). Anything that interferes with the development of peak bone density places the individual at greater risk of osteoporosis, because any bone loss that might occur after the attainment of peak bone density will begin from a lower level. There is no question that genetics plays an important role in the maximum level of bone density that is achieved, but perhaps 20% of the determinants of peak bone density are not genetically related. Dietary calcium deficiency and lack of exercise

**Excess mortality refers to the number or percentage of deaths that occur over and above that expected for any given age group.

††The terms peak bone density and peak bone mass are used interchangeably in this context. This value is also called the average young adult bone mass or density.

are two factors that have been implicated in the failure to achieve an average peak bone density (16,17).

Maintenance of Bone Density

Once peak bone density has been reached, the density of the skeleton is maintained by the coordinated efforts of the bone remodeling cells, the osteoblast and osteoclast. The osteoclast actually initiates the resorption or removal of old bone. The osteoblast forms new bone to replace the old bone that has been removed by the osteoclast. In the adult, after the attainment of peak bone density, these processes are balanced or coupled. The amount of bone removed by the osteoclast is replaced by the same amount under the direction of the osteoblast. When these actions are no longer balanced or become uncoupled, bone loss will begin either because excessive bone is being resorbed by the osteoclast or because too little bone is being replaced by the osteoblast, or both.

Bone loss tends to occur with advancing age. Consequently, the term age-related bone loss is often used to describe the bone loss that occurs in the absence of an obvious disease process. This bone loss should not be mistakenly considered either normal or desirable. It is also quite likely that as more is learned about the factors that cause bone loss, less will be attributed to age alone. The list of known factors that can cause either an increase in osteoclastic bone resorption or decrease in osteoblastic bone formation is lengthy. Such factors include calcium deficiency, smoking, estrogen deficiency, testosterone deficiency, Cushing's Disease, hyperthyroidism, insulin-dependent diabetes, alcohol abuse, malabsorption, use of corticosteroids, anticonvulsants, lithium, GnRH agonists, and long-term heparin.

When the bone density is sufficiently low, little provocation is required to cause a fracture. In the spine, coughing, sneezing, or maintaining a flexed posture can cause fractures. Most hip fractures occur after a fall, although most falls are from a standing height or less (18). Any factor that increases the risk of falling can increase the risk for hip fracture. Such factors include poor eyesight, poor balance, muscle weakness, seizure disorders, postural hypotension, and use of sedating medications.

The risk of osteoporotic fractures is not the same in men and women or among different races. The reasons for this are not entirely clear. There may be genetic differences that result in the attainment of greater or lesser values for peak bone density. Factors that can cause bone loss may be more prevalent in some populations and in some geographical areas than others. Women have a higher risk of osteoporotic fracture than do men.

This is almost certainly attributable in large part to estrogen-deficient bone loss that occurs at menopause. Caucasians, as a race, have the highest risk for osteoporotic fracture, whereas African-Americans have the lowest (18).

GUIDELINES FOR BONE MASS MEASUREMENTS

Several society and organizations have issued guidelines for bone mass measurements in clinical practice. There are far more similarities among the guidelines than differences. The differences that do exist often reflect the unique patient populations served by the members of a particular society rather than disagreement with the recommendations of another society or organization.

The National Osteoporosis Foundation Guidelines for Bone Mass Measurements

In 1998, the National Osteoporosis Foundation (NOF) issued guidelines for physicians to help determine which patients should undergo bone density testing (19). These guidelines were not intended to supersede the judgment of physicians regarding the care of individual patients. They are extremely useful, however, in ensuring that the women who should have a measurement are referred for a measurement. The guidelines were written after a lengthy process that involved consultation with many experts and extensive reviews of the medical literature. The majority of the literature available for review at the time dealt with findings in postmenopausal Caucasian women. Like the WHO criteria, because these guidelines were based on information obtained in postmenopausal Caucasian women, they were primarily intended for postmenopausal Caucasian women and not women of other races. Nevertheless, it is not uncommon or considered inappropriate to utilize these guidelines in the care of women of other races.

The 1998 NOF guidelines are summarized in Table 9-2. The list of risk factors that may be considered in determining whether a woman under age 65 should have a measurement is extensive. It is so extensive, in fact, that it is unusual to find a woman who does not have at least one risk factor. Recommending testing women who had been on hormone replacement therapy for prolonged periods was a departure from earlier recommendations. In the past, it was generally assumed that these women were protected

Table 9-2
The 1998 National Osteoporosis Foundation (NOF) Recommendations
for Bone Mass Measurement Testing

-
1. Postmenopausal women under 65 with one or more risk factors other than being postmenopausal.
 2. All women age 65 and over. Consideration of other risk factors is not necessary.
 3. Postmenopausal women who present with fractures.
 4. Women in whom knowledge of their BMD would influence their decision to begin treatment for osteoporosis.*
 5. Women who have been on hormone replacement therapy for long periods of time.*
-

*These recommendations were deleted from the 2003 NOF recommendations.

from bone loss and less likely to obtain useful information from a bone density study. It became clear, however, that many of these women did have low bone density in spite of prolonged use of hormone replacement therapy. In making this recommendation, the NOF was attempting to ensure that these women were not arbitrarily and inappropriately excluded from testing.

In 2003, the NOF reissued guidelines for bone density testing (20). The 2003 guidelines were identical to the 1998 guidelines except that testing was no longer recommended for women who had been on long-term hormone replacement therapy. The reason for this deletion remains unclear and in retrospect, is perhaps unwise in the face of the findings from the Women's Health Initiative in which the risk-benefit ratio of one of the more commonly used forms of hormone replacement was clearly undesirable (21).

Guidelines From Specialty Societies

The 1998 NOF guidelines formed the basis for guidelines from other major medical organizations. In 2001, the American Association of Clinical Endocrinologists (AACE) issued guidelines that were essentially identical to the first three points of the 1998 NOF guidelines (22). AACE reissued guidelines in 2003, although these guidelines did not contain changes to their previous recommendations regarding the use bone densitometry (23). In 2002, the American College of Obstetricians and Gynecologists (ACOG) and The North American Menopause Society (NAMS) also issued similar guidelines (24,25). In late 2002, the United States Preventative Services Task Force (USPSTF) issued guidelines that dealt only with the prevention of osteoporosis (26). As a consequence,

women with fractures were not included in these guidelines. In the USPSTF guidelines, bone density testing was once again recommended for all postmenopausal women aged 65 and older. Testing was also recommended for postmenopausal women aged 60 to 64 at high risk of osteoporosis.

In 2004, the ISCD (27) updated and expanded guidelines for bone density testing that had been previously issued in 2002 (28,29). These guidelines reiterate the NOF position that postmenopausal women aged 65 and older and postmenopausal women under age 65 with one or more risk factors should be tested. ISCD also recommended that men aged 70 and older undergo bone density testing. The Society also recommended testing in both men and women with a presumed fragility fracture or a disease, condition, or history of medication use associated with low bone mass or bone loss. It was also noted that anyone being considered for pharmacologic therapy for osteoporosis should have a bone density measurement and that monitoring of such therapy was also an appropriate indication for bone density testing.

The guidelines for women from all these organizations are compared in Table 9-3. The various organizations agree that DXA is the technique of choice for the diagnosis of osteoporosis based on a measurement of bone density. The 2001 AACE guidelines also suggest that quantitative computed tomography (QCT) of the spine may be used. There is also general agreement that the diagnosis of osteoporosis should be based on a measurement of bone density at either the PA lumbar spine or proximal femur. Peripheral sites should not be used for this purpose, even if measured by DXA. A corollary of this statement is that the WHO Criteria for diagnosis of osteoporosis based on a measurement of BMD should only be used with measurements of bone density at the spine and proximal femur.

THE 1997 BONE MASS MEASUREMENT ACT

The cost of a bone density test has generally fallen over the last 10 years as the devices have become more numerous and widespread. Nevertheless, the cost of testing can deter a woman from undergoing the measurement in some circumstances. In 1998, the Health Care Financing Administration (HCFA) proposed regulations for Medicare coverage of bone mass measurements based on the passage of the 1997 Bone Mass Measurement Act by Congress (30). These regulations went into effect in July 1998. There were five circumstances described in

Table 9-3
Comparison of Major Guidelines for Bone Density Testing for the Detection
of Osteoporosis in Women

	Women ≥65	Postmenopausal women ≤64 and at least 1 risk factor	Postmenopausal women with fractures	Technique for diagnosis	Site for diagnosis ^d	Against using peripheral sites for monitoring
NOF 1998/2003	√	√	√	DXA	Hip preferred	—
WHO 1999	√ ^b	√ ^b	√ ^c	DXA	Hip preferred	—
IOF 2000	—	—	—	—	Total hip	—
AACE 2003	√	√	√ ^c	DXA/QCT	Spine, proximal femur	√
ACOG 2002	√	√	√	DXA	—	—
NAMS 2002	√	√	√	DXA	Total hip preferred, femoral neck or spine	√
USPSTF 2002	√	√ ^d	—	—	—	—
ISCD 2004	√	√	√	DXA ^e	PA spine, hip (not Ward's area)	√

^aThe term hip indicates that a specific region in the proximal femur was not specified.

^bThe WHO noted that hypogonadism, possibly to include all postmenopausal women, was justification for a measurement.

^cConsideration was limited to low-trauma fractures.

^dThis recommendation was limited to postmenopausal women age 60 to 64.

^eMethodologies other than DXA were not considered in these guidelines.

—, indicates no comment; NOF, National Osteoporosis Foundation; WHO, World Health Organization; IOF, International Osteoporosis Foundation; AACE, American Association of Clinical Endocrinologists; ACOG, American College of Obstetricians and Gynecologists; NAMS, North American Menopause Society; USPSTF, United States Preventative Services Task Force; ISCD, International Society for Clinical Densitometry.

Table 9-4
Medicare Coverage for Bone Mass Measurements From the Bone Mass
Measurement Act (BMMA) of 1997

-
1. A woman who has been determined by her treating physician or treating qualified nonphysician practitioner to be estrogen-deficient and at clinical risk for osteoporosis, based on her medical history and other findings.
 2. An individual with vertebral abnormalities on X-ray suggestive of osteoporosis, osteopenia, or fracture.
 3. An individual receiving or expected to receive glucocorticoid therapy equivalent to 7.5 mg of prednisone or greater per day for more than 3 months.
 4. An individual with primary hyperparathyroidism.
 5. An individual being monitored to assess the response to or efficacy of an Food and Drug Administration (FDA)-approved drug therapy for osteoporosis.
-

which Medicare would potentially cover the bone mass measurement. These are summarized in Table 9-4. Notice that four of the five circumstances refer to an “individual” rather than a “woman.” This means, of course, that men as well as women should be covered. Prior to late 2000, there were no Food and Drug Administration (FDA)-approved treatments for osteoporosis in men so coverage for monitoring therapy was limited to women. In late 2000, alendronate was approved for the treatment of osteoporosis in men so that Medicare should now cover men in this circumstance as well. Legislation has been introduced in both houses of the U.S. Congress to change Medicare coverage for bone mass measurements to clearly indicate that men, as well as women, who are considered at risk for osteoporosis, should be tested. This legislation has yet to pass.

Medicare will cover a bone density measurement at one skeletal site by one technique every 23 months. Two exceptions to this “frequency” limitation were specifically noted by HCFA. The first exception was in patients on glucocorticoid therapy for more than 3 months. In this situation, the bone mass measurement could be repeated sooner than 23 months to monitor the bone density. The second exception was when the bone density measurement that lead to the initiation of treatment was made with a technique that would not be used for monitoring. In this case, a second bone mass measurement could be made quickly with the monitoring technique in order to establish the baseline for monitoring. HCFA did not exclude the possibility that coverage might be allowed for more frequent measurements in other circumstances, but these were the only two exceptions actually noted in the *Federal Register*. The covered circumstances described by Medicare do not have specific International Classification of Disease 9 (ICD-9)

codes.^{§§} Several different ICD-9 codes are potentially applicable to each circumstance. Which code a Medicare carrier accepts as justifying coverage can vary from state to state. HCFA has approved the use of a combination of two ICD-9 codes to indicate “an estrogen-deficient woman at clinical risk for osteoporosis.” The codes are V82.81, which is the code for special screening for osteoporosis, and V49.81, which is the status code for postmenopausal women. The CPT codes^{¶¶} necessary for billing Medicare for various types of bone density testing are listed in Appendix V.

TREATMENT GUIDELINES FOR POSTMENOPAUSAL OSTEOPOROSIS

NOF Guidelines

The NOF also published guidelines for prescription intervention to prevent or treat osteoporosis based on the bone density measurement (19). It was emphasized that women over age 70 with multiple risk factors did not necessarily need a bone density measurement before therapy was initiated. The recommendations for prescription intervention based on the bone density measurement utilize the T-score. The NOF recommended that therapy be initiated in women with T-scores poorer than -2 even if no other risk factors were known to exist. In women with T-scores poorer than -1.5 and at least one other risk factor, the NOF also recommended that prescription intervention be considered. These intervention thresholds suggested by the NOF do not correspond with the diagnostic thresholds suggested by the WHO. Even though the diagnostic threshold for osteoporosis as proposed by the WHO was set at a T-score of -2.5 , the risk for fracture is present at higher levels of bone density. The NOF intervention thresholds recognize this and consequently intervention is recommended at T-scores of -1.5 or -2.0 , depending on the presence of other risk factors.

Treatment Guidelines From AACE and NAMS

AACE and NAMS originally issued treatment guidelines based on the T-score in 2001 and 2002, respectively (22,25). AACE reiterated these guidelines in 2003 (23). Both sets of guidelines differ slightly from the NOF recommendations, but there is considerable overlap. Like the NOF,

^{§§}ICD-9 codes are diagnostic codes used to justify the performance of procedures.

^{¶¶}CPT (Current Procedural Terminology) codes are codes used to identify procedures.

Table 9-5
Treatment Guidelines for Postmenopausal Osteoporosis Based on the T-Score

<i>Organization</i>	<i>T-score criteria</i>		<i>Prior fragility fracture</i>
	<i>Without risk factors</i>	<i>With risk factors</i>	
NOF 2003	Poorer than -2	Poorer than -1.5	Yes
AACE 2003	-2.5 or poorer	-1.5 or poorer	Yes
NAMS 2002	Poorer than -2.5	-2 or poorer	Yes

NOF, National Osteoporosis Foundation; AACE, American Association of Clinical Endocrinologists; NAMS, North American Menopause Society.

AACE recommends pharmacologic intervention for postmenopausal osteoporosis if the T-score is -1.5 or poorer and any other risk factor is present, but they do not recommend treatment in the absence of other risk factors until the T-score is -2.5 or poorer. NAMS does not recommend pharmacologic intervention until the T-score is -2 or poorer when other risk factors are present, but NAMS does recommend intervention when the T-score is -2.5 or poorer, irrespective of the presence of risk factors, as does both the NOF and AACE. All three organizations recommend pharmacologic intervention in women with a prior fracture that is believed to be a fragility fracture. These guidelines are compared in Table 9-5.

INTERVENTIONS IN OSTEOPOROSIS

Interventions in osteoporosis are divided into two basic categories: nonprescription and prescription. The nonprescription interventions can be further divided into lifestyle modifications and over-the-counter supplements or medications.

Nonprescription Interventions

LIFESTYLE MODIFICATIONS

Many lifestyle modifications recommended to prevent bone loss and fractures are modifications that are appropriate for everyone in general, not just the woman concerned about osteoporosis. In some cases, however, the recommendations are different if the woman already has a very low bone density or fracture compared to the woman who has a normal

bone density and is concerned about future bone loss. Recommendations that are appropriate for everyone include:

1. Avoidance of cigarette smoke
2. Moderation in alcohol intake
3. Moderation in caffeine intake
4. Moderation in salt (sodium) intake
5. Modification of the home environment to reduce the risk of falls

Cigarette smoke, alcohol, caffeine, and sodium are all associated with bone loss to some degree (31–35). Modification of the home environment does not have to be extensive to reduce the risk of falls. Measures include removal of throw rugs, elimination of electrical extension cords from walk areas, installation of automatic night-lights in the bedroom, bath, and kitchen, and installation of safety bars in the bath. Only the installation of safety bars in the bath requires any expertise or potential expense. The bars themselves are not expensive but they must be installed into the studs of the wall with long screws in order to support the weight of the body. These are relatively simple measures that can be life saving.

CALCIUM, VITAMIN D, AND EXERCISE

Nonprescription interventions that are appropriate for most, but not all, women are obtaining adequate calcium and vitamin D and regular weight bearing or resistance exercise. There are several different sets of recommendations for calcium intake. The differences between them tend to be small and following any one of them is appropriate. Table 9-6 lists the recommendations for calcium intake from the 1994 National Institutes of Health Consensus Conference on Calcium Intake (36). Table 9-7 lists the 1997 recommended intakes according to the National Academy of Science (37). The NOF has issued a blanket recommendation of 1200 mg a day for all adults (19).

Obtaining these amounts of calcium from the diet alone is often difficult, although it is the desirable means of obtaining the recommended amounts of calcium. Over-the-counter calcium supplements are an acceptable means of supplementing dietary calcium to ensure that the intake goals are met. Calcium supplements are relatively inexpensive. Most supplements are forms of calcium carbonate but supplements of calcium citrate, calcium phosphate, and combinations of calcium lactate and gluconate are also available. All of these supplements with the exception of calcium citrate should be taken with food. Calcium citrate is best taken on an empty stomach. It is also important to note the milligrams of

Table 9-6
1994 National Institutes of Health Recommendations for Calcium Intake

<i>Group/age (years)</i>	<i>Recommended calcium intake (mg)</i>
Adolescents/young adults	
11–24	1200–1500
Women	
25–50	1000
Over 50 (postmenopausal)	
On estrogen	1000
Estrogen deficient	1500
Over 65	1500
Pregnant or Nursing	1200–1500
Men	
25–65	1000
Over 65	1500

Table 9-7
1997 National Academy of Science Recommendations for Calcium Intake

<i>Group/age (years)</i>	<i>Recommended calcium intake (mg)</i>
Adolescents/adults (both sexes)	
9–18	1300
19–50	1000
≥51	1200
Pregnant or nursing women	
≤18	1300
19–50	1000

elemental calcium per tablet, as this is the important amount, not the milligrams of calcium salt. For example, a common strength of calcium carbonate tablet is 1250 mg of calcium carbonate. This tablet size provides 500 mg, not 1250 mg, of elemental calcium. Calcium fortified foods and beverages are also useful in increasing dietary calcium intake. There are a variety of fruit juices that are now fortified with calcium as well as calcium-fortified bread, rice, and cereal. Obtaining excessive amounts of calcium is not recommended. There is no proof that consuming amounts in excess of those recommended is beneficial. It may also be possible to increase the likelihood of developing a kidney stone if excessively large amounts of calcium are excreted into the urine.

Patients should always be asked if they have ever had a kidney stone or been told to avoid foods high in calcium before recommending an increase in dietary calcium or calcium supplements. If they have, they should be encouraged to discuss this issue with their physician before proceeding on their own.

Vitamin D is important for calcium absorption and metabolism but it is not always necessary to consume a vitamin D supplement. It is certainly not necessary to have vitamin D and calcium in the same tablet. The 1997 National Academy of Science recommendations for vitamin D intake called for 200 International Units (I.U.) per day for both sexes from ages 14 to 50 and 400 I.U. for ages 51 to 70 (37). After age 70, 600 I.U. was recommended. Most over-the-counter multivitamin preparations contain 400 I.U. of vitamin D. Such a multivitamin is a reasonable choice for women aged 51 and older to ensure adequate vitamin D intake. Most experts believe that the intake recommendations for vitamin D will increase to as much as 1000 I.U. per day for older individuals. This amount appears to be safe and warranted, given that vitamin D deficiency is more widespread than previously believed. In addition, recent evidence suggests that vitamin D supplementation reduces the risk of falls by an average of 22% (38). Although such a statement initially seems strange, vitamin D apparently has beneficial effects on neuromuscular function through which the risk of falls is reduced (39). The vitamin D in over-the-counter preparations must undergo chemical conversions in the liver and kidney before becoming biologically active. Because of this delay in becoming active, any vitamin D combined with a calcium supplement does not actually affect the absorption of the calcium in that supplement. Its actions will begin later.

Exercise is important in bone health. The most beneficial forms of exercise for the skeleton are weight bearing exercise and resistance exercise. Weight bearing exercise is any type of exercise that forces the skeleton to support the weight of the body. For example, walking is a weight bearing exercise, whereas swimming is not. Resistance exercise is exercise in which the muscles push or pull against a resistance. Such resistance can be in the form of weight, tension, or air pressure. This is the type of exercise that is performed with the use of machines or free weights. There are restrictions on the type of exercise that women with osteoporosis should perform. High impact exercises may place a fragile spine at risk for fracture and should be avoided. This includes running, rope jumping, and high-impact aerobics. Any type of exercise in which the risk of falling is increased should be avoided. Exercises that require

repeated or resisted trunk flexion*** should also be avoided since this may increase the risk of spine fracture. Such exercises include traditional sit-ups and toe-touches. Trunk or spine extension exercises are both safe and recommended.

Prescription Interventions

The prescription medications used in osteoporosis are either antiresorptive or anabolic agents. Antiresorptive agents are approved by the FDA for the prevention of osteoporosis, for the treatment of osteoporosis, or both. An antiresorptive agent is a medication that primarily inhibits bone loss rather than stimulating new bone formation. Increases in the measured bone density are observed with these agents, which may seem contradictory if the agents primarily inhibit bone loss. Part of this increase is attributed to the agent stopping additional bone loss while the skeleton rebuilds bone naturally. The bone rebuilding is not being directly stimulated by the antiresorptive agent. Recently, the term *anticatabolic* agent has been proposed to replace the term antiresorptive agent. This new descriptive term for antiresorptive agents has not been widely adopted yet, but its use may be encountered in clinical practice in the near future. Estrogen, raloxifene, calcitonin, and the bisphosphonates are antiresorptive or anticatabolic agents. There is only one anabolic agent, teriparatide, which is currently approved by the FDA for the treatment of osteoporosis. Anabolic agents stimulate bone formation rather than inhibit bone loss.

Agents that have been approved by the FDA for the prevention of bone loss or the prevention of osteoporosis are agents that have been shown to inhibit bone loss. Agents that are FDA-approved for the treatment of osteoporosis have been shown in clinical trials to reduce the risk of fractures. Physicians are not restricted by these approvals from using a medication to treat osteoporosis that has been approved only for prevention and vice versa if it is deemed medically appropriate to do so.

ESTROGEN REPLACEMENT

A number of estrogen replacement preparations are approved for the prevention of osteoporosis. The list has grown rapidly over the last few years and will continue to grow. The approval for the prevention of osteoporosis does not extend to every form of estrogen replacement that

***Trunk flexion refers to bending forward from the waist with the back rounded.

Table 9-8
 FDA-approved Estrogen Preparations for the Prevention of Osteoporosis

Premarin [®]	Vivelle Dot [®]
Prempro [®]	Menostar [™]
Premphase [®]	Ortho-Est [®]
Alora [®]	Climara [®]
Estrace [®]	Ortho-Prefest [™]
Estraderm [™]	femHRT [®]
Prefest [™]	Activella [™]

is available by prescription. It is given only to those preparations that have provided information from clinical trials to the FDA demonstrating that the particular preparation at a specific dose inhibits bone loss. A list of approved preparations is shown in Table 9-8. Premarin was previously approved for the treatment of osteoporosis as well. This approval was rescinded, not because the preparation was shown to be ineffective, but because there was inadequate data to prove its efficacy by current standards. Many physicians will appropriately use estrogen preparations in the treatment of osteoporosis as well its prevention. However, because of findings from the Women's Health Initiative (40), in which the risks associated with oral combined-continuous hormone replacement using conjugated equine estrogen and medroxyprogesterone acetate outweighed the benefits, all forms of estrogen now carry FDA-mandated warnings regarding the use of estrogen for the prevention of osteoporosis. In essence, the warning suggests that other prescription interventions be considered, if estrogen is being prescribed solely to prevent osteoporosis.

THE SELECTIVE ESTROGEN RECEPTOR MODULATOR RALOXIFENE

Raloxifene, or Evista[®], was approved for the prevention of osteoporosis in 1997 and the treatment of osteoporosis in 1999. The recommended dose is one 60-mg tablet by mouth once a day. In a very large clinical trial known as the Multiple Outcomes of Raloxifene Evaluation (MORE) study, women who received 60 mg of raloxifene a day for 3 years had a 2.1% increase in PA lumbar spine bone density and a 2.6% increase in femoral neck bone density compared to women who received a placebo (41). Compared to their baseline bone density, women receiving 60 mg of raloxifene a day had an increase of approximately 3% at the PA lumbar spine and 1% at the femoral neck. Most important, there was a 30%

reduction in the risk of new spine fractures in these women over the course of the 3-year study. Raloxifene does not stimulate the endometrium and cause menstrual bleeding. It does not appear to have any beneficial effect on hot flashes and conveys a risk of thromboembolic events similar to estrogen (42).

SYNTHETIC SALMON CALCITONIN

Synthetic salmon calcitonin in an injectable form has been available for the treatment of osteoporosis in the United States since 1984. In 1995, a nasal spray formulation was approved for the treatment of osteoporosis in women more than 5 years postmenopausal. Both the injectable and nasal spray are available by prescription. The injectable synthetic salmon calcitonin is given in a dose of 100 I.U. subcutaneously daily. The recommended dose of the nasal spray is 200 I.U. once a day. One spray delivers the recommended dose. The results of a 5-year clinical trial evaluating the efficacy of nasal spray synthetic salmon calcitonin were published in 2000 (43). This trial is called the Prevent Recurrence of Osteoporotic Fractures (PROOF) trial. The women who received 200 I.U. of nasal spray synthetic salmon calcitonin had small increases of slightly greater than 1% in PA lumbar spine bone density compared to their baseline value over the course of the 5 years. This increase was significantly different from the placebo group at the end of years 1 and 2 only. Over the course of the 5-year study, however, the women receiving 200 I.U. of nasal spray synthetic salmon calcitonin had a 33% reduction in the risk of new spine fractures.

At present, Miacalcin® is the only brand of nasal spray synthetic salmon calcitonin that is available for prescription use in the United States. The medication is delivered by a pump-spray assembly. The vial should be kept refrigerated prior to first use, after which it can remain at room temperature. The medication can be used without regard to meals or time of day. There are no known drug interactions and no adjustments are necessary based on age or kidney function.

BISPHOSPHONATES

Bisphosphonates are very similar to pyrophosphate, a substance normally found in bone. The first bisphosphonate was etidronate or Didronel®. Although etidronate has never been approved for the prevention or treatment of osteoporosis in the US early research using etidronate to treat osteoporosis helped spur the development of more potent bispho-

sphonates for use in osteoporosis (44,45). Three bisphosphonates are FDA-approved for both the prevention and treatment of osteoporosis. They are alendronate or Fosamax[®], risedronate, or Actonel[™] and ibandronate or Boniva[™].

Alendronate. Alendronate is approved for the prevention and treatment of osteoporosis in women and is also approved for the treatment of osteoporosis in men. When used to treat osteoporosis, the recommended dose was originally one 10-mg tablet given once a day. It appears to be equally effective to give 70 mg only once a week, based on findings from a bioequivalency^{†††} trial of 10 mg daily and 70 mg once weekly, in which changes in bone density and bone turnover were compared (46). Both the 10 mg daily and 70 mg once weekly doses are now approved for the treatment of osteoporosis. The recommended dose when used for the prevention of osteoporosis is one 5-mg tablet given once a day or one 35-mg tablet given once a week. The medication must always be given before breakfast, after an overnight fast. It must be taken with a full glass of water alone, and no other beverage, food, or medication should be consumed for at least 30 minutes. It is also important that the patient remains awake after taking the medication and does not go back to bed. These instructions are necessary to ensure that the medication is absorbed properly and that any chance of reflux of the medication into the esophagus where it could cause irritation is minimized. There are no known adverse drug interactions with alendronate but it is not recommended for individuals with renal insufficiency.^{§§§}

The efficacy of alendronate is unquestioned. In the 3-year Fracture Intervention Trial (FIT), women receiving 10 mg of alendronate daily had a 47% reduction in their risk of having a new or worsening spine fracture compared to women receiving a placebo (47). There was also a 51% reduction in the risk of hip fractures. Bone density at the PA lumbar spine increased by more than 8% and at the femoral neck by approximately 3% compared to baseline in women receiving alendronate over the 3-year

^{†††}Bioequivalency and non-inferiority trials are similar. When these are done for bone-active agents for the treatment of osteoporosis, these trials compare changes in bone density and bone turnover markers caused by different doses of the drugs. These trials do not compare reductions in fracture risk for a particular dose. Bone density and bone turnover are considered acceptable surrogates in these trials.

^{§§§}Renal insufficiency is defined here as a creatinine clearance less than 35 cc per minute

period of the study. The effects of 7 years of continuous treatment with 10 mg of alendronate daily have been published showing an average increase of 11.4% at the spine from baseline (48). Ten years of continuous 10 mg daily use has been reported to result in a 13.5% increase in lumbar spine bone density (49). Alendronate has also been shown to be effective in preventing bone loss in recently menopausal women with lumbar spine bone densities within 2 SDs of the young adult peak bone density (50). In this 3-year study, alendronate given in a dose of 5 mg or 10 mg per day prevented bone loss from the spine and hip.

The effectiveness of adding alendronate to ongoing hormone replacement was investigated in a 2-year study known as the Fosamax Addition to Continuing Estrogen Therapy (FACET) study (51). In the women in whom 10 mg of alendronate was added to their ongoing hormone replacement, there was a 2.6% greater increase in PA spine BMD and a 2.7% greater increase in trochanteric BMD compared to the women who simply continued hormone replacement. The combination appeared safe as well. This study was not designed to evaluate potential reductions in fracture risk from combination therapy.

Alendronate has been approved for the treatment of osteoporosis in men. In a 2-year study of 241 men with osteoporosis, alendronate in a dose of 10 mg a day resulted in significant increases in bone density at the spine and hip (52). The average increase from baseline at the PA lumbar spine was 7.1% and at the femoral neck, 2.5%. The incidence of vertebral fracture was also reduced in the men receiving alendronate. Testosterone levels had no apparent influence on the effectiveness of alendronate.

Risedronate. Risedronate is also approved for the prevention and treatment of osteoporosis in women. A dose of 5 mg daily or 35 mg once weekly is recommended for either prevention or treatment. Like alendronate, risedronate should be given after an overnight fast, with only a full glass of water. Nothing other than water should be consumed for at least 30 minutes after taking risedronate and the patient should remain awake after taking it. There are no significant drug interactions known to occur with risedronate and no alterations in dose are necessary solely on the basis of age. Like alendronate, risedronate is not recommended in individuals with renal insufficiency.

The efficacy of risedronate in reducing spine fracture risk has been demonstrated in two large clinical trials, collectively called the Vertebral Efficiency with Risedronate Therapy (VERT) trials (53,54). Both of these trials were 3-year studies that involved several thousand women

with pre-existing spine fractures. In the United States trial, women who received 5 mg of risedronate had a 41% reduction in their risk of new spine fracture (53). Bone density increased at the lumbar spine by 5.2% and at the femoral neck by 1.6% compared to baseline over the 3 years. In the multinational or European trial, women who received 5 mg of risedronate had a 49% reduction in the risk of new spine fractures (54). Bone density at the spine increased by approximately 7% and at the femoral neck by approximately 2% from baseline by the end of the study. Long-term changes in bone density from risedronate have been reported by Mellstrom et al. (55) in 2004. After 7 years of continuous use of 5 mg of risedronate daily, the increase in lumbar spine bone density from baseline was reported to be 11.5%. Risedronate also prevents bone loss in recently menopausal women. In a 2-year study of women within 3 years of menopause, 5 mg of risedronate per day resulted in small but significant increases in lumbar spine and femoral neck bone density, whereas women receiving a placebo lost bone density at those sites (56).

Risedronate can also be given once a week for either the prevention or treatment of postmenopausal osteoporosis in a dose of 35 mg. The equal efficacy of this dose, based on changes in bone density and bone turnover, was demonstrated in a non-inferiority trial, similar to that done for alendronate.

Although risedronate is FDA-approved to reduce the risk of nonvertebral fracture in general, it is not approved specifically to reduce hip fracture risk. A very large trial, called the Hip Intervention Program (HIP) was performed in which two doses of risedronate or placebo were given to women aged 70 to 79 with very low proximal femoral bone densities or to women aged 80 and older with clinical risk factors for hip fracture. Although a statistically significant reduction in hip fracture risk was demonstrated for the women receiving risedronate in the 70 to 79 year old group, it could only be demonstrated when both risedronate dose groups were combined for the purposes of the statistical analysis. A significant reduction in hip fracture risk could not be shown when the 5 mg (the FDA-approved dose) dose group alone was compared to the placebo group.

Ibandronate. Ibandronate was approved by the FDA for the prevention and treatment of postmenopausal osteoporosis in 2003 in a dose of 2.5 mg by mouth daily. In a 2-year study of postmenopausal women without osteoporosis, 2.5 mg of ibandronate taken daily increased lumbar spine bone density by 3.1% compared to placebo (57). Bone density was

increased 1.8% at the total hip, 2.0% at the femoral neck, and 2.1% at the trochanter in the ibandronate-treated women compared to placebo. In a 3-year trial of postmenopausal women with osteoporosis called the Oral Ibandronate Osteoporosis Vertebral Fracture Trial in North America and Europe (BONE) trial, 2.5 mg of ibandronate daily reduced the risk of new vertebral fractures by 52% compared to placebo (58). PA lumbar spine BMD increased by 6.5% from baseline at the end of 3 years in the women receiving 2.5 mg of ibandronate daily.

The 2.5 mg daily dose of ibandronate was recently marketed in the United States. In addition, FDA-approval has been obtained for a 150 mg, once a month tablet. The pharmacokinetics of ibandronate are such that a larger dose, given much less frequently, appears to have equal efficacy to the smaller, daily dose as measured by changes in bone density and bone turnover markers. This has been demonstrated for ibandronate in a non-inferiority trial called the Monthly Oral Ibandronate in Ladies (MOBILE) (59,60) trial.

Dosing, Contraindications, and Safety. All bisphosphonates must be taken only with water. This is because bisphosphonates are very poorly absorbed when taken by mouth. It is imperative that nothing other than water be used when taking the tablet and that nothing else other than water be consumed for at least 30 minutes for alendronate and risedronate and for 1 hour for ibandronate. Any other beverage or food consumed during that time would potentially result in a failure to absorb an adequate amount of the medication. The stomach must be empty at the time the medication is taken so that no previously consumed food, beverage, or medication is present to interfere with the absorption of the bisphosphonate. That is why the medication should be taken after an overnight fast and before breakfast.

The bisphosphonates have the potential to cause irritation of the esophagus. It is for this reason that patients are encouraged to consume a full glass of water to ensure passage of the tablet from the esophagus into the stomach. This is also why patients are advised to remain upright after taking the medication in order to reduce any risk of reflux of the medication into the esophagus. Because of the potential for esophageal irritation, oral bisphosphonates are not recommended for use in individuals who have difficulty swallowing or pre-existing esophageal disorders that might make passage of the tablet into the stomach more difficult. These are disorders such as delayed esophageal emptying, esophageal strictures, or esophageal ulceration.

Although these restrictions on the use of bisphosphonates are appropriately emphasized, it should also be noted that bisphosphonates are very safe overall. In all of the major trials in which women taking alendronate or risedronate or ibandronate were compared to women taking a placebo, no increase in gastrointestinal side effects was demonstrated in women taking the bisphosphonate. Gastrointestinal complaints occur fairly frequently in such research trials but they are equally frequent in women not taking the bisphosphonate as in the women who are (47,53,54). This suggests that gastrointestinal complaints are common in the age group of women in whom these drugs are likely to be used. It does not suggest that the drugs are the cause. There does not seem to be any reason to prefer one bisphosphonate over another based on the likelihood of gastrointestinal side effects. In a recent trial (61) in which 70 mg of alendronate and 35 mg of risedronate given once per week were compared in postmenopausal women with low bone mass, there was no difference in the number of overall adverse events or specifically in the number of gastrointestinal adverse events between the two groups of women. The bisphosphonates are some of the most efficacious and well-studied drugs available for the prevention and treatment of osteoporosis. Their use should not be discontinued prematurely because of minor gastrointestinal complaints that are just as likely to occur in the absence of treatment with a bisphosphonate.

TERIPARATIDE

Teriparatide is marketed under the trade name Fortéo®. The FDA-approved dose for the treatment of women with postmenopausal osteoporosis who are at high risk of fracture is 20 µg injected subcutaneously daily for a maximum of 2 years. Teriparatide is also approved to increase bone mass in men with osteoporosis who are high risk of fracture. This drug is essentially the first 34 amino acids found in parathyroid hormone, which is an 84 amino acid polypeptide. As a consequence, teriparatide is also called recombinant human 1-34 parathyroid hormone (PTH). In 2001, the results of a planned 3-year trial were published in the *New England Journal of Medicine* (62). The trial involved postmenopausal women with either one spine fracture and a low bone density or two spine fractures. Women who received 20 µg of teriparatide daily for an average of 18 months increased their lumbar spine bone density by 9.7% from baseline. Femoral neck bone density increased by 2.8% from baseline. Compared to placebo, the risk of new spine fracture was decreased 62% in the women receiving 20 µg of teripartide in the same time frame.

The planned duration of this trial was 3 years, but it was stopped prematurely because of the finding of an increased incidence of osteosarcoma in rats. Although teriparatide carries a warning about rat osteosarcoma in the prescribing information, it should be noted that these rats were given very large, virtually lifetime daily injections of the drug. The relevance of this finding to human medicine is unclear. Nevertheless, the current data for the efficacy and safety of teriparatide administered daily is limited to 2 years. As a result, treatment with teriparatide should not currently exceed 2 years.

A practical issue that has arisen with the approval of teriparatide is when to use it as opposed to any of the members of the antiresorptive class. This issue was addressed by Miller et al. (63). The authors acknowledge that their recommendations are largely opinions based on practical experience. They note, however, that teriparatide could be considered for use in patients with a pre-existing fracture, patients with a T-score less than -3 , and patients losing bone or sustaining fractures on other therapies. In keeping with the labeling of the product, the authors note that teriparatide is contraindicated in anyone with a increased risk of osteosarcoma^{¶¶¶}, prior external beam or implant radiation involving the skeleton, or other types of bone cancer.

Because treatment with teriparatide is currently limited to 2 years, a logical question is what treatment, if any, should be offered after 2 years of teriparatide therapy are completed? Based on findings from a study called the Parathyroid Hormone and Alendrone (PaTH) trial, it appears that teriparatide should be followed by antiresorptive therapy (64). Teriparatide was not used in the PaTH trial. Instead, a form of 1-84 PTH was used. Although it cannot be said with certainty that the results would have been the same had teriparatide been used instead of 1-84 PTH, results from the PaTH trial are clear that 1-84 PTH should be followed by an antiresorptive agent to prevent bone loss after discontinuation of 1-84 PTH. In the absence of information to the contrary, it would seem reasonable to apply these findings to teriparatide at the present time.

PATIENT EDUCATION MATERIALS

Densitometry facilities may wish to develop their own patient education materials in osteoporosis and densitometry, but many brochures and

^{¶¶¶}Patients with Paget's disease, unexplained increases in alkaline phosphatase, or open epiphyses.

pamphlets are available at no cost from local pharmaceutical representatives. In some instances, these materials can be personalized for the densitometry facility. Such materials will also generally contain some mention of the particular product or medication manufactured by the company but these references are usually kept to a minimum. There are also publications available from the National Osteoporosis Foundation suitable for patients (see Appendix I). A variety of books on osteoporosis are available at local books stores, including *The Osteoporosis Handbook* by Sydney Lou Bonnick, MD.

REFERENCES

1. Consensus Development Conference. (1991) Prophylaxis and treatment of osteoporosis. *Am. J. Med.* **90**, 107–110.
2. Peck, W. A. (1993) Consensus development conference: diagnosis, prophylaxis, and treatment of osteoporosis. *Am. J. Med.* **94**, 646–650.
3. World Health Organization. (1994) Assessment of fracture risk and its application to screening for postmenopausal osteoporosis: report of a WHO study group. WHO Technical Report Series. WHO, Geneva.
4. NIH Consensus Development Panel. (2001) National Institutes of Health Consensus Development Conference statement: osteoporosis prevention, diagnosis, and therapy. *JAMA* **285**, 785–795.
5. Melton, L. J., Chrischilles, E. A., Cooper, C., Lane, A. W., Riggs, B. L. (1992) How many women have osteoporosis? *J. Bone Miner. Res.* **7**, 1005–1010.
6. Melton, L. J. (1995) How many women have osteoporosis now? *J. Bone Miner. Res.* **10**, 175–177.
7. National Osteoporosis Foundation. (2002) America's Bone Health: The State of Osteoporosis and Low Bone Mass in Our Nation. NOF, Washington, D.C.
8. Chrischilles, E. A., Butler, C. D., Davis, C. S., Wallace, R. B. (1991). A model of lifetime osteoporosis impact. *Arch. Intern. Med.* **151**, 2026–2032.
9. Ray, N. F., Chan, J. K., Thamer, M., Melton, L. J. (1997) Medical expenditures for the treatment of osteoporotic fractures in the United States: a report from the National Osteoporosis Foundation. *J. Bone Miner. Res.* **12**, 24–35.
10. Schlaich, C., Minne, H. W., Bruckner, T., et al. (1998) Reduced pulmonary function in patients with spinal osteoporotic fractures. *Osteoporos. Int.* **8**, 261–267.
11. Marotolli, R. A., Berkman, L. F., Cooney, L. M. (1992) Decline in physical function following hip fracture. *J. Am. Geriatr. Soc.* **40**, 861–866.
12. Cummings, S. R., Kelsey, J. L., Nevitt, M. C., O'Dowd, K. J. (1985) Epidemiology of osteoporosis and osteoporotic fractures. *Epidemiol. Rev.* **7**, 178–208.
13. Bonnick, S. L., Nichols, D. L., Sanborn, C. F., et al. (1997) Dissimilar spine and femoral z-scores in premenopausal women. *Calcif. Tissue Int.* **61**, 263–265.
14. Hansen, M. A. (1994) Assessment of age and risk factors on bone density and bone turnover in healthy premenopausal women. *Osteoporos. Int.* **4**, 123–128.
15. Rodin, A., Murby, B., Smith, M. A., et al. (1990) Premenopausal bone loss in the lumbar spine and neck of the femur: a study of 225 Caucasian women. *Bone* **11**, 1–5.

16. Lloyd, T., Martel, J. K., Rollings, N., et al. (1996) The effect of calcium supplementation and Tanner stage on bone density and area in teenage women. *Osteoporos. Int.* **6**, 276–283.
17. Slemenda, C. W., Miller, J. Z., Hui, S. L., Reister, T. K., Johnston, C. C. (1991) The role of physical activity in the development of skeletal mass in children. *J. Bone Miner. Res.* **6**, 1227–1233.
18. Melton, L. J. (1993) Epidemiology of age-related fractures, in *The Osteoporotic Syndrome*. (Avioli, L. V., ed.), Wiley-Liss, New York, pp. 17–38.
19. National Osteoporosis Foundation. (1998) Physician's guide to prevention and treatment of osteoporosis. Excerpta Medica, Inc., Belle Mead, NJ.
20. National Osteoporosis Foundation. (2003) Physician's guide to prevention and treatment of osteoporosis. NOF, Washington, D.C.
21. Women's Health Initiative Investigators. (2002) Risks and benefits of estrogen plus progestin in healthy postmenopausal women. Principal results from the Women's Health Initiative randomized controlled trial. *JAMA* **288**, 321–333.
22. Osteoporosis Task Force. (2001) American Association of Clinical Endocrinologists 2001 medical guidelines for clinical practice for the prevention and management of postmenopausal osteoporosis. *Endocr. Prac.* **7**, 293–312.
23. AACE. (2003) American Association of Clinical Endocrinologists medical guidelines for clinical practice for the prevention and treatment of postmenopausal osteoporosis: 2001 edition, with selected updates for 2003. *Endocr. Pract.* **9**, 545–564.
24. (2002) ACOG releases recommendations for bone density screening for osteoporosis. American College of Obstetricians and Gynecologists, Washington, D.C. (Accessed March 26, 2002, at http://www.acog.org/from_home/publications/press_release/nr02-28-02-1.htm).
25. (2002) Management of postmenopausal osteoporosis: position statement of The North American Menopause Society. *Menopause* **9**, 84–101.
26. U.S. Preventative Services Task Force. (2002) Screening for osteoporosis in postmenopausal women: recommendations and rationale. *Ann. Intern. Med.* **137**, 526–528.
27. The Writing Group for the ISCD Position Development Conference. (2004) Indications and reporting for dual-energy x-ray absorptiometry. *J. Clin. Densitom.* **7**, 37–44.
28. Hamdy, R. C., Petak, S. M., Lenchik, L. (2002) Which central dual x-ray absorptiometry skeletal sites and regions of interest should be used to determine the diagnosis of osteoporosis? *J. Clin. Densitom.* **5**, S11–S17.
29. Binkley, N. C., Schmeer, P., Wasnich, R. D., Lenchik, L. (2002) What are the criteria by which a densitometric diagnosis of osteoporosis can be made in males and non-Caucasians? *J. Clin. Densitom.* **5**, S19–S27.
30. Health Care Financing Administration, Department of Health and Human Services. (1998) Medicare program: Medicare coverage of and payment for bone mass measurements. Federal Register 42 CFR, Part 410.
31. Kiel, D. P., Baron, J. A., Anderson, J. J., Hannan, M. T., Felson, D. T. (1992) Smoking eliminates the protective effect of oral estrogens on the risk for hip fracture among women. *Ann. Intern. Med.* **116**, 716–721.
32. Cornuz, J., Feskanich, D., Willett, W. C., Colditz, G. A. (1999) Smoking, smoking cessation and risk of hip fracture in women. *Am. J. Med.* **106**, 311–314.
33. Barger-Lux, J. J., Heaney, R. P., Stegman, M. R. (1990) Effects of moderate caffeine intake on the calcium economy of premenopausal women. *Am. J. Clin. Nutr.* **52**, 722–725.

34. Bikle, D. D., Genant, H. K., Cann, C., Recker, R. R., Halloran, B. P., Strewler, G. J. (1985) Bone disease in alcohol abuse. *Ann. Intern. Med.* **103**, 42–48.
35. Burger, H., Grobbee, D. E., Drucke, T. (2000) Osteoporosis and salt intake. *Nutr. Metab. Cardiovasc. Dis.* **10**, 46–53.
36. (1994) Optimal calcium intake. *NIH Consensus Statement* **12**, 1–31.
37. Yates, A. A., Schlicker, S. A., Suitor, C. W. (1998) Dietary reference intakes: the new basis for recommendations for calcium and related nutrients, B vitamins, and choline. *J. Am. Diet. Assoc.* **98**, 699–706.
38. Bischoff-Ferrari, H. A., Dawson-Hughes, B., Willett, W. C., et al. (2004) Effect of Vitamin D on falls: a meta-analysis. *JAMA* **291**, 1999–2006.
39. Dhesi, J. K., Jackson, S. H., Bearne, L. M., et al. (2004) Vitamin D supplementation improves neuromuscular function in older people who fall. *Age Ageing* **33**, 589–595.
40. Writing Group for the Women's Health Initiative Investigators. (2002) Risks and benefits of estrogen plus progestin in healthy postmenopausal women. Principal results from the women's Health Initiative randomized controlled trial. *JAMA* **288**, 321–333.
41. Ettinger, B., Black, D. M., Mitlak, B. H., et al. (1999) Reduction of vertebral fracture risk in postmenopausal women with osteoporosis treated with raloxifene. *JAMA* **282**, 637–645.
42. Delmas, P. D., Bjarnason, N. H., Mitlak, B. H., et al. (1997) Effect of raloxifene on bone mineral density, serum cholesterol concentrations, and uterine endometrium in postmenopausal women. *N. Engl. J. Med.* **337**, 1641–1647.
43. Chesnut, C. H., Silverman, S., Andriano, K., et al. (2000) A randomized trial of nasal spray salmon calcitonin in postmenopausal women with established osteoporosis: the prevent recurrence of osteoporotic fractures study. *Am. J. Med.* **109**, 267–276.
44. Watts, N. B., Harris, S. T., Genant, H. K., et al. (1990) Intermittent cyclical etidronate treatment of postmenopausal osteoporosis. *N. Engl. J. Med.* **323**, 73–79.
45. Storm, T., Thamsborg, G., Steiniche, T., Genant, H. K., Sørensen, O. H. (1990) Effect of intermittent cyclical etidronate therapy of bone mass and fracture rate in women with postmenopausal osteoporosis. *N. Engl. J. Med.* **322**, 1265–1271.
46. Schnitzer, T., Bone, H. G., Crepaldi, G., et al. (2000) Therapeutic equivalence of alendronate 70 mg once-weekly and alendronate 10 mg daily in the treatment of osteoporosis. *Aging Clin. Exp. Res.* **12**, 1–12.
47. Black, D. M., Cummings, S. R., Karpf, D. B., et al. (1996) Randomised trial of effect of alendronate on risk of fracture in women with existing fractures. *Lancet* **348**, 1535–1541.
48. Tonino, R. P., Meunier, P. J., Emkey, R., et al. (2000) Skeletal benefits of alendronate: 7-year treatment of postmenopausal osteoporotic women. Phase III osteoporosis treatment study group. *J. Clin. Endocrinol. Metab.* **85**, 3109–3115.
49. Bone, H. G., Hosking, D., Devogelaer, J. P., et al. (2004) Ten years' experience with alendronate for osteoporosis in postmenopausal women. *N. Engl. J. Med.* **350**, 1189–1199.
50. McClung, M., Clemmesen, B., Daifotis, A., et al. (1998) Alendronate prevents postmenopausal bone loss in women without osteoporosis. *Ann. Intern. Med.* **128**, 253–261.
51. Lindsay, R., Cosman, F., Lobo, F. A., et al. (1999) Addition of alendronate to ongoing hormone replacement therapy in the treatment of osteoporosis: a randomized, controlled clinical trial. *J. Clin. Endocrinol. Metab.* **84**, 3076–3081.
52. Orwoll, E., Ettinger, M., Weiss, S., et al. (2000) Alendronate for the treatment of osteoporosis in men. *N. Engl. J. Med.* **343**, 604–610.

53. Harris, S. T., Watts, N. B., Genant, H. K., et al. (1999) Effects of risedronate treatment on vertebral and nonvertebral fractures in women with postmenopausal osteoporosis. *JAMA* **282**, 1344–1352.
54. Reginster, J. Y., Minne, H. W., Sorensen, O. H., et al. (2000) Randomized trial of the effects of risedronate on vertebral fractures in women with established postmenopausal osteoporosis. *Osteoporos. Int.* **11**, 83–91.
55. Mellstrom, D. D., Sorensen, O. H., Goemaere, S., et al. (2004) Seven years of treatment with risedronate in women with postmenopausal osteoporosis. *Calcif. Tissue Int.* **75**, 462–468.
56. Hooper, M., Ebeling, P., Roberts, A., et al. (1999) Risedronate prevents bone loss in early postmenopausal women. *Calcif. Tissue Int.* **64**, Abstract P-80.
57. McClung, M. R., Wasnich, R. D., Recker, R., et al. (2004) Oral daily ibandronate prevents bone loss in early postmenopausal women without osteoporosis. *J. Bone Miner. Res.* **19**, 11–18.
58. Chesnut III, C. H., Skag, A., Christiansen, C., et al. (2004) Effects of oral ibandronate administered daily or intermittently on fracture risk in postmenopausal osteoporosis. *J. Bone Miner. Res.* **19**, 1241–1249.
59. Miller, P. D., Drezner, M. K., Delmas, P. D., et al. (2004) Monthly oral ibandronate is at least as effective as daily oral ibandronate in postmenopausal osteoporosis: 1-year results from MOBILE. *J. Bone Miner. Res.* **19**, S94.
60. Recker, R. R., Kendler, D. L., Adami, D. S., et al. (2004) Monthly oral ibandronate significantly reduces bone resorption in postmenopausal osteoporosis: 1-year results from MOBILE. *J. Bone Miner. Res.* **19**, S94.
61. Rosen, C. J., Hochberg, M. C., Bonnick, S. L., et al. (2005) Treatment with once-weekly alendronate 70 mg compared with once-weekly risedronate 35 mg in women with postmenopausal osteoporosis: a randomized double-blind study. *J. Bone Miner. Res.* **20**, 141–151.
62. Neer, R. M., Arnaud, C. D., Zanchetta, J. R., et al. (2001) Effect of parathyroid hormone (1-34) on fractures and bone mineral density in postmenopausal women with osteoporosis. *N. Engl. J. Med.* **344**, 1434–1441.
63. Miller, P. D., Bilezikian, J. P., Deal, C., Harris, S. T., Ci, R. P. (2004) Clinical use of teriparatide in the real world: initial insights. *Endocr. Prac.* **10**, 129–148.
64. Black, D. M., Rosen, C. J., Palermo, L., et al. (2004) The effect of 1 year of alendronate following 1 year of PTH 1-84: second year results from the PTH and alendronate (PaTH) trial. *J. Bone Miner. Res.* **1**, S26.

10 Interpretation of Bone Densitometry Data

CONTENTS

- THE RESULTS
 - THE SKELETAL IMAGE
 - MEASURED AND CALCULATED BONE DENSITY PARAMETERS
 - COMPARISONS TO THE REFERENCE DATABASE
 - STANDARDIZED BMD
 - AGE-REGRESSION GRAPH
 - ASSIGNMENT OF DIAGNOSTIC CATEGORY BASED ON WHO CRITERIA
- CONFLICTING DIAGNOSES FROM THE MEASUREMENT OF MULTIPLE SITES
- REPORT REVIEW
- REFERENCES

The physician is always ultimately responsible for the interpretation of bone densitometry data. The ability of the technologist to perform his or her duties, however, is only enhanced by understanding what the physician will attempt to do with the data that they provide. The circumstances in which bone densitometry is often performed are also quite different from the circumstances in which other diagnostic procedures are usually performed. Unlike having a chest X-ray for example, in which the procedure is over in a few seconds, the patient is often asked to sit or lie down for several minutes during a bone density study. The technologist is not physically separated from the patient by a protective barrier but usually seated only a few feet away. It is inevitable that the patient will ask questions about the test and the nature of the results. The technologist should be able to respond to these questions appropriately while ultimately deferring to the diagnostic judgment of the physician. It is also true that occasionally the technologist must make decisions

independently regarding the choice of skeletal site to measure, the technical acceptability of the study and the timing of return visits. An understanding of how the data is to be used is crucial to making these decisions.

THE RESULTS

The type of information obtained from the various bone densitometry devices may appear different, but the nature of the information is the same. With only a few exceptions, the information can be categorized as follows:

- The skeletal image.
- The measured and calculated bone density parameters.
- Comparisons to the reference database.
 - % Comparisons.
 - Standard score comparisons.
- Standardized bone mineral density (sBMD).
- Age-regression graph.
- Assignment of diagnostic category based on World Health Organization (WHO) criteria.

The exact location of this information on the computer screen or on the printout will vary from device to device, but the nature of the information does not.

The Skeletal Image

All of today's X-ray densitometers provide an image of the region of the skeleton being studied. Some, but not all, ultrasound densitometers do so as well. These images should always be closely examined for the possible presence of artifacts that would affect the accuracy of the study and the interpretation of the data. If problems are suspected from a review of the image, it is appropriate for the technologist to contact the physician to ask if another site should be studied. At the very least, it is appropriate for the technologist to flag the study in some way, to alert the physician to possible problems. The skeletal images created during a bone densitometry study are not approved by the Food and Drug Administration (FDA) to be used to make structural diagnoses*. Plain films are required if it is necessary to confirm the suspected skeletal

*Spine images acquired during a DVA™, IVA™, or RVA™ study are FDA-approved for use in structural diagnosis.

abnormalities. Nevertheless, it is important that the images be reviewed for possible structural problems. This situation occurs most often with studies of the PA lumbar spine. As noted in Chapter 3, the presence of osteophytes, facet sclerosis, or compression fractures will increase the measured BMD. Although the device is accurately measuring the amount of mineral in the beam path such that the measurement cannot truly be said to be inaccurate, clearly the interpretation of the bone density data in the context of osteoporosis will be affected. The precision of future measurements at that site will also be poorer. Consequently, if the technologist is aware that the study is being done to establish a baseline value for future measurements, it would be appropriate to contact the physician to explain the potential problem to ask if another skeletal site should be measured. The presence of a suspected fracture has additional significance in assigning the patient's diagnosis and the interpretation of risk for future fracture. In a postmenopausal Caucasian woman, the presence of a fracture combined with a bone density that is 2.5 standard deviations (SDs) or more below the average peak bone density of the young adult will result in a diagnosis of severe osteoporosis rather than just osteoporosis. In addition, many studies have shown that the risk for future fracture is greater than that implied by the bone density alone once a fracture has occurred (1-4). For example, the posteroanterior (PA) lumbar spine image from the dual-energy X-ray absorptiometry (DXA) study shown in Fig. 10-1 clearly suggests the presence of a compression fracture at L3. A review of the individual BMD values for each vertebra also clearly shows a dramatic increase in the BMD between L2 and L3, which is much greater than expected. The presence of a fracture at L3 should be confirmed with plain X-rays since this image is not FDA-approved for use in making structural diagnoses. Nevertheless, suspicion should be aroused by these findings. The increase in BMD at L3 will increase the L2-L4 BMD, on which comparisons to the reference database will be made. The higher T-score could result in an incorrect diagnosis. It is quite likely that this patient is actually osteoporotic rather than osteopenic as the T-score in Fig. 10-1 suggests. The presence of a fracture also implies that the patient is at much greater risk of future fracture than the bone density alone implies. It would be entirely appropriate for the technologist to note that there appears to be a structural problem at L3 and that the BMD at L3 is unusually high compared to L2 and L4. Without going any further, the technologist has alerted the physician to potential problems in the interpretation of the data.

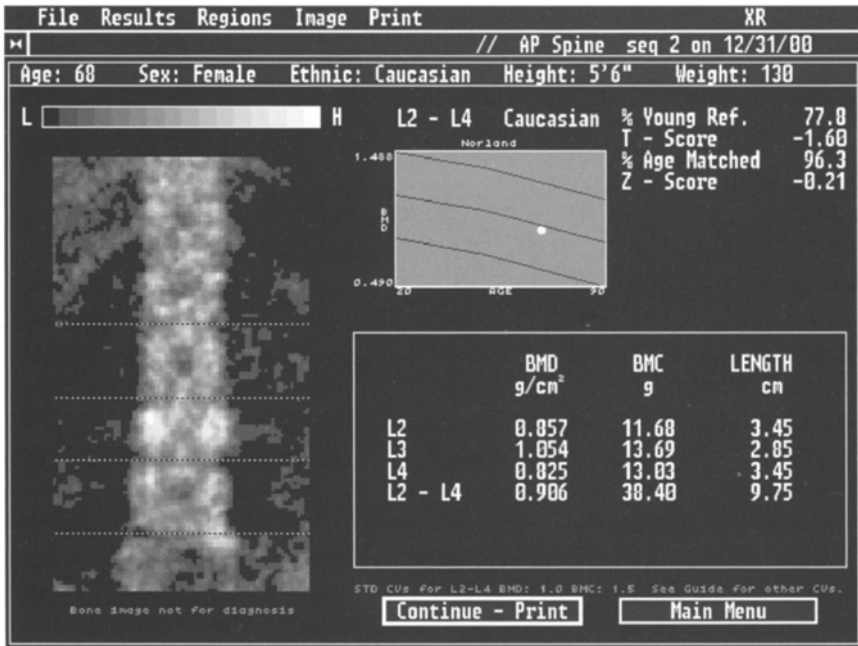


Fig. 10-1. Norland XR-series posteroanterior lumbar spine study. A review of the skeletal image suggests a loss of height and increased density at L3. The values for the individual vertebrae also suggest a much greater increase in density between L2 and L3 than normal. These findings are suggestive of fracture at L3 although plain films would be required to prove this. The L2-L4 BMD will be increased by the process at L3.

Structural diagnoses can be made using the IVA™ or RVA™ application from Hologic, Inc. and the DVA™ application from GE Lunar, in which the entire spine is imaged. These applications are available only on specific models from the respective manufacturers. If these applications are available and a structural abnormality in the spine is suspected, the physician can be contacted for permission to proceed with spine imaging to confirm the presence and nature of the suspected abnormality. Figure 10-2 is an IVA image from the Hologic Delphi that shows a wedge fracture at L1.

Measured and Calculated Bone Density Parameters

The measured and calculated parameters for the regions of interest will be displayed on the computer screen at the conclusion of the analysis phase of the bone density study. Remember that BMD is actually calculated from the measurements of BMC and area or volume as described in

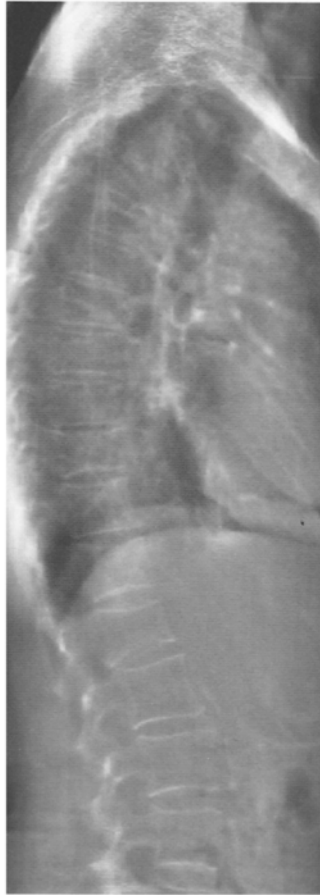


Fig. 10-2. Delphi IVA image of the lateral spine. The remarkable clarity of this image allows structural diagnoses to be made. A compression fracture is seen at L1 as well as aortic calcification anterior to the lower lumbar spine. This is a single-energy X-ray image. (Photo courtesy of Hologic, Inc., Bedford, MA.)

Chapter 1. When multiple regions of interest have been measured during a single study, the technologist must decide which region's parameters to emphasize. The calculated parameter for the region that is picked will be highlighted and plotted on an age-regression graph. It is this value that will likely receive the attention of the physician. As a consequence, it is imperative that the technologist selects the correct region and the correct parameter for that region.

At the PA spine, the measured and calculated values for each vertebra are listed in Fig. 10-3. Also shown are the values for each combination of

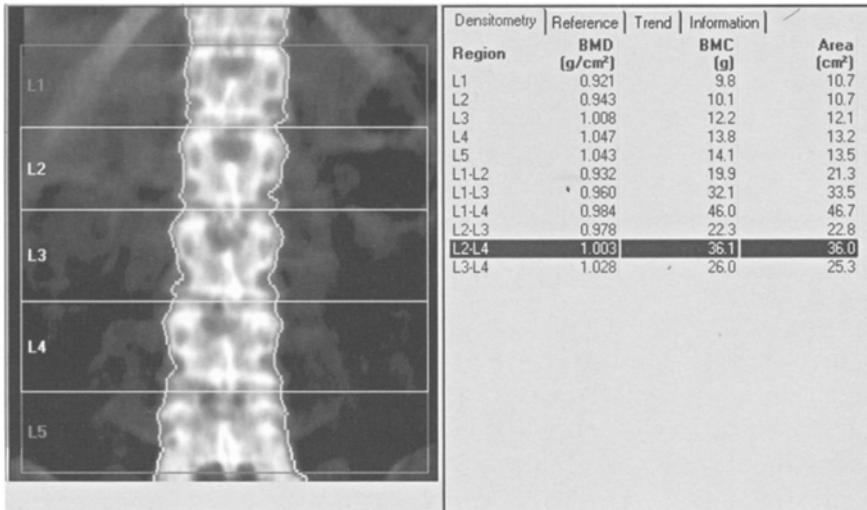


Fig. 10-3. Posteroanterior lumbar spine GE Lunar Prodigy DXA study. The measured parameters of bone mineral content (BMC) and area are shown for each individual vertebra and every possible combination of contiguous vertebrae. The bone mineral density (BMD) that is calculated by dividing the BMC by the area is also shown for each individual vertebra and every combination of contiguous vertebrae. The technologist can choose to emphasize any value although the L1–L4 or L2–L4 BMD is preferred for reasons of statistical accuracy and precision.

contiguous vertebrae. On most devices, a “default” region of interest will be programmed into the software. This is the region of interest that will be emphasized unless changed by the technologist. On the study shown in Fig. 10-3, the L2–L4 BMD is highlighted by default. If unchanged by the technologist, this value will be plotted on the age-regression graph and displayed prominently on the printout. For PA spine studies, it is preferable to use the BMD that is calculated from the measurement of three or four contiguous vertebrae as long as none of those vertebrae are affected by artifacts. The reason for selecting the three- or four-vertebral BMD over the BMD for only one or two vertebrae is that the accuracy and precision of the measurement are superior. The default region of interest on central GE Lunar and Norland DXA devices at the spine is the L2–L4 BMD and on Hologic central DXA devices, L1–L4. If one of the vertebra in these default regions is suspected of being structurally abnormal, it should be excluded from the calculation or the average from another set of contiguous vertebrae chosen. The approach that is preferable will depend on the type of densitometry device.

In the proximal femur, five different regions of interest can be measured: the total hip (or total femur), the femoral neck, Ward's area, the trochanter, and the shaft, as shown previously in Fig. 3-21 A and B. The total hip region of interest combines the femoral neck, Ward's area, the trochanter, and the shaft into one measurement. Because the combined area of all these regions that contribute to the total hip measurement is greater than the area of any one of these regions alone, the precision of the total hip measurement tends to be the best of any of the five regions. For this reason, many authorities prefer to emphasize the total hip region of interest over the other regions in the proximal femur. This enthusiasm must be tempered by the recognition that any anticipated rate of change in the total hip region of interest will tend to be slower than in the femoral neck or trochanter. The combination of precision and rate of change, not precision alone, determines a site's utility for serial measurements[†]. Excellent precision can be obtained at the femoral neck in which greater rates of change are generally seen than in the total hip. Both regions are similarly useful in the prediction of fracture risk (5). Consequently, the authors prefer to emphasize the femoral neck over the total hip. The technologist should consult with the supervising physician to determine which region of interest is preferred. Ward's area is virtually never emphasized, as it is not used for either diagnosis, fracture risk assessment, or monitoring of bone density. In research studies, Ward's area is a good predictor of fracture risk. Nevertheless, its utility in an individual is quite limited. The area defined by the densitometry computer software as Ward's area is so small that the accuracy and precision of the measurement are extremely poor compared to the total hip, femoral neck, or trochanter.

At the forearm, many densitometers will measure several different skeletal sites. It is also possible to obtain a measurement at one site of either the radius or ulna or of both bones combined. The combined measurement, again because of the larger area being measured, generally offers better accuracy and precision than the single bone measurement. This makes the combined bone measurement preferable. The preferred site on either bone or both bones combined is highly dependent on the reason the measurement is being performed. The more distal regions in the forearm such as the ultradistal, 8-mm, 10%, and distal region of interest are generally preferred for the diagnosis of osteoporosis[§]. If a patient

[†]See Chapter 6 for a discussion of the interaction between precision and rate of change.

[§]See Chapter 3 for a discussion of naming conventions for forearm bone density sites.

is being evaluated for hyperparathyroidism, the proximal, 1/3, or 33% sites are preferred. The choice of site is influenced by the percentage of trabecular and cortical bone found at those sites. In diseases such as osteoporosis, in which trabecular bone loss is an early feature, the more trabecular distal sites are preferred. Hyperparathyroidism tends to have a pronounced effect on cortical bone, making the highly cortical proximal sites the better sites to measure in the forearm. If the patient has had a distal radial fracture or Colles' fracture, the BMD at the distal site may be increased by as much as 20%, whereas the proximal site tends to be unaffected (6). In this circumstance, if the opposite arm cannot be measured for some reason, the proximal site is the site that more accurately reflects the patient's bone mineral status. For the prediction of fracture risk, any of the distal or proximal sites can be used. None of the forearm sites are generally used for monitoring therapy. This is not because of either poor accuracy or poor precision at any of the sites. This is because the rate of change at the forearm sites tends to be so slow that the time needed before the least significant change (LSC) will have occurred is much too long to be clinically useful[¶].

Measurements of bone density at the calcaneus, phalanges, and metacarpals do not present the technologist with a variety of regions of interest from which to choose. These are normally predetermined by the computer software. Total body bone density studies can be subdivided into all the various regions of the skeleton. The accuracy and precision of the total body bone density measurement is excellent. When the skeleton is divided into smaller regions (smaller within the context of the total body measurement) such as the lumbar spine or legs, the accuracy and precision of the measurement suffer. Because of this, it is not recommended that the various regions of the skeleton from a total body bone density measurement be used for diagnosis or monitoring of therapy. The total body bone density measurement itself is, as noted in Chapter 3, a measure of predominantly cortical bone. As such, it is not particularly useful in the diagnosis of diseases that affect the more trabecular areas of the skeleton or in monitoring changes in trabecular bone from the therapeutic agents used in the treatment of osteoporosis.

Comparisons to the Reference Database

The percentage comparisons and standard score comparisons were discussed in Chapter 1. The region of interest that is selected by the technologist to be emphasized on the printout also determines which set of

[¶]See Chapter 6 for a discussion of LSC.

comparisons will be emphasized as well. The percentage comparisons and standard score comparisons are different expressions of the same thing. The % Young Adult comparison and the T-score both compare the patient's BMD to the peak BMD value that is expected for a healthy individual of the same sex. The % Age-Matched comparison and the z-score both compare the patient's BMD to the BMD that is expected for an individual of the same age and sex. One comparison is simply in the form of a percentage, whereas the other indicates the number of SDs above or below the reference value. In clinical practice, the standard score comparisons have been given more importance than the percentage comparisons in diagnosis and fracture risk prediction. This is largely the result of the application of the WHO criteria for diagnosis of osteoporosis, which are based on the number of SDs from the average peak bone density of the young adult. These criteria are readily converted to T-scores as shown in Appendix II. In addition, most of the data from fracture trials demonstrating the utility of bone mass measurements in predicting fracture risk are expressed as the increase in risk per SD decline in bone density. Once again, this data is easily used in conjunction with the T- or z-score.

It is just as important to avoid misinterpreting the percentage comparisons and standard scores as it is to interpret them correctly. The % Young Adult comparison and T-score should never be interpreted as indicating a certain magnitude of bone loss. For example, although a patient may be found to have a bone density that is 15% below the average peak BMD for a young adult, a 15% bone loss could only be proven if it was known that the patient's peak BMD was in fact identical to the average peak BMD to which the patient is being compared. It is, after all, quite possible that the patient developed a lower than average peak BMD and that they have lost no bone density at all. On the other hand, if they had developed a better than average peak bone density as a young adult, they might have actually experienced an ever greater loss than 15%. It is simply not possible to come to any conclusion in this regard from a single bone mass measurement. The % Age-Matched comparison and the z-score can also be misinterpreted. Patients often ask how they compare to others their same age. This question generally follows being told that their % Young Adult comparison or T-score is relatively poor. It is possible to have a favorable age-matched comparison or z-score while having a poor % Young Adult comparison or T-score. This is because bone loss tends to occur with advancing age. Simply because lower levels of bone density are expected at older ages should not be misconstrued as indicating the absence of a

problem. This loss of bone is not desirable and certainly not beneficial. A good % Age-Matched comparison and good z-score can provide a false sense of security in the presence of the more important low young-adult comparisons.

These comparisons to the reference database should never be used in serial bone mass measurements to determine if a change has occurred in the patient's bone density. When a patient is being followed over time to determine if bone loss is occurring or if a therapy has caused an increase in bone density, it is the actual BMD values that should be compared from study to study. As discussed in Chapter 6, the significance of the change in the BMD is determined by the precision of the measurement and the desired level of statistical confidence.

The T-score is readily used to determine the WHO diagnostic category if the patient is a postmenopausal Caucasian woman. If the patient is a healthy premenopausal Caucasian woman, the WHO criteria should not be applied. This is because, in an otherwise healthy woman, a low bone mass may not indicate bone loss. It may only indicate a lower than average peak bone density that is being maintained. Although there may be less mass in her bones, it is highly unlikely that there is anything wrong with the architecture of her bones. The 1991 and 1993 Consensus Conference definitions of osteoporosis require microarchitectural deterioration of bone tissue in addition to low bone mass**. Microarchitectural deterioration is presumed in older women with low bone mass, but it should not be presumed in otherwise healthy younger women. Labeling such a woman as having a disease is inappropriate. It is useful to make her aware that her bone mass is lower than average so that she takes all necessary steps to prevent bone loss in the future. In the absence of other criteria, the WHO criteria for postmenopausal Caucasian women are used in conjunction with bone density measurements in postmenopausal African-American, Hispanic, and Asian women, although it is not entirely clear if this is appropriate. Similarly, the criteria are also being used in mature Caucasian men. The z-score is not used for diagnostic purposes.

In predicting fracture risk, the guiding principle is that the risk of fracture approximately doubles for each SD decline in bone density (7). This is generally true for any type of fracture or all fractures as measured at any skeletal site. Therefore, because the T-score indicates how many SDs

**See Chapter 9 for a discussion of the 1991 and 1993 Consensus Conference definitions of osteoporosis.

below the average peak BMD the patient's bone density actually lies, the T-score can be used to predict fracture risk. This is an exponential relationship. For example, if the T-score is -3 , and the risk of fracture doubles for each SD decline in bone density, the patient's risk of fracture is increased eightfold ($2 \times 2 \times 2$) compared to the individual who still has the bone density of a young adult. If the z -score was -2 , then the patient's risk of fracture is increased fourfold (2×2) compared to an individual of the same age. Neither of these approaches is ideal. Using the T-score in this fashion likely overestimates the patient's actual fracture risk. Using the z -score almost certainly underestimates the patient's fracture risk. The use of the T-score is common, although better ways of expressing fracture risk are actively being pursued.

Predictions of fracture risk that refer to the risk of having any type of osteoporotic fracture are called *global fracture risk predictions*. Predictions of the risk of having a specific type of fracture are called *site-specific fracture risk predictions*. For example, the prediction of the risk of spine fracture is a site-specific fracture risk prediction. Similarly, the prediction of the risk of hip fracture is a site-specific fracture risk prediction. Site-specific fracture risk predictions do not have to be based on the measurement of BMD at the potential fracture site. For example, a site-specific spine fracture risk assessment can be made based on the measurement of BMD at the femoral neck as well as at the spine. A doubling of fracture risk for each SD decline in bone density is used for global fracture prediction almost irrespective of where the measurement is being made. For site-specific fracture predictions the increase in fracture risk per SD decline in bone density that is used does depend on where the measurement is being made. For the prediction of hip fracture, the increase in risk is 2.6-fold for each SD decline in bone density at the femoral neck and 2.7-fold at the total hip (5). If the measurement is made at the heel the increase in risk is twofold and at the distal radius, 2.6-fold (8). For the prediction of spine fracture, the increase in risk is 1.9-fold for each SD decline in PA spine bone density (8). If the measurement is made at the femoral neck, the increase in risk is 1.8-fold and at the midradius, 2.2-fold. The available information on the increase in fracture risk per SD decline in bone density comes from studies in women aged 60 or older. It is not known if such information is directly applicable to younger, postmenopausal women or certainly, younger, premenopausal women. For this reason, assessments of fracture risk based on bone mass measurements are most appropriately made in women aged 60 and older.

Standardized BMD

The sBMD, reported in mg/cm^2 , is available as an option for the DXA L2–L4 PA spine BMD and the total hip BMD. The technologist can usually activate or deactivate this option by adjusting the settings of the software. As noted in Chapter 1, it was hoped that the sBMD would make possible direct comparisons of spine and proximal femur BMDs that were obtained on central devices from different manufacturers. The sBMD is not used for diagnosis, fracture risk assessment, or serial monitoring. In using the sBMD to compare values from two different machines, both machines native BMD values should be converted to the sBMD value. The two sBMD values can then be compared. Because there is a margin of error in these conversions, at least 3% difference in the sBMD values should be anticipated even when the bone density has not changed between the two measurements. This margin of error makes the sBMD difficult to use clinically because the conclusions that are drawn from such comparisons remain uncertain. One can only say that “there doesn’t appear to have been any change” or that “this difference is larger than expected.” More precise conclusions cannot be reached on the basis of the sBMD. The equations for the conversion of the manufacturer’s PA spine and total hip BMD values to the sBMD are listed in Appendix VII.

Age-Regression Graph

The age-regression graph that is found on the printouts for all the different devices actually provides no additional information that cannot be obtained from the actual BMD and standard score comparisons. Patients often ask for an explanation of these colorful graphs, and, therefore, the technologist should be able to provide some insight into their meaning. Some recent additions to these graphs are also easily misinterpreted.

The horizontal axis of the age-regression graph reflects advancing age. The vertical axis indicates BMD in the units of the measurement. On some graphs, the vertical axis on the right indicates the T-score. The BMD of the default region of interest or the region of interest that has been selected by the technologist will be plotted on the graph above the patient’s age. A line indicating the expected value of BMD of the selected region of interest for the age range represented on the graph will be seen. On some devices, depending on the skeletal site, this line tends to be flat in young adulthood and then drop sharply after the age of 45 or 50. On other devices, the line is more curvilinear. This line is called the *regression of*

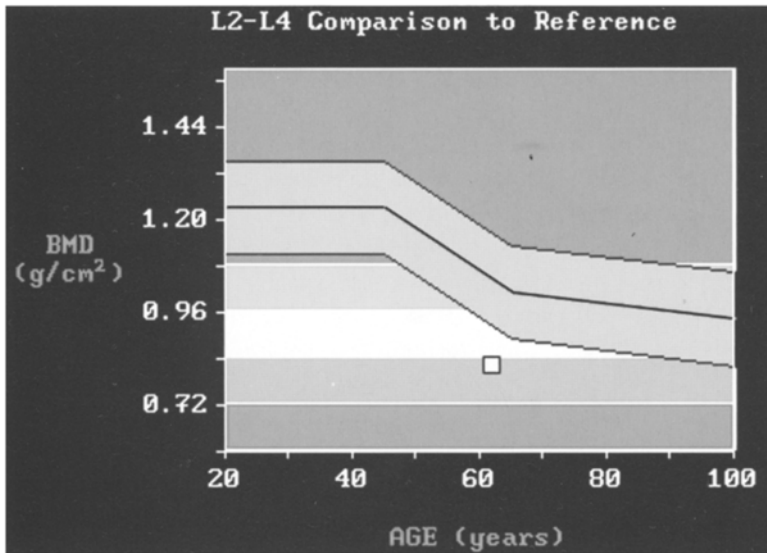


Fig. 10-4. Age-regression graph. The age-regression line is linear and flanked on either side by limits indicating change in bone density of ± 1 standard deviation from the age-matched predicted value. The patient's bone mineral density (BMD) is plotted above her age. From the graph, the patient appears to be approximately 62 years of age with a BMD slightly less than 0.84 g/cm^2 . The T-score is poorer than -3 while the z-score is approximately -2 .

bone density on age or the *age-regression*. The highest point on this line will represent the peak bone density of the young adult. On some graphs, two other lines will parallel the age-regression line on either side. These lines denote a change of either 1 or 2 SDs from the predicted value for any given age. The operator's manual must be consulted to determine whether a change of 1 or 2 SDs is being indicated. The patient's bone density can be visually compared to the peak bone density and the value that is predicted for their age. The actual bone density and the T- and z-scores could just as easily be read from printout however. Examples of age-regression graphs with linear or curvilinear age-regression lines are shown in Figs. 10-4 and 10-5.

On some of the newer versions of software the background of these graphs has been divided into areas that are colored red, yellow, and green, as shown in Figs. 10-6. The dividing line between green and yellow is at a T-score of -1 , and the dividing line between yellow and red is at a T-score of -2.5 . These T-score cut points are intended to represent the dividing lines between the WHO categories of normal, osteopenia, and

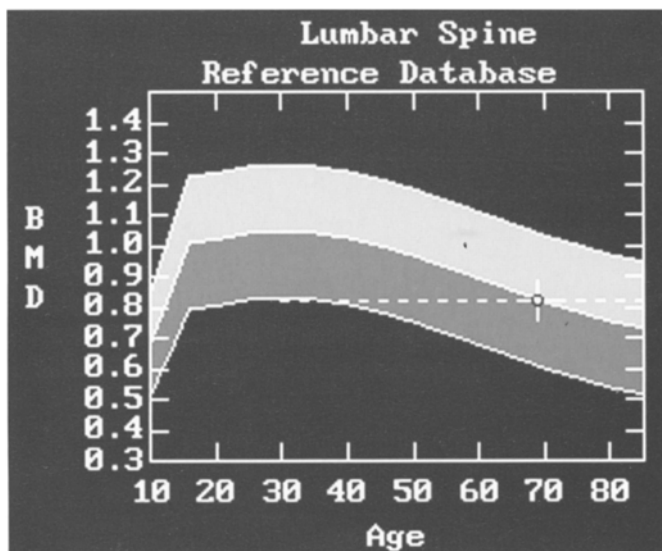


Fig. 10-5. Age-regression graph for a posteroanterior lumbar spine study. The age-regression line is curvilinear and flanked by limits indicating a change of ± 2 standard deviations from the age-matched predicted value. The highest point on the age-regression appears to occur at approximately age 30, suggesting that is the age of attainment of peak bone density at this site. The patient appears to be approximately 70 years of age with a bone mineral density of 0.8 g/cm^2 . The T-score is approximately -2 while the z-score is 0.

osteoporosis. This would allow the technologist and physician to immediately know which WHO diagnostic category applies based on the measured bone density. Although this can be helpful, it can also be inappropriate. Notice on the generic graph in Fig. 10-6 that the divisions denoting the various diagnostic categories extend across the entire age range of the graph even though the WHO criteria are not intended for premenopausal women. Such graphs may also be seen in conjunction with bone density studies on men for whom the WHO criteria were not originally intended. An inappropriate diagnosis assigned by the computer can cause undue mental distress if not recognized and explained by the technologist or physician. Fracture risk assessments, based on the WHO diagnostic categories, are also appearing on age-regression graphs. Instead of the diagnostic categories of normal, osteopenia, and osteoporosis, risk assessments of low, medium, and high appear in the green, yellow, and red areas that are again created by using the T-score cut points of -1 and -2.5 . Unfortunately, like the WHO diagnostic category assignments, these colored areas representing levels of fracture risk extend across the entire age

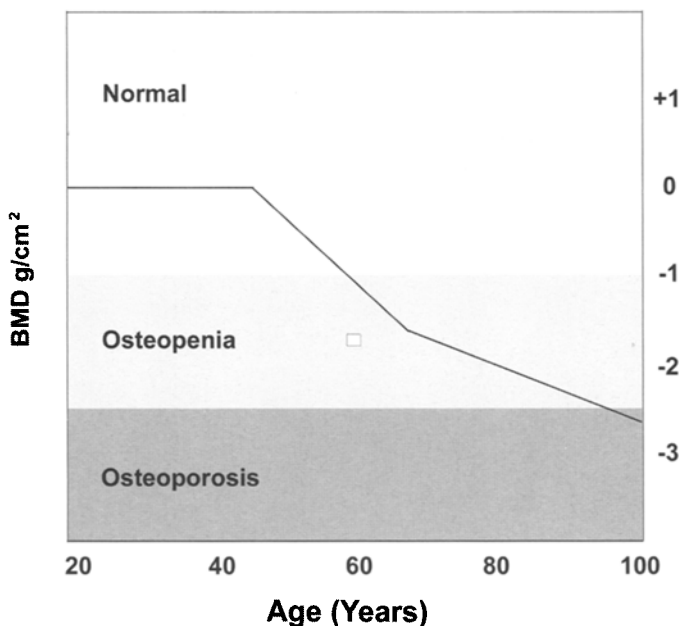


Fig. 10-6. Generic age-regression graph in which the background has been divided into three sections based on the T-score values of -1 and -2.5 . This makes possible the assignment of the patient's bone mineral density value to a World Health Organization diagnostic category depending on where the BMD is plotted on the graph. Although appropriate for postmenopausal Caucasian women, this may not be appropriate for others.

range represented on the graph. There is no data to support such an approach to the characterization of fracture risk in younger individuals. Consequently, this aspect of the age-regression graph must be interpreted with extreme caution.

Assignment of Diagnostic Category Based on WHO Criteria

As noted above, the assignment of diagnostic category has been incorporated into the age-regression graph on many bone densitometry devices. This can also be presented in a tabular form, as shown in Fig. 10-7. The diagnostic assignment on any computer printout should not automatically be accepted. It must be considered in light of the patient's age, sex, and race, the presence or absence of fractures, and the potential presence of confounding factors that might increase or decrease the measured bone mineral density. Considerations of age, sex, and race have been previously discussed. If it is known that a fracture exists and the bone density is 2.5 SDs or more below the average peak bone density, the patient's diagnostic

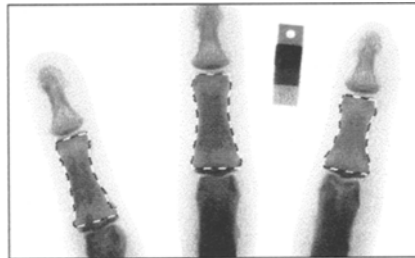
MetriScan Bone Mineral Density Report

Software Version 1.19

Exam Date	19/10/00 09:47 AM	Patient ID	01
Calibration Date	19/10/00 09:43 AM	Gender	Female
Instrument Serial #	100181	Age	50 years
Operator ID	1	Ethnic Group	Caucasian
Physician	_____	Patient Name	_____

Comments:

Image not for diagnosis



60.46 66.07 53.61
 BMD results for individual fingers

BMD Test Results

	Estimated Relative BMD ¹ (arbitrary units)	T-score (normative data)	Z-score (peer-matched data)
Result	60.04	0.75	0.84
Analysis	Normal ²	105%	107%

¹CV = +/-1.1%

²Based on WHO guidelines

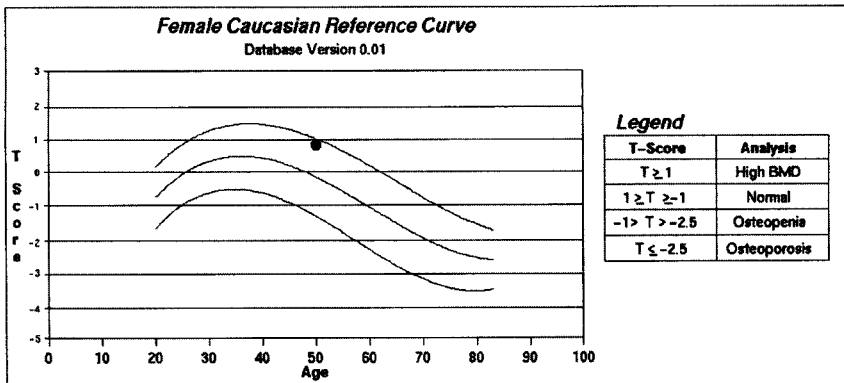


Fig. 10-7. Alara MetriScan™ bone density report of a radiographic absorptiometry study of the phalanges. The middle phalanges of the index, long, and ring fingers are analyzed. The aluminum wedge is seen between the index and long fingers. The bone mineral density (BMD) is reported in arbitrary RA units along with the percentage comparisons and standard scores. A diagnostic assignment is made based on the T-score using World Health Organization criteria. The curvilinear age-regression graph is seen, on which the patient's BMD is plotted above her age. Because the patient's z-score is given as 0.84, it is reasonable to assume that the limits surrounding the age-regression line represent a change in BMD of ±1 standard deviation.

category should change from osteoporosis to severe osteoporosis. On PA lumbar spine studies, suspected osteophytes, facet sclerosis, or other degenerative processes may increase the measured bone density resulting in the assignment of a better diagnostic category than is justified (9). There is no substitute for clinical judgment when it comes to conveying what these numbers really mean. This does not mean that the measured and calculated parameters from these devices are not accurate or precise—they are. The medical implications of these numbers, however, must always be placed in the context of the individual patient.

CONFLICTING DIAGNOSES FROM THE MEASUREMENT OF MULTIPLE SITES

If a patient undergoes bone density testing of multiple skeletal sites or even of the same site by different techniques, it is quite likely that the various T-scores from the different tests will result in different diagnoses when the WHO criteria are used. For example, a postmenopausal Caucasian woman may undergo a DXA study of the PA lumbar spine and the proximal femur. The T-score at the PA lumbar spine is -1.5 and at the femoral neck, -2.6 . Looking at each site individually and applying the WHO criteria, a diagnosis of osteopenia is appropriate at the spine, whereas a diagnosis of osteoporosis would be appropriate at the femoral neck. Another woman may have a DXA bone density measurement of her forearm and be found to have a T-score at the 33% combined forearm site of -0.9 . A day later she may have an ultrasound study of the calcaneus done at which time the T-score is found to be -2.0 . A DXA study of the proximal femur in this same woman is -2.8 . Depending on the site and technique, this woman could be classified as normal, osteopenic, or osteoporotic. The recognition of this dilemma is not new. The World Health Organization observed in 1994 that individuals would be classified differently depending on the site that was measured and the technique that was employed to make the measurement (10). This situation is created by three basic problems. First, the various skeletal sites need not do exactly the same thing at the same time. In fact, they may, be quite different from one another because of the differences in weight bearing or differences in the percentages of cortical and trabecular bone. Some disease processes may preferentially affect one type of bone over the other. Second, different techniques may actually measure biologically different quantities. For example, the three-dimensional measurement of the spine made with

quantitative computed tomography (QCT) can isolate trabecular from cortical bone. The two-dimensional spine measurement made with DXA cannot. The QCT measurement, then, is 100% trabecular bone, whereas the DXA measurement may contain only 66% trabecular bone. The measurement of speed of sound or BUA with ultrasound may be biologically quite different from the measurement of bone mass with DXA. Finally, there are differences in the reference databases that are the basis for the calculation of the percentage comparisons and the standard scores. Remember that the T-score reflects the number of SDs above or below the average peak bone density of the young adult that the patient's bone density lies. The T-score is therefore dependent on two quantities that are derived from the reference database: the value for the average peak bone density of the young adult and the value for the SD. The calculation of the SD itself is, in part, dependent on the number of individuals that were studied to create the reference database. In creating the reference databases for all of the various bone density devices, each manufacturer has, of necessity, used a different population of individuals for each skeletal site. The criteria for participation in the reference population could vary from manufacturer to manufacturer, as could the number of individuals that were included. And finally, once the studies were completed, different statistical methods may have been used to ultimately create the reference databases. When all three of these issues are considered, it is not surprising that different T-scores are encountered when measurements are made at multiple skeletal sites.

Differences in the percentage comparisons at the proximal femur between central devices were noted in the medical literature as early as 1992 (11,12). Concern was raised in 1996 about the differences in T-scores and diagnostic assignments based on those T-scores at the proximal femur when different devices were used (13). This led to the incorporation of the National Health and Nutrition Examination Survey III femur database by the manufacturers of central devices as discussed in Chapter 1. With this common database, and therefore the same peak BMD and SD on which to base the calculation of the T-score, the diagnostic discrepancies were minimized.

The diagnostic discrepancies between other sites when measured by the same type of device from different manufacturers or by different techniques still remain a clinical problem. In a study using one central DXA device and the manufacturer-supplied databases, the percentage of women diagnosed as osteoporotic varied from 19.3% to 75%, depending on which skeletal site was used to make the diagnosis (14). In another study in

Table 10-1
Equivalent T-Score at Peripheral Sites by Specific Devices for Osteoporosis
at the PA Lumbar Spine and/or Proximal Femur

<i>Device</i>	<i>Site/ROI</i>	<i>Osteoporosis</i>
pDEXA ^a	Distal	" -0.74
	Proximal	" -0.73
accuDEXA	Phalanges	" -1.0 ^b / " -1.65 ^c
UBIS ^d	Heel BUA	" -1.3
	Heel SOS	" -1.5
PIXI ^{e,f}	Heel	" -1.3
Apollo ^g	Heel	" 0

Adapted with permission from Bone Densitometry in Clinical Practice (2004), Humana Press, Totowa NJ.

which only one central device was used but a common database for all sites was created by the researchers, the percentages of women diagnosed as osteoporotic still varied widely from 11% to 45.7%, depending on which site was measured (15). In a similar study that included ultrasound measurements of the calcaneus as well as DXA measurements of other regions of the skeleton, significant differences in the percentages of women diagnosed as osteoporotic again resulted depending on the site and technique that were used (16).

One approach to reducing the potential for different diagnoses depending on the site and technique used has been the position taken by major organizations like the International Osteoporosis Foundation (17) and the International Society for Clinical Densitometry (18) that the WHO criteria for the diagnosis of osteoporosis should be used only with DXA measurements of the PA lumbar spine or proximal femur. Similarly, when measuring bone density at a peripheral site by any technique, the concept of what level of bone density is actually low must be adjusted upwards. Table 10-1 summarizes data from multiple studies in which the bone density was measured at a peripheral site and at a central site as well. The T-score cut point at the peripheral site that was necessary to identify the majority of patients with osteopenia or osteoporosis at the central site is noted in the table. It is clear from these types of studies that the WHO criteria for the diagnosis of osteoporosis should not be used with bone density measurements at peripheral sites. Measurements of bone density at peripheral sites are often appropriately performed to select individuals who should then be referred for a central measurement. Even in this situation, however, it must be recognized that a T-score found on a peripheral

measurement that would ordinarily be considered in the upper range of osteopenia may indicate osteoporosis centrally. Such an individual should undergo a central measurement. As a general rule, a T-score of -1.5 or poorer on a peripheral study warrants further evaluation.

REPORT REVIEW

A review of several different types of densitometry printouts will illustrate the similarities in the type of information provided on each report and also provide an opportunity to review some of the attributes of the various skeletal sites and techniques.

Figure 10-7 is a report from an Alara Metriscan™ study of the phalanges. This peripheral device employs radiographic absorptiometry (RA) and measures the middle phalanges of the index, long, and ring fingers. The radiation exposure to the patient is $<0.001 \mu\text{Sv}$, according to the manufacturer^{††}. The phalanges themselves can be characterized as being part of the appendicular, peripheral, non-weight bearing skeleton and predominantly cortical in composition. The skeletal image of the phalanges can be seen as well as the aluminum wedge that is used for comparison. The BMD in arbitrary RA units is reported as 60.04. Standard score and percentage comparisons are given as well as the WHO diagnostic classification that is based on the reported T-score. The WHO criteria are given in tabular form in the lower right-hand corner of the report. The age-regression graph is seen on which the patient's BMD is plotted above her age. The age-regression line has a curvilinear rather than linear shape. The highest point on the line appears to be around the age of 35, implying that peak BMD at this site is reached around age 35. The lines paralleling the center age-regression line appear to indicate a limit of ± 1 SD. Visually, then, it is clear that the patient's phalangeal BMD is both above the average peak BMD and above the value predicted for her age. The BMD is not more than 1 SD above the age-matched predicted value based on the graph. In fact, the T-score is 0.75 and the z-score is 0.84.

Figure 10-8 is a printout from a Norland Apollo™ study of the calcaneus. This is a peripheral DXA bone densitometer. According to the manufacturer, the radiation exposure to the patient during this study is <0.2 mrem. The calcaneus can be characterized as being an appendicular, peripheral, weight bearing and predominantly trabecular bone. The

^{††}See Chapter 4 for the manufacturer descriptions of the various technologies.

Clinical Research Center of North Texas

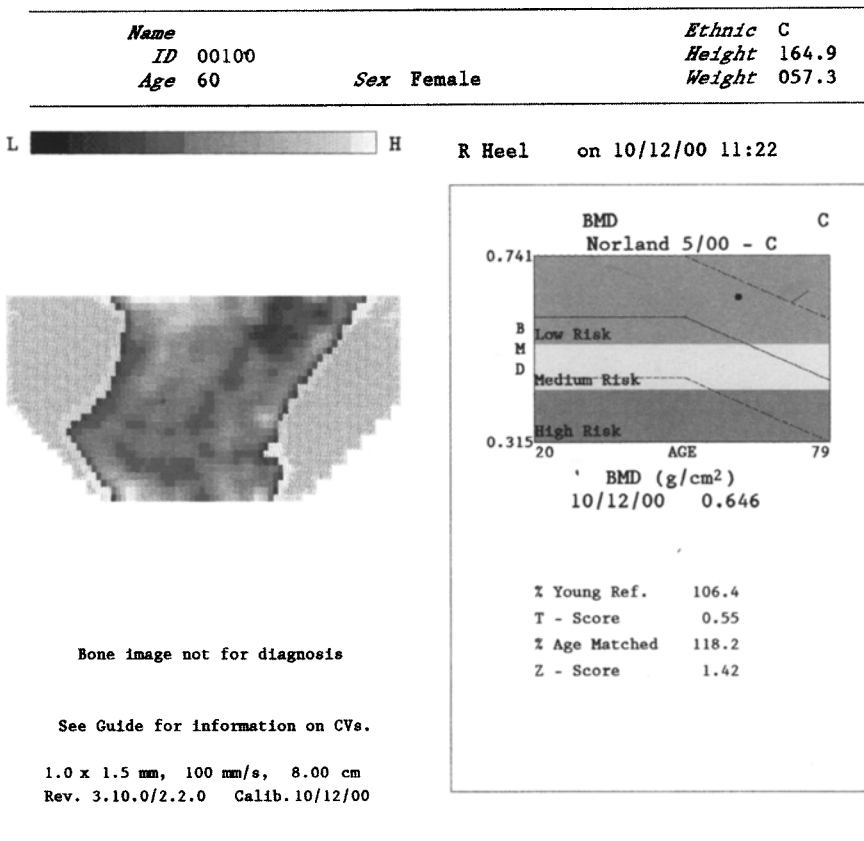


Fig. 10-8. Norland Apollo™ DXA study of the calcaneus. Although the appearance of this report is quite different from the report in Fig. 10-7, the information provided is basically the same. Fracture risk categories are seen on the age-regression graph that correspond to the World Health Organization categories of normal, osteopenia, and osteoporosis. The patient's z -score is given as 1.42. It is reasonable to assume that the limits surrounding the age-regression line indicate a change of ± 2 standard deviations.

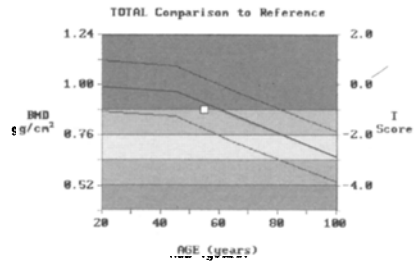
appearance of this printout is quite different from that seen in Fig. 10-7, but the basic information is the same. The skeletal image of the calcaneus is seen on the left as the printout is viewed. The age-regression graph is seen on the right. The age-regression line is linear in appearance. Peak BMD appears to have been reached by the youngest age represented on the age range given on the horizontal axis of the graph, age 20. This BMD is maintained until approximately age 50 when it begins to decline. The lines paralleling the age-regression line denote a change of ± 2 SDs from the age-predicted value. Once again, the patient's calcaneal BMD is

Clinical Research Center of North Texas
Denton, Texas

Right FEMUR BONE DENSITY

Facility: CRC
55 years
68 in 130 lbs White Female
Physician: Bonnick

Acquired: 10/09/1999 (4.6b)
Analyzed: 10/09/1999 (4.6b)



Region	BMD g/cm ²	Young-Adult %	T	Age-Matched %	Z
TOTAL	0.881	88	-1.0	97	-0.2

Image not for diagnosis
3.00ma:Hi-Res Fast DPX10 0.6x1.2mm 1.68mm
761097:437021 275.34:204.52:145.50
%fat = 14.6(1.363) Neck Angle = 53

- 1 - See appendix on precision and accuracy.
Statistically 68% of repeat scans will fall within 1 SD. (± 0.02 g/cm²)
- 2 - USA Femur Reference Population: Young Adult Ages 20-45. See Appendices.
- 3 - Matched for Age, Weight(25-100kg), Ethnic.
- 7 - Standardized BMD for TOTAL is 831 mg/cm². See J Bone Miner Res 1994; 9:1503-1514

Fig. 10-9. GE Lunar DPX IQ™ DXA study of the proximal femur. The technologist selected the total hip region of interest and this value is plotted on the age-regression graph. Note that the standardized bone mineral density (sBMD) for the total hip BMD of 0.881 g/cm² is 831 mg/cm².

plotted above her age on the graph. The actual BMD is given below the graph and is 0.646 g/cm². The percentage comparisons and standard scores for this BMD are listed below the graph. On this graph, the green, yellow, and red color scheme is used. The cut points that determine the color changes correspond to the WHO cut points of T-scores of -1 and -2.5. A fracture risk assessment of low risk, medium risk, or high risk is given for the green, yellow, and red areas, respectively. The patient's BMD clearly falls in the green, or low risk area. With a T-score of 0.55, the WHO diagnostic classification would be normal.

Figure 10-9 is a printout from a GE Lunar IQ™ DXA study of the proximal femur. This is a pencil-beam, DXA, central device. The

image of the proximal femur is seen on the left and the age-regression graph is seen on the right. The proximal femur itself is part of the appendicular skeleton as well as part of the central skeleton. It is clearly a weight bearing site. The radiation exposure to the patient for this study according to the manufacturer is <3 mrem. Although the technologist could have chosen any one of five different regions within the proximal femur to emphasize, the total hip was chosen. The total hip itself is considered to be predominantly cortical bone although the exact percentage of cortical bone is difficult to estimate. The choice of left hip versus right hip was arbitrary in this case. There was no reason to suspect a difference in bone densities between the two sides because leg dominance does not appear to affect BMD in the proximal femur as arm dominance does in the forearm.

The BMD for the total hip that was calculated from the measurement of BMC and area is given under the graph along with the percentage-comparisons and standard scores for the total hip region of interest. The total hip BMD is plotted above the patient's age on the age-regression graph. On this graph, the vertical axis on the left indicates the BMD in g/cm^2 . The vertical axis on the right indicates the T-score. The lines paralleling the age-regression line indicate a change of ± 1 SD from the age-predicted value. The total hip BMD is given as $0.881 \text{ g}/\text{cm}^2$. This value is 88% of the average peak bone density of a young adult and 97% of the value that was predicted for this 55-year-old Caucasian woman. The interpretation of these values would be that the BMD of $0.881 \text{ g}/\text{cm}^2$ is 12% below the average peak BMD of a young adult and 3% below the value that would otherwise be predicted for a 55-year-old Caucasian woman. It cannot be said that a 12% loss of BMD has occurred because it is not known what this patient's peak BMD as a younger woman was. Her BMD actually compares quite favorably to the BMD that is expected for a 55-year-old woman, although this only suggests that she does not have any secondary causes of bone loss present. The T-score of -1 indicates that the BMD of $0.881 \text{ g}/\text{cm}^2$ is 1 SD below the average peak bone density of the young adult. Applying the WHO criteria for diagnosis, this bone density is still normal. The z -score of -0.2 indicates that the BMD of $0.881 \text{ g}/\text{cm}^2$ is only 0.2 SDs below the value predicted for her age and sex. This is again a favorable comparison to her age-matched peers. If necessary, the BMD at the total hip of $0.881 \text{ g}/\text{cm}^2$ could be converted to the sBMD by using the equation found in Appendix VII. The sBMD is $831 \text{ mg}/\text{cm}^2$.

REFERENCES

1. Nevitt, M. C., Ross, P. D., Palermo, L., et al. (1999) Association of prevalent vertebral fractures, bone density and alendronate treatment with incident vertebral fractures: effect of number and spinal location of fractures. *Bone* **25**, 613–619.
2. Davis, J. W., Grove, J.S., Wasnich, R. D., Ross, P. D. (1999) Spatial relationships between prevalent and incident spine fractures. *Bone* **24**, 261–264.
3. Black, D. M., Arden, N. K., Palermo, L., et al. (1999) Prevalent vertebral deformities predict hip fractures and new vertebral deformities but not wrist fractures. *J. Bone Miner. Res.* **14**, 821–828.
4. Melton, L. J., Atkinson, E. J., Cooper, C., et al. (1999) Vertebral fractures predict subsequent fractures. *Osteoporos. Int.* **10**, 214–221.
5. Cummings, S. R., Black, D. M., Nevitt, M. C., et al. (1993) Bone density at various sites for prediction of hip fracture. *Lancet* **341**, 72–75.
6. Akesson, K., Gardsell, P., Sernbo, I., Johnell, O., Obrant, K. J. (1992) Earlier wrist fracture: a confounding factor in distal forearm bone screening. *Osteoporos. Int.* **2**, 201–204.
7. Marshall, D., Johnell, O., Wedel, H. (1996) Meta-analysis of how well measures of bone mineral density predict the occurrence of osteoporotic fractures. *BMJ* **312**, 1254–1259.
8. Melton, L. J., Atkinson, E. J., O'Fallon, W. M., Wahner, H. W., Riggs, B. L. (1993) Long-term fracture prediction by bone mineral assessed at different skeletal sites. *J. Bone Miner. Res.* **8**, 1227–1233.
9. Liu, G., Peacock, M., Eilam, O., Dorulla, G., Braunstein, E., Johnston, C. C. (1997) Effect of osteoarthritis in the lumbar spine and hip on bone mineral density and diagnosis of osteoporosis in elderly men and women. *Osteoporos. Int.* **7**, 564–569.
10. World Health Organization. (1994) Assessment of fracture risk and its application to screening for postmenopausal osteoporosis: report of a WHO study group. WHO Technical Report Series. WHO, Geneva.
11. Laskey, M. A., Crisp, A. J., Cole, T. J., Compston, J. E. (1992) Comparison of the effect of different reference data on Lunar DPX and Hologic QDR-1000 dual-energy X-ray absorptiometers. *Br. J. Radiol.* **65**, 1124–1129.
12. Pocock, N. A., Sambrook, P. N., Nguyen, T., Kelly, P., Freund, J., Eisman, J. A. (1992) Assessment of spinal and femoral bone density by dual X-ray absorptiometry: comparison of Lunar and Hologic instruments. *J. Bone Miner. Res.* **7**, 1081–1084.
13. Faulkner, K. G., Roberts, L. A., McClung, M. R. (1996) Discrepancies in normative data between Lunar and Hologic DXA systems. *Osteoporos. Int.* **6**, 432–436.
14. Greenspan, S. L., Maitland-Ramsey, L., Myers, E. (1996) Classification of osteoporosis in the elderly is dependent on site-specific analysis. *Calcif. Tissue Int.* **58**, 409–414.
15. Arlot, M. E., Sornay-Rendu, E., Garnero, P., Vey-Marty, B., Delmas, P. D. (1997) Apparent pre- and postmenopausal bone loss evaluated by DXA at different skeletal sites in women: the OFELY cohort. *J. Bone Miner. Res.* **12**, 683–690.
16. Varney, L. F., Parker, R. A., Vincelette, A., Greenspan, S. L. (1999) Classification of osteoporosis and osteopenia in postmenopausal women is dependent on site-specific analysis. *J. Clin. Densitom.* **2**, 275–283.
17. Kanis, J. A. and Gluer, C-C. (2000) An update on the diagnosis and assessment of osteoporosis with densitometry. Committee of Scientific Advisors, International Osteoporosis Foundation. *Osteoporos. Int.* **11**, 192–202.
18. Hamdy, R. C., Petak, S. M., Lenchik, L. (2002) Which central dual x-ray absorptiometry skeletal sites and regions of interest should be used to determine the diagnosis of osteoporosis? *J. Clin. Densitom.* **5**, S11–S17.

11 Considerations in Pediatric Densitometry

CONTENTS

SCAN ACQUISITION AND ANALYSIS CONSIDERATIONS
BONE AGE
SEXUAL MATURATION STAGE
CONSIDERATIONS OF BONE SIZE AND SHAPE
SKELETAL DEVELOPMENT AND THE USE OF STANDARD SCORES IN PEDIATRIC DENSITOMETRY
SKELETAL DEVELOPMENT
USE OF STANDARD SCORES IN PEDIATRIC DENSITOMETRY
PEDIATRIC REFERENCE DATABASES
INTERNATIONAL SOCIETY FOR CLINICAL DENSITOMETRY GUIDELINES FOR CHILDREN
THE SPECIALTY OF PEDIATRIC DENSITOMETRY
REFERENCES

Pediatric densitometry is a rapidly growing field. The rapidity of its growth, however, increases the likelihood of technical errors and misinterpretation of the results. One of the most important lessons to remember in pediatric densitometry is the admonition (1) from an expert in the field that “children are not simply small adults.”

There are many issues in pediatric densitometry that are not concerns in adult densitometry, or minimally, much less of a concern. The pediatric skeleton is constantly changing in terms of size and even shape. Ossification centers fuse in different bones at different ages. A child’s chronological age does not necessarily reflect his or her bone age. The onset of puberty, at whatever age it occurs in the child, has a pronounced effect on the development of the skeleton. The densitometry software in pediatric densitometry must be able to detect bone edges in the setting of

lower densities than often seen in adult densitometry. Reference databases for adults are not appropriate in pediatric densitometry. Similarly, the use of T-scores in pediatric densitometry is not appropriate. Finally, the diagnosis of any degree of low bone mass or density should not be made on the basis of the mass or density measurement alone.

SCAN ACQUISITION AND ANALYSIS CONSIDERATIONS

The technical aspects of the performance of pediatric densitometry are not entirely different from those aspects in adult densitometry. The greatest challenge in scan acquisition may indeed be keeping the child still during the scan. The shorter scan times needed by newer densitometers have helped to alleviate, but not completely eliminate, this problem. The manufacturer's directions for positioning and analysis should be followed for any given type of scan. It is preferable, however, that the acquisition software is specifically designed for a pediatric population.

Bone edge detection algorithms that are unique to each manufacturer's dual-energy X-ray absorptiometry (DXA) device enable the separation of bone from soft tissue. Edge detection algorithms designed with an adult population that has an expected range of bone densities in mind, may fail when used in a pediatric population with an anticipated lower body weight and lower bone mineral density (BMD). In essence, the machine may be unable to tell where the bone stops and starts. This will cause a failure in appropriate edge detection, which can be identified by the technologist. The bone edges or bone map should be verified by the technologist during the analysis and corrected, if necessary. In a review of 34 pediatric bone density studies in which a diagnosis of osteoporosis, osteopenia, or low bone density was made, Gafni and Baron (2) found errors in bone mapping in seven or 21%. After recognition of these errors, three of the seven bone densities were found to be normal and two of the seven could not be classified because of other errors.

Pediatric densitometry must be performed with these edge detection issues in mind. In 1993, Hologic, Inc. introduced a low density spine (LDS) software option to be used in children as well as adults with low bone density. This was an operator-selected analysis mode rather than a scan acquisition mode. The effects of low density edge detection became apparent when 100 bone density studies in children ages 2 to 18 years were analyzed using the LDS option as well as the standard analysis option (3). When the LDS option was used, the measured bone area and bone mineral content

(BMC) increased significantly. Because the bone area increased to a greater degree than the BMC, the BMD decreased an average of 8.7% with the LDS option. Norland systems such as the XR-46™ and Excell™ utilize a dynamic filtration system that automatically adjusts the photon flux to accommodate differences in body size during scan acquisition. Systems like the GE Lunar Prodigy™ automatically select the best scan mode based on the height and weight of the patient and also employ specialized analysis algorithms for low bone density in the pediatric spine.

BONE AGE

Bone age is not automatically the same as a child's chronological age. Bone age is a reflection of the developmental maturity of the skeleton. The presence of unfused and fused epiphyses is a reflection of developmental maturity. The epiphyses are secondary ossification centers at the ends of long bones. The epiphyses are responsible for longitudinal growth. The epiphyseal plate deposits cartilage, which is subsequently changed to bone. Ultimately, the epiphysis itself becomes engulfed in bone. Longitudinal growth stops and the epiphysis is said to be "fused" with the rest of the bone. After fusion, the only remnant of the ossification center is a line of demarcation called the epiphyseal line. The presence of unfused epiphyses will cause a DXA image that appears bizarre to the technologist accustomed to adult images such as the proximal femur image in Fig. 11-1. The greater trochanter is not completely formed or fused with the rest of the proximal femur. Ossification in the greater trochanter begins around the age of 3, but is not complete until around the age of 18 (4). Fusion of the femoral head and lesser trochanter to the proximal femur is also generally not complete until around the age of 18. The typical adult appearance of the vertebrae is not seen in young children. There are ring-like epiphyses on the upper and lower surfaces of the vertebral bodies that appear around the age of 16, which do not fuse with the rest of the vertebral body until around the age of 25. Other regions that are commonly studied with DXA in which unfused epiphyses may be seen are the heel and the forearm. The secondary ossification center in the posterior calcaneus appears around the age of 7 and fuses at puberty. At the distal radius and ulna, secondary ossification centers appear by ages 1 and 5, respectively, although neither fuses until around the age of 20.

The state of the secondary ossification centers in the hand is used to determine bone age. There are two techniques traditionally used to make

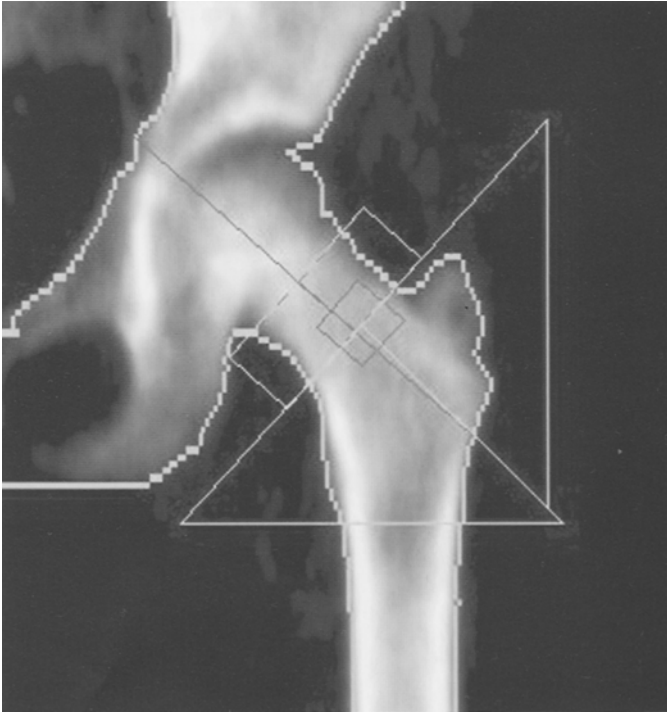


Fig. 11-1. Dual-energy X-ray absorptiometry image of a proximal femur in a child. The greater trochanter in particular appears unusual. The greater trochanter is not fully formed and will not completely fuse to the femoral neck and shaft until approximately 18 years of age. Case courtesy of GE Healthcare, Madison, WI.

this determination: the Greulich and Pyle method and the Tanner and Whitehouse method (5,6). The Greulich and Pyle method requires a comparison of all the bones in the hand and wrist against reference X-rays for a wide range of ages. The technique has been modified in many centers to a comparison of the overall appearance of the child's hand to a set of reference radiographs. The Tanner and Whitehouse method* requires a systematic assessment of the maturity of all the bones in the hand and wrist and employs a point scoring system to determine skeletal maturity. Although studies (7,8) have suggested that the two techniques give similar results, some authorities prefer the Tanner and Whitehouse method.

*The Tanner and Whitehouse method is often indicated by the abbreviation TW2 to indicate the method proposed in 1983 rather than an earlier method proposed in 1975.

Bone age is not determined from a DXA study. However, the interpretation of the bone density seen on a DXA study may well be affected by knowledge of the child's bone age. For example, if the child's bone age is less than their chronological age, their bone density would not be expected to be the same as their chronological peers.

SEXUAL MATURATION STAGE

Another important element in the interpretation of pediatric bone density measurements is knowledge of the level of sexual development of the child. This assessment is usually made by determining the Tanner[†] stage (9). Tanner assigned five stages to puberty for both boys and girls, with stage 1 indicating prepubertal development and stage 5 indicating mature sexual development. The five stages in girls are based on the development of the breasts and pubic hair. For boys, the stages are based on the development of the genitalia and pubic hair. Tanner stages are associated with different rates of linear growth (changes in height). In girls, the peak rate of linear growth is generally seen in Tanner stage 3 around the age of 11.5 years. In boys, the maximum rate of linear growth occurs in conjunction with Tanner stage 4 around the age of 13.5 years. In clinical practice, representative drawings are often used to allow the child to pick the body image that most closely matches their own. This is generally thought to be the least intrusive manner in which to make this determination. Parental permission is, of course, mandatory. Given that the Tanner stage represents pubertal development, it is not surprising that it is linked to skeletal maturity and rates of increases in height. This is relevant information, then, to the interpretation of a pediatric bone density study.

CONSIDERATIONS OF BONE SIZE AND SHAPE

The potential effect of changes in size on bone density is discussed in Chapter 1. Because the BMD obtained with DXA is a two-dimensional areal measurement, a larger bone may have a greater BMD than a smaller bone in spite of both having identical volumetric BMDs (10,11). This concept is illustrated in Fig. 1-4. The maturation of the skeleton and

[†]This is the same James Mourilyan Tanner, as in the Tanner and Whitehouse bone age method.

increases in height will cause changes in the shape and size of the bones, making this issue particularly relevant to pediatric densitometry. In addition, children with chronic diseases are often smaller than healthy children of the same age. The interpretation of areal density in such children must be made cautiously to avoid incorrectly diagnosing a child who simply has small bones from any cause as having an abnormally low bone mass for their age. Mølgaard et al. (12) proposed a three-step method to address the potential for misdiagnosis in a pediatric population because of changes in the size or shape of the bones. The authors noted that BMD was the ratio of the BMC divided by the bone area and that if the bone area was small, the BMC would potentially be reduced. They pointed out that it was important to know whether the low BMC was the result of a small bone area. Mølgaard et al. (12) proposed the concept of BMC adjusted for bone area which is also called *BMC for bone area*. They also proposed an assessment of bone area adjusted for height or *bone area for height* and an assessment of height adjusted for age, also called *height for age*. They suggested that this would address three potential causes of an apparent low BMD in a child: "light bones," "narrow bones," and "short bones." In essence, these three parameters address the following questions: Is the height appropriate for the age or does the child have short bones? Is the bone size or area appropriate for the child's height or does the child have narrow bones? Is the BMC appropriate for the bone area or does the child have light bones? The relevance of each of these findings to the health of the child may be quite different to the pediatrician. Fig. 11-2 shows the plot of these three parameters on centile scales[§] for the child whose total body bone density study is shown in Fig. 11-3. Data for the comparison of height for age comes from the U.S. Centers for Disease Control (13) growth statistics. BMC for bone area and bone area for height data are derived from the manufacturer's pediatric

[§]A centile scale reflects values from 0 to 100. The terms *centiles* and *percentiles* are often used interchangeably. The location of the value plotted on the scale indicates the percentage of individuals in the population in question who have a similar or poorer value. For example, if the centile scale reflects a value of 40, 40% of individuals in that population have the same or poorer value for the quantity in question. Conversely, 60% will have a higher value. If the value on the centile scale is 50, an appropriate interpretation is that 50% of the population will have a better value and 50% will have a poorer value. A centile value of 5 or less is generally cause for concern although some circumstances may dictate concern at higher centile values.

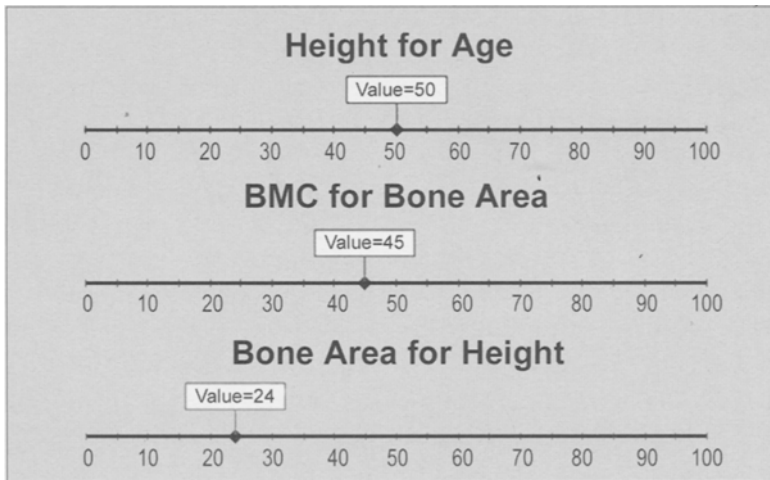


Fig. 11-2. Ancillary data provided as part of the pediatric total body study seen in Fig. 11-3. These centile line graphs provide necessary comparisons of the child's height for his or her age, bone area for his or her height, and bone mineral content (BMC) for his or her bone area. This is useful in determining whether a low bone mineral density in a child is the result of a truly decreased BMC or simply the result of bones that are smaller in size than an average child of the same age, sex, and ethnicity. Case courtesy of GE Healthcare, Madison, WI.

reference database. In this particular example, the total body bone density z -score shown in Fig.11-3 is -2.2 . Why might this be? The centile scales shown in Fig. 11-2 suggest that the bone area for height is only in the 24th percentile, whereas the height for age and BMC for bone area centiles are better. This suggests that the low BMD z -score may be in part determined by what Mølgaard et al. (12) called “narrow bones” and not solely a result of a truly low BMC.

SKELETAL DEVELOPMENT AND THE USE OF STANDARD SCORES IN PEDIATRIC DENSITOMETRY

As noted in Chapter 1, the standard score called the T-score in densitometry indicates the number of standard deviations above or below the average peak bone density that the patient's bone density lies. The z -score, on the other hand, is the standard score comparison to the bone density that is predicted for the patient's age. Both are used in adult densitometry, although the T-score commands greater attention for its role in the diagnosis of osteoporosis based on the World Health Organization

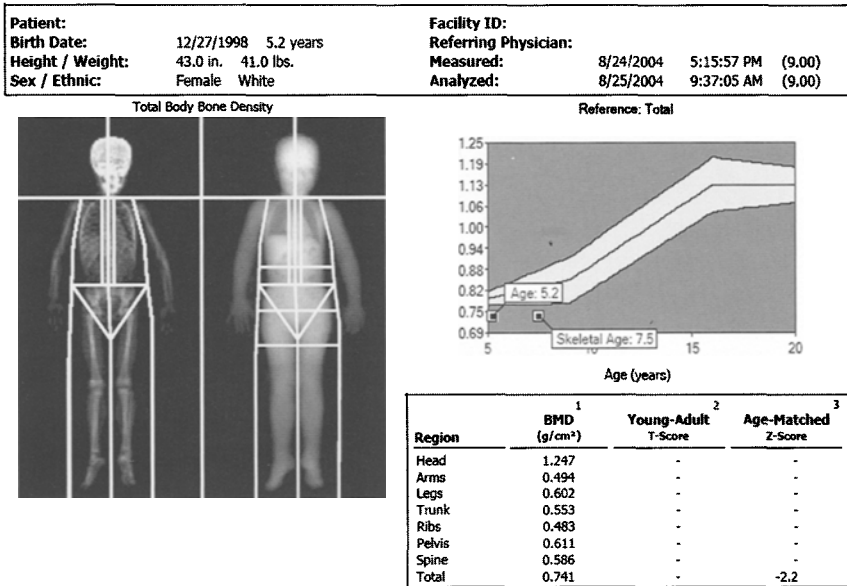


Fig. 11-3. Pediatric DXA total body study performed on the GE Lunar Prodigy™ for a 5-year-old girl. The total body bone image is on the left and the body composition image is on the right. Note that only the z-score is shown for the total body bone density. The bone age is also plotted on the age-regression graph and is shown as 7.5 years. This age was determined using the Tanner-Whitehouse method and inputted by the technologist prior to data acquisition. Case courtesy of GE Healthcare, Madison, WI.

criteria[¶] as well as for fracture risk prediction. Authorities in pediatric densitometry agree, however, that the use of T-scores in children for any purpose is not appropriate. To find that a child has a bone density that is less than the average peak bone density is expected because the child may not have reached the age by which peak bone density is achieved. Such a finding, then, carries no particular significance.

Skeletal Development

The exact age at which peak bone density is reached at any given skeletal site remains somewhat controversial. It is clear, however, that the age of peak bone density may be different between boys and girls and that the age of peak bone density may vary by skeletal site (14,15). The age at

[¶]See Chapter 9 for a discussion of the World Health Organization criteria for the diagnosis of osteoporosis based on the measurement of bone density.

which peak bone density is achieved at any site may also be determined not only by the patient's chronological age, but also by their bone age and pubertal status as well.

Changes in bone density in 778 Caucasian boys and girls ages 2 to 20 years were determined in a cross-sectional** study by Zanchetta et al. (16) using DXA of the posteroanterior (PA) lumbar spine, proximal femur, and total body. In this study, BMD at the PA lumbar spine and proximal femur did not increase significantly after the age of 14 in girls. In boys, however, BMD at the spine increased throughout the age range of the study, but significant increases in proximal femur BMD were not seen in boys after the age of 16. Total body BMD in girls did not increase after the age of 16 but increased throughout the age range in boys. Nguyen et al. (14) also reported that total body peak BMD was reached earlier in girls than in boys, although at a later age than reported by Zanchetta et al. In a longitudinal study of 94 males and 92 females ages 6–36 years with an average follow-up of 4.29 years, peak total body bone density was reached by the age of 20.8 years in females and 25.2 years in males.

Teegarden et al. (17) looked specifically at total body BMC and BMD with DXA in 247 girls and young women aged 11 to 32. They concluded that 99% of peak total body BMD and total body BMC is achieved by 22.1 years and 26.2 years of age, respectively. Based on a study (15) of 300 girls and women aged 6 to 32, these same authors concluded that peak BMD was achieved at the PA lumbar spine by age 23 although BMC and bone area continued to increase at the spine across the age range of this study. Peak BMD at the femoral neck was reached by the age of 18.5 years.

In another very large cross-sectional study by Sabatier et al. (18) changes in BMD, BMC, and bone area were determined in 574 girls, aged 10 to 24 years. In this study, bone density measurements were made at the lumbar spine with DXA. Bone age was determined for girls less than age 20 using plain radiographs of the left hand and wrist and the Greulich and Pyle (5) method. Pubertal status was assessed using Tanner stages (6). Sabatier et al. found that the BMD and BMC in the lumbar spine increased dramatically between the bone ages of 10 and 14 or until the first year after menarche.†† Between the bone ages of 14 and 17, the PA lumbar spine

**A cross-sectional study is a study in which subjects are assessed at a single point in time. This is in contrast to a longitudinal study in which subjects are followed over a period of time.

††Menarche is defined as the age at which the first menstrual period occurs.

BMD and BMC continued to increase, but at a slower rate. After the bone age of 17, or the 4th year after menarche, no additional significant increases in PA lumbar spine BMD or BMC were seen. The authors noted that bone age and pubertal status appeared to be more useful than chronological age in assessing skeletal status. They noted that lumbar spine BMC roughly doubled between the bone ages of 10 and 17 and that the period between the bone ages of 10 and 14 was particularly critical in the development of BMC.

The effect of pubertal state on the accumulation of bone mass had previously been observed by Theintz et al. (19) In a study of 98 girls and 100 boys ages 9–19 years, Theintz et al. found that BMC and BMD increased rapidly between the ages of 11 and 14. The rate of increase dropped dramatically, however, after the age of 16, or 2 years after menarche. In this study, 16 appeared to be the age of peak bone mass at the lumbar spine and femoral neck in girls. These findings are very similar to those from Sabatier (18). In boys, the increase in both BMC and BMD at the lumbar spine and proximal femur was greatest between the ages of 13 and 17. The rate of increase declined markedly after the age of 17 at both sites. No additional significant increases were seen at the femoral neck after the age of 17 in boys, although significant increases in spine BMD were still seen.

Although there are slight differences among the various studies that have attempted to determine the age of peak bone mass and density at various skeletal sites, the majority of these studies have concluded that peak bone mass is achieved at most sites by the age of 20. There is little disagreement that the overwhelming majority of peak bone density is attained by the age of 20. Increases in BMC and bone area may indeed continue, particularly at the spine, after the age of 20 (15). This would not necessarily be reflected as an increase in BMD because BMD is the ratio of BMC to area, as noted in Chapter 1.

Use of Standard Scores in Pediatric Densitometry

An appreciation of the timing of peak bone density is critical to understanding why T-scores must not be used in the interpretation of bone density in children. This would be analogous to comparing the height of a 7-year-old to the height of a 35-year-old and concluding that the 7-year-old was abnormally short. Unfortunately, this misuse of the T-score is not widely appreciated. In the study cited earlier from Gafni and Baron (2) in 2002, the results of a review of 34 DXA bone density studies and the accompanying interpretations in children aged 4 to 17

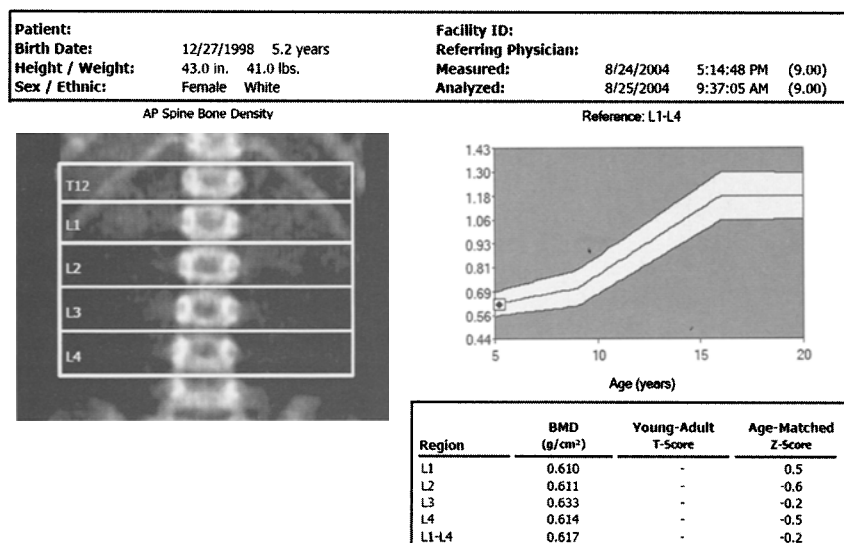


Fig. 11-4. Pediatric dual-energy X-ray absorptiometry posteroanterior lumbar spine study performed on the GE Lunar Prodigy™ for a 5-year-old girl. The L1–L4 bone mineral density is 0.617 g/cm². The z-score is –0.2. No T-score is provided. The use of the T-score in pediatric densitometry is not appropriate. The ancillary data for this study is seen in Fig. 11-5. Case courtesy of GE Healthcare, Madison, WI.

years were reported. These children had been referred to the National Institutes of Health as possible participants in an osteoporosis treatment trial. All 34 children had a diagnosis of osteoporosis, osteopenia, or low bone mass based on the original bone density study interpretation. Gafni and Baron found that 88%, or 30 of the 34 studies, had at least one error in interpretation. In 21 of the 30 studies, the T-score had been used for diagnosis even though the z-score was also present on the printout. When the appropriate interpretation was made based on the z-score, 12 of these 21 children actually had a normal bone density. In 5 of the 21, an accurate diagnosis could not be made because of a lack of necessary information.

Printouts of DXA studies from major DXA manufacturers in which pediatric software is used do not display a T-score. This is seen in the printout from the total body study in Fig. 11-3 and the PA lumbar spine bone density study in Fig. 11-4. Note that only z-scores appear on the report. In the ancillary data for this study shown in Fig. 11-5, both the T-score and the % Young Adult comparisons are appropriately absent. This should prove extremely helpful in preventing this type error in interpretation.

Patient:			Facility ID:		
Birth Date:	12/27/1998	5.2 years	Referring Physician:		
Height / Weight:	43.0 in.	41.0 lbs.	Measured:	8/24/2004	5:14:48 PM (9.00)
Sex / Ethnic:	Female	White	Analyzed:	8/25/2004	9:37:05 AM (9.00)

ANCILLARY RESULTS [AP Spine]

Region	BMD (g/cm ²)	Young-Adult (%)	T-Score	Age-Matched (%)	Z-Score	BMC (g)	Area (cm ²)	Width (cm)	Height (cm)
T12	0.589	-	-	-	-	2.6	4.4	2.4	1.82
L1	0.610	-	-	106	0.5	3.0	4.8	2.4	1.99
L2	0.611	-	-	94	-0.6	3.3	5.3	2.5	2.10
L3	0.633	-	-	98	-0.2	3.7	5.8	2.7	2.14
L4	0.614	-	-	95	-0.5	4.0	6.5	3.0	2.14
L1-L2	0.611	-	-	102	0.2	6.2	10.2	2.5	4.09
L1-L3	0.619	-	-	100	0.0	9.9	16.0	2.6	6.23
L1-L4	0.617	-	-	98	-0.2	13.8	22.4	2.7	8.37
L2-L3	0.622	-	-	96	-0.4	6.9	11.1	2.6	4.24
L2-L4	0.619	-	-	95	-0.4	10.9	17.6	2.8	6.38
L3-L4	0.623	-	-	96	-0.4	7.6	12.3	2.9	4.28

Fig. 11-5. Ancillary dual-energy X-ray absorptiometry posteroanterior lumbar spine data for the study shown in Fig. 11-4. Note that no T-score or % Young Adult comparison is provided. Case courtesy of GE Healthcare, Madison, WI.

PEDIATRIC REFERENCE DATABASES

Even with the removal of the T-score from consideration, the validity of the z-score comparison is dependent on the validity of the reference database. In the study from Gafni and Baron (2), the second most common error in interpretation of pediatric densitometry results was the use of a reference database that did not correctly reflect the patient's sex or ethnicity. As noted earlier, the BMD is expected to differ between boys and girls, particularly in adolescence. Use of a pediatric database that combines both genders as though there were no expected differences in BMD will lead to erroneous interpretations (2,20). In particular, boys may be misclassified as having low bone mass. It is also clear from studies from Bachrach et al. (21) that the expected BMD differs among pediatric ethnic groups as well as between boys and girls. In general, she found that Blacks had a greater areal bone density than non-Blacks at the PA lumbar spine, proximal femur, and total body. For any age, the average BMD at the spine was 10% greater in Black females and 3% greater in Black males than in non-Blacks. There were also differences among Asian, Hispanic, and Caucasian males and females, although the differences were not as great as those seen between Blacks and non-Blacks. Among the males, spine BMD was lower in Hispanics than in Asians or Caucasians. Total hip BMD and total body BMD was greater in Caucasian males than in Hispanic or Asian males. Among the females, Asians had a lower average femoral neck and total body BMD than Hispanics and Caucasians.

Bachrach and colleagues also found that gender rather than ethnicity played a significant role in the timing of increases in BMD.

In the report from Gafni and Baron (2) noted earlier, there were seven instances in which an incorrect database had been used to interpret the pediatric bone density findings. When Gafni and Baron applied the correct database to determine the z -score, five of the seven children were no longer considered osteopenic or osteoporotic. They were, in fact, considered normal. In the other two cases, a determination could still not be made because of missing information. Gafni and Baron recommended that any reference database used to interpret pediatric bone density studies be specific for age, sex, and ethnicity. They also noted that an ideal database would consider body size and pubertal status as well.

INTERNATIONAL SOCIETY FOR CLINICAL DENSITOMETRY GUIDELINES FOR CHILDREN

In 2004, the International Society for Clinical Densitometry (ISCD) (22) published guidelines for the diagnosis of osteoporosis in individuals less than 20 years of age. The ISCD emphasized that T-scores should not be used and that the diagnosis of osteoporosis should not be based on the bone density measurement alone. They also noted that the degree to which BMD in children was predictive of fracture was not proven. ISCD recommended the use of the spine and total body as the preferred sites for the measurement of bone density. They also emphasized that z -score comparisons should only be made using the best available pediatric reference database. Finally, ISCD pointed out that there is no consensus yet as to the best method of interpreting or adjusting the measured BMD based on bone size, pubertal state, bone age, or body composition in children, although the need to do so is clear.

THE SPECIALTY OF PEDIATRIC DENSITOMETRY

In addition to studies of the development of peak bone density in children and its relationship to osteoporosis in later life, there is an ever growing number of diseases in childhood in which the bone density may be adversely affected. One primary cause of osteoporosis in children is juvenile idiopathic osteoporosis (23). This disease is considered relatively rare. It usually occurs before puberty and is manifested by back pain, long bone fractures, and loss of height. There is often spontaneous resolution after 2 to 4 years but some individuals may develop permanent disabilities. Osteogenesis imperfecta

(OI) is another cause of primary osteoporosis in children. OI is also often called *brittle bone disease*, as is adult osteoporosis. OI is the result of a genetic defect in collagen synthesis that results in skeletal fragility. Signs and symptoms of OI include a bluish discoloration of the sclerae, hearing loss, short stature, and fractures. There are 6 or more variants of OI (24). Type I is considered mild, Type II is fatal, and Type III is the most severe, nonfatal form of OI. Bisphosphonates are being evaluated as potential therapies in both juvenile idiopathic osteoporosis and OI (25,26). Other genetic defects that are associated with low bone density in childhood include Turner's syndrome, Down's syndrome, and Klinefelter's syndrome (24).

Secondary causes of osteoporosis or low bone mass in childhood are numerous, just as they are in adults (27). The list includes Cushing's syndrome, hyperthyroidism, hypopituitarism and hypogonadism, as well as various nutritional deficiencies. Rheumatoid arthritis and inflammatory bowel disease in children are also associated with low bone density. Other diseases include sickle cell anemia, hemophilia, and cystic fibrosis. As in adults, certain drugs, such as corticosteroids and anticonvulsants, may cause bone loss. As the number of childhood cancer survivors increases, the effects of antineoplastic agents on bone mass has also become a concern. As in adult densitometry, the increasing application of densitometry in the pediatric population has resulted in an increasing number of diseases now known to have an adverse effect on the skeleton of a child. This, in turn, will further increase the number of pediatric densitometry studies that are performed.

Perhaps the greatest problem faced in pediatric densitometry today is not its underutilization but rather, its misinterpretation when it is performed. It must always be remembered that "children are not simply small adults" (1). There is much more to consider in the interpretation of pediatric bone density results than the BMD itself, or even the z-score. Excellence in adult densitometry does not automatically confer excellence in pediatric densitometry. A technologist who is cognizant of the nuances necessary for the proper performance and interpretation of pediatric densitometry can provide invaluable assistance to the interpreting physician.

REFERENCES

1. Bachrach, L. K. Bare-bones fact—children are not small adults. (2004) *N. Engl. J. Med.* **351**, 924–926.
2. Gafni, R. I. and Baron, J. (2004) Overdiagnosis of osteoporosis in children due to misinterpretation of dual-energy X-ray absorptiometry (DEXA). *J. Pediatr.* **144**, 253–257.

3. Leonard, M. B., Feldman, H. I., Zemel, B. S., et al. (1998) Evaluation of low density spine software for the assessment of bone mineral density in children. *J. Bone Miner. Res.* **13**, 1687–1690.
4. Abrahams, P. H., Marks, S. C., Hutchings, R. T. (2003) *McMinn's Color Atlas of Human Anatomy*. 5th ed. Elsevier Science Limited, Edinburgh.
5. Greulich, W. W., Pyle, S. I., Waterhouse, A. M. (1971) A radiographic standard of reference for the growing hand and wrist. Case Western Reserve University, Chicago.
6. Tanner, J. M., Whitehouse, R. H., Cameron, N., et al. (1983) *Assessment of skeletal maturity and prediction of adult height*, 2nd ed. Academic Press, London.
7. Milner, G. R., Levick, R. K., Kay, R. (1986) Assessment of bone age: a comparison of the Greulich and Pyle and the Tanner and Whitehouse methods. *Clin. Radiol.* **37**, 119–121.
8. King, D. G., Steventon, D. M., O'Sullivan, M. P., et al. (1994) Reproducibility of bone ages when performed by radiology registrars: an audit of Tanner and Whitehouse II versus Greulich and Pyle methods. *Br. J. Radiol.* **67**, 848–851.
9. Tanner, J. M. (1967) *Growth of adolescents*. Blackwell Scientific Publishing, Oxford.
10. Carter, D. R., Bouxsein, M. L., Marcus, R. (1997) New approaches for interpreting projected bone densitometry data. *J. Bone Miner. Res.* **7**, 137–145.
11. Jergas, M., Breitenseher, M., Gluer, C. C., Yu, W., Genant H. K., (1995) Estimates of volumetric bone density from projectional measurements improve the discriminatory capability of dual X-ray absorptiometry. *J. Bone Miner. Res.* **10**, 1101–1110.
12. Mølgaard, C., Thomsen, B. L., Prentice, A., Cole, T. J., Michaelsen, K. F. (1997) Whole body bone mineral content in healthy children and adolescents. *Arch. Dis. Child* **76**, 9–15.
13. CDC, National Center for Health Statistics. Clinical growth charts. Accessed January 5, 2005, at http://www.cdc.gov/nchs/about/major/nhanes/growthcharts/cliical_charts.htm.
14. Nguyen, T. V., Maynard, L. M., Towne, B., et al. (2001) Sex differences in bone mass acquisition during growth: the Fels Longitudinal Study. *J. Clin. Densitom.* **4**, 147–157.
15. Lin, Y. C., Lyle, R. M., Weaver, C. M., et al. (2003) Peak spine and femoral neck bone mass in young women. *Bone* **32**, 546–553.
16. Zanchetta, J. R., Plotkin, H., Alvarez Filgueira, M. L. (1995) Bone mass in children: normative values for the 2-20-year old population. *Bone* **16**, 393S–399S.
17. Teegarden, D., Proulx, W. R., Martin, B. R., et al. (1995) Peak bone mass in young women. *J. Bone Miner. Res.* **10**, 711–715.
18. Sabatier, J. P., Guaydier-Souquières, G., Laroche, A., et al. (1996) Bone mineral acquisition during adolescence and early adulthood: a study in 574 healthy females 10–24 years of age. *Osteoporos. Int.* **6**, 141–148.
19. Theintz, G., Buchs, B., Rizzoli, R., et al. (1997) Longitudinal monitoring of bone mass accumulation in healthy adolescents: evidence for a marked reduction after 16 years of age at the levels of lumbar spine and femoral neck in female subjects. *J. Clin. Endocrinol. Metab.* **75**, 1060–1065.
20. Leonard, M. B., Propert, K. J., Zemel, B. S., Stallings, V. A., Feldman, H. I. (1999) Discrepancies in pediatric bone mineral density reference data: potential for misdiagnosis of osteopenia. *J. Pediatr.* **135**, 182–188.
21. Bachrach, L. K., Hastie, T., Wang, M. C., Narasimhan, B., Marcus, R. (1999) Bone mineral acquisition in healthy Asian, Hispanic, Black, and Caucasian youth: a longitudinal study. *J. Clin. Endocrinol. Metab.* **84**, 4702–4712.

22. Khan, A. A., Bachrach, L., Brown, J. P., et al. (2004) Standards and guidelines for performing central dual-energy X-ray absorptiometry in premenopausal women, men, and children: a report from the Canadian Panel of the International Society for Clinical Densitometry. *J. Clin. Densitom.* **7**, 51–63.
23. Krassas, G. E., Idiopathic juvenile osteoporosis. (2000) *Ann. N.Y. Acad. Sci.* **900**, 409–412.
24. Saggese, G., Baroncelli, G. I., Bertelloni, S. (2001) Osteoporosis in children and adolescents: diagnosis, risk factors, and prevention. *J. Pediatr. Endocrinol. Metab.* **14**, 833–859.
25. Shaw, N. J., Boivin, C. M., Crabtree, N. J. (2000) Intravenous pamidronate in juvenile osteoporosis. *Arch. Dis. Child* **83**, 143–145.
26. Glorieux, F. H. (2000) Bisphosphonate therapy for severe osteogenesis imperfecta. *J. Pediatr. Endocrinol. Metab.* **13**, 989–992.
27. van der Sluis, I. M., de Muinck Keizer-Schrama, S. M. P. F. (2001) Osteoporosis in childhood: bone density of children in health and disease. *J. Pediatr. Endocrinol. Metab.* **14**, 817–832.

12 Moving Beyond Bone Density With Bone Densitometers

Skeletal Morphometry and Body Composition Assessments

CONTENTS

SKELETAL MORPHOMETRY FOR STRUCTURAL DIAGNOSES AND PREDICTION OF FRACTURE RISK
VERTEBRAL MORPHOMETRY AND FRACTURES
PROXIMAL FEMUR MORPHOMETRY
BODY COMPOSITION ANALYSIS
THE BODY MASS INDEX
BODY COMPOSITION METHODS
REFERENCES

SKELETAL MORPHOMETRY FOR STRUCTURAL DIAGNOSES AND PREDICTION OF FRACTURE RISK

Densitometry has primarily been a quantitative measurement technique. The first skeletal images from a densitometer, such as that seen in Fig. 2-7, were only vaguely reminiscent of the actual bone. The poor image quality had little effect on the ability to quantify the bone density, which was the primary purpose of the various techniques. With the advent of dual-energy X-ray absorptiometry (DXA) and quantitative computed tomography (QCT), skeletal imaging as a potential application of densitometry has been anticipated for over 10 years. Continued improvements in the technology combined with modern computer capabilities have resulted in spine images with more than sufficient clarity to diagnose fractures. Truly remarkable images of the spine such as the RVA™ image

from a Hologic Discovery* seen in Fig. 12-1 are possible today. The physical dimensions of the vertebrae and proximal femur can be measured from densitometry images using morphometric software applications. These imaging applications have potential effects on both diagnosis and fracture risk assessment. Recognition of a vertebral fracture may result in a different diagnosis than would otherwise result based on the bone density alone. In addition, the presence of vertebral fracture and proximal femur geometry have been recognized as independent predictors of fracture risk.

Vertebral Morphometry and Fractures

RELATIONSHIP BETWEEN PREVALENT SPINE FRACTURES AND FUTURE FRACTURE RISK

A number of individual studies have demonstrated that the presence of a spine fracture is predictive of future fractures, independent of bone density (1-6). In 2000, Klotzbuecher et al. (7) reviewed the available literature to summarize the known associations between prevalent fracture and future fracture risk of all types. They performed a literature search that spanned 1966-1999, identifying 15 publications that reported associations between prevalent spine fractures and subsequent fractures. Based on this review, Klotzbuecher et al. concluded that prevalent spine fracture increases the risk for future spine fracture 4.4-fold. The risk of subsequent hip fracture increases 2.3-fold and the risk of subsequent wrist fracture increases 1.4-fold. The authors noted that in 5 of the 15 studies reviewed, the associations between prevalent spine fracture and subsequent fracture were reduced by only 20% or less when adjustments were made for the level of bone mineral density (BMD). Nevertheless, BMD is also a strong predictor of future fractures, independent of prior fractures. The strongest association is between existing spine fractures and future spine fractures, with estimates of the increase in risk from only one prevalent spine fracture of 3- to 11.1-fold. Klotzbuecher et al. concluded that BMD and prevalent fractures were complementary in the prediction of future fracture risk.

DIAGNOSING VERTEBRAL FRACTURES

Authorities today believe that the assessment of fracture risk is clearly incomplete without an assessment of the presence of vertebral fracture.

*RVA™ is a trademarked reference for Radiographic Vertebral Assessment from Hologic. Specifications for the Hologic Discovery can be found in Chapter 4.



Fig. 12-1. RVA image from the Hologic Discovery. The vertebrae are seen with remarkable clarity enabling structural diagnoses to be made at a fraction of the radiation exposure of plain spine films. Vertebral fracture assessment with DXA is now reimbursable under Medicare under CPT code 76077. Case provided courtesy of Hologic, Inc., Bedford, MA.

Only 33% of vertebral fractures are symptomatic (8). Of those fractures that are not clinically symptomatic, 78% remain unrecognized (9). A more aggressive effort to evaluate patients for vertebral fracture is clearly indicated.

A change in the size or shape of a vertebral body is characterized generically as a deformity. The lack of a clear “gold standard” for defining the

types of vertebral deformities that are the result of bone fragility and thus fractures, remains controversial. Semiquantitative and quantitative approaches for defining vertebral fractures are used clinically. Either can be applied to plain radiographs or densitometric spine images.

VERTEBRAL FRACTURE ASSESSMENT WITH GENANT'S SEMIQUANTITATIVE TECHNIQUE

The semiquantitative technique of Genant relies on the expertise of the observer rather than direct measurements of the physical dimensions of the vertebrae (10). Based on the physical appearance, vertebrae are characterized as being normal or deformed. The types of deformation are mild (grade 1), moderate (grade 2), and severe (grade 3). Deformed vertebrae are also described based on the shape of the deformation as wedged (anterior fracture), biconcave (middle fracture), or crushed (posterior fracture). These deformities are illustrated in Fig. 12-2. Although physical measurements are not made with this technique, a grade 1 deformity roughly corresponds with a 20 to 25% reduction in the anterior, middle, or posterior height of the vertebra and a 10 to 20% reduction in vertebral area. A grade 2 deformity is the result of a 25 to 40% reduction in any of the three heights and a reduction in vertebral area of 20 to 40%. A grade 3 deformity occurs when there is a 40% reduction in any of the three heights and a 40% reduction in vertebral area. This technique has been traditionally used with plain radiographs of the spine but semiquantitative vertebral fracture assessments can be performed with fan-array DXA spine images as well. In fact, some DXA software will automatically assign a fracture type and grade to a vertebral deformity, based on the Genant semiquantitative technique.

VERTEBRAL FRACTURE ASSESSMENT WITH QUANTITATIVE TECHNIQUES

Quantitative techniques rely on physical measurements to diagnose vertebral fracture. Reference points are placed on each vertebral body. A common method is the placement of six points, one point at each corner of the vertebral body and one point at the midpoint of each of the endplates. Using these points, the anterior, middle, and posterior heights (h_a , h_m , and h_p , respectively) of the vertebra are measured. The vertebral area is calculated as the polygon area defined by the six points. In addition to the heights themselves, the anterior-posterior height ratio ($h_a:h_p$) and the mid-posterior height ratio ($h_m:h_p$) are calculated. Other ratios include the wedge index ($I_w = h_p/h_a$) (11) and the biconcavity index (h_m/h_a) (12).

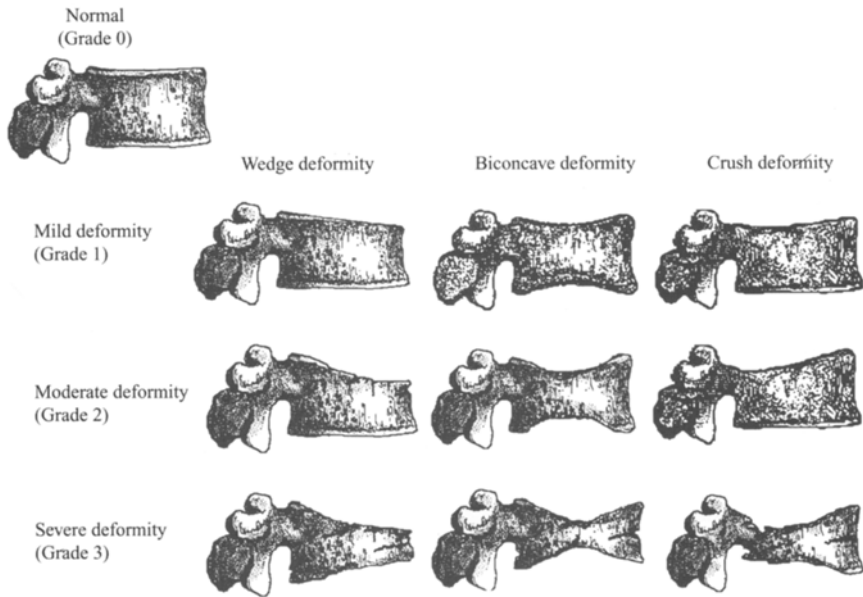


Fig. 12-2. Genant semiquantitative vertebral fracture grading system. (Reproduced courtesy of Dr. Harry Genant, San Francisco, CA.)

These measurements were originally made from plain radiographs. In recent years, measurements were made from digitized films. With the advent of fan-array DXA spine imaging and morphometry software, quantitative vertebral morphometry can be performed by the densitometry technologist as well.

Different criteria have been proposed for the diagnosis of prevalent or incident[†] fracture based on quantitative morphometry. Several authorities have proposed that a prevalent fracture should be considered present if there is a 15% or greater reduction in the $h_a:h_p$ or $h_m:h_p$ ratio or the ratio of the posterior height of one vertebra to the posterior height of an adjacent vertebra ($h_p:h_{pa}$) when compared to the mean value for a normal population (13–15). A more stringent 20% reduction in these ratios has been proposed as well. A reduction of 3 standard deviations (SDs) in the $h_a:h_p$

[†]A prevalent fracture is a fracture that is already present at the time the patient is seen. An incident fracture is a fracture that develops at some point in time after the initial evaluation.

or $h_m:h_p$ compared to normative data to define vertebral fracture was proposed by Ross et al. and Eastell et al. (16,17). McCloskey and Kanis (18,19) also proposed utilizing a 3 SD reduction in any of the ratios combined with reductions in ratios calculated using a predicted posterior height. These morphometric definitions of vertebral fracture require comparisons to normative reference data for a population. Heights may also be adjusted for body size using the dimensions of the fourth thoracic vertebra (T4). In other words, the h_p for T12 can be adjusted or normalized for size by dividing it by the h_p at T4 in the individual. The resulting posterior dimension for T12 is then abbreviated nh_p , reflecting the normalization for size. Minne et al. (20) proposed defining vertebral fracture as being present when any of the three normalized heights was below the third percentile of the normal range. Because vertebrae are expected to have slightly different shapes depending on the vertebral level, individual heights must be compared to normal values that are specific for that vertebral level.

The definition of incident fractures tends to be more straightforward. A decrease of 15% in the h_a , h_m , or h_p from the baseline film is indicative of an incident fracture. Other authorities have proposed a reduction of 20 to 25% alone for the definition of an incident fracture (21) or this amount of reduction in any of the three heights in combination with a minimum absolute reduction of 4 mm (22).

PERFORMANCE COMPARISONS OF SEMIQUANTITATIVE AND QUANTITATIVE TECHNIQUES

Quantitative techniques rely heavily on the accuracy of point placements as well as comparisons to reference databases. Point placement can be subjective and affected by the deformity itself or patient positioning. Differences of opinion exist regarding the validity and design of reference databases for vertebral morphometry, just as they do for bone densitometry. Genant's semiquantitative technique is based on the visual recognition of quantitative changes in vertebral shape. The performance of quantitative and semiquantitative techniques in identifying vertebral fractures has been compared in several studies (23–28). In order to compare the techniques, a "gold standard" for the diagnosis of vertebral fracture was generally created by a consensus reading of radiographs by experts. When done in this manner, the semiquantitative and quantitative approaches generally perform equally well, but the quantitative morphometry fracture criteria profoundly effect the agreement between the two techniques. The combination of a semiquantitative and quantitative technique may be better than either alone. Spine imaging with fan-array densitometry combined

with precise, computerized measurements make it possible for the densitometry technologist to utilize both.

FAN-ARRAY SPINE IMAGING WITH DXA

Fan-array DXA spine imaging is one of the newer applications for DXA. The spine can be imaged from T4–L5 in the lateral or posteroanterior (PA) projection. DXA spine imaging can be performed in seconds to minutes, depending on the scan mode, but always at a fraction of the radiation exposure of conventional spine radiographs. Fan-array DXA imaging also largely avoids the problem created by parallax[§] in plain radiography of the spine. Because the movement of the scan arm allows the DXA beam to be passed parallel to the vertebral endplates throughout the entire length of the spine, the vertebral dimensions are not distorted by the angle of the beam. If the patient has severe scoliosis, some parallax effect may be unavoidable.

Lateral spine images, such as the DVA[™] image from a GE Lunar Prodigy[¶] shown in Fig. 12-3, can be evaluated using Genant's semiquantitative method. Morphometric software can also be used to define and measure vertebral heights, as shown in Fig. 12-4. This technique is called morphometric X-ray absorptiometry (MXA) in contrast to the use of conventional radiographs for morphometric measurements, which is called morphometric radiography (MRX). In 1998, Rea et al. (29) evaluated 161 postmenopausal women for fracture using conventional lateral spine radiographs and fan-array lateral spine imaging. Both image types were evaluated using the Genant semiquantitative method. MXA correctly identified 91.9% of the grade 2 and grade 3 spine fractures. When the grade 1 (mild) fractures were included in the total, MXA correctly identified 77.4%. MXA also correctly identified 98.4% of the unfractured vertebrae. This suggests that DXA spine imaging and applying the Genant semiquantitative method was an excellent means of excluding the diagnosis of vertebral fracture. If a fracture was not seen using this technique, it

[§]Parallax refers to an apparent displacement of an object because of a change in the observer's position. In the case of spine radiography, it refers to the angle at which the X-ray beam passes through the vertebral bodies. If the X-ray beam is not parallel to the vertebral endplates, the shape of the vertebrae may be distorted, making morphometric measurements inaccurate.

[¶]DVA[™] is a trademarked reference to Dual-Energy Vertebral Assessment as performed on GE Lunar fan-array DXA devices. Specifications for the GE Lunar Prodigy may be found in Chapter 4.

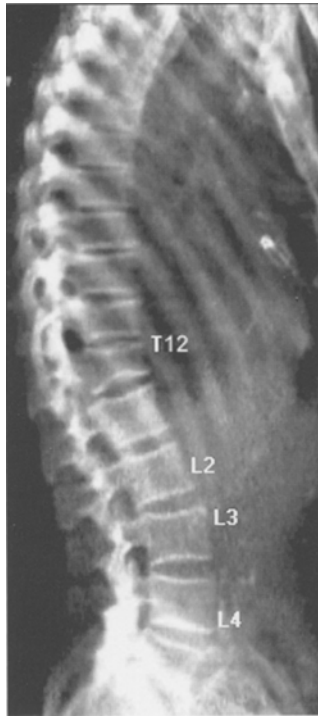


Fig. 12-3. Lateral spine DVA™ image from a Lunar Prodigy showing a grade 2 fracture at T12. (Case courtesy of GE Healthcare, Madison, WI.)

was highly unlikely that a fracture was present at all, and extremely unlikely that a grade 2 or grade 3 fracture was present. The agreement in fracture diagnoses between the visual assessment of DXA spine images and the semiquantitative assessment of standard spine radiographs for vertebrae that could be evaluated with both techniques was 96.3%.

Although DXA spine imaging spans T4 to L5, it is not uncommon for the uppermost thoracic vertebrae to be poorly visualized. In the study noted above from Rea et al. (29), 94.9% of the vertebrae could be evaluated. T4 and T5 were the most common vertebrae that were too poorly visualized to be evaluated. In a study from Schousboe et al. (30) in which 342 women underwent DXA lateral spine imaging, 92.1%, or 4096 of the 4446 vertebrae studied, could be evaluated. In this study, T4–T6 were less likely to be adequately visualized.

The inability to consistently evaluate T4–T6 on lateral DXA spine images does not present a significant problem in osteoporotic fracture identification. Several studies have demonstrated that the majority of fractures



Fig. 12-4. Computerized morphometric analysis of vertebral heights for T12, as seen in Fig. 10-6. (Case courtesy of GE Healthcare, Madison, WI.)

occur below these levels. The most common locations for vertebral fractures would appear to be T11–L1, followed by T7–T8 (2,27,30,31). In studies that have utilized DXA spine imaging for spine fracture diagnosis, a surprising percentage of women with nonosteoporotic bone densities have been found to have fractures. In the study from Schousboe et al. (30), 27.4% of the patients aged 60 and older with osteopenic bone densities according to World Health Organization (WHO) criteria were found to have vertebral deformities consistent with a diagnosis of fracture on DXA spine images. Forty-two percent of the patients aged 60 and older with osteoporotic bone densities were found to have vertebral deformities as well. In this study, the diagnosis of fracture on the DXA image was based primarily on the Genant semiquantitative method. Faulkner et al. (32) evaluated 231 women with a mean age of 65 with DXA spine imaging utilizing proprietary morphometric software in which a diagnosis of spine fracture was based on a reduction in vertebral height or height ratio of 3 SDs or more from the expected mean value. Using this definition of prevalent fracture, more than half of the women were found to have vertebral fractures. Based on bone density at the PA lumbar spine or proximal femur, 46.7% of the women had osteopenia and 26.4% had osteoporosis.

Of the women with osteopenia, 49.1% were found to have spine fractures. Over 72% of the women with osteoporosis were also found to have spine fractures based on MXA measurements.

The significance of these findings to the diagnosis of osteoporosis, prediction of fracture risk, and thus the decision to intervene with prescription medications must not be overlooked. Even though a patient may have an osteopenic bone density, using WHO criteria^{**}, the presence of a fracture implies that they have met the conceptual definitions of osteoporosis proposed by consensus conferences over the last decade. If a patient has an osteoporotic bone density by WHO criteria and also has a fracture, the patient's diagnosis would change to the WHO diagnostic category of severe osteoporosis. In addition, the presence of a fracture clearly increases the risk of fracture fractures, over and above that implied by the bone density alone. These additional considerations must become part of the decision-making process for treatment. Consequently, vertebral fracture imaging with DXA should be considered an indispensable part of the evaluation of the patient's skeletal status. Vertebral fracture imaging or vertebral fracture assessment with DXA has recently been assigned its own CPT^{††} code of 76077 and is now reimbursable under Medicare.

MXA, like densitometry, is a quantitative measurement technique. Like densitometry, then, the utility of MXA can be assessed in part, by its reproducibility or precision.^{§§} After studying 48 normal postmenopausal women and 50 osteoporotic postmenopausal women, Ferrar et al. (33) concluded that the long-term precision of MXA was comparable to that of MXR. In this study, the root mean square (RMS)-SD was 0.60 mm in the normal women and 0.77 mm in the osteoporotic women. The RMS-SD for height ratios in the normal women was 0.03. These values were obtained using the "compare" feature. Use of the compare feature resulted in better precision than when the compare feature was not used. Rea et al. (34) also evaluated the long-term precision of MXA. They noted, as did Ferrer et al. (33), that the precision errors for MXA were substantially smaller than the 20 to 25% reduction in vertebral height often used as a criteria for the diagnosis of incident vertebral fracture. The diagnosis of incident fracture from these images based on quantitative spine morphometry is therefore not adversely affected by the precision of the measurement technique.

^{**}See Chapter 9 and Appendix II for a discussion of the WHO criteria for the diagnosis of osteoporosis based on the measurement of bone density.

^{††}See Appendix V for a listing and discussion of relevant CPT codes.

^{§§}See Chapter 6 for a discussion of precision.

Proximal Femur Morphometry

Interest in the measurement of the dimensions and geometry of the proximal femur as part of the assessment of fracture risk was spurred by the initial recognition of hip axis length (HAL) as an independent predictor of hip fracture risk. Other measures have also come under scrutiny as predictors of hip fracture risk. These are measures such as the neck-shaft angle and femoral neck width, as well as individual segments of the hip axis length.

HIP AXIS LENGTH

HAL was originally demonstrated to be a predictor of hip fracture risk that was independent of bone mineral density based on measurements made with a goniometer on proximal femur bone density printouts by Faulkner et al. (35). HAL was defined as the distance from the inner pelvic brim to the outer edge of the greater trochanter along the femoral neck axis as shown in Fig. 12-5. In this study, each SD increase in length resulted in a 1.9-fold increase in the risk of femoral neck fracture and a 1.6-fold increase in the risk of trochanteric fracture. Other investigators (36) have also found HAL to be a significant predictor of femoral neck fracture risk, but not trochanteric fracture risk.

HAL has also been portioned into segments, to determine if any particular segment of HAL is more predictive of hip fracture than HAL itself. One such segment is the femoral neck axis length (FNAL), which is a segment of HAL that spans the base of the greater trochanter to the apex of the femoral head, as shown in Fig. 12-6. Another segment of interest is the intertrochanteric-head center distance, also shown in Fig. 12-6. Of these two, the intertrochanteric-head center distance, although more difficult to measure with good precision than HAL, remains the focus of interest as an independent predictor of hip fracture risk (37,38)

Automation of the HAL measurement was originally proposed by Faulkner et al. in 1994 (39). This automated measurement is now offered commercially as part of proximal femur bone density studies by some manufacturers. Figure 12-7 is a DualFemur[®] DXA study performed on a Lunar Prodigy showing the HAL measurement. The scale indicates the patient's value in comparison to the mean value predicted for height. Although this is clearly a nonmodifiable risk factor, HAL can be useful for hip fracture risk stratification. Using the Lunar Prodigy, Bonnick and Lewis (40) reported RMS-SD and RMS-percent coefficient of variation (%CV) precision values for HAL measurements of the left femur of 0.7 mm, or 0.67%, in women aged 20 to 49 and 0.6 mm, or 0.53%, in women aged 50 to 70.

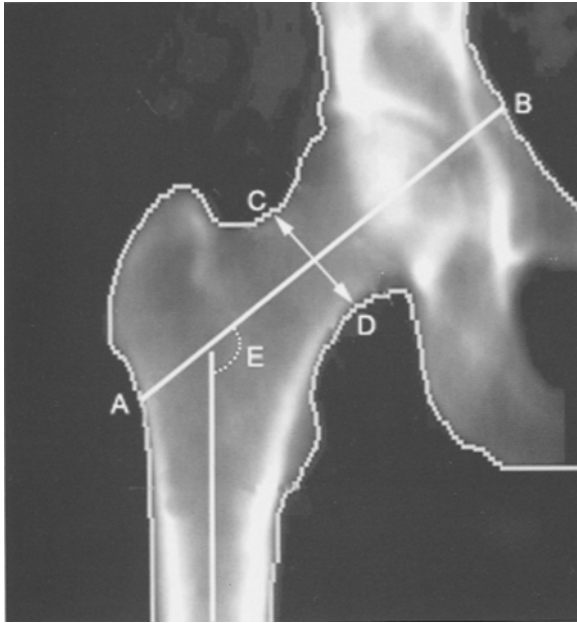


Fig. 12-5. Proximal femur image showing the HAL (A-B), femoral neck width (C-D), and neck-shaft angle (E).

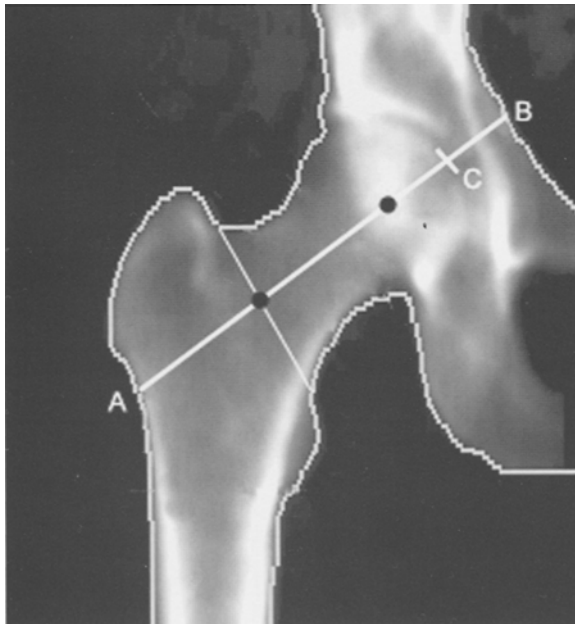


Fig. 12-6. Proximal femur showing the HAL (A-B) and its segments: the femoral neck axis length (A-C), and the intertrochanteric-head distance (■-●).

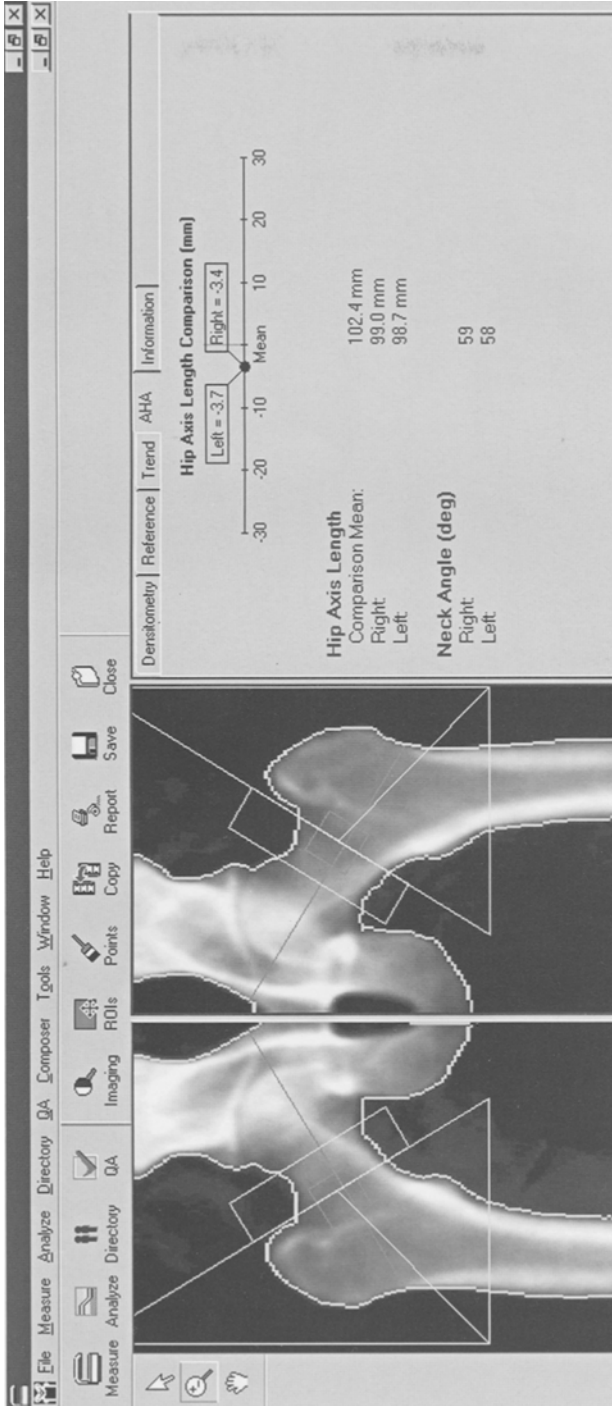


Fig. 12-7. Lunar Prodigy DualFemur™ study with the hip axis length (HAL) measurement. The HAL in both femurs is slightly shorter than predicted for height.

THE FEMORAL NECK-SHAFT ANGLE

The femoral neck-shaft angle is another geometric measure that has been studied as a predictor of hip fracture risk. This angle is indicated by the letter "E" in Fig. 12-5. The studies to date have provided mixed results on the utility of this measure. Several studies (41-44) have found significantly greater femoral neck-shaft angles in hip fracture patients than in controls, whereas others (35,38,45) have not.

FEMORAL NECK WIDTH

Femoral neck width is measured at the narrowest part of the femoral neck as indicated by line C-D in Fig. 12-5. An increase in neck width from periosteal bone apposition has been postulated as a compensatory response to a decrease in bone density. The result of the width increase should be an increase in the cross-sectional moment of inertia (CSMI). This would potentially compensate for the reduction in endosteal bone and theoretically reduce the risk of hip fracture. If this is so, the increase in femoral neck width in the presence of a low bone density should indicate a reduction in fracture risk compared to individuals with an average or reduced neck width and the same low bone density. Findings from various researchers, however, have been mixed (38,41,42).

THE UPPER FEMORAL NECK

The upper femoral neck is a relatively new region of interest in the proximal femur. It is the superior half of the traditional femoral neck region of interest as shown in Fig. 12-8. Yoshikawa et al. (46) suggested that there was a greater decrease in bone density in the superior region of the femoral neck in women. They suggested that this would cause the center of mass to move in such a way as to place greater stress on the femoral neck, increasing the risk of fracture. The upper femoral neck region of interest was compared to the entire femoral neck region and to the lower femoral neck region for the prediction of neck and trochanteric hip fracture in the study from Duboeuf et al. (36). In this study, upper femoral neck BMD was highly predictive of femoral neck fracture and actually outperformed the more traditional total femoral neck measurement. The lower femoral neck BMD was not predictive of femoral neck fracture. All three regions were predictive of trochanteric fracture and hip fracture in general. The upper femoral neck as a predictor specifically of femoral neck fracture is receiving increasing scrutiny in both research and clinical practice. In Fig. 12-9, the upper femoral neck region has a significantly

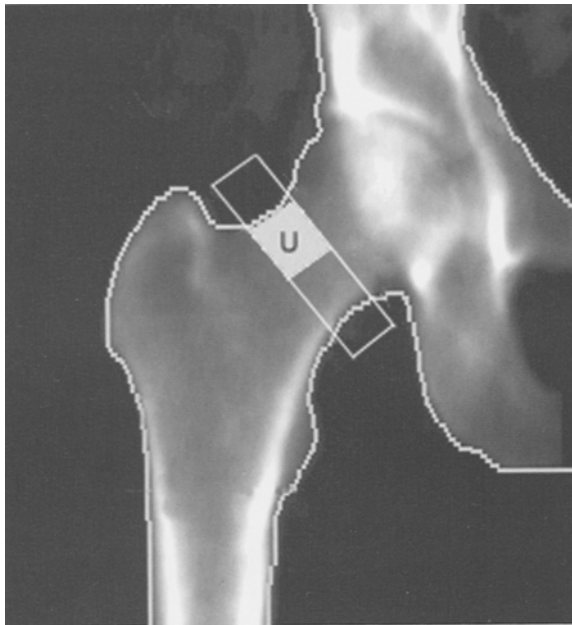


Fig. 12-8. Upper neck region of interest in the proximal femur.

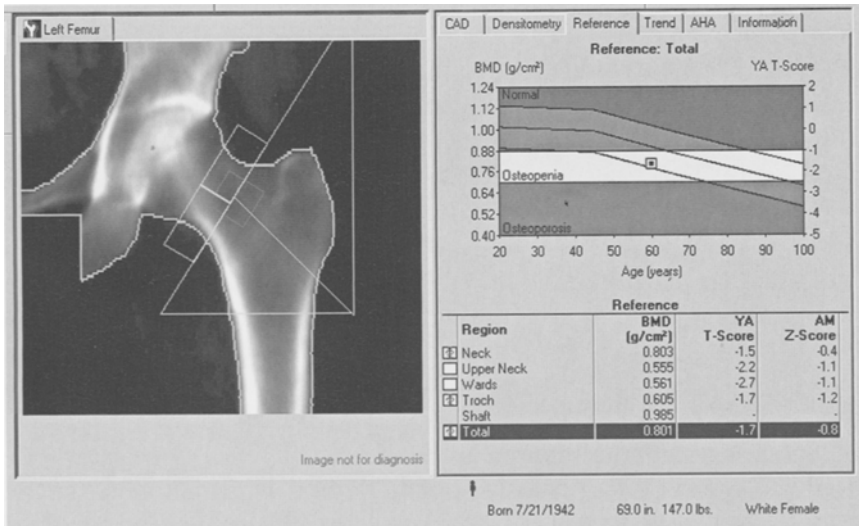


Fig. 12-9. GE Lunar Prodigy study of the proximal femur showing the measurement of bone density in the upper femoral neck. Note that the upper femoral neck has a T-score of -2.2 in comparison to the T-score of -1.5 for the entire femoral neck.

lower T-score than the total femoral neck, -2.2 vs -1.5 , respectively. It is also lower than the total hip or trochanteric region of interest.

HIP STRENGTH ANALYSIS

Yoshikawa et al. (46) developed algorithms to calculate the CSMI, as well as other measures of hip strength based on the measurement of proximal femur bone density with DXA. Yoshikawa et al. noted that although BMD was an important predictor of hip fracture risk, BMD accounted for only 50% of the bone strength estimated from the CSMI. This suggested that the CSMI reflected elements of bone strength not captured in the measurement of BMD. In 2002, Crabtree et al. (47) reported the application of a test version of proprietary DXA software (GE Medical Systems) designed to assess hip strength. The hip strength analysis (HSA) software uses the proximal femur DXA study to calculate measures reflecting the geometry and bone distribution within the proximal femur. In addition to standard measurements of proximal femur BMD, the program calculated the upper and lower femoral neck BMD, HAL, Cstress, and Fall Index (FI). Cstress reflected the compressive stress from a fall on the greater trochanter. The FI was a dimensionless quantity that reflected the resistance to fracture from forces generated during a fall on the greater trochanter. In this study, HAL was significantly longer in the fracture patients than in the controls. Cstress was also significantly greater and the FI was significantly lower in the fracture patients than in the controls. Femoral neck BMD, whether measured as a total, upper, or lower neck value, was significantly lower in the fracture patients than in the controls. Unlike the earlier study from Duboeuf et al. (36), Crabtree et al. could not show that the upper femoral neck BMD was a better predictor of femoral neck fracture than total femoral neck BMD.

In 2004, Faulkner et al. (48) reported the results of a study utilizing Hip Strength Analysis software on the GE Lunar Prodigy in which 365 women with a prior hip fracture and 2141 nonfractured women were studied. As originally described by Yoshikawa, the FI combines density, CSMI, age, height, and weight to estimate the ability of a hip to withstand a fall on the greater trochanter. The FI itself is the ratio of the patient's estimated femoral strength to the expected force of a fall on the greater trochanter. As a consequence, larger FI values indicate a femoral strength greater than the fall force, which should indicate a lower risk of fracture.

In this study from Faulkner et al. (48), the femoral neck bone density, HAL, and the FI were all significant predictors of hip fracture risk. They

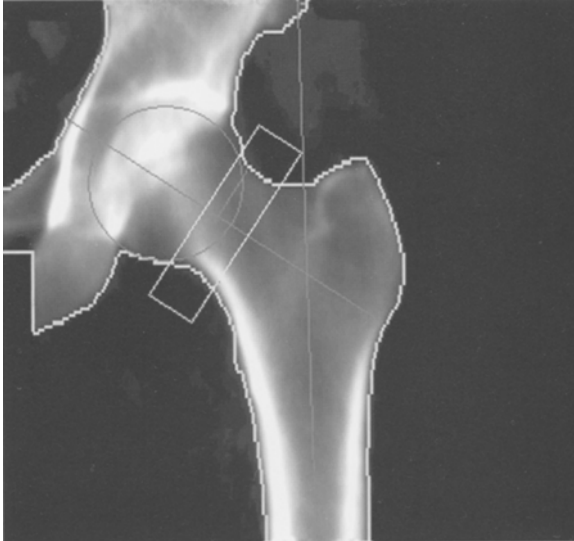


Fig. 12-10. GE Lunar Prodigy proximal femur image produced during hip strength analysis. The femoral head is identified during the data analysis. A line that is parallel to the long axis of the femoral shaft is shown bisecting the femoral shaft. This line intersects the line that is parallel to the long axis of the femoral neck and bisects the femoral neck, creating the neck-shaft angle. The line bisecting the femoral neck is also used to measure hip axis length.

also found that the ability to discriminate the hip fracture patients from the nonfractured controls was significantly improved when HAL and the FI were considered in addition to femoral neck BMD. The proximal femur analysis image used to calculate the FI is shown in Fig. 12-10. The results of the hip strength analysis for both proximal femurs is shown in Fig. 12-11. Hip Strength Analysis software is available commercially for the GE Lunar Prodigy.

BODY COMPOSITION ANALYSIS

Most full-size central DXA densitometers offer software that can be used to determine body composition from a total body bone density study. This application was first developed for dual-photon absorptiometers but the almost 1 hour scan time made such measurements clinically impractical. In contrast, modern DXA devices can perform total body scans in only a few minutes. In spite of this dramatic improvement in

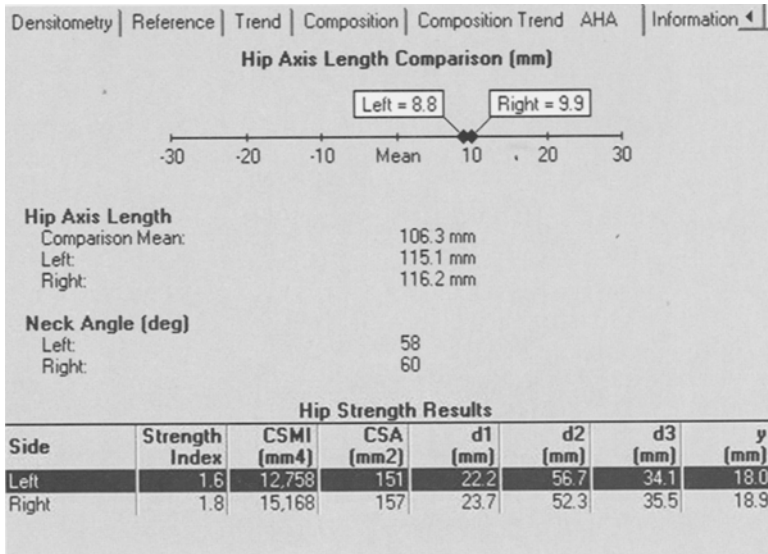


Fig. 12-11. Hip strength analysis results from a DualFemur™ study from a GE Lunar Prodigy. Data is provided for the hip axis length, neck-shaft angle, and the Fall Index (FI), as well as the various parameters used in calculating the FI, such as the cross-sectional moment of inertia. (Data provided courtesy of GE Healthcare, Madison, WI.)

speed, body composition assessment with DXA remains an underutilized application.

The assessment of body composition is much different from the measurement of weight, although certainly the two are related. The assessment of body composition is concerned with the percentage and distribution of fat and lean tissue in the body. Although many studies have associated extremes of weight with disease states, it is increasingly recognized that the percentage and distribution of fat and lean tissue is as or even more important than total body weight in various disease states. Although the densitometry technologist is primarily concerned with the measurement of body composition using DXA, a working knowledge of other techniques used to assess body composition will prove useful as the technologist encounters patients who have previously been measured with other techniques.

The Body Mass Index

The body mass index (BMI) is only first step in the assessment of body composition but it goes beyond the simple measurement of total body

weight. The BMI relates the patient's weight to their height, using the following formula:

$$\text{BMI} = \left(\frac{\text{Weight (lbs)}}{\text{Height (in)}^2} \right) \times 703 \quad (1)$$

For example, if a woman weighs 120 lbs and has a height of 62 in., her BMI is:

$$\text{BMI} = \left(\frac{120}{62^2} \right) \times 703 \quad (2)$$

$$\text{BMI} = 21.95 \text{ lbs/sq.in.} \quad (3)$$

If you are using the metric system to measure height and weight, the formula changes to:

$$\text{BMI} = \left(\frac{\text{Weight (kg)}}{\text{Height (cm)}^2} \right) \times 10,000 \quad (4)$$

Here, the calculated BMI will have the units of kg/cm^2 . The formula for calculating BMI is also called Quetelet's formula or index (49).

In 1995, the World Health Organization used the BMI to define obesity in adults (50). The WHO criteria for obesity based on the BMI are shown in Table 12-1. These criteria are for both women and men. Some of the newer software for DXA body composition assessments calculate and plot the patient's BMI on a graphic scale that indicates the WHO classification. This is shown in Fig. 12-12.

Although the BMI is an improvement over the assessment of weight alone, it does not address the actual percentage of total body fat or the distribution of fat in the body. More sophisticated methods are required for that.

Body Composition Methods

The body can be divided into two major compartments: fat and fat-free. The fat-free compartment can be further divided into water, protein, and mineral. The various techniques used to measure body composition are characterized by the number of compartments that they measure. A two-compartment method measures fat and fat-free mass. If a method is described as a three or four-compartment method, it is measuring fat mass and two or three of the components of the fat-free mass.

Table 12-1
World Health Organization Criteria for Obesity Based
on the BMI for Adults Aged 20 and Older

<i>BMI</i>	<i>Weight status</i>
<18.5	Underweight
18.5–24.9	Normal
25.0–29.9	Overweight
≥30.0	Obese

This BMI scale is based on the English measures of lbs and in.

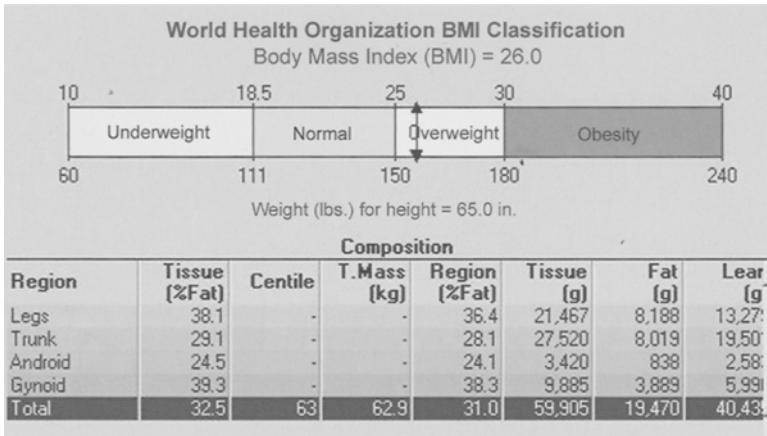


Fig. 12-12. Ancillary body composition data from a GE Lunar Prodigy body composition study in which the patient’s BMI has been plotted on a scale representing the World Health Organization classification system for obesity.

The traditional “gold standard” for measuring body composition has been a two-compartment technique called underwater weighing (UWW).⁹⁹ Other two compartment methods include measurement of skinfold thickness, bio-electrical impedance and air displacement plethysmography. Near infrared interactance (NIR) and DXA body composition assessments are three-compartment methods.

In spite of the appropriate medical concern for the health consequences of too much body fat, it should be noted that some fat is desirable in the

⁹⁹This technique is also known as hydrostatic weighing or hydrodensitometry.

human body. A portion of the fat mass is considered essential fat. This is the fat found in the bone marrow, internal organs, muscles, and central nervous system. Essential fat is necessary for the normal function of these organs and organ systems. Storage fat is the fat found in adipose tissue, around the internal organs, and subcutaneously. Because some fat is essential, it is never desirable to have 0% body fat. The minimum percentage of essential fat for men is estimated to be 5% and for women, 8%. Below these levels, organ function may not be normal. Total body fat ranges for optimal health are 18 to 30% for women and 10 to 25% for men.

TWO-COMPARTMENT BODY COMPOSITION MEASUREMENT TECHNIQUES

Underwater Weighing. Underwater weighing (UWW) is one of the most widely used methods for assessing body composition, and, as noted earlier, has long been considered the gold standard for these types of techniques. The overriding principle behind UWW is that there is an inverse relationship between body fat and body density. That is, as one goes up, the other goes down. The major assumption in UWW is that the densities of the fat and fat-free mass in the body are constant (51). It is generally agreed that fat mass has a density of 0.9 g/cm^3 but the density of the fat-free mass is controversial. In the past, the density of the fat-free mass was assumed to be a relatively constant 1.1 g/cm^3 . This does not appear to be true. Recall that the fat-free mass consists of water, protein, and bone mineral. Variations in any of these components may cause the density of the fat-free mass to change. Although the bone mineral is a small percentage of the fat-free mass, it contributes significantly to the density of the fat-free mass. Consequently, changes in the amount of bone mineral have a greater influence on the total density of the fat-free mass than might otherwise be expected. This creates potential inaccuracies in the measurement of total body fat with UWW in which the amount of bone mineral is assumed, rather than measured. If the density of the fat-free mass is lower because of a decreased total body bone mineral content, the total body percent fat will be overestimated by UWW (52). The converse is also true; if the density of the fat-free mass is higher because the total body bone mineral is greater than assumed, UWW will underestimate total body percent fat.

The UWW technique calls for the complete submersion of the individual in a tank of water. The individual is asked to exhale as much as possible and then, while holding their breath, they are submerged and weighed

under water. Under ideal circumstances, no clothing of any kind is allowed for the measurement. This requirement is often waved, for obvious reasons, but this will affect the accuracy of the measurement to a small extent. The amount of air left in the lungs after completely exhaling, the residual lung volume, must be measured because this is expected to provide some buoyancy to the body while underwater. In some institutions the residual lung volume is estimated, rather than measured, using equations that are specific for age, height, and gender.

The person's weight underwater can be calculated based on the Archimedes principle that there is a buoyant counterforce equal to the weight of the water that is displaced by the body. Consequently, the weight of the body under water reflects the weight of the body minus the weight of the fluid that is displaced by the volume of the body. When combined with knowledge of the residual lung volume, the volume and density of the body can be estimated. The classic equation used to calculate the density of the fat mass from the total body density is the equation from Siri (53) in which

$$F = \left[4.95 \times \left(\frac{1}{D} \right) - 4.50 \right] \quad (5)$$

where F is the density of the fat mass and D is the density of the total body. In recent years, however, age- and gender-specific equations have been developed for the calculation of fat density.

Skinfold Measurements. Body fat can be estimated from multiple measurements of skinfold thickness. This is also considered a two-compartment method. In this method, it is assumed that the distribution of subcutaneous fat and internal fat is similar in everyone. This is a major assumption that is not necessarily valid. Nevertheless, there are equations that allow the calculation of percent body fat from skinfold thickness for men and women.

The technique requires that the skinfold thickness be measured at multiple sites. There are calipers made specifically for this purpose, such as the Lange Skinfold Caliper and the Harpenden Skinfold Caliper. The number of sites measured varies from three to seven. The seven-site method calls for measurements of skinfold thickness at the chest, triceps, subscapular region, axilla, suprailiac region, abdomen, and thigh. The more commonly used three-site method calls for measurements at the chest, abdomen, and thigh in men and at the triceps, thigh, and suprailiac region in women.

The measurement of skinfold thickness at the various sites is then used in an equation to calculate the total body density. Equations have been developed by Durnin and Womersley (54) as well as Jackson and Pollock (55,56) for this purpose, although Jackson and Pollock also combined gluteal or waist circumference with skinfold measurements to calculate body density. The classic formula to calculate total body density from the seven-skinfold thickness measurement in men is:

$$D = 1.112 - 0.00043499(x) + 0.00000055(x)^2 - 0.00028826(A) \quad (6)$$

in which D is the total body density, x is the sum of the seven skinfolds in mm, and A is the age in years. In women, the corresponding formula is:

$$D = 1.097 - 0.00046971(x) + 0.00000056(x)^2 - 0.00012828(A) \quad (7)$$

For the three-skinfold thickness measurement, specific equations also exist for men and women. For men:

$$D = 1.109380 - 0.0008267(x) + 0.0000016(x)^2 - 0.0002574(A) \quad (8)$$

in which D is again the total body density, x is now the sum of the chest, abdomen, and thigh skinfolds, and A is age in years. For women, the corresponding equation is:

$$D = 1.099421 - 0.0009929(x) + 0.0000023(x)^2 - 0.0001392(A) \quad (9)$$

in which x is the sum of the triceps, thigh, and suprailiac skinfolds. Variations of these equations from other authors exist as well. With any of these equations, once the total body density is known, an equation such as Eq. 5 from Siri can be used to calculate the percentage of total body fat. Today, these calculations are readily performed by computer programs. The accuracy and reproducibility of skinfold measurements is highly dependent on the skill of the individual making the measurements.

Bioelectrical Impedance Analysis. Bioelectrical impedance analysis (BIA) is also considered a two-compartment method. In this technique, the individual commonly stands barefoot on a metal foot plate from which an extremely low voltage electric current is sent up one leg and then down the other. The individual may also be asked to lie on a table with electrodes connected to both legs after which an undetectable low voltage electric current is transmitted through the body from the electrodes. Because fat is a very poor conductor of electricity and water, a component of the fat free mass is a very good conductor of electricity, the resistance to the electric current can be used to estimate the percent body fat.

BIA is a popular method, often found in health clubs because of its ease of use and short measurement time (<1 minute). It is generally considered to overestimate body fat in lean individuals and underestimate body fat in obese individuals. Because BIA results are highly dependent on total body water, the hydration status of the individual can profoundly affect the results. Consequently, individuals are advised to abstain from eating or drinking 4 hours before the test, avoid exercise within 12 hours of the test, and abstain from alcohol for 48 hours before the test. Immediately before testing, the individual is asked to empty their bladder. Diuretic use can also affect the results obtained with BIA.

Air Displacement Plethysmography. Air displacement plethysmography can be considered analogous to underwater weighing, except that it is the displacement of air instead of the displacement of water that is used to measure the density and volume of the body. One technique using air displacement is called the BOD POD[®] (Life Measurements Instruments, Concord, CA). This is an enclosed, egg-shaped, capsule-like structure. An individual undergoing the measurement must sit very still within the capsule and breathe quietly during the 5- to 8- minute measurement. A swim cap and tight fitting clothing are generally worn. Although the individual is completely enclosed within the capsule, a clear window through which the individual can see, and be seen, lessens any anxiety. As in underwater weighing, it is necessary to determine the residual lung volume, either by measurement or estimation. The equipment is relatively expensive which limits its availability, although less expensive models have become available. Measurements of body fat with the BOD POD[®] have been reported to be highly correlated with those made by underwater weighing (57). In a review of the published literature from December 1995 to August 2001, the average percent body fat in children and adults differed by less than 1% between the BOD POD[®] and underwater weighing and by less than 1% between the BOD POD[®] and DXA in adults and less than 2% in children (58).

THREE-COMPARTMENT BODY COMPOSITION MEASUREMENT TECHNIQUES

Near Infrared Interactance. NIR for body composition analysis relies on the principles of infrared spectroscopy. A computerized spectrophotometer is used in this method. A probe that emits an infrared light is placed on the body. The infrared light passes through the fat and muscle and is then reflected back to the probe. The reflected light is quantified

and used to calculate body density. The method is considered quite safe and is fast, convenient, and inexpensive. It requires no particular patient preparation. The NIR unit itself is generally small and portable. The Futrex-5000® (Futrex Inc., Gaithersburg, MD) is a commercial brand of a NIR body composition device. The accuracy of NIR has been compared to skinfolds and BIA using underwater weighing as the reference technique (59–61). In general, the results obtained from skinfold measurements, BIA, and NIR were all highly correlated with the results from UWW. At the extremes of weight, skinfold measurements appeared to be more accurate than BIA or NIR, when UWW was used as the reference measurement, but all three performed reasonably well in individuals of normal weight.

Dual-Energy X-Ray Absorptiometry. DXA is considered a three-compartment method for the assessment of body composition because bone mineral is measured as well as the fat and fat free mass. Unlike underwater weighing or air displacement plethysmography, no assumption needs be made as to the amount of bone mineral because it is measured with the technique. Values are also not affected by the residual lung volume, making it unnecessary to either measure or estimate this value. The hydration status of the patient is still important (62,63). DXA body composition studies go beyond the measurement of total body fat or fat free mass. Unlike any other body composition technique, the distribution of fat in the body can be evaluated.

Although body composition software was originally developed for dual-photon absorptiometry, DXA's predecessor, the scan times approached an hour, making the study clinically impractical. The dramatically faster scan times of today's DXA units have reduced the time needed for DXA body composition studies to several minutes. This technique employs ionizing radiation. Radiation exposure is reported as 0.037 mrem for the GE Lunar Prodigy™ (Madison, WI) and as low as 0.01 mGy for the Hologic Discovery™ (Bedford, MA) model A. In either case, radiation exposure is extremely low. Body composition software is generally offered as an option with full-size central DXA devices.

The positioning and acquisition of data for a body composition study is identical to that for a total body bone density study. As is recommended for following changes in bone density, changes in body composition assessed by DXA should be made on the basis of serial measurements on the same DXA device. In one study from Soriano et al. (64), although body composition measurements on 78 adults were highly

correlated*** when performed on a GE Lunar DPX, GE Lunar DPX-L, GE Lunar Prodigy, and Hologic Dephi, there were significant differences in the percentage of fat and bone mineral measurements among the devices.

DXA total body bone and soft tissue images from a GE Lunar Prodigy are shown in Fig. 12-13. The images seen in Fig. 12-13 are from the same woman, acquired during a total body bone and body composition study. The soft tissue image generally tends to be unflattering, even for a slim individual. The various regions of the body are defined by the cuts on the image placed by the technologist. Figure 12-14 is the bone density data from this study and Fig. 12-15 is the body composition data. Note that in the body composition data in Fig. 12-15, regional values as well as total body values are provided for the grams of fat, lean, and bone mineral. If the grams of fat, lean, and bone mineral are added, the total gram weight provides an extremely accurate assessment of the actual weight of the patient. In this particular case, adding the grams of fat, lean, and bone mineral results in a total gram weight of 56,440 grams or 56.4 kg. This is the derivation of the value listed in the column titled Total Mass and in the row for Total values at the bottom of the printout. The total grams of tissue refer to the combined weight of the fat and lean mass. The Region % Fat values indicate the percentage of fat found in the indicated region when the gram weight of fat, lean, and bone mineral is considered. The Tissue % Fat refers to the percent of fat found in the indicated region when only the fat and lean gram weight is considered.

Fig. 12-16 shows the total body image from a Hologic Discovery. The bone density data from this study is shown in Fig. 12-17 and the body composition data in Fig. 12-18. The presentation of the data is similar but note that on the Discovery total body bone density and body composition data, a subtotal for every column is provided that excludes data from the head region. This is useful because it is often desirable to exclude the head from these analyses because of the marked density of the skull.

***Correlation is a measure of the strength of a relationship. It does not imply cause and effect. The statistical value that measures correlation is called Pearson's correlation coefficient and is abbreviated as r . A perfect correlation is expressed as $r = +1$ or $r = -1$. If one value increases as the other decreases, the correlation is a negative number. If one value increases as the other increases, the correlation is a positive number. As in this case, two measurements may be highly correlated, but the actual values may be significantly different. This suggests that the machines are indeed measuring the same thing, but the calibration for each machine produces a different result.

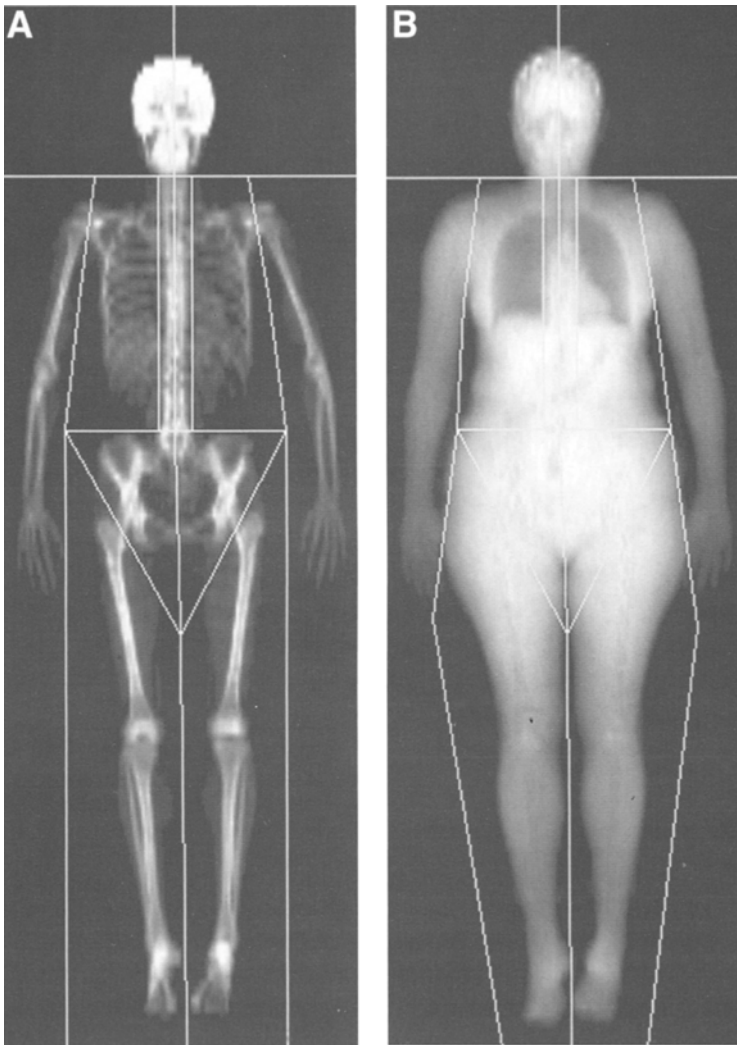


Fig. 12-13. Total body bone image and body composition image from a total body study on a GE Lunar Prodigy.

In addition to the standard regions of interest shown in the body composition studies in Figs. 12-13 and 12-16, it is also possible to define unique regions of interest for analysis to describe more android or more gynoid distributions of fat. This is commonly done in research studies focusing on cardiovascular disease and the effect of fat distribution. The technologist may be asked to create region of interest boxes that are placed

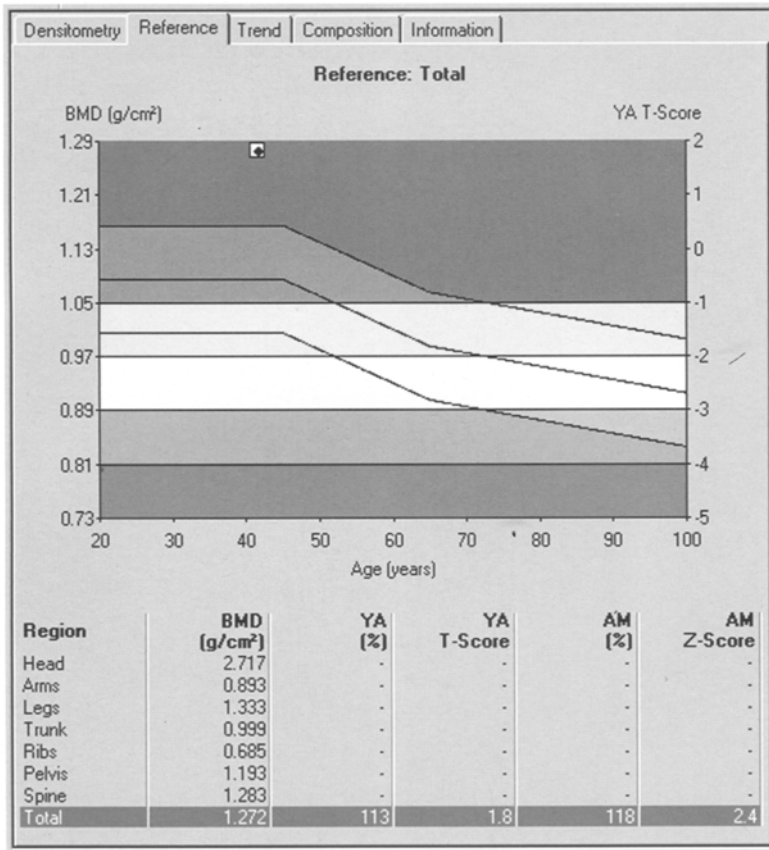


Fig. 12-14. Total body bone density data for the image shown in Fig. 12-13.

over the abdomen and thighs to make this type of assessment. Some versions of body composition software also provide these highly specialized regions of interest, as shown in Fig. 12-19.

DXA body composition assessments of total body fat are highly correlated with those from UWW and skinfold measurements. In a study from Dalsky et al. (65), there were no significant differences in the average body fat results obtained in 63 men and women using all three techniques and the measurements were highly correlated. The correlation coefficient for UWW and DXA was 0.864 and for DXA and skinfolds, 0.917.

The precision of body composition measurements with DXA is excellent. In a study of 20 individuals measured four times on consecutive days,

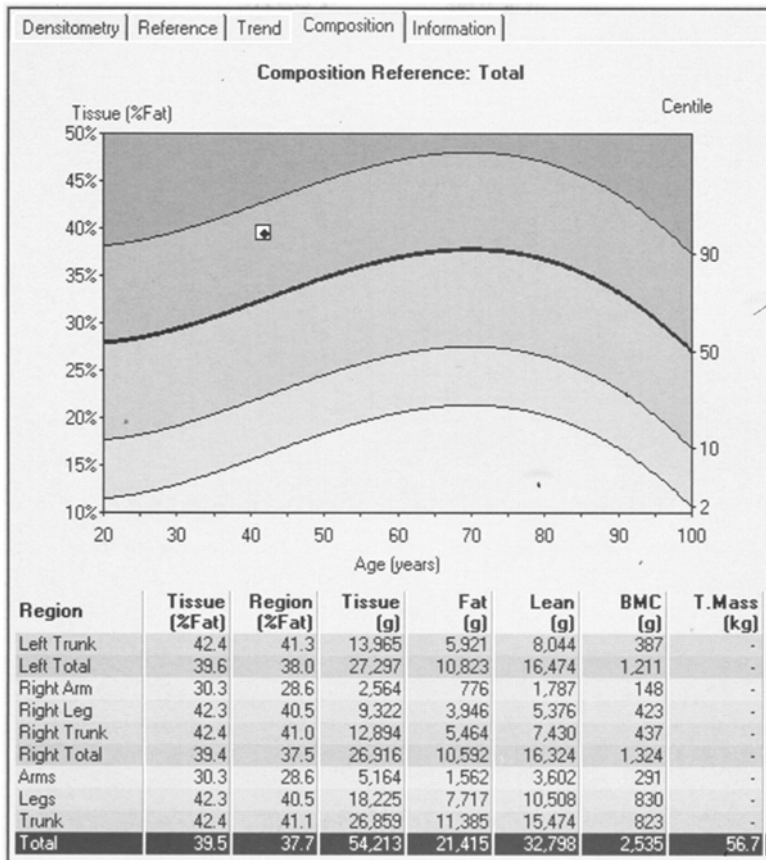


Fig. 12-15. Body composition data for the image shown in Fig. 12-13B. The total grams of tissue reflect the grams of fat and lean tissue combined, excluding the grams of bone mineral. The % Tissue Fat thus reflects the percentage of fat in tissue only, exclusive of bone mineral. The % Region Fat reflects the percentage of fat in a region that includes both tissue and bone mineral. The total tissue mass, in kg, is an accurate measure of the patient's weight. Here, the value is 56.7 kg or 125 lbs.

the percent coefficient of variation^{†††} for total body BMD was 0.62% and for total body percent fat, 1.89% (66). The precision of the total body fat mass, lean mass, and bone mineral content, expressed as the %CV, was 2.0, 1.11, and 1.09%, respectively. Regional measurement precision tended not to be as good as total body measurement precision. The authors

^{†††}See Chapter 6 for a discussion of the percent coefficient of variation and the number of subjects and studies needed for a valid precision study.

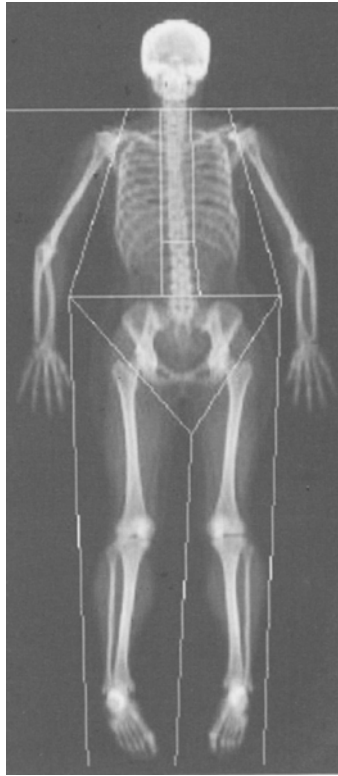


Fig. 12-16. Image from a total body study performed on the Hologic Discovery. (Case provided courtesy of Hologic, Inc., Bedford, MA.)

also noted that, just as in following changes in bone density, the same scan mode should always be used when performing total body DXA studies to follow changes in body composition. Use of different scan modes is expected to reduce the precision of repeat measurements (67).

Using the same device for serial measurements of body composition is equally imperative in achieving good precision, just as it is in the measurement of bone density. Although the body composition measurements performed on one manufacturer's device will be highly correlated with those from another, there will be differences in the absolute results because of differences in the manner in which the machines are calibrated. In a comparison of body composition measurements from devices from three different DXA manufacturers, differences of 2.6 to 6.3% in the total body fat and as much as 13% in trunk fat were found (68). Even among

DXA Results Summary:

Region	Area (cm ²)	BMC (g)	BMD (g/cm ²)	T-Score	PR (%)	Z-Score	AM (%)
L Arm	197.48	150.33	0.761				
R Arm	220.23	176.76	0.803				
L Ribs	105.72	81.56	0.771				
R Ribs	113.70	77.81	0.684				
T Spine	148.41	150.10	1.011				
L Spine	53.06	63.93	1.205				
Pelvis	207.06	261.46	1.263				
L Leg	363.05	426.29	1.174				
R Leg	369.04	435.21	1.179				
Subtotal	1777.76	1823.45	1.026				
Head	221.82	609.89	2.749				
Total	1999.58	2433.34	1.217	1.3	110	2.3	119

Total BMD CV 1.0%

Fig. 12-17. Total body bone density data for the image seen in Fig. 12-16. Note that a subtotal is provided for total body bone density, bone mineral content, and area that excludes the head. (Case provided courtesy of Hologic, Inc., Bedford, MA.)

DXA Results Summary:

Region	BMC (g)	Fat (g)	Lean (g)	Lean+BMC (g)	Total Mass (g)	% Fat
L Arm	150.33	808.4	1941.2	2091.5	2899.9	27.9
R Arm	176.76	1010.0	2202.4	2379.2	3389.1	29.8
Trunk	634.86	5659.2	20279.8	20914.7	26573.9	21.3
L Leg	426.29	1921.0	6859.0	7285.3	9206.3	20.9
R Leg	435.21	2195.1	7379.5	7814.8	10009.8	21.9
Subtotal	1823.45	11593.7	38661.9	40485.4	52079.1	22.3
Head	609.89	792.2	2829.2	3439.1	4231.3	18.7
Total	2433.34	12385.9	41491.1	43924.4	56310.4	22.0

Fig. 12-18. Body composition results for the image seen in Fig. 12-16. The % Fat indicates the percentage of fat of the total tissue mass. The total mass in grams reflects the grams of bone mineral, lean, and fat tissue and is thus a measure of the patient's weight. A subtotal for each column is provided that excludes the head data. (Case provided courtesy of Hologic, Inc., Bedford, MA.)

devices from the same manufacturer, small differences have been found that could adversely affect the precision of serial measurements (69,70).

A final practical consideration is the height and weight of the patient to be studied. It is imperative that the entire body be included in the scan

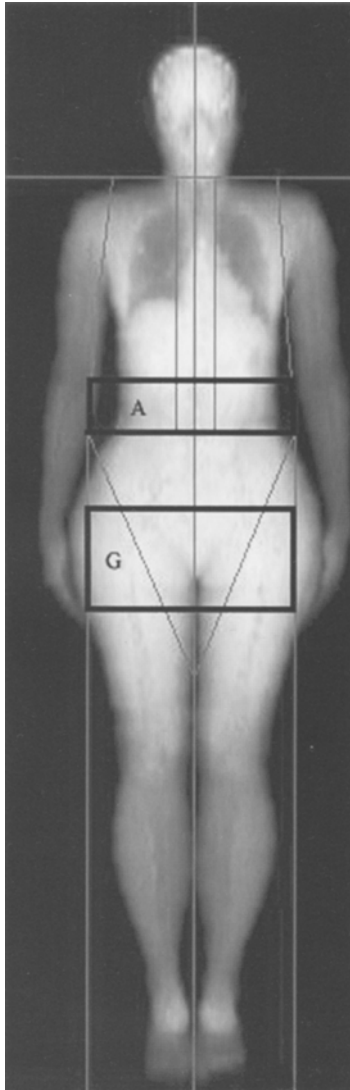


Fig. 12-19. Specialized regions of interest on a GE Lunar Prodigy body composition study. A indicates the android region of interest. G indicates the gynoid region of interest. (Image provided courtesy of GE Healthcare, Madison, WI.)

field. Therefore, the maximum height that can be accommodated will be determined by the table length and maximum scan length. In general, heights less than six feet (1.83 m) can be accommodated. The maximum weight that can be accommodated is largely a function of the construction

of the scan table and may vary from manufacturer to manufacturer. Any height and weight limitations for a total body study should be provided by each manufacturer.

The assessment of body composition in medicine, particularly by DXA, is relatively new. The list of diseases or conditions in which body composition assessments may assist in clinical management continues to grow. Body composition measurements are playing an increasing role in the management of obesity and anorexia nervosa as well as Crohn's Disease, celiac disease, and cystic fibrosis (71). Body composition measurements have been an integral part of sports medicine for some time.

REFERENCES

1. Ross, P. D., Davis, J. W., Epstein, R. S., Wasnich, R. D. (1991) Pre-existing fractures and bone mass predict vertebral fracture incidence in women. *Ann. Intern. Med.* **114**, 919–923.
2. Nevitt, M. C., Ross, P. D., Palermo, L., Muslinger, T., Genant, H. K., Thompson, D. E. (1999) Association of prevalent vertebral fractures, bone density and alendronate treatment with incident vertebral fractures: effect of number and spinal location of fractures. *Bone* **25**, 613–619.
3. Ross, P. D., Genant, H. K., Davis, J. W., Miller, P. D., Wasnich, R. D. (1993) Predicting vertebral fracture incidence from prevalent fractures and bone density among non-black, osteoporotic women. *Osteoporos. Int.* **3**, 120–126.
4. Black, D. M., Arden, N. K., Palermo, L., Pearson, J., Cummings, S. R. (1999) Prevalent vertebral deformities predict hip fractures and new vertebral deformities but not wrist fractures. *J. Bone Miner. Res.* **14**, 821–828.
5. Melton, L. J., Atkinson, E. J., Cooper, C., O'Fallon, W. M., Riggs, B. L. (1999) Vertebral fractures predict subsequent fractures. *Osteoporos. Int.* **10**, 214–221.
6. Burger, H., van Daele, P. L. A., Algra, D., et al. (1994) Vertebral deformities as predictors of non-vertebral fractures. *BMJ* **309**, 991–992.
7. Klotzbuecher, C. M., Ross, P. D., Landsman, P. B., Abbott, T. A., Berger, M. (2000) Patients with prior fractures have an increased risk of future fractures: a summary of the literature and statistical synthesis. *J. Bone Miner. Res.* **15**, 721–739.
8. Cooper, C., Atkinson, E. J., O'Fallon, W. M., Melton, L. J. (1992) Incidence of clinically diagnosed vertebral fractures: a population-based study in Rochester, Minnesota, 1985–1989. *J. Bone Miner. Res.* **7**, 221–227.
9. Ensrud, K. E., Nevitt, M. C., Palermo, L., et al. (1999) What proportion of incident morphometric vertebral fractures are clinically diagnosed and vice versa? Abstract. *J. Bone Miner. Res.* **14**, S138.
10. Genant, H. K., Wu, C. Y., Van Kuijk, C., Nevitt, M. C. (1993) Vertebral fracture assessment using a semiquantitative technique. *J. Bone Miner. Res.* **8**, 1137–1148.
11. Fletcher, H. (1947) H. Anterior vertebral wedging—frequency and significance. *AJR* **57**, 232–238.
12. Barent, E. and Nordin, B. E. C. (1960) The radiological diagnosis of osteoporosis: a new approach. *Clin. Radiol.* **11**, 166–174.

13. Black, D. M., Cummings, S. R., Stone, K., Hudes, E., Palermo, L., Steiger, P. (1991) A new approach to defining normal vertebral dimensions. *J. Bone Miner. Res.* **6**, 883–892.
14. Melton, L. J., Kan, S. H., Frye, M. A., Wahner, H. W., O'Fallon, W. M., Riggs, B. L. (1989) Epidemiology of vertebral fractures in women. *Am. J. Epidemiol.* **129**, 1000–1011.
15. Smith-Bindman, R., Cummings, S. R., Steiger, P., Genant, H. K. (1991) A comparison of morphometric definitions of vertebral fracture. *J. Bone Miner. Res.* **6**, 25–34.
16. Ross, P. D., Davis, J. W., Epstein, R. S., Wasnich, R. D. (1992) Ability of vertebral dimensions from a single radiograph to identify fractures. *Calcif. Tissue Int.* **51**, 95–99.
17. Eastell, R., Cedel, S. L., Wahner, H. W., Riggs, B. L., Melton, L. J. (1991) Classification of vertebral fractures. *J. Bone Miner. Res.* **2**, 207–214.
18. McCloskey, E., Spector, T. D., Eyres, K. S., et al. (1993) The assessment of vertebral deformity: a method for use in population studies and clinical trials. *Osteoporos. Int.* **3**, 138–147.
19. McCloskey, E. V. and Kanis, J. A. (1995) The assessment of vertebral deformity, in Vertebral Fracture in Osteoporosis (Genant, H. K., Jergas, M., Van Kuijk, C., eds.), Radiology Research and Education Foundation, University of California, San Francisco, pp. 215–233.
20. Sauer, P., Leidig, G., Minne, H. W., et al. (1991) Spine deformity index versus other objective procedures of vertebral identification in patients with osteoporosis: a comparative study. *J. Bone Miner. Res.* **6**, 227–238.
21. Black, D. M., Palermo, L., Nevitt, M. C., Genant, H. K., Christensen, L., Cummings, S. R. (1999) Defining incident vertebral deformity: a prospective comparison of several approaches. *J. Bone Miner. Res.* **14**, 90–101.
22. Lunt, M., Ismail, A. A., Felsenberg, D., et al. (2002) Defining incident vertebral deformities in population studies: a comparison of morphometric criteria. *Osteoporos. Int.* **13**, 809–815.
23. National Osteoporosis Foundation Working Group on Vertebral Fractures. (1995) Assessing vertebral fractures. *J. Bone Miner. Res.* **10**, 518–523.
24. Leidig-Bruckner, G., Genant, H. K., Minne, H. W., et al. (1994) Comparison of a semiquantitative and quantitative method for assessing vertebral fractures in osteoporosis. *Osteoporos. Int.* **3**, 154–161.
25. Genant, H. K., Jergas, M., Palermo, L., et al. (1996) Comparison of semiquantitative visual and quantitative morphometric assessment of prevalent and incident vertebral fractures in osteoporosis. The Study of Osteoporotic Fractures Research Group. *J. Bone Miner. Res.* **11**, 984–996.
26. Grados, F., Roux, C., de Vernejoul, M. C., Utard, G., Sebert, J. L., Fardellone, P. (2001) Comparison of four morphometric definitions and a semiquantitative consensus reading for assessing prevalent vertebral fractures. *Osteoporos. Int.* **12**, 716–722.
27. Li, J., Wu, C. Y., Jergas, H., Genant, H. K. (1995) Diagnosing prevalent vertebral fractures: a comparison between quantitative morphometry and a standardized visual (semiquantitative) approach, in Vertebral Fracture in Osteoporosis (Genant, H. K., Jergas, M., Van Kuijk, C., eds.), Radiology Research and Education Foundation, University of California, San Francisco, pp. 271–279.
28. Wu, C. Y., Li, J., Jergas, M., Genant, H. K. (1995) Diagnosing incident vertebral fractures: a comparison between quantitative morphometry and a standardized visual (semiquantitative) approach, in Vertebral Fracture in Osteoporosis (Genant, H. K.,

- Jergas, M., Van Kuijk, C., eds.), Radiology Research and Education Foundation, University of California, San Francisco, pp. 281–291.
29. Rea, J. A., Li, J., Blake, G. M., Steiger, P., Genant, H. K., Fogelman, I. (2000) Visual assessment of vertebral deformity by X-ray absorptiometry: a highly predictive method to exclude vertebral deformity. *Osteoporos. Int.* **11**, 660–668.
 30. Schousboe, J. T., DeBold, C. R., Bowles, C., Glickstein, S., Rubino, R. K. (2002) Prevalence of vertebral compression fracture deformity by X-ray absorptiometry of lateral thoracic and lumbar spines in a population referred for bone densitometry. *J. Clin. Densitom.* **5**, 239–246.
 31. Davis, J. W., Grove, J. S., Wasnich, R. D., Ross, P. D. (1999) Spatial relationships between prevalent and incident spine fractures. *Bone* **24**, 261–264.
 32. Faulkner, K. G., Barden, H. S., Weynand, L., Burke, P. (2002) Frequency of spine fractures assessed with LVA in normal, osteopenic, and osteoporotic postmenopausal women. *J. Bone Miner. Res.* **17**, S110.
 33. Ferrar, L., Jiang, G., Eastell, R. (2001) Longitudinal evaluation of morphometric X-ray absorptiometry for the identification of vertebral deformities. *Osteoporos. Int.* **12**, 661–671.
 34. Rea, J. A., Chen, M. B., Li, J., et al. (2001) Vertebral morphometry: a comparison of long-term precision of morphometric x-ray absorptiometry and morphometric radiography in normal and osteoporotic subjects. *Osteoporos. Int.* **12**, 158–166.
 35. Faulkner, K. G., Cummings, S. R., Black, D., Palermo, L., Glüer, C. C., Genant, H. K. (1993) Simple measurement of femoral geometry predicts hip fracture: the study of osteoporotic fractures. *J. Bone Miner. Res.* **8**, 1211–1217.
 36. Duboeuf, F., Hans, D., Schott, A. M., et al. (1997) Different morphometric and densitometric parameters predict cervical and trochanteric hip fracture: the EPIDOS study. *J. Bone Miner. Res.* **12**, 1895–1902.
 37. Center, J. R., Nguyen, T. V., Pocock, N. A., et al. (1998) Femoral neck axis length, height loss and risk of hip fracture in males and females. *Osteoporos. Int.* **8**, 75–81.
 38. Bergot, C., Bousson, V., Meunier, A., Laval-Jeantet, M., Laredo, J. D. (2002) Hip fracture risk and proximal femur geometry from DXA scans. *Osteoporos. Int.* **13**, 542–550.
 39. Faulkner, K. G., Mcclung, M., Cummings, S. R. (1994) Automated evaluation of hip axis length for predicting hip fracture. *J. Bone Miner. Res.* **9**, 1065–1070.
 40. Bonnick, S. L. and Lewis, L. A. (2002) The precision of PA spine, dualfemur and single femur bone density studies on the GE Lunar Prodigy, a DXA fan-array device. *J. Clin. Densitom.* **5**, S48.
 41. Gomez Alonso, C., Diaz Curiel, M., Hawkins Carranza, F., Perez Cano, R., Diez Perez, A. (2000) Femoral bone mineral density, neck shaft angle and mean femoral neck width as predictors of hip fractures in men and women. *Osteoporos. Int.* **11**, 714–720.
 42. Gnudi, S., Ripamonti, C., Gualtieri, G., Malavolta, N. (1999) Geometry of proximal femur in the prediction of hip fracture in osteoporotic women. *Br. J. Radiol.* **72**, 729–733.
 43. Karlsson, K. M., Sernbo, I., Obrant, K. J., Redlund-Johnell, I., Johnell, O. (1996) Femoral neck geometry and radiographic signs of osteoporosis as predictors of hip fracture. *Bone* **18**, 327–330.
 44. Partanen, J., Jämsä, T., Jalovaara, P. (2001) Influence of the upper femur and pelvic geometry on the risk and type of hip fractures. *J. Bone Miner. Res.* **16**, 1540–1546.
 45. Peacock, M., Turner, C. H., Liu, G., et al. (1995) Better discrimination of hip fracture using bone density geometry and architecture. *Osteoporos. Int.* **5**, 167–173.

46. Yoshikawa, T., Turner, C. H., Peacock, M., et al. (1994) Geometric structure of the femoral neck measured using dual-energy X-ray absorptiometry. *J. Bone Miner. Res.* **9**, 1053–1064.
47. Crabtree, N. J., Kroger, H., Martin, A., et al. (2002) Improving risk assessment: hip geometry, bone mineral distribution and bone strength in hip fracture cases and controls. The EPOS Study. *Osteoporos. Int.* **13**, 48–54.
48. Faulkner, K. G., Wacker, W. K., Simonelli, C., et al. (2004) Fall index and hip axis length predict hip fracture independent of bone density. Abstract. *J. Bone Miner. Res.* **19**, S68.
49. Garrow, J. S. and Webster, J. (1985) Quetelet's index (W/H²) as a measure of fatness. *Int. J. Obes.* **9**, 147–153.
50. World Health Organization. (1995) Physical status: the use and interpretation of anthropometry. World Health Organization, Geneva, Switzerland, WHO Technical Report Series.
51. Wang, J., Heymsfield, S. B., Aulet, M., Thornton, J. C., Pierson, R. N. (1989) Body fat from body density: underwater weighing vs. dual photon absorptiometry. *Am. J. Physiol.* **256**, E829–E834.
52. Heymsfield, S. B., Wang, J., Lichtman, S., et al. (1989) Body composition in elderly subjects: a critical appraisal of clinical methodology. *Am. J. Clin. Nutr.* **50**, 1167–1175.
53. Siri, W. E. (1956) Body composition from fluid spaces and density: analysis of methods. University of California Radiation Laboratory Report 3349.
54. Durnin, J. V. G. A. and Womersley, J. (1974) Body fat assessed from total body density and its estimation from skinfold thickness: measurements on 481 men and women aged from 16 to 72 years. *Br. J. Nutr.* **32**, 77–97.
55. Jackson, A. S. and Pollock, M. L. (1978) Generalized equations for predicting body density of men. *Br. J. Nutr.* **40**, 497–504.
56. Jackson, A. S., Pollock, M. L., Ward, A. (1980) Generalized equations for predicting body density of women. *Med. Sci. Sports Exerc.* **12**, 175–182.
57. McCrory, M. A., Gomez, T. D., Bernauer, E. M., Molé, P. A. (1995) Evaluation of a new air displacement plethysmograph for measuring human body composition. *Med. Sci. Sports Exerc.* **27**, 1686–1691.
58. Fields, D. A., Goran, M. I., McCrory, M. A. (2002) Body-composition assessment via air-displacement plethysmography in adults and children: a review. *Am. J. Clin. Nutr.* **75**, 453–467.
59. McLean, K. P. and Skinner, J. S. (1992) Validity of Futrex-5000 for body composition determination. *Med. Sci. Sports Exerc.* **24**, 253–258.
60. Brodie, D. A. and Eston, R. G. (1992) Body fat estimations by electrical impedance and infra-red interactance. *Int. J. Sports Med.* **13**, 319–325.
61. Heyward, V. H., Cook, K. L., Hicks, V. L., et al. (1992) Predictive accuracy of three field methods for estimating relative body fatness of nonobese and obese women. *Int. J. Sports Nutr.* **2**, 75–86.
62. Horber, F. F., Thomi, F., Casez, J. P., Fonteille, J., Jaeger, P. (1992) Impact of hydration status on body composition as measured by dual energy X-ray absorptiometry in normal volunteers and patients on haemodialysis. *Br. J. Radiol.* **65**, 895–900.
63. Pietrobelli, A., Wang, Z., Formica, C., Heymsfield, S. B. (1998) Dual-energy X-ray absorptiometry: fat estimation errors due to variation in soft tissue hydration. *Am. J. Physiol.* **274**, E808–E816.

64. Soriano, J. M., Ioannidou, E., Wang, J., et al. (2004) Pencil-beam vs fan-beam dual-energy X-ray absorptiometry comparisons across four systems: body composition and bone mineral. *J. Clin. Densitom.* **7**, 281–289.
65. Dalsky, G. P., Kraemer, W., Zetterlund, A. E., et al. (1990) A comparison of methods to assess body composition. Abstract. American College of Sports Medicine, Salt Lake City, UT, May 22–25.
66. Kiebzak, G. M., Leamy, L. J., Person, L. M., Nord, R. H., Zhang, Z. Y. (2000) Measurement precision of body composition variables using the Lunar DPX-L densitometer. *J. Clin. Densitom.* **3**, 35–41.
67. Black, E., Petersen, L., Kreutzer, M., et al. (2002) Fat mass measured by DXA varies with scan velocity. *Obes. Res.* **10**, 69–77.
68. Tothill, P., Avenell, A., Love, J., Reid, D. M. (1994) Comparisons between Hologic, Lunar, and Norland dual-energy X-ray absorptiometers and other techniques used for whole-body soft tissue measurements. *Eur. J. Clin. Nutr.* **48**, 781–794.
69. Ellis, K. J. and Shypailo, R. J. (1998) Bone mineral and body composition measurements: cross-calibration of pencil-beam and fan-beam dual-energy X-ray absorptiometers. *J. Bone Miner. Res.* **13**, 1613–1618.
70. Abrahamsen, B., Gram, J., Hansen, T. B., Beck-Nielsen, H. (1995) Cross calibration of QDR 2000 and QDR 1000 dual energy X-ray densitometers for bone mineral and soft-tissue measurements. *Bone* **16**, 385–390.
71. Albanese, C. V., Diessel, E., Genant, H. K. (2003) Clinical applications of body composition measurements using DXA. *J. Clin. Densitom.* **6**, 75–85.

Appendix I

Contacts for Bone Densitometry Manufacturers and Organizations of Interest

MANUFACTURERS

The products listed by manufacturer refer to the products discussed in Chapter 4 and do not necessarily represent the entire line of densitometers available from the manufacturer.

Alara, Inc.
47505 Seabridge Drive
Fremont, CA 94538-6546
Tel.: 800-410-2525
Fax: 510-315-5201
Web site: www.alara.com
E-mail: through Web site
Product: MetriScan™

CompuMed, Inc.
5777 W. Century Blvd., Suite 1285
Los Angeles, CA 90045
Tel.: 310-258-5000
Tel. (Osteo-systems): 310-258-5027
Fax: 310-645-5880
Web site: www.compumed.net or www.osteogram.com
E-mail: osteo@compumed.net
Product: Automated Osteogram®

CooperSurgical, Norland
95 Corporate Drive
Trumbull, CT 06611

Corporate

Toll-free tel.: 800-645-3760

Tel.: 203-601-5200

Fax: 203-601-1007

Customer service: 800-243-2974

Fax: 800-262-0105 (customer service)

Web site: www.coopersurgical.com

E-mail: e-mail@coopersurgical.com (U.S.)

E-mail: intl@coopersurgical.com (International)

Products: XR-46™, Excell™, Excell™ plus, Apollo™, pDEXA®,
McCue C.U.B.A. Clinical™

GE Medical Systems, Lunar

726 Heartland Trail

Madison, WI 53717-1915

Tel.: 608-828-2663

Toll-free tel.: 1-888-795-8627

Fax: 608-826-7106

Web site: www.gemedicalsystems.com or www.lunarcorp.com

Products: EXPERT®-XL, DPX Bravo®, DPX Duo®, DPX-IQ™, DPX
MD™, DPX MD+™, DPX- NT™, DPX Pro™, Prodigy™,
Achilles+™, Achilles Express™, Achilles Insight™, PIXI®

Hologic, Inc.

35 Crosby Drive

Bedford, MA 01730-1401

Toll-free tel.: 800-343-XRAY

Tel.: 781-999-7300

Fax: 781-280-0669

Web site: www.hologic.com

Customer support

Tel.: 800-321-HOLX

E-mail: support@hologic.com

Products: QDR® 4500 A, QDR® 4500 C, QDR® 4500 SL, QDR® 4500 W,
Delphi®, Discovery®, Sahara Clinical Bone Sonometer®

Image Analysis, Inc.

1380 Burkesville Street

Columbia, KY 42728

Tel.: 800-548-4849

Tel.: 270-384-6400

Fax.: 270-384-6405
Web site: www.image-analysis.com
E-mail: info@image-analysis.com
Products: QCT-5000 DICOM

Orthometrix, Inc.
106 Corporate Park Drive, Suite 102
White Plains, NY 10604
Tel.: 914-694-2285
Fax.: 914-694-2286
Web site: www.orthometrix.net
E-mail: info@orthometrix.net
Products: Distributor in North America of the Stratec XCT 2000

Osteometer MediTech, Inc.
12515 Chadron Ave.
Hawthorne, CA 90250
Tel.: 310-978-3073
Toll-free tel.: 866-421-7762
Fax: 310-676-0948
Website: www.osteometer.com
E-mail: info@osteometer.com
Products: DTX-200 DEXACare[®], DTU-one Ultrasure[™], DEXACare[®]G4

Quidel Corporation
10165 McKellar Court
San Diego, CA 92121
Tel.: 800-874-1517 (U.S. only)
Tel.: 858-552-1100 (outside U.S.)
Fax: 858-455-4960
Web site: www.quidel.com
E-mail: through Web site
Product: QUS-2[®]

Schick Technologies, Inc.
30-00 47th Avenue
Long Island City, New York 11101
Tel.: 718-937-5765
Fax: 718-937-5962
Product support
Tel.: 877-724-4254

Fax: 718-482-2030
Web site: www.schicktech.com
E-mail: through Web site
Product: accuDEXA™

Sectra North America, Inc.
4 Corporate Dr., Suite 197
Shelton, CT 06484
Tel.: 203-925-0899
Fax: 203-925-0906
Web site: www.sectra.com
Products: Sectra Osteoporosis Package™ IDS5™ Workstation Clinical
Application

Sectra Imtec AB
Teknikringen 20
SE-583 30 Linköping, Sweden
Tel.: 46 13 23 52 00
Fax.: 46 13 21 21 85
Web site: www.sectra.com

Stratec Medizintechnik
Durlacher Strasse 35
D-75172 Pforzheim, Germany
Tel.: 49 0 7231 145420
Fax.: 49 0 7231 145422
Web site: www.stratec-med.com
E-mail: info@stratec-med.com
Products: XCT™ 2000

Sunlight Medical, Inc.
5 Tuval Street
P.O. Box 25222
Tel-Aviv 61251, Israel
Tel.: 972 3-684-2626
Fax.: 972 3-684-2627
Web site: www.sunlightnet.com
E-mail: info@sunlightnet.com
Product: Omnisense™ 7000S

Wallach Surgical Devices, Inc.
235 Edison Road

Orange, CT 06477

Tel.: 800-243-2463

Fax: 203-799-2002

Web site: www.sunlightnet.com or www.wallachsurgical.com

E-mail: wallach@wallachsurgical.com

Product: Distributors in the United States for Sunlight Omnisense™ 7000S

ORGANIZATIONS OF INTEREST

American Society of Radiologic Technologists

15000 Central Avenue, S.E.

Albuquerque, NM 87123-3917

Toll-free tel.: 800-444-2778

Fax: 505-298-5063

Web site: www.asrt.org

E-mail: customerinfo@asrt.org

Foundation for Osteoporosis Education and Research

300 27th Street, Suite 103

Oakland, CA 94612

Tel.: 510-832-2663

Fax.: 510-208-7174

Web site: www.fore.org

E-mail: beverley@fore.org

International Society for Clinical Densitometry

342 North Main Street

West Hartford, CT 06117-2507

Tel.: 860-586-7563

Fax: 860-586-7550

Web site: www.iscd.org

E-mail: iscd@iscd.org

National Osteoporosis Foundation

1232 22nd St., N.W.

Washington, DC 20037-1292

Tel.: 202-223-2226

Web site: www.nof.org

E-mail: through Web site

Appendix II

World Health Organization Criteria for the Diagnosis of Osteoporosis Based on the Measurement of Bone Density^a

<i>Diagnosis</i>	<i>Bone density criteria</i>	<i>T-score criteria</i>
Normal	Not more than 1 SD below the young adult peak bone density	-1 or better
Osteopenia	More than 1 but less than 2.5 SDs below the young adult peak bone density	Between -1 and -2.5
Osteoporosis	2.5 SDs or more below the young adult peak bone density	-2.5 or poorer
Severe or established osteoporosis	2.5 SDs or more below the young adult peak bone density and a fracture	-2.5 or poorer + a fracture

^aThe World Health Organization criteria were intended to be applied to measurements of bone density made in postmenopausal Caucasian women only. In the absence of other criteria, they are often applied to postmenopausal women of other races and to men of any race over the age of 50. They should not be applied to healthy premenopausal women of any race, however.

World Health Organization. (1994) Assessment of fracture risk and its application to screening for postmenopausal osteoporosis: report of a WHO study group. *WHO Technical Report Series*. WHO, Geneva.

Appendix III

Guidelines for Bone Density Testing

1998 AND 2003 NATIONAL OSTEOPOROSIS FOUNDATION GUIDELINES FOR BONE DENSITY TESTING IN POSTMENOPAUSAL WOMEN

Bone density should be measured in:

- All postmenopausal women age 65 and older
- All postmenopausal women under age 65 with one or more risk factors
- Postmenopausal women who present with fractures

The 1998 Guidelines also contained the following two circumstances, which were omitted from the 2003 Guidelines:

- Women who have been on ERT or HRT for prolonged periods of time
- Women who are considering therapy for osteoporosis if bone mineral density testing would aid the decision

National Osteoporosis Foundation. (1999) *Physician's Guide to Prevention and Treatment of Osteoporosis*. Excerpta Medica, Belle Meade, NJ.

National Osteoporosis Foundation. (2003) *Physician's guide to prevention and treatment of osteoporosis*. NOF, Washington, DC.

AMERICAN ASSOCIATION OF CLINICAL ENDOCRINOLOGISTS 2003 MEDICAL GUIDELINES FOR THE PREVENTION AND MANAGEMENT OF POSTMENOPAUSAL OSTEOPOROSIS

BMD measurements should be performed in the following settings:

- For risk assessment in perimenopausal or postmenopausal women who have risk factors for fractures and are willing to consider available interventions

- In women who have X-ray findings that suggest osteoporosis
- In women beginning or receiving long-term glucocorticoid therapy or other drugs associated with bone loss
- In all adult women with symptomatic hyperparathyroidism or other diseases or nutritional conditions associated with bone loss in whom evidence of bone loss would result in adjustment of management
- For establishing skeletal stability and monitoring therapeutic response in women receiving treatment for osteoporosis (baseline measurements should be made before intervention)
- In all women 40 years old or older who have sustained a fracture
- In all women 65 years of age and older
- In younger postmenopausal women who have risk factors

AACE. (2003) American Association of Clinical Endocrinologists medical guidelines for clinical practice for the prevention and treatment of postmenopausal osteoporosis: 2001 edition, with selected updates for 2003. *Endocr. Pract.* 9, 545–564.

AMERICAN COLLEGE OF OBSTETRICIANS AND GYNECOLOGISTS GUIDELINES FOR BONE DENSITY MEASUREMENTS

Bone density measurements should be made in:

- All postmenopausal women 65 years of age or older
- Postmenopausal women under 65 years of age who have one or more risk factors
- All postmenopausal women who have sustained a fracture

Bone density measurements may be useful in:

- Pre- or postmenopausal women with diseases or conditions associated with an increased risk of osteoporosis

(2002) ACOG releases recommendations for bone density screening for osteoporosis. Washington, D.C.: American College of Obstetricians and Gynecologists. Accessed March 26, 2002, at http://www.acog.org/from_home/publications/press_releases/nr02-28-02-1.htm.

POSITION STATEMENT ON MANAGEMENT OF POSTMENOPAUSAL OSTEOPOROSIS FROM THE NORTH AMERICAN MENOPAUSE SOCIETY

Bone density should be measured in:

- All women who are at least 65 years of age regardless of risk factors
- All postmenopausal women younger than 65 with one or more risk factors
- Premenopausal women with low trauma fractures or known secondary causes of bone loss

(2002) Management of postmenopausal osteoporosis: position statement of The North American Menopause Society. *Menopause* 9, 84–101.

UNITED STATES PREVENTIVE SERVICES TASK FORCE RECOMMENDATIONS FOR BONE DENSITY TESTING

Bone density should be measured in:

- All postmenopausal women 65 years of age and older
- All postmenopausal women aged 60 to 64 at high risk for osteoporosis

U.S. Preventive Services Task Force. (2002) Screening for osteoporosis in postmenopausal women: recommendations and rationale. *Ann. Intern. Med.* 137, 526–528.

GUIDELINES FROM THE INTERNATIONAL SOCIETY FOR CLINICAL DENSITOMETRY

Bone density should be measured in:

- Women aged 65 and older
- Postmenopausal women under age 65 with risk factors
- Men aged 70 and older
- Adults with a presumed fragility or low trauma fracture
- Adults with a disease, condition, or history of medication use associated with low bone mass
- Individuals being considered for pharmacologic intervention to prevent bone loss or treat osteoporosis

- Individuals receiving pharmacologic treatment to prevent bone loss or treat osteoporosis to monitor therapeutic efficacy

The Writing Group for the ISCD Position Development Conference. (2004) Indications and reporting for dual-energy x-ray absorptiometry. *J. Clin. Densitom.* 7, 37–44.

Appendix IV

Bone Mass Measurement Act of 1997

Medicare recipients are potentially eligible for reimbursement of bone mass measurements performed in the following circumstances:

- An estrogen-deficient woman at clinical risk for osteoporosis, based on medical history and other findings
- An individual with vertebral abnormalities demonstrated by X-ray suggesting osteoporosis, osteopenia, or fracture
- An individual being monitored to assess efficacy of a Food and Drug Administration-approved drug therapy
- An individual receiving or expected to receive corticosteroids ≥ 7.5 mg of prednisone for >3 months
- An individual with primary hyperparathyroidism

Frequency Standards

At least 23 months must have passed since the month the last measurement was performed except:

- For monitoring patients on long-term glucocorticoid therapy
- For allowing a confirmatory baseline measurement to permit future monitoring if the initial test was performed with a technique that is different from the proposed monitoring method

Appendix V

CPT Codes for Bone Densitometry

<i>Technique</i>	<i>Type of study</i>	<i>CPT code</i>
Dual-energy X-ray absorptiometry ^a	PA spine bone density	76075
	Lateral spine bone density	
	Proximal femur bone density	
	Total body bone density	
Dual-energy X-ray absorptiometry	Forearm bone density	76076
	Heel bone density	
	Phalanges bone density	
Dual-energy X-ray absorptiometry	Vertebral fracture assessment	76077
Single-energy X-ray absorptiometry	Heel bone density	G0130
Quantitative ultrasound Radiographic absorptiometry	Heel bone density	76977
	Phalanges bone density	76078
Computer-assisted radiogrammetry	Phalanges bone density	76078
	Forearm bone density	
Quantitative computed tomography ^a	PA spine bone density	76070, G0131
	Proximal femur bone density	
Quantitative computed tomography	Forearm bone density	G0062
	Heel bone density	
Single-photon absorptiometry	Forearm bone density	78350
Dual-photon absorptiometry ^a	PA spine bone density	78351
	Proximal femur bone density	
	Total body bone density	

^aIn the description of the code, the skeletal sites noted are characterized as axial sites, even though anatomically the proximal femur is part of the appendicular skeleton. PA, posteroanterior.

CPT™ codes are Level I codes developed and maintained by the American Medical Association. These are five digit codes that are widely accepted for reporting services by healthcare providers. The modifier “-TC” is attached to the code to indicate billing for the technical component.

HCPCS codes, pronounced “hick-picks,” are Level II codes that are developed and assigned by the Health Care Finance Administration (HCFA). They are intended to meet the needs of Medicare and Medicaid and allow coordination of government programs by providing a uniform reporting system of procedures. HCPCS codes begin with a letter and are followed by four digits. “G” codes are assigned to procedures and services that are under review for inclusion in the AMA CPT™ coding system. Once a CPT™ code is assigned, the “G” code is eliminated.

REFERENCES

- AMA. HCPCS 2000. (1999) *Medicare's national Level II Codes*. 12th edition. AMA, Dover DE.
- AMA. (2004) *CPT™ 2005*. AMA, Chicago, IL.

Appendix VI

Dual-Energy X-Ray Absorptiometry Posteroanterior Spine Labeling Guidelines

1. Approximately 91% of women have five lumbar vertebrae.
2. The most common finding is five lumbar vertebrae with the lowest set of ribs on T12.
3. When five lumbar vertebrae are present, if the ribs are not on T12, they are usually on T11.
4. Six lumbar vertebrae are uncommon. Five lumbar vertebrae with the lowest set of ribs on T11 are more common.
5. Approximately 75% of the time, the tops of the iliac crests will be in the vicinity of the L4–L5 disc space.
6. L4 is shaped like a block H or X, and L5 is shaped like a block I on its side. L1, L2, and L3 tend to be U-shaped.
7. The lowest bone mineral content and bone mineral density is generally found at L1.
8. When in doubt, determine L4 and/or L5 by the shape and label from the bottom up.

Appendix VII

Conversion Formulas

PA SPINE CONVERSIONS BETWEEN CENTRAL DXA DEVICES* (1)

$$\text{Hologic QDR-2000 Spine}_{\text{BMD}} = (0.906 \times \text{Lunar DPX-L Spine}_{\text{BMD}}) - 0.025$$

$$\text{Hologic QDR-2000 Spine}_{\text{BMD}} = (0.912 \times \text{Norland XR-26 Spine}_{\text{BMD}}) + 0.088$$

$$\text{Lunar DPX-L Spine}_{\text{BMD}} = (1.074 \times \text{Hologic QDR-2000 Spine}_{\text{BMD}}) + 0.054$$

$$\text{Lunar DPX-L Spine}_{\text{BMD}} = (0.995 \times \text{Norland XR-26 Spine}_{\text{BMD}}) + 0.135$$

$$\text{Norland XR-26 Spine}_{\text{BMD}} = (0.983 \times \text{Lunar DPX-L Spine}_{\text{BMD}}) - 0.112$$

$$\text{Norland XR-26 Spine}_{\text{BMD}} = (1.068 \times \text{Hologic QDR-2000 Spine}_{\text{BMD}}) - 0.070$$

FEMORAL NECK BMD CONVERSIONS BETWEEN CENTRAL DXA DEVICES* (1)

$$\text{Hologic QDR-2000 Neck}_{\text{BMD}} = (0.836 \times \text{Lunar DPX-L Neck}_{\text{BMD}}) - 0.008$$

$$\text{Hologic QDR-2000 Neck}_{\text{BMD}} = (0.836 \times \text{Norland XR-26 Neck}_{\text{BMD}}) + 0.051$$

$$\text{Lunar DPX-L Neck}_{\text{BMD}} = (1.013 \times \text{Hologic QDR-2000 Neck}_{\text{BMD}}) + 0.142$$

$$\text{Lunar DPX-L Neck}_{\text{BMD}} = (0.945 \times \text{Norland XR-26 Neck}_{\text{BMD}}) + 0.115$$

$$\text{Norland XR-26 Neck}_{\text{BMD}} = (0.961 \times \text{Lunar DPX-L Neck}_{\text{BMD}}) - 0.037$$

$$\text{Norland XR-26 Neck}_{\text{BMD}} = (1.030 \times \text{Hologic QDR-2000 Neck}_{\text{BMD}}) + 0.058$$

*Although specific models of the central dual-energy X-ray absorptiometry devices are noted in the equations, the formulas may be used to convert bone mineral density (BMD) measured on any model for a given manufacturer to the BMD for any model of the other manufacturer. It must be recognized however that the error in these conversions is too great to allow serial monitoring of BMD to be done using devices from different manufacturers.

STANDARDIZED BMD (sBMD) CALCULATIONS FOR PA SPINE FOR CENTRAL DXA DEVICES[†] (2)

$$\text{sBMD}_{\text{SPINE}} = 1000 (1.0761 \times \text{Norland XR-26 BMD}_{\text{SPINE}})$$

$$\text{sBMD}_{\text{SPINE}} = 1000 (0.9522 \times \text{Lunar DPX-L BMD}_{\text{SPINE}})$$

$$\text{sBMD}_{\text{SPINE}} = 1000 (1.0755 \times \text{Hologic QDR-2000 BMD}_{\text{SPINE}})$$

STANDARDIZED BMD (sBMD) CALCULATIONS FOR TOTAL HIP FOR CENTRAL DXA DEVICES[§] (3)

$$\text{sBMD}_{\text{TOTAL HIP}} = 1000 [(1.012 \times \text{Norland XR-26 BMD}_{\text{TOTAL HIP}}) + 0.006]$$

$$\text{sBMD}_{\text{TOTAL HIP}} = 1000 [(0.979 \times \text{Lunar DPX-L BMD}_{\text{TOTAL HIP}}) - 0.031]$$

$$\text{sBMD}_{\text{TOTAL HIP}} = 1000 [(1.008 \times \text{Hologic QDR-2000 BMD}_{\text{TOTAL HIP}}) + 0.006]$$

STANDARDIZED BMD (sBMD) CALCULATIONS FOR HIP SUB-REGIONS FOR CENTRAL DXA DEVICES[¶] (4)

$$\text{sBMD}_{\text{FEMORAL NECK}} = 1000 [(1.087 \times \text{Hologic BMD}_{\text{FEMORAL NECK}}) + 0.019]$$

$$\text{sBMD}_{\text{FEMORAL NECK}} = 1000 [(0.939 \times \text{Lunar BMD}_{\text{FEMORAL NECK}}) - 0.023]$$

$$\text{sBMD}_{\text{FEMORAL NECK}} = 1000 [(0.985 \times \text{Norland BMD}_{\text{FEMORAL NECK}}) + 0.006]$$

$$\text{sBMD}_{\text{TROCHANTER}} = 1000 [(1.105 \times \text{Hologic BMD}_{\text{TROCHANTER}}) - 0.017]$$

$$\text{sBMD}_{\text{TROCHANTER}} = 1000 [(0.949 \times \text{Lunar BMD}_{\text{TROCHANTER}}) - 0.042]$$

$$\text{sBMD}_{\text{TROCHANTER}} = 1000 [(0.961 \times \text{Norland BMD}_{\text{TROCHANTER}}) + 0.057]$$

[†]All equations are multiplied by 1000 to express the sBMD in mg/cm² instead of g/cm².

[§]All equations are multiplied by 1000 to express the sBMD in mg/cm² instead of g/cm². The term total hip and total femur are interchangeable.

[¶]All equations are multiplied by 1000 to express the sBMD in mg/cm² instead of g/cm².

$$sBMD_{WARD'S} = 1000 [(0.940 \times \text{Hologic BMD}_{WARD'S}) + 0.101]$$

$$sBMD_{WARD'S} = 1000 [(0.980 \times \text{Lunar BMD}_{WARD'S}) - 0.106]$$

$$sBMD_{WARD'S} = 1000 [(1.091 \times \text{Norland BMD}_{WARD'S}) + 0.001]$$

**STANDARDIZED BMD CALCULATIONS FOR THE
ULTRADISTAL (su), MID (sm), AND PROXIMAL (sp)
FOREARM FOR FOUR DXA DEVICES (5)**

$$suBMD = (0.945 \times \text{PIXIBMD}) + 0.015$$

$$suBMD = (1.158 \times \text{Hologic Radius} + \text{Ulna Ultradistal BMD}) - 0.019$$

$$suBMD = (0.802 \times \text{Osteometer BMD}) + 0.071$$

$$suBMD = (1.027 \times \text{Norland Distal BMD}) + 0.084$$

$$smBMD = (1.011 \times \text{PIXI BMD}) + 0.033$$

$$smBMD = (0.894 \times \text{Hologic Radius} + \text{Ulna Mid BMD}) - 0.030$$

$$smBMD = (0.856 \times \text{Osteometer BMD}) + 0.094$$

$$smBMD = (1.106 \times \text{Norland Distal BMD}) + 0.105$$

$$spBMD = (1.091 \times \text{PIXI BMD}) + 0.119$$

$$spBMD = (0.861 \times \text{Hologic Radius} + \text{Ulna } \frac{1}{3}\text{BMD}) + 0.020$$

$$spBMD = (0.917 \times \text{Osteometer BMD}) + 0.188$$

$$spBMD = (0.596 \times \text{Norland Proximal BMD}) + 0.114$$

**METRIC/ENGLISH CONVERSIONS
FOR UNITS OF MEASURE**

English to Metric

1 inch = 2.54 centimeters

1 lb = 0.45 kg

Degrees in F = (1.8 C°) + 32

1 rad = 100 Gy

1 rem = 100 Sv

Metric to English

1 centimeter = 0.39 inches

1 kg = 2.20 lb

Degrees in C = (F° - 32) × 0.555

1 Gy = 0.01 rad

1 Sv = 0.01 rem

MATHEMATICAL SYMBOLS AND DESIGNATIONS OF MULTIPLES

<i>Symbol</i>	<i>Designation</i>	<i>Factor</i>
G	giga-	10^9
M	mega-	10^6
k	kilo-	10^3
d	deci-	10^{-1}
c	centi-	10^{-2}
m	milli-	10^{-3}
μ	micro-	10^{-6}
n	nano-	10^{-9}
p	pico-	10^{-12}

REFERENCES

1. Genant, H. K., Grampp, S., Gluer, C. C., et al. (1994) Universal standardization for dual X-ray absorptiometry: patient and phantom cross-calibration results. *J. Bone Miner. Res.* **9**, 1503–1514.
2. Steiger, P. (1995) Standardization of spine BMD measurements. *J. Bone Miner. Res.* **10**, 1602–1603.
3. Hanson J. (1997) Standardization of femur BMD. *J. Bone Miner. Res.* **12**, 1316–1317.
4. Lu, Y., Fuerst, T., Hui, S., Genant, H. K. (2001) Standardization of bone mineral density at femoral neck, trochanter and Ward's triangle. *Osteoporos. Int.* **12**, 438–444.
5. Shepherd, J. A., Cheng, X. G., Lu, Y., et al. (2002) Universal standardization of forearm bone densitometry. *J. Bone Miner. Res.* **17**, 734–745.

Appendix VIII

Recommended Procedures for Short-Term Precision Studies

GENERAL PROCEDURES

1. Complete all scans within 1 month.
2. Determine precision values for each skeletal site to be used for serial measurements. The same individuals may be used for each site, however.
3. For assessing the skill level of the technologist, choose a group of individuals of normal body size in whom a normal bone density is anticipated.
4. For establishing precision values for a facility, choose a group of individuals that are representative of the type of patients seen at the facility.
5. Utilize an appropriate combination of number of individuals and scans per individual to give the study sufficient validity.
6. Each technologist should perform a precision study.
7. If more than one technologist performs bone density studies at a facility, a precision study should also be done in which all technologists participate.
8. Precision studies should be repeated if a new technologist begins work or if there is a major equipment change.

**RECOMMENDED NUMBER OF INDIVIDUALS
AND NUMBER OF SCANS/INDIVIDUAL FOR
A SHORT-TERM PRECISION STUDY**

<i>Number of individuals</i>	<i>Number of scans/individual</i>
10	4
15	3
30	2

CALCULATIONS*

1. Calculate the average in g/cm² for each set of scans on an individual:

$$\bar{X}_j = \frac{\sum_{j=1}^i X_{ij}}{n}$$

where \bar{X}_j is the average for an individual, Ms. J; $\sum_{j=1}^i$ means to sum the first through the i th measurement; X_{ij} is each of the measured values; and n is the number of scans.

2. Calculate the SD in g/cm² for each set of scans on an individual.

$$SD_j = \sqrt{\frac{\sum_{j=1}^i (X_{ij} - \bar{X})^2}{n - 1}}$$

3. Calculate the percent coefficient of variation (%CV) for each individual.

$$\%CV_j = 100 \left(\frac{SD_j}{\bar{X}_j} \right)$$

*These calculations will be performed automatically by the Precision Calculator on the accompanying CD-ROM for a precision study involving 15 individuals who undergo three scans each.

4. Calculate the average value in g/cm² for the entire group.

$$\bar{X}_G = \frac{\sum_{m=1}^i \bar{X}_{im}}{m_G}$$

where \bar{X}_G is the average for the entire group; $\sum_{m=1}^i$ means to sum the first through the i th average; \bar{X}_{im} is the average for each set of measurements; and m_G is the number of individuals in the group.

5. Find the root mean square-standard deviation (RMS-SD) in g/cm² for the entire group.

$$SD_{RMS} = \sqrt{\frac{\sum_{m=1}^i (SD_{im})^2}{m_G}}$$

where SD_{im} is the standard deviation for each set of measurements.

6. Find the root mean square percent coefficient of variation (RMS-%CV) for the entire group.

$$\%CV_{RMS} = \sqrt{\frac{\sum_{m=1}^i (CV_{im})^2}{m_G}} \times 100$$

where CV_{im} is the coefficient of variation for each set of measurements.

Appendix IX

Least Significant Change

CALCULATION OF LEAST SIGNIFICANT CHANGE (LSC)*

For 1 × 1 Measurements

<i>For a confidence level of</i>	<i>Multiply precision value by</i>
99%	3.65
95%	2.77
90%	2.33
80%	1.81

For 2 × 2 Measurements

<i>For a confidence level of</i>	<i>Multiply precision value by</i>
99%	2.58
95%	1.96
90%	1.65
80%	1.28

CALCULATION OF TIME TO LSC

The time required to achieve the LSC is the time interval that should be allowed before repeating a study.

$$\text{Time to LSC} = \text{LSC} \div \text{Anticipated Rate of Change}$$

*The calculations of the LSC for 1 × 1 measurements at 95% confidence is performed automatically using the Precision Calculator found on the CD-ROM that accompanies this book.

Appendix X

Quality Control Shewhart Rules

<i>Rule name</i>	<i>Description</i>
3 SD or 1.5% rule	A phantom value exceeds the average ± 3 SDs or 1.5%.
2 SD twice or 1.0% twice rule	Two consecutive phantom values on the same side of the average exceed the average ± 2 SDs or 1%.
Range of 4 SD or range of 2% rule	Two consecutive phantom values differ by more than 4 SDs or 2%.
4 ± 1 SD or 4 $\pm 0.5\%$ rule	Four consecutive phantom values on the same side of the average exceed the average ± 1 SD or 0.5%.
Mean $\times 10$ rule	Ten consecutive phantom values fall on the same side of the average, regardless of the distance from the average.

Appendix XI

Glossary of Computer Terms

Many of these terms and phrases are discussed in Chapter 5, but some are not. It is likely that the technologist will encounter all of these terms and phrases at some point in the practice of densitometry.

Applet—A very small program or application.

Application(s)—A set of instructions or a program that performs work unrelated to the actual operation of the computer itself. The programs that operate bone densitometers and analyze the data are applications. Other examples are word processors, photo editors, and spreadsheet programs.

Apps—Short for application.

ARF—An abbreviation and acronym for a common computer message indicating three possible courses of action when an attempted action has failed. The possible actions are abort, retry, or fail.

Autoexec.bat file—This is the file that contains instructions that must be loaded every time the computer is started. It is normally found on the C drive.

Backslash—A character on the keyboard often used in computer commands. It is important to distinguish the backslash, “\,” from the forward slash, “/.”

Bit—A binary digit, either 0 or 1.

Boot—To start the computer. The term comes from the old expression of “pulling yourself up by the bootstraps.” In this case, the computer has to pull up or load its operating system in order to start and then load other programs.

BSOD—The abbreviation for blue screen of death. This results when the Windows operating system freezes and a blue screen appears with an error message. To restore the computer to working status, a reboot is usually required.

Bug—An error in a computer program. The first bug was a real moth.

Bundled software—Software that is sold in conjunction with hardware.

Burn—Slang for writing data to a CD-R, CD-RW, or DVD-R, or DVD-RW.

Bus—A mode of communication within the computer. Different modes of communication or languages are described as having different bus architectures. The bus transmits data between the input-output devices and the computer memory and CPU. A computer may utilize different bus architectures to communicate with various peripheral devices. Some of these different bus architectures are called ISA, PCI, VESA, USB, and FireWire. The term *bus* comes from the analogy of a bus carrying many people back and forth to different destinations. In the case of the computer, the bus carries information between the CPU and the various peripheral devices (like a printer or optical scanner) in both directions.

Byte—The number of bits required to indicate one character. Usually eight bits equal one byte.

Card—This is a small circuit board that can be added to a computer by fitting or inserting it into a special slot. These circuit boards are often required in order for some peripheral devices to communicate with the computer.

CD—The abbreviation for compact disk.

CD-E—The abbreviation for compact disk-erasable. This is the same type of optical storage media as a CD-RW. CD-RW has become the preferred term.

CD-ROM—The abbreviation for compact disk read only memory. This is a type of optical storage media from which information can only be retrieved. Information cannot be written to the CD-ROM nor can it be erased by the user.

CD-R—The abbreviation for compact disk-writable. A compact disk to which data or audio can be written by the user, if the computer is equipped with a CD-R drive.

CD-RW—The abbreviation for compact disk-rewritable. A compact disk to which data can be written, erased, and re-written by the user if the computer is equipped with a CD-RW drive. This type of CD is also sometimes called a CD-E, for compact disk-erasable.

Click—To briefly depress a button on the mouse.

Coaster—A CD that is no longer usable.

Compact Flash Card—A small, flash memory card that may hold up to 6 GB of data. There are two types: type I and type II.

Config.sys file—A computer file that contains information on how the various devices will communicate with the computer and how computer memory is to be used. This file is normally found on the C drive.

Control-Alt-Del—A combination of keys on the keyboard, which when depressed simultaneously, will re-boot the computer or shut down a program.

Cookie—A file from a Web site with which you have communicated that is sent to your Internet browser and stored on the hard drive that allows the Web site to identify you when you visit that web site again. Some cookies may also provide additional information about you to the Web site.

CPU—The abbreviation for central processing unit. The CPU controls the operation of the computer. The microprocessor in the computer contains the CPU. The computer is often characterized by the type of CPU that it contains. For example, Celeron, AMD-64, and Pentium IV are all types of CPUs. Depending on the CPU that it contains, a computer may be called an AMD or Pentium computer.

Crash—The term indicating that the hardware has failed or an error has occurred in a program that causes the computer to become inoperable.

CRT—The abbreviation for cathode ray tube. Many computer monitors and televisions utilize CRT displays. Phosphor dots inside a glass tube are excited by an electron beam, creating an image on the screen. CRT displays are generally curved and such monitors are much heavier than LCD displays.

Daemon—A software program that is automatically triggered by some event, but not by the user and which runs in the background of other computer programs.

Defrag—To use a defragmenter program.

Defragmenter—A type of utility program that organizes files on the hard drive or diskettes, making computer operations smoother.

Degauss—The act of neutralizing electromagnetic energy. For example, some monitors may automatically degauss when turned on to prevent image distortion.

Desktop—A term used to describe computers that are rectangular in shape, with much greater width and depth than height, such that sitting them on a desktop is feasible. The monitor will often sit on top of this computer. The term is also used to describe the opening screen of a graphical interface operating system like Microsoft® Windows.

DICOM—The abbreviation for the Digital Imaging and Communications in Medicine. This term is commonly used to refer to an image file format that meets Part 10 of the DICOM standard created by the National Electrical Manufacturers Association to facilitate the sharing and viewing of medical images.

DIMM—The abbreviation for dual inline memory module, a type of RAM circuit board. It is pronounced like the word dim.

Disc, Disk—Short for diskette.

Disk or disc drive—A device used to access and write data to a disk.

Diskette—A type of magnetic data storage media. Although this term could apply to any of several different types of magnetic storage media, in common use, it refers to a 3½-in. square diskette.

Download—When a file or program is sent from a Web site to a user's computer.

Double click—To briefly and in succession depress a button on a mouse twice.

DPI—The abbreviation for dots per inch. This refers to the resolution of a monitor, optical scanner or printer. The value that is expressed is actually the dots per square inch.

DVD—The abbreviation for digital video disk. This is a type of optical storage media that can hold such large amounts of data that it is usually described in GB. DVD is synonymous with DVD-ROM.

DVD-ROM—The abbreviation for digital video disk-read only memory. This is a DVD from which data can only be read. Data cannot be written to this DVD by the user.

DVD-R—See DVD-RAM.

DVD-RAM—The abbreviation for digital video disk-random access memory. This is a DVD to which data can be written by the user in DVD writable drives. This type of optical storage media is not yet in common use by personal computer users, but it offers the potential of storing GBs of data on one disc.

E-mail—Short for electronic mail which are text messages sent over the Internet or other type of network.

Executable files—A file with the extension “.exe” (pronounced dot-e-x-e) or “.com” (pronounced dot-com). These files initiate programs when run by a user rather than store data. Consequently, they are also called program files.

Extensions—Usually three or four letters that follow the period (.) in the name of a file that indicate the type of file. For example, “.doc” is a document file. The extensions “.tif,” “.pcx,” and “.gif” indicate that the files are graphics files.

Firewall—This is software or hardware that prevents unwanted access to computer files from an outside source.

Flash memory—This refers to memory devices that utilize solid state electronics.

Floppy—A type of diskette that is 3½ square in. with a hard plastic outer covering. A typical floppy disk holds approximately 1.44 MB of data.

Floppy drive—A drive that can read and write data to a floppy diskette. This drive is traditionally assigned the letter “a.”

Footprint—The area or size of the space on the desktop or floor that is required by the computer.

Format—To prepare a storage media to accept data.

GB—Abbreviation for gigabyte. A measure of computer storage that contains 1 billion bytes or 1000 megabytes.

GUI—The abbreviation for graphical user interface. This refers to operating systems that use icons to carry out commands instead of written characters. Microsoft® Windows and Macintosh® operating systems are GUIs as opposed to DOS®, which is a character-based interface.

Hacker—An individual who accesses computer data without authorization. A computer that has been accessed illegally is said to have been “hacked.”

Hard drive—This is the computer’s internal magnetic storage media and the drive that writes data to it. It is traditionally assigned the capital letter “C” to distinguish it from drives for which there is an external access for the user, such as a floppy disk drive that is usually assigned the lower case letter “a.” The term hard drive is used to refer both to the drive and to the storage media that the drive contains. The hard drive (or really the storage media within the hard drive) can be sub-divided (or partitioned). One subdivision will retain the “C” designation, whereas the other subdivisions will be assigned other letters, such as “D” or “E.” The lower case letters of “a” and “b” are reserved for disk drives with external user access.

Hardware—This refers to any and all of the physical components of the computer such as the motherboard, circuitry, microprocessor, and disk drives.

Http—The abbreviation for hypertext transport protocol. This designation is normally part of the URL for a Web site or document.

Input device—Any device that allows the input of information into the computer. Examples of input devices are the keyboard, mouse, and optical scanners.

Internet—A network of smaller networks and individual computers worldwide.

ISA—The abbreviation for industry standard architecture. A type of bus communication.

ISP—The abbreviation for Internet service provider. An organization or company that provides access to the Internet by allowing the user to connect to its own computers, usually for a fee.

JPEG—The abbreviation for Joint Photographic Experts Group. A file extension for photographs.

KB—The abbreviation for kilobytes. 1 kilobyte = 1025 bytes.

Kbps—The abbreviation for kilobits per second. A unit of measure for the speed of a modem to indicate how fast data is being transmitted over a phone line. 1 Kbps is equal to 1000 bits.

Laptop—A small computer, generally weighing under 7 lbs, that opens like a notebook to reveal a screen and keyboard.

Launch—To start a program.

LCD—The abbreviation for liquid crystal display. This is a display technology used in calculators, laptop computers and now in full size computer monitors. LCD displays are flat and lightweight by comparison to CRT monitors.

Mac—Short for Macintosh, a type of computer operating system.

MB—The abbreviation for megabyte. A measure of computer storage that contains approximately 1 million bytes.

MHz—The abbreviation for megahertz. The speed of the CPU is measured in megahertz with one megahertz equal to approximately 1 million cycles per second. Today's computers typically have CPUs of 500 MHz or faster.

Minitower—A tower style computer that is generally half as tall as a regular tower.

MMC—An abbreviation for multi-media card.

Modem—An acronym for modulator-demodulator. This device encodes data for transmission over phone lines, fiber optic cable, or other types of communications media.

Moiré—Refers to the distortion of an image by electronic interference or differences in resolution.

Motherboard—The main circuit board of the computer.

Mouse—An input device that allows the user to point to areas on the monitor screen and by depressing or clicking a button on the mouse initiate actions by the computer.

Multimedia card—A small flash memory module.

OCR—The abbreviation for optical character recognition. This is a type of software that allows text that has been converted to a digital image by a scanner to be converted back into text so that it can be edited on a computer.

Optical storage media—This refers to storage media such as CD-ROM, CD-R, CD-RW, and DVD in which a laser is used to read and write data to the media.

Output device—Any device that displays the end result of the computer's calculations or actions. A monitor and printer are examples of output devices.

Parallel port—This port is reserved for a cable having parallel wires, which allows data transfer at a speed of 8 bits (1 byte) at a time. This port is commonly used by printers and is designated LPT1 or LPT2. It will generally have two rows of pins receptacles for a total of 25 pin receptacles to which the printer cable will attach.

PC— personal computer. The abbreviation also implies an IBM-compatible computer rather than a Macintosh.

PCI—The abbreviation for peripheral component interconnect, a type of bus.

Peripherals—Devices that are attached to the computer by cables. Examples are devices such as a printer, optical scanner, keyboard, mouse, and monitor.

PCMCIA—The abbreviation for Personal Computer Memory Card International Association, which developed standards for flash memory. The abbreviation is also applied to small flash memory cards and flash memory card slots on laptop computers.

Pixel—The smallest fragment of an image that a monitor or printer can display. Pixel is a contraction of picture element. Each pixel on a color monitor contains a red, green, and blue dot.

Ports—These are the openings or connectors on the back of the computer to which are attached the cables of the various peripheral devices, like printers and monitors.

PS/2 port—This is a small round six-pin receptacle port that is designed to accept the cable from a mouse or keyboard. It was originally developed by IBM for its line of PS/2 computers but has since become the standard for other manufacturers as well.

RAM—The abbreviation and acronym for random-access memory. This is the temporary or short-term memory in the computer into which program instructions are loaded. The amount of RAM is normally measured in MB. Most computers today will have a minimum of 128 MB of RAM.

Reboot—Re-starting the computer.

Resolution—The clarity of an image on a printer or monitor. This can be measured in DPI or pixels.

ROM—The abbreviation and acronym for read only memory. Data can be retrieved from this memory location but data cannot be written to it or erased by the user.

Scanner—This term refers to an input device that converts an image or text document into a digital image that can be transferred to the computer. Text that is converted to a digital image can be changed back to text with optical character recognition (OCR) software so that it can be edited like any other document.

Serial port—A port that allows data transfer at a rate of 1 bit at a time. This port is generally used for input devices like a mouse, keyboard or bone densitometer. This port generally has two rows of pins for a total of nine pins.

Smart media card—A small flash memory card. Also called a solid state floppy disk card, as it resembles a miniature floppy disk. It may hold up to 128 MB of data.

SCSI—Pronounced “skuzzy,” the abbreviation for small computer systems interface. This is a type of bus architecture. Devices that utilize SCSI to communicate with the computer are often called SCSI or “scuzzy” devices.

SDRAM—A type of RAM circuit board.

SD—An abbreviation for secure digital.

Secure digital cards—A solid-state flash memory module similar to a multimedia card in technology but that can be copy controlled.

SIMM—The abbreviation for single inline memory module. This is a type of RAM circuit board that will be found inserted into the motherboard of the computer. A computer may have more than 1 SIMM.

Slot(s) —A socket in the computer designed to accept add-in circuit boards. Slots are often designated by the type of communication or bus that they employ, such as PCI or ISA.

Software—A set of instructions or program.

Spam—Junk e-mail. Someone who has received junk e-mail is said to have been spammed.

Spyware—Software that records and transmits internet activity on your computer. This type of software may be installed on the computer without your knowledge as a consequence of visiting some Web sites. Software programs also now exist that will identify and remove such programs from your computer.

SSP—An abbreviation for service storage provider. This is a business that stores data for other businesses.

Star-Dot-Star—A description of the key combination of “*.*” (the key sequence of asterik-period-asterik) that is used in writing the name of a file to substitute for “all files.”

Super floppy—A type of diskette that contains a much greater amount of data than the traditional 1.44 MB floppy disk. Super floppies may contain over 100 MB of data.

TIFF—A tagged image format file. This is a graphics file type that can be viewed on an IBM-compatible computer or a MAC, regardless of which type of operating system was used to create the file.

Tower—This term describes a computer that is much taller than it is wide such that it is generally placed on the floor, rather than on a desktop.

Upload—The opposite of download. When the user sends a file or program to a Web site.

URL—The abbreviation for universal resource locator. The URL is the system used for addresses on the Internet.

USB—Universal serial bus. This was introduced in 1995 as a means of standardizing the types of connections or bus used by peripheral devices to communicate with the computer, rather than having various devices use ISA, PCI, or VESA connections.

USB port—A port using USB.

UPS—The abbreviation for uninterruptible power supply. This is a device that will provide power to the computer in the event of a general power failure in order to allow the user to safely shut down the computer. The UPS will generally provide 20 minutes or more of additional power depending on the type of device purchased.

Virus—A program that is designed to disrupt computer operation or alter or destroy data. Viruses are transmitted from computer to computer when files from an infected computer are loaded onto another computer, either by disk or by downloading from the Internet.

WAV—A file format for sound files.

Web—Short for World Wide Web.

Wi-Fi—A contraction of wireless fidelity. This is a standard created by the Wireless Ethernet Compatibility Alliance to ensure compatibility in wireless data transfer.

World Wide Web—The interface for the Internet.

Worm—A highly destructive software program often hidden in or attached to other programs, which will replicate itself until the capacity of the drive or network is exhausted, causing major malfunctions.

www—The abbreviation for World Wide Web.

Zip disk—A type of magnetic storage media that will hold 100 to 750 MB of data. It is approximately 3¼ square in. with a hard plastic shell.

Zip drive—A disk drive designed to read and write data to zip disks.

Zip file—A computer file that has been compressed in size in order to facilitate storage or transfer. It will usually have the file extension “.zip.” When file is compressed it is said to have been “zipped.”

Appendix XII

The CD-ROM Companion

There are three folders in the CD-ROM: Precision Calculator Companion, the Patient Questionnaire, and the CME Review. Put the CD-ROM into the CD-ROM drive of your computer. The CD is self-launching and will open automatically. All the folders can be accessed from the opening page. This is the simplest way to access the contents of the CD-ROM Companion. The folders may also be accessed through My computer or through Windows Explorer. The Precision Calculator Companion requires Microsoft® Excel. To view the Patient Questionnaire, Microsoft Word must be installed on your computer. The CME Review is a stand-alone program. Microsoft® Word and Microsoft® Excel may also be used to open their respective programs directly.

Precision Calculator Companion

There is only one Microsoft® Excel workbook file in this folder. There are two spreadsheets in the workbook. The first spreadsheet is the Precision Calculator Companion. Instructions are given on the spreadsheet. This spreadsheet will allow you to calculate precision as the root mean square-standard deviation (RMS-SD) and RMS-percent coefficient of variation (RMS-%CV) for a group of 15 patients studied 3 times each. The spreadsheet will also calculate the $_{1x1}LSC^{95}$ for this level of precision.

The second spreadsheet is the Statistical Confidence Calculator. The instructions are included on the spreadsheet. This spreadsheet will allow you to calculate the absolute and percent change from baseline for two studies as well as the level of statistical confidence for that change and any precision value.

Each spreadsheet can be printed once the calculations are completed. The instructions will not be visible on the printout. The spreadsheets are locked but not password protected. This was done to prevent inadvertent erasure of the formulas. As long as the spreadsheets are not deliberately unlocked, it is not possible to erase the formulas embedded in the spreadsheets.

Patient Questionnaire

There is only one file in the Patient Questionnaire folder, the Patient Questionnaire. The questionnaire is not protected in any way and can be altered to suit your practice's needs.

Continuing Education Review for Bone Densitometry for Technologists, Second Edition

To begin the review, click on the link from the Companion CD launch page. Follow the on-screen instructions. This is a 116-question review that consists of both multiple choice and true-false questions. Each question has only one right answer. You may stop the review at any time and resume at a later date. After completing the review, print out the answer sheet and sign and date it in the spaces indicated. Identifying data must be entered on the answer sheet before printing. A score of 75% or higher will result in the awarding of 15 hours of Category A credit acceptable to the American Society of Radiologic Technologists.

The following 3 items must be included with any submission:

1. A completed answer sheet.
2. A self-addressed, stamped envelope.
3. A processing fee of \$15 in the form of a money order, cashier's check, or personal check, made payable to Lori Lewis.

Send your submission to:

Lori Lewis, MRT
Clinical Research Center of North Texas
2921 Country Club Road, Suite 101
Denton, Texas 76210-8625

Please allow 4 weeks for processing.

INDEX

A

- accuDEXA™, specifications, 138, 139
- Accuracy, definition, 2–4
- Achilles+™, specifications, 148, 149
- Achilles Express™, specifications, 149
- Achilles InSight™, specifications, 150, 152
- Actonel™, osteoporosis prevention and treatment, 280, 281
- AGCT, *see* Army General Classification Test
- Age, percent comparison and standard score adjustment, 17, 18
- Age-regression graph, interpretation, 19, 300–303
- Air displacement plethysmography, body composition analysis, 352
- Alendronate (Fosamax®), osteoporosis prevention and treatment, 279, 280
- Aortic calcification, effects on densitometry measurements, 75–79
- Apollo™, specifications, 139–141
- Appendicular skeleton, definition, 5, 6
- Arm dominance, effects on densitometry measurements, 97, 98
- Army General Classification Test (AGCT), score, 16, 17
- Artifacts,
 - aortic calcification, 75–79
 - miscellaneous causes, 84
 - osteophytes, 75–77, 93
 - vertebral fracture, 73–75
 - vertebral rotation, 81–83
- Automated Osteogram®, specifications, 107, 108
- Axial skeleton, definition, 4, 5

B

- Baseline phantom value, determination, 240, 241

- BIA, *see* Bioelectric impedance analysis
- Bioelectric impedance analysis (BIA),
 - body composition analysis, 351, 352
- Bisphosphonates,
 - alendronate, 279, 280
 - dosing, 282
 - ibandronate, 281, 282
 - risedronate, 280, 281
 - safety, 283, 283
- BMAD, *see* Bone mineral apparent density
- BMC, *see* Bone mineral concentration
- BMD, *see* Bone mineral density
- BMI, *see* Body mass index
- Body composition analysis,
 - air displacement plethysmography, 352
 - bioelectric impedance analysis, 351, 352
 - body mass index, 346, 347
 - clinical applications, 361
 - dual-energy X-ray absorptiometry, accuracy, 356–358
 - advantages, 345, 346, 353
 - examples, 354–356
 - height and weight considerations, 359–361
 - precision, 358, 359
 - scan acquisition, 353, 354
 - fat functions and ranges, 348, 349
 - near infrared interactance, 352, 353
 - skinfold measurements, 350, 351
 - underwater weighing, 349, 350
- Body mass index (BMI),
 - calculation, 346, 347
 - classification, 347, 348
- Bona Fide Spine Phantom, features, 234
- Bone marrow, radiation damage, 219
- Bone Mass Measurement Act of 1997, 268, 270, 379

- Bone mineral apparent density (BMAD),
 - calculation, 10, 11
- Bone mineral concentration (BMC),
 - bone area adjustment, 318, 319
 - developmental changes, 320–322
 - measurement and bone mineral density
 - calculation, 8, 9, 292
- Bone mineral density (BMD),
 - average spine bone density
 - determination, 11
 - bone size effect on areal density, 9, 10
 - calculation, 8, 9, 292
 - developmental changes, 320–322
 - report review, 308–311
- Boniva™, osteoporosis prevention
 - and treatment, 281, 282
- C**
- Calcaneus, anatomy, 100
- Calcar femorale thickness, measurement, 32, 33
- Calcium supplements, osteoporosis
 - prevention and treatment, 273–275
- Central skeleton, definition, 6
- Coefficient of variation (CV),
 - calculation, 192
 - precision expression, 4
- Computers,
 - components,
 - central processing units, 167, 168
 - disk drives, 169, 170
 - hard drives, 168, 169
 - keyboard, 170, 171
 - monitors, 173, 174
 - motherboard, 167
 - mouse, 172
 - overview, 166, 167
 - ports,
 - keyboard and mouse, 175
 - modem, 178
 - monitor, 178
 - network, 178
 - parallel ports, 175, 176
 - power cord, 177, 178
 - serial ports, 176, 177
 - USB ports, 177
 - printers, 174, 175
 - random access memory, 167
 - slots, 167
 - trackball, 172
 - instrument coupling, 163, 164
 - maintenance, 186, 187
 - storage media,
 - data protection, 184, 185
 - flash memory, 183, 184
 - magnetic media, 180–182
 - optical storage media, 182, 183
 - types,
 - desktop, 164
 - laptop, 164
 - PC vs Macintosh, 165
- Continuing education, resources, 408
- Cortical bone, sites, 6–8
- CPT codes, bone densitometry, 381, 382
- Cross-sectional moment of inertia
 - (CSMI), proximal femur
 - morphometry, 342, 344
- CSMI, *see* Cross-sectional moment of inertia
- Curie, radiation unit, 214
- CUSUM charts, quality control, 245, 246, 248, 249
- CV, *see* Coefficient of variation
- D**
- Delphi™, specifications, 109–111
- DexaCare® G4, specifications, 141, 142
- Diagnostic category,
 - assignment based on World Health
 - Organization criteria, 303, 305
 - conflicting diagnosis from
 - measurement of multiple sites, 305–308
- Discovery™, specifications, 111–114
- DPX Bravo®, specifications, 114, 115
- DPX Duo®, specifications, 115–117
- DPX MD™, specifications, 119, 120
- DPX MD+™, specifications, 120, 121
- DPX-IQ™, specifications, 117–119
- DPX-NT™, specifications, 121–123
- DTU-one UltraSure®, specifications, 152–154
- DTX-200 DexaCare®, specifications, 142–144
- Dual-energy X-ray absorptiometry (DXA),

- artifacts, *see* Artifacts
- body composition analysis,
 - accuracy, 356–358
 - advantages, 345, 346, 353
 - examples, 354–356
 - height and weight considerations, 359–361
 - precision, 358, 359
 - scan acquisition, 353, 354
- fan-array spine imaging, 335–338
- instrumentation,
 - see* specific instruments
- NHANES III proximal femur data, 23–25
- posteroanterior spine labeling
 - guidelines, 383
- printout, *see* Reporting
- skeletal image features, 290–292
- DXA, *see* Dual-energy X-ray absorptiometry

E

- Effective dose equivalent, radiation unit, 216
- European Spine Phantom, features, 233, 234
- Evista®, *see* Raloxifene
- Excel™, specifications, 123, 124
- Excel™plus, specifications, 124, 125
- Exercise, osteoporosis prevention and treatment, 275, 276
- EXPERT@-XL, specifications, 126, 127
- Explorer™, specifications, 127–129

F

- Facet sclerosis, effects on densitometry measurements, 80
- Femur, *see* Proximal femur densitometry
- Film badge, personnel monitoring, 228
- Forearm densitometry,
 - arm dominance effects, 97, 98
 - artifacts, 98, 99
 - nomenclature, 94, 95
 - sites, 95, 295, 296
- Fortéo®, osteoporosis prevention and treatment, 283, 284
- Fosamax®, osteoporosis prevention and treatment, 279, 280

- Fracture,
 - effects on densitometry measurements, 73–75, 93
 - risks,
 - global fracture risk prediction, 299
 - osteoporosis, 265, 291
 - site-specific fracture risk prediction, 299
 - vertebral morphometry,
 - fan-array spine imaging, 335–338
 - fracture diagnosis, 330–332
 - Genat technique for fracture assessment, 332
 - prevalent fractures and future fracture risk prediction, 330
 - quantitative techniques for fracture assessment, 332–335

G, H

- Genat technique, fracture assessment, 332
- HAL, *see* Hip axis length
- Hip axis length (HAL), proximal femur morphometry, 339
- Hologic hip phantom, features, 235
- Hologic spine phantom, features, 235

I

- Ibandronate (Boniva™), osteoporosis prevention and treatment, 281, 282
- International Society for Clinical Densitometry (ISCD),
 - bone mass measurement guidelines, 268, 377, 378
 - contact information, 371
 - nomenclature guidelines, 25, 26
 - pediatric densitometry guidelines, 325
 - precision assessment guidelines, 203, 209–211
 - quality control guidelines, 231, 253, 255
- ISCD, *see* International Society for Clinical Densitometry

L

- LDS, *see* Low density spine
- Least significant change (LSC),
 - case study, 201–203

- determination, 197–200
 timing of repeat measurements, 200, 201, 210
- Leg dominance, effects on densitometry measurements, 93
- Low density spine (LDS), bone edge detection, 314, 315
- LSC, *see* Least significant change
- Lunar spine phantom, features, 235, 237
- M**
- Manufacturers, contact information, 367–371
- McCue C.U.B.A. Clinical™, specifications, 154–156
- Medicare,
 bone mass measurement reimbursement, 268, 270, 271, 379
 CPT codes for bone densitometry, 381, 382
- Metacarpals, anatomy, 100
- Metriscan™, specifications, 108, 109
- Miacalcin®, *see* Synthetic salmon calcitonin
- Morphometry, *see* Skeletal morphometry
- N**
- Near infrared interactance (NIR), body composition analysis, 352, 353
- NHANES III, proximal femur data, 23–25
- NIR, *see* Near infrared interactance
- Non-weight bearing skeleton, definition, 4
- O**
- Omnisense™ 7000S Ultrasound Bone Sonometer, specifications, 156–158
- Osteoarthritis, effects on densitometry measurements, 93, 94
- Osteogenesis imperfecta, types, 326
- Osteopenia, diagnostic criteria, 373
- Osteophytes, effects on densitometry measurements, 75–77, 93
- Osteoporosis,
 bone loss in aging, 265, 266
 bone mass measurement guidelines, American Association of Clinical Endocrinologists, 267, 375, 376
 American College of Obstetricians and Gynecologists, 267, 376
 International Society for Clinical Densitometry, 268, 377, 378
 National Osteoporosis Foundation, 266, 267, 375
 United States Preventive Services Task Force, 267, 377
- consequences, 263, 264
- definitions,
 consensus development conferences, 258, 259
 National Institutes of Health, 261, 262
 World Health Organization, 259–261, 373
- fracture risk, 265, 291
- organizations of interest, 371
- patient education materials, 284, 285
- peak bone density attainment, 264, 265
- pediatrics, 325, 326
- prevalence, 262, 263
- race differences, 266
- sex differences, 265
- treatment,
 antitabolic agents, 276
 bisphosphonates,
 alendronate, 279, 280
 dosing, 282
 ibandronate, 281, 282
 risedronate, 280, 281
 safety, 283, 283
 calcium supplements, 273–275
 estrogen replacement therapy, 276, 277
 exercise, 275, 276

- guidelines,
 - American Association of Clinical Endocrinologists, 271, 272
 - National Osteoporosis Foundation, 271
 - North American Menopause Society, 271, 272, 377
- lifestyle modification, 272, 273
- raloxifene, 277, 278
- teriparatide, 283, 284
- vitamin D supplements, 275
- Ovaries, radiation damage, 218, 219
- P**
- pDEXA®, specifications, 144, 145
- Peak bone density, attainment, 264, 265, 321
- Pediatric densitometry,
 - apron protection, 227
 - bone age determination, 315–317
 - bone edge detection, 313–315
 - bone size and shape considerations, 317–319
 - International Society for Clinical Densitometry guidelines, 325
 - reference databases, 324, 325
 - scan acquisition and analysis considerations, 314, 315
 - skeletal development and density changes, 320–322
 - specialization, 325, 326
 - standard score utilization, 322, 323
 - Tanner stages, 317
- Percent age-matched comparison, evaluation, 15
- Percent Young Adult comparison, evaluation, 14, 15
- Peripheral skeleton, definition, 6
- Phalanges, anatomy, 100
- Phantoms,
 - anthropomorphic phantoms, 233
 - automated procedures, 249–253
 - baseline phantom value determination, 240, 241
 - Bona Fide Spine Phantom, 234
 - CUSUM charts, 245, 246, 248, 249
 - European Spine Phantom, 233, 234
 - Hologic hip phantom, 235
 - Hologic spine phantom, 235
 - instrument manufacturers as suppliers, 232, 233
 - Lunar spine phantom, 235, 237
 - Shewart control chart,
 - generation, 238, 240, 243
 - interpretation, 240
 - Shewart rules,
 - origins, 242
 - percentage differences, 244, 245
 - setting, 243, 244
- PIXI®, specifications, 145–147
- Precision,
 - calculator on CD-ROM, 407
 - concept, 2–4, 189, 190
 - confidence interval between two measurements, 204–206
 - least significant change,
 - case study, 201–203
 - determination, 197–200
 - timing of repeat measurements, 200, 201, 210
 - level of confidence determination, 203, 204
 - studies,
 - coefficient of variation calculation, 192
 - importance, 206, 207
 - instrument consistency, 211
 - long-term studies, 197
 - root-mean-square coefficient of variation calculation, 193–196
 - root-mean-square standard deviation calculation, 193–196
 - short-term studies, 192–197
 - skeletal sites for monitoring, 207–210
 - standard deviation calculation, 191
- Pregnancy, radiation safety, 226, 229
- Prodigy™, specifications, 129–131
- Proximal femur densitometry,
 - anatomy, 88, 89
 - artifacts in densitometry measurements, 93, 94

- NHANES III data, 23–25
 regions of interest, 295
 rotation effects on densitometry
 measurements, 89, 91–93
- Proximal femur morphometry,
 cross-sectional moment of inertia,
 342, 344
 femoral neck width, 342
 femoral neck-shaft angle, 342
 hip axis length, 339
 hip strength analysis, 344, 345
 upper femoral neck, 342, 344
- Q**
- QDR@ 4500 A, specifications, 131–133
 QDR@ 4500 C, specifications, 133, 134
 QDR@ 4500 SL, specifications, 134, 135
 QDR@ 4500 W, specifications, 135, 136
- Qualitative morphometry,
 Singh index, 31, 32
 spinal morphometry, 30
- Quality control,
 automated procedures, 249–253
 baseline phantom value determination,
 240, 241
 control table creation, 237, 238
 CUSUM charts, 245, 246, 248, 249
 guidelines, 231, 232, 253
 instrument replacement, 254, 255
 out of control machines, 237, 238
 phantom, *see* Phantoms
 Shewart control chart,
 generation, 238, 240, 243
 interpretation, 240
 Shewart rules,
 origins, 242
 percentage differences, 244, 245
 setting, 243, 244
- Quantitative ultrasound (QUS),
 instrumentation, *see* specific
 instruments
 measurement parameters, 11, 12
- Questionnaire, sample for patients, 408
- QUS, *see* Quantitative ultrasound
- QUS-2@ Calcaneal Ultrasonometer,
 specifications, 158, 159
- R**
- RA, *see* Radiographic absorptiometry
- Race,
 osteoporosis differences, 266
 percent comparison and standard score
 adjustment, 17, 18
- Rad, radiation unit, 215
- Radiation safety,
 exposure in densitometry, 220–222
 harmful effects of ionizing radiation,
 acute lethal radiation syndromes,
 217, 218
 late effects, 219, 220
 local tissue damage,
 bone marrow, 219
 gonads, 218, 219
 skin, 218
 ionizing radiation sources, 217, 220
 patient protection,
 aprons, 227
 pregnancy, 226
 repeat studies, 225, 226
 public protection,
 posting, 223
 radiation survey, 223, 224
 technologist protection,
 distance, 227, 228
 exposure time, 227
 monitoring devices, 228, 229
 pregnancy, 227
 shielding, 227, 228
 units of radiation,
 Curie, 214
 effective dose equivalent, 216
 rad, 215
 rem, 215, 216
 Roentgen, 214, 215
- Radiogrammetry,
 instrumentation, 105, 106
 principles, 33–35
 radiologic osteoporosis score, 35
- Radiographic absorptiometry (RA),
 instrumentation, 107–109
 principles, 37, 38
- Radiographic photodensitometry,
 principles, 36, 37
- Radiologic osteoporosis score,
 determination, 35
- Raloxifene (Evista®), osteoporosis
 prevention and treatment,
 277–278

- Reference databases,
 - comparisons with patient data, 296–299
 - NHANES III proximal femur data, 23–25
 - pediatric densitometry, 324, 325
- Rem, radiation unit, 215, 216
- Reporting,
 - age-regression graph, 19
 - examples, 12, 13
 - percentage comparisons, 13–15
 - review of reports, 308–311
 - standard score comparisons, 15–17, 19
- Ribs, lowest rib position, 71, 72
- Risedronate (Actonel™), osteoporosis prevention and treatment, 280, 281
- RMS-CV, *see* Root-mean-square standard deviation
- Roentgen, radiation unit, 214, 215
- Root-mean-square coefficient of variation (RMS-CV), calculation, 193–196
- Root-mean-square standard deviation (RMS-SD), calculation, 193–196
- RVA™, image resolution, 330, 331
- S**
- Sahara Clinical Bone Sonometer®, specifications, 159, 161
- sBMD, *see* Standardized bone mineral density
- Scoliosis, effects on densitometry measurements, 93
- SD, *see* Standard deviation
- Sectra Osteoporosis Package™ IDS5™ Workstation Clinical Application, specifications, 105, 106
- Shewart control chart,
 - generation, 238, 240, 243
 - interpretation, 240
- Shewart rules,
 - origins, 242
 - percentage differences, 244, 245
 - setting, 243, 244
- Singh index, 31, 32
- Skeletal morphometry,
 - image resolution, 329, 330
 - proximal femur morphometry,
 - cross-sectional moment of inertia, 342, 344
 - femoral neck width, 342
 - femoral neck-shaft angle, 342
 - hip axis length, 339
 - hip strength analysis, 344, 345
 - upper femoral neck, 342, 344
 - vertebral morphometry,
 - fan-array spine imaging, 335–338
 - fracture diagnosis, 330–332
 - Genant technique for fracture assessment, 332
 - prevalent fractures and future fracture risk prediction, 330
 - quantitative techniques for fracture assessment, 332–335
- Skin, radiation damage, 218
- Skinfold measurements, body composition analysis, 350, 351
- Spine,
 - anatomy, 68–73
 - average spine bone density determination, 11
 - fracture effects on densitometry measurements, 73–75
 - lateral projection and vertebrae identification, 84, 85, 87, 88
 - lumbar vertebrae posterior elements, 68, 69
 - morphometry, *see* Vertebral morphometry
 - regions of interest, 293, 294
 - T12 mislabeling effects on densitometry measurements, 73
 - vertebral rotation effects on densitometry measurements, 81–84
- Standard deviation (SD),
 - calculation, 191
 - precision expression, 4
- Standardized bone mineral density (sBMD),
 - calculation and interpretation, 20–22, 300
 - utility, 22, 23

Synthetic salmon calcitonin
(Miacalcin®),
postmenopausal
osteoporosis treatment, 278

T

Tanner stage, determination, 317
Teriparatide (Fortéo®), osteoporosis
prevention and treatment,
283, 284
Testes, radiation damage, 218, 219
Thermoluminescence dosimeter (TLD),
personnel monitoring,
228, 229
TLD, *see* Thermoluminescence dosimeter
Trabecular bone, sites, 6–8
T-score,
conflicting diagnosis from
measurement of multiple
sites, 306–308
pediatric densitometry utilization,
322, 323
reference database comparisons,
297–299
report review, 308–311
scale, 16, 17
Ultrasound, *see* Quantitative ultrasound
Underwater weighing, body composition
analysis, 349, 350

V

Vertebral morphometry,
fan-array spine imaging, 335–338
fracture diagnosis, 330–332
Genant technique for fracture
assessment, 332
prevalent fractures and future fracture
risk prediction, 330
quantitative techniques for fracture
assessment, 332–335
Vertebral rotation, effects on densitometry
measurements,
81–84, 98
Vitamin D supplements, osteoporosis
prevention and treatment,
275

W–Z

Weight bearing skeleton, definition, 4
XCT 2000™, specifications, 147, 148
X-ray, radiographic densitometry, 30
XR-46™, specifications, 136–138
z-score,
pediatric densitometry utilization,
322, 323
reference database comparisons,
297–299
scale, 16, 17

About the Authors

Sydney Lou Bonnick, MD, FACP

Dr. Bonnick is a native of Dallas, Texas and a graduate of Southern Methodist University and the University of Texas Southwestern Medical School. She is board certified in internal medicine and a fellow in the American College of Physicians. She has worked in the field of women's health with an emphasis on osteoporosis and bone densitometry for 20 years.

Dr. Bonnick is one of the founders and past Secretary of the International Society for Clinical Densitometry. She is the 1999 winner of the International Society for Clinical Densitometry President's Award and a past recipient of the American Medical Women's Association President's Recognition Award and the AMWA's Calcium Education Nutrition Award. She is a member of the American Society for Bone and Mineral Research and the North American Menopause Society and a former member of the osteoporosis advisory committee for the Texas Department of Health. She also serves as an associate editor for the *Journal of Clinical Densitometry*.

She has served as a primary investigator in numerous research trials in the field of the prevention and treatment of osteoporosis and has published extensively. In addition to this volume, she is the author of *The Osteoporosis Handbook*, now in its third edition, from Taylor Publishing in Dallas, Texas; *Bone Densitometry in Clinical Practice* from Humana Press in Totowa, NJ, now in its second edition; and the *Pocket Reference for Bone Densitometry* from Science Press in London.

Dr. Bonnick is the medical director of the Clinical Research Center of North Texas and an adjunct professor at the University of North Texas in Denton, Texas.



Lori Ann Lewis, MRT, CDT



Ms. Lewis is a medical radiologic technologist and recognized by the International Society for Clinical Densitometry as a certified densitometry technologist. She is one of the original members of the technologist teaching faculty for ISCD and the 1997 winner of the ISCD technologist of the year award. She is the clinical research coordinator for Dr. Sydney Bonnick and bone density technologist at the Clinical Research Center of North Texas in Denton, Texas. She has extensive experience in bone densitometry on all types of equipment over the last 20 years. She lives in Denton, Texas.